



IPR 2021

The International Pediatric Radiology

8th Conjoint Congress & Exhibition

October 11 – October 15, 2021

& Pre-course Colloquia October, 10-11, 2021

Rome, Italy - Marriott Park Hotel



IPR 2021: BUILDING THE CLASSICS: HISTORY, INNOVATION AND INSPIRATION

Presented by

The European Society of Paediatric Radiology (ESPR)
The Society for Pediatric Radiology (SPR)

Under the Patronage of

Associazione Italiana di Neuroradiologia Diagnostica e Interventistica (AINR)
African Society of Paediatric Imaging (AfSPI)
Asian and Oceanic Society for Paediatric Radiology (AOSPR)
Società Italiana di Radiologia Medica e Interventistica (SIRM)
Sociedad Latino Americana de Radiología Pediátrica (SLARP)
The World Federation of Pediatric Imaging (WFPI)

This supplement was not sponsored by outside commercial interests; it was funded by the Societies' own resources.

TABLE OF CONTENTS

Welcome Message.....	S1
IPR Organization/Committees /Scientific Board.....	S2
Abstract Evaluation Committees.....	S2
ESPR Abstract Review Committee – Papers.....	S2
ESPR Abstract Review Committee - Posters.....	S2
SPR Abstract Review Committee - Papers.....	S3
SPR Abstract Review Committee – Posters.....	S3
Continuing Medical Education	S3
Program at a Glance.....	S4

Acknowledgements.....	S6
2021 Jacques Lefèbvre/Edward B. Neuhauser Lecture.....	S6
ESPR 2021 Honorary Member	S6
SPR 2021 Honorees	S6
Social Activities.....	S13
Scientific Paper Abstracts.....	S13
Educational and Scientific Posters	S82
Authors Index by abstracts.....	S219

WELCOME MESSAGE

Dear friends and colleagues,

After the chaos, heartache and tragedy of the coronavirus pandemic, we are delighted to welcome you to the 8th International Pediatric Radiology (IPR) Congress which will be held in Rome from October 10 to 15th 2021. We welcome not only members from the two organizing societies but all pediatric radiologists and imaging specialists from all over the world to liaise professionally, to meet old friends and to make new ones as well as engage in high-level interdisciplinary exchange.

The motto for the 2021 IPR remains, “Building on the Classics: History, Innovation and Inspiration” and highlights the continuity of growth in knowledge in the pediatric imaging field.

Although the meeting will be hybrid, with live streaming and on-demand access to the program, we are expecting a large in-person contingent now that the pandemic restrictions are lifting. We will be offering rapid covid testing on site at the Marriott Park Hotel, our conference venue.

The IPR congress is a joint effort of the European and the American societies for pediatric radiology (ESPR and SPR). The congress is held once every 5 years and rotates between a North American location and a European location. Since the inaugural IPR was convened in Toronto in 1987, the IPR has grown into a global event which defines the current state of pediatric radiology. The IPR is the most important meeting for pediatric radiologists as it brings together the key figures and scientific leaders in the field of pediatric imaging from all around the world.

The scientific planning committee has put together an exciting program consisting of >100 hours of educational content. Our world-renowned faculty will present a bench-to-bedside overview of the field of pediatric radiology with special focus sessions on advanced technology, artificial intelligence, personalized medicine, and emerging diseases. There will be two concurrent Categorical Courses that will run throughout the meeting. One Categorical Course – “Pediatric Radiology Essentials” - will focus on basic pediatric imaging and is designed for trainees, general

radiologists, and as a review for pediatric radiologists. The second Categorical Course – “Tips for the Specialists” - is designed for pediatric radiologists who are well versed in the field and will concentrate on controversies and advanced concepts.

The scientific program consists of 24 sessions running in parallel, and 180 oral papers will be presented. Other features include sunrise sessions dedicated to specific topics of current interest. Additionally, there will be over 400 Poster presentations, including 117 educational exhibits and 277 scientific exhibits.

The Pre-course Colloquia, which will be held on the 10 and the morning of the 11 of October, are designed for learning in small groups and will present innovative and controversial papers in five separate programs, including the imaging of child abuse, post-mortem imaging, fetal and placental imaging, advanced pediatric MR imaging and the work of the World Federation of Pediatric Imaging. Another highlight will be the IPR Olympics hosted by Thierry Huisman, a jeopardy-style format that will challenge the best and brightest from both societies. It is sure to be a fun and educational event. On Tuesday afternoon, Paolo Tomà (from Rome, Italy) will present the Jacques Lefèbvre/Edward B. Neuhauser Lecture titled “Lessons of a life as a pediatric radiologist”.

Welcome to Rome and to a truly extraordinary scientific program, both virtual and on-demand... “a presto!”



Andrea Rossi, MD
ESPR, Co-President IPR



Damien Grattan-Smith, MD
SPR, Co-President IPR

IPR ORGANIZATION

IPR Co-Presidents

Andrea Rossi, ESPR - Co-President IPR (Genoa, Italy)
Damien Grattan-Smith, SPR - Co-President IPR (Atlanta, USA)

Special Assistant to the Presidents

Rutger-Jan Nievelstein (Utrecht, The Netherlands)

Categorical Course:

Owen Arthurs (London, United Kingdom)
Jean-François Chateil (Bordeaux, France)
Jeanne (Mei-Mei) Chow (Boston, USA)
Josee Dubois (Montreal, Canada)

Sunrise Sessions

Maria Argyropoulou (Ioannina, Greece)
Franz-Wolfgang Hirsch (Leipzig, Germany)
Jeannette Perez-Rossello (Boston, USA)
Mahesh Thapa (Seattle, USA)

Scientific Sessions Directors

Brandon Brown (Indianapolis, USA)
Maria Beatrice Damasio (Genoa, Italy)
Maarten Lequin (Utrecht, The Netherlands)
Lil-Sofie Ording-Muller (Oslo, Norway)
Erika Rubesova (Stanford, USA)
Teresa Victoria (Philadelphia, USA)

IPR Olympics

Thierry A.G.M. Huisman (Houston, USA)
Rutger-Jan Nievelstein (Utrecht, The Netherlands)

Pre-course Colloquia

Advanced Pediatric MRI: Richard Jones (Atlanta, USA), Antonio Napolitano (Rome, Italy)
Child abuse: Arabinda Choudhary (Little Rock, USA), Amaka Offiah (Sheffield, United Kingdom)
Feto-placental imaging: Gabrielle Colleran (Boston, USA), Mariana Meyers (Aurora, USA),
Postmortem imaging: Owen Arthurs (London, United Kingdom),

World Federation of Pediatric Imaging: Joanna Kasznia-Brown (Bristol, United Kingdom)

Junior IPR

Maddy Artunduaga (Dallas, USA)
Pablo Caro (Seville, Spain)
Julian Jürgens (Hamburg, Germany)
Fiammetta Sertorio (Genoa, Italy)
Elizabeth Snyder (Nashville, USA)

Cases of the Day Organizers

Neil D. Johnson (Cincinnati, USA)
Aurelio Secinaro (Rome, Italy)
Christopher Sternal-Johnson (Cincinnati, USA)

Abstract Evaluation Committees

ESPR – Abstract Review Committee – Papers and Electronic Posters

Michael Aertsen
Alexopoulou Efthymia
Maria Argyropoulou
Owen Arthurs
Loukas Astrakas
Fred Avni
Shivaram Avula
Ignasi Barber
Süreyya Burcu Görkem
Pablo Caro
Marie Cassart
Greg Chambers
Jean-François Chateil
Pierluigi Ciet
Giorgio Conte
Felice D’Arco
Maria Beatrice Damasio
Charlotte De Lange
Marjolein Dremmen
Catherine Garel
Maria Carmen Garganese
Ralph Gnannt
Daniel Gräfe
Claudio Granata
Franz-Wolfgang Hirsch
Julian Jürgens
Willemijn Klein
Damjana Kljucsevsek
Martin Kyncl
Tim Leiner
Maarten Lequin
Annemieke Littooi
Maria Luisa Lobo

Lucia Manganaro
 Kshitij Mankad
 Kieran McHugh
 Fernando Gómez Muñoz
 Rutger Jan Nievelstein
 Catherine Owens
 Premal Patel
 Annie Paterson
 Giulia Perucca
 Philippe Petit
 Maria Raissaki
 William Ramsden
 Monica Rebollo
 Andrea Righini
 Karen Rosendahl
 Maria Camilla Rossi Espagnet
 Aurelio Secinaro
 Mariasavina Severino
 Susan Shelmerdine
 Erich Sorantin
 Laura Tanturri De Horatio
 Eilish Twomey
 Rick Van Rijn
 Jens Vogel-Claussen
 Thekla Von Kalle

SPR – Abstract Review Committee – Papers

Dianna Bardo
 Heather Bray
 Teresa Chapman
 Govind Chauvin
 Kassa Darge
 Lane Donnelly
 Josee DuBois
 Laura Fenton
 Donald Frush
 Cristian Garcia Bruce
 Michael Gee
 Damien Grattan-Smith
 Roger Harned
 Beth Kline-Fath
 Rajesh Krishnamurthy
 Neil Lall
 Henrique Lederman
 Stephen Little
 GraceMa
 John MacKenzie
 Beverly Newman
 Jie Nguyen
 Janet Reid
 Cynthia Rigsby
 Victor Seghers
 Dennis Shaw
 Ethan Smith
 Andrew Trout
 Jason Weinman

SPR – Abstract Review Committee – Electronic Posters

Anjum Bandarkar
 Richard Bellah
 Sarah Bixby
 Hans Blickman
 Kiery Braithwaite
 Micheal Breen

Lorna Browne
 Hisham Dahmouh
 Nilesh Desai
 Paula Dickson
 Steven Don
 Judith Gadde
 Anne Elizabeth Gill
 Jared Green
 Leslie Hirsig
 Thierry Huisman
 Pinar Karakas-Rothey
 Neha Kwatra
 Maria and Ladino-Torres
 Shailee Lala
 Jonathan Loewen
 Yu Luo
 Jonathan Mumick
 Helen Nadel
 Dhananjaya Kotebagilu Narayana Vamyanmane
 Srikala Narayanan
 Hansel Otero
 Daniel Podberesky
 Maura Ryan
 Raja Shaikh
 Susan Sharp
 Manrita Sidhu
 Aylin Tekes-Brady
 Stephanie Theut
 Alexander Towbin
 Nghia Vo
 Ewa Wasilewska
 Arash Zandieh

CONTINUING MEDICAL EDUCATION

Accreditation Statement

An application has been made to the UEMS EACCME for CME accreditation of this event.

The request of accreditation was submitted in accordance with the requirements and policies of the European Board of Radiology – Accreditation Council in Imaging.

“The **IPR2021 - The International Pediatric Radiology 8th Conjoint Congress & Exhibition, Rome (hybrid), Italy, 10/10/2021-15/10/2021** has been accredited by the European Accreditation Council for Continuing Medical Education (EACCME[®]) with **33** European CME credits (ECMEC[®]s).


Each medical specialist should claim only those hours of credit that he/she actually spent in the educational activity.”

“Through an agreement between the Union Européenne des Médecins Spécialistes and the American Medical Association, physicians may convert EACCME[®] credits to an equivalent number of AMA PRA Category 1 Credit(s)TM.

Information on the process to convert EACCME[®] credit to AMA credit can be found at "<http://www.ama-assn.org/education/earn-credit-participation-international-activities>" www.ama-assn.org/education/earn-credit-participation-international-activities.

“Live educational activities, occurring outside of Canada, recognised by the UEMS-EACCME[®] for ECMEC[®]s are deemed to be Accredited Group Learning Activities (Section 1) as defined by the Maintenance of Certification Program of the Royal College of Physicians and Surgeons of Canada.”

PROGRAM AT A GLANCE



IPR 2021
The International Pediatric Radiology
8th Conjoint Congress & Exhibition
October 11–15, 2021
Pre-course Colloquia October 10–11, 2021
Rome Marriott Park Hotel

PROGRAM AT A GLANCE


IPR 2021 PRE-COURSES - OCTOBER 10-11, 2021

SUNDAY, OCTOBER 10, 2021

	MICHELANGELO PLENARY ROOM	TIZIANO 1 ROOM	TIZIANO 2 ROOM	TIZIANO 3 ROOM	CARAVAGGIO ROOM	BRAMANTE ROOM	TIZIANO FOYER	LOBBY	
08:00-11:00							EXHIBITION COMMON AREA	REGISTRATION	08:00-11:00
11:00-13:00		Pre-Course Colloquium	Pre-Course Colloquium	Pre-Course Colloquium	Pre-Course Colloquium NOT CME ACCREDITATION	Pre-Course Colloquium			11:00-13:00
13:00-14:15	Break								13:00-14:15
14:15-15:45		Pre-Course Colloquium	Pre-Course Colloquium	Pre-Course Colloquium	Pre-Course Colloquium NOT CME ACCREDITATION	Pre-Course Colloquium			14:15-15:45
15:45-16:15	Break								15:45-16:15
16:15-17:45		Pre-Course Colloquium	Pre-Course Colloquium	Pre-Course Colloquium	Pre-Course Colloquium NOT CME ACCREDITATION	Pre-Course Colloquium			16:15-17:45

MONDAY, OCTOBER 11, 2021

	MICHELANGELO PLENARY ROOM	TIZIANO 1 ROOM	TIZIANO 2 ROOM	TIZIANO 3 ROOM	CARAVAGGIO ROOM	BRAMANTE ROOM	TIZIANO FOYER	LOBBY	
08:30-10:00		Pre-Course Colloquium	Pre-Course Colloquium	Pre-Course Colloquium	Pre-Course Colloquium NOT CME ACCREDITATION	Pre-Course Colloquium	EXHIBITION COMMON AREA	REGISTRATION	08:00-11:00
10:00-10:30	Break								11:00-13:00
10:30-12:00		Pre-Course Colloquium	Pre-Course Colloquium	Pre-Course Colloquium	Pre-Course Colloquium NOT CME ACCREDITATION	Pre-Course Colloquium			13:00-14:00
12:00-13:00	Break								14:15-15:45




IPR 2021
The International Pediatric Radiology
8th Conjoint Congress & Exhibition
October 11–15, 2021
Pre-course Colloquia October 10–11, 2021
Rome Marriott Park Hotel

PROGRAM AT A GLANCE

IPR 2021 CONGRESS - OCTOBER 11-15, 2021

MONDAY, OCTOBER 11, 2021

	MICHELANGELO PLENARY ROOM	TIZIANO 1 ROOM	TIZIANO 2 ROOM	TIZIANO 3 ROOM	CARAVAGGIO ROOM	BRAMANTE ROOM	TIZIANO FOYER	LOBBY	
13:00-14:50		Categorical Course			Categorical Course		EXHIBITION COMMON AREA	REGISTRATION	13:00-14:50
15:00-15:30	Break								15:00-15:30
15:30-16:50		Categorical Course			Categorical Course				15:30-16:50
17:00-19:00	Opening Ceremony & Opening Lectures								17:00-19:00
19:00-22:00	WELCOME RECEPTION								19:00-22:00




IPR 2021
The International Pediatric Radiology
8th Conjoint Congress & Exhibition
October 11–15, 2021
Pre-course Colloquia October 10–11, 2021
Rome Marriott Park Hotel

PROGRAM AT A GLANCE

IPR 2021 CONGRESS - OCTOBER 11-15, 2021

TUESDAY, OCTOBER 12, 2021

	MICHELANGELO PLENARY ROOM	TIZIANO 1 ROOM	TIZIANO 2 ROOM	TIZIANO 3 ROOM	CARAVAGGIO ROOM	BRAMANTE ROOM	TIZIANO FOYER	LOBBY	
08:00-09:30		Categorical Course			Categorical course		EXHIBITION COMMON AREA	REGISTRATION	08:00-09:30
09:30-10:00	Break								09:30-10:00
10:00-11:45	Scientific Session	Scientific Session	Scientific Session		Scientific Session				10:00-11:45
12:00-13:00	Break		INDUSTRY Sponsored Session						12:00-13:00
13:10-14:15	Jacques Lellouche/ Edward B. Reibman Lecture								13:10-14:15
14:15-15:15		Categorical Course			Categorical course				14:15-15:15
15:15-15:45	Break								15:15-15:45
15:50-16:50	Scientific Session	Scientific Session	Scientific Session		Scientific Session				15:50-16:50
17:00-18:15	ESPR & SPR Awards and Honorary Members Ceremony								17:00-18:15



INTERNATIONAL PEDIATRIC RADIOLOGY CONGRESS


IPR 2021
The International Pediatric Radiology
8th Conjoint Congress & Exhibition
 October 11–15, 2021
 Pre-course Colloquia October 10–11, 2021
 Rome Marriott Park Hotel

PROGRAM AT A GLANCE

IPR 2021 CONGRESS - OCTOBER 11-15, 2021

WEDNESDAY, OCTOBER 13, 2021

	MICHELANGELO PLENARY ROOM	TIZIANO 1 ROOM	TIZIANO 2 ROOM	TIZIANO 3 ROOM	CARAVAGGIO ROOM	BRAMANTE ROOM	TIZIANO FOYER	LOBBY		
07:30-08:20	Sunrise Session	Sunrise Session	Sunrise Session				EXHIBITION COMMON AREA	REGISTRATION	07:30-08:20	
08:30-10:00		Categorical Course			Categorical Course				08:30-10:00	
10:00-10:30	Break									10:00-10:30
10:30-11:30		Categorical Course			Categorical Course				10:30-11:30	
11:35-13:15	Scientific Session	Scientific Session	Scientific Session		Scientific Session				11:35-13:15	
13:30-14:30	Break									13:30-14:30
	FREE AFTERNOON									
	FREE AFTERNOON									



INTERNATIONAL PEDIATRIC RADIOLOGY CONGRESS


IPR 2021
The International Pediatric Radiology
8th Conjoint Congress & Exhibition
 October 11–15, 2021
 Pre-course Colloquia October 10–11, 2021
 Rome Marriott Park Hotel

PROGRAM AT A GLANCE

IPR 2021 CONGRESS - OCTOBER 11-15, 2021

THURSDAY, OCTOBER 14, 2021

	MICHELANGELO PLENARY ROOM	TIZIANO 1 ROOM	TIZIANO 2 ROOM	TIZIANO 3 ROOM	CARAVAGGIO ROOM	BRAMANTE ROOM	TIZIANO FOYER	LOBBY		
07:30-08:20	Sunrise Session	Sunrise Session	Sunrise Session				EXHIBITION COMMON AREA	REGISTRATION	07:30-08:20	
08:30-10:00		Categorical Course			Categorical Course				08:30-10:00	
10:00-10:30	Break									10:00-10:30
10:30-11:55	Scientific Session	Scientific Session	Scientific Session		Scientific Session				10:30-11:55	
12:00-12:30	JOSPAR Lecture								12:00-12:30	
12:45-13:45	Break		INDUSTRY Sponsored Session						12:45-13:45	
13:50-15:15	IPR Olympics Panel								13:50-15:15	
15:20-16:20		Categorical Course			Categorical Course				15:20-16:20	
16:20-16:50	Break							16:20-16:50		
16:50-18:00	Scientific Session	Scientific Session	Scientific Session		Scientific Session		16:50-18:00			



INTERNATIONAL PEDIATRIC RADIOLOGY CONGRESS

IPR 2021
The International Pediatric Radiology
8th Conjoint Congress & Exhibition
 October 11–15, 2021
 Pre-course Colloquia October 10–11, 2021
 Rome Marriott Park Hotel

PROGRAM AT A GLANCE

IPR 2021 CONGRESS - OCTOBER 11-15, 2021

FRIDAY, OCTOBER 15, 2021

	MICHELANGELO PLENARY ROOM	TIZIANO 1 ROOM	TIZIANO 2 ROOM	TIZIANO 3 ROOM	CARAVAGGIO ROOM	BRAMANTE ROOM	TIZIANO FOYER	LOBBY		
07:30-08:20	Sunrise Session	Sunrise Session	Sunrise Session				EXHIBITION COMMON AREA	REGISTRATION	07:30-08:20	
08:30-10:00		Categorical Course			Categorical Course				08:30-10:00	
10:00-10:30	Break									10:00-10:30
10:30-11:55	Scientific Session	Scientific Session	Scientific Session		Scientific Session				10:30-11:55	
12:00-13:00									12:00-13:00	
13:00-14:00	Break									13:00-14:00
14:10-15:30	Scientific Session	Scientific Session	Scientific Session		Scientific Session				14:10-15:30	
15:30-16:00	Break									15:30-16:00
16:00-17:20	Scientific Session	Scientific Session	Scientific Session		Scientific Session		16:00-17:20			
17:25-17:45	Closing Ceremony						17:25-17:45			

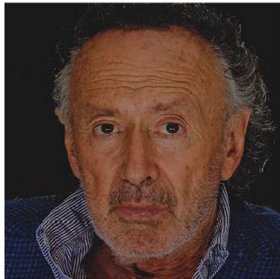
ACKNOWLEDGEMENTS

As the host Society, the European Society for Pediatric Radiology gratefully acknowledges the promotional supporters of the 8th International Pediatric Radiology Conjoint Congress & Exhibition.

BAYER Italia
BAYER AG
BRACCO SUISSE
DOMED
FUJIFILM ITALIA
LMT Medical Systems
PHILIPS Healthcare
PLANMED

As of July 30, 2021

2021 JACQUES LEFÈBVRE/EDWARD B. NEUHAUSER LECTURE



Paolo Tomà, MD

Professor Paolo Tomà is one of the giants of paediatric radiology in Italy and in Europe. He worked at the G. Gaslini Institute from 1980 until 2009 where he became radiologist-in-chief, and then moved to the Bambin Gesù Children's Hospital in Roma, where he has chaired the Department of Radiology since 2010. A prolific scholar, Paolo has published more than 228 peer reviewed articles on a broad range of topics including paediatric ultrasound, radiation protection, hip dysplasia and cardiothoracic imaging. In addition to his many academic accomplishments, Paolo has been a leader in the Italian Radiological and Paediatric societies as well as the ESPR and was awarded the Gold Medal of the ESPR in 2016. Paolo's career has also been celebrated by the Society of Paediatric Radiology honouring him with their Honorary Membership in 2021. His lecture on "Lessons of a life as a Paediatric Radiologist" will be a highlight of this year's IPR.

ESPR 2021 HONORARY MEMBER



Rick R. van Rijn, MD, PhD

Professor Rick R. van Rijn, MD, PhD was born in Leiden, the Netherlands and attended medical school, trained in radiology and defended his PhD thesis at the University of Rotterdam. Since 2001 he has worked in Amsterdam; from 2003 to date as a pediatric radiologist at the Amsterdam University Medical Center (AMC). From 2010 onwards, he has also held the position of forensic radiologist at the Netherlands Forensic Institute, the Hague, and from 2014 as a professor in forensic radiology with an emphasis on forensic pediatric radiology.

Rick is a dedicated pediatric radiologist and researcher. Early in his career Rick gained an interest in pediatric musculoskeletal radiology. Following his PhD thesis "Radiological strength assessment of the proximal femur", he gradually developed an interest in inflicted trauma in children and initiated numerous studies to define the problem and understand the mechanisms of abusive trauma. Subsequently, this work has helped establish guidelines on how to deal with suspected inflicted trauma.

Amongst other roles, Rick is the vice-secretary of the World Federation of Pediatric Imaging, secretary of the European Society of Paediatric Radiology and Board member of the Dutch Expertise Centre for Child Abuse. He supervises several research groups on abusive trauma and forensic imaging, has published more than 230 original and review articles in peer reviewed journals, edited or co-edited four books and written 24 book chapters. He has also contributed to the publication of 4 national/international guidelines.

Rick has been a huge source of inspiration over the years and has mentored 15 PhD candidates, 8 on-going and 7 of whom have successfully defended their theses. He is currently a member of the Editorial Board for Pediatric Radiology and a member of the Child Abuse Task Force of ESPR. In both roles, his enthusiasm for our specialty, work ethic and attention to detail are all of tremendous benefit.

Despite his busy work schedule, Rick finds the time to be a cheerful, reliable and helpful colleague and friend (and I speak from personal knowledge, having known him since 2002, when he came as a visitor to Great Ormond Street Hospital). He is also a loving and supportive husband and father to Melanie and their two boys.

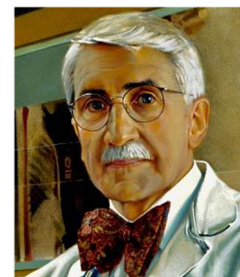
It is a great privilege to award the ESPR Honorary membership to such a special radiologist, and our society, and children of Europe have greatly benefited and will continue to benefit from his enthusiasm, consistent dedication and hard work.

Karen Rosendahl and Amaka C. Offiah

SPR 2021 HONOREES

SPR 2021 GOLD MEDALIST

The Gold Medal of The Society for Pediatric Radiology is our most distinguished honor. The SPR Gold Medal is awarded to pediatric radiologists who have contributed greatly to the SPR and our subspecialty of pediatric radiology as a scientist, teacher, personal mentor and leader.



Kenneth E. Fellows, MD

Kenneth E. Fellows, one of our 2021 Gold Medalists, was born in Grand Rapids, MI in 1938. His father was a Radiologist. He attended Grand

Rapids Junior College for two years in his hometown. He then finished his college studies at the University of Michigan in Ann Arbor, where he also attended Medical School and received his MD degree in 1963. A rotating Internship at The University of Oregon Hospitals followed. Under the Berry Plan Ken joined the US Navy for 2 years and served both on a destroyer and at Balboa Naval Medical Center in San Diego. This posting in California was providential as it is where he met and subsequently married Kristen Thorsdale. They recently celebrated their 55th wedding anniversary.

Their oldest child, Ian, died suddenly and unexpectedly in 2006 of heart disease at age 37. Their daughter Maria is a Social Worker, doing Marriage and Family Counseling. Their daughter Hannah is a Registered Nurse, and the mother of Ken's and Kristen's granddaughter Ella. Their son Jesse is married and is a Food Research Scientist.

After the Navy, Ken was a Resident in Radiology at Children's Hospital Medical Center in Boston and then a Radiology Resident at the University of Michigan Hospitals in Ann Arbor. When he completed his residency, he became a Research Fellow in Pediatric Radiology under the auspices of the Max Kade Foundation in Hamburg, Germany.

Returning to Boston after a year abroad, Ken joined the staff of Boston Children's under the Chairmanship of Dr. EBD Neuhauser. His colleagues in the Department included Drs. GBC (Clif) Harris, N.T. (Thorne) Griscom, Robert (Bob) Wilkinson, Roy Strand, and S.T. (Ted Treves). Ken also rose to the rank of Associate Professor at Harvard Medical School.

While at Boston Children's, Ken began to specialize in Pediatric Cardiac Radiology. He worked intimately on clinical cardiac problems in infants and children with colleagues from Pediatric Cardiac Surgery, Pediatric Cardiology, and Pediatric Pathology, such as Alexander Nadas, Aldo Castenada, Amnon Rosenthal, William Norwood, Roberta Williams, Richard Van Praagh, and Barry Keane. In 1984 Ken was made an Honorary Member of The Society of Pediatric Cardiovascular Surgery. In 1984, Ken left Boston Children's to become Professor of Radiology at The University of Pennsylvania and Radiologist-in-Chief (and Associate in Cardiology) at Children's Hospital of Philadelphia (CHOP); in 1992, he became President of the Medical Staff there.

In 1995 Ken received the Charles Dotter Memorial Award from The American Heart Association Council on Cardiovascular Radiology.

In our Society Ken served as Chairperson of The Pediatric Cardiovascular and Interventional Committee, The R and E Fund Committee, The Finance Committee, and in 1994-5 The Meeting Site Committee and The Program Committee. In 1995-96 Ken was The President of our Society and was The co-Chair for the 3rd conjoint Meeting of The SPR, The European Society of Pediatric Radiology, and The Australasian Society of Pediatric Radiology, held in Boston in 1996.

Ken served as Co-Editor-in-Chief of the journal *Cardiovascular and Interventional Radiology*, and he is now Editor Emeritus.

Between 1989 and 1992, he received three Siemens Research Grants for his Department in Philadelphia.

In 1992 Ken began to think of retirement. Always a careful planner, he began to prepare by enrolling in drawing and painting courses at the Wallingford, PA, Art Center, and the Philadelphia College of the Arts.

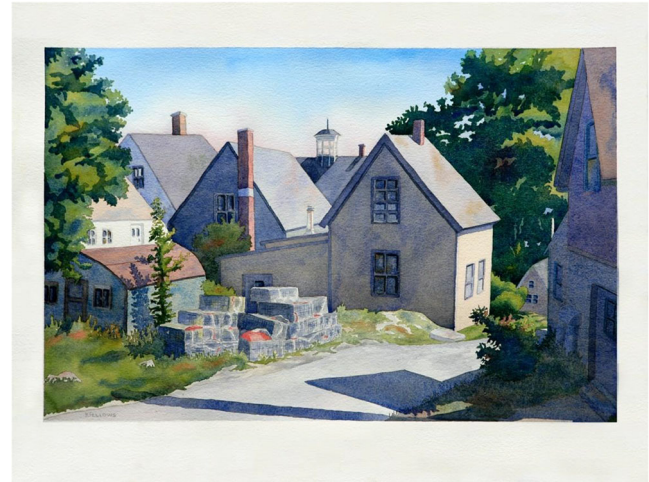
Following retirement in 2001, Ken and Kristen moved to Kittery Point, Maine, on the coast. When the wind is from the East, one can smell the salt air. In addition to playing pond hockey and pick-up basketball, Ken continued his art instruction and education and attended many watercolor workshops.

Always an artist in his career in Diagnostic Radiology and Cardiovascular Radiology, Ken is a talented artist in his retirement. Painting is his "second act." He paints Maine landscapes, portraits, including many of Ella, and whatever else captures his attention. One of his many paintings is shown below. He says that painting is pure pleasure for him, and that is his incentive. He loves the things he paints and hopes they may be interesting or pleasurable to those who view them.

"Within organizations, trust is usually built by leaders who create environments that encourage people to behave with integrity, competence,

and benevolence," and this is just what Ken did, wherever he was. After such an exemplary career in Pediatric Radiology and his dedicated efforts on behalf of our specialty and our Society, congratulations and best wishes to our friend and colleague, Ken Fellows.

Robert L. Lebowitz, MD



Lobster Traps and Houses by Ken Fellows

SPR 2021 GOLD MEDALIST



The Rev. Joanna J. Seibert, MD

"Variety of form and brilliancy of color in the object presented to patients are an actual means of recovery."

– Florence Nightingale

Joanna Johnson grew up in the small town of West Point, Virginia where her dad (Bud) was a forester and mom (Florence) a homemaker. She benefitted from unconditional love from her maternal grandparents who lived a block away and farmed land across the York River. While attending the women's University of North Carolina-Greensboro, Joanna worked summers as a medical technologist. She believed this was her career path, but when her husband's training in Optometry led to a move to Memphis, Joanna realized she enjoyed working with patients; she applied and was accepted as one of eight females in the class at the University of Tennessee College of Medicine. Midway through medical school Joanna had to deal with two major setbacks – a divorce followed by a life-altering car wreck. Bilateral ankle fractures and knee/back injuries delayed Joanna's medical school studies (now the only female in her class), but helped steer her toward Radiology training over Pediatrics. Later in medical school, Joanna met her second husband Robert Seibert on an Obstetrics rotation and they married in 1969. They never would have met if she had not had that accident and dropped back into Robert's class.

During her Radiology residency years at the University of Tennessee, Dr. Seibert was fortunate to spend a year at LeBonheur and St Jude's children's hospitals under the mentoring of Memphis's first trained pediatric radiologist, Dr. William Webster Riggs, Jr. Dr. Riggs recalls a "fabulous, soft spoken, highly intelligent trainee with a serene atmosphere" whom he encouraged to pursue a career in pediatric radiology. He remembers Joanna working hard while raising two children at a time her husband Robert was in Vietnam with military duty. Dr. Riggs helped jumpstart an academic career when he collaborated with Joanna on her first two publications in *AJR* (Cockayne's syndrome) and *Radiology* (Pseudoectopic ureter) in the early 1970s. Dr. Riggs, godfather to Joanna's son Robert, considers training Dr. Seibert as his "claim to fame!"

When Dr. Robert Seibert was accepted into Otolaryngology training at the University of Iowa, radiologist Dr. Jim Christie appointed pediatric radiologist Dr. Joanna Seibert as their first woman faculty member. Both Doctors Seibert were subsequently recruited to Arkansas by Dr. Robert Fiser, a visionary Chair of Pediatrics, who was planning to move the Pediatrics department from the university campus into what had previously been an indigent Orthopedic hospital. Joanna vividly recalls driving their 3 children (Robert, John and Joanna) into Little Rock on the Fourth of July 1976, the bicentennial year. With Robert's parents nearby in Memphis and helping with child rearing duties in the Natural State, the Seiberts now had a chance of a lifetime: they could help develop a high-quality children's hospital from the ground up.

Dr. Joanna Seibert started by reading films right off the developer, in a department with one X-ray room and a fluoroscopy unit where you viewed the screen through a mirror. Over her 23 years of Chief of Radiology at Arkansas Children's Hospital, Joanna collaborated to develop a full-service Radiology department, developing ultrasound technologists and introducing the full range of state-of-the-art modalities. She remembers the endless hours spent recruiting colleagues, physicians typically unfamiliar with Arkansas, who often spent part of their recruitment visit with the Seibert family. Joanna had a different management style (she did not believe in hierarchy) and recruited others into the department who then became equal participants in decision making. Her scholarly contributions were numerous including 140 peer-reviewed articles, 20 book chapters and a widely popular textbook, *Pediatric Radiology: Casebase*. Dr. Seibert chose Sickle Cell Doppler as her research focus because she was already interested in Doppler and the leader in this field, Dr. Robert Adams had gone to school in Arkansas. He quickly connected with Joanna and their ultrasound teams developed a lasting relationship. Beyond all of her achievements in Radiology, Dr. Joanna Seibert was always beloved by the housestaff at a rapidly growing Arkansas Children's Hospital for incorporating radiologic findings into clinical decision making. Respect for Dr. Seibert outside of Radiology is evident in numerous awards such as Outstanding Teacher by the Pediatrics housestaff in 1977, Friend of the Housestaff award in 1983 and her election into the Arkansas Women's Hall of Fame in 2017. Her leadership often extended beyond the Radiology Department, such as the years serving as Chief of Staff for Arkansas Children's Hospital from 1990–1992. Before completing her tenure at ACH Radiology her departmental mentoring skills became evident in her outstanding Chief replacement (Dr. Richard Leithiser) and pediatric radiologists that would serve as president of their subspecialty societies (Dr. Charles Glasier – ASPNR, Dr. Bruce Greenberg – NASCI, Dr. Charles James – SPIR, and Dr. Mary Beth Moore – MIRS). Arkansas Children's gives an award biennially to physicians who embody a practice of teamwork named the Joanna and Robert Seibert Award.

A glimpse of Dr. Seibert's career impact as a pediatric radiologist is provided in the words of two past SPR Gold Medalists. According to Dr. Diane Babcock (Gold Medalist 2004), "My thought is that of course she contributed so much to the use of ultrasound for diagnosis and follow-up of pediatric patients – but what comes to mind is her development and

teaching others to use TCD in diagnosis of cerebral vascular disease in sickle cell patients. It is so difficult and tedious to perform, but she mastered the technique and taught so many of us – radiologists and ultrasound technologists – to do it. And it benefitted the patients by suggesting successful treatment with transfusions." Dr. Dorothy Bulas (Gold Medalist 2018) states "Joanna Seibert has been such an inspirational role model throughout her career! Compassionate and brilliant, she showed so many of us how to do it all regarding teaching, research, writing, clinical care while balancing it with a life filled with family and spirituality. A true original!!"

Dr. Joanna Seibert feels her greatest career accomplishment was becoming connected to the SPR at the beginning of her career. This is where she met some of the most outstanding physicians she will ever know as well as constantly learning new ideas and examining old ways of doing things. In her words, "The SPR was a constant place of learning and friendship and collaboration". SPR Executive Director Jennifer Boylan (Gold Medalist 2016) recalls her second year with the SPR when Dr. Seibert ran "an exceptional meeting" in 1994 in Colorado Springs despite an unexpected snowstorm which cancelled many planned outdoor events. "The Board meeting was held in her Presidential Suite – which was a room with windows on three sides. We were nestled in a warm room watching the snow fall on the mountains." This meeting was the first where SPR video recorded talks as an educational resource for members preparing for the first CAQ exam in 1995. In addition, the SPR Foundation was established that year as an official, separate 501c3 organization. Jennifer fondly recalls in the winter of that same year when her dad was a patient at Johns Hopkins being treated for leukemia. "I accompanied my grandmother, his mom – to Baltimore so we could visit him. Joanna was a Visiting Professor at Hopkins – found out I was there and why – and came and visited with me and my dad. I'll never forget that kindness. My dad was thrilled to meet someone from my professional life."

Joanna Seibert's spiritual journey began in childhood where she attended Sunday morning services at a Methodist church (her paternal grandfather was a Methodist minister) and Sunday evening Baptist services with her maternal grandparents. In medical school both Joanna and Robert Seibert became Episcopalians where the Dean of the Episcopal Cathedral in Memphis offered the spiritual guidance they were seeking. In the early 1990s in Little Rock, the Seiberts helped establish St Margaret's Episcopal Church. During these years, Joanna overheard a friend discussing a school for deacons, prompting Joanna's interest and eventual ordination as a deacon in 2001. In an April 2021 Arkansas Democrat-Gazette High Profile article by Rachel O'Neal on The Reverend Joanna Johnson Seibert, M.D., Reverend Danny Schieffler, Rector of St. Mark's Episcopal Church is quoted saying "Part of her strength and power in her ministry is because she is open about her vulnerabilities and struggles and she is very relatable when she is teaching and preaching." Part of Seibert's ministry through the Episcopal Church is helping people in alcohol and substance abuse recovery. Reverend Seibert comments "I do think it is important to let people know that the church really cares about those caught in addiction, and that it is not a moral failing. It is a disease."

Learning to play the harp when her daughter Joanna was a child, Dr. Seibert feels putting this instrument against your body helps one "feel the music in your body." Reverend Seibert strives to play the harp on most days, often setting the tone for the congregation before the early morning church service. She would often go to the Arkansas Children's NICU and play the harp, where once a parent asked Dr. Seibert to play the harp to provide comfort while her baby was dying.

In the words of former United States Secretary of State Hillary Rodham Clinton: "Dr. Joanna Seibert has been a stalwart champion for the children and families of Arkansas for 45 years now. Over that time, she has shaped, changed, and saved countless lives. I am proud to be her friend, and to have partnered with her on advancing the health and wellbeing of

our most vulnerable and precious citizens throughout her trailblazing career in medicine.”

Joanna Seibert feels her greatest accomplishment in life has been marrying her amazing partner Robert Seibert of over 52 years and raising three caring children with six just-as-thoughtful-grandchildren. Her favorite paraphrased quote is from American writer, theologian and Presbyterian minister Frederick Buechner: “The place God calls us to is where our greatest bliss meets the world’s greatest need.” Joanna states: “My bliss was always working with children and trying to improve their lives and teaching and sharing with others what I had learned. The greatest need was for children’s health and having a children’s advocate. Now I have learned from children more about the needs of the world.”

“Where the spirit does not work with the hand there is no art.”

– Leonardo da Vinci

Dr. Joanna Seibert practiced the art of medicine at the highest level, elevating the Society for Pediatric Radiology along her journey. Using her artistic gift of playing the harp and cultivating years of spiritual ministry, Reverend Joanna Seibert continues to provide wellness and healing benefitting the community at large. The SPR is grateful for these unique contributions and pleased to bestow with enthusiasm this highest societal honor, a Gold Medal, to a deserving Renaissance woman!

Charles A. James, MD, FACR

SPR 2021 PIONEER AWARD

Pioneer Honorees were first acknowledged in 1990 as a means to honor certain physicians who made special contributions to the early development of our specialty. The Pioneer Award now honors individuals who have advanced pediatric radiology through innovation, forethought and leadership.



Ramiro J. Hernandez, MD, MS

Ramiro Hernandez arrived in the United States in 1971 from Valencia, Spain where he was raised, educated, and graduated from medical school. Following an internship at Vassar Brothers Hospital in Poughkeepsie, NY, he commenced radiology residency at Oakwood Hospital, Dearborn, Michigan and was introduced to pediatric radiology while rotating through Children’s Hospital of Michigan (aka Detroit Children’s Hospital) with Joe Reed and company. Following residency, Ramiro joined Andy Poznanski, Jack Holt, and Larry Kuhns for a one year fellowship at C.S. Mott Children’s Hospital, University of Michigan, Ann Arbor. A post fellowship private practice position at Oakwood Hospital was cut short at 6 months upon Ramiro accepting a University of Michigan faculty appointment. When Andy Poznanski moved to Children’s Memorial Hospital, Northwestern University, Chicago, Ramiro soon followed. His career flourished at Northwestern from 1979 to 1984 where he published several papers and authored the body CT section of what I recall as the first pediatric imaging book that included body CT - Sty JR, Hernandez RJ, Starshak R: *Body Imaging in Pediatrics* (1984).

In 1984 Ramiro returned to the University of Michigan to become Section Chief at C.S. Mott Children’s Hospital, holding that position until 2006. Ramiro is now Emeritus Professor at University of Michigan and lives in Chicago with his wife Mary, Professor Emerita of Pediatrics and Communicable Diseases at the University of Michigan.

Pioneer – the first or among the first ... that originates or helps to open up a new line of thought, activity, new method, or new technical development. Merriam – Webster Dictionary

Although Ramiro has considerable expertise in most aspects of pediatric imaging, his work in congenital heart disease and the musculoskeletal system stands out in particular relative to this award.

Ramiro, by invitation of the Chief of Pediatric Cardiology, reviewed and reported all the pediatric cardiac angiograms for many years and presented them at their weekly preoperative conference, much in the manner that this year’s Gold Medalist Ken Fellows did for years at Boston Children’s Hospital. Ramiro “learned the lingo” at these conferences and noted specific problems which he would later address with cross sectional imaging, first CT, and later MR. Rather than duplicate what echocardiography already did well, Ramiro focused on difficult to image anatomy such as Tetralogy of Fallot with diminutive pulmonary arteries. Ramiro also published on anomalies of the aorta, pulmonary arteries and pulmonary veins, hypoplastic left heart syndrome, endocardial fibroelastosis, and fast CT and MR techniques. In 2000 Ramiro was appointed to the SPR Cardiac Imaging Committee.

In the early 1980s Ramiro introduced us to the immediate post-spica cast, low mA, few-slices CT to verify DDH reduction before the patient is discharged home. This definitive image, which Ramiro taught us to read when the femoral head was not yet ossified (“soccer ball and clog” analogy), was a substantial improvement from the hard to read radiographs obtained through wet plaster which, even if clear, could have false negatives, as he dramatically demonstrated.

Ramiro also described the use of CT to determine femoral neck version and tibial torsion more precisely and reproducibly, replacing an otherwise clever method of using fluoroscopy and a protractor. Ramiro was the first to describe the utility of MRI in the management, diagnosis and follow up of dermatomyositis. Prior to MRI the diagnosis and follow-up of children with dermatomyositis required invasive testing (EMG and biopsy) and less reliable assessments. Ramiro followed this highly cited Journal of Pediatrics paper with papers establishing that MRI sequences with fat suppression was the optimal technique to evaluate these muscle disorders as is now standard technique.

Multiple publications on using CT and MRI for assorted musculoskeletal entities led to Ramiro’s election to the International Skeletal Society (ISS). Ramiro was one of the few pediatric radiologists in this select multidisciplinary society which once included/includes such SPR greats as EBD Neuhauser, John Caffey, John A. Kirkpatrick, Fred Silverman, John Dorst, John Gwinn, Andrew Poznanski, H. Ted Harcke, and Paul Kleinmann. In 1997 Ramiro delivered the ISS Founder’s Lecture, “Bone Marrow MRI in Children” in honor of Andy Poznanski.

Recognized expertise in oncologic and bone marrow imaging led to Ramiro being named Primary Investigator or Co-Investigator on several funded grants, including an NIH funded multicenter grant on CT and MR for staging children with neuroblastoma.

To my recollection, in 1991 Ramiro was the first radiologist at the University of Michigan to complete the Master of Science degree program in Clinical Research Design and Statistical Analysis through the University of Michigan School of Public Health, across the street from C.S. Mott Children’s Hospital. Many subsequent department faculty have since followed his path.

Among the papers arising from this experience were: Hernandez RJ, Cornell RG, Hensinger RN: Ultrasound diagnosis of neonatal congenital dislocation of the hip: A decision analysis assessment. *Bone and Joint Surgery [Br]* 1994; 76B:539-543, which recommended that infants

suspected of or evaluated for DDH would benefit from radiographs of the pelvis at 6 months of age; and Schlesinger AE, Hernandez RJ, Zerin JM, Marks TI, Kelsch RC: Inter- and Intraobserver variations in sonographic renal length measurements in children. *AJR* 1991; 156:1029-1032.

Ramiro was a superb division leader and colleague. He would like to tease and keep us on our toes. Although he would staff our Ultrasound service, he preferred reading CT and MR and used to joke that “ultrasound makes the palpable visible.”

Ramiro speaks his mind. He often challenged us to think differently about a problem and to support our contentions. Lively discussions with a younger Dr. Jonathan Dillman at morning interesting case conferences were particularly enjoyable and educational for all. Ramiro was polite but did not back down without a convincing opposing opinion, whether in our reading room or at an international conference. His points were always worthy of consideration and were often correct.

Yet, what Ramiro is most known for among those who have worked with him is his incredibly fast eye which, coupled with his superb intuition and power of deduction, make him a superb diagnostician as I have observed firsthand for almost four decades: a description of Ramiro with which many radiological and clinical colleagues and generations of trainees would agree.

When challenged by Ramiro on a diagnosis, “Do you want to bet a Coke on it?” we learned that we might as well save time and just answer, “Will you want regular or diet?” Ramiro was occasionally wrong, but those occurrences were rare. Somehow, when the answer finally came back in those few situations, Ramiro was uncannily away in Spain. Did he know? As Alan Schlesinger would joke in such situations, “I won a bet with Ramiro, and walked away thirsty.” Go figure.

Michael DiPietro, MD

Professor Emeritus of Radiology and Pediatrics

University of Michigan

CS Mott Children’s Hospital

Ann Arbor

SPR 2021 SINGLETON-TAYBI AWARD

The Edward B. Singleton-Hooshang Taybi Award is given in honor of Edward B. Singleton and Hooshang Taybi, in recognition of their personal commitment to the educational goals of the SPR. Initiated in 2006, the award is presented annually to a senior member of the SPR whose professional lifetime dedication to the education of medical students, residents, fellows, and colleagues has brought honor to him/her and to the discipline of pediatric radiology.



Harris L. Cohen, MD, FACR

This award acknowledges a “... *lifetime dedication to education in the discipline of pediatric radiology.*”

What makes a great teacher: knowledge, scholarship, curiosity, engagement, delivery, availability, motivation, inspiration, and love of sharing?

Harris Cohen has exhibited such qualities in planning, preparing, and presenting hundreds of talks, during informal teaching and discussion, and in hundreds of publications he wrote and edited over 4 decades. I witnessed his spark of curiosity and love of teaching as we planned and shared teaching events in SPR and in other societies throughout that timespan. Like SPR legends Ed Singleton, who continued teaching and loving it well into his 90s, and Hoosh Taybi, who kindly and generously shared his scholarship with all who sought it, Harris has a wealth of knowledge, is curious, likes people, and likes discussion: interactive discussion. He wants to know what you think. He enjoys sharing his knowledge while also learning from you.

Harris is a New Yorker. His father was a legendary long time appetizing clerk/lox slicer at the world famous Zabar’s gourmet market in upper Manhattan who was portrayed in New Yorker magazine and memorialized in the New York Times. Harris studied at Stuyvesant High School, Brooklyn College, and State University of New York Downstate (medical school and radiology residency). There he met and was inspired by radiologists Joshua Becker, E. George Kassner, and Jack Haller. Following a fellowship at Children’s Hospital-National Medical Center, Washington, D.C., Harris returned to New York commencing a span of appointments at SUNY Downstate, Cornell Medical College, and SUNY Stony Brook. He was awarded tenure at SUNY Downstate and Stony Brook, and is now Professor Emeritus at SUNY Stony Brook. A 2000-2002 Visiting Professor appointment at Johns Hopkins afforded Harris the opportunity to lead a pediatric division in a world class department complimenting his already widely recognized expertise in ultrasound: pediatric, fetal, and adult.

As a recognized expert in multiple areas of ultrasound, Harris has been on the “hot seat” of unknown case panels before large audiences at national conferences where I witnessed his noble performances. Ironically, his ultrasound expertise led some SPR colleagues to not realize that Harris was actually a pediatric radiologist!

In 2008 Harris was recruited to University of Tennessee, Memphis, where he is a Professor with tenure of Radiology, Pediatrics, and Obstetrics, as well as Chair, University of Tennessee Health Science Center, Department of Radiology, Medical Director and Radiologist-in-Chief, LeBonheur Children’s Hospital, and Director of their CAQ accredited Pediatric Radiology Fellowship program.

Harris’ CV lists a myriad of presentations, and lectures for numerous organizations including SPR, The Society for Radiologists in Ultrasound (SRU), The American Institute of Ultrasound in Medicine (AIUM), The American Academy of Pediatrics (AAP), and RSNA. He has served on the SPR and AIUM governing boards and has chaired the Radiology section of AAP. For over 10 years Harris was in charge of planning the entire educational programming at the AIUM annual conferences, a huge commitment. He planned pediatric sessions at SRU where he often asked us to present practical “How I Do It” talks.

Harris has been an “ambassador” of pediatric radiology, especially pediatric ultrasound, among other societies. His planning and teaching at AIUM, SRU, and AAP helped pediatric radiology maintain a strong presence in their broad educational curricula. He continues to be a valued resource at the planning sessions of the pediatric and neuro sections of AIUM which include several SPR members. Harris has chaired the pediatric, emergency, and neuro sections of AIUM. A major function of these sections is to propose educational sessions for the AIUM conventions. He has been an RSNA International Visiting Professor on three occasions serving as the pediatric and ultrasound expert during stints in India, Kenya, and Bosnia-Herzegovina

Harris edited 5 books in the American College of Radiology (ACR) Syllabus Series. That decades long series ended and was replaced by the ACR Continuous Professional Improvement (CPI) Series, an ongoing series of monographs (modules and self-assessment modules), with

Harris continuing as Editor-in Chief. Over the past 13 years Harris has edited 67 of these monographs in all areas of radiology. He introduced several new pediatric related module topics including a co-authored one on perinatal imaging and others on pediatric oncologic, pediatric head and neck and pediatric neuroradiologic imaging.

Harris has edited 10 books. A favorite of mine for teaching pediatric US was: Cohen HL, Sivit CJ (eds) *Fetal & Pediatric Ultrasound. A casebook approach*. McGraw Hill. New York 2001. Entities encountered in pediatric and fetal US are presented in accessible, clear, and concise segments designed for efficient educational engagement. Harris serves or has served on several editorial boards including: Ultrasound Quarterly, Journal of Ultrasound in Medicine (AIUM), Journal of Diagnostic Medical Sonographers, and RadioGraphics. He was co-editor with Paul Babyn of the October 2017 RadioGraphics, its first special edition devoted to pediatric imaging. In addition, Harris has served on RSNA's Radiographics pediatric scientific and educational exhibit review committee for over 20 years with 5 years as Chair.

Harris is curious, intellectual, devoted, productive, and loves to teach in person and through writing. He has an extensive experience teaching pediatric imaging in multiple societies. His long CV cites hundreds of publications and presentations, many of which relate to teaching pediatric imaging especially sonography.

Harris Cohen, a model educator and an inquisitive scholar, loves to discuss almost anything, including movies and sports. Have a chat.

Michael DiPietro, MD

Professor Emeritus of Radiology and Pediatrics
University of Michigan
CS Mott Children's Hospital
Ann Arbor

SPR 2021 PRESIDENTIAL RECOGNITION AWARD

The Society bestows Presidential Recognition Awards on members or other individuals whose energy and creativity have made a significant impact on the work of the Society and its service to its members.



Richard Jones, PhD

"I've been lucky. I've had the great pleasure to work with a fantastic MR physicist for most of my career. Richard Jones is a marvel." Steve Little, Pediatric Radiologist and Neuroradiologist

"Always humble, never seeking the spotlight, Richard is not only a brilliant and dedicated scientist; he possesses the rare ability to bridge the divide from the arcane language of MR physics and basic science and incorporate it into clinical practice". Ann Schechter – Pediatric Radiologist

This year's Presidential Recognition Award goes to Dr. Richard Jones for his scientific contributions that have improved clinical MRI for children and ultimately advanced our specialty of pediatric radiology. Richard is a truly remarkable phenomenon – an extra-ordinary MR physicist, mountain climber, yoga devotee, fluent in five languages, raconteur and gourmand. He is equally comfortable regaling and educating one over the scanner console as over a glass of beer.

Richard was born and raised in the north of England helping to foster his deep love of soccer and a predisposition to hard work. In 1980, after studying Physics at the University of Nottingham (where he did a course in MR spectroscopy) Richard's first foray into the job market was working for British Telecom. He quickly decided that wasn't for him, having secured a scholarship to do an MSc. in Medical Physics at Aberdeen he left British Telecom and spent 6 months backpacking in South and Central America. His course at Aberdeen finished with a 3 month practical in which he worked on fast MR imaging on the departments 0.04T magnet, the start of a career long interest in fast MRI imaging. After the MSc. he was offered a post as a "undergraduate technician under training" and worked on the 0.08T scanner in the hospital, working with his mentor, Tom Redpath, to optimize the clinical studies and implement projects such as flow imaging, rapid MRI imaging (including the introduction of an early version of the the DESS sequence, which they called FADE) and cardiac imaging. When he wasn't working, he spent most of his time climbing, on the local sea cliffs in the evenings and in the mountains at the weekends.

After 6 years at Aberdeen, he left to take a job in Norway working in Trondheim. This involved contract research on a 2.35T animal scanner as well as protocol and sequence development on the clinical scanner in the adjacent hospital. The contract research included contrast agent development and testing for Nycomed and drug testing in animal models for pharmaceutical companies. The MR work in these areas included the development of diffusion imaging and DSC imaging. For the latter he developed a K-space sharing dynamic sequence which was a forerunner of sequences such as TRICKS & TWIST. He didn't do as much climbing in Norway but became a proficient cross-country skier. As this didn't take up as much of his time as climbing, he was able to complete his PhD. He worked with the head of the clinical group, Peter Rinck to write an early MRI textbook.

Even for someone from Northern England the long dark winters eventually became too much, and he had enough of animal models and wanted to focus on work with patients so he took a post at the Max-Planck institute for Psychiatry in Munich. Here the focus was initially on fMRI and optimizing the clinical studies. His doctoral student, Timo Schirmer, also developed an early version of a multi-element coil to improve the sensitivity of fMRI. All of this, plus running the fMRI studies and optimizing the clinical sequences, occupied most of his time but the head of the department then wanted to do diffusion imaging, quantitative DSC imaging, spectroscopy and various other projects; an impossible proposition given the size of the group so once his doctoral student had finished it was time to move on. He had gotten back into climbing while in Munich and at the end of his time there did his first trip to the Himalayas with some old climbing buddies.

For his next position he had an EU scholarship to work with the group led by Chrit Moonen in Bordeaux. Life in Bordeaux was good, climbing in the Dordogne and Pyrenees, beaches close by and, of course, excellent wine. The group worked together well and did research in several areas including diffusion imaging in the spine and kidneys and yet more fMRI. We are very lucky that he met Rebecca, an American and his future wife who was also living in Bordeaux and they held many memorable parties at their flat. When the possibility of a job in a Pediatric hospital in his wife's hometown of Atlanta came up they thought they would go there for a few years, but that turned into many.

Richard started working at the Scottish Rite campus of Children's Healthcare of Atlanta in 2001. For this next chapter in his career, Richard worked with a small group of private practice Pediatric Radiologists. The outstanding work done in our department was built around Richard's expertise and his desire to improve the health of children. Richard's first priority has always been to produce consistently high-quality images, particularly when imaging the small, often moving parts we encounter in pediatric radiology. Although Richard masks his gentle and thoughtful nature behind the curmudgeonly facade of a Northern Englishman, he is a patient and resourceful colleague. The radiologists, sometimes with a crazy idea, would walk over to

Richard's office first thing in the morning, describe what they were trying to achieve and wait. Most often, Richard had built a new sequence or tailored an existing sequence to meet the need by late afternoon. I remember saying to Richard shortly after he started working in Atlanta that we need to measure renal function, especially GFR with MR urography. He initially said it couldn't be done with the current technology but within a week he came back with several innovative solutions that have subsequently driven MR urography forward. Sometimes optimizing a new sequence requires a little back and forth, but Richard is a patient man. Forever surrounded by obsessive-compulsive radiologists, Richard has developed a Zen-like attitude. Novel pulse sequences and techniques to shorten scan time while maintaining diagnostic quality are constantly being developed. To make use of them not only requires an investment in 'the latest and greatest' equipment but also in a unique individual such as Richard capable of harnessing that equipment. But Richard doesn't only respond to Radiologists requests for higher quality and greater speed. He often leads the way, educating us on new developments in MR and helping us coax sometimes reluctant administrators into making the necessary investment. He also spends time educating the techs about new developments and how to get the most out of them.

Richard has published 66 peer reviewed research papers and won the Caffey award for the best clinical paper at the SPR meetings of 2003 and 2007 as well as at the IPR in 2016. However, what is truly remarkable about Richard is not his academic output but his desire to help sick children and his willingness to work with the radiologist to achieve this goal. Richard is the paradigm for the medical physicist all departments aspire to have as a member of their team, but few possess. Several radiologists working with MR at other institutions appreciate Richard's talents, some of whom have developed what can best be termed "Richard Envy".

In addition to the many accomplishments already mentioned, Richard is a great cook, an avid reader, wonderful gardener, devoted father of two teenage daughters, Fiona and Phoebe, and many times the winner of the husband-of-the-year award. He has two brothers one older and one younger and his father, a world war 2 veteran, is 95 years old and still lives in the house Richard grew up in.

J. Damien Grattan-Smith, MBBS

SPR 2021 HONORARY MEMBER

The Society extends Honorary Membership to individuals outside of the SPR who have made outstanding contributions to the care of children.



Andrea Rossi, MD

Professor Andrea Rossi is a pediatric neuroradiologist and a leader among European pediatric radiologists and neuroradiologists. He is Professor of Neuroradiology at the University of Genoa, Italy and has been the Division Head of Neuroradiology at the famous Istituto Giannina Gaslini Children's Hospital, Genoa, Italy since 2007, having recently been appointed to chair the whole Imaging Department. Andrea is also co-president of the 2021 International Congress of

Pediatric Radiology where his leadership and diplomatic skills have been demonstrated organizing such a complex meeting during the Covid Pandemic of 2020 and 2021. In his spare time, Andrea is also serving as the President of the Italian Association of Neuroradiology, as well as Secretary General of the European Society of Neuroradiology and Chief Operative Officer, European Board of Neuroradiology. He has been a Board member of the European Society of Paediatric Radiology since 2019.

Andrea had initially wanted to be a pediatric surgeon but thankfully serendipity took a hand and Andrea became a neuroradiologist because of an unexpected opportunity – it can be said that Neuroradiology chose Andrea. Andrea's mentors were Paolo Tortori-Donati who taught him all he knows about neuroradiology and Paolo Tomà who first hired him as a pediatric radiologist. Andrea is a prolific researcher and writer being the author and editor of 4 textbooks with more than 400 peer reviewed publications, earning him an H index of 47 on Google Scholar. Andrea's renown as a pediatric neuroradiologist has led observers from around the world to seek him out, to learn from his encyclopedic knowledge and to glean wisdom at his side.

Andrea has been married to his wife Rita for 26 years and has one daughter, Erika, aged 16. He is a lover of cats with 2 cats since he was married. Andrea is a true Renaissance man with an eclectic knowledge and wide-ranging interest in the world. His interests include traveling, particularly in Norway, Iceland and the Faroe Islands where he has taught himself to be fluent in Norwegian. He loves to read, especially Icelandic sagas as well as 20th century Scandinavian writers such as Halldór Laxness or William Heinesen. In his youth Andrea demonstrated less-than-prodigious talent as a young tennis player who occasionally let his temper and desire for perfection interfere with his success. His sporting interests now include hiking, swimming and running. True to his fondness for everything Norwegian, he loves to watch ski jumping and biathlon races. His diverse musical tastes run from the Australian rock group "The Church" to St Matthew's Passion by Bach. Andrea has also taught himself to play the piano by ear; he considers himself a keyboard torturer but could entertain you with a range of classic rock ballads as well as a sizable original production, much to the dismay of both wife and daughter.

Although Andrea may initially seem serious, he is in fact a humble and self-effacing man. He has a sharp sense of humor and once the façade drops, he reveals his beguiling personality, as one who values loyalty and seriousness of intent. Andrea has an eye for talent and considers that his proudest achievement is the team he has chosen and assembled at Gaslini Children's hospital. The best affirmation of who Andrea is and why he deserves to be an honorary member of the Society for Pediatric Radiology comes from those who know him best, his colleagues at Gaslini Children's Hospital:

"Andrea is a brilliant neuroradiologist, with a huge knowledge in the field of pediatric neuroradiology and great communication skills. His lectures inspired me to become a pediatric neuroradiologist, and it is now a privilege to work with him at Gaslini Children's Hospital. Discussing cases with him is always an exciting learning experience! He is a dear friend and a special mentor. He is humble and always ready to question himself with a very open-minded attitude." - Dr Mariasavina Severino

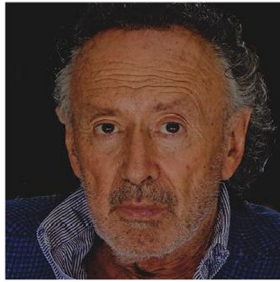
"Andrea is an inspiring doctor with great assertive leadership skills. I admire his way of trusting and promoting collaborators, with a very generous attitude. I am impressed by his vast culture and knowledge in every field (especially regarding the Icelandic sagas!). It is always a pleasure to have a chat with him!" - Dr Domenico Tortora

"Andrea is the foundation stone of the Imaging Department of the Gaslini Institute. A fascinating neuroradiologist with a deepest culture and profound human skills. A dear and honest friend with listening capacities and problem-solving skills. A stimulating guide for young trainees. A passionate clinician and radiologist." - Dr. Beatrice Damasio

"A perfect man, as Valentino Rossi" - Dr. Paolo Tomà

J. Damien Grattan-Smith, MBBS

SPR 2021 HONORARY MEMBER



Paolo Tomà, MD

Professor Paolo Tomà qualified in medicine from the University of Genoa in 1976 and went on to train in both clinical paediatrics and then radiology, explaining his sound knowledge base into what really matters for the best care of sick children, in turn helping parents and clinicians. He then worked as a radiologist in the department of Imaging at G. Gaslini Institute, first as a registrar – later in a more senior position from 1980 until 1994. He was then promoted to the post of Director of the Ultrasound division at Gaslini where his scientific focus and attention to detail changed the profile of the unit. Due to his tireless dedication, major focus on clinical excellence and superb leadership by example, in 1995 he was appointed as Director of Radiology. In 2005 he was promoted to the post of Director of the Department of Imaging at the G. Gaslini Institute in Genoa until 2009.

In 2010, he was appointed to transform and revamp the Imaging department at the Bambino Gesù Hospital in Rome. Since his appointment he has restructured the department replacing all of the equipment to state of the art standards (4 latest generation MRI scanners (2/4 3T) and 3 CTs totally dedicated to paediatric imaging. He is currently upgrading nuclear medicine with PET, SPECT and metabolic radiotherapy unit.

He has initiated one of the busiest paediatric cardiac imaging units, with an excellent international reputation and recruiting world class staff.

In 2019 he was made honorary member of the Italian Society of Paediatrics.

Prof. Toma has published widely on many topics, and has made major contributions within ultrasound, radiation protection, early screening for hip dysplasia, and within cardiothoracic imaging. He has published over 220 papers in peer reviewed journals, several book chapters and books and has given a substantial number of invited lectures across the world. He was President of the Italian Society of Paediatric Radiology from 1996 to 2000. He has been a member of the Editorial Board in *Pediatric Radiology* from 2011.

Paolo has served as a member of the ESR Subspecialties Committee from 2008 to 2011, and contributed to the annual ESRP meetings over nearly four decades.

Internationally, he served as Vice-President of the European Society of Paediatric Radiology (ESPR) from 1999–2002, as President from 2002–2003, as senior councillor from 2006–11 and as one of three Trustees from 2014–2018 supporting and guiding with the governance of the ESPR Board. Indeed, Prof Toma is sage, with the gentle ability to differentiate between important and unimportant matters. He is intensely focused on his passion for imaging in children and is a hands on hard working clinical radiologist in his busy departments where he personally performs a substantial number of cases. He is deeply respected and indeed loved by his staff and his mentorship is legendary. Many of his students, residents and fellows are now leading the major paediatric radiology departments in Italy, and see him as their father figure.

Paolo is a very popular, calm, focused doctor with a real love for his profession. He is a 'go to' person for inspiration for many of the ESRP leaders including myself. We all benefit from his wisdom and guidance which led to his appointment as ESRP Gold Medallist at IPR 2016.

Dr. Catherine Owens
July 2021

SOCIAL ACTIVITIES

Welcome Reception

Monday October 11
19:00–22:00
Marriott Park Hotel
Hors d'oeuvres and Refreshments
Business Casual Attire

Junior IPRun for Fun

Wednesday October 13
06:30–08:30
Villa Pamphili
Attendees from all ages are welcome to run or walk with us the 5.4Km, an energizing and friendly race that take place in one of the most beautiful Park of Rome!

Explore Rome

Wednesday October 13
Get your afternoon off and take a walk in Rome with one of our guided tours!
More information on the website www.ipr2021.org

Farewell Banquet

Friday October 15
20:30–23:30
Casina di Macchia Madama
Reception, Dinner and Dancing
Business Casual Attire

SCIENTIFIC PAPERS

S1.1.1

HIGH-RESOLUTION NEUROSONOGRAPHIC EXAMINATION OF THE LENTICULOSTRIATE VESSELS IN NEONATES WITH HYPOXIC-ISCHEMIC ENCEPHALOPATHY

SHAWN Lyo^{1,2}, LUIS OCTAVIO Tierradentro-Garcia², ANGELA Viaene³, MISUN Hwang^{2,4}

¹ Department of Radiology, SUNY Downstate Health Sciences University, Brooklyn, NYC, USA

² Department of Radiology, Children's Hospital of Philadelphia, Philadelphia, USA

³ Department of Pathology and Laboratory Medicine, Children's Hospital of Philadelphia, University of Pennsylvania, Philadelphia, USA

⁴ Department of Radiology, Perelman School of Medicine, University of Pennsylvania, Philadelphia, USA

Purpose: To assess the feasibility of visualizing lenticulostriate vessels (LV) using a linear high frequency ultrasound probe and characterize LV morphology to determine whether morphological alterations in LV are present in neonatal hypoxic-ischemic encephalopathy (HIE) as compared to the unaffected infants.

Methods: We manually annotated and characterized LV by their echogenicity, width, length, tortuosity, and numbers of visualized stems and branches in neurosonographic examinations of 80 total neonates (Fig. 1). Our population included 45 unaffected (Non-HIE) and 35 with clinical and/or imaging diagnosis of HIE. Of the neonates with clinical diagnosis of HIE based on the Sarnat Grading Scale, 16 had positive MRI findings for HIE (HIE+MRI) and 19 had negative MRI findings (HIE-MRI). Annotations were performed twice with shuffled datasets at a one-month interval and intra-rater reliability was assessed. Characteristics of the visualized LV were assessed overall. Focused comparison was

conducted between non-HIE, HIE+MRI and HIE-MRI neonates whose images were acquired with a high-frequency linear transducer.

Results: The LV were visualized in 78 of 80 examinations (44 of 45 normal controls) in the cohort. In general, a greater number of branches ($p=0.002$) with thicker ($p=0.007$), more echogenic ($p=0.009$) vessels was seen with the higher resolution linear transducer compared to the lower resolution linear transducer. Groupwise comparison of vessels imaged with our higher resolution linear transducer found significantly fewer branches in HIE+MRI patients compared to HIE-MRI patients and non-HIE patients ($p=0.005$) (Fig. 2). There was strong intra-rater reliability for stems ($r=0.88$, $p<0.001$), branches ($r=0.90$, $p<0.001$), width ($k=0.75$, $p<0.001$) and echogenicity ($k=0.77$, $p<0.001$). However, reliability was moderate ($r=0.60$, $p<0.001$) for vessel length and non-significant for tortuosity ($p=0.27$).

Conclusion: With modern high resolution neurosonography, the LV can be visualized in the absence of pathology. Interestingly, our results demonstrate that fewer LV branches were visualized in high-resolution neurosonography of HIE+MRI neonates as compared to HIE-MRI neonates and unaffected neonates. Further research into the diagnostic and prognostic utility of LV morphology in various neurologic conditions affecting neonates is warranted.

S1.1.2

NEONATAL DEVELOPMENTAL VENOUS ANOMALIES: CLINICAL-RADIOLOGICAL CHARACTERIZATION AND FOLLOW-UP

ANA Geraldo¹, SIMONA Messina², DOMENICO Tortora³, ALESSANDRO Parodi⁴, MARIYA Malova⁴, GIOVANNI Morana³, CARLO Gandolfo⁵, ALESSANDRA D'Amico⁶, ELLEN Herkert⁷, PAUL Govaert⁷, LUCA Ramenghi⁴, ANDREA Rossi³, MARIASAVINA Severino³

¹ Diagnostic Neuroradiology Unit, Imaging department, Vila Nova de Gaia, PORTUGAL

² Radiology Unit, Casa di Cura Regina Pacis, Palermo, ITALY

³ Neuroradiology Unit, IRCCS Istituto Giannina Gaslini, Genoa, ITALY

⁴ Neonatal Intensive Care Unit, IRCCS Istituto Giannina Gaslini, Genoa, ITALY

⁵ Interventional Unit, IRCCS Istituto Giannina Gaslini, Genoa, ITALY

⁶ Dipartimento di Scienze Biomediche Avanzate, Università Federico II Napoli, Napoli, ITALY

⁷ Division of Neonatology, Department of Paediatrics, Erasmus University Medical Centre, Rotterdam, THE NETHERLANDS

Background and Purpose: Although developmental venous anomalies have been frequently studied in adults and occasionally in children, data regarding these entities are scarce in neonates. We aim to characterize clinical and neuroimaging features of neonatal developmental venous anomalies, and to evaluate any association between MR abnormalities in their drainage territory and corresponding angioarchitectural features. Methods: We reviewed associated parenchymal abnormalities and angioarchitecture features of 41 newborns with developmental venous anomaly (20 males; mean corrected age 39.9 weeks) selected through radiology report text search from 2135 newborns who underwent brain MRI between 2008-2019. Fetal and longitudinal MRI were also reviewed. Neurological outcomes were collected. Statistics were performed using chi-squared, Fisher exact, Mann-Whitney or t-tests corrected for multiple comparisons.

Results: Developmental venous anomalies were detected in 1.9% of neonatal scans. These were complicated by parenchymal/ventricular abnormalities in 15/41 cases (36.6%), improving at last follow-up in 8/10 (80%), with normal neurological outcome in 9/14 (64.2%). Multiple collectors ($P=0.008$), and larger collector(s) caliber ($P<0.001$) were significantly more frequent in complicated developmental venous anomalies. At a patient level, multiplicity

($P=0.002$) was significantly associated with presence of more than 1 complicated developmental venous anomaly. Retrospective fetal detection was possible in 3/11 subjects (27.2%).

Conclusion: One third of neonatal developmental venous anomalies may be complicated by parenchymal abnormalities, especially if with multiple and larger collector(s). Neuroimaging and neurological outcomes were favorable in the majority of cases, suggesting a benign, self-limited nature of these vascular anomalies. A congenital origin could be confirmed in one quarter of cases with available fetal MRI.

S1.1.3

EXPANDING THE SPECTRUM OF NEONATE SUBPIAL HEMORRHAGE : MORE COMMON THAN YOU THINK

JOANNE Rispoli¹, SANJAY Prabhu²

¹ NYU Langone Health, New York City, USA

² Boston Children's Hospital, Boston, USA

Purpose:

Subpial hemorrhage is an underrecognized imaging finding in neonates and is often mischaracterized as subarachnoid hemorrhage. Little is known regarding risk factors for developing subpial hemorrhage or the clinical outcomes of patients with subpial hemorrhage beyond studies involving handful of patients. Our aim is to better investigate the related antecedent etiologies of this entity and clinical outcomes for these patients using a larger cohort of patients at a tertiary care institution.

Materials and Methods:

A retrospective chart review was performed identifying cases from 2010-2020 with the words "subpial hemorrhage" in the final radiology report. Images were reviewed confirming subpial hemorrhage and clinical chart review for gestational age, delivery mechanism, coagulation profile, and neurologic symptoms at clinical follow-up was performed. Inclusion criteria included large subpial hemorrhage (defined as >1 sulcus) and imaging within the first month of life.

Results:

Upon review, 178 cases of subpial hemorrhage were identified in our database and 68 cases met criteria for inclusion. The average gestational age for patients with the diagnosis of subpial hemorrhage was 39.5 weeks, with the majority of patients being full term. The most common location for subpial hemorrhage was the temporal lobe (32/68) with up to 24% of patients having multi-focal subpial hemorrhage. Associated radiographic findings included infarct (59%), medullary vein thrombosis (27%) and parenchymal hemorrhage (45%). Associations with previously identified possible risk factors in our population were trauma (14%), coagulopathy (14%), and history of congenital cardiac disease (10%). Of the patients, 60 patients had follow-up with 41% having neurologic symptoms at follow-up ranging from hypotonia to hemiparesis.

Conclusions:

This study involving the largest series of patients with subpial hemorrhage to date indicates that this is not an uncommon entity in the neonatal population. Most common etiologies include trauma and coagulopathy, but rates of coagulopathy in our population were lower than previously reported. Long term neurologic sequelae are variable and further investigation should be focused on correlating size and location of subpial hemorrhage to clinical outcomes.

S1.1.4

CEREBELLAR HEMORRHAGE IN EXTREMELY PREMATURE INFANTS COMPARED TO VERY PREMATURE INFANTS

ELIZABETH Snyder, SUMIT Pruthi, MARTA Hernanz-Schulman
Monroe Carell Jr. Children's Hospital at Vanderbilt, Department of Radiology, Nashville, TN, USA

Purpose. Extremely premature infants (EPIs 22–28w GA) survive due to advances in neonatology. These fragile infants are at increased risk of CNS injury, including hemorrhage in the larger germinal matrix, and cerebellar injury. Our aim was to determine the prevalence of cerebellar hemorrhage (CH) on head US in EPIs, compared to a control population of very premature infants (VPIs, 28–32w GA).

Materials and methods. IRB-approved retrospective study. Consecutive EPIs less than 28 weeks GA presenting 2013–2018 were included. A consecutive group of VPIs 28–32 weeks served as control. Head scans include linear images of the posterior fossa through the mastoid fontanelle, bilateral whenever possible. Review for the presence of CH included consensus read of two pediatric radiologists and one pediatric neuro-radiologist. Demographic data were extracted from the EHR.

Results. The study included 459 EPIs, mean GA 26 weeks (Range: 22–27). There were 30 EPIs with CH (6.5%). The control group included 456 VPIs, mean GA 29.5 (Range 28–31). There were only 2 CH in this population (0.4% [$p < 0.001$]). CHs in EPIs were bilateral in 12 (40%). Among the EPIs, 22/30 (73%) had either Grade I, II or no other bleeds, with no other bleeds in 16/30 (53%). Most CHs in the EPIs (17/30 [57%]) occurred in the 114 infants in the 22–24 week GA population 17/114 (15%). Both CHs in the VPI group were unilateral; neither infant had other bleeds.

Conclusions. EPIs are much more likely to have CH than VPIs, reaching a prevalence as high as 15% in the youngest infants (22–24 week), and are more likely to be bilateral. In most patients the CHs are not associated with supratentorial bleeds, underscoring the importance of high-resolution posterior fossa images in routine head ultrasounds. The prognostic significance of these injuries correlated to the extent, laterality and age of onset needs to be determined.

S1.1.5

PERI-ROLANDIC INVOLVEMENT IN HYPOXIC ISCHEMIC INJURY MAY ALSO OCCUR WITH PARTIAL PROLONGED INSULTS

ANILAWAN S Fleury, SAVVAS Andronikou

Children's Hospital of Philadelphia, Radiology department, Philadelphia, USA

Background

MRI patterns of hypoxic ischemic injury (HII) include the Watershed (WS) (partial prolonged injury) and Basal-ganglia-thalamus (BGT) patterns (profound injury). BGT and WS can occur concurrently and in these patients it is not clear if Peri-Rolandic MRI changes result from profound insults and include the paracentral gyri (accessory motor areas) or are part of watershed damage due to a prolonged insult.

Objective

To compare distribution of Peri-Rolandic injury between the different MRI categories of HII.

Materials and methods

Retrospective review of delayed MRI in cerebral palsy patients with Peri-Rolandic injury regarding distribution and comparison of different MRI based HII groups. Patients with diffuse brain involvement were excluded.

Results

25 of the 105 patients with CP and Peri-Rolandic injury considered were excluded and 80 evaluated (mean age: 6.7 years (1–17.8)).

There were an equal number of patients in the combined BGT-WS group (46.3%) and BGT group (46.3%), a small minority with WS alone (5%), and 2.5% had Peri-Rolandic without other findings.

Peri-Rolandic distribution:

Isolated BGT pattern: 91.9% precentral, 86.5% postcentral, 94.6% paracentral lobule and 78.4% posterior part of superior frontal gyrus.

Combined BGT-WS pattern: 97.3% precentral, 94.6% postcentral, 94.6% paracentral lobule and 59.5% posterior part of superior frontal gyrus.

Distribution in the WS group: 50% precentral, 100% postcentral, 100%

paracentral lobule and 66.7% posterior part of superior frontal gyrus. Combined BGT-WS group had statistically more frequent precentral gyrus injury; WS group had statistically more frequent postcentral, and paracentral gyrus injury ($p < 0.0001$). The BGT group showed statistically more frequent invol posterior frontal gyrus injury ($p < 0.0001$).

Conclusion

Over 90% of peri-Rolandic injury in children with CP accompanies the BGT pattern of injury, with or without accompanying WS injury. 5% occurs in WS injury without BGT - therefore peri-Rolandic abnormality should not automatically be considered profound injury. Statistically differences in distribution between BGT and BGT-WS supports the notion that peri-Rolandic injury may be part of a watershed injury.

Injury to the paracentral gyrus and posterior frontal gyrus are commonly associated with Peri-Rolandic injury in all groups, and the latter should not be considered a watershed injury.

S1.1.6

INTRANASAL DEXMEDETOMIDINE FOR SEDATION OF CHILDREN IN MRI-EXAMINATION

GABRIELLA Lewis¹, MARIA Liljeroth¹, SANDRA Diaz^{1, 2}

¹ Karolinska University Hospital, Stockholm, SWEDEN

² Skanes University Hospital, Lund, SWEDEN

Purpose:

To evaluate the feasibility of sedating children with intranasal (IN) Dexmedetomidine to obtain diagnostic imaging of the brain when examined by Magnetic Resonance (MR) and reduce long waiting lists.

Material and Method:

Retrospective study of 99 children between 6 months and 6 years old (yo), 43 girls and 56 boys, sedated with IN Dexmedetomidine who underwent MR of the brain. Referrals were classified by a pediatric anesthesiologist. A MR-radiographer administered a dose of IN Dexmedetomidine of 4µg/kg-weight and a second dose of 2µg/kg if the children did not fall asleep. MR examinations were performed at 1.5 and 3 T magnetic field. A neuroradiologist graded the amount of motion artifacts using a 1–3 scale. Time of appearance of movement artifacts and gender was analyzed with a t-student test. Relationship between age and time of appearance of movement artifacts was evaluated with Pearson's test.

Results:

23% of the children (7 girls and 16 boys) required and extra IN Dexmedetomidine dose; 13 before and 10 after the beginning of the examination. No major or minor adverse events were registered. 98 out of 99 examinations were of diagnostic quality. A total of 43% of the examinations did not have motions artifacts, 37% had mild and 30% had major. No motion artifacts were found in 60% of children between 6 months–2 yo, 36% between 2–4 yo and 30% between 4–6 yo. Mild motion artifacts were found in 18%, 39% and 24% and major in 21%, 24% and 45% respectively. There was no statistically significant difference between age, gender and movement artifacts.

Conclusion:

IN Dexmedetomidine sedation is feasible, safe and reduces the use of deep sedation in children between 6 months to 6 yo when examined with brain MR. Implementing this sedation method in a target population can reduce long waiting lists.

S1.1.7

DROP IN SEDATION EXAMINATIONS BY ADOPTING REAL-TIME CMRI SEQUENCES

DANIEL Gräfe¹, INA Sorge¹, DIRK Voit², JENS Frahm², MATTHIAS Krause³, CHRISTIAN Roth¹, PETER Zimmermann⁴,

FRANZ WOLFGANG Hirsch¹

¹ University Hospital Leipzig - Pediatric Radiology, Leipzig, GERMANY

² Biomedizinische NMR - Max-Planck-Institut für biophysikalische Chemie, Göttingen, GERMANY

³ University Hospital Leipzig - Neurosurgery, Leipzig, GERMANY

⁴ University Hospital Leipzig - Pediatric Surgery, Leipzig, GERMANY

Background

Rapid volume coverage sequences based on real-time MRI allow for scanning the entire brain within a few seconds. Movements of the children become almost irrelevant due to the fast acquisition of 30 ms per slice. The adoption of these sequences in an ultra-fast cranial real-time MRI protocol (RT-cMRI) is expected to reduce the frequency of examinations requiring anesthesia in infants and toddlers.

Objective

The aim of the study was to determine whether the novel cMRI real-time protocol significantly reduced the number of anesthesia examinations.

Material and methods

cMRI studies of children up to 6 years in the first 12 months after the establishment of the RT-cMRI 2019/2020 were retrospectively compared to a matched group of the same period in 2017/2018. The frequency of examinations under anesthesia vs. non-sedation examinations was analyzed. In addition, the number of follow-up examinations and the effectiveness of RT-cMRI was determined.

Results

The launch of RT-cMRI led to a significant decrease in the proportion of cMRI under anesthesia from 92% to 55%. Only 2% of the RT-cMRI failed and required conventional MRI under sedation in the follow-up. The ease of use of RT-cMRI increased the number of repeat examinations from 1.3 to 1.5 examinations per child.

Conclusion

The innovative real-time MRI allows a drastically reduction of studies under anaesthesia for suitable cranial pathologies. However, cautious selection of indications as well as adjustments to the workflow in the radiological department are required.

S1.1.8

PORTABLE LOW FIELD STRENGTH MRI: PRELIMINARY EXPERIENCE IN NEONATES AND CHILDREN

JOHNSTON Fite¹, AMIE Robinson¹, MAURA Sien¹, AMIT Jain¹, HARRY Hu³, JOHN Pitts³, SHERWIN Chan^{1,2}

¹ Children's Mercy Hospital, Kansas City, USA

² University of Missouri Kansas City, Kansas City, USA

³ Hyperfine, Guilford, USA

Background:

High field strength MRI (HF-MRI) is a pediatric imaging staple. However, HF-MRI access is limited by strong (1.5 – 3.0 T) magnetic fields with associated safety concerns, space requirements, and cost. To address these limitations, Hyperfine (Guilford, CT) developed a low magnetic field (0.064 T) portable MRI device, named Swoop. Preliminary data in adults shows benefits despite decreased image quality. In this study, initial evaluation of Swoop's image quality in pediatric patients was assessed.

Methods:

The study was a single-site prospective cohort evaluating the quality of the Swoop's adult sequences in pediatric subjects (0–4 years) at a tertiary pediatric medical center. NICU/PICU patients with standard of care (SOC) brain imaging (CT, HF-MRI or US) were considered for the study. Axial FLAIR T2, T2, T1 and DWI/ADC Swoop sequences were performed within +/- 24 hours of SOC imaging. 10 consecutive scans were evaluated independently by 5 attending pediatric radiologists. They graded image quality of each sequence

on a five-point Likert scale from: 1) none (no artifact) to 5) extensive (images are non-diagnostic). They also graded if each total scan was diagnostic. Radiologists were blinded to clinical picture and SOC findings.

Results:

Individual quality scores (average +/- SD) for each sequence were FLAIR: 3.6 +/- 0.8, T2: 3.6 +/- 0.7, T1: 4.6 +/- 0.6, and DWI/ADC 4.2 +/- 0.6. 48% of scans were of diagnostic quality. Written feedback stated that the sequences were adequate for diagnosis of large or global processes but lacking detail for smaller or subtle abnormalities.

Conclusion:

In conclusion, Swoop's adult sequences were suboptimal in a pediatric population. T2 and T2 FLAIR sequences performed better than T1 and DWI sequences. This initial data demonstrates the pressing need for development of neonatal and pediatric specific sequences for the Swoop. Overall, we feel the Swoop is a promising technology with further research efforts warranted by its potential to provide quick, safe, accessible, and cost-effective MRI.

S1.1.9

SIBLING SCREENING IN SUSPECTED ABUSIVE HEAD TRAUMA: A PROPOSED GUIDELINE

KSHITIJ Mankad¹, JAI Sidpra², ADAM J Oates³, ALISTAIR Calder¹, AMAKA C Offiah⁴, ARABINDA K Choudhary⁵

¹ Department of Radiology, Great Ormond Street Hospital for Children NHS Foundation Trust, London, UNITED KINGDOM

² University College London Medical School, London, UNITED KINGDOM

³ Department of Radiology, Birmingham Childrens Hospital, Birmingham, UNITED KINGDOM

⁴ Academic Unit of Child Health, University of Sheffield, Western Bank, Sheffield, UNITED KINGDOM

⁵ Department of Radiology, University of Arkansas for Medical Sciences, Little Rock, USA

Purpose:

To develop a guideline for the assessment of siblings and cohabiting contacts of children with suspected abusive head trauma (AHT).

Materials and Methods:

Despite the strong association between abuse in one child and abuse in siblings and cohabiting children, there is a paucity of literature outlining how to screen this vulnerable group for abusive injuries. We established an international working group and, based on a review of the literature and our collective clinical experience, developed a standardised protocol for sibling screening in suspected AHT.

Results:

We recommend a skeletal survey for cohabiting children under the age of 2 years. Children over 2 years should have targeted radiographs as indicated by clinical findings. Contacts under 2 years of age with evidence or suspicion of trauma should be screened with a computed tomography (CT) scan of the head and magnetic resonance imaging (MRI) of the brain and spine. Even in the absence of abusive symptomatology, cohabiting children under 1 year should have a CT head with follow-up MRI brain and spine if the CT raises concerns. In children aged 1–2 years, with no evidence or suspicion of AHT, skeletal survey should be followed by a CT head and MRI brain and spine if there are calvarial concerns. In all instances, if a CT head has been or will be performed, skull radiographs may be omitted from skeletal survey. Imaging is not indicated in cohabiting children over 2 years if age if there is no evidence or suspicion of trauma.

Conclusions:

The radiologist plays a central role in the multidisciplinary identification of abusive injuries. Despite ongoing challenges, our framework offers the vital first steps towards a standardised guideline for the screening of these

at-risk infants. To garner further consensus on this subject, we have released an international modified Delphi consensus survey, the preliminary results of which will be presented at the IPR.

S1.2.1

CHEST IMAGING IN CHILDREN WITH COVID-19, A SYSTEMATIC REVIEW

MONICA Miranda Schaeubinger¹, KAREN Ramirez Suarez¹, JORDAN Rapp¹, DAVID Saul², KUSHALJIT Sodhi³, SAVVAS Andronikou¹

¹ Children's Hospital of Philadelphia, Department of Radiology, Philadelphia, PA, USA

² Nemours/Alfred I. DuPont Hospital for Children, Wilmington, DE, USA

³ Postgraduate Institute of Medical Education and Research, Department of Radio Diagnosis and Imaging, Chandigarh, INDIA

Purpose: Amid the Coronavirus disease 2019 (COVID-19) pandemic, numerous publications of imaging findings in children have surfaced in a short period of time. Publications often discuss overlapping study populations or describe different imaging patterns. We aim to show an overview of the quantity and type of literature available regarding COVID-19 imaging findings in children in 2020.

Materials and Methods: A systematic review was conducted in compliance with preferred reporting items for systematic reviews and meta-analyses (PRISMA). Appropriate terminology was used in the search to include terms related to COVID-19, chest, children, and imaging modalities, using PubMed and Embase. Studies were included if they were published online in the year 2020, described imaging findings specific to pediatric cases, and reported 5 or more cases. Each abstract was reviewed by two researchers, and disagreements were resolved by a senior radiologist. Eligible study designs included original articles, case series (> 5 cases), systematic reviews, and meta-analysis. We excluded case reports, non-English manuscripts, retracted articles, and those without available full text. Articles were divided and evaluated independently by four different pediatric radiologists, who summarized COVID-19 imaging findings in US, X-Ray, CT and MRI for each included article.

Results: Title and abstract screening was conducted for 293 studies. Of those, 179 underwent full text review and 97 articles were included in the final analysis. Of those, 24 are from radiology journals and 73 from clinical journals. Included publications were: 52 (53%) original articles (with > 10 pediatric cases), 22 (23%) review articles, 19 (19%) case series (5-10 cases), and 4 (4%) meta-analysis. August was the month with the highest number of publications (n=11), followed by October (n=10) and June (n=10). Overall, 83 (85%) articles described CT, 37 (40%) discussed X-ray, 17 (18%) discussed US and 2 (3.3%) discussed MRI findings.

Conclusions: A myriad of information on pediatric COVID-19 chest imaging has become rapidly available over a short period of time. Most publications are original articles; however, they are predominantly from clinical journals and lack accepted Fleischner Society terminology used in radiology. This review shows that continued collation of high-quality radiologic data is necessary to formulate expert opinion consensus guidelines for pediatric chest imaging of COVID-19.

S1.2.2

CHEST IMAGING IN COVID-19 INFECTION IN CHILDREN: A DIAGNOSTIC CROSS-SECTIONAL STUDY

MARK Bishay¹, RICHARD Gagen¹, ZHIA Lim², LISA van Geyzel², DEEPTHI Jyothish², SIMON McGuirk¹

¹ Birmingham Children's Hospital - Department of Radiology, Birmingham, UNITED KINGDOM

² Birmingham Children's Hospital - Department of Paediatrics, Birmingham, UNITED KINGDOM

Purpose:

- Evaluate the use of chest imaging in children with suspected COVID-19.
- Assess the diagnostic utility of chest x-ray (CXR) in paediatric COVID-19.

Materials & Methods:

Retrospective cohort study.

Children undergoing laboratory testing (SARS-CoV2 RT-PCR assay on nasal/throat swab) for clinically suspected COVID-19 at a specialist children's hospital between 15 March 2020 and 24 April 2020 were included. Chest imaging was performed as deemed clinically indicated by the clinical/radiology teams.

CXRs and CT thorax examinations obtained 7 days before to 30 days after PCR test were reviewed.

Radiographs were evaluated and categorised according to British Society of Thoracic Imaging (BSTI) CXR proforma.

Diagnostic odds ratio (OR) and its 95% confidence interval were calculated for each CXR feature.

SARS-CoV2 RT-PCR was taken as the reference standard for diagnosis of COVID-19.

Results:

398 consecutive patients with suspected COVID-19 were included.

Median age 2 years (range 0 - 17), 53% male. 226 children (57%) had comorbidities.

SARS-CoV2 RT-PCR was positive in 46 patients (12%).

CXR was obtained in 215 patients (54%), with no significant difference in CXR availability between COVID positive and negative groups (Fisher's exact test [FET] p = 0.9).

A higher proportion of children with comorbidities had CXR compared to those without (60% vs 47%, FET p = 0.01).

Consolidation on initial CXR was negatively correlated with COVID-19 PCR [OR 0.34 (0.12 - 0.95); p = 0.046]. No significant correlation was identified for other CXR features: collapse, bronchial thickening, hyperexpansion and effusion.

Classic COVID-19 features were seen in just 4 patients on initial CXR (only 1 with COVID-19).

CT thorax was obtained in 19 children (5%). Comorbidities were present in 18, and all 3 children with COVID-19 who underwent CT thorax had leukaemia.

CT availability was not associated with COVID-19 status (FET p = 0.5). No CT showed classic COVID features.

Conclusions:

- Chest imaging was not deemed clinically indicated in almost half of children with suspected COVID-19.
- Children with comorbidities were more likely to undergo chest imaging.
- Few children (5%) required cross-sectional imaging, for non-COVID-19 indications.
- Very few children demonstrated classic COVID-19 features on CXR.
- Consolidation on initial CXR had negative correlation with COVID-19 PCR.
- No other radiographic findings had significant correlation with COVID-19 PCR; CXR in paediatric COVID-19 is non-specific.

S1.2.3

PREVALENCE AND PATTERN OF THROMBOEMBOLIC DISEASE IN PEDIATRIC PATIENTS WITH COVID-19

IVEY Royall, HAITHUY Nguyen, MARLA Sammer
Texas Children's Hospital, Houston, USA

Purpose: While there has been recent literature investigating increased thrombotic risk in adults with coronavirus disease (COVID-19), similar studies have not been done in pediatric populations. Our purpose was to evaluate the prevalence and pattern of thrombotic events in pediatric patients infected with the severe acute respiratory syndrome coronavirus 2 (SARS-CoV-2).

Materials and Methods: An institutional database with all patients with positive SARS-CoV-2 PCR tests from 3/1/20 through 9/30/20 was obtained. From the database, exams targeted to evaluate for thromboembolism, including computed tomography (CT) and magnetic resonance (MR) angiography/venography of the head, neck, chest, and abdomen and arterial and venous Doppler ultrasounds (US) were reviewed by a pediatric radiology fellow. Medical history and demographics were extracted from the medical record.

Results: 3849 pediatric patients were positive for SARS-CoV-2. A total of 79 imaging studies from 42 patients were performed for evaluation of thromboembolism (1.1%). Nine studies (11%) from six patients were positive for thrombus and/or embolus. The average age of the patients with positive exams was 14.6 years (range 5-17) with 1:1 male to female ratio. Of the nine positive imaging studies, two were on CT angiography of the chest (pulmonary embolism protocol) and seven were on extremity venous Doppler US. Of these six patients with thrombus, only one was previously healthy prior to COVID-19 diagnosis. The other five patients had preexisting conditions including four with malignancy, either in process of treatment or with suspected recurrent disease and one with short gut syndrome and prior central line related thrombosis.

Conclusion: The prevalence of thromboembolic disease in children with COVID-19 is low but not insignificant, especially in patients with comorbidities such as malignancy. CT angiography of the chest and venous Doppler US of the extremities were the exams most likely to yield positive results.

S1.2.4

CHEST IMAGING IN PAEDIATRIC MULTISYSTEM INFLAMMATORY SYNDROME – TEMPORALLY ASSOCIATED WITH SARS-COV-2(PIMS-TS)

REBECCA Spruce, DIPALEE Durve, SHEMA Hameed, ALICE Roueche, JAMES Wong, MARIO Sa, EVELINA PIMS TS Working Group
Evelina London Children's Hospital, London, UNITED KINGDOM

Purpose: Between April-June 2020 the United Kingdom witnessed an unprecedented increase in children presenting with a multisystem hyperinflammatory syndrome which bore Kawasaki-like features. This led to a national alert and subsequent case definition by the Royal College of Paediatrics and Child Health of this novel condition, Paediatric Multisystem Inflammatory Syndrome – Temporally associated with SARS-CoV-2 (PIMS-TS).

We describe the thoracic imaging findings in PIMS-TS, their evolution and correlation with biochemical markers.

Methods: A PIMS-TS database was accessed containing all patients with relevant imaging performed between April and September 2020. Admission radiographs, cardiac CT and follow up imaging was reviewed blindly by two Consultant Paediatric Radiologists, with consensus agreement, for manifestations of PIMS-TS. Findings were correlated with patients' symptoms, biochemistry and clinical progression.

Results: At the Evelina London Children's Hospital 62 patients underwent imaging for PIMS-TS with the majority having chest radiographs at presentation and subsequent cardiac CTs. Few had dedicated thoracic CT for respiratory deterioration, however, cardiac CT images were used to assess the lungs and soft-tissues for the purposes of this study. Mean age at presentation was 8.5 years.

Preliminary imaging review revealed 73% of admission chest radiographs to be abnormal; perihilar bronchial cuffing/interstitial thickening were common findings. 77% of initial CTs were abnormal with manifestations including pleural effusions, ground glass opacification and consolidation. A single case of pulmonary embolism and of lymphadenopathy were noted. 25% of CTs demonstrated cardiac aneurysms with a z-score >2.5 in at least 1 location and the majority had resolved on subsequent imaging. Follow up CTs demonstrated minor sequelae (e.g. bronchial wall thickening/cardiomegaly).

Conclusions: To our knowledge this is the largest single site study looking specifically at paediatric thoracic imaging findings in PIMS-TS with correlation with clinical course, medium term follow-up imaging and outcomes. Common findings in the chest include inflammatory airway disease, pulmonary oedema and less commonly, acute respiratory distress syndrome. Our findings will aid the radiologist in the interpretation of chest imaging manifestations in both the acute and chronic phases of this novel disease.

S1.2.5

LOW DOSE LUNG CT – PUSHING FOR THE LOWEST RADIATION DOSE NECESSARY FOR ENSURING ADEQUATE DIAGNOSTIC IMAGE QUALITY IN CHILDREN

MICHAEL Zellner¹, SEBASTIAN Tschauner⁴, MATHIAS S. Weyland², GERD Lutters³, ISMAIL Özden³, STEPHAN Scheidegger², CHRISTIAN Kellenberger¹

¹ University Children's Hospital, Zurich, SWITZERLAND

² Zürich University of Applied Sciences, Winterthur, SWITZERLAND

³ Cantonal Hospital Aarau AG, Aarau, SWITZERLAND

⁴ Medical University of Graz, Graz, AUSTRIA

Purpose

To investigate a quantitative method for assessing image quality of low dose lung CT and find the lowest exposure dose providing diagnostic images in children.

Material and Methods

Axial volumetric CT (256 slice scanner) was performed on anthropomorphic phantoms (paediatric chest and adult-sized phantom) at different dose levels and with deep learning image reconstruction (DLIR, TrueFidelity, GE Healthcare). The steepness (maximum slope) of sigmoid curves fitted to line density profiles was measured at lung-to-pleura interfaces. Image sharpness was calculated as the median steepness from 18 different locations. Diagnostic image quality was rated by three radiologists as 1 (unacceptable), 2 (limited), 3 (adequate) and 4 (higher than needed). The image sharpness cut-off for obtaining adequate image quality was determined by comparing steepness with qualitative ratings. Lung CT from 18 children (age range 3 weeks to 17.6 years) were reviewed for image quality and radiation dose.

Results

Image sharpness increased with higher CT DIvol. Adequate diagnostic quality was reached at median steepness of 862 HU/mm in the paediatric and 515 HU/mm in the adult phantom, with corresponding CT DIvol \geq 0.1 mGy in the paediatric and \geq 0.15 mGy in the adult phantom. Patient studies obtained with low dose (median CT DIvol 0.13 mGy, median effective dose 0.12 mSv) were subjectively rated as adequate for diagnosis while image sharpness was below the adult cut-off in 1/12 cases and below the paediatric cut-off in 12/18 cases.

Conclusion

Determination of image sharpness on line density profiles can be used as measure for image quality of lung CT using DLIR. Adequate diagnostic image quality requires a CT DIvol \geq 0.1 mGy in a child and \geq 0.15 mGy in adult-sized patients. Our current protocol needs to be refined to ensure

diagnostic image quality in children of all sizes with estimated effective dose ranging from 0.1 mSv in a neonate to 0.3 mSv in a teenager.

S1.2.6

LOW DOSE LIMITED REGION CHEST CT FOR PREOPERATIVE EVALUATION OF PECTUS EXCAVATUM

GRACE Ma, DOROTHY Bulas, SUNIL Valaparla, TIMOTHY Kane, MIKAEL Petrosyan, JEFFREY Lukish
Children National Hospital, Washington, D.C., USA

Purpose: Pectus excavatum is a congenital chest wall deformity resulting in a concave depression of the sternum. Pre-operative imaging includes chest radiographs or CT to evaluate the severity of the depression, which is assessed using the Haller index (HI) (maximal transverse diameter/narrowest anterior-posterior length of chest). CT currently remains the gold standard. This study compares the radiation exposure from a limited chest CT protocol that comprises of thicker slices and only includes the region surrounding the depression needed to calculate the HI with that of a full low dose noncontrast CT chest typically used for preoperative evaluation of pectus excavatum.

Materials and Methods: Prospective study of 7 patients who have undergone a limited chest CT protocol for evaluation of pectus excavatum between May to Oct 2020. A marker is placed at the deepest point of depression and 5mm slices are obtained 3cm above and below the marker. Dose length product (DLP) and effective dose were compared to patients of similar ages who had undergone a full non-contrast pectus low dose chest CT protocol and with average values of non-contrast chest CT performed for other reasons.

Results: 7 patients with mean age of 15.4 years and weight of 68.8kg underwent the limited chest CT protocol. Mean DLP and effective doses were lower compared to patients who had a full low dose pectus chest CT and to those who had CT for other reasons (DLP: 17.9 vs 48.9 and 67.8 mGycm, $p < 0.001$; effective dose: 0.32 vs 0.88 and 1.22mSv, $p < 0.001$). Age and weight of the patients who underwent the limited protocol did not significantly differ from those who underwent the full chest CT for pectus excavatum ($p > 0.22$).

Conclusion: Limited chest CT comprising of only the region immediate to the deepest point of depression offers a lower dose (<50%) alternative for calculation of Haller index in the pre-operative evaluation of pectus excavatum.

S1.2.7

CT AND MRI FINDINGS OF LYMPHOID THYMIC HYPERPLASIA AND THYMOMA IN CHILDREN

KAREN I Ramirez-Suarez¹, DAVID M Biko^{1,2}, REBECCA A Dennis^{1,2}, HANSEL J Otero^{1,2}, AMMIE M White^{1,2}, JORDAN B Rapp^{1,2}

¹ Department of Radiology, Children's Hospital of Philadelphia, 3401 Civic Center Blvd, Philadelphia, PA, USA

² University of Pennsylvania, Perelman School of Medicine, Philadelphia, USA

Purpose: To characterize common CT and MRI features of thymic lymphoid hyperplasia (TLH) and demonstrate thymic and extra-thymic masses are not exclusive of thymic epithelial tumors (TETs).

Materials and Methods: All children with available chest CT or MRI and excisional or incisional biopsy of the thymus from 2011 to 2020 were included. Diagnoses of thymoma, lymphoma, teratoma, and TLH were established by pathology. All images were retrospectively reviewed by two pediatric radiologists and disagreements were evaluated by a senior pediatric radiologist. The presence of mass, size, location, margins, internal composition, homogeneity, and enhancement were evaluated. Clinical information was also reviewed from medical charts.

Results: Thirty-one patients (16 boys) with a median age of 12 years (IQR=10) were included in the sample. Fourteen (45%) patients had MRI and 17 (55%) had CT. Twenty (64.5%) patients had biopsy findings of TLH, 2 (6.5%) thymoma, 5 (16%) germ cell tumor, and 4 (13%) lymphoma. There were no cases of thymic cysts, thymic carcinoma, or thymolipoma. Diagnosis of myasthenia gravis was present in 16 patients with TLH (52%). 26 (84%) patients underwent surgical resection, 6 (19%) received chemotherapy, and none has had tumor recurrence to date. TLH findings were classified according to presence (n=11) or absence of mass (n=9) and were categorized by size and extension. Seven patients (64%) had small masses, 3 (27%) moderate, and 1 (9%) large. Localized mass was seen in 5 (45%) children, extra-thymic extension was seen in 4 (36%), and an extra-thymic mass in one case (9%). Margins were circumscribed in most cases (64%), and composition was solid in 7 cases (64%), cystic in 2 (18%), and mixed in 2 (18%). Masses were heterogenous in 7 cases and homogenous in 4 cases, all enhanced without calcifications and internal fat. TLH patients without mass (n=9) showed a diffusely enlarged thymus in 6 cases (67%) and a normal thymus in 3 (33%). Thymomas (n=2) were described as enhancing heterogeneous masses with extra-thymic extension and lobulated margins without calcifications or internal fat.

Conclusion: In our experience, thymic lymphoid hyperplasia is the most common biopsy proven finding in patients with focal mass or thymic enlargement on imaging. Pediatric TLH has varying imaging appearances from normal thymus to an extra-thymic mass and is vastly more common than thymic epithelial tumors.

S1.2.8

CORRELATION BETWEEN CLINICAL PRESENTATION, HIGH RESOLUTION COMPUTED TOMOGRAPHY (HRCT) FINDINGS AND HISTOLOGIC FINDINGS IN CHILDREN'S INTERSTITIAL LUNG DISEASE (CHILD)

CHIARA Sileo¹, NADIA Nathan², ANNICK Clement², AURORE Coulomb L Herminé³, HUBERT Ducou le Pointe¹

¹ APHP Hôpital Trousseau, Sorbonne Université - Pediatric Radiology Department, Paris, FRANCE

² APHP Hôpital Trousseau, Sorbonne Université - Pediatric Pulmonology Department, Paris, FRANCE

³ APHP Hôpital Trousseau, Sorbonne Université - Pediatric Histopathology Department, Paris, FRANCE

Purpose: To determine the correlation between clinical presentation, chest radiography findings, High Resolution Computed Tomography (HRCT) findings and histologic findings in Children's Interstitial Lung Disease (chILD).

Materials and Methods: As a reference center for rare lung diseases, we reviewed in our chILD cohort the cases of chILD who benefited from a lung sample through biopsy or autopsy. Their clinical data, chest radiography findings, HRCT findings and histologic findings were reviewed and compared according to the last American Thoracic Society (ATS) classification.

Results: Among 122 patients, 47 underwent a lung biopsy [some under extracorporeal membrane oxygenation (ECMO)], autopsy or both. The most frequent diagnosis were diffuse developmental disorders (n=10), growth abnormalities (n=8), specific conditions of undefined aetiology (n=9) [pulmonary interstitial glycogenosis (n=5) and neuroendocrine cell hyperplasia of infancy (n=4)], surfactant dysfunction mutations and related disorders (n=5). Only 5 patients met pulmonary fibrosis criteria.

Conclusions: ChILD is a rare condition and covers heterogeneous disorders in the immunocompetent host. A better understanding of the correlation between clinical presentation, imaging and histopathologic

findings is of utmost importance to improve patient care in this population with high morbidity and mortality.

S1.2.9

THE ROLE OF THE DIFFUSION-WEIGHTED IMAGING (DWI) IN THE DIAGNOSIS OF PULMONARY COLONIZATION BY PSEUDOMONAS AERUGINOSA

ALESSANDRA Ottavianelli¹, TERESA PIA Santangelo², MARIA LUISA Mennini¹, DAVIDE Curione¹, VERONICA Bordonaro¹, PAOLO Tomà¹, AURELIO Secinaro²

¹ Department of Imaging Bambino Gesù Children Hospital IRCCS, Rome, ITALY

² Advanced Cardiovascular Imaging Unit Department of Imaging, Bambino Gesù Children Hospital IRCCS, Rome, ITALY

PURPOSE: to evaluate Diffusion-Weighted Imaging (DWI) characteristic of the mucus plugs in chest MRI during airway colonization by *Pseudomonas Aeruginosa* (PA) in a young and adult patient with Cystic Fibrosis (CF).

METHOD AND MATERIALS: we retrospectively evaluated Chest MRI of patients with CF, who referred to our hospital from January 2018 to March 2020. During imaging analysis, the spots of hyperintensity on DWI scans corresponding to mucus plugs were signed and were subsequently evaluated according to ADC maps. Imaging data were correlated with a cultural analysis of respiratory secretions, especially with the presence of PA and PA mucoid in patients' sputum.

RESULTS: chest MRI of twenty-one patients were evaluated (9 males and 12 females; median age 26.5 years old, range 6 - 44). On DWI images 12 patients showed areas of restriction of diffusion corresponding to mucus plugs; while 14 patients presented PA in sputum cultures (10 patients were positive for PA mucoid, 11 patients for PA other than mucoid and 7 patients were colonization by both of them). In the subgroup of patients with diffusion restricted signal of the mucus plugs, 11 presented positivity to PA in sputum culture (p-values 0.005 both when $p < 0.05$ and 0.01); of these 8 patients were positive for PA mucoid (p-values 0.043 when $p < 0.05$) and 4 patients were positive for PA other than mucoid (p-values not statically significant). The presence of mucus plug with diffusion restriction in DWI sequences showed a sensitivity of 78.6% and a specificity of 85.7% for the diagnosis of PA infection in the sputum.

CONCLUSION: mucus plugs with diffusion restriction signals on DWI were significantly associated with the presence of PA colonies in sputum analysis, especially in the case of mucoid type.

S1.3.1

ESTABLISHING THE NORMAL ECHODENSITY RATIO BETWEEN RENAL CORTEX AND PYRAMID IN THE NEONATE/INFANT POPULATION AND THE EFFECT OF UTILIZED RECEIVER GAIN

TIN YAU Li¹, DENISE A. Castro¹, WILMA M. Hopman², DONALD A. Soboleski¹

¹ Kingston Health Sciences Centre, Kingston, CANADA

² Kingston General Hospital Research Institute, Kingston, CANADA

Purpose- Establish the normal echodensity ratio between renal cortex and pyramid in the normal neonatal/infant population and the effects of utilized receiver gain as a variable. Disease processes causing transmission of increased collecting system pressures into the pyramid tubules may potentially disturb this ratio and could be studied after establishing normal values.

Methods & Materials- 196 data points from 57 normal infant kidneys were collected consisting of mid-renal pyramid and adjacent cortex ROI measurements at similar depths using a 9L MHz transducer. Data collected included

gestational age, sex, sidedness and receiver gain. Additional data with gain being the only variable was obtained using an ex vivo porcine kidney. ROI's were acquired mirroring the infant kidney methods. Measurements and ratios were recorded at gains ranging from 47-90.

Results- Median ratio value was 2.51 (IQR 1.99, 3.39). The preterm population (2.80) had the highest median value, though not significantly different from term (2.54) or >44 weeks (2.37, $p = 0.360$, Kruskal-Wallis). No significant variation existed based on sex (median male 2.55, female 2.48; $p = 0.128$, Mann-Whitney U) or sidedness (median left 2.56, right 2.48; $p = 0.535$). Mean porcine model ROI's were inherently higher in the pyramid and lower in the cortex compared to neonates. ROI measurements and ratios from the porcine model demonstrated a strong non-linear correlation to gain ($p < 0.001$, Spearman). Patient data reflected this, where gain >50 was significantly correlated with renal cortex ROI ($p = 0.008$), and even more so renal pyramid ($p < 0.001$), resulting in decreasing cortex to pyramid ratios ($p < 0.001$). Utilized receiver gain <50 demonstrated no significant association with echodensity ratio.

Conclusion- A significant association exists between utilized receiver gain and echodensity at higher levels of gain (>50). We therefore recommend a utilized receiver gain of 50 or less when assessing cortical-medullary ratios. Within this gain range, the median renal cortex to pyramid ratio in our study of healthy neonates/infants was 2.51.

S1.3.2

PEDIATRIC MODIFICATION OF THE BOSNIAK CLASSIFICATION FOR COMPLEX RENAL CYSTS IN CHILDREN: IS MR NECESSARY?

STEPHANIE Cajigas-Loyola, AMY Farkas, RICHARD Bellah, HANSEL Otero
Children's Hospital of Philadelphia, Philadelphia, USA

BACKGROUND/OBJECTIVE:

The adult Bosniak classification for complex renal cyst has been validated for CT & MR but not ultrasound. In children, a proposed modification still relies in CT and/or MR for intermediate risk lesions, while recent studies have also challenged its interreader reliability. We aim to evaluate the interreader reliability of the modified Bosniak classification for ultrasound and MR as well as to determine the number of lesions that are upstage during MR after ultrasound.

MATERIALS & METHODS:

This IRB-approved retrospective study included 30 patients with complex renal cysts. Ultrasound images of all lesions were independently reviewed by two pediatric radiology fellows and two pediatric radiologists to determine a modified Bosniak category (Wallis, C et al 2008). Similar evaluation was carried for 14 patients with follow-up MR. Discrepancies were resolved by consensus. In addition to descriptive statistics, Inter-observer agreement was evaluated using kappa statistics.

RESULTS: Thirty patients (median age: 14 years -IQR: 10.5-17 years-; 17 girls) were included in the final sample. On ultrasound the lesions were classified as category I, II, and III in 3 (10%), 22 (73.3%), and 5 (16.6%), respectively. Lesions were classified on MR as category I, II and III in 6, 7 and 2 cases, respectively. There were no category IV lesions. The interreader agreement was substantial for both ultrasound ($\kappa = 0.71$ between fellows and 0.76 between attendings) and MR substantial ($\kappa = 0.74$ between fellows and 0.69 between attendings). When comparing Bosniak classification for US and subsequent MR, the category did not change for 8 (57%) patients and was lowered in 6 (42.9%).

CONCLUSION:

The modified Bosniak classification for children has substantial agreement between radiologists (1 to 32 years of experience). No lesion was upgraded into a more worrisome category after MR. Moreover, ultrasound provided a higher category in almost half the cases compared to

MR. This suggests that ultrasound is a reliable tool to evaluate complex renal cysts while MR provides little additional value.

S1.3.3

LIMITED ABDOMINOPELVIC MRI FOR APPENDICITIS: CAN WE RULE OUT OVARIAN TORSION?

SHARON Gould¹, TEJAL Mody¹, MARY Gould², HEIDI Kecskemethy¹, SIMONE Veale², ARABINDA Choudhary³

¹ Nemours/Alfred I duPont Hospital for Children, Department of Radiology, Wilmington, DE, USA

² Nemours/Alfred I duPont Hospital for Children, Department of Biomedical Research, Wilmington, DE, USA

³ University of Arkansas for Medical Sciences, Department of Radiology, Little Rock, AR, USA

Improved diagnosis of ovarian torsion is needed because 30% of ovaries are torsed at laparoscopy for acute pelvic pain, yet only 14% of torsed ovaries are salvaged. We evaluate ovarian appearance on short MRI studies performed for possible appendicitis versus ovarian torsion, proposing that symmetric adnexal appearance can exclude ovarian torsion.

Medical records of girls who had completed limited MRI between 2013 and 2019 were reviewed. Three radiologists measured the ovaries and calculated ovarian volume ratios, stromal T2 signal ratios, and stromal apparent diffusion coefficient (ADC) ratios. Adnexal cysts were measured. Statistical analysis of these measurements and presence of torsion was performed.

651 girls (1–19 years) were evaluated including 8 surgically proven torsion cases (prevalence 1.2%). Ninety-three (14%) patients had an adnexal cyst/follicle > 1 cm. Torsed cases had significantly higher volume ratios versus non-torsed cases ($p < 0.001$). Six of 8 torsion cases had a volume ratio > 3:1. Four of 8 torsion cases had large cysts > 7 cm, including both torsion cases with a volume ratio < 3:1. Four of 5 cases with cysts > 7 cm were torsed. The median T2 signal ratios with torsion were higher than without torsion ($p = 0.01$), but the two groups overlapped. A volume ratio < 3:1 had a 99.6% negative predictive value for torsion with 75% sensitivity, 87% specificity, but only a 6.7% positive predictive value. Stromal ADC ratio differences were not statistically significant ($p = 0.46$).

Our population had a low prevalence of torsion, likely because highly suspicious patients did not undergo MRI. All torsed cases had either a volume ratio > 3:1 and/or a large adnexal cyst. We conclude that ovarian torsion is very unlikely when the ovaries are symmetric in size and there is no large adnexal cyst in patients with low suspicion of torsion. Further evaluation of MRI compared to US when there is high suspicion of torsion is needed.

S1.3.4

ULTRASOUND BASED RENAL PARENCHYMA AREA AND KIDNEY FUNCTION DECLINE IN INFANTS WITH CONGENITAL ANOMALIES OF THE KIDNEY AND URINARY TRACT

BERNARDA Viteri^{1,2,3}, MOHAMED Elsingerly², JENNIFER Roem⁴, DEREK Ng⁴, BRADLEY Warady⁶, SUSAN Furth^{1,3}, GREGORY Tasian^{3,5}

¹ Department of Pediatrics, Division of Nephrology, Childrens Hospital of Philadelphia, Philadelphia, USA

² Department of Radiology, Division of Body Imaging, Childrens Hospital of Philadelphia, Philadelphia, USA

³ Perelman School of Medicine, University of Pennsylvania, Philadelphia, USA

⁴ Department of Biostatistics, John Hopkins University Hospital, Baltimore, USA

⁵ Department of Surgery, Division of Urology, Childrens Hospital of Philadelphia, Philadelphia, USA

⁶ Department of Pediatrics, Division of Nephrology, Childrens Mercy Hospital, Kansas City, USA

Background: Congenital anomalies of the kidney and urinary tract (CAKUT) are the leading cause for development of chronic kidney disease (CKD) in children worldwide.

Purpose: To determine the association between renal parenchymal area (RPA) on post-natal renal ultrasound (US) and CKD progression in infants with CAKUT.

Method: Ancillary study of children with CAKUT who had a kidney US in the first 10 months of life and estimated glomerular filtration rate (eGFR) measurement at enrollment and most recent follow-up visit nested in the prospective Chronic Kidney Disease in Children cohort (CKiD). RPA was measured by subtracting the area of the collecting systems from the total renal area in the midline on longitudinal axis (both kidneys if present or single kidney if solitary kidney). Both areas were manually segmented on the US image using ImageJ software. Each participant's eGFR annual percent change and total RPA z-score were plotted with a least-squares line of best fit (linear regression model) to quantify the association.

Results: 14 participants with CAKUT were included from two CKiD sites. 11 male and 3 female participants had their US exam at a median age of 3.41 months, IQR [1.33, 7.93] and kidney dysplasia related entities were the most common form of CAKUT (28.6%; $n = 4$) reported. Median total RPA at baseline was 16.55 cm², IQR [13.84, 19.90] (z score -1.01). After a median follow up of 7.4 years IQR [6.8, 8.2] eGFR decreased from a median of 49.4 mL/min/1.73m² at baseline visit to 29.4 mL/min/1.73m² showing an annual eGFR percent decline of -4.68%. Anthropometric and blood pressure measurements were normal at both visits.

RPA z-scores and annual eGFR percent showed slightly positive correlation (Spearman's coefficient of 0.33; $p = 0.272$) such that cases with higher total RPA z-scores had slower annual decline in eGFR. Participants with baseline eGFR < 60 mL/min/1.73m² had a lower RPA z-score and substantial annual eGFR decline (> 2.5% decline) compared to patients with baseline eGFR > 60 mL/min/1.73m² with < 3% annual eGFR decline.

Conclusion: RPA may have utility as a potential ultrasound based anatomical marker of CKD progression in children with CAKUT. Further studies with larger sample sizes are required to confirm and clarify this association.

S1.3.5

SENSITIVITY OF IMAGING FOR PREDICTING PEDIATRIC ADNEXAL TORSION

MARIA Velez-Florez, AARON Chen, ERON Friedlaender, GARY Nace, ELENA Tsemberis, CHRISTOPHER Hoffman, ROSA Hwang, SUMMER Kaplan

The Children's Hospital of Philadelphia, Philadelphia, USA

Purpose: Adnexal (ovarian and tubal) torsion is a surgical emergency affecting patients of all ages. The incidence of adnexal torsion in the pediatric emergency department (ED) is 0.5 to 2 per 10,000 patients, and its diagnosis is often delayed due to nonspecific symptoms and physical exam findings common to other frequently diagnosed conditions. Pelvic ultrasound (US) is the primary modality for assessing adnexal torsion (AT), but computed tomography (CT) and magnetic resonance (MR) may also be used. Although studies report surgical confirmation rates from 26% to 79% for US, most data are lacking regarding added value of CT and MR. Tubal torsion is not commonly addressed in imaging reports. The purpose of this study is to determine the sensitivity of imaging in the diagnosis of adnexal torsion at our institution.

Materials and Methods: We retrospectively reviewed US, MR, and CT exam reports from patients age 1–19 years old in the ED who underwent

surgery for adnexal pathology between 1/1/15-12/31/19. We coded radiology report impression as positive, negative, or equivocal for adnexal torsion, considering equivocal reports to be positive for purposes of clinical management. We calculated sensitivity for adnexal torsion for US alone, US + MR, and US + CT based on true positive and false negative reports. As our cohort did not include true negative or false positive imaging we did not calculate specificity or predictive value.

Results: The cohort included 198 patients with a median age of 14-years old and 27% premenarchal girls. based on intra-operative findings, ovarian (N=99), tubal (N=7), or tubo-ovarian (N=10) torsion was present in 54% patients. All patients had imaging prior to surgery. For adnexal torsion, US alone in 127 patients was 97% sensitive, US + MR in 41 patients was 80% sensitive, US with CT in 18 patients was 82% sensitive.

Conclusion: In our practice, pelvic US alone is 97% sensitive for adnexal torsion, but specificity remains to be calculated. MR and CT are secondary modalities for adnexal imaging used in select cases in which clinical signs or US findings are inconclusive, representing a different cohort than those in whom US findings are clear. CT findings of AT suggest imaging obtained for concerns other than AT and this was an unanticipated finding, with US used secondarily to further characterize the adnexa. Future study is needed to define specificity of imaging for AT in a pediatric population.

S1.3.6

VALIDITY OF PARENCHYMAL THICKNESS FOR PRE AND POST OPERATIVE MONITORING IN INFANT PYELOPLASTY

PRASANNA Karpaga Kumaravel, ABIRAMI KRITHIGA Jayakumar
Rainbow Childrens Hospital, Hyderabad, INDIA

Purpose

To compare the parenchymal thickness before and after pyeloplasty in infants with Ureteropelvic junction obstruction.

Materials and Methods

Retrospective and prospective study from January 2017 to October 2020 including infants (n = 107) who have undergone pyeloplasty at Rainbow Children's Hospital, Hyderabad, India, a tertiary care centre. The parenchymal thickness is measured by ultrasound, pre and post pyeloplasty in infants.

Results

A total of hundred and seven (N=107) infants were diagnosed with ureteropelvic junction obstruction and underwent laparoscopic pyeloplasty. Since the study included both retrospective and prospective data, few of the infants from retrospective records (N=19) did not have preoperative parenchymal thickness. So those infants were excluded while analysing the parenchymal thickness. Preoperative parenchymal thickness is compared with postoperative scan in 88 patients, the minimum preop parenchymal thickness was 1 and maximum preop parenchymal thickness was 7, postoperative minimum parenchymal thickness was 4 and maximum postoperative parenchymal thickness was 12.8. Parenchymal thickness was measured at the mid portion of the kidney in all patients. 88 (82.24%) patients had both preoperative and postoperative parenchymal thickness. There was a statistically significant difference (p=0.001) between the average of preop and post op parenchymal thickness.

Conclusions

Parenchymal thickness (PT) is the first portion of renal parenchyma that is affected in high-grade hydronephrosis. Very few studies have included PT to define the hydronephrosis severity due to UPJO. Early surgery helps in recover of the parenchymal thickness. Being a slowly growing part of the parenchyma, PT can be a good measurable parameter to predict pyeloplasty. Measurement of PT in hydronephrosis is reliable.

S1.3.7

USING GONAD SHIELDS IN PAEDIATRIC X-RAYS

FADI Maghrabia

Bradford Teaching hospitals, Bradford, UNITED KINGDOM

Background:

The problem of inaccurate placement of gonad shields in children has been highlighted by several publications nationally and internationally [3]. A written departmental protocol, with regular audit, will:

- Avoid confusion over when and where gonad protection is required
- Reduce gonad dose without significant loss of radiographic information

Standards:
Gonad protection should be used according to the local policy in all cases [1,2].

Initial Hip/Pelvic x-ray doesn't require gonad shield but it should be used in all subsequent images and should be positioned accurately.

Methodology:

PACS search for Hip/Pelvic X-ray in patients under 16 years old at BRI hospital

Patients who had 2 images (2 views) at the same session.

Audit:

Information of 100 patients were retrospectively collected from April 2018.

Re-audit:

Information were collected during the period from May 2018 to August 2018.

Assess:

The presence or absence of gonad protection

Whether the protection was placed correctly

Audit results:

Gonad shields were used and placed correctly in 33% of the patients.

Gonad shields were used but misplaced in 37% of the patients.

Gonad shields were not used at all in 30% of the patients.

Changes that have been done

The results were discuss at the radiological clinical governance meeting. A course has been conducted to the new radiographers by a senior staff. The local guidelines have been reviewed and simplified to make it easier to follow.

Re-audit results

Gonad shields were used and placed correctly in 60% of the patients.

Gonad shields were used but misplaced in 13% of the patients.

Gonad shields were not used at all in 27% of the patients.

References

- 1.The Ionising Radiations (Protection of Persons Undergoing Medical Examination or Treatment) Regulations 1988 (POPUMET). London: HMSO, 1988.
- 2.National Radiological Protection Board. Occupational, public and medical exposure: guidance on the 1990 recommendations of the ICRP. Didcot: NRPB, 1990.

S1.3.8

REFERENCE RANGES OF AGE BASED PORTAL VEIN, RENAL VEIN AND VENA CAVA INFERIOR SIZE IN CHILDREN IN CONJUNCTION WITH WAIST CIRCUMFERENCE

ZUHAL Bayramoglu, BERKE Ersoy, HAKAN Ayyildiz

Istanbul University, Istanbul Medical Faculty, Radiology Department, Istanbul, TURKEY

We aimed to provide a nomogram of solid intraabdominal organ size by age for Turkish children on contrast-enhanced abdominal computed tomography images in conjunction with waist circumference(WC).

800 pediatric patients (468 male; mean age:8.68±5.2 years,332 female; mean age:9.12±5.04) previously underwent abdominal computed tomography examinations were enrolled. The largest diameters of the right, left

and main portal vein, splenic and superior mesenteric vein, right-left renal veins, and vena cava inferior were measured. Descriptive statistics of the data were expressed as mean, standard deviation, and percentiles. Differences in mean diameters among age groups were compared with the ANOVA test. Pearson correlation analysis and regression equations were assessed to depict the association of diameters with age and WC parameters.

There has been statistically significant positive correlations of all measured size parameters with age ($p:0.001$; $r:0.34-0.56$) and WC ($p:0.001$; $r:0.45-0.7$). WC was significantly correlated with age ($p:0.001$, $r:0.77$). We documented 5th, 50th, 90th and 95th percentiles of solid organ diameters for age groups. Age (years) dependant regression equations for diameters (mm) of main portal vein ($0.279 \times \text{age} + 6.43$), splenic vein ($0.19 \times \text{age} + 3.8$), superior mesenteric vein ($0.28 \times \text{age} + 5.4$), right and left renal veins ($0.19 \times \text{age} + 3.9$; $0.194 \times \text{age} + 3.75$) and vena cava inferior ($0.72 \times \text{age} + 10.36$) have been calculated. There was no statistically significant difference among the mean ratios of main portal vein to vena cava inferior (0.54 ± 0.15 (median: 0.53), right to left renal vein (1.03 ± 0.14 (median: 1.02)) and main portal vein to splenic vein (1.65 ± 0.45 (median: 1.62)) ($p:0.4$) by age groups. Age dependant regression equation for WC (mm) was depicted as " $22 \times \text{age (years)} + 408$ ". WC (mm) dependant diameters (mm) of main portal vein ($0.009 \times \text{WC} + 3.6$), splenic vein ($0.006 \times \text{WC} + 1.8$), superior mesenteric vein ($0.009 \times \text{WC} + 2.3$), right and left renal veins ($0.007 \times \text{WC} + 1.25$; $0.007 \times \text{WC} + 1.26$) and vena cava inferior ($0.022 \times \text{WC} + 3.12$) were also depicted. Main portal vein (MPV; mm) dependant vena cava inferior ($1.8 \text{ MPV} + 0.6$) and splenic vein ($0.59 \text{ MPV} + 0.14$) diameters were calculated in mm by regression equations. Age and WC would be reliable parameters to predict reference ranges for deep vein diameters.

S1.3.9

URODYNAMICS AND WHITAKER TESTS: A NEW LOOK AT OLD TOOLS

DARSHAN Variyam, MATT Hawkins, ANNE Gill, JAY Shah
Emory University School of Medicine + Children's Healthcare of Atlanta, Atlanta, USA

Purpose:

First conceived in the early 1970s, combining antegrade pyelography and urodynamic concepts, the Whitaker test offers a dynamic diagnostic evaluation to differentiate between structural and functional obstruction. With a recent return to popularity in urology literature, the purpose of this abstract is to (re)acquaint Pediatric / Interventional Radiologists with the technical and diagnostic concepts necessary to providing comprehensive genitourinary service line.

Materials and Methods / Educational Objectives

1. Indications for Whitaker Test or Urodynamics study (UDS).
2. Urogenital anatomy/pathology
3. Concepts of access (Needles, Sheaths, Seldinger technique, etc.)
4. Obstructive vs. Nonobstructive uropathy
5. Equipment

1. Digital (Air-charged catheters, etc.)
2. Manual

Results

Whitaker tests can provide a crucial complement to surgical planning in patients with equivocal concerns of obstructive uropathy, especially in the upper renal collecting system. Urodynamic testing is helpful in patients with incontinence and other lower urinary tract systems. These evaluations are also useful in helping to determine postoperative course.

Conclusions

Whitaker tests and urodynamic testing is utilized to provide clarity in cases concerning for obstruction. Although minimally invasive in nature, In comparison to other modalities, dynamic testing offers visual and

physiologic information valued by surgical colleagues. The use of Whitaker testing and UDS to inform definitive urologic options and for pre and postoperative planning is a long-standing concept which has recently become more accessible due to new equipment and options available on the market. Familiarity with the indications, concept, and process of this evaluation is a must for any pediatric radiology department offering a comprehensive genitourinary service line.

S1.4.1

PEDIATRIC TUMORS WITH NTRK FUSION TRANSCRIPT: FOR A BETTER IMAGING CHARACTERIZATION

ANNE-LAURE Hermann¹, LAURIANE Lemelle², ARNAUD Gauthier³, GAËLLE Pierron⁴, NAYLA NICOLAS⁵, LIESBETH Cordoen⁵, SALMA Moalla⁶, SARAH Watson⁷, PAUL Freneaux³, DELPHINE Guillemot⁴, MATTHIEU Carton⁸, ISABELLE Aerts², FRANÇOIS Doz², GUDRUN Schleiermacher², BIRGIT Geogerger⁹, PABLO Berlanga⁹, OLIVIER Delattre², DANIEL Orbach², HERVÉ Brisse⁵

¹ Department of Radiology, Armand Trousseau Hospital, Sorbonne University, Paris, FRANCE

² SIREDO Oncology Center, Institut Curie, PSL University, Paris, FRANCE

³ Department of Pathology, Institut Curie, PSL University, Paris, FRANCE

⁴ Department of Somatic Genetics, Institut Curie, PSL University, Paris, FRANCE

⁵ Department of Radiology, Institut Curie, PSL University, Paris, FRANCE

⁶ Department of Radiology, Gustave Roussy, Villejuif, FRANCE

⁷ Department of Oncology, Institut Curie, PSL University, Paris, FRANCE

⁸ Department of Biostatistics, Institut Curie, PSL University, Paris, FRANCE

⁹ Department of Pediatric and Adolescent Oncology, Gustave Roussy, Villejuif, FRANCE

Purpose

Chromosomal rearrangements leading to NTRK1-3 (neurotrophic receptor tyrosine kinase) fusions are major genetic hallmarks of infantile fibrosarcoma (IFS) and cellular congenital mesoblastic nephroma (cCMN) but are also described in other rare tumors. The recent development of NTRK inhibitors has enhanced the need for a better identification of these tumors. The objective of the study was to describe the imaging features of unselected tumors with NTRK fusion transcript (NTRK-FTT).

Materials and Methods

Eligible patients were children (< 18 yo) with NTRK-FTT tumors as identified by RT-qPCR or RNA sequencing at Institut Curie Biobank between 2001 and 2019. Retrospective radiological analysis (US, CT or MRI) of tumors' characteristics at diagnosis was performed independently by two different radiologists.

Results

63 NTRK-FTT pediatric tumors were identified. 42 tumors with available imaging data were included. Median patients' age at diagnosis was 0.3 yo [0–15.4] with 81% < 2 yo. The fusion gene involved NTRK3 in 33 cases (including 29 NTRK3-ETV6), NTRK2 in 3 cases and NTRK1 in 6 cases, with 12 different histotypes. 24 tumors (57%) were located in soft-tissues including 20 infantile fibrosarcoma (IFS) while 10 tumors (24%) were located in the kidney including 9 cCMN. Median tumor volume was 58.6 cm³ (IQR 0.6–847). Among IFS, 9/20 (45%) had ill-defined margins, 15/20 (75%) were heterogeneous with necrosis or hemorrhage, 14/20 (70%) showed perilesional invasion and 16/19 (84%) displayed enlarged intratumoral vessels. Unlike infantile hemangiomas, intra-tumoral vessels demonstrated anarchic distribution. cCMN were also heterogeneous

(n=8/9, 89%) with necrosis (n=6/9, 67%) and 8/9 (89%) demonstrated enlarged intra-tumoral vessels.

Conclusion

NTRK-FTT are rare tumors in children occurring mainly in infants. They encompass a variety of different histotypes, the most frequent being IFS and cCMN, but also numerous others subtypes. Although nonspecific, rich intra-tumoral vascularization is a recurrent finding. Non-necrotic small-size tumors within soft tissues may mimic infantile hemangiomas.

S1.4.2

COMPARISON OF DIFFUSION-WEIGHTED MRI AND 18F-FDG PET FOR THE DETECTION OF BONE MARROW METASTASES IN CHILDREN WITH SOLID MALIGNANCIES

ELTON Greene, ALI Rashidi, LUCIA Baratto, ASHOK Theruvath, RONG Lu, MICHAEL Link, SHERI Spunt, HEIKE Daldrup-Link
Stanford University School of Medicine, Stanford, USA

Purpose: The bone marrow in children is characterized by high metabolic activity on 18F-FDG-PET, which can impede the detection of metastases. We evaluated the diagnostic accuracy of 18F-FDG-PET and diffusion-weighted (DW) MRI for the detection of bone marrow metastases in children.

Experimental Design: We investigated 23 children and young adults (7–25 years, 16 males, 7 females) with bone marrow metastases who underwent 66 simultaneous 18F-FDG PET and DW-MRI scans, including 23 baseline scans and 43 follow up scans after chemotherapy. We measured the radiotracer uptake and MRI signal of the normal bone marrow and focal tumors and calculated the tumor-to-bone marrow contrast. In addition, three readers determined the presence or absence of bone marrow metastases in 9 anatomical regions on 18F-FDG PET and DW-MRI. Results were compared with the McNemar's test and a receiver operating characteristic (ROC) analysis. Bone marrow biopsies and follow-up imaging served as standard of reference.

Results: Sensitivities, specificities and diagnostic accuracies were 84%, 100% and 93%, respectively, for DW-MRI, and 83%, 100% and 94%, respectively, for 18F-FDG PET. There was no significant difference between the two imaging modalities. Two of 23 patients demonstrated remission after chemotherapy and 21 of 23 patients progressed. We found several bone marrow metastases that demonstrated reduced 18F-FDG PET metabolism after chemotherapy, but increased in size, as measured on DW-MRI.

Conclusion: The diagnostic accuracy of 18F-FDG-PET and diffusion-weighted (DW) MRI for the detection of bone marrow metastases in children is not significantly different. DW-MRI and 18F-FDG PET provide complementary information on imaging studies of pediatric cancer patients. The addition of DW-MRI can be valuable for patients with low metabolically active tumors or highly metabolically active marrow on 18F-FDG PET.

S1.4.3

COMBINED METABOLIC AND FUNCTIONAL TUMOR VOLUMES ON PET/MRI IN NEUROBLASTOMA: COMPLEMENTARY OR REDUNDANT INFORMATION BY 18F-FDG UPTAKE AND DIFFUSION RESTRICTION?

MARYANNA Chaika¹, SIMON Männlin¹, SEBASTIAN Gassenmaier¹, STEVEN Warmann², CRISTIAN Urla², MICHAEL Esser¹, ILIAS Tsiflikas¹, SERGIOS Gatidis¹, JÜRGEN Schäfer¹

¹ Department of diagnostic and interventional Radiology, Tübingen, GERMANY

² Pediatric Surgery and Urology, Tübingen, GERMANY

Purpose: In Neuroblastoma (NB), high metabolic 18F-FDG tumor volume is associated with highly viable tissue and poor prognosis. MR studies including diffusion-weighted imaging (DWI), have shown that the extent of diffusion restriction is related to tumor cell differentiation and response to chemotherapy. Simultaneous acquisition of both modalities is feasible using PET/MRI. The purpose of our study was to evaluate the correlation between standard uptake value (SUV) and apparent diffusion coefficient (ADC) in neuroblastic tumors by voxel-wise analysis.

Methods: From our prospective observational PET/MRI study, all patients diagnosed with NB at baseline and after chemotherapy were included. After image registration and tumor segmentation, metabolic and functional tumor volumes were calculated from ADC and SUV values using a dedicated software allowing voxel-wise analysis. Under the means of thresholds each voxel was assigned to one of 3 virtual tissue groups: highly viable (v) (low ADC and high SUV), possibly benign (b) (high ADC and low SUV), and intermediate (i) with high ADC and high SUV or low ADC and low SUV. Additionally, values of ADC and SUV were correlated after clustering of multiple Gaussian distributions.

Results: From 43 PET/MR, 17 examinations of 14 patients (age range from 1–17 years, five nMyc positive) met the inclusion criteria. Eight examinations were performed at baseline, 9 for response assessment. The proportion of tumor volumes were 16, 35, 48% (v,b,i) at baseline and 6, 68, 26% after treatment, respectively. ADC and SUV showed a negative correlation prior and after to treatment ($R=-0.332,-0.401$; $P<0.0001$) in the cluster, which contains more than 70% highly viable voxels. Interestingly, post treatment only patients with progression under therapy had a relevant part in this cluster. In contrast, ADC and SUV correlated positively in the cluster containing possibly benign or intermediate voxels ($R=0.326,0.295$; $P<0.0001$).

Conclusion: Our preliminary results indicate that voxel-wise analysis of ADC and SUV can quantify different quality of tumor tissue before and after therapy. Only in volumes, which correspond to highly viable tissue, the expected negative correlation of low ADC and high SUV was found representing a redundant information. However, the positive correlation in “equivocal” voxels could be due to cell differentiation or inflammatory/necrotic processes. Further investigations in larger cohorts have to validate this hypothesis.

S1.4.4

WHOLE-BODY MRI VERSUS AN FDG-PET/CT-BASED REFERENCE STANDARD FOR EARLY RESPONSE ASSESSMENT AND RESTAGING OF PAEDIATRIC HODGKIN LYMPHOMA: A PROSPECTIVE MULTICENTRE STUDY

SUZANNE Spijkers¹, ANNEMIEKE S. Littoojij^{1,2}, THOMAS C. Kwee³, NELLEKE Tolboom^{1,2}, AUKE Beishuizen^{2,4}, MARRIE C.A. Bruin², GOYA Enriquez⁵, CONSTANTINO Sabado⁶, ELKA Miller⁷, CLAUDIO Granata⁸, CHARLOTTE de Lange⁹, FEDERICO Verzeznassi¹⁰, BART de Keizer^{1,2}, RUTGER A.J. Nievelstein^{1,2}

¹ Department of Radiology and Nuclear Medicine, University Medical Centre Utrecht/Wilhelmina Childrens Hospital, Utrecht, THE NETHERLANDS

² Princess Máxima Centre for Paediatric Oncology, Utrecht, THE NETHERLANDS

³ Medical Imaging Centre, Department of Radiology, University Medical Centre Groningen, Groningen, THE NETHERLANDS

⁴ Department of Paediatric Oncology/Haematology, Erasmus Medical Centre-Sophia Childrens Hospital, Rotterdam, THE NETHERLANDS

⁵ Department of Pediatric Radiology, University Hospital Vall d'Hebron, Institut de Recerca Vall d'Hebron, Barcelona, SPAIN

⁶ Department of Paediatric Oncology and Haematology, University Hospital Vall d'Hebron, Barcelona, SPAIN

⁷ Department of Medical Imaging, CHEO, University of Ottawa, Ottawa, CANADA

⁸ Department of Radiology, Institute for Maternal and Child Health IRCCS Burlo Garofolo, Trieste, ITALY

⁹ Department of Diagnostic Imaging and Intervention, Oslo University Hospital, Rikshospitalet, Oslo, NORWAY

¹⁰ Oncohematology Unit, Institute for Maternal and Child Health IRCCS Burlo Garofolo, Trieste, ITALY

Purpose: To compare WB-MRI with an FDG-PET/CT-based reference for early response assessment and restaging in children with Hodgkin lymphoma (HL).

Materials and Methods: 51 children (ages 10-17) with HL were included in this prospective, multicentre study. All participants underwent WB-MRI and FDG-PET/CT at early response assessment. 13 of the 51 patients also underwent both WB-MRI and FDG-PET/CT at restaging. Two radiologists independently evaluated all WB-MR images in two separate readings: with and without DWI. The FDG-PET/CT examinations were evaluated by a nuclear medicine physician. An expert panel assessed all discrepancies between WB-MRI and FDG-PET/CT to derive the FDG-PET/CT-based reference standard. Inter-observer agreement for WB-MRI was calculated using kappa statistics. Concordance for correct assessment of the response of WB-MRI and the reference standard was calculated as well as PPV, NPV, sensitivity and specificity for both nodal and extra-nodal disease presence and total response evaluation.

Results: Inter-observer agreement of WB-MRI including DWI between both readers was moderate (κ 0.46-0.60). For early response assessment, WB-MRI DWI agreed with the reference standard in 33/51 patients (65%, 95%CI 51-77%) versus 15/51 (29%, 95%CI 19-43%) for WB-MRI without DWI. For restaging, WB-MRI including DWI agreed with the reference standard in 9/13 patients (69%, 95%CI 42-87%) versus 5/13 patients (38%, 95%CI 18-64%) for WB-MRI without DWI.

Conclusions: The addition of DWI to the WB-MRI protocol in early response assessment and restaging of paediatric HL improved agreement with the FDG-PET/CT-based reference standard. However, WB-MRI remained discordant in 30% of the patients compared to standard imaging for assessing residual disease presence.

S1.4.5

ACCELERATING WHOLE-BODY MRI IN PEDIATRIC PATIENTS WITH CANCER PREDISPOSITION SYNDROME: PRELIMINARY RESULTS

JUDITH Herrmann¹, MICHAEL Esser¹, ILIAS Tsiflikas¹, MARCEL DOMINIK Nickel², RALPH Strecker², INES Brecht³, JÜRGEN Schäfer¹

¹ University of Tuebingen, Department of Diagnostic and Interventional Radiology, Tuebingen, GERMANY

² Siemens Healthcare GmbH, Erlangen, GERMANY

³ University of Tuebingen, Department of Pediatric Hematology and Oncology, Tuebingen, GERMANY

Purpose:

Over the last decades, whole-body magnetic resonance imaging (WB-MRI) has gained significant importance in diagnosis, follow-up, and prevention of cancer and cancer predisposition syndromes (CPS) in pediatric patients. As a potential “one-stop-shop”-examination, WB-MRI is an alternative to standard multi-modality staging strategies. Nonetheless, one major disadvantage of WB-MRI is its long acquisition time (TA) with the need for sedation or general anesthesia. However, latest technological advances with new reconstruction techniques such as compressed sensing (CS) enabled a WB-MRI acceleration. The purpose of our prospective study was to evaluate the feasibility and diagnostic confidence of a novel MR protocol using CS to accelerate and improve the image quality for WB-MRI in oncologic staging of pediatric patients.

Materials and Methods:

A total of 90 patients (inclusion criteria: >7 years-old, diagnosis of cancer or CPS) are to be included in this institutional review board-approved, prospective study (registration code: 685/2019BO1). To date, 10 patients were included, who underwent WB-MRI staging in an advanced 3T MR scanner with an abbreviated WB protocol consisting of 1) T2-weighted (T2w) HASTE in coronal orientation with CS (HASTE_CS) 2) standard axial DWI sequence 3) axial post-contrast T1-weighted (T1w) Volume Interpolated Breathhold Examination (VIBE) Dixon with CS (VIBE_CS). Additionally, standard T2w Turbo-Inversion Recovery-Magnitude (TIRM) in coronal orientation (T2w-TIRM) and standard axial post contrast T1w VIBE Dixon (VIBE_S) were acquired. Three readers independently evaluated the images concerning image quality and diagnostic confidence (image quality overall and organ-based, sharpness, and artifacts) on a Likert-Scale ranging from 1 to 5.

Results:

HASTE_CS and VIBE_CS were successfully acquired in all patients and were compared to standard T2w-TIRM and VIBE_S. Overall image quality for both sequences HASTE_CS and VIBE_CS was comparable to standard T2w-TIRM and VIBE_S. Scan time depends on the size of the patient examined. For a normal sized adolescent, scan time could be reduced from 9:39min (T2w-TIRM) to 3:30min (HASTE_CS) and from 1:27min (VIBE_S) to 1:10min (VIBE_CS), which results in a time saving of about 60%.

Conclusion:

The accelerated WB-MRI protocol using CS is feasible, yielding comparable image quality and diagnostic confidence to standard protocol and may allow for a remarkable time saving in pediatric WB imaging.

S1.4.6

IMPACT OF RESIDUAL DISEASE ANALYSIS BY MRI IN NEUROBLASTIC TUMORS ON TUMOR PROGRESSION EVENTS

SEBASTIAN Gassenmaier¹, ILIAS Tsiflikas¹, JOERG Fuchs², CHRISTIAN Urla², STEVEN Warmann², JÜRGEN Schäfer¹

¹ Eberhard-Karls-University Tuebingen - Department of Diagnostic and Interventional Radiology, Tuebingen, GERMANY

² Eberhard-Karls-University Tuebingen - Department of Pediatric Surgery and Pediatric Urology, Tuebingen, GERMANY

Purpose

In neuroblastoma, it is uncertain whether the tumor bed should be routinely irradiated after complete resection. Therefore, the purpose of this study was to analyze residual tumor volume and the occurrence of tumor progress events without tumor bed radiation therapy.

Methods and materials

Pediatric patients, who underwent total tumor resection of neuroblastic tumors between 2012-2018 and who received a pre- and postoperative MRI of the tumor region, were included in this retrospective single-center study. Tumor volumes were segmented on a dedicated workstation. The event of tumor progression was analyzed regarding residual tumor as well as preoperative risk factors.

Results

34 patients (neuroblastoma: n=20; ganglioneuroblastoma: n=12; ganglioneuroma: n=2) with a mean age of 4.2±2.8 years were evaluated. Preoperative risk group analysis resulted in 7 low-, 7 intermediate- and 20 high-risk patients (LR, IR, HR). The MRI scans were performed with a mean of 27±35 days before and 113±101 days after resection. Residual tumor was found in 13 cases (4 LR, 1 IR, 8 HR) with a median volume of 2.8 ml. Seven out of eight events occurred in HR patients (1 LR). There was a significant difference in the occurrence of events regarding the existence of residual tumor as six events were located in patients with residual tumor (p=0.014). Event-free survival is shown in Figure 1. Two patients with residual

tumor had local events, three patients local and metastatic events and one patient metastatic event only.

Conclusion

As expected all events except for one occurred in high-risk patients. However, residual tumor is significantly associated with local tumor relapse.

S1.4.7

MULTIMODAL VOXEL-WISE ANALYSIS OF EARLY RESPONSE TO CHEMOTHERAPY IN CHILDHOOD RHABDOMYOSARCOMA

SIMON Maennlin¹, SEBASTIAN Gassenmaier¹, ANDREAS Schmidt², JOERG Fuchs², ROBERT Grimm³, MONIKA Scheer⁴, SERGIOS Gatidis¹, JUERGEN FRANK Schaefer¹

¹ University Hospital Hospital Tuebingen, Diagnostic and Interventional Radiology, Tuebingen, GERMANY

² University Hospital Tuebingen, Kinderheilkunde 5, Tuebingen, GERMANY

³ Siemens Healthcare MR, Erlangen, GERMANY

⁴ Olgahospital, Hospital Stuttgart, Stuttgart, GERMANY

Introduction:

Rhabdomyosarcoma is the most common soft tissue tumor in childhood. In clinical trials evaluating new treatment regimens, event-free survival at three years and overall survival are the main endpoints, so data collection often lasts up to ten years. In contrast, changes in tumor volume with therapy is not a reliable marker. Planned therapy protocols (e.g., EPSSG or CWS) now include functional image parameters such as SUV on FDG PET studies. As a first step, a method of voxel-wise analysis of functional tumor volumes from 18F-FDG PET and simultaneous diffusion-weighted MRI will be investigated. For this purpose, all patients were included from the prospective PET/MRI observational study who received existing imaging before and after two cycles of neoadjuvant chemotherapy according to the CWS protocol. In addition, several patients who had undergone PET-CT and MRI as part of the CWS registry study were included in the analysis.

Methods:

Volume of interest (VOI) included total tumor volume before or after therapy. ADC (apparent diffusion coefficient) and SUV values were determined voxel-wise. Each tumor voxel was assigned to one of three groups: highly viable (ADC less than 1000 mm²/s and SUVmax greater than 2.5), intermediate (ADC less than 1000 mm²/s or SUVmax greater than 2.5), and possible necrosis (ADC greater than 1000 mm²/s and SUVmax less than 2.5).

Results:

Twenty examinations in ten patients who had received PET-MRI and fourteen examinations in seven patients who had been examined by PET-CT and MRI could be evaluated (10 M +/- 70 M, 12 m, 5 w).

There was an increase in average ADC values and a decrease in SUVmax values after chemotherapy compared to baseline.

The proportion of voxels in the highly viable group in the total number of voxels per patient decreased significantly from an average of 21.1% to 0.8% (p = 0.0002).

The proportion of voxels in the intermediate group to total voxel number did not change significantly, from an average of 41.5% to 28.6% (p = 0.14).

There was a significant increase in the proportion of voxels in the possible necrosis group, from an average of 36.3% to 70.6% (p = 0.0026).

Conclusion:

Our initial results demonstrate the feasibility of voxel-based evaluation. In particular, the ratio/change in sub-tumor volumes with increased FDG with concomitant diffusion restriction should be investigated as a target

parameter for its prognostic significance in a larger collective.

S1.4.8

THE EVOLUTION OF MRI IN THE DIAGNOSIS AND FOLLOW UP OF PAEDIATRIC EXTRACRANIAL SOLID TUMOURS - A 10 YEAR REVIEW IN A TERTIARY PAEDIATRIC HOSPITAL

SPARSH Prasher, AMY Price, JOSHUA Taylor, SRIKRISHNA Harave Alderhey Children's Hospital, Liverpool, UNITED KINGDOM

Purpose:

We are carrying out a retrospective study in a major paediatric tertiary oncology centre to assess the evolution of paediatric oncology imaging over the last 10 years.

Methods:

Retrospective analysis of the imaging strategy used in the diagnosis and follow up of 5 solid tumours (lymphoma, neuroblastoma, hepatoblastoma, Wilms' tumour and sarcoma) was performed.

Results:

A snapshot of children diagnosed with lymphoma in 2009-2010, 2014-2015 and 2019-2020 demonstrated increasing use of MRI for imaging the neck and abdomen-both for diagnosis and post treatment follow up. CT remains the most common modality for thoracic imaging owing to superior assessment of the lungs and pulmonary nodules.

Conclusions:

A comprehensive imaging strategy is essential in the management of solid extracranial paediatric tumours. The aim of imaging is to characterise lesions and quantify disease burden including metastasis. Follow up imaging is essential in assessing response to treatment.

CT has traditionally been the most popular cross-sectional imaging modality in the staging and follow-up of solid extracranial tumours due to its widespread availability and rapid acquisition of images. Some modern multi-detector row scanners can acquire images so fast that sedation may not be required. However, concerns remain about cumulative stochastic effects of repeated exposure to ionising radiation, which is especially important in the paediatric population.

MRI is an important alternative to CT due to its excellent soft tissue contrast, spatial resolution and lack of ionising radiation. In addition newer techniques such as whole body MRI with narrow and wide field of view and whole-body DWI can provide both high quality characterisation of lesions as well as identifying distant metastatic disease. Furthermore, emerging techniques such as PET MR combines functional and anatomical information of tumours and reduces the need for CT.

However, it is important to note that MRI is not sensitive in identifying pulmonary nodules and low dose CT thorax remains a vital modality in the follow-up of oncology patients. Furthermore, it is important to recognise that prolonged scanning times, the need for general anaesthesia, and higher costs often strain limited resources. Recent developments in faster and newer scanning techniques have partially addressed this issue and over the last decade MRI has had an increasing role in the diagnosis and follow up of solid extracranial tumours in children.

S1.4.9

IMAGING FEATURES OF CONGENITAL INFANTILE FIBROSARCOMA

ELETI Saigeet¹, NASIM Tahir²

¹ Department of Radiology - Great Ormond Street Hospital, London, UNITED KINGDOM

² Department of Radiology - Leeds Children's Hospital, Leeds, UNITED KINGDOM

Background

Congenital-infantile fibrosarcoma (CIFS) is a rare soft tissue childhood tumour which constitutes 5-10% of all sarcomas in children under 1 year of age. Tumours usually involve the extremities and may be misdiagnosed as benign vascular lesions. Unlike the adult counterpart, prognosis is usually excellent. Given their rarity, there is a lack of literature on imaging features.

Purpose

To review imaging features of biopsy proven CIFS across two tertiary institutions and determine any characteristic findings that may aid in differentiating between CIFS and other tumours.

Materials and methods

Patients with histologically proven CIFS were identified and retrospective review of patient demographics, clinical features and imaging findings was performed.

Results

During the period January 2010 - October 2020, 16 patients were identified, of which 7 were female and 9 were male. The t(12;15) chromosomal translocation, characteristic of CIFS compared to other soft tissue neoplasms, was present in 15 patients. 7 patients had lesions apparent at birth. The median age of presentation was 3 weeks and the mean was 4.25 months. Anatomically, the lesions were most often located in the limbs (10 patients). In the remaining patients, 2 were on the head, 2 in the thorax, 1 was intra-abdominal and 1 was over the lumbosacral spine.

6 patients had plain films on presentation which demonstrated a soft tissue opacity in 4 cases. Of these, 2 patients had irregularity of the underlying bone associated with the opacity and in 1 patient there were areas of dystrophic calcification within the opacity. 14 patients had ultrasound at presentation. 6 of these showed complex solid / cystic masses; 5 demonstrated solid masses, 1 showed a solid mass with punctate calcification, 1 showed a solid mass with irregularity of the underlying bone and 1 showed a solid mass with echogenic strands in the periphery. 13 lesions demonstrated hypervascularity on doppler US while 1 was hypovascular. All patients had MRI which typically depicted well circumscribed masses, isointense to muscle on T1 weighting and hyperintense on T2 with enhancement and diffusion restriction. In 3 patients areas of haemorrhage were noted.

Conclusion

Our cohort demonstrates that while imaging findings of CIFS are non-specific, it should be considered in the differential for a mass presenting on a limb during infancy which mimics a vascular lesion on US and appears as a discrete, enhancing and diffusion restricted mass on MR.

S2.1.1

CONCURRENT CT ANGIOGRAPHY AND DYNAMIC AIRWAY CT IN CHILDREN IN THE EVALUATION OF EXTRINSIC AIRWAY COMPRESSION

JORDAN B. Rapp^{1, 2}, KAREN I. Ramirez¹, HANSEL J. Otero^{1, 2}, SETH E. Vatsky^{1, 2}, AMMIE M. White^{1, 2}, DAVID M. Biko^{1, 2}

¹ Children's Hospital of Philadelphia, Philadelphia, USA

² University of Pennsylvania, Perelman School of Medicine, Philadelphia, USA

Purpose: Tracheobronchomalacia can be the result of extrinsic or intrinsic causes. Dynamic Airway CT (DACT) can evaluate the entire respiratory cycle in the assessment of airway compression or collapse. CT angiography (CTA) offers information regarding vascular abnormalities. Here we show that with a combined study, the cause and effect of an airway abnormality can often be determined in a single setting.

Materials and Methods: All children with dynamic airway CT performed in conjunction with a CTA of the chest between January 2019 and December 2020 were included. All images were retrospectively reviewed by a pediatric cardiothoracic radiologist. CTAs were viewed in conjunction with DACT to assess for vascular abnormality, mass effect, and

presence and degree of fixed airway compression or dynamic airway collapse. Clinical information including study indication, history of congenital heart disease, and if performed, bronchoscopy results were reviewed.

Results: Thirty-one children (12 boys) with a median age of 5.3 months (IQR=16.9) with thirty-two exams were identified. Nineteen (61.3%) had a known diagnosis of vascular anomalies, 4 (12.9%) had TE fistula, and 4 (12.9%) had chronic lung disease. Ten (32.2%) had fixed airway compression only, 16 (51.6%) had dynamic airway collapse only, and 4 (12.9%) had both fixed and dynamic collapse of the same segment. The most common causes of mass effect were dilated pulmonary artery (6/32) and vascular ring (5/32). Four (12.5%) with a vascular ring did not demonstrate airway compression or collapse. Fifteen (46.9%) had recent bronchoscopy confirming 5 cases of fixed extrinsic compression.

Conclusion: Dynamic Airway CT, when used in conjunction with CTA, can effectively detect and characterize the underlying etiology and degree of airway collapse.

S2.1.2

BRONCHOPULMONARY MALFORMATIONS. PRE AND POSTNATAL IMAGING AND FOLLOW-UP OF NON-OPERATIVE CASES

BEVERLEY Newman, CLAUDIA Mueller, MATIAS Bruzoni, MODUPEOLA Diyaoalu, RICHARD Barth
Stanford Childrens Hospital at Stanford University, Stanford, USA

Purpose: Review imaging & clinical features of lung malformations managed non-operatively.

Materials & methods: From 2011-2018, 19 infants with bronchopulmonary malformations on prenatal US &/or MR were managed nonoperatively. 13 had postnatal CT, 6 only had postnatal CXR so were excluded from the study. All imaging was reviewed jointly by two experienced pediatric radiologists and clinical charts evaluated.

Results: 13 cases included: 13/13 had prenatal US and postnatal CTA, 10/13 second trimester MR. Newborns (6M,7F) were asymptomatic except for unrelated symptoms in a small premature infant. Early CXRs 11/13 were normal or with vague opacity, 1 paraspinal mass and 1 large lung opacity. Prenatal MR/US and postnatal CT largely agreed on lesion location (56% right, 44% left), features, and diagnoses. 4 infants had more than one lesion, 4 of these lesions were resected in 3 infants (2 CPAM /bronchial atresia (BA) hybrids and 2 duplication cysts); in each case 1 lesion remained in situ; in one infant with 2 lesions, neither was removed. Only lesions treated conservatively (14 lesions in 13 infants) were included in further analysis. 5 lesions enlarged, 4 were smaller and 1 unchanged from prenatal MR (10) to postnatal CT. Lesion volume (earliest CT) ranged from 0.4 to 28ml, mean 9ml. 6 lesions were partially aerated at initial CT (2-13months mean 5), 11 showed air trapping; mucoid impaction in 12/14; small macroscopic cysts in 4; 2 with small systemic artery. Lesions enlarged on later CT (4) with more complete aeration. Imaging-based diagnoses included segmental BA (10); CPAM with BA (2); CPAM /sequestration /BA hybrid (2). Clinical and CXR follow-up was performed for 2-7 years in 6 patients; CT follow up between 7 months- 4 years in 4; and MR at 8 & 11 months in 2. Others were told to call back if they had clinical symptoms. In 13/14 no later problems were documented. One premature infant with chronic lung disease had RSV bronchiolitis.

Conclusions. 1. Lack of symptoms, small size, segmental hyperinflation and mucoid impaction (BA) with minimal macroscopic cysts favored nonoperative management. 2. Careful imaging evaluation is essential. Lesions called CPAM tend to be removed while BA are less likely. 3. The risk of infection or other complications related to lesions left in situ were very small in our cases although follow-up was incomplete. 4. A

more organized consistent diagnostic approach and standardized follow-up are needed.

S2.1.3

LOW DOSE CHEST CT FOR DIAGNOSIS OF PEDIATRIC ESOPHAGEAL FOREIGN BODIES

VICTOR Seghers, HERMAN Kan, RAY Somcio, PAUL Guillerman, CARLY Hansen, RAYMOND Pahlka, ANDY Sher, MARLA Sammer Texas Children's Hospital, Houston, USA

Foreign body ingestion is a common problem in children. Radiography is the mainstay of imaging, but many radiolucent items go undetected without further imaging by fluoroscopic esophagram. While studies in adults support the use of computed tomography (CT) for esophageal foreign body ingestion, CT has historically not been used in children, especially given the typically higher radiation doses on CT compared with fluoroscopy. In distinction to an esophagram, CT does not require administration of oral contrast, eliminating the need for placement of a nasogastric in an uncooperative patient and the risk of contrast aspiration. Additionally, CT does not require the presence of an onsite radiologist and can be interpreted remotely. At our institution, a dedicated CT protocol has been used for airway foreign bodies since 2015. Given the advantages of CT over esophagram, we retrospectively reviewed our institutional radiation dose data from 2017–2020 for esophagrams, airway foreign body CT (FB-CT), and routine CT Chest (RCTC) to compare effective doses for each modality. For ages 1 year and older, effective dose was lowest using the FB-CT protocol; esophagram mean dose showed the most variability, and was over double the dose of FB-CT for ages 5+ years. Routine CT chest doses were uniformly highest across all age ranges. Given these findings, we instituted a CT foreign body (FB-CT) imaging protocol as the first-line imaging modality for radiolucent esophageal foreign body across our institution. Here, we describe our experience which can guide others.

Fig 1. Comparison of findings of esophageal foreign bodies on routine noncontrast chest CT (a,c) and simulated low-dose CT foreign body (b, d). Images a and b refer to a 6 year old male with persistent emesis secondary to esophageal obstruction from food impaction. Images c and d refer to a 12 year old male presenting with multiple episodes of emesis after accidentally swallowing a plastic bottle cap.

S2.1.4

THE ROLE OF SUPERB MICROVASCULAR IMAGING AND SHEAR WAVE ELASTOGRAPHY IN DIFFERENTIATION OF THYROID NODULES FROM INTRATHYROIDAL ECTOPIC THYMUS IN CHILDREN

ZUHAL Bayramoglu, IGOR Ihezagire, YUNUS EMRE Akpınar, İBRAHİM Adaletli Istanbul University, Istanbul Medical Faculty, Radiology Department, Istanbul, TURKEY

We aimed to investigate differences in stiffness and vascularity properties among thyroid nodules and intrathyroidal ectopic thymus (IET) by obtaining quantitative data in children.

Twenty-seven thyroid nodules and 20 IET in children were evaluated in terms of vascularity index (VI) via superb microvascular imaging (SMI) and stiffness by shear wave elastography (SWE).

Differences in the volume, VI, and SWE parameters of the lesions were assessed by using the Mann-Whitney U test. Association of the age, lesion volume, SWE, and VI parameters were investigated by using Spearman's correlation analysis. The optimal cut-off values for stiffness and vascularity in the differentiation of nodules from IET were calculated with ROC analysis. The median (range) age of the participants with thyroid nodules and IET were

15.6 (10–18) years and 8.8 (3–14) years, respectively. The median (range) VI of the IET and thyroid nodules were 4.7 (0.2–16) % and 23.8 (7.5–40)%, respectively. The median SWE values were 7.6 (4.4–9.5) kPa and 15.58 (8.5–23.4) kPa for IET and nodules, respectively. There have been highly significant differences among medians of volume, SWE, and VI values of the lesions. Significant positive correlations were found between VI and SWE parameters ($p=0.001$, $r=0.64$), and volume with VI ($p=0.018$, $r=0.34$) and SWE ($p:0.001$, $r= 0.5$). The diagnostic accuracies were 93%, 91% with the cut-off values as 9.2 kPa, 13% for the SWE and SMI, respectively.

IETs were found to be less vascular and less stiff than thyroid nodules. IETs could be easily and confidently differentiated from nodules using SWE and SMI quantifications. This discrimination prompts the reduction of unnecessary interventional procedures.

S2.2.1

FERUMOXYTOL-ENHANCED 4D FLOW MRI FOR INTERROGATION OF RENAL BLOOD FLOW: COMPARATIVE ASSESSMENT IN CHILDREN WITH AND WITHOUT END-STAGE RENAL DISEASE

EVAN Zucker, AYA Kino, RICHARD Barth, SHREYAS Vasanawala Stanford University, Department of Radiology, Stanford, USA

Purpose: To compare 4D flow-derived renal blood flow hemodynamics in children with and without end-stage renal disease (ESRD) and correlate with renal function.

Materials & Methods: Consecutive pediatric patients with ESRD or normal kidneys who underwent ferumoxytol-enhanced abdominal 4D flow MRI at 3T from 2/2019–11/2020 were retrospectively identified. Two pediatric cardiovascular radiologists in consensus measured flow and peak systolic velocity (PSV) at the origins of the right and left renal arteries and veins (RRA, LRA, RRV, LRV, respectively) and at the suprarenal aorta and inferior vena cava. Differences in flow and PSV between the ESRD and normal renal groups were compared using the Wilcoxon rank-sum test and multivariate linear regression, adjusting for patient age and gender. Pearson correlation (r) was also used to assess associations between renal flow/PSV and glomerular filtration rate (GFR) derived from serum creatinine using the Shull equation.

Results: 38 children were included, 28 (73.7%) male, with mean \pm SD age of 9.8 ± 6.3 years, 23 (60.5%) with ESRD. Renal artery and vein flows were all significantly decreased in the ESRD compared to the normal renal group (RRA: 0.1 ± 0.1 L/min vs. 0.4 ± 0.3 L/min, $p < 0.001$; LRA: 0.04 ± 0.06 L/min vs. 0.2 ± 0.2 L/min, $p < 0.001$; RRV: 0.1 ± 0.1 L/min vs. 0.4 ± 0.5 L/min, $p = 0.002$; LRV: 0.2 ± 0.2 L/min vs. 0.6 ± 0.5 L/min, $p < 0.001$), as were renal artery PSVs (RRA: 40.3 ± 27.0 cm/s vs. 54.8 ± 16.2 cm/s, $p = 0.03$; LRA: 31.6 ± 16.8 cm/s vs. 47.5 ± 11.9 cm/s, $p = 0.002$). These relationships persisted in multivariate models. Greater renal flow and arterial PSVs were also correlated with higher GFR (RRA flow: $r = 0.5$, $p = 0.002$; LRA flow: $r = 0.4$, $p = 0.007$; RRV flow: $r = 0.3$, $p = 0.04$; LRV flow: $r = 0.4$, $p = 0.02$; RRA PSV: $r = 0.5$, $p = 0.01$; LRA PSV: $r = 0.4$, $p = 0.04$).

Conclusions: Ferumoxytol-enhanced 4D flow MRI is feasible for pediatric renal hemodynamic evaluation, showing decreased renal flow and arterial PSV in patients with ESRD, associated with lower GFR. Such measurements may serve as unique noninvasive biomarkers of renal function in children.

S2.2.2

SAFETY AND ACCEPTANCE OF ULTRASOUND CONTRAST AGENTS IN CHILDREN AND ADOLESCENTS - CONTRAST ENHANCED VOIDING UROSONOGRAPHY AND CONTRAST ENHANCED ULTRASOUND

KATJA Glutig, JOSEFINA Seelbach, PAUL -C Krüger, MATTHIAS Wäger, DIANE M. Renz, HANS -JOACHIM Mentzel
Section of Pediatric Radiology, University hospital Jena, Jena, GERMANY

Objectives To evaluate the safety of the CEUS and contrast enhanced voiding urosonography (ceVUS) in children and adolescence and to receive data about parents' acceptance of intravesical and intravenous application of sulfur hexafluoride.

Methods Within a one-year period, the parents of 56 children (f/m=32/24; mean age 3.1 years; range 3 weeks - 15.9 years) with ceVUS and of 30 children (f/m=15/15; mean age 10.5 years; range 2 months - 17.7 years) with CEUS agreed to be included in this prospective single-center study. A standardized telephone survey about the acceptance of the parents during and after the procedure as well as the adverse events (AE) was conducted three days after the examination.

Results The parents would agree with the use of both ceVUS and CEUS as a diagnostic tool again in 96 % (54/56) or 100 % (30/30) of the cases, respectively. 92.9 % (52/56) would prefer ceVUS to voiding cystourethrography (VCUG). In addition, 83.3 % (25/30) would prefer CEUS to CT and 73.3 % (22/30) would prefer CEUS to MRI. AE were reported in 3.6 % after ceVUS (2/56; skin rash, mild fever) and in 3.3 % after CEUS (1/30; vomiting). AE were subacute and self limited.

Conclusions The vast majority of parents prefers ceVUS and CEUS to VCUG, CT or MRI because of agents safety and diagnostic accuracy.

S2.2.3

CONTRAST-ENHANCED ULTRASOUND (CEUS) IN THREE PATIENTS WITH MULTISYSTEM INFLAMMATORY SYNDROME IN CHILDREN (MIS-C)

MISUN Hwang^{1,2}, LUIS OCTAVIO Tierradentro-García¹, LAURA Poznick¹, TODD Kilbaugh^{2,3}, KATHLEEN Chiotos^{2,3}

¹ Department of Radiology, Children's Hospital of Philadelphia, Philadelphia, USA

² Perelman School of Medicine, University of Pennsylvania, Philadelphia, USA

³ Department of Anesthesiology and Critical Care Medicine, Children's Hospital of Philadelphia, Philadelphia, USA

Purpose: MIS-C an emerging post-infectious condition that develops after exposure to SARS-CoV-2. MIS-C is associated with shock requiring vasoactive agents in approximately half of cases. Previous studies have shown that echocardiogram demonstrates impaired ejection fraction in one-third of patients and coronary artery aneurysms in 8%. As part of a pilot study, we report for the first time the use of CEUS for assessing the microvascular flow of the heart and kidneys in children with MIS-C.

Methods: We included patients with diagnosis of MIS-C (including fever, laboratory evidence of inflammation, clinically evidenced multisystemic involvement, and positive SARS-CoV-2 IgG). After biparental consent, the contrast agent LUMASON® was administered. Real-time imaging of the heart (focusing on the left ventricular wall perfusion) and left kidney was performed. Static and cine clip images were acquired after US contrast agent (UCA) injection until wash-out. B-FLOW and MicroFlow Imaging HD were performed in the kidney. Images were interpreted qualitatively by a board-certified pediatric radiologist with expertise on use of CEUS for potential microvascular perfusion abnormalities.

Results: Three patients: A, B, and C (ages 8, 10, and 6 years, respectively) were evaluated. All of them had cardiovascular compromise (hypotension requiring vasopressors and/or abnormal echocardiography) and were receiving immunoglobulin and corticosteroid therapy. Contrast-enhanced echocardiography (CE Echo) and renal CEUS were performed between days 2 and 6 after admission. In patients A and B, CE Echo and renal CEUS demonstrated homogeneous perfusion without perfusion defect or

areas of prolonged and/or delayed enhancement in the left ventricular wall or the left kidney. In patient C, CE Echo and renal CEUS showed diffuse diminished microvascular perfusion of the left ventricular wall and kidney.

Conclusion: We provide the initial feasibility data of using CEUS to assess microvascular perfusion of the heart and kidney in MIS-C. Our cohort of MIS-C patients did not exhibit severe microvascular perfusion defects in the heart or the kidney, but whether this is due to the small sample, the timing of CEUS, concomitant medications, or the differing pathophysiology between MIS-C and primary COVID-19 infection in adults warrants further exploration. Further work will be needed to investigate the potential microvascular dysfunction in MIS-C and its long-term implications.

S22:4

ADAPTING THE REALIZING IMPROVEMENT THROUGH TEAM EMPOWERMENT (RITE) PROGRAM TO A VIRTUAL FORMAT IN THE MIDST OF THE COVID-19 PANDEMIC

MONICA Miranda Schaeubinger¹, ETHAN Larsen¹, KANDICE Garcia Tomkins², VALERIE Rigby¹, AMMIE White¹, RAYMOND Sze¹, DAVID Larson²

¹ Children's Hospital of Philadelphia, Department of Radiology, Philadelphia, USA

² Stanford University School of Medicine, Department of Radiology, Stanford, USA

Purpose:

Process improvement, a valuable tool in complex health care environments such as radiology departments, uses effective improvement methods that involve the participation of all potential stakeholders (personnel, patients, students, referring physicians) to achieve sustainable improvement. The Realizing Improvement through Team Empowerment (RITE) program was developed in 2016. Previously exclusively taught through an in-person flipped-classroom approach, the RITE program has shifted the improvement culture in different clinical departments through its team-based, project-based improvement approach. During 2020, and due to the COVID-19 pandemic, the RITE training program was adapted to a virtual format. In this abstract, we describe the multi-institutional implementation of RITE during a pandemic.

Materials and Methods:

The virtual RITE program took place from July to December of 2020. The program was reconfigured to an online format using Zoom, which allowed two hospitals to become one cohort and attend sessions together. An every-other-week session was facilitated by the RITE Program Manager. All other in-person meetings and site visits were cancelled. Ten 2-hour sessions were scheduled from July to December to go through the learning material, advance improvement projects and present results. The project progress scale was used to track the progress of the projects throughout the cohort.

Results:

The virtual platform facilitated simultaneous multi-institutional training while presenting with additional challenges. The cohort consisted of six teams (37 participants) from 2 institutions. Each team completed a Quality Improvement project following the RITE methodology in subjects including MRI, US, CT, DR and ACR certification. All projects reached levels of 3.0-4.0, all met graduation criteria for project completion, with evidence of at least modest improvement.

Conclusions:

Having a structured problem-solving method that is learned along with applicable, timely and focused QI education materials ensures that teams not only complete projects successfully but also teaches them skills that can be used for subsequent improvements within the department. This was not only a useful test of bringing multiple hospitals together in one training program, but it was a testament to the strength of the principles of

the RITE program, with the unexpected benefit of positive peer pressure and momentum to foster improvement culture across institutions.

S3.1.1

STRUCTURAL HETEROGENEITY IN ADOLESCENT BRAIN AGE ASSOCIATED WITH DISTINCT COGNITIVE PROFILES

SUSAN Sotardi¹, MONICA Truelove-Hill², GURAY Erus², JIMIT Doshi², RAQUEL Gur², RUBEN Gur², DANIEL Wolf², TYLER Moore², THEODORE Satterthwaite², CHRISTOS Davatzikos²

¹ Childrens Hospital of Philadelphia, Philadelphia, USA

² University of Pennsylvania, Philadelphia, USA

Background

Brain age prediction models may be useful as indicators of divergence from typical development. Previously, we used structural and functional MRI data from pediatric datasets to produce a brain-age based neural maturation index (NMI) that characterizes typical brain maturation patterns and identifies those who deviate from this trajectory (Truelove-Hill, et al. 2020). Here, we examined the association between brain age and cognitive scores.

Methods

We stratified 1710 participants (aged 8-23; 819 males) into three age groups and split participants based on their structural NMI scores, with those above the 70th percentile being high, those below the 30th percentile being low, and the remaining being typical. We then performed HYDRA analysis, which categorizes the extreme (high/low) groups from the typical, and then identifies heterogeneity within the extremes. HYDRA revealed two clusters each for both high and low groups, regardless of age. We then performed between cluster comparisons with respect to neurocognitive scores.

Results

We found distinct cognitive differences, both between high performing clusters and low performing clusters. Participants in the high clusters showed significant ($p < 0.05$) differences in language reasoning (LAN), nonverbal reasoning (NVR), working memory (WM) and spatial ability (SPA) scores, across both young and middle age groups. Participants in the low clusters showed significant differences in LAN across middle and old age groups. Generally, one cluster performed better than or equivalently to the typical group and one performed worse.

Discussion

Our results indicate a heterogeneity in brain aging, which may have a significant impact on cognition. Our NMI clusters were particularly different with respect to language reasoning, as an indicator of episodic memory (Moore, et al. 2015). Therefore, NMI scores reflect an individual's deviation from typical brain development and may be helpful in the early detection and intervention of abnormalities in neurocognitive function.

S3.1.2

THE PEDIATRIC MILD TRAUMATIC INJURY DIFFUSION-TENSOR IMAGING STUDY AT 3 TESLA

ANDREI Manzhurtsev¹, MAXIM Ublinskiy^{1,2}, ALEXEY Yakovlev¹, OLGA Bozhko¹, TOLIB Akhadov¹, NATALIA Semenova^{1,2}

¹ Clinical and Research Institute of Emergency Pediatric Surgery and Trauma, Moscow, RUSSIA

² Emanuel Institute of Biochemical Physics of the Russian Academy of Sciences, Moscow, RUSSIA

Computed tomography and magnetic resonance imaging (MRI) are not sensitive to mild traumatic brain injury (mTBI). However, mTBI may cause changes in cerebral microstructure that could be found using diffusion tensor imaging (DTI). The aim of this study is to reveal possible microstructural disorders in grey and white cerebral matters of children in

the acute phase of mTBI (no more than 72 hours), not accompanied by any structural brain injury.

Materials and methods

Subjects: 11 healthy subjects and 11 patients with mTBI (up to 41+19 hours since the injury), mean age 16+2. Philips Achieva dStream 3.0T and 32-channel SENSE head coil were used. The standard TBI MRI protocol was applied. No pathological changes in brain tissue of any subject were found.

DTI was performed in 32 directions and was processed in Philips Intellispace Portal software. The fractional anisotropy (FA) and apparent diffusion coefficient (ADC) values were obtained in corpus callosum (CC), corticospinal tract (CST) and in thalamus.

Statistical analysis was performed in STATISTICA 12 (Statsoft). The nonparametric Mann-Whitney criterion was used to reveal the significance of group differences, p -value < 0.05 was considered significant.

Results

FA and ADC measured in thalamus are sensitive to acute mTBI: FA is increased and ADC decreases. The trend to the FA increase in corpus callosum in mTBI group and the absence of any changes in this parameter in corticospinal tract were observed. ADC in both CC and CST is unchanged.

Discussion

The results of this study signify the presence of microstructural damage in thalamus. The changes in diffusion parameters arise from the cytotoxic swelling that happens because of the alterations in metabolic processes caused by the traumatic impact [1]. The trend to the growth of FA revealed in this work may witness for the process of microstructural damage "maturation", causing these changes to be observed as significant at a later stage after injury [1, 2, 3].

References

1. Z. Chu. Voxel-Based Analysis of Diffusion Tensor Imaging in Mild Traumatic Brain Injury in Adolescents. *AJNR Am J Neuroradiol.* 2010 Feb;31(2):340-6
2. Henry LC, Tremblay J, et al. (2011) Acute and chronic changes in diffusivity measures after sports concussion. *J Neurotrauma.* (10):2049-59.
3. Mayer AR, Ling J, Mannell MV, et al. (2010) A prospective diffusion tensor imaging study in mild traumatic brain injury. *Neurology.*;74(8):643-50.

S3.1.3

EVALUATING BRAIN ELASTOGRAPHY CORRELATIONS IN A PEDIATRIC PORCINE MODEL OF ASPHYXIA ASSOCIATED CARDIAC ARREST

KRISTINA Khaw¹, ANUSH Sridharan², SUNIL Unnikrishnan², TODD Kilbaugh³, MISUN Hwang²

¹ University of Pennsylvania - Department of Bioengineering, Philadelphia, USA

² Children's Hospital of Philadelphia - Department of Radiology, Philadelphia, USA

³ Children's Hospital of Philadelphia - Department of Anesthesiology and Critical Care Medicine, Philadelphia, USA

Purpose

To evaluate changes in brain tissue stiffness in a pediatric porcine model of asphyxia-associated cardiac-arrest.

Methods

In 6-week-old, 10kg swine ($n=8$), cardiac-arrest was induced by clamping the endotracheal tubes for 7-minutes, followed by CPR for 10-minutes or until return of spontaneous circulation (ROSC). Cortex elastography samples including 5 regions of interest were collected during baseline (10 minutes pre-asphyxia), 1-hour post-ROSC, and 3-hour post-ROSC. Due to challenges with transducer footprint making sufficient contact with brain tissue in the cranial window, only images with $>50\%$ of the

elastography box filled were used for analysis. Mean arterial pressure (MAP) and intracranial pressure (ICP) were collected continuously. Hemodynamics, elastic modulus (E), and velocity (V) were compared using multivariate linear regression.

Results

Of the swine, 5 survived and 3 did not survive the arrest. The baseline mean V and E of surviving swine (2.44 ± 0.80 m/s and 19.74 ± 12.62 kPa) were significantly higher than non-surviving (1.71 ± 0.46 m/s and 9.29 ± 7.02 kPa) with $p < 0.001$. The mean V and E of 3-hours post-ROSC (2.04 ± 0.63 m/s and 13.63 ± 8.77 kPa) were significantly higher than baseline (1.88 ± 0.63 m/s and 11.74 ± 9.64 kPa) and 1-hour post-ROSC (1.76 ± 0.63 m/s and 10.48 ± 8.27 kPa) with $p = 0.080$ and $p = 0.010$ respectively. The 1-hour post-ROSC elastography parameters were insignificantly lower than baseline, suggesting increased stiffness developing post-ROSC. ICP and elastography parameters were significantly correlated at the 1-hour post-ROSC period ($p < 0.001$), and MAP correlated significantly with elastography parameters at the 1-hour (positive, $p = 0.024$) and 3-hour (negative, $p < 0.001$) post-ROSC period. Baseline had no correlations.

Conclusion

In this preliminary investigation, there appears to be changes in brain tissue stiffness associated with cardiac-arrest that ultrasound elastography can identify. The findings indicate brain elastography may serve as an important biomarker for assessing cerebral health during the acute to subacute periods post-cardiac-arrest, but the quantitative parameter derived likely represents a more complex pathophysiology affected by cerebral perfusion, ICP, and brain injury. Further mechanistic work will advance the clinical utility of brain elastography in hypoxic ischemic injury.

S3.1.4

CEREBRAL pH IN ACUTE MILD TRAUMATIC BRAIN INJURY MEASURED BY 1H MAGNETIC RESONANCE SPECTROSCOPY

PETR Bulanov¹, ANDREI Manzhurts^{1,2,3}, ALEXEY Yakovlev^{1,3,5}, PETR Menshchikov^{3,4}, MAXIM Ublinskiy^{1,3}, NATALIA Semenova^{1,2,3,5}, TOLIB Akhadov^{1,2}

¹ Clinical and Research Institute of Emergency Pediatric Surgery and Traumatology, Moscow, RUSSIAN FEDERATION

² Lomonosov Moscow State University, Moscow, RUSSIAN FEDERATION

³ Emanuel Institute of Biochemical Physics of RAS, Moscow, RUSSIAN FEDERATION

⁴ Philips Healthcare, Moscow, RUSSIAN FEDERATION

⁵ Semenov Institute of Chemical Physics of the Russian Academy of Sciences, Moscow, RUSSIAN FEDERATION

Introduction

Concussion (or mild traumatic brain injury (mTBI)) is a common pediatric trauma. The long-term consequences of an mTBI may be: headaches, attention deficit, sleep problems, etc. [1]. However, no anatomical changes and abnormalities are observed in standard MRI or CT scans, which indicates the necessity to search for biochemical changes in brain by alternative methods. One of these methods is Magnetic Resonance Spectroscopy (MRS).

The aim of present work is to find the effect of mTBI in acute phase on the cerebral pH value in posterior cingulate cortex. In 1H MRS the pH value is determined using standard PRESS spectra by measuring the chemical shift in «aromatic» region: 7-8 ppm.

Materials and methods

The study was performed at the Clinical and Research Institute of Emergency Pediatric Surgery and Trauma. The research involved 16

patients with mTBI (up to 3 days after injury), mean age was 15 ± 3 years, and 17 healthy subjects forming the control group.

Philips Achieva dStream 3.0T MRI and a 32-channel SENSE quadrature coil were used. The study protocol included PRESS pulse sequence with the following parameters: TR = 2 s, TE = 80 ms, N points = 2048, BW = 2000 Hz, NSA = 288. The voxel ($50 \times 25 \times 25$ mm) was located in the posterior cingulate cortex (PCC).

The values of the central frequency of the signal in the region of 7 ppm were calculated and the pH values were calculated using the expression from [2].

Results

The shift in the resonance of the imidazole rings by 7 ppm is observed in trauma. The chemical shifts of creatine (Cr) signals are the same in normal conditions and in mTBI, which confirms the reliability of the shift in the 7 ppm region.

A significant decrease by 1.2% in the pH value of the posterior cingulate cortex in the acute phase after concussion was discovered. Despite the relatively low absolute change, it may cause biochemical disturbances in PCC, because pH directly affects the activity of enzymes. One hypothesis explaining this effect is a disruption of microcirculation in the cerebral vessels, resulting in activation of the anaerobic stage of glycolysis with subsequent accumulation of lactate and consequent lowering of the pH.

Literature:

- DOI: 10.1007/s12178-019-09536-8.
- DOI: 10.1002/mrm.1910380611

S3.1.5

WILL THE REAL PAPILLEDEMA PLEASE COME FORWARD: DIFFERENTIATING CONCERNING AND CONGENITAL OPTIC NERVE DISK ELEVATION

ADAM Goldman-Yassen¹, ANNA Shifrin², AVRUM Pollock³, TAMARA Feygin³

¹ Children's Healthcare of Atlanta, Atlanta, USA

² North Shore Radiological Associates, Winchester, USA

³ Children's Hospital of Philadelphia, Philadelphia, USA

Purpose: 1. Describe imaging features defining papilledema (PE) versus pseudo-PE and 2. Determine imaging finding associations with visual outcomes.

Material and Methods We performed a retrospective cohort study, searching the radiology database for patients referred for clinically suspected PE. We reviewed brain/orbit MRIs with focus on the appearance of the optic nerve head (ONH), specifically protrusion into the vitreous, calcification, enhancement, and restricted diffusion (RD); flattening of the posterior sclera; and dilation of peri-optic nerve spaces. We reviewed the electronic medical record for initial and final (ie, following complete resolution of PE) visual acuity and visual field testing. Patients with PE were categorized depending on their visual outcome as normal, subnormal, or abnormal. Final visual acuity and visual fields were defined and recorded as normal, abnormal, or subnormal. Comparisons between subjects with true and pseudo-PE with regards to imaging findings and vision outcomes were performed using the Fisher's exact test.

RESULTS: We identified 52 patients referred for MRI evaluation of suspected PE. 38/52 had true PE and 14/52 had pseudo-PE based on neuroimaging features. RD was the most reliable sign to distinguish these two entities, present in 28/38 patients with clinical PE and 3/14 with pseudo-PE (cases of optic glioma and optic neuritis, where RD was unilateral and also seen in the rest of the optic nerve) ($p = 0.001$). Of the patients with PE, pseudotumor cerebri was the most common underlying etiology (17/28). Patients with clinical PE had RD of the ONH in both eyes. Visual outcomes were subnormal or normal in 33/38 patients with PE, with no statistically significant association between visual outcome and prevalence of diffusion restriction ($p = 0.77$).

CONCLUSIONS: ONH RD was the findings most strongly differentiating with PE from pseudo-PE. Visual outcomes were not significantly different in patients with ONH RD compared to those without restricted diffusion, which argues for reversible metabolic disruption causing RD instead of ischemia.

S3.1.6

MRI-GUIDED LASER ABLATION FOR CHILDREN WITH REFRACTORY EPILEPSY RELATED TO HYPOTHALAMIC HAMARTOMA (HH): TECHNIQUE, PITFALLS AND INITIAL RESULTS IN 11 PATIENTS

JORDI Muchart¹, SANTIAGO Candela², MONICA Rebollo¹, MARTA Gomez-Chiari¹, JAVIER Aparicio³, SILVIA Serrano⁴, MARIANA Alamar², ALIA Ramirez³, MARIA VICTORIA Becerra², ALBA Carrillo¹, FERRAN Pifarre¹, JOSE Hinojosa², JOSEP Munuera¹

¹ Diagnostic Imaging Department, Sant Joan De Deu Barcelona Children's Hospital, Barcelona, SPAIN

² Neurosurgery Department, Sant Joan De Deu Barcelona Children's Hospital, Barcelona, SPAIN

³ Neuropediatric Department, Sant Joan De Deu Barcelona Children's Hospital, Barcelona, SPAIN

⁴ Anaesthesiology Department, Sant Joan De Deu Barcelona Children's Hospital, Barcelona, SPAIN

INTRODUCTION

Real-time MRI-guided laser ablation is a promising technique for HH approved in 2018 by the European Medicines Agency. We present our experience, safety and follow-up in 11 patients.

METHODS

Patients were selected in the Epilepsy Unit based on drug-resistance and HH type/size.

MRI studies & treatment were performed in a 3T or 1.5T Philips Ingenia magnet. Fiber trajectory was planned with Voxim® software and performed with robotic arm Neuromate-Renishaw®. Treatment was designed to achieve disconnection, and if possible complete ablation.

Ablation was performed with the Visualase® system. Therapy was monitored by real-time MR-thermography during ablation and DWI, FLAIR and T2 in-between cooling times to identify complications and assess disconnection/ablation.

RESULTS

We treated 11 patients from April 2018-February 2021, 15m-18y old, 4-23m follow-up. All patients had mostly gelastic seizures. 14 procedures (including 3 re-ablations) were performed.

No fiber repositioning was needed.

Intraop MRI changes included lesion increase, restricted DWI, intralesional bleeding and high FLAIR/T2 signal, and high FLAIR/T2 signal and tumefaction in surrounding tissues that persisted or were more extensive at 24h. At 6 months, lesion tumefaction diminished but bleeding and high FLAIR/T2 signal persisted. Surrounding tissue changes improved.

1 patient suffered a transient hemiparesis, 1 postop somnolence and SIADH and 1 patient an oculomotor (III) palsy.

In 3 patients epilepsy relapsed and underwent a second procedure, at least two months later they are seizure-free.

CONCLUSIONS

1. Real time MRI-guided laser treatment for HH is a complex technique that requires tight multidisciplinary teamwork for optimal precision in treatment planning, execution and monitoring for patient safety and treatment success.

2. System's MRI thermography is very useful for monitoring estimated lesion and surrounding tissue temperature but currently lacks whole anatomic coverage, so conventional MRI sequences are needed to evaluate

safety out of treatment planes and assess treatment-related changes that may ensure complete HH disconnection/ablation.

3. Further studies are needed but, in our experience, it seems a safe technique. Accuracy of fiber path planning and positioning is crucial, as well as cautious supervision of correct pump functioning.

4. In terms of efficacy some patients may need more than 1 procedure for seizure control, which seems related to HH size and attachment.

S3.1.7

IMAGING OF PEDIATRIC SPINAL CORD INFARCT ASSOCIATED WITH FIBROCARILAGINOUS EMBOLISM

ALIREZA Zandifar¹, LUIS O. Tierradentro-García¹, JORGE DU UB Kim¹, LAUREN A. Beslow², ARASTOO Vossough¹

¹ Department of Radiology, Children's Hospital of Philadelphia, Philadelphia, USA

² Department of Neurology, Children's Hospital of Philadelphia, University of Pennsylvania, Philadelphia, USA

Purpose:

Fibrocartilaginous Embolism (FCE) is a rare cause of pediatric ischemic myelopathy and the proposed mechanism is fragmentation and migration of fibrocartilaginous nucleus pulposus into spinal microvasculature. Fewer than 30 pediatric patients have been reported in the literature, mostly as single case reports. The presence of a T2 hypointense disc near the cord infarct is taken as presumptive evidence of FCE in some reports. We assessed imaging features predictive of FCE in a pediatric cohort.

Materials and Methods:

We evaluated patients with spinal cord infarct over a 15-year period. A definitive diagnosis of FCE can only be made at autopsy. The presumptive diagnosis of spinal cord infarct due to FCE in our patients was made based on clinical, laboratory and imaging features. Spinal imaging was compared to 120 age-group matched controls. Disc abnormalities, including annular fissure and T2-hypointense intervertebral disc were reviewed and prevalence and association of these abnormalities were evaluated using Chi-Square or Fisher exact tests.

Results:

There were 12 patients with a diagnosis of FCE. Seven were female (58.3%). The mean age was 10.8 years (range 6-17). A disc annular fissure was seen in 10/11 (91.6%) of FCE cases vs 3/120 (2.5%) of controls; odds ratio=429 (95%CI:41-4480, p<0.000001), the majority present at cervical levels. The annular fissure was at or within one level of the spinal cord infarct in all patients. A T2-hypointense disc was observed in 1/12 (8.3%) infarct patients vs 2/120 (1.6%) of controls; odds ratio=5.1 (95%CI:0.44-63, p=0.25). In the single patient with a T2-hypointense disc near the cord infarct level, location was adjacent to a disc level with an annular fissure.

Conclusions:

In pediatric patients with cervicothoracic spinal cord infarction, an adjacent disc annular fissure is associated with a greatly elevated odds of FCE. A T2-hypointense disc adjacent to the spinal cord infarct was not associated with an elevated odds of FCE in our cohort.

S3.1.8

RED FLAGS OF TORTICOLLIS: RETROSPECTIVE STUDY OF 540 CHILDREN ADMITTED TO EMERGENCY DEPARTMENT

ANTONIO Marrazzo¹, ALESSIA Carboni¹, ALESSANDRO Ferretti², FRANCESCO Dotta¹, CARLO Gandolfo¹, UMBERTO Raucci³, PAOLO Tomà⁴, G. STEFANIA Colafati¹

¹ Neuroradiology Unit, Department of Imaging, Bambino Gesù Children's Hospital, IRCCS, Rome, ITALY

² Rare and Complex Epilepsy Unit, Department of Neurosciences, Bambino Gesù Children's Hospital, IRCCS, Rome, ITALY

³ Emergency Department, Bambino Gesù Children's Hospital, IRCCS, Rome, ITALY

⁴ Department of Imaging, Bambino Gesù Children's Hospital, IRCCS, Rome, ITALY

Purpose

Torticollis in childhood is a common cause of medical examination in the Emergency Department (ED) and the literature on its specific evaluation is poor. Our aim is (i) to describe the etiological spectrum responsible for torticollis, (ii) to identify “red flags” that might recommend further investigations, including radiological ones and (iii) to detect atypical and underestimated causes.

Materials and Methods

540 children admitted to ED for torticollis over six-years are retrospectively reviewed. History and physical examination findings, imaging, laboratory tests and management are analyzed. Torticollis is classified as postural, traumatic, infectious, neurological, congenital, ophthalmological, neoplastic, vascular or miscellaneous.

Results

Postural torticollis (43.7%) is the most frequent, followed by traumatic (26.5%) and infective (22.2%). Neurological, congenital, ophthalmological, neoplastic, vascular and other causes represented less common pathologies but, for this reason, they must not be underestimated. The age is statistically significantly lower ($p < 0.001$) in neurologic and congenital categories. Symptoms present a period of time longer ($p < 0.001$) in neurologic, tumor and congenital categories than in others (red flag). Fever is statistically more frequent in children with infectious torticollis (red flag) ($p < 0.001$). Neuroimaging (TC and MRI) is performed more frequently in children with a longer period of time of symptoms ($p < 0.001$). On the other hand, no parameters correlate directly with a positive CT and/or MRI.

Conclusions

There is not yet a standard management for children with torticollis admitted to the ED due to the etiological variability of the pathology. The prompt identification of “red flags” such as (i) neurological associated signs/symptoms, (ii) no response to medical therapy, (iii) no history of trauma, (iv) time more than 7-10 days, is mandatory to identify atypical and less frequent causes (tumor, neurological, etc.) and rule out life-threatening conditions.

S3.2.1

BIOMECHANICAL FLOW MODELING USING PATIENT-SPECIFIC 3D PRINTED MODELS FOR SURGICAL DECISION-MAKING IN ANOMALOUS AORTIC ORIGIN OF THE CORONARY ARTERIES (AAOCA)

YASAMAN Farsiani¹, JAYANTHI Parthasarathy¹, SILVANA Molossi², CARLOS Mery³, ATEFE Razavi⁴, LAKSHMI PRASAD Dasi⁴, RAJESH Krishnamurthy¹

¹ Nationwide Children's Hospital, Columbus, USA

² Baylor College of Medicine, Houston, USA

³ University of Texas Austin, Austin, USA

⁴ Georgia Institute of Technology, Atlanta, USA

Background: AAOCA is the second most common cause of sudden cardiac death (SCD) in the young. Surgery is being offered for patients with documented evidence of ischemia, and increasingly, in patients without ischemia based on “high-risk” features on CTA, including long intramural course and ostial stenosis, without guidance regarding preoperative risk, whether surgery is directed at the offending mechanism causing ischemia, and how surgery may alter risk. Biomechanical flow modeling allows improved risk stratification and surgical decision making.

Methods: IRB approval was obtained for case studies in 2 patients: 1. AAOCA-L, and a short 3.5 mm intramural course passing through a thickened intercoronary pillar. Patient presented with repeat SCD after initial unroofing, and a second surgery, coronary translocation, was performed to treat recurrent ischemia related to the pillar. 2. patient with AAOCA-R, a high origin, and a long 7.8 mm intramural course, s/p successful unroofing of the intramural segment. Patient-specific biomechanical 3D-printed models incorporating morphological features derived from CTA were created preop- and postoperatively, and connected to a left heart flow simulator. Hemodynamic parameters such as fractional flow reserve (FFR), and instantaneous coronary flow rate (IFR) were recorded at rest and simulated exercise, and location of FFR drop and pressure recovery were identified.

Results: In patient 1, flow studies showed FFR of 0.7 in the distal intramural segment preoperatively consistent with ischemia, FFR less than 0.8 in the proximal mediastinal segment after unroofing, consistent with persistent ischemia related to compression by the thickened pillar, and normal FFR at all locations after translocation. In patient 2, FFR fell to 0.4 on the preop modeling study, whereas in the post-operative study, FFR recovered to >0.87 , consistent with resolution of ischemia after surgery.

Conclusion: Importance of resolving patient-specific mechanism of ischemia during surgery for AAOCA is illustrated using biomechanical flow-modeling, which may allow improved surgical decision-making and determine biomarkers of surgical success.

S3.2.2

UNDERSTANDING FONTAN ASSOCIATED LIVER DISEASE (FALD): CORRELATION OF VASCULAR FLOW IN THE LIVER WITH FONTAN HEMODYNAMICS IN CHILDREN

KAREN I Ramirez-Suarez¹, ENSAR Yekeler¹, SURAJ D Serai¹, JORDAN B Rapp^{1,3}, SARA L Partington², MATTHEW A Harris², KEVIN K Whitehead^{2,3}, JACK Rychik^{2,3}, DAVID M Biko^{1,3}

¹ Department of Radiology, Children's Hospital of Philadelphia, Philadelphia, USA

² Division of Cardiology, Children's Hospital of Philadelphia, Philadelphia, USA

³ University of Pennsylvania, Perelman School of Medicine, Philadelphia, USA

PURPOSE: Fontan associated liver disease (FALD) begins in childhood, but the underlying mechanism of this condition is unknown. Our purpose is to evaluate vascular flow to the liver in children post-Fontan palliation and to compare this to functional and hemodynamic data from magnetic resonance imaging (MRI).

MATERIALS AND METHODS: All children (< 18 yo) post Fontan palliation who presented for cardiac MRI with measurement of hepatic flows by velocity mapping between 2019 and 2020 were evaluated. Cardiac function, caval, pulmonary artery and veins, and main portal vein flows were reviewed. Total hepatic flow was calculated by comparing infrahepatic IVC to IVC flow. Total caval return, pulmonary venous return, systemic to pulmonary collateral flow, and pulmonary-to-systemic blood flow ratio (Qp/Qs) were calculated. Flows were indexed to body surface area (BSA). Clinical information including cardiac diagnosis, type of Fontan procedure (lateral tunnel or extracardiac) presence of fenestration, and Fontan associated pathology were assessed. Descriptive data were presented as median (IQR) or mean (SD) as corresponding, Pearson correlation was used for parametric values, and non-parametric tests were used to evaluate hepatic flow between group differences. P value < 0.05 was considered significant.

RESULTS: 22 Patients (13 male) were included, with a median age of 13 years (IQR = 4.1) at MRI, and 2.8 (IQR = 1.5) at Fontan operation. Mean BSA was 1.32 (SD 0.35). 16 patients (73%) had single right ventricle

physiology and 6 (27%) single left ventricle. 17 (77%) had fenestration, 6 (27%) underwent lateral tunnel procedure and 16 (73%) extracardiac conduit. 6 children (27%) had diagnosis of FALD by MRI or liver elastography. Pearson correlation demonstrated significant correlation of indexed hepatic flow with indexed pulmonary artery flow ($p < 0.001$) and cardiac index ($p < 0.001$) No correlation was demonstrated with collateral flow ($p = 0.619$) nor Q_p/Q_s ($p = 0.510$). Non-parametric tests showed no correlation between hepatic flow and FALD, and neither for type of Fontan. Indexed hepatic flow was not statistically different between patients with right and left single ventricle, nor between patients with and without fenestration.

CONCLUSION:

Hepatic flow in children post-Fontan palliation correlates with cardiac index and pulmonary arterial flow. Understanding the liver hemodynamics in children post-Fontan can lead to treatment strategies to decrease FALD.

S3.2.3

FREE-BREATHING NON-CONTRAST MR ANGIOGRAPHY IN CHILDREN USING 3D DUAL-ECHO DIXON TECHNIQUE: INITIAL CLINICAL EXPERIENCE

MADELEINE Fischer¹, JAN-MALTE Ambs¹, MISCHA Sommer¹, UNDINE Wilke², MASAMI Yoneyama³, SHUO Zhang², CARL-MARTIN Junge¹

¹ Altonaer Kinderkrankenhaus gGmbH, Hamburg, GERMANY

² Philips Healthcare, Hamburg, GERMANY

³ Philips Healthcare, Tokyo, JAPAN

Purpose

MR imaging is considered a valuable diagnostic tool for noninvasive imaging of the vasculature in children and adults. However, simple, non-ECG-gated MR angiography/venography with high resolution without contrast is still challenging. We aimed to investigate the clinical utility of the recently introduced Relaxation-Enhanced Angiography without Contrast or Triggering (REACT) method in pediatric patients.

Materials and Methods

Patients with various indications for MR vascular exams were examined (1.5T Ingenia Ambition, Philips Healthcare). The scan protocol included REACT using a 3D dual-echo Dixon acquisition with T2- and inversion-recovery pre-pulses. Typical scan time was 2 to 4 min with 1 to 1.5-mm in-plane resolution and 2.8-mm slice thickness. Conventional CE- and non-CE-MRA such as TOF and PCA were performed for comparison. Images were assessed visually according to general quality, artifacts, diagnostic confidence and visualization of the anatomical structures as well as pathologies.

Results

Thirty patients (3mo to 17yo; median age 8.2yo; 11 female) were included. In general, REACT showed good image quality with sufficient background tissue suppression and was comparable to TOF and PCA if not better. Vascular malformations consisting of dilated tortuous vessels and intramuscular infiltration shown in CE-MRA as well as stenosis, thrombus and collateral circulation were also well depicted by REACT without contrast administration. It is noteworthy that a helicopter overview of the vasculatures including veins from REACT was deemed particularly helpful for pre-surgery or intervention check. Furthermore, REACT was found to be useful as a scout sequence or fallback for CE-MRA in case of technical or operation failure.

Conclusions

Non-contrast MRA in children using REACT benefited from simple examination with high-resolution anatomical information of the vasculature of the body and extremities without the need for contrast material or

breathhold. The obtained vasculatures overview may be helpful in screening for negative workup or unexplained causes.

S3.2.4

QUANTITATIVE CT IN INFANTS WITH BRONCHOPULMONARY DYSPLASIA ASSOCIATED WITH AND WITHOUT PULMONARY HYPERTENSION

KAREN I Ramirez-Suarez¹, CHRISTIAN A Barrera¹, ERIK A Jensen^{2,3}, JORDAN B Rapp^{1,3}, DAVID M Biko^{1,3}, AMMIE M White^{1,3}, HANSEL J Otero^{1,3}

¹ Department of Radiology, Children's Hospital of Philadelphia, 3401 Civic Center Blvd, Philadelphia, PA, USA

² Division of Neonatology, The Children's Hospital of Philadelphia, 3401 Civic Center Blvd, Philadelphia, PA, USA

³ University of Pennsylvania, Perelman School of Medicine, Philadelphia, PA, USA

Purpose: To evaluate the quantitative CT parameters in infants with severe bronchopulmonary dysplasia (BPD) associated with and without pulmonary hypertension.

Materials and Methods: All infants with confirmed BPD diagnosis and available non-contrast enhanced chest CT from 2012 and 2020 were included. Diagnosis of pulmonary hypertension was established by echocardiography soon after birth. Lung parenchyma was segmented using a semi-automated technique with an open-source software by two researchers. Patients with collapsed lung and thoracic malformations that limited the segmentation were excluded. Hounsfield units (HU) were measured and plotted in a histogram to obtain different values. Low attenuation areas < -950 HU (LAA), high attenuation areas > -250 HU (HAA), mean lung density (MLD), kurtosis, skewness, lung mass (grams), and volume (liters) were obtained. Descriptive data were presented as mean \pm standard deviation. Non-parametric tests were used to evaluate group differences. P value < 0.05 was considered significant.

Results: 135 patients (82 boys) with BPD with a mean age of 4.7 ± 1.5 months were included in the sample. The mean gestational age at birth was 25.6 ± 2.0 weeks of gestation. 99 (73%) infants were diagnosed with pulmonary hypertension. 17 (12%) infants died during hospitalization, with a mean age of 10.5 ± 10.4 months; all of them had pulmonary hypertension. Based on the analysis, there were no significant difference between BPD infants with and without pulmonary hypertension in terms of LAA% (0.1 vs 0.2, $p = 0.12$), HAA% (13.2 vs 10.7, $p = 0.12$), MLD (-527.5 vs -554.3 HU, $p = 0.26$), kurtosis (2.1 vs 2.1, $p = 0.18$), skewness (1.2 vs 1.4, $p = 0.69$), volume (0.2 vs 0.2, $p = 0.64$), and mass (89.7 vs 83.8, $p = 0.71$).

Conclusion: The presence of pulmonary hypertension in patients with severe BPD is not correlated with quantitative lung parenchymal changes, as measured with qCT.

S3.2.5

NON-CONTRAST PULMONARY MRI: LONG-TERM MONITORING OF STRUCTURAL LUNG DISEASE IN PATIENTS WITH CYSTIC FIBROSIS

MAREEN Kraus¹, MICHAEL Esser¹, LENA Kiefer¹, RICARDA Schwarz¹, PHILIPP Utz², UTE Graepler Mainka², ILIAS Tsiflikas¹, JÜRGEN F Schäfer¹

¹ Diagnostic and interventional Radiology, Tübingen, GERMANY

² Paediatrics, Tübingen, GERMANY

Purpose: Phenotypic expression and pulmonary impairment varies substantially across cystic fibrosis (CF) patients. The purpose of this study was to evaluate the change in structural lung disease over 6 years assessed

by pulmonary MRI (pMRI) and correlated to pulmonary function testing with forced expiratory volume in 1 s (FEV1).

Material and methods: In this retrospective study CF patients were included with biennial pMRI continuing over at least 6 years and with pulmonary function testing. All pMRIs consisted of the same protocol and were conducted on a 1.5 T scanner (PDw Flash 3D in breath-hold, coronal T2w TSE with double-triggering and functional sagittal PDw Flash 2D sequence in submaximal in- and expiration). Structural lung disease was assessed per lung lobe using the semi-quantitative MR-CF-S score, which comprises bronchiectasis/peribronchial wall thickening, mucus plugging, centrilobular opacities, consolidation, sacculation, and air trapping. For better comparison, z-scores were calculated for each patient's examination and pulmonary function testing, which were correlated to time.

Results: 41 patients (mean age 10.2±5.2 years, 19 males, 22 females) were included. Over a 6 year period, an overall decrease of FEV1 of -0.77 % per year (SD 2.1) was observed with a baseline FEV1 of 91.1% (SD 14.3). Concurrently the baseline MR-CF-S with an average of 5.6 ±5.0 showed an increase of 6.4 points (SD 3,69) over the 6 years. There was a significant difference in the z-scores that were correlated to the examination time points: z- FEV1 (-1) showed a slope of 0.03 (p=0.38) and z-MR-CF-S 0.14 (p<0.001). The most significant categorical differences in z-MR-CF-S were seen for bronchiectasis and air trapping.

Conclusion: The increase in MR-CF-S over the 6 years showed a significantly swifter disease progression than FEV1, suggesting that the pMRI is more sensitive than pulmonary function testing. CF patients can therefore benefit from biennial pulmonary MRIs.

S3.2.6

LUNG MR-IMAGING WITH 3D ULTRASHORT-TE IN FREE BREATHING IN COMPARISON WITH CONVENTIONAL T2 SEQUENCES IN PEDIATRIC RADIOLOGY

FRANZ-WOLFGANG Hirsch¹, REBECCA Anders¹, THOMAS Benkert², DANIEL Gräfe¹

¹ Department of Pediatric Radiology, University of Leipzig, Leipzig, GERMANY

² Siemens Healthcare GmbH, Erlangen, GERMANY

Objectives

Recent lung-MR sequences with ultra-short TE time (UTE) coupled with respiratory compensation promise to overcome the typical problems in lung imaging regarding respiratory motion, low proton density and rapid T2* decay. So far, there are very few studies on the relevance of these sequences in children. We compared the diagnostic value of the respiratory-self-gated 3D UTE sequence versus conventional respiratory-triggered T2-weighted Turbo Spin Echo (T2-TSE) sequence in a pediatric collective.

Methods

71 patients between 0 and 18 years of age, who were scheduled for a thoracic MRI based on different clinical indication, were examined on a 3T MRI system. The UTE and T2-TSE sequences were evaluated by two readers regarding quality features and visualization of 8 common pathology patterns.

Results

UTE was superior to T2-TSE for so-called 'MR-negative pathologies', significant for air trapping, and in tendency for bullae and cysts. In all remaining pathologies, T2-TSE proved to be at least equivalent and occasionally better as UTE. The image quality of both sequences was equally high, with UTE depicting pleural and central bronchi more clearly.

Conclusions

3D-ultrashort-TE time sequences have a substantial benefit in the context of hyperinflation, emphysema, cysts, or pathologies of the bronchial

system. However at present UTE cannot serve as universal replacement for conventional T2-TSE for all pathologies.

S3.2.7

FAST LUNG MRI AS A DIAGNOSTIC IMAGING TOOL FOR CONGENITAL DIAPHRAGMATIC HERNIA

SUREYYA BURCU Gorkem¹, HAZAL BERCEM Gurleyen²

¹ Erciyes University Department of Pediatric Radiology, Kayseri, TURKEY

² Erciyes University Department of Pediatric Surgery, Kayseri, TURKEY

Purpose: We aimed to demonstrate congenital diaphragmatic hernias (CDHs) by using a fast lung MRI technique. **Methods:** Between, 2019-2020, children (9 patients (7 boys, 1 girl), age range, 1 year 7 months-3 years; median age, 23.5 months) who were presented with diaphragm hernia were selected for fast lung MRI examination. The imaging protocol was performed on an MRI unit (1.5 T Aera; Siemens, Erlangen, Germany) with T2-weighted free-breathing rapid sequences by using a body coil.

Results: Imaging findings were confirmed in the operation rooms as Bochdaleck Hernia (n=5), and sliding hernia (n=1). One patient with diaphragmatic eventration due to an unknown etiology. Two patients (Morgagni (n=1) and sliding hernia (n=1) were not operated on due to his comorbidities (severe epilepsy, etc.). Patients who were operated on recovered well and were discharged without any symptoms. **Conclusion:** Fast Lung MRI technique is a promising, fast, and alternative imaging method to diagnose CDH without any radiation exposure or contrast use in children.

S3.2.8

THORACIC IMAGING FEATURES OF ANTI-MDA5 JUVENILE DERMATOMYOSITIS

HAITHUY Nguyen¹, DAVID Moreno-McNeill², MANUEL Silva-Carmona², TIPHANIE Vogel³, R. PAUL Guillerman¹

¹ Texas Children's Hospital - Department of Radiology, Houston, USA

² Texas Children's Hospital - Department of Pediatrics, Pulmonology, Houston, USA

³ Texas Children's Hospital - Department of Pediatrics, Rheumatology, Houston, USA

Purpose: A subtype of juvenile dermatomyositis (JDM) is associated with anti-melanoma differentiation-associated protein 5 (anti-MDA5) autoantibodies and interstitial lung disease (ILD), including the rapidly progressive subtype (RP) of ILD. The purpose of this study is to describe the thoracic imaging features of anti-MDA5 JDM.

Materials & Methods: Patients with anti-MDA5 JDM-related lung disease were identified from an institutional pulmonology registry. Two pediatric radiologists conducted a consensus retrospective review of the findings on chest radiography (CXR) and CT. Demographics, clinical presentation, and pulmonary function testing results were extracted from the electronic medical records.

Results: 11 children (6:5 male:female; 8 Caucasian/3 African-American) with chest imaging available for review were identified. The mean ages were 10.4 years (range 2.1 - 17.6) at presentation and 12.3 years (range 3.1 - 18.1) at first chest CT. Presenting signs and symptoms included cutaneous manifestations (11/11), mild muscle weakness (9/11), dyspnea (4/11), and impaired diffusing capacity, with mean DLCO/VA of 64%. Mean FEV1 was normal at baseline. 3/11 had abnormal CXRs. 10/11 had abnormalities on CT: ground-glass opacities (7/10), patchy consolidation (7/10), poorly-defined nodules (5/10), subpleural septal thickening (5/10), fibrosis (honeycombing or architectural distortion, 2/10), pleural thickening (2/10), subpleural cysts (1/10), pneumomediastinum (3/10),

hilar/mediastinal lymphadenopathy (2/10), or axillary lymphadenopathy (6/10). Lung disease was predominantly distributed at the juxta-pleural anterior upper and posterior lower lobes. Of 8 with follow-up chest CT, lung disease progressed in 4/8, regressed in 2/8, and remained stable in 2/8. The youngest patient presented with RP-ILD and pneumomediastinum and had a fatal outcome.

Conclusions: The most common features of anti-MDA5 JDM thoracic disease are juxta-pleural consolidations and ground-glass opacities of the anterior upper and posterior lower lobes, axillary lymphadenopathy, and impaired diffusing capacity in the setting of mild muscle weakness. Pneumomediastinum with RP-ILD is associated with a higher risk of mortality.

S3.3.1

MRI-CHARACTERISTICS OF PEDIATRIC RENAL TUMORS: A SIOP-RTSG RADIOLOGY PANEL DELPHI STUDY

JUSTINE N. van der Beek^{1,2}, TOM A. Watson³, RUTGER A.J. Nievelstein^{1,2}, RONALD R. de Krijger^{2,4}, NORBERT Graf⁵, ØSTEIN E. Olsen³, JENS-PETER Schenk⁶, MARRY M. van den Heuvel-Eibrink², ANNEMIEKE S. Littoojij^{1,2}

¹ Department of Radiology and Nuclear Medicine, University Medical Center Utrecht/Wilhelmina Children's Hospital, Utrecht, THE NETHERLANDS

² Princess Máxima Center for Pediatric Oncology, Utrecht, THE NETHERLANDS

³ Department of Paediatric Radiology, Great Ormond Street Hospital NHS Foundation Trust, London, UNITED KINGDOM

⁴ Department of Pathology, University Medical Center Utrecht, Utrecht, THE NETHERLANDS

⁵ Department of Paediatric Oncology&Hematology, Saarland University Medical Center-Saarland University Faculty of Medicine, Homburg, GERMANY

⁶ Clinic of Diagnostic and Interventional Radiology, Division of Pediatric Radiology, Heidelberg University Hospital, Heidelberg, GERMANY

Purpose: The International Society of Pediatric Oncology-Renal Tumor Study Group (SIOP-RTSG) does not advocate invasive procedures to determine histology before start of therapy. This may induce misdiagnosis-based treatment initiation, but only for the relatively small percentage of non-Wilms tumors (non-WTs). Even though magnetic resonance imaging (MRI) is the preferred modality for diagnosis and pre-operative assessment of pediatric renal tumors, no consensus has been reached on which indicators are able to differentiate tumor subtypes. The aim of the current study is to identify MRI-characteristics that may be used for discrimination of newly diagnosed pediatric renal tumors.

Materials and Methods: A two-round Delphi procedure, consisting of online questionnaires, was initiated by the SIOP-RTSG radiology panel. Participants had >4 years of experience in MRI of pediatric renal tumors and/or assessed >49 MRI-scans of pediatric renal tumors in the past 5 years. The cut-off value for consensus and agreement among the majority was >74% and >59%, respectively.

Results: The first round was completed by 23 participants, the second round by 20 participants. Consensus or an agreement among the majority on a variety of characteristics specific for certain types of renal tumors mainly concerned the discrimination between WTs and non-WTs, and between WTs and nephrogenic rest(s)/nephroblastomatosis.

Conclusions: Although the discrimination of pediatric renal tumors based on MRI remains challenging, this study identified some specific characteristics, based on the shared opinion of carefully selected experts. These results may guide future validation studies and innovative efforts, including the potential value of MRI-techniques such as diffusion-weighted

imaging (DWI).

S3.3.2

ROLE OF INTRA-VOXEL INCOHERENT DIFFUSION (IVIM) MRI IN SURVEILLANCE OF KIDNEY TRANSPLANT DYSFUNCTION: PRELIMINARY FINDINGS

ADARSH Ghosh, BERNARDA Viteri, ERUM A Hartung, TRICIA Bhatti, DMITRY Khrichenko, MOHINI Dutt, ROBERT Carson, HANSEL J. Otero, SURAJ Serai
Children's Hospital of Philadelphia, Philadelphia, USA

Purpose: Appropriate management of kidney transplant dysfunction entails early detection of rejection and identification of fibrosis progression. Blood flow is reduced in rejection, as inflammatory damage to blood vessels causes vasoconstriction and progressive fibrosis. Diffusion of protons in tissue is affected by the random motion of protons in cells (diffusion coefficient D) and microcapillary motion (Pseudo-diffusion coefficient D*). IVIM can quantify both D and D* and provides perfusion fraction (f), a dimensionless percent of pixels occupied by capillary flow. We compared IVIM-based perfusion in healthy control subjects to that of pediatric kidney transplant recipients.

Materials and Methods: As part of this IRB-approved prospective study, five healthy controls and four kidney transplant recipients were scanned using 8 b-values ranging from 0 to 1000 s/m² using SS-EPI DWI on a 3T MRI scanner. D, D* and f were calculated using ROIs drawn on the renal cortex and whole kidney. Kidney transplant recipients underwent surveillance allograft biopsy on the same day of the scan. IVIM values obtained were then compared between participants with stable/"normal" kidney allograft, acute rejection and fibrosis on biopsy.

Results: The age (mean±std. dev) of the healthy controls and kidney transplant recipients were 28±13 years and 16±4 years, respectively. Renal biopsies demonstrated stable allograft histology in 2 patients, one patient with acute antibody mediated rejection and one patient with grade 1 fibrosis. Amongst the healthy controls the IVIM parameters were as follows: f = 23.08±1.98%; D = 1607.14±63.25 m/s² and D* = 29197.4±6079.83 m/s². No significant difference was observed in the values obtained from the cortex and the whole kidney (p>0.05). Allografts with stable renal histology had IVIM parameters comparable to the control population. In comparison, the allograft with acute rejection had a perfusion fraction of 18.8%, and the allograft with grade 1 fibrosis had a perfusion fraction of 21.29%, demonstrating the decrease in vascularity secondary compression by inflamed tissue/ fibrosis. D and D* were lower in the participant having acute rejection.

Conclusion: IVIM diffusion shows promise in quantifying perfusion changes in transplanted kidneys and a subset of histological changes associated with rejection. IVIM diffusion can potentially be developed as a non-invasive surveillance marker of kidney transplant health and dysfunction.

S3.3.3

FUNCTIONAL MAGNETIC RESONANCE UROGRAPHY (FMRU) IN URETEROPELVIC JUNCTION OBSTRUCTION (UPJO): PROPOSAL FOR A PEDIATRIC QUANTITATIVE SCORE

FIAMMETTA Sertorio¹, MARIA BEATRICE Damasio¹, IRENE Campo², LUCA Basso¹, LORENZO Anfigno³, MICHELA CING YU Wong⁴, ANGELA Pistorio⁵, MONICA Bodria⁶, GIORGIO Piaggio⁶, GIROLAMO Mattioli⁴

¹ IRCCS Giannina Gaslini, Radiology Department, Genova, ITALY

² UOC di Radiologia Ospedale Civile Conegliano Veneto, ULSS 2, Conegliano, ITALY

³ Università degli Studi di Genova, DISSAL, Radiology Department, Genova, ITALY

⁴ IRCCS Giannina Gaslini, Pediatric Surgery Department, Genova, ITALY

⁵ IRCCS Giannina Gaslini, Epidemiology and Biostatistics Unit, Genova, ITALY

⁶ IRCCS Giannina Gaslini, Nephrology and Renal Transplantation Department, Genova, ITALY

Purpose

Uretero-pelvic junction obstruction (UPJO) is one of the most frequent causes of congenital hydronephrosis due to intrinsic or extrinsic anomalies. It is essential to distinguish UPJO which needs surgical treatment from those that remain stable or even resolve over time. In UPJO framework, functional magnetic resonance urography (fMRU) combines high quality morphological details of the kidney and excretory pathways with functional data. The study aim was to identify a new radiological score based on fMRU findings able to differentiate surgical from non-surgical kidneys.

Material and Methods

We retrospectively selected patients with hydronephrosis due to UPJO who underwent fMRU (January 2009–June 2018). A multidisciplinary team identified a list of fMRU morpho-functional predictive variables to be included in the analysis.

To evaluate the role of different independent variables in predicting the outcome, a multivariable logistic regression model has been performed; the outcome variable was the surgical intervention. The variables included in the model were those parameters significant in the bivariate analysis or clinically relevant. For each predictive variable, Odds Ratio and 95% Confidence Intervals were calculated. The Likelihood Ratio test was used to assess the significance of the variables. Using the regression model, we assigned a numerical value (score) to each predictive variable, rounding up the beta-coefficients. Finally, the cut-off value of the total score that would be able to discriminate between surgical and non-surgical kidneys was obtained from the ROC curve analysis.

Results

According to inclusion and exclusion criteria 192, patients were enrolled, corresponding to 200 pathological kidneys. All of them underwent fMRU; 135 were surgically treated, while 65 underwent US or MRU follow-up. Predictive variables significantly associated with surgery resulted to be the urographic phase, the presence of abnormal vessels and a baseline antero-posterior pelvic diameter greater than 23 mm. Beta coefficient of the logistic regression model were then converted in scores. The ROC curve of the score showed high sensitivity (84.3%) and specificity (81.3%) with a cut-off > 2.5.

Conclusion

We propose a new highly sensitive and specific fMRU score able to identify surgical versus non-surgical kidneys with UPJO.

S3.3.4

FEASIBILITY OF QUANTITATIVE ASSESMENT OF RENAL FUNCTION USING MOTION-INSENSITIVE MR UROGRAPHY IN PEDIATRIC PATIENTS

RAMKUMAR Krishnamurthy ¹, DMITRY Khrichenko ², TOBIAS Block ³, SILA Kurugol ⁴, JEANNE Chow ⁴, RAJESH Krishnamurthy ¹

¹ Nationwide Children's Hospital - Radiology, Columbus, USA

² Children's Hospital of Philadelphia - Radiology, Philadelphia, USA

³ NYU Langone Health - Radiology, New York, USA

⁴ Boston Children's Hospital - Radiology, Boston, USA

Background: Quantitative assessment of kidney function in children using functional MR urography (fMRU) is challenging due to 1) long

scan times, 2) respiratory/bulk motion artifact, and 3) non-availability of validated open-use software for analysis.

In this study, we demonstrate the feasibility of quantitative assessment of renal function from motion-insensitive MR imaging using freely available validated software.

Methods: In 6 patients (mean age: 5 years, range: 4 months–19 years) referred to fMRU from April 2019 until November 2020, MR imaging of the renal system was performed on a 3T scanner (Siemens Prisma or Skyra). After obtaining anatomy and T2W scans, contrast-enhanced imaging (single dose gadavist, 0.1 or 0.2 cc/s) of the kidneys was performed 15 minutes after injection of furosemide.

A golden-angle radial sparse parallel (GRASP) technique was used to acquire 3D coronal images. Acquisition parameters: TR = 3.3 ms; TE = 1.5 ms; flip angle = 13; 288x288 acquisition matrix; slice thickness = 2–3 mm; 6000–9000 radial spokes; acquisition time = 8–10 minutes. Dynamic images were reconstructed at 6.8 s temporal resolution using the freely available Yarra framework (<http://yarraframework.com/>).

Dynamics were loaded into freely available and validated pMRI software (www.parametricmri.com) for quantitative analysis. Semi-automated segmentation of aorta, kidney parenchyma, and excretory system was performed to obtain the following functional metrics: volume, Patlak scores, volumetric and Patlak differential renal function (vDRF, pDRF), calyceal transit time (CTT), and renal transit time (RTT). Maps showing Patlak KPS map and fractional blood volume were also generated.

Results: Reconstruction/analysis was successful in all patients. Figure 1 shows the results. The differences in RTT, CTT, and DRF demonstrate the differences between two kidneys. Patlak scores serve as measure of GFR.

Conclusion: In this study, we demonstrate the technical feasibility of performing free-breathing and unsedated quantitative assessment of kidney function using the freely available Yarra framework and pMRI software, a process that is reproducible in most pediatric centers.

S3.3.5

DIFFUSION-WEIGHTED MRI IN THE EVALUATION OF RENAL PARENCHYMAL INVOLVEMENT DURING FEBRILE URINARY TRACT INFECTIONS IN CHILDREN: PRELIMINARY DATA

LORENZO Anfigeno ¹, FIAMMETTA Sertorio ¹, LUCA Basso ¹, ANDREA Fontana ², MONICA Bodria ³, ANGELA Pistorio ⁴, GIAN MARCO Ghiggeri ³, MARIA BEATRICE Damasio ¹

¹ Radiology Department, IRCCS Giannina Gaslini, Genova, ITALY

² Postgraduation School in Radiodiagnostics, Università degli Studi di Milano, Milan, ITALY

³ Nephrology Department, IRCCS Giannina Gaslini, Genova, ITALY

⁴ Epidemiology and Biostatistics Department, IRCCS Giannina Gaslini, Genova, ITALY

Purpose: Urinary tract infection (UTI) is the most common infection in pediatric age. Acute pyelonephritis (PNA) represents a worrying situation in pediatric patients related to the risk of sepsis and long-term cicatricial consequences.

The purpose of this retrospective study is to investigate the diagnostic role of Diffusion-Weighted MRI (DW-MRI) in febrile urinary tract infections (fUTIs).

Materials and Methods: According to inclusion and exclusion criteria we enrolled 51 patients less than 15 years old admitted to our Institute between September 2012 and April 2020 with febrile UTI who underwent DW-MRI evaluation. Clinical, laboratory and imaging data were collected. Statistical analysis was performed.

Results: 34 of 51 patients with fUTI (66.7%) showed signs of acute parenchymal involvement at DW-MRI study. In 27/34 (79.4%) DW-

MRI showed multiple areas of pyelonephritis. A statistically significant relationship ($p = 0.0004$) between older age at admission and pyelonephritis was demonstrated. No statistically significant relationship was found between the other clinical, anamnestic and laboratory parameters and the outcome of DWI.

Only 2 ultrasound examinations allowed the identification of pathologic areas on the renal parenchyma.

Conclusions: DW-MRI has proved to be a very promising imaging technique for the early detection of renal parenchymal involvement in patients with febrile UTI.

S3.3.6

MULTIPARAMETRIC QUANTITATIVE RENAL MRI IN CHILDREN AND YOUNG ADULTS: COMPARISON BETWEEN HEALTHY PARTICIPANTS AND PATIENTS WITH CHRONIC KIDNEY DISEASE

JONATHAN Dillman, STEFANIE Benoit, DEEP Gandhi, PRASAD Devarajan, JEAN Tkach, ANDREW Trout
Cincinnati Children's Hospital Medical Center, Cincinnati, OH, USA

Purpose: To obtain normative multiparametric quantitative MRI data from the kidneys of healthy children and young adults, and to compare measurements between healthy children and patients with chronic kidney disease (CKD).

Methods: We recruited 20 pediatric/young adult healthy controls (median age=18.6 years [IQR: 14.9-22.9]) to undergo research quantitative MRI of the kidneys including T1 mapping, T2 mapping, MR elastography, and diffusion-weighted imaging. 12 patients with CKD (median age=17.8 years [IQR: 12.8-18.8]) were imaged using the same protocol. Clinical and laboratory data were obtained at the same visit, including serum creatinine (sCr), estimated glomerular filtration rate (eGFR), cystatin C, and urine protein/creatinine ratio (UPCR). Images were analyzed by a research scientist, blinded to clinical and laboratory data. Measurements were made in the upper, mid, and lower portions of the kidneys (cortex, medulla, and whole kidney) and averaged. Mann-Whitney U tests were used to compare continuous data between groups; Spearman correlation was used to assess bivariate associations.

Results: Healthy control subjects had a median eGFR of 112.3 ml/min/1.73 m² (IQR: 108.6-130.9) vs. 55.0 ml/min/m² (IQR: 32.0-76.1) for CKD patients ($p < 0.0001$). Whole kidney and cortical T1 values were higher in CKD patients vs. control subjects (1333 vs 1291 ms [$p = 0.018$] and 1212 vs 1137 ms [$p < 0.0001$]). There were no differences in renal T2 values or stiffness measurements between groups. Whole kidney, cortical, and medullary ADC values were lower in CKD patients vs. control subjects (e.g., whole kidney ADC 1.87 vs. 2.02 10⁻³ mm²/s [$p = 0.007$]). Whole kidney and cortical T1 measurements correlated with sCr, eGFR, cystatin C, and UPCR (e.g., cortical T1 vs. eGFR $\rho = -0.62$ [$p = 0.0003$]). Whole kidney, cortical, and medullary ADC values correlated with sCr, eGFR, and cystatin C (e.g., whole kidney ADC vs. cystatin C $\rho = -0.46$ [$p = 0.009$]).

Conclusion: Renal T1 and DWI ADC measurements significantly differ between healthy controls and patients with CKD and may be useful noninvasive biomarkers of pediatric CKD.

S3.3.7

COMPARISON OF DEEP LEARNING RECONSTRUCTION OF UNENHANCED CT FOR URINARY TRACT STONE DETECTION

SAMJHANA Thapaliya, ELANCHEZHIAN Somasundaram, SAMUEL Brady, CHRISTOPHER Anton, BRIAN Coley, ALEXANDER Towbin, JONATHAN Dillman, ANDREW Trout

Cincinnati Children's Hospital Medical Center Department of Radiology, Cincinnati, USA

Background: Deep learning Computed Tomography (CT) reconstruction (DLR) algorithms promise to improve image quality but their impact on diagnosis has not been studied. We aimed to study the impact of DLR on urinary tract stone detection.

Methods: This was a retrospective study involving post-hoc reconstruction of clinically acquired unenhanced abdomen/pelvis CT scans obtained to detect and characterize urinary tract calculi on a Canon Aquilion ONE/Genesis CT scanner. Images were reconstructed with six different, manufacturer standard DLR algorithms and reformatted in 3 planes (axial, sagittal, coronal). De-identified reconstructions were randomized and loaded into a research PACS as independent examinations for review by 3 blinded radiologists (R1, R2, R3) tasked with identifying and measuring all urinary tract stones. Intra-class correlation coefficients (ICC) and kappa (κ) statistics were used to quantify inter-agreement for total number of stones and largest stone diameter.

Results: CT data from 14 patients (mean age: 17.3±3.4 years, 5 males and 9 females, weight class: 31-70 kg (n=6), 71-100 kg (n=7), >100 kg (n=1)) were reconstructed as 84 total exams. Reported number of stones ranged from 0-10 and reported stones sizes ranged from 1-8 mm. Patient-level agreement between R1 and R3 for presence/absence of stones was near-perfect ($\kappa = 1$) for all algorithms. Agreement between R1 and R2 and R2 and R3 was substantial to near perfect ($\kappa = 0.71-1$) for all algorithms. ICCs for number of stones ranged from 0.73 to 0.90 and ICCs for largest stone size ranged from 0.85 to 0.96 for the 6 DLR algorithms. The body sharp standard algorithm provided the highest absolute ICC for both total number of stones (ICC=0.90) and largest stone size (ICC=0.96), although the 95% confidence intervals overlapped for all algorithms.

Conclusion:

Type of CT DLR algorithm appears to have a minor effect on the detection and characterization of genitourinary stone disease on non-contrast CT.

S3.3.8

ROLE OF ELASTOSONOGRAPHY IN THE MANAGEMENT OF POST-OPERATIVE UNDESCENDED TESTES IN CHILDREN

SILVIA Storer¹, COSTANZA Bruno¹, SIMONE Patanè², NICOLA Zampieri², STEFANIA Montemezzi¹, FRANCESCO Camoglio²
¹ Radiology Unit, Department of Pathology and Diagnostics, AOUI, Verona, ITALY
² Pediatric Surgery Unit, Department of Surgery, Dentistry, Pediatrics and Gynaecology, AOUI, Verona, ITALY

Undescended testes (UDT) is the most common genital malformation in male infants, encountered in about 33% of preterm and 2-8% of full-term boys.

Cryptorchidism can predispose to infertility and testicular cancer, so boys with persistent UDT at the 6th month of life should undergo orchiopexy by 12 months.

Progressive peritubular fibrosis and atrophy can delay germ cell development, due to improper environment. Elastography is a non-invasive method that can provide information regarding the histological properties of tissues by assessing stiffness.

The aim of our study was to compare the changes in elasticity and volume of UDT with the contralateral descended testis in order to assess differences that may reflect the histological condition. Strain elastography (SE) results were graded using a color-coded map from 1 (elastic tissue, A) up to 3 (stiffer tissue, B).

A total of 42 patients (age at surgery 7 months-8 years) with unilateral UDT that underwent orchiopexy in our Institution between January 2014 and September 2019 were included. Clinical examination evaluated the

position of both testes. Ultrasound and SE were performed to assess testicular volume and stiffness.

The mean testicular volume of post-operative UDT was 0.68 ml (95% IC 0.44–0.92 ml) and the mean volume of contralateral testes was 0.96 ml (95% IC 0.69–1.22 ml) ($p < 0.0001$, Wilcoxon).

The post-operative UDT group showed a higher stiffness than contralateral testis group ($p = 0.02$, Mann-Whitney). Among the UDT group, testes with a higher stiffness score demonstrated lower volumes ($p = 0.03$, Chi-square). Children that underwent orchiopexy after 24 months of age exhibited lower testicular volumes and a higher frequency of score 2–3 at SE than boys treated prior 24 months of age ($p < 0.05$, Fisher).

Postoperative UDT exhibited lower volume and increased stiffness than contralateral testes. Elastography can be used as a reliable tool in the follow up of post-operative UDT to assess indirect signs of histological damage that can precede morphological changes.

S3.4.1

RADIOGENOMICS PREDICTION OF MYCN STATUS IN NEUROBLASTOMA: A HYPOTHESIS GENERATING STUDY

PIER LUIGI Di Paolo¹, DAVIDE Curione¹, ANGELA Di Giannatale², JACOPO Lenkowitz³, ANTONIO Napolitano¹, FRANCO Locatelli², PAOLO Tomà¹, LUCA Boldrini³, AURORA Castellano², AURELIO Secinaro¹

¹ Bambino Gesù Children's Hospital IRCCS, Department of Imaging, Rome, ITALY

² Bambino Gesù Children's Hospital IRCCS, Department of Pediatric Onco-Hematology, Rome, ITALY

³ Fondazione Policlinico Universitario A. Gemelli IRCCS, Department of Radiology, Rome, ITALY

Introduction

MYCN amplification represents a powerful prognostic factor in neuroblastoma patients and may occasionally account for intratumoral heterogeneity.

We aimed to create a radiogenomics model correlating CT quantitative image features with MYCN amplification status in neuroblastoma patients and overall survival (OS).

Materials and Methods

Pre-therapy computed tomography (CT) scans were retrieved from OPBG institutional archive and gross tumor volumes were manually segmented by two pediatric radiologists using a dedicated segmentation platform (Eclipse, Varian Medical Systems).

Radiomics features have been extracted using the MODDICOM radiomics and advanced image analysis platform and later processed through dimensionality reduction/features selection approaches.

Logistic regression models have been developed for the considered outcome and the OS prediction obtained using the two selected radiomics features was then plotted with actual OS data.

Results

A total of 78 patients diagnosed with neuroblastoma were included in this retrospective study, with a MYCN amplified prevalence of 30% (24 pts) in the whole dataset.

232 radiomics features have been firstly extracted, divided as follows for the single feature classes: 20 statistical features, 14 morphological features, 198 texture features.

After the Boruta selection procedure, 8 features were selected and addressed to further analysis.

After Pearson correlation analysis, 2 features were lastly chosen: $F_stat.mean$ (mean of voxel intensity histogram, $p = 0.0082$) and $F_szm_2.5D.zsnu$ (zone size non-uniformity, $p = 0.038$).

Five-times repeated 3-fold cross-validation logistic regression models with the 2 selected features yielded a AUC value of 0.879 on the training and 0.865 on the testing set (prediction cut off = 0.3) for MYCN. No

statistical significant difference has been observed comparing radiomics predicted and actual OS data ($p = \text{not significant}$).

Conclusions

CT based radiomics appeared to be able to predict MYCN amplification status and OS in neuroblastoma, paving the way to the in depth analysis of imaging based biomarkers that could enhance outcomes prediction in disease.

S3.4.2

QUANTITATIVE CT TEXTURE FEATURES CAN NON-INVASIVELY PREDICT MYCN GENE AMPLIFICATION STATUS IN NEUROBLASTOMA

EELIN Tan¹, KHURSHID Merchant², SEYED EHSAN Saffari³, JOSEPH Zhao⁴, EDNA Aw¹, KENNETH Chang², PHUA HWEI Tang¹

¹ KK Womens and Childrens Hospital - Diagnostic and Interventional Imaging, Singapore, SINGAPORE

² KK Womens and Childrens Hospital - Department of Pathology and Laboratory Medicine, Singapore, SINGAPORE

³ Duke NUS Medical School - Centre for Quantitative Medicine, Singapore, SINGAPORE

⁴ National University of Singapore - Yong Loo Lin School of Medicine, Singapore, SINGAPORE

Introduction: MYCN oncogene amplification in neuroblastoma confers patients to the high-risk disease category for which prognosis is poor and more aggressive multimodal treatment is indicated. This study explores if quantitative tumour texture features on contrast-enhanced CT (CECT) can non-invasively predict MYCN gene status.

Methods: From 2009–2019, fifty consecutive patients treated for neuroblastoma at a tertiary paediatric hospital with pre-operative CECT and MYCN gene status were identified. MYCN amplification was positive in 16 tumours and negative in 34. Following manual whole tumour segmentation, 107 radiomic features were extracted. Feature selection was performed with univariate analysis, removal of highly correlated features and finally with a wrapper algorithm. Scan parameters (aortic enhancement, slice width, kV, mA, kernel, machine) were treated as potential confounding factors. Predictive accuracy of the machine learning algorithms was estimated with leave-one-out cross validation.

Results: None of the scan parameters were significantly associated with MYCN status. The final radiomics signature consisted of 3 texture features: “Busyness”, “Strength” and “MajorAxisLength”. The eXtreme Gradient Boosting (XGBoost) algorithm returned the highest area under the receiver operating characteristics curve (AUC) of 0.86 (95% confidence interval [CI], 0.74–0.98); at this threshold, sensitivity was 0.88 (95% CI, 0.64–0.97) and specificity was 0.79 (95% CI, 0.63–0.90).

Conclusion: The CT radiomics signature was able to reliably and non-invasively classify MYCN gene status. The main limitations of the study were small sample size which precluded data splitting and lack of a separate data set for external validation.

S3.4.3

VALIDATION OF LOW DOSE CHEST CT EQUIVALENT TO TWO TWO-VIEW CHEST RADIOGRAPHS FOR DETECTION OF LUNG NODULES

SAMJHANA Thapaliya¹, LEAH Gilligan², SAMUEL Brady¹, CHRISTOPHER Anton¹, MICHAEL Nasser¹, ERIC Crotty¹, JONATHAN Dillman¹, ANDREW Trout¹

¹ Cincinnati Children's Hospital Medical Center, Department of Radiology, Cincinnati, USA

² Northwestern University Feinberg School of Medicine; Department of Radiology, Chicago, USA

Background: Low dose (LD) chest computed tomography (CT) has potential applications in pediatric and young adult patients if diagnostic performance can be proven to be similar to routine CT.

Methods: This was an IRB approved prospective study of patients <21 years old undergoing chest CT for solid tumor staging or follow-up. Immediately following routine diagnostic CT (R-CT), a low dose chest CT (100 kVp, 25 mA, ~0.3 mSv effective dose) was acquired. The R-CT and LD-CT exams were de-identified and loaded to PACS for blinded review by 2 pediatric radiologists. Cohen's kappa statistics and intra-class correlation coefficients (ICC) were used to calculate interobserver and intra-observer (LD-CT vs. R-CT) agreement.

Results: 76 patients (44/32 M/F, mean 14.7±4 years) were enrolled. Depending on observer and CT technique, 22-38 patients were reported as having lung nodules. Nodules ranged in size from 1-105 mm.

Kappa statistics (95%CI) for intra-observer agreement regarding the presence of any nodule were 0.68 (0.52-0.85) and 0.68 (0.51-0.85) for R1 and R2. LD-CT had 76% sensitivity and 92% specificity for the presence of any nodule for R1 and 69% sensitivity and 96% specificity for R2.

For number of nodules and size of largest nodule, intra-observer ICCs (95%CI) were 0.95 (0.92-0.97) and 0.93 (0.89-0.96) for LD-CT and were 0.83 (0.74-0.89) and 0.63 (0.47-0.75) for R-CT for R1 and R2 respectively.

For interobserver agreement, kappa statistics (95%CI) were 0.55 (0.36-0.74) and 0.71(0.56-0.86) for the presence of any nodule on LD-CT and R-CT, respectively. For number of nodules and largest nodule, interobserver ICCs (95%CI) were 0.95 (0.92-0.97) and 0.85 (0.77-0.90) for LD-CT and 0.84 (0.76-0.90) and 0.32 (0.11-0.51) for R-CT.

Conclusion: A LD-CT equivalent to two chest radiographs has moderate sensitivity and high specificity for lung nodules with good intra-observer agreement to R-CT on number of nodules and size of largest nodule. Agreement between observers was only moderate for both LD-CT and R-CT.

S3.4.5

E-CIGARETTE OR VAPING PRODUCT USE ASSOCIATED LUNG INJURY (EVALI) IN ADOLESCENTS

JiHYUN Kang, BRANDON Lei, RYAN Webb, HANEEN Ali, AMI Gokli

Staten Island University Hospital, Staten Island, USA

Purpose: Since late 2019 there has been an emerging nationwide epidemic involving e-cigarette or vaping product use associated lung injury (EVALI), also known as vaping-associated pulmonary injury (VAPI), resulting in significant morbidity and mortality. Despite new reports and data continuing to surface in the literature, the pathophysiology of EVALI remains poorly understood. We discuss our experience from a large community-based hospital setting regarding clinical symptoms and imaging findings in pediatric patients with suspected EVALI, as well as review what is currently known in the literature about treatment and histopathology.

Materials and methods: Seventeen patients (ages 18-24, male = 14, female = 3) with acute pulmonary and/or gastrointestinal symptoms and associated radiographic or CT findings of EVALI were reviewed separately by two pediatric radiologists. Clinical and laboratory values were reviewed by two radiology residents via electronic medical records and discussions with the pulmonology team.

Results: Predominant presenting symptoms included cough (n = 10), shortness of breath (n = 10), chest pain (n = 10), abdominal pain (n = 3), nausea and vomiting (n = 8), diarrhea (n = 5) and fever (n = 6). Predominant radiographic findings included reticular or interstitial opacities with basilar predominance in nearly all cases. The most common CT

findings included central ground glass opacities and subpleural sparing (n = 12) with some patients presenting with interlobular septal thickening, reverse halo sign or pneumomediastinum. A slight majority of patients reported use of THC products (n = 11). These observations are concordant with current EVALI literature. A steroid taper was the most common treatment (n = 11), with antibiotics (n = 9), antihistamines (n = 3) and bronchodilators (n = 3) used in some cases.

Conclusion: The long-term sequelae and treatment of EVALI are still unknown. The radiologist is uniquely poised to play a central role in the diagnosis and characterization of EVALI.

S3.4.6

MR-EVALUATION OF WHITE MATTER AFTER THERAPY WITH HIGH-DOSE METHOTREXATE USING QUANTITATIVE T2 RELAXATION TIME AND ADC VALUES IN PEDIATRIC PATIENTS WITH LEUKEMIA

LUCIANA Porto, RAFAEL Willems

Goethe Frankfurt University, Frankfurt, GERMANY

Aim: To investigate the detectability of toxic leukoencephalopathies after therapy with high-dose methotrexate (MTX) using quantitative T2 relaxation time and ADC values.

Method: 9 children (between 6 and 17 years old), who were first diagnosed with ALL and received treatment with MTX as part of the AIEOP-BFM therapy study without radiation therapy, were evaluated. MRI scan was performed before starting the induction therapy and after completing the high-dose therapy. CNS-manifestation was ruled out in all patients. Quantitative T2 relaxation time and ADC values were compared to conventional imaging using MP-RAGE and TIRM sequences in voxel-based ROI analyzes.

Results: In all but one of the 9 examined patients no significant white matter changes after therapy with methotrexate could be detected. The one patient in question showed also new white matter changes on conventional sequences after completing the high-dose therapy.

Conclusion: A significant increase of the T2 relaxation time after completing the high-dose therapy MTX could only be measured in one of the 9 patients. We assume that the presence of white matter changes in this patient was a single event due probably to an underlying predisposition. Collective evaluation showed no statistical significance. However, further studies with a larger number of subjects should be carried out for a more detailed investigation.

S3.4.7

EXTERNAL VALIDATION OF THE 2017 CHILDREN'S HEPATIC TUMORS INTERNATIONAL COLLABORATION-HEPATOBLASTOMA STRATIFICATION (CHIC-HS) SYSTEM IN PATIENTS WITH HEPATOBLASTOMA

PYEONG HWA Kim¹, HEE MANG Yoon¹, HYUN JOO Shin², AH YOUNG Jung¹, YOUNG AH Cho¹, JIN SEONG Lee¹

¹ Asan Medical Center, Seoul, SOUTH KOREA

² Severance Children's Hospital, Seoul, SOUTH KOREA

Purpose: In 2017, Children's Hepatic tumors International Collaboration-Hepatoblastoma Stratification (CHIC-HS) system was introduced. We aimed to externally validate CHIC-HS system, and to develop a simplified novel risk stratification system.

Materials and Methods: This bi-center retrospective study included consecutive pediatric patients with histopathologically confirmed hepatoblastoma. We compared EFS between four risk groups according to CHIC-HS system. Associated factors of EFS were explored. Classification and regression tree (CART) analysis was used to develop

the novel risk stratification systems and optimism-corrected C-statistics were compared with CHIC-HS system.

Results: 129 patients (mean age, 2.6±3.3 years; female:male, 63:66) were included. 5-year EFS in very low, low, intermediate, and high-risk group according to CHIC-HS system were 90.0%, 82.8%, 73.5%, and 51.3%, respectively. Age group, PRETEXT stage, and presence of metastasis were independently associated with EFS. CART analysis separated patients into four strata (model I; very low, absence of metastasis & age younger than 8; low, presence of metastasis & PRETEXT I or II; intermediate, absence of metastasis & age of 8 or older; high, presence of metastasis & PRETEXT III or IV). In the model II, intermediate and low risk category in the model I were integrated. Optimism-corrected C index of CHIC-HS, model I, and model II were comparable to be 0.644 (95% CI, 0.561–0.727), 0.671 (95% CI, 0.587–0.755), and 0.682 (95% CI, 0.598–0.766), respectively.

Conclusions: CHIC-HS system demonstrated significant association with EFS. Our simplified risk stratification systems using age, PRETEXT stage, and presence of metastasis showed the comparable performance. Large-scale prospective studies may be required for further validation.

S34:4

VIRTUAL SURGICAL PLANNING AND PATIENT-SPECIFIC 3D-PRINTED MODELS FROM MULTIMODAL IMAGING FOR IMPROVED OUTCOMES IN PEDIATRIC ORTHOPEDIC TUMOR RESECTION

JAYANTHI Parthasarathy, MITCHELL Rees, BHAVANI Selvaraj, THOMAS Scharschmidt

Nationwide Children's hospital, Columbus, USA

Purpose: We evaluated the early surgical outcomes of multimodal imaging derived virtual surgical planning (VSP) and patient-specific 3D-printed models (3DPM) in pediatric orthopedic tumor resection and reconstruction.

Materials and Methods: After IRB approval, 10 patients with Ewing's sarcoma or osteosarcoma were chosen for the study. CT and contrast-enhanced MR imaging were acquired as standard of care. Bony and soft tissue components of the tumor and the adjacent bone were derived and a 3D model of the region was created. VSP was performed on the computer-generated 3D model with the surgeon and radiologist as part of the team. Patient specific (preprint) model with the planned osteotomies was created and printed on an Objet 350TM Stratasys polyjet printer. The 3DPM was used by the surgeon for presurgical planning, intraoperative reference and for family education. Reconstruction was performed with osseous or soft free flaps, allografts, or metallic implants. Clinical impact, was assessed by the surgeon in a survey, rating the model utility for preoperative planning, patient/family education, intraoperative guidance of the 3DP model and the accuracy of its representation of his intraoperative findings on a Likert scale of 1-5. 3DPM accuracy was assessed by comparing the 3DPM with the preprint model as a surface contour map and histogram.

Maximum length of the resected tumor was measured from the pathological specimen and compared with that of 3DP model in the cranio-caudal direction.

Results: In all the cases the surgeon strongly agreed the model helped in preop planning and intra operative orientation and could reduce surgical time. Average surface contour difference between the preprint model and 3DPM was -0.18 +/- 0.28mm. An average difference of 4 +/- 2mm (5 +/- 3%) was found between the resected tumor and the printed model.

Conclusion: VSP produced patient-specific 3DPM accurately represented the patients' tumor and proved very useful to the orthopedic oncologic

surgeon caring for these children, in the preoperative and operative phases.

S34:8

DIRECT CORRELATION OF MRI WITH HISTOPATHOLOGY IN PEDIATRIC RENAL TUMORS THROUGH THE USE OF A PATIENT-SPECIFIC 3D-PRINTED CUTTING GUIDE: A PILOT STUDY

JUSTINE N. van der Beek^{1,2}, MATTHIJS Fitski³, RONALD R. de Krijger^{1,4}, MARC H.W.A. Wijnen³, MARRY M. van den Heuvel-Eibrink¹, ALIDA F.W. van der Steeg³, ANNEMIEKE S. Littooi^{1,2}

¹ Princess Máxima Center for Pediatric Oncology, Utrecht, THE NETHERLANDS

² Department of Radiology and Nuclear Medicine, University Medical Center Utrecht/Wilhelmina Children's Hospital, Utrecht, THE NETHERLANDS

³ Department of Pediatric Surgery, Princess Máxima Center for Pediatric Oncology, Utrecht, THE NETHERLANDS

⁴ Department of Pathology, University Medical Center Utrecht, Utrecht, THE NETHERLANDS

Purpose: In pediatric renal tumors there is no histopathological assessment until after surgery. Imaging could play a crucial role in the pre-operative characterization of renal tumor types. Direct correlation of radiology and pathology could reveal imaging features in these frequently highly heterogeneous lesions. With this pilot study the feasibility of a patient-specific 3D-printed cutting guide is investigated to ensure corresponding orientation between magnetic resonance imaging (MRI) and histopathology.

Materials and Methods: Based on the preoperative MRI-scan prior to total nephrectomy, a 3D-model of the kidney and tumor was manually developed in 3D Slicer. This allowed us to create a cutting guide enabling an MRI-orientated transversal slicing of the specimen. The pathologist used the cutting guide for gross dissection of the specimen, ensuring macroscopic slices of 5 millimeters each. The feasibility of this technique was determined using structured measurements including overlap calculation with the dice similarity coefficient and qualitatively through questionnaires among involved experts.

Results: In this pilot, the cutting guide has been applied to five Wilms tumor patients. Their median age at diagnosis was 50 months (range 4-100 months). Digital correlation in a total of 20 slices resulted in a median dice similarity coefficient of 0.91 (range 0.76-0.94). The positioning and slicing of the specimen was overall rated as 'easy' and the median macroscopic slice thickness of each specimen ranged from 5-6 millimeters. Tumor consistency strongly influenced the practical application of the cutting guide.

Conclusions: A patient-specific 3D-printed cutting guide seems to provide a feasible tool for the direct correlation of MRI and histopathology of pediatric renal tumors. The clinical implementation and design of the cutting guide are currently optimized, to ensure a methodological workflow for future prospective studies.

S4.1.1

GENETIC, CLINICAL, AND IMAGING PREDICTORS OF ATAXIA IN PEDIATRIC PRIMARY MITOCHONDRIAL DISORDERS

LUIS OCTAVIO Tierradentro-García¹, JUAN SEBASTIAN Martin-Saavedra^{1,2,3}, SARA REIS Teixeira¹, CESAR AUGUSTO Alves¹, FABRÍCIO Gonçalves¹, MARTIN Kidd⁴, COLLEEN Muraresku⁵, AMY Goldstein^{5,6}, ARASTOO Vossough^{1,7}

¹ Division of Neuroradiology, Department of Radiology, Children's Hospital of Philadelphia, Philadelphia, USA

² Department of Pediatrics, St. Christopher's Hospital for Children, Philadelphia, USA

³ Clinical Research Group, Escuela de Medicina y Ciencias de la Salud, Universidad del Rosario, Bogota, COLOMBIA

⁴ Central for Statistical Consultation, Stellenbosch University, Stellenbosch, SOUTH AFRICA

⁵ Mitochondrial Medicine Frontier Program, Division of Human Genetics, Department of Pediatrics, CHOP, Philadelphia, USA

⁶ Department of Pediatrics, University of Pennsylvania Perelman School of Medicine, Philadelphia, USA

⁷ Department of Radiology, University of Pennsylvania Perelman School of Medicine, Philadelphia, USA

Purpose: Evaluation of ataxia in children is challenging in clinical practice. This is particularly true for highly heterogeneous conditions such as primary mitochondrial disorders (PMD). In this study, we aim to explore cerebellar and brain abnormalities identified on MRI as potential predictors of ataxia in patients with PMD. Likewise, we aim to determine the effect of the patient's genetic profile on these predictors as well as the establishment of the temporal relationship of clinical ataxia with MRI findings.

Methods: We evaluated clinical, radiological, and genetic characteristics of 111 PMD patients younger than 21 years of age at our institution. Clinical and genetic data were extracted from patient charts. The Scale for the Assessment and Rating of Ataxia (SARA) was used to define ataxia in our cohort. Imaging studies were reviewed by two neuroradiologists blinded to clinical history and genetic diagnosis. A third senior neuroradiologist was consulted in case of disagreement and results were collated by final consensus. Cerebellar atrophy was considered if any of the following was identified: abnormally deep or wide sulci, or thin cerebellar folia in the cerebellar hemispheres and/or vermis. Signal abnormality was categorized topographically in the dentate nuclei, white matter, or cerebellar peduncles; other brain structures were also evaluated. Multivariate logistic regression and generalized estimating equations were used for analysis.

Results: Ataxia was identified in 41% of patients. Cerebellar atrophy or putaminal involvement with mitochondrial DNA (mtDNA) mutations (OR 1.18, 95% CI 1.1-1.3, $p < 0.001$), and on the other hand, nuclear DNA mutation without atrophy of the cerebellum (OR 1.14, 95% CI 1.0-1.3, $p = 0.007$) were associated with and predicted an increased likelihood of having ataxia per year of age. Central tegmental tract predicted the presence of ataxia independent of age and pathogenic variant origin (OR 9.8, 95% CI 2-74, $p = 0.009$). Ataxia tended to precede the imaging finding of cerebellar atrophy.

Conclusions: Cerebellar atrophy and putaminal involvement on MRI of pediatric-onset PMD may predict the presence of ataxia with age in patients with mtDNA mutations. This was not the case for nuclear DNA mutations. This study provides predicted probabilities of having ataxia per year of age, which may help in family counseling and future research of this population.

S4.1.2

WIDENING THE NEUROIMAGING FEATURES OF ADENOSINE DEAMINASE 2 DEFICIENCY

ANA Geraldo¹, ROBERTA Caorsi², DOMENICO Tortora³, CARLO Gandolfo⁴, ROSA Ammendola³, MARIA Alessio⁵, GIOVANNI Conti⁶, ANTONELLA Insalaco⁷, SERENA Pastore⁸, SILVANA Martino⁹, ISABELLA Ceccherini¹⁰, SARA Signa², MARCO Gattorno², ANDREA Rossi¹, MARIASAVINA Severino¹

¹ Diagnostic Neuroradiology Unit, Centro Hospitalar Vila Nova de Gaia/Espinho EPE, Vila Nova de Gaia, PORTUGAL

² Center for Autoinflammatory diseases and Immunodeficiencies, IRCCS Istituto Giannina Gaslini, Genoa, ITALY

³ Neuroradiology Unit, IRCCS Istituto Giannina Gaslini, Genoa, ITALY

⁴ Interventional Unit, IRCCS Istituto Giannina Gaslini, Genoa, ITALY

⁵ Department of Translational Medical Sciences Federico II University of Naples, Naples, ITALY

⁶ Pediatric Nephrology and Rheumatology Unit, AOU G Martino, Messina, ITALY

⁷ Division of Rheumatology, IRCCS Ospedale Pediatrico Bambino Gesù, Rome, ITALY

⁸ Department of Pediatrics, Institute for Maternal and Child Health - IRCCS Burlo Garofolo, Trieste, ITALY

⁹ Division of Pediatric Immunology and Rheumatology, Department of Public Health and Pediatrics, Regina Margherita Childre, Turin, ITALY

¹⁰ UOSD Genetics and Genomics of Rare Diseases, IRCCS Istituto Giannina Gaslini, Genoa, ITALY

Introduction: Adenosine deaminase 2 deficiency (OMIM #615688) is an autosomal recessive disorder characterized by a wide clinical spectrum, including small- and medium-sized vessel vasculopathies, but data focusing on the associated neuroimaging features are still scarce in the literature.

Materials and Methods: Review of imaging, clinical and genetic findings of patients with with genetic-proven adenosine deaminase 2 deficiency identified in 6 Italian observed between 2014 and 2019 in six Italian hospitals.

Results: Twelve patients (6 males, median age at disease onset and at genetic diagnosis 1.3 and 15.5 years, respectively) were included. Neuroimaging review demonstrated multiple ($n = 9/12$), frequently recurrent brain lacunar ischemic and/or hemorrhagic strokes ($n = 2/12$), spinal infarcts ($n = 1/12$), and intracranial aneurysms ($n = 1/12$), but also new phenotypes characterized by cerebral microbleeds ($n = 3/12$) and a peculiar, likely inflammatory, perivascular tissue in the basal and peripontine cisterns ($n = 3/12$).

Discussion/Conclusion: Together with early clinical onset, positive family history, inflammatory flares and systemic abnormalities, these imaging findings should raise the suspicion of adenosine deaminase 2 deficiency, thus prompting genetic evaluation and institution of TNF inhibitors, with a potential great impact on neurological outcome.

S4.1.3

SWALLOWING DIFFICULTIES AND BREATHING DIFFICULTIES IN CHILDREN WITH SPINA BIFIDA- ARE THESE A COMPLICATION OF COMPRESSION AT THE FORAMEN MAGNUM OR OF DYSPLASTIC BRAIN DEVELOPMENT?

MATYLYDA Sheehan¹, FIONA Healy², AOIBHINN Walsh², IRWIN Gill², JANE Leonard², KIERON Sweeney³, STEPHANIE Ryan¹

¹ Children's Health Ireland at Temple Street, Dept of Radiology, Dublin, IRELAND

² Children's Health Ireland at Temple Street, Dept of Paediatrics, Dublin, IRELAND

³ Children's Health Ireland at Temple Street, Dept of Neurosurgery, Dublin, IRELAND

PURPOSE: The pathogenesis of swallowing difficulties and sleep disordered breathing (SDB) in children with spina bifida is not fully understood. Brainstem herniation and compression in the upper cervical spinal canal is considered a major etiological factor. Surgical management is focused on this hypothesis. Feeding and breathing difficulties may however be secondary to dysplastic brain development rather than brain stem compression alone. We aimed to correlate feeding and breathing complications in children with spina

bifida with the MRI findings of hindbrain compression and MRI findings of dysplastic development to evaluate their relative role.

MATERIALS AND METHODS: In our National Centre for Care of Children with Spina Bifida, all children with spina bifida who underwent videofluoroscopic swallowing studies (VFSS) over a 10-year period and those with confirmed or suspected SDB were identified. We compared the MRI findings of these patients with a control group of spina bifida patients without feeding or breathing difficulties.

RESULTS: MRI scans of 64 children with spina bifida and VFSS studies of 23 of these, were reviewed. 39 children who had SDB +/- swallowing abnormalities formed the symptomatic group and 25 without SDB or VFSS abnormalities formed the control group.

When MRIs of symptomatic children are compared with those of controls, cerebellar volume was significantly smaller ($p=0.001$), the fourth ventricle was significantly more likely to be slit like ($p=0.04$), the CSF space at the foramen magnum was significantly more likely to be effaced ($p=0.029$) and the mean extent of vermian herniation was greater ($p=0.008$) in the symptomatic children.

Of the brain malformations remote from the brain stem, the presence of stenogryria was significantly commoner in symptomatic patients than in the control group ($p=0.001$). There was also more periventricular nodular heterotopia (PVNH) and more abnormalities of the corpus callosum in symptomatic patients, but this did not reach statistical significance.

CONCLUSIONS: Among children with spina bifida, those with feeding difficulties +/- SDB are more likely to have smaller posterior fossa structures and more hindbrain compression than those who are asymptomatic. They are, however, also more likely to have markers of brain dysplasia. The pathogenesis of feeding difficulties and SDB is likely to be multifactorial and may not respond to treatment focused solely on reducing pressure on the brain stem.

S4.1.4

KRABBE DISEASE AND METACHROMATIC LEUKODYSTROPHY: COMPARISON OF INITIAL MRI FINDINGS FOR DIFFERENTIAL DIAGNOSIS

YOUNGHUN Choi¹, SEULBI Lee¹, SEUNGHYUN Lee¹, YEON JIN Cho¹, JUNG-EUN Cheon¹, WOO SUN Kim¹, JAE-YEON Hwang²

¹ Seoul National University Children's Hospital, Seoul, SOUTH KOREA

² Pusan National University Yangsan Hospital, Seoul, SOUTH KOREA

Objective

The purpose of this study was to identify characteristic MRI features for differentiation between Krabbe disease (KD) and metachromatic leukodystrophy (MLD) in young children.

Methods

After searching electronic medical charts between October 2004 and September 2020 to identify confirmed cases of KD and MLD, 11 children with KD and 13 with MLD with available initial MR images were included in the study. The MRI images at initial presentation were retrospectively reviewed for the following parameters: extent of white matter signal abnormality and volume change, presence of Tigroid sign, presence of volume decrease and signal alteration in the thalamus, presence of optic nerve hypertrophy.

Results

The two patient groups did not differ significantly in age and symptoms at onset. KD showed T2-high signal in the internal capsule and brainstem more frequently than MLD (internal capsule, 82% in KD, 31% in MLD, $p=0.012$; midbrain, 45% in KD, 0% in MLD, $p=0.011$; pons, 55% in KD, 0% in MLD, $p=0.003$). T2-high signal intensities in the splenium and genu of the corpus callosum were noted in 45% and 0% in KD while 92% and 77% in MLD ($p=0.023$ and <0.001 , respectively). Volume decrease in the involved area of the corpus callosum was more frequently observed in KD than MLD (36% in KD, 0% in MLD, $p=0.031$) Volume loss in the

thalamus was also more frequently noted in KD (55% in KD, 8% in MLD, $p=0.023$). Other MR findings, including Tigroid sign showed no significant difference between two group (Tigroid sign, 45% in KD, 62% in MLD, $p=0.431$)

Conclusion

Signal abnormalities in the internal capsule and brainstem, decreased thalamus volume, decreased splenial volume accompanied by signal changes, absence of signal changes in the callosal genu portion were MRI findings suggesting KD rather than MLD at initial MRI. Other MR findings such as Tigroid sign did not help with differential diagnosis.

S4.1.5

CORPUS CALLOSUM THICKNESS IN NF1 AND ITS CORRELATION WITH COGNITIVE, DEVELOPMENTAL, INTELLECTUAL ASSESSMENT, AUTISM SPECTRUM, AND ADHD

MONICA Miranda Schaeubinger, LUIS Tierradentro Garcia, JORGE Kim, CESAR Alves, SAVVAS Andronikou

Children's Hospital of Philadelphia, Department of Radiology, Philadelphia, USA

Purpose: A number of neurological disorders are associated with Neurofibromatosis type I (NF1). Studies seeking to establish associations between these and brain characteristics lack sufficient sample sizes for robust statistical conclusions. Thickened corpus callosum (CC) is a known feature of NF1. We explored CC thickness and its association with cognitive, learning and developmental disorders, intellectual assessment, autism spectrum disorder (ASD) and attention-deficit/hyperactivity (ADHD).

Materials and Methods: CC thickness of NF1 patients aged 1 to 15 years was retrospectively measured from midline T1 sagittal MR images using a customized semi-automated MATLAB tool. Thickness at each location was compared to age-appropriate reference standards. Patient demographics and clinical evaluations were obtained from the electronic medical record. Mann-Whitney tests were used to compare the CC thickness at the level of the genu, body, isthmus, and splenium with different evaluation parameters.

Results: Ninety patients were included (median age 7 [5-7 IQR], 48 female [53.3%]). CC median thickness at all locations was significantly thicker than reference standards, except for the body in infancy and the splenium in early adolescence. Notable differences in CC thickness were found at the isthmus in infancy (1.9 mm median difference, p value = 0.037), splenium in infancy (3.1 mm median difference, p value = 0.037) and early childhood (1.7 mm median difference, p value = 0.003), and genu in infancy (3.9 mm median difference, p value = 0.037). Eleven children (12.2%) had ASD, and 38 (42.2%) ADHD; of these, 6 children (6.7%) had both ASD and ADHD. Median CC thickness was significantly larger at the genu ($p=0.005$) and body ($p=0.005$) in children with learning disorders; and at the body in children with behavioral or cognitive disorders ($p=0.07$) and those with global cognitive delay ($p=0.044$). Median isthmus was thicker in children with ADHD ($p=0.008$).

Conclusion: Semi-automated evaluation of CC thickness demonstrated thicker CC median values than published reference standards. The CC was significantly thicker in patients with learning disorders, behavioral or cognitive development disorders, and ADHD. Further studies with larger sample sizes, longitudinal assessments, and control comparison could expound the relationship between CC thickness and these disorders in children with NF1.

S4.1.6

CERVICAL INTERNAL CAROTID ARTERIOPATHY IN CHILDREN WITH SICKLE CELL ANEMIA. TEN-YEAR

FOLLOW-UP

SUZANNE Verlhac¹, ALEXANDRA Ntorkou¹, GHISLAINE Ithier², CAMELIA Oloukoi¹, MARIANE Alison¹

¹ Pediatric Imaging Department, Robert Debre Hospital, APHP, Paris, FRANCE

² Referral center for sickle cell disease, Robert Debre Hospital, APHP, Paris, FRANCE

Purpose: SCA arteriopathy is not limited to the Willis-circle, but also affects the cervical ICA. It can be detected by Doppler-US via submandibular approach. We previously showed that an acceleration of flow in cICA is associated with a MRA-depicted stenosis. The aim of this work is to retrospectively evaluate the outcome of cICA abnormalities.

Material: SCA patients with abnormal velocity in a cICA and concomitant MRA and at least 1-year follow-up. Kinkings, location and severity of stenoses were collected.

Results: 54 patients, median age 5.2 years (1.6–17.1) at inclusion, median follow-up 5.3 years (1.1–9.3). Right ICA was affected in 16 patients, left ICA in 15 patients and both in 17 patients (65 stenoses). 58 stenoses (89%) were located in the middle third of the artery length, 4 (6%) were proximal, 2 (3%) distal and 1 artery was occluded. 43/58 middle-third-stenoses were associated with kinking. Patients were treated by chronic transfusions and/or hydroxyurea according to their condition. At the last assessment, 25 patients (46%) still had abnormal velocity and angiography was still abnormal in 39 patients (72%). Improvement of arterial stenosis occurred in 18 patients with reduction of kinking in 11 patients, worsening of stenosis in 11 patients with occlusion in 3 patients all with proximal web-like stenosis, despite chronic transfusions.

Conclusions: This study confirms the severity of cICA stenoses related to SCA, which can lead to occlusion. Moreover, we confirm the association between stenosis and kinking. The etiology of kinking is probably both congenital and acquired. Remodeling of the ICA could be related to hemodynamic disturbances with high blood flow due to chronic anemia as shown by recent animal models studies. Extensive screening for cerebral arteriopathy in SCA children including cICA should improve stroke prevention.

S4.2.1

MULTI-INSTITUTIONAL SPR-VENDOR COLLABORATION FOR PEDIATRIC FREE-BREATHING ABDOMINAL MRI PROTOCOL OPTIMIZATION

CARA Morin¹, VIBHAS Deshpande², LINDSAY Griffin³, PEDRO Itriago Leon², BRIAN Dale², SHERWIN Chan⁴, GOVIND Chavhan⁵, MICHAEL Gee⁶, SURAJ Serai⁷, SUSAN Sotardi⁷, TERESA Victoria⁷, MICHAEL Moore⁸

¹ St. Jude Childrens Research Hospital, Memphis, USA

² Siemens Healthineers, Malvern, USA

³ Ann & Robert H Lurie Childrens Hospital of Chicago, Chicago, USA

⁴ Childrens Mercy Hospital, Kansas City, USA

⁵ Hospital for Sick Children, University of Toronto, Toronto, CANADA

⁶ Mass General Hospital/Harvard Medical School, Boston, USA

⁷ Childrens Hospital of Philadelphia, Philadelphia, USA

⁸ Penn State Children's Hospital, Hershey, USA

Motion mitigation is a crucial challenge in pediatric MRI. Motion reduction techniques such as radial acquisition and compressed-sensing can improve image quality. Pediatric radiologists from the Society of Pediatric Radiology MRI committee collaborated with an MRI vendor to test a free-breathing (FB) abdominal MRI protocol for children, including 4 age-groups and 7 sequences, including PDFF/R2*, T1 and T2 mapping, DWI, elastography, and dynamic post-contrast T1. Iterative feedback is provided for works-in-progress (WIPs) optimization.

We pilot-tested the process with two WIPs for fat/iron quantification (WIP963, breath-held cartesian and WIP991, FB radial) in 45 patients (age 5 - 26 years, mean 14.7 years) at a single institution. Eight pediatric radiologists reviewed the sequences side-by-side, comparing them to the routine product sequence. Radiologists judged if images were “diagnostic” or “non-diagnostic” based on clinical judgment, scored artifacts from 1 to 5 (lower score for better quality), and indicated which sequence they preferred. Ratings were compared using logistic regression and a mixed-effects linear model.

The frequency of non-diagnostic rating was not significantly different between WIPs; 12.0% for WIP963, 95% CI [8.9, 15.6%] and 10.7% for WIP991, 95% CI [7.2, 14.9%] (p=0.608). Mean artifact scores were 2.6 for WIP991 (IQR 2-3), 2.9 for WIP963 (IQR 2-4), and 3.9 for product (IQR 3-5) (p<0.001). Compared to product, WIP991 reduced artifact levels by -1.37, 95% CI [-1.50, -1.24] and WIP963 by -0.98, 95% CI [-1.09, -0.87]. Both WIPs were preferred over product (p<0.001). WIP 963 had the fastest acquisition time (21.7 s, 95% CI [13.3 s, 30.0 s]), significantly faster than product (p<0.001).

Results will be used to optimize WIPs, decreasing non-diagnostic rates and making sequences shorter. The vendor - multi-institutional collaboration will be used to create a robust protocol that is ready for use in pediatric practice without the site-specific optimization often required to make adult-specific sequences work for children.

S4.2.2

SURVEY OF PEDIATRIC RADIOLOGY DEPARTMENTS REGARDING THE USE OF RAPID MRI FOR ABDOMINAL PAIN

PINAR Karakas Rothey¹, GOVIND Chavhan², TAYLOR Chung¹, CARA Morin³, LARA Farras², SUBRAMANIAN Subramanian⁴, SUMMER Kaplan⁵, JAMES Brian⁶, MICHAEL Aquino⁷

¹ UCSF Benioff Childrens Hospital Oakland, Oakland, CA, USA

² The Hospital for Sick Children, Toronto, CANADA

³ St. Jude Hospital, Memphis, TN, USA

⁴ UPMC Children's Hospital of Pittsburgh, Pittsburgh, PA, USA

⁵ Childrens Hospital of Philadelphia, Philadelphia, USA

⁶ Penn State Hershey Medical Center, Hershey, PA, USA

⁷ Cleveland Clinic, Cleveland, OH, USA

Purpose

To survey pediatric radiology departments regarding the use of rapid MRI (RMR) for abdominal pain in the emergency department (ED) or urgent care setting to assess practice specifics and protocols.

Materials and Methods

A survey was developed by the Society for Pediatric Radiology (SPR) MR and Trauma & ER Imaging Committees and distributed via email to SPR members. Respondents were requested to coordinate to provide a single response from each institution. Respondents were contacted to obtain consensus responses if multiple surveys were submitted from the same institution.

Results

80 surveys were received representing 65 institutions. 11 institutions had multiple respondents comprising 26/80 surveys for which consensus responses were obtained.

38.4% (25/65) of institutions reported utilizing RMR to evaluate pediatric abdominal pain in the ED and urgent care. Of these, 60.0% (15/25) had 24/7 in-house MRI technologists, and 40.0% (10/25) had MRI technologists available via pager.

Most institutions provide a preliminary report by trainees 60.0% (15/25). Preliminary reports were produced by an attending in 8.0% (2/25), and by contracted nighthawk in 12.0% (3/25). 56.0% (14/25) of institutions provided finalized reports by an attending, and 12.0% (3/25) by internal nighthawk.

Of the 19 institutions that detailed RMR practice specifics, 10.5% (2/19) had immediate access to the magnet that serves the ED or urgent care. Estimated wait times for magnet access for RMR cases in the remaining institutions was ½-1 hour in 31.5% (6/19), >1-2 hours in 47.3% (9/19), and >2-3 hours in 10.5% (2/19).

Exams most commonly were reported to take 10-19 minutes (78.9%, 15/19). The exam was reported to take <10 minutes at 2 institutions (10.5%, 2/19), and >19 minutes in the remaining 2 institutions (10.5%, 2/19).

The most commonly utilized sequences were axial and coronal T2W SS SE (both 94.7%, 18/19), the majority of which were acquired with and without fat-saturation (66.7%, 12/18). The next most utilized sequence was axial diffusion imaging (57.8%, 11/19).

Most institutions did not administer IV contrast (84.2%, 16/19).

Conclusion:

RMR for the evaluation of pediatric abdominal pain in the ED and urgent care is utilized by 38.4% of respondent institutions with the majority having 24/7 in-house MRI technologists. Protocols predominantly take less than 19 minutes, most commonly utilize T2W SS SE sequences with and without fat saturation, and rarely use gadolinium.

S4.2.3

SHEAR WAVE ELASTOGRAPHY HAS POTENTIAL TO CLASSIFY NON-FIBROTIC LIVER TISSUE IN CHILDREN WITH SUSPECTED OR ESTABLISHED LIVER DISEASE NON-INVASIVELY: A PROSPECTIVE STUDY WITH HISTOLOGIC CORRELATION

HANNA Hebelka¹, CHARLOTTE De Lange¹, HÅKAN Boström¹, JENNY Ahlin¹, MELA Brink¹, NILS Ekvall³, KERSTIN Lagerstrand²

¹ Institute of Clinical Sciences, Sahlgrenska Academy, University of Gothenburg, Dept. of Pediatric Radiology, Gothenburg, SWEDEN

² Institute of Clinical Sciences, Sahlgrenska Academy, University of Gothenburg, Dept. of Medical Physics and Techniques, Gothenburg, SWEDEN

³ Institute of Clinical Sciences, Sahlgrenska Academy, University of Gothenburg, Dept. of Pediatric Medicine, Gothenburg, SWEDEN

Purpose

To reduce the need for biopsy in children with chronic liver disease, non-invasive methods for detection of liver fibrosis are warranted. Ultrasound shear-wave elastography (SWE) is a promising tool to distinguish between no/mild and moderate/severe fibrosis in children but the diagnostic performance needs to be validated prospectively. This prospective study aimed to evaluate the diagnostic performance of SWE and to determine cutoff-value for non-fibrotic tissue in children with suspected or established liver disease.

Materials&Methods

In 90 consecutive patients (0-18years), two-dimensional SWE was performed during anesthesia and free breathing. Liver stiffness, estimated with SWE, was measured (median of 10 registrations) and followed by a percutaneous biopsy from the corresponding area. Fibrosis severity was scored according to the Batts&Ludwig classification (grade 0-4=F0-F4). If the biopsy scoring included more than one grade of fibrosis, the highest grade was registered. SWE-values (kPa) were compared to both histology and hepatic serological markers.

Results

Four patients with interquartile range/median>30%kPa were excluded. Remaining 86 children (59% males) had mean age=10.2years (range:0.1-18). SWE-values within each fibrosis grade are displayed in Table1. Overall, SWE-values were different between fibrosis grades (p<.0001). The receiver operating characteristic area for differentiation of F0-1 from F2-4 was 0.77(95% CI:0.67-0.87). A cutoff SWE-value of 4.5kPa yielded 90% sensitivity and 68% specificity to classify F0-1. Out of the 18 children (21%) with SWE-value<=4.5kPa, 12 had grade F0-1 and 6 had F2 (steatosis n=2/auto-immune-hepatitis n=1/hepatitisB n=1/transplants n=2). No correlation was

found to hepatic serological markers. Intra-class correlation coefficient for both intra- and interobserver was 0.96.

Conclusion

With free breathing, SWE can robustly distinguish no/mild from moderate/severe fibrosis in children with suspected/established liver disease with good sensitivity and specificity. Results imply that biopsy could potentially be re-considered in up to 20% of cases. It remains to evaluate if the diagnostic performance could be improved by including ultrasound exam, laboratory findings, age and long-time follow up.

S4.2.4

IMPACT OF PREOPERATIVE CT-BASED BODY METRICS ON POSTOPERATIVE COMPLICATIONS IN PEDIATRIC LIVER TRANSPLANT RECIPIENTS

MARTIJN Verhagen¹, STEF Levolger¹, JAN BINNE Hulshoff¹, MAUREEN Werner², HUBERT van der Doef³, ALAIN Viddeleer¹, RUBEN de Kleine², ROBBERT de Haas¹

¹ UMCG, Department of radiology, Groningen, THE NETHERLANDS

² UMCG, Department of hepatobiliary surgery, Groningen, THE NETHERLANDS

³ UMCG, Department of pediatric gastroenterology, Groningen, THE NETHERLANDS

Background:

Computed tomography (CT) derived body metrics such as skeletal muscle index (SMI), psoas muscle index (PMI), and subcutaneous fat index (ScFI) are considered measurable components of sarcopenia, frailty, and nutrition. This study aimed to determine the relation between preoperative CT-based body metrics and postoperative short-term clinical outcomes in pediatric liver transplant (LT) recipients.

Methods:

Patients aged 0-18 years who underwent a primary LT in a national pediatric liver transplantation center in The Netherlands were retrospectively included (n=117, median age 0.6 years, range 0.2-17.1). SMI, PMI, and ScFI were derived from preoperative axial CT slices. Postoperative outcomes and complications within 90 days were correlated with the CT-based body metrics. To classify postoperative infections the Clavien-Dindo (CD) classification was used. Subgroup analyses were performed for age groups (<1, 1-10, and >10 years old), and cirrhotic and biliary atresia subgroups. An optimal threshold for test performance was defined using Youden's J-statistic and receiver operating characteristic curve as appropriate.

Results:

ScFI was significantly (p=0.001) correlated with moderate to severe postoperative infections (CD grade 3-5) in children <1 year old, with the optimal ScFI threshold less than 27.1 cm²/m² (sensitivity 80.4% and specificity 77.8%). A weak negative correlation between SMI and the total duration of hospital stay (r=-0.310, p=0.016) and intensive care unit stay (r=-0.299, p=0.020) was observed in children <1 year old. No other associations between CT-based body metrics and postoperative outcomes were observed.

Conclusion:

In the most vulnerable pediatric group, children <1 year old, CT-based body metrics were correlated with moderate to severe postoperative infections (ScFI), and with longer duration of hospital and ICU stay (SMI), and thus can be considered important warning tools for pre-LT risk assessment.

S4.2.5

ULTRASOUND LIVER STIFFNESS IS A GOOD BIOMARKER OF GRAFT CONDITION AT THE EARLY PHASE FOLLOWING PAEDIATRIC LIVER TRANSPLANTATION

DAVID Missud, CLÉMENT Escallard, HÉLÈNE Agostini, INÈS Mannes, DANIELLE Pariente, CATHERINE Adamsbaum, STÉPHANIE Franchi-Abella
Hôpital Bicêtre - APHP, Le Kremlin-Bicêtre, FRANCE

Background: Liver stiffness measurement (LSM) in the context of liver transplantation (LT) has been poorly studied until now. Even if the acute post-transplantation period is complex, ultrasound LSM may be interesting to evaluate early graft condition and detect complications.

Patients and methods: Prospective study including paediatric liver recipients with collection of clinical and biological data and liver stiffness measurement (LSM) every week until week 6. Statistical analysis comparing groups with and without complication (Student's t-test) and evaluating the performance of liver stiffness for the diagnosis of complications (Receiver Operating Characteristic curves).

Results: 56 liver recipients were studied, median age 2.8 y (from 0.3 to 15.2 y). 25 had no significant complication. 31 had one or several significant complications including: 14 acute rejection, 7 septic liver on histology, 8 severe sepsis, 10 biliary complications, 4 vascular complications, 2 compartment syndrome and 2 digestive complications. In the uncomplicated group LSM decreased regularly from 16.5 kPa [7.8 to 40.2 kPa] at week 1 to 9.9 kPa [4.9 - 21.4 kPa] at week 6. Median LSM was significantly higher in the complicated group compared to uncomplicated from 23.6 kPa [7.1 - 76.9 kPa] at week 1 to 12.4 kPa [6.4 - 25.3 kPa] at week 6. Diagnostic performance for the diagnosis of complications were: Area Under the Curve between 0.66 and 0.74. Sensitivities between 0.58 and 0.81. Specificities between 0.60 and 0.80. Optimal cut-offs decreased from 19.9 at week 1 to 9.6 kPa at week 6.

Conclusion: LSM is a good biomarker of complications following LT in children. LSM decreases after LT without complication. LSM above weekly cut-off is a good indicator of possible complication.

S4.2.6

CORRELATION BETWEEN QUANTITATIVE MRI BIOMARKERS AND CLINICAL RISK SCORES IN CHILDREN AND YOUNG ADULTS WITH AUTOIMMUNE LIVER DISEASE

JOSEPH McCrary¹, JONATHAN Dillman^{1,2}, NEERAJA Mahalingam¹, RUCHI Singh³, ANDREW Trout^{1,2}, CYD Castro Rojas³, ALEXANDER Miethke^{3,4}

¹ Cincinnati Children's Hospital Medical Center, Department of Radiology, Cincinnati, USA

² University of Cincinnati College of Medicine, Department of Radiology, Cincinnati, USA

³ Cincinnati Children's Hospital Medical Center, Division of Pediatric Gastroenterology, Hepatology and Nutrition, Cincinnati, USA

⁴ University of Cincinnati College of Medicine, Department of Pediatrics, Cincinnati, USA

Purpose: There are multiple clinical tools for monitoring the progression of autoimmune liver disease (AILD), including the Mayo Risk Score and SCOPE index. The purpose of this study was to correlate these clinical risk scores with quantitative magnetic resonance imaging (MRI) biomarkers of chronic liver disease in a pediatric and young adult cohort with AILD.

Materials and Methods: Fifty-eight pediatric and young adult patients with AILD (mean age=15.1 years; range: 6-24 years) underwent research liver MRI examinations that included multiple quantitative techniques: MR elastography, iron-corrected T1 (cT1; LiverMultiScan), and quantitative magnetic resonance cholangiopancreatography (MRCP+). Using temporally-related laboratory and clinical data, the Mayo risk score and SCOPE index were calculated for each patient. For each clinical risk score, Spearman correlation was used to evaluate univariate associations with quantitative MRI biomarkers.

Results: Mean Mayo risk score was -1.12 ± 0.85 (range: $-2.86 - 1.06$). Mean SCOPE index was 2.69 ± 2.17 (range: $0 - 9$). Mean liver stiffness was 2.84 ± 1.05 kPa. Mean whole liver cT1 was 874.7 ± 77.7 ms, while mean cT1 interquartile range (IQR) was 150.8 ± 55.6 ms. Mayo risk score significantly correlated with cT1 IQR ($r=0.58$; $p<0.0001$), MRE liver stiffness ($r=0.56$; $p<0.0001$), whole liver cT1 ($r=0.31$; $p=0.02$), and multiple quantitative MRCP measures (including left hepatic duct maximum diameter – $r=0.45$, $p=0.0006$; and right hepatic duct maximum diameter – $r=0.36$; $p=0.005$). SCOPE index significantly correlated with MRE liver stiffness ($r=0.68$; $p<0.0001$), cT1 IQR ($r=0.51$; $p<0.0001$), and multiple quantitative MRCP measures (including left hepatic duct median diameter – $r=0.49$, $p=0.0001$; and left hepatic duct maximum diameter – $r=0.47$, $p=0.0003$).

Conclusion: Multiple quantitative liver MRI-based biomarkers are associated with the Mayo risk score and SCOPE index in children and young adults with AILD. Given this correlation, there is a high likelihood that MRI will perform well in stratifying patients based on likelihood to develop clinical endpoints.

S4.3.1

THE USE OF MAGNETIC RESONANCE LYMPHANGIOGRAPHY TO IMPROVE OUR UNDERSTANDING OF LYMPHATIC DISEASE IN NOONAN SYNDROME

LOTTE ELISABETH Kleimeier, JOS MT Draaisma, WILLEMIJN M Klein

Radboud university medical centre, Nijmegen, THE NETHERLANDS

Introduction: Dynamic contrast-enhanced magnetic resonance lymphangiography (DMRL) is a relatively new method to visualize the central conducting lymphatic system and flow. This modality gives new insights in previously poorly understood mechanisms. In Noonan syndrome (NS) the prevalence of lymphatic flow abnormalities is about 20%, however without clear pathophysiologic mechanism. NS is caused by mutations encoding for proteins of the RAS/MAPK pathway; patients with a SOS2 mutations have a higher prevalence of lymphatic disease. To get a better understanding of the clinical lymphatic disorders in patients with NS, we imaged SOS2 NS patients using DMRL.

Methods: We selected three NS patients based on SOS2 mutation, severe lymphedema. Non-contrast Heavily T2-weighted MR lymphangiography was performed to visualize fluid collections and edema. After intranodal contrast injections, dynamic T1 sequences were performed to visualize the central lymphatic vessels and lymphatic flow. The FOV consisted of thorax, abdomen and pelvis.

Results: The first patient, 11 years, presented with lymphedema of the lower extremities starting at the age of 6. DMRL showed a partially developed thoracic duct; extensive network of lymphatic vessels; effusion in lungs; pulmonary edema; intrahepatic periportal fluid and retrograde flow; diffusion of lymphatic flow toward lungs, mesenteric and intercostal cavities. The second patient, 17 years, presented with severe lymphedema of the lower extremities and pelvis since the age of 9. DMRL showed absence of the thoracic duct; multiple smaller tortuous lymphatic tracts retroperitoneal and mesenteric; pleural effusion; peritoneal lymphatic cysts; no development of larger lymphatic vessels; diffuse edema; intrahepatic periportal fluids with retrograde flow; diffusion of lymphatic flow towards lungs, mesenteric and intercostal cavities. The third patient, 32 years, had severe lymphedema of the upper and lower extremities during infancy and which redeveloped at the age of 16. DMRL showed no edema or fluid collections, and a normal central lymphatic system with a normal flow.

Conclusion: DMRL of the central conducting lymphatic system can show central conducting lymphatic anomalies in patients with NS and lymphedema. The correlation of the resulting images to the lymphedema symptoms is still poorly understood and needs further research. This is especially important since therapeutic options are becoming available.

S4.3.2

FERUMOXYTOL-ENHANCED DYNAMIC MR LYMPHANGIOGRAPHY: A NOVEL ALTERNATIVE METHOD TO GADOLINIUM-BASED CONTRAST AGENTS IN MR LYMPHATIC IMAGING IN CHRONIC KIDNEY DISEASE

ENSAR Yekeler¹, GANESH Krishnamurthy², CHRISTOPHER L Smith³, FERNANDO A Escobar², ERIN Pinto⁴, JORDAN B Rapp², HANSEL J Otero², AMMIE M White², YOAV Dori³, DAVID M Biko²

¹ Department of Radiology, Children's Hospital of Philadelphia, Philadelphia, USA

² Department of Radiology, Children's Hospital of Philadelphia, University of Pennsylvania Perelman School of Medicine, Philadelphia, USA

³ Division of Cardiology, Children's Hospital of Philadelphia, University of Pennsylvania Perelman School of Medicine, Philadelphia, USA

⁴ Center for Lymphatic Imaging and Interventions, Children's Hospital of Philadelphia, Philadelphia, USA

Purpose:

Dynamic contrast-enhanced MR lymphangiography (DCMRL) is routinely performed using gadolinium-based contrast agents (GBCAs) via intra-nodal and less commonly with intra-hepatic, or intra-mesenteric techniques but in some patients GBCA are contraindicated due to underlying renal disease. Our purpose is to describe a novel technique of direct intra-lymphatic administration of ferumoxytol in place of GBCAs to visualize the central lymphatics with MR lymphangiography in children with renal disease.

Methods:

Initially, an in-vitro dose optimization was performed determining a ferumoxytol concentration of 1 to 1.5 mg/mL with the dilution factor of 1:20 to 1:30 to be optimal for DCMRL. A ferumoxytol enhanced DCMRL was then performed in 4 children (ages 7 months, 11 months, 2 years, and 3 years) with renal disease. Indications were postoperative chylothorax following heart transplant, chylous ascites, and protein losing-enteropathy. Intra-hepatic, intra-mesenteric, and intranodal lymphatic access was performed using ultrasound guidance and fluoroscopy. Following transfer to the MR suite, a coronal T2-weighted 3D imaging was followed by DCMRL using coronal time-resolved dynamic and high-resolution 3D GRE sequences with the lowest TE values (1 to 1.5 ms) during the administrated diluted ferumoxytol via intra-mesenteric followed intra-hepatic and intranodal route by slow hand injection (0.5 to 1.0 mL/min).

Results:

DCMRL with direct lymphatic ferumoxytol injection was successful in all four patients in terms of diagnostic quality and clarity. The contrast conspicuity was sufficient within the lymphatic channels without subtracted images. Ferumoxytol DCMRL revealed diagnostic quality equivalent to gadolinium enhanced DCMRL according to our familiarity and experience with it. There was no discontinuity or signal loss in the lymphatic channels. There were no short-term complications during or after the studies.

Conclusion:

Magnetic resonance lymphangiography using ferumoxytol via IN, IH, and IM access is a new method to directly visualize the lymphatic system and can be applied safely in patients with renal failure. FDCMRL shows excellent contrast resolution by using 3D GRE sequences with the lowest TE value and appropriate dilution of the ferumoxytol.

S4.3.3

THE USE OF INTRANODAL MR LYMPHANGIOGRAPHY IN PEDIATRIC UNIVERSITY HOSPITAL

CAROLINE van Schaik, JAN JAAP Janssen, SJOERD Jenniskens, LEO Schultze Kool, WILLEMJIN Klein

Radboudumc, Nijmegen, THE NETHERLANDS

Introduction

Lymph flow problems, resulting in symptoms such as chylothorax, percutaneous lymph leakage, lymph edema and protein losing enteropathy, have long been out of the scope of the diagnostic pediatric radiologist. The innovative method of intranodal contrast injection and dynamic MR imaging, called intranodal dynamic MR lymphangiography (IDMRL), has made a major change in the visualization and understanding of central lymph flow disorders. In this presentation we will demonstrate the technique, typical cases and therapeutic options, to familiarize the pediatric radiologists with this upcoming modality.

Methods

In our university hospital and referring centers, patients suspected of abnormalities in the central lymph vessels and potential therapeutic options, had an indication for IDMRL. Most patients had general anaesthesia. After ultrasound guided placement of 25G needles in the bilateral inguinal lymph nodes, the patient was positioned in the MR. T1 and T2 sequences were made; then, contrast injection was started and the dynamic sequences scanned. Postprocessing included timelapse movies of the contrast flow.

Results

We imaged 30 pediatric and congenital cases during 3 years, including 4 cases of generalized lymphatic anomaly (GLA), 6 venolymphatic malformations, 7 cases of Noonan(-like) or yellow nail syndrome. Symptoms for indication were scrotal / vaginal chyle leakage, chylothorax, protein losing enteropathy and lymph edema. In 24 cases the abnormalities in the lymphatic anatomy or flow were visualized with IDMRL. In all cases IDMRL was helpful in the therapeutic decision making such as embolization, surgery or prolonged conservative treatment.

Conclusion

IDMRL is an innovative technique to image the central lymph vessels and visualize the lymph flow. It is indicated in case of suspected abnormal lymphatic flow. The IDMRL images are a guidance for improving and personalizing the therapy. We encourage pediatric radiologists to get familiar with this modality.

S4.3.4

DYNAMIC CONTRAST-ENHANCED MAGNETIC RESONANCE LYMPHANGIOGRAPHY IN A PEDIATRIC TERTIARY HOSPITAL IN SWITZERLAND

RALPH Gnannt, HITENDU Dave, LUREGN Schlapbach, CHRISTIAN Kellenberger

Children's Hospital Zurich, Zurich, SWITZERLAND

INTRODUCTION:

Dynamic Contrast-Enhanced Magnetic Resonance Lymphangiography (DCMRL) in neonates as a routine diagnostic procedure is not well established in Switzerland. We present our experience of this technically challenging imaging modality and patient outcome.

MATERIAL & METHODS

All DCMRL at our institution were performed on a 1.5T GE scanner and retrospectively analyzed. Patient demographics (sex, age, and weight of the patient), referring hospital/department, clinical indication (congenital chylothorax, post-cardiac surgery, Gorham Stout Disease, Generalized Lymphatic Anomaly), and imaging findings were noted. Technical success was defined as visible ascending contrast media within the lymphatic system on both iliacal axis and above the cisterna chyli.

RESULTS

Since May 2017 we performed 18 DCMRL scans, 13 with the above mentioned indication: 4 with a congenital chylothorax, 7 post-cardiac surgery, 1 with Gorham Stout Disease and one with Generalized Lymphatic Anomaly. Technical success rate was 92%. 7 girls and 6 boys were scanned with a

median age of 5 months (range 1 mo – 128 mo) and a median body weight of 4.2 kg (range 2.5 kg – 35 kg). 4 (31%) patient showed a Central Lymphatic Flow Disorder (CLFL), 3 (23%) patient a Pulmonary Lymphatic Perfusion Syndrome (PLPS), 1 (8%) patient a surgical complication, 4 (31%) patient showed normal lymphatic flow and in 1 (8%) patient the DCMRL was non-diagnostic. Out of the 4 patient with CLFL 2 died, whereas patient with a PLPS 3 out of 3 patient survived with interventional radiology guided (2/3) or conservative (1/3) treatment.

CONCLUSION

Outcome of this chylothorax cohort is consistent with recent publications. DCMRL predict patient outcome and may guide to possible treatment options.

S4.3.5

IMAGING FINDINGS OF COPA SYNDROME

HAITHUY Nguyen¹, TIPHANIE Vogel², MANUEL Silva-Carmona³, MARIETTA DeGuzman², R. PAUL Guillermin¹

¹ Texas Children's Hospital - Department of Radiology, Houston, USA

² Texas Children's Hospital - Department of Pediatrics, Rheumatology, Houston, USA

³ Texas Children's Hospital - Department of Pediatrics, Pulmonology, Houston, USA

Purpose: Autosomal dominant mutations in the coatamer subunit alpha (COPA) gene cause an immune dysregulation disorder with interstitial lung disease including pulmonary capillaritis, arthritis, and glomerulonephritis. The purpose of this study is to describe the thoracic, musculoskeletal (MSK), and renal imaging findings of COPA syndrome.

Materials & Methods: COPA syndrome patients were identified from an institutional rheumatology registry. Two pediatric radiologists conducted a consensus retrospective review of findings on chest radiography (CXR) and computed tomography (CT), MSK radiography and magnetic resonance imaging (MRI), and renal ultrasound (US). Demographics were extracted from the medical records.

Results: 17 COPA syndrome patients (12 children, 5 adults; 9:8 M:F) with imaging were identified. Mean age at first imaging exam for children was 7 years (0.7-15 years) and for adults was 42 years (32-51 years). 4/11 had abnormal CXRs at presentation. 14/17 had chest CT which demonstrated ground-glass opacities (GGO) (13/14), interlobular septal thickening (13/14), hilar/mediastinal lymphadenopathy (11/14), intralobular septal thickening (10/14), cysts (9/14), fibrosis (honeycombing or architectural distortion) (8/14), chest wall deformity (5/14), nodules (6/14), and crazy-paving (3/14). 8/17 had at least one follow-up chest CT which showed improvement in GGO, nodules, and hilar/mediastinal lymphadenopathy but worsening of septal thickening, cyst formation, and fibrosis. 7/17 had MSK imaging later in childhood or adulthood which revealed joint synovitis (3/7), tenosynovitis (1/7), enthesitis (1/7) and subcutaneous nodules (1/7). 7/17 had at least one renal US later in childhood or adulthood which revealed nephromegaly or atrophy (6/7) and cortical hyperechogenicity (3/7).

Conclusions: The most prevalent imaging findings of COPA syndrome relate to early childhood-onset recurrent pulmonary hemorrhage and lymphoid hyperplasia leading to pulmonary fibrosis. Less prevalent imaging findings manifesting later in life include synovitis, enthesitis, and renal cortical and size abnormalities. Genetic testing for COPA syndrome is warranted in the setting of diffuse hemorrhagic lung disease, particularly in the setting of accompanying arthritis, nephritis or family history.

S4.3.6

THORACIC MDCT FINDINGS OF DOCK8 IMMUNODEFICIENCY SYNDROME IN CHILDREN

EDWARD Lee¹, SARA Vargas², JONATHAN Gaffin³, JANET Chou³, ABBEY Winant¹

¹ Boston Children's Hospital and Harvard Medical School, Department of Radiology, Boston, USA

² Boston Children's Hospital and Harvard Medical School, Department of Pathology, Boston, USA

³ Boston Children's Hospital and Harvard Medical School, Department of Pediatrics, Boston, USA

Purpose: To investigate the characteristic thoracic MDCT findings of DOCK8 immunodeficiency syndrome, a rare autosomal recessive form of hyperimmunoglobulin E syndrome, in children.

Materials and Methods: All pediatric patients (less than 18 years) with a known diagnosis of DOCK8 immunodeficiency syndrome (based on genetic testing) who underwent thoracic MDCT studies from October 2004 to October 2020 were included. Two pediatric thoracic radiologists independently evaluated MDCT studies for the presence of thoracic abnormalities in the lung parenchyma (ground-glass opacity (GGO), consolidation, nodule, mass, cyst, and bronchiectasis), pleura (pleural effusion, pleural thickening, and pneumothorax), and mediastinum (lymphadenopathy). When a pulmonary parenchymal abnormality was present, laterality, distribution (upper, mid, and lower lung zone), and extent were also evaluated. When a pleural abnormality was identified, size of the abnormality was also assessed. When mediastinal lymphadenopathy was present, its location and size were also evaluated. Interobserver agreement between two independent reviewers was evaluated with kappa statistics. **Results:** 17 pediatric patients were identified (5 male (29%), 12 female (71%); mean age 7.4 years). All patients underwent MDCT studies (contrast-enhanced MDCT studies in 11/17 (65%) and noncontrast-enhanced MDCT studies in 6/17 (35%)). Bilateral symmetric bronchiectasis with a mid and lower lung zone predominance (11/17; 65%) was the most frequently detected lung parenchymal abnormality, followed by GGO in 9/17 patients (53%). Among 11 patients who underwent contrast-enhanced MDCT studies, the majority (9 patients, (82%)) had mediastinal adenopathy. There was excellent interobserver kappa agreement between two independent reviewers for detecting abnormalities on thoracic MDCT studies ($k > 0.90$).

Conclusion: Children with DOCK8 immunodeficiency syndrome have characteristic thoracic MDCT findings, including bilateral symmetric bronchiectasis, with a mid and lower lung zone predominance, GGO, and mediastinal lymphadenopathy. Clear knowledge of these characteristic thoracic MDCT findings of DOCK8 immunodeficiency syndrome is important for timely diagnosis and optimal care of children with this rare genetic disorder.

S4.4.1

ROLE OF LOW DOSE 18F-FDG-PET/MRI IN THE DETECTION OF INFLAMMATORY AIRWAY CHANGES IN CHILDREN WITH CYSTIC FIBROSIS

RICARDA Schwarz¹, MAREEN Kraus¹, PHILIPP Utz², UTE Graepler-Mainka², HELMUT Dittmann³, ILIAS Tsiflikas¹, SERGIOS Gatidis¹, JÜRGEN Schäfer¹, MICHAEL Esser¹

¹ Radiology Department, University Hospital Tübingen, Tübingen, GERMANY

² Pediatric Department, University Hospital Tübingen, Tübingen, GERMANY

³ Department for Nuclear Medicine, University Hospital Tübingen, Tübingen, GERMANY

Purpose

Research on PET/CT in patients with cystic fibrosis is rare, and so far nothing on PET/MRI has been published. With this retrospective study, we aim to investigate the impact of 18F-FDG PET/MRI on individual therapy of pediatric patients with cystic fibrosis.

Materials and Methods

Indications for PET/MRI were the pre-transplantation exclusion of inflammatory focus (n=2), worsening of lung function (n=3), prolonged infection despite therapy (n=2), and follow-up (n=4).

FDG was administered intravenously at a dose of 1,3 MBq/kgKG (min 0,97, max 2,79). Standardized Uptake Values (SUV) were used to classify areas with low, moderate, or high increased FDG uptake compared to the liver and blood pool.

We assessed if PET/MRI had an impact on the therapeutic regime, such as a start, change or stop in medication, or conduction of therapy lately started before the PET/MRI study. If the therapy was continued without any change despite pathological findings in PET/MRI, it was deemed to have had no impact.

Results

11 FDG PET/MRI studies of the lung in 7 patients in the age of 8-21 years (15,8 ± 5 years, 3 female, 4 male) were included. Our cohort had a mean BMI of 18,7 ± 3, which resulted in an effective dose of 1,35 ± 0,5 mSV (following IRCP 106). PET/MRI showed a high increased SUV in 4 cases, moderate increased SUV in 2 cases, and 1 case without an increased SUV of the airways. The results of the PET/MRI affected the patient's therapy in all cases (100 %): A new medication/therapy was started in 63 % (n=7), continued in 27% (n=3), and suspended in 10 % (n=1) of the cases.

Conclusion

FDG PET/MRI of the lung impacted the patient's therapy plan significantly in all children with cystic fibrosis. Compared to the gold standard of chest CT, FDG PET/MRI has a remarkably low radiation dose. Therefore, we suggest that FDG PET/MRI should be considered as a good alternative diagnostic tool in specific cases.

S4.4.2

GASTROINTESTINAL INVOLVEMENT OF POST-TRANSPLANT LYMPHOPROLIFERATIVE DISORDER (PTLD) AND THE UTILITY OF 18F-FDG POSITRON EMISSION TOMOGRAPHY (PET)

JENNIFER Gillman, J. CHRISTOPHER Davis, LISA J. States
Children's Hospital of Philadelphia, Philadelphia, USA

Purpose:

Post-transplant lymphoproliferative disorder (PTLD) is the most common malignancy in children with solid-organ transplants, related to the immunosuppression needed to prevent graft rejection. Early diagnosed PTLD is more common in children, demonstrating more extra-nodal involvement. Approximately 32% of children develop gastrointestinal PTLD (GI-PTLD). 18F-FDG PET imaging is important for staging and treatment response. The purpose of this study is to compare FDG bowel activity in PTLD patients with and without bowel involvement on biopsy.

Methods:

This IRB-approved study examines PTLD patients at a tertiary children's hospital between January 1 2010 and October 30 2020. Patient characteristics include age at PTLD diagnosis, sex, organ transplant type, inflammatory bowel disease (IBD), diabetes, metformin use, or *C. difficile* colitis. Patients with gastrointestinal pathology specimens within 40 days of FDG-PET were evaluated for the distribution of GI metabolism (diffuse vs. focal/multifocal), bowel SUVmax (BSUV), liver SUVmax (Lmax) and liver SUVmean (Lmean). Descriptive statistics and Mann-Whitney U tests were performed.

Results:

46 patients were diagnosed with PTLD, 56.5% male with an average age of 7.9 years at diagnosis. 146 FDG PET exams were performed (average 3.2 per patient) with 118 PET-CT (80.8%) and 28 PET-MR (19.2%). 23 patients (50%) had specimens within 40 days of PET imaging, with 32 pathology-PET pairings (pathology: 21 GI-PTLD(+), 9 GI-PTLD(-), 2 equivocal).

Overall 20 patients had GI-PTLD (43.5%), 15% of GI-PTLD patients (n=3) also had IBD; only 3 patients in total had known IBD. After excluding 4 patients concomitant *C. difficile*, median BSUV, BSUV/Lmax, BSUV/Lmean for GI-PTLD positive versus GI-PTLD negative pairings were 4.4 vs 4.0 (p=.70), 3.7 vs 2.4 (p=.12), 4.0 vs 2.8 (p=.16).

Conclusion:

GI-PTLD is common in children however the diagnosis requires a multidisciplinary approach, and comparing BSUV with GI pathology is challenging. IBD and *C. difficile* colitis are important confounding factors, and interestingly all patients in our study with IBD also had GI-PTLD.

S4.4.3

IMAGING CHEMOTHERAPY-INDUCED BRAIN DAMAGE IN PEDIATRIC CANCER SURVIVORS

DIANA LOPEZ, LUCIA Baratto, FLORIAN Siedek, ALI Rashidi, MICHAEL Iv, HIEKE Dandrup
Stanford University, Palo Alto, USA

Purpose: Chemotherapy with methotrexate (MTX) is associated with chronic neurotoxicity. Many pediatric cancer survivors face chronic neurological problems ranging from mild symptoms to severe headaches, seizures, motor problems and cognitive impairment. Currently, it is impossible to predict who will develop long-term neurocognitive effects after MTX. Our goal was to detect early imaging signs of chemotherapy-induced brain damage, that can be associated with chronic neurocognitive problems.

Methods: In an IRB approved, retrospective study, we investigated 10 children (2-24 years), with osteosarcoma (n=6) and lymphoma (n=4), who underwent 18F-FDG-PET/MR scans of (3-5 MBq/kg), before and after chemotherapy with IV high-dose-MTX (3000-144,000 mg/m2). The 18F-FDG uptake of different brain regions was measured using MIM vista 6.5 software. Hyper- or hypometabolic brain areas were defined by a z-score of ± 1.65. Baseline scans were compared to follow up scans.

Results: Of 10 patients who received high dose MTX, 9 patients demonstrated abnormal brain metabolism on 18F-FDG-PET/MR scans after high-dose-MTX compared to baseline: Hypometabolic areas were seen in 8 patients in the frontotemporal cortex (n=8), parietal cortex (n= 3) and basal ganglia (n=2). Executive functions areas were affected: the middle frontal gyrus (n=3), fusiform gyrus (n=1), and the inferior frontal gyrus (n=1). Hypermetabolic areas were seen in 8 patients in the frontotemporal cortex (n=8), parietal cortex (n= 2) and basal ganglia (n=3). Executive functions areas were also affected: middle frontal gyrus (n=3), fusiform gyrus (n=1), inferior frontal gyrus (n=4), and the insula (n=1). More patients had bilateral (6) than unilateral (n=3) regional uptake differences. Ongoing studies are correlating the hypometabolism in the dorsolateral frontal cortex with reduced school performance and hypometabolism in the temporoparietal cortex with reading problems.

Conclusion: PET/MRI can detect early signs of chemotherapy-induced brain damage. Since there is a window of time between drug exposure and morbidity, this early detection could enable non-invasive monitoring of interventions, which can improve clinical outcomes

S4.4.4

ULTRASOUND DETERMINATION OF PEDIATRIC THYROID MASS

ABIGAIL Crothers¹, JANET Chuang², SUSAN Sharp³, SARAH Szabo⁴, BIN Zhang⁵, ANDREW Trout³

¹ University of Cincinnati College of Medicine, Cincinnati, USA

² Cincinnati Children's Hospital Medical Center, Division of Endocrinology, Cincinnati, USA

³ Cincinnati Children's Hospital Medical Center, Department of Radiology, Cincinnati, USA

⁴ Cincinnati Children's Hospital Medical Center, Division of Pathology and Laboratory Medicine, Cincinnati, USA

⁵ Cincinnati Children's Hospital Medical Center, Division of Biostatistics and Epidemiology, Cincinnati, USA

Background

Radioiodine therapy for pediatric Graves' disease can be achieved with empiric dosing or with patient-specific dosing based on thyroid mass. Thyroid mass can be estimated by calculating thyroid volume from measurements by ultrasound adjusted by a correction factor. Different factors will impact estimated thyroid mass and thus administered radioiodine dose. The objective of this study was to define the relationship between thyroid volume measured by ultrasound and thyroid mass following thyroidectomy.

Methods

This was a retrospective study that included all patients <18 years of age with <6 months between thyroid ultrasound and thyroidectomy (total or hemithyroidectomy) between January 2010 and June 2020. Thyroid dimensions measured by ultrasound, thyroid mass measured at thyroidectomy, and histopathologic diagnosis were collected. Five correction factors derived from the literature (0.479, 0.494, 0.554, 0.524, 0.523) were used to estimate thyroid volume by ultrasound. Pearson correlations and Bland Altman difference analyses were used to define the relationship between calculated ultrasound volume and specimen weight. Linear regression was used to calculate the optimal correction factor for thyroid volume. Variables predictive of thyroid mass were examined by univariate analysis.

Results

We included 86 patients, 19 (22%) male, with mean age 14.5 ± 3.15 years. All correction factors had equal strong, positive correlation with thyroid mass ($r=0.95$). Mean difference between estimated volume and measured mass ranged from -0.54 ± 8.98 (factor:0.554) to 2.56 ± 9.13 (factor:0.479). Sex ($p=0.054$), age ($p=0.13$), interval to surgery ($p=0.65$), disease category ($p=0.074$), and presence of nodules ($p=0.15$) were not significantly associated with thyroid mass. Based on linear regression the optimal factor for estimation of thyroid volume was 0.52.

Conclusion

Estimated thyroid mass based on calculated thyroid volume from ultrasound does not vary substantially based on conversion factor used. Errors in estimated mass are less than 3 grams on average. Based on our sample, the optimal conversion is 0.52, assuming a 1 g/ml density

S4.4.5

CLINICAL SIGNIFICANCE OF MULTIPLE COLLOID NODULES IN CHILDREN

ZUHAL Bayramoglu, ZEYNEP NUR Akyol Sari

Istanbul University, Istanbul Medical Faculty, Radiology Department, Istanbul, TURKEY

Polycystic thyroid disease (PCTD) is a recently defined entity and the clinical significance has yet to be clarified especially in children. We aimed to investigate the association of the colloidal nodules with thyroid diseases and dysfunctions. This study included 150 consecutive children diagnosed with PCTD. Thyroid volumes, associated parenchymal diseases, and nodules along with thyroid-stimulating hormone (TSH), free thyroxine (f-T4), anti-thyroglobulin (anti-TG), and anti-thyroid peroxidase (anti-TPO) were evaluated. Descriptive statistics were expressed as a minimum, maximum, mean, standard deviation, median with range, and frequencies were expressed as a percentage.

Results: Fifty-nine male (mean age; 12.3 ± 3.7 years) and 91 female (mean age; 12.5 ± 3.6 years) patients were evaluated. The mean thyroid volume was 7.50 ± 6.3 lcc and the mean colloidal nodule diameter was 4.36 ± 2.34 mm. Colloidal nodules were found commonly in both thyroid lobes (90.5%). Nodules were found in 5.3% of the patients. TSH values were elevated (>4 mIU/L) in 61.3% (mean: 6.76 m IU/L) of the patients. Normal levels of anti-TG, anti-TPO, and f-T4 were found in 58%, 56%, and 65% of the patients, respectively. Significant positive correlations were found among age with thyroid volume ($p=0.001$, $r=0.4$), TSH with anti-TG ($p:0.001$, $r:0.76$), TSH with anti-TPO ($p:0.001$, $r:0.86$), left lobe volume with f-T4 ($p:0.049$, $r:0.2$), colloidal nodule diameter with f-T4 levels ($p:0.036$, $r:0.51$)

Conclusion: PCTD is a common endocrinological disorder in children mostly associated with subclinical hypothyroidism. Coexistent autoimmune thyroid disorders may contribute to hypothyroidism. The PCTD patients would be closely monitored in terms of overt hypothyroidism.

S4.4.6

A META-ANALYSIS ON THE DIAGNOSTIC PERFORMANCE OF WHOLE-BODY MRI VERSUS FDG-PET/CT FOR THE INITIAL STAGING OF HODGKIN LYMPHOMA

SUZANNE Spijkers¹, ANNEMIEKE S. Littooi^{1,2}, AUKE Beishuizen², MARNIX G.E.H. Lam^{1,2}, RUTGER A.J. Nijelstein^{1,2}

¹ Department of Radiology and Nuclear Medicine, University Medical Centre Utrecht/Wilhelmina Childrens Hospital, Utrecht, THE NETHERLANDS

² Princess Máxima Center for Pediatric Oncology, Utrecht, THE NETHERLANDS

Purpose: To meta-analyse all published data on the diagnostic performance of WB-MRI compared to FDG-PET/CT for the initial staging of Hodgkin lymphoma.

Materials and methods: Both the PubMed/MEDLINE and EMBASE databases were systematically searched (updated until 7 September 2020) for studies that compared WB-MRI with FDG-PET/CT for staging Hodgkin lymphoma. All search results were reviewed for eligibility. The "quality assessment of diagnostic accuracy studies" tool (QUADAS-2) was used to assess the methodological quality of the studies. Pooled staging accuracy, sensitivity and specificity of WB-MRI compared to FDG-PET/CT was calculated for determining stage and for both nodal and extra-nodal staging. A sensitivity analysis for children and adults was performed.

Results: A total of nine studies with a combined total of 297 Hodgkin lymphoma patients were included. Pooled sensitivity and specificity for nodal staging were 94% (95%CI 0.92-0.96) and 99% (95%CI 0.98-1.00) respectively. For extra-nodal staging sensitivity and specificity were 90% (95%CI 0.74-0.96) and 100% (95%CI 0.99-1.00). For disease stage, the pooled accuracy was 92% (95%CI 0.87-0.96).

Conclusion: In comparison with FDG-PET/CT, WB-MRI shows high sensitivity and specificity for both nodal and extra-nodal staging and for determining disease stage.

S5.1.1

MOST OF WHAT YOU NEED TO KNOW ABOUT THE PEDIATRIC LITERATURE IN 6 MINUTES OR LESS

BRENDAN Kelly¹, RONAN Killeen¹, AONGHUS Lawlor², GABRIELLE Collieran³

¹ St Vincents University Hospital, Dublin, IRELAND

² Insight @ UCD, Dublin, IRELAND

³ CHI @ Temple Street University Hospital, Dublin, IRELAND

Introduction

There has been a large amount of research in the field of artificial intelligence as applied to clinical radiology. However these studies address a narrow range of tasks with a narrow pallet of techniques

Methods

In a PRISMA registered systematic review we identified all papers that apply artificial intelligence techniques to paediatric radiology, both to survey the literature and to evaluate their methods. We aimed to identify the key questions being addressed in the literature and to identify the most effective methods employed and trends in use over time.

Results

1091 titles and abstracts were screened. 180 full texts were reviewed and 156 articles were included for analysis. The median number of patients in each study was 149.5 and the median number of images per patient was 6.2. Two main kinds of papers accounted for over 90% of included studies: those that used basic machine learning to separate classes using radiomics or texture features and those that used deep learning techniques. Segmentation, identification, classification and regression tasks accounted for 87% of papers with 8% image generation and dose reduction, 3% on prediction and 2% on biomarker identification. Most papers were in the subspecialties of neuroradiology (49%) and musculoskeletal imaging (24%) and 60% of studies were undertaken on MRI. 22% of papers focussed on image quality/processing, 18.5% on age assessment and 10.5% on brain development. The remaining 49% of papers investigated a wide range of diverse use cases. Only 17% of papers externally validated their results.

Conclusion

Due to the narrow focus of the included papers we have identified that the review of only a small number concepts can allow a paediatric radiologist to meaningfully interact with the AI literature relevant to their practise. This presentation gives a tour of the literature and introduces these key concepts.

S5.1.2

DEEP LEARNING ASSISTED DIAGNOSIS OF PEDIATRIC SKULL FRACTURE ON PLAIN RADIOGRAPHY

SEUL BI Lee, YEON JIN Cho, JAE WON Choi, SEUNGHYUN Lee, YOUNG HUN Choi, JUNG-EUN Cheon, WOO SUN Kim
Seoul National University Hospital-Department of Radiology, Seoul, SOUTH KOREA

Objectives: This study aimed to develop and evaluate a deep learning model that detects pediatric skull fractures on plain radiography.

Materials and Methods: This retrospective multi-center study consisted of data sets 1 (n=157) and 2 (n=264) for model development and internal test, and data set 3 (n=95) for the external test. The combined data sets 1 and 2 was split into training, validation, and internal test sets at a 7:1:2 ratio. The data sets included pediatric skull radiography underwent for head trauma. The reference standard for data sets 1 and 2 was radiographic finding, while for data set 3, that was cranial CT findings. We used a YOLOv3 that predicts bounding boxes and scores for candidate lesions. An observer study was performed by radiologists on the external test set. To evaluate the diagnostic performance of the model and radiologists, we calculated the area under the receiver operating characteristic curve (AUC), sensitivity, specificity, positive predictive value (PPV), and negative predictive value (NPV). The cut-off point for diagnostic performance evaluation was calculated from the internal test set.

Results: Our model showed an AUC of 0.984 (95% CI, 0.966–1.000) in the internal test set, and 0.782 (95% CI, 0.642–0.922) in the external test set. The AUCs of the radiologists were in the range of 0.765–0.908. At the optimal cut-off point, the model had sensitivity of 90.6% (95% CI, 0.750–0.980), specificity of 94.3%

(95% CI, 0.843–0.988), PPV of 90.6% (95% CI, 0.762–0.967), and NPV of 94.3% (95% CI, 0.850–0.980) for the internal test set; for the external test set, it had sensitivity of 68.4% (95% CI, 0.435–0.874), specificity of 88.2% (95% CI, 0.787–0.944), PPV of 76.9% (95% CI, 0.421–0.741), and NPV of 91.8% (95% CI, 0.851–0.956).

Conclusions: Our study is the first to demonstrate a deep learning model for the diagnosis of pediatric skull fracture on plain radiography.

S5.1.3

CONVOLUTIONAL NEURAL NETWORK FOR AUTOMATIC QUANTIFICATION OF LOWER EXTREMITY ALIGNMENT IN CHILDREN

ANDY Tsai

Boston Children's Hospital, Boston, USA

Purpose: Lower extremity deformity in children is common, the most frequent of which are genu varum and genu valgum. The imaging workup of this deformity is to acquire full-length radiographs of bilateral lower extremities, and to assess the hip-knee-ankle angles (HKAA), also referred to as the mechanical femoral-tibial angles. Measuring this angle from a radiograph requires identifying three anatomical landmarks: the centers of the femoral head, tibial spine, and tibial plafond. This study's objective is to develop a convolutional neural network (CNN) capable of predicting these three landmarks to accurately predict the HKAA in quantifying lower extremity alignment.

Material and methods: A search of the image archive at a large tertiary children's hospital was conducted to identify standing, full-length, anteroposterior radiographs of both lower extremities performed during 7/2019-10/2019 for the indication of lower extremity alignment. The inclusion criteria were 1) children ≤ 18 years-old; 2) adequate image quality; and 3) imaging field-of-view that included bilateral femoral heads, tibial spines, and tibial plafonds. The six anatomical landmarks of each radiograph (three from each limb) were manually labeled by a pediatric radiologist and the resultant labels were defined as the ground-truth. A 2D heatmap was generated for each ground-truth landmark to encode the pseudo-probability of a landmark being at a particular location. A CNN was developed for indirect landmark localization by regressing across a collection of these 2D heatmaps. The landmarks predicted from this model were used to calculate the prediction HKAA.

Results: The study cohort consisted of 528 radiographs. The average age at the time of imaging was 10.8 ± 4.2 years. Evaluation of this CNN showed few prediction outliers (12/1056 [1.1%]), defined as having an absolute prediction error of $>10^\circ$. Excluding these outliers, the study cohort's mean absolute prediction error for the HKAA was $0.94^\circ \pm 0.84^\circ$; and the intraclass correlation between the ground-true and prediction was 0.974 (excellent agreement).

Conclusion: The proposed CNN generated promising results in quantifying lower extremity alignment. The results of this study offer the potential use of this model as a computer-aided diagnostic tool to increase the efficiency of the clinical workflow, reduce the variability of assessing lower extremity alignment, and improve the diagnostic confidence of the interpreting radiologist.

S5.1.4

CAN A DEEP LEARNING MODEL AUTOMATE RADIOLOGICAL ANGLE MEASURES USED TO EVALUATE AND MANAGE CLUBFOOT?

DANIELLA Patton¹, ADARSH Ghosh¹, AMY Farkas¹, SUSAN Sotardi^{1,2}, MICHAEL Francavilla^{1,2}, SHYAM Venkatakrishna¹, MINUHI Ouyang³, HAO Huang^{1,3}, RICHARD Davidson¹, RAYMOND Sze^{1,2}, JIE Nguyen^{1,2}

¹ Department of Radiology, The Children's Hospital of Philadelphia, Philadelphia, USA

² University of Pennsylvania School of Medicine, Philadelphia, USA

³ Department of Radiology, Perelman School of Medicine, University of Pennsylvania, Philadelphia, USA

Purpose: Although angle measurements are routinely performed on radiographs to diagnose and manage clubfoot, these metrics are time-consuming and subjective to obtain (Kamath, 2018). However, a convolutional neural network (CNN) model may be a more reliable alternative method since angles are the mathematical relationship between bones. We aimed to develop and compare a CNN to automate angle measures for management of clubfoot.

Materials and Methods: In this IRB approved retrospective study, we acquired 461 radiographs (Anteroposterior, AP: n=231, Lateral, LAT: n=230) from 217 studies obtained between 2000–2020 from our PACS (children <3 years). Data was split into training, validation, and test sets (60:15:25 ratio-split). The 1st metatarsal, calcaneus, and talus were manually segmented and a multiclass U-Net model with a ResNet-50 backbone was trained to segment these bones. The talo-1st metatarsal and talocalcaneal angles were computationally derived to mimic clinical methods (Simons, 1977). Dice coefficients, Bland-Altman bias tests (after outlier removal), limits of agreement (LOAs), and intraclass correlation coefficients (ICC) for two radiologists in comparison to the CNN algorithm and CNN were reported on the test set.

Results: High spatial overlap between manual and CNN segmentations were achieved for all bones with mean Dice values of 0.94 for AP and 0.91 for LAT radiographs. Besides the AP talocalcaneal angle ($p < 0.01$), no significant bias was found for radiologist-radiologist or mean radiologist-CNN model angle comparisons. Talo-1st metatarsal: LOAs for the radiologists was (LAT) -10.3° to 11.0° and (AP) -12.7° to 12.4° and for the radiologist-CNN model was (LAT) -22.2° to 21.2° and (AP) -34.6° to 28.6° . Talocalcaneal: LOAs for the two-radiologist comparison was (LAT) -13.4° to 9.3° and (AP) -12.2° to 13.4° versus (LAT) -19.4° to 21.5° and (AP) -31.9° to 18.9° for the radiologist-CNN model. ICC values ranged from 0.50–0.83 for two radiologists and CNN angle comparisons. Mean time to compute angles per study was 100 versus 2.2 seconds for the radiologists and CNN, respectively.

Conclusion: Our CNN reliably calculates clubfoot measurements with significant time-savings for radiologists. ICC values and bias tests indicate moderate to high similarity between CNN and radiologist angle measures, despite an increase in LOAs. These findings indicate that our computational methods may have utility in clubfoot angle determination.

S5.1.5

INFERRING PEDIATRIC KNEE SKELETAL MATURITY FROM MRI USING DEEP LEARNING

JOHN Zech¹, GIUSEPPE Carotenuto¹, DIEGO Jaramillo²

¹ New York Presbyterian - Columbia University Irving Medical Center, New York, USA

² New York Presbyterian - Columbia University Children's Hospital of New York, New York, USA

Purpose

Hand radiographs are used to determine skeletal maturity. Deep learning performs competitively with radiologists at this task. For children who have suffered lower extremity trauma, skeletal maturity of the involved bones determines appropriate management, and may differ from the hands. We evaluated how accurately skeletal maturity could be inferred from knee MRI using deep learning.

Materials and Methods

Retrospective data from 913 patients were obtained (mean age 13.0, 48% female). Coronal and sagittal sequences that were T1/PD-weighted were

included and resized to 224x224 pixels. Data were divided into train (n=686), tune (n=49), and test (n=178) sets.

Chronologic age was predicted using deep learning approaches based on (1) features extracted from a single coronal slice through the center of the distal femur using a DenseNet-121 ("Single Slice CNN") and (2) a long-short-term-memory model which took as input DenseNet-121-extracted features from all T1/PD coronal and sagittal slices ("Multislice-LSTM") trained using PyTorch.

Each test case was manually assigned a bone age by two radiology residents and an experienced pediatric radiologist using a reference atlas provided by Pennock and Bomar. The radiologist's assigned bone age served as ground truth.

Results

Residents were more accurate at predicting bone age than the best performing machine learning method (mean M.S.E. 0.63 vs. 1.76, paired t-test 6.99, $p < 0.001$), although the model predicted chronological age competitively with radiology residents (M.S.E. 1.22 vs 1.01, t-test 1.30, $p = 0.257$) and radiologist (M.S.E. 1.22 vs 1.82, t-test 2.49, $p = 0.014$).

Conclusion

A deep learning-based approach demonstrated ability to infer skeletal maturity from knee MRI sequences, and may offer a method for automatically evaluating lower extremity skeletal maturity as part of every MRI examination. Accuracy can likely be refined by training directly to radiologist-assigned bone ages.

S5.3.1

FOLLOW-UP MRI AFTER INTRA-ARTERIAL CHEMOTHERAPY FOR RETINOBLASTOMA: SIGNIFICANCE OF OPTIC NERVE ENHANCEMENT

LIESBETH Cardoen¹, ARNAUD Gauthier¹, ALEXANDRE Matet¹, NAYLA Nicolas¹, LIVIA Lumbroso-Le Rouic¹, ISABELLE Aerts¹, PAUL Freneaux¹, NATHALIE Cassoux¹, FRANÇOIS Doz¹, RAPHAËL Blanc², HERVÉ J. Brisse¹

¹ Institut Curie, Paris, FRANCE

² Hôpital Fondation Adolphe de Rothschild, Paris, FRANCE

Purpose

Follow-up MRI after intra-arterial chemotherapy (IAC) for conservative treatment of retinoblastoma (RB) is performed to assess both the tumor shrinkage and the normality of optic nerve (ON), especially for tumors located close to the optic disk. ON enhancement may be observed and needs appropriate interpretation.

Material and Methods

Retrospective review of all children with RB without extraocular invasion treated with IAC at our institution since 2010 (n=139). Eligible patients were children with at least 1 MRI before and 1 MRI during or after IAC.

Results

Among the 35 eligible children, ON enhancement without ON enlargement was identified in 7 (20%). The interval between the last IAC and MRI varied between 1 to 12 months.

Secondary enucleation was decided in 6/7 patients and histopathological analysis never identified ON tumor invasion but showed fibrotic and inflammatory modifications.

For the conservatively treated patient, the enhancement of the optic nerve has completely disappeared after 21 months.

All 7 patients are currently in complete remission (follow-up range between 9 months and 7 years).

Conclusion

ON enhancement on follow-up MRI after IAC for RB is a common finding and should not be interpreted as tumor invasion.

S5.3.2

MAGNETIC RESONANCE ELASTOGRAPHY OF PEDIATRIC GLIOMAS: A PRELIMINARY EXPERIENCE

RAHUL Nikam¹, GRACE Mcilvain², VINAY Kandula¹, GURCHARANJĒET Kaur¹, ANDREW Walter¹, LAUREN Averill¹, ARABINDA Choudhary³, CURTIS Johnson²

¹ Nemours Alfred I. duPont Hospital for Children, Wilmington, USA

² University of Delaware, Newark, USA

³ University for Arkansas for Medical Sciences, Little Rock, USA

Purpose/Aim:

Compare the stiffness of pediatric gliomas with stiffness of uninvolved/contralateral white matter.

Materials and Methods:

Imaging technologies capable of “virtual histology” offer some of the best prospects for detecting and assessing neuropathology noninvasively. Accordingly, quantitative measures of neural tissue microstructure are at the forefront of neuroimaging technology development. Magnetic resonance elastography (MRE) is a promising technique for sensitively evaluating the health of the brain and characterizing pediatric gliomas through their viscoelastic mechanical properties.

We prospectively enrolled 7 pediatric patients (3–18 years) with pediatric gliomas and minimum tumor dimension of 15 mm. For each subject, brain MRE data were collected as an add-on scan at the end of clinical MRI scan protocol. All studies were performed using a GE 3T MR/PET scanner. Single-shot echoplanar imaging (EPI) sequence was used for fast, motion-robust imaging of MRE displacement data with whole-brain coverage and 2.5 mm isotropic spatial resolution. The MRE sequence is synchronized with external vibration at 50 Hz delivered to the head by a pneumatic actuator system and soft pillow driver (Resoundant; Rochester, MN). The MRE imaging scan time is 3 min 15 s. MRE data are input to nonlinear inversion (NLI) algorithm that returns the viscoelastic shear stiffness.

Our preliminary data suggest that pediatric gliomas are softer than normal uninvolved white matter, with average tumor stiffness ranging from 1.99 +/- 0.48 kPa to 2.55 +/- 0.78 kPa. The average brain stiffness (excluding the tumor) ranged from 2.64 +/- 0.68 kPa to 2.83 +/- 0.72 kPa. In all cases examined, the tumor was softer than surrounding tissue, and in most cases significant heterogeneity in properties was observed.

Conclusion:

To our knowledge, this is the first study evaluating the role of MRE in pediatric gliomas. Our preliminary data suggest that pediatric gliomas are softer than normal uninvolved white matter. Further work will compare MRE measures with tumor grade and histopathology.

S5.3.3

MAGNETIC RESONANCE FEATURES AND CRANIAL NERVE INVOLVEMENT IN PEDIATRIC HEAD AND NECK RHABDOMYOSARCOMA

GIACOMO Talenti¹, STEFANIA Picariello², CAROLINE Robson³, RUSSO Carmela⁴, SLATER Olga⁵, MERTIRI Livja⁶, BISDAS Sotirios⁷, MASSIMO ERALDO Abate⁸, PERROTTA Silverio⁸, RICHARD Hewitt⁹, KSHITIJ Mankad⁶, FELICE D'Arco⁶

¹ Azienda Ospedaliera Universitaria di Verona, Neuroradiology Unit, Verona, ITALY

² Department of Woman, Child and General and Specialized Surgery, University of Campania Luigi Vanvitelli, Naples, ITALY

³ Boston Children's Hospital, Department of Radiology, Boston, Massachusetts, USA, Boston, USA

⁴ Neuroradiology Department, Santobono Childrens Hospital, Naples, ITALY

⁵ Neuro Oncology Department, Great Ormond Street Hospital for Children, London, UNITED KINGDOM

⁶ Great Ormond Street Hospital for Sick Children, Neuroradiology Department, London, UNITED KINGDOM

⁷ Lysholm Department of Neuroradiology, The National Hospital for Neurology and Neurosurgery, Queen Square 8-11, London WC, London, UNITED KINGDOM

⁸ Pediatric Oncology, AORN Santobono-Pausilipon, Naples, ITALY

⁹ Ear, Nose and Throat Surgery Department, Great Ormond Street Hospital for Children NHS Trust, London, UNITED KINGDOM

BACKGROUND AND PURPOSE
Rhabdomyosarcoma (RMS) is a high-grade malignant tumor composed of small round blue cells resembling skeletal muscle. Although it has been previously reported, the frequency and characteristics of cranial nerve involvement in pediatric head and neck RMS have been scarcely investigated. The aim of this study is to review the radiological features of a large cohort of pediatric head and neck RMS reported with a special focus on cranial nerve involvement in relation to location and magnetic resonance (MR) features of the tumors.

MATERIALS AND METHODS

We retrospectively searched the electronic patient record system of 3 tertiary hospitals for MR studies of pathologically confirmed pediatric head and neck rhabdomyosarcomas over a 10 years period. Cranial nerve involvement was defined as radiologically apparent macroscopic tumor extension along a nerve and/or the presence of secondary signs such as fat pads obliteration or muscle denervation. Scans were reviewed by two pediatric neuroradiologists, blinded to clinical data, and a consensus agreement was reached in case of discordant findings.

RESULTS

Among 68 cases meeting inclusion criteria, 52 had diagnostic images. Histologically, 39/52 were Embryonal RMS while 13/52 were Alveolar RMS. Lymph nodes metastases were present 19.2%. Cranial nerve involvement was present in 36.5%. Nerves were mainly involved as a direct extension of the mass through skull base foramina or after invasion of cavernous sinus, Merkel's cave, orbital apex or stylomastoid foramen, which appeared enlarged.

CONCLUSIONS

Cranial nerve involvement is frequent in pediatric H&N RMS, but is secondary to “geographic” invasion due to direct extension through skull base foramina or cavernous sinus. These tumors never showed distant perineural metastatic disease like in cases of adult H&N carcinomas. This implies a different biological interaction between the nerves and these tumours in comparison.

S5.3.4

RADIOLOGIC CHARACTERIZATION OF PEDIATRIC POSTERIOR FOSSA EPENDYMOMAS: THE ROLE OF NEUROIMAGING IN DISTINGUISHING MOLECULAR SUBTYPES

JORGE Kim¹, FABRICIO Goncalves¹, LUIS Tierradentro-Garcia¹, ALIREZA Zandifar¹, ADARSH Ghosh², DMITRY Khrichenko¹, ANGELA Viaene³, CESAR Alves¹, SARA Teixeira¹, SAVVAS Andronikou^{1,4}, ARASTOO Vossough^{1,4}

¹ Department of Radiology, Division of Neuroradiology, The Children's Hospital of Philadelphia, Philadelphia, USA

² Department of Radiology, Division of Body Imaging, The Children's Hospital of Philadelphia, Philadelphia, USA

³ Department of Pathology and Laboratory Medicine, Perelman School of Medicine, University of Pennsylvania, Philadelphia, USA

⁴ Department of Radiology, Perelman School of Medicine, University of Pennsylvania, Philadelphia, USA

Purpose: There are two well-defined posterior fossa ependymoma (PF-EPN) molecular subgroups, PF-EPN-A and PF-EPN-B, with overlapping imaging features. We aim to determine the neuroimaging role in distinguishing PF-EPN molecular subgroups in children.

Methods: 19 biopsy-proven PF-EPN cases were retrospectively reviewed. Demographic and clinical data were retrieved from electronic charts. A neuropathologist determined the molecular subgroups by H3K27me3 immunohistochemical staining. A pediatric neuroradiologist, blinded to clinical and molecular data, reviewed preoperative features (MRI and, when available, CT). Features were tumor volume(TV), contrast-enhancing component volume(CETV), location/extension, T1WI/T2WI/FLAIR signal, contrast enhancement(CE), apparent coefficient diffusion(ADC), cysts/necrosis, hemorrhage, calcification, mass effect, edema, invasion, hydrocephalus, and metastases. Fisher's exact test was used for statistical analysis. Data are presented as median(IQR).

Results: 12(63.2%) male and 7(36.8%) female aged 2.7(1.2-5.0)years (range 0-17) were found. There were 12(63.2%) PF-EPN-A, 6(31.6%) PF-EPN-B, and 1(5.2%) with unknown status. TV was 25.5(17.3-38.6)cm³, CETV was 8.1(3.4-18.9)cm³ with CETV/TV ratio of 40.4(9.5-73)%. Tumors were centered in the 4th ventricle(4V) (n=15) and the cerebellopontine angle(CPA) cistern (n=4). Within the 4V and in relation to the fastigial point, tumors were either caudal (27.8%), mostly caudal with rostral extension (72.2%), but never rostrally alone. From the 4V, tumors extended to the CPA cistern (n=3), cisterna magna(CM) (n=11), Luschka/Magendie foramina(L/MF) (n=13), cervical spine(CS) (n=9), and prepontine cistern(PPC) (n=1). From the CPA cistern, extension occurred to the 4V (n=2), CM (n=2), L/MF (n=2), supratentorial compartment (n=1), CS (n=3), and PPC (n=2). 36.8% were purely solid, and 63.2% had cyst/necrotic components. ADC was 1118.5(1068-1193) in PF-EPN-A and 1086.6(1033-1132) in PF-EPN-B. CE was seen in PF-EPN-A (91.7%) and in all PF-EPN-B. Hemorrhage (42%), calcification (37%), mass effect (84%), edema (11%), and hydrocephalus (89%) were also found. None had metastases or invasion. Calcification was seen in PF-EPN-A (63.6%) and absent in PF-EPN-B, which showed statistical significance to distinguish molecular subgroups (p<0.05).

Conclusion: Many qualitative/quantitative features did not distinguish between PF-EPN subgroups. Absence of calcification could potentially predict PF-EPN-B in children.

S5.3.5

PATIENTS DOSE COMMUNICATIONS IN PEDIATRIC SETTING FOR COMMONS RADIOLOGICAL EXAMINATIONS: WHAT THE PARENTS WANT TO KNOW

MARIO Pace¹, DOMENICO Gagliano¹, CLAUDIO Granata², ANDREA Magistrelli³, SERGIO Salerno¹, PAOLO Toma³

¹ Dipartimento di Biomedicina, Neuroscienze e Diagnostica avanzata, Policlinico Università di Palermo, Palermo, ITALY

² SCR di Radiologia Institute for Maternal and Child Health - IRCCS Burlo Garofolo, Trieste, ITALY

³ Dipartimento Diagnostica per Immagini IRCCS Ospedale pediatrico Bambino Gesù Roma, Rome, ITALY

Purpose:

The directive 59/2013 provides that patients in Europe are informed about the radiation dose received for radiological procedure; furthermore, the International Atomic Energy Agency (IAEA) affirms that the professionals must to inform patients about the potential benefit of the radiological procedure and the risks.

Purpose of this study was to investigate the interest of children's parents in knowing the exposure dose to ionizing radiation for radiological examinations and to identify a simple explanatory way in communicate the personal and possible variables.

Materials and methods:

Parents of patients that undergo to non-urgent radiological procedures were recruited. After

an informative text, an anonymous questionnaire was administered to parent's including personal data sheet (sex, age, educational qualification and occupation), to assess the understanding of the information sheet, interest in knowing the radiation dose with 4 different communication

modalities. First modality include dose amount derived from the x ray apparatus; second modality include dose amount with a referee range derived from the national DRL; thirds modality include a comparison with x-ray equivalent dose and the natural background; fourth modality the x-ray symbol and a colorimetric scale ranging from green to red.

Results

30 parents in two paediatric centres, participated in the study. The informative text was clear for all parents. Almost all patients were interested in knowing x-ray dose used.

The second modality with dose amount and referee range derived from the national DRL was preferred by graduated and working parents. Fourth modality with x-ray symbol and a colorimetric scale was instead preferred by ungraded and unemployed.

Conclusions

There is in general an interest knowing the dose exposure. Different choice in our sample demonstrated that communication should be individualized and must take in account the socio-cultural differences.

S5.4.1

EFFICIENCY OF RADIOLOGISTS WORKING FROM HOME DURING A PANDEMIC AT A QUATERNARY PEDIATRIC ACADEMIC HOSPITAL

ANDREW Sher, SIDDHARTH Jadhav, VICTOR Seghers, NILESH Desai, THIERRY Huisman, MARLA Sammer

Texas Children's Hospital - Department of Radiology, Baylor College of Medicine, Houston, USA

Purpose:

Secondary to the Covid-19 pandemic, Neuroradiologists worked assignments from at-home workstations. To determine the effect of working from home on efficiency, productivity, quality and safety, we evaluated turn-around time (TAT), volume of studies, and error rates from at-home workstations compared to in-hospital.

Materials and Methods:

For each neuroradiologist, number of CT and MRI studies, TATs, and error rates were evaluated from 4/1/2020 thru 9/30/2020. TAT were defined as interval between "study completed" and "final read" timestamps. Studies requiring 3D post-processing, performed overnight, or performed on trainee rotations were excluded. As a group, median TATs and error rates were compared for studies read at-home vs in-hospital. For radiologists who worked >5 rotations at-home and in-hospital, mean and median TATs and volumes were compared. Two-tailed T-test was used for statistical significance of differences in means, Fisher's exact for error rates.

Results:

2597 CTs (1897 at-home, 700 in hospital) and 3685 MRIs (2601 at-home, 1084 in-hospital) met inclusion criteria. For CT's, the median TAT for all neuroradiologists combined was 34 minutes +/- 106 minutes at-home and 31 minutes +/- 85 minutes in-hospital. For MRIs, median TAT was 81 minutes +/- 129 minutes at-home and 79 +/- 109 minutes in-hospital. For individual radiologists meeting inclusion criteria, most had statistically significantly shorter TAT at-home and with an increase in mean number of studies read at-home, though some were fewer (Table 1). There was a statistically significant decrease in error rates at-home (p=0.0082), with 18 peer reviews on 4498 studies read at-home (.4%) compared to 18 on 1784 read in-hospital (1%).

Conclusion:

There was variability in individual radiologists' productivity and efficiency when working from home vs in-hospital. As a group, near equivocal TATs were appreciated with no decrease in quality. The decision to work at-home vs in-hospital may best be based on local factors, balancing variability among individual radiologist's and the institution's needs and preferences.

S5.4.2

A PHANTOM STUDY FOR DEEP LEARNING BASED CT IMAGE CONVERSION IMPROVING REPRODUCIBILITY OF RADIOMICS FOR PEDIATRIC ABDOMEN CT

SEUL BI Lee¹, YEON JIN Cho¹, SEUNGHYUN Lee¹, YOUNG HUN Choi¹, JUNG-EUN Cheon¹, WOO SUN Kim¹, YOUNGTAEK Hong², HACKJOON Shim², DAWUN Jeong³

¹ Seoul National University Hospital, Seoul, SOUTH KOREA

² CONNECT-AI Research Center, Yonsei University College of Medicine, Seoul, SOUTH KOREA

³ Division of Biomedical Engineering, Hankuk University of Foreign Studies, Yongin, Seoul, SOUTH KOREA

Objectives: This study aimed to evaluate the usefulness of deep learning based image conversion to improve reproducibility of CT radiomics feature

Materials and Methods: This study was conducted with pediatric body phantom with liver nodules. We obtained CT images under various CT parameters and reconstruction kernel. Total 12 different kind of images (a. 100 kVp/30 mAs with iterative reconstruction (IR), b. 100 kVp/30 mAs with filtered back projection (FBP), c. 100 kVp/60 mAs with IR, d. 100 kVp/60 mAs with FBP, e. 100 kVp/120 mAs with IR, f. 100 kVp/120 mAs with FBP, g. 120 kVp/30 mAs with IR, h. 120 kVp/30 mAs with FBP, i. 120 kVp/60 mAs with IR, j. 120 kVp/60 mAs with FBP, k. 120 kVp/120 mAs with IR, l. 120 kVp/120 mAs with FBP) was obtained 10 times each. We developed image conversion algorithm using residual feature aggregation network to reproduce radiomics feature. To evaluation of variability of radiomic features, region of interest was drawn by single radiologist with targeting liver parenchyme and live nodules. Measurement variability was assessed by concordance correlation coefficient (CCC). In total, 18 types of the first order intensity features and 68 types of texture features were evaluated by CCC.

Results: Original images without image conversion with algorithm showed excellent CCC in the first order intensity features (CCC, 0.9704–0.9998) but, poor CCC in texture features (CCC, 0.176–0.919). After applying developed algorithm, converted images showed improvement of the reproducibility of texture features (CCC, 0.9100 – 0.9806), regardless of CT parameters and types of kernels/

Conclusions: Our study demonstrated a deep learning model for the image conversion could reduce the effect of CT parameters and types of kernels and may improve the reproducibility of radiomic features in pediatric abdomen CT.

S5.4.3

AI IN PAEDIATRIC RADIOLOGY: AN INTERNATIONAL SURVEY OF HEALTHCARE PROFESSIONALS' OPINIONS

SUSAN Shelmerdine, OWEN Arthurs

Great Ormond Street Hospital for Children, London, UNITED KINGDOM

Purpose

Despite widespread hype and interest in artificial intelligence (AI) for adult radiology, less is known about how AI might impact paediatric radiology. The aim of this study was to evaluate the attitudes, perceptions and suggested areas for future development relating to AI amongst healthcare professionals working within children's imaging services.

Methods

A web-based questionnaire was designed using Google Forms and distributed to the membership of several paediatric and general radiological societies (ESPR, SPR, ANZSPR, BMUS, SoR) over a 4 month period

(Feb – June 2020). The survey was voluntary and responses were anonymous. Survey questions covered participant demographics, attitudes towards AI in general, future impacts and suggested areas for development within paediatric imaging.

Results

A total of 240 responses were collected (113/240, 47.1% male), with the majority being radiologists (159/240, 66.3%), or allied healthcare professionals 31.3% (75/240). Respondents agreed that AI could potentially alert radiologists to abnormal pathologies in radiological examinations (61.7%, 148/240) but felt that results should still be checked by a human. The majority did not believe jobs in paediatric radiology would be replaced by AI (85.4%, 205/240), nor that paediatric radiology would be more adversely affected than other radiological subspecialties (54.6%, 131/240). Important driving forces behind development of AI tools should focus on improved diagnostic accuracy (77/240, 32.1%), workflow efficiencies (60/240, 25%) and patient safety (54/240, 22.5%). The majority of ESPR members who responded (82.7%, 67/81) welcomed the idea of a dedicated ESPR AI taskforce, to lead on specific AI imaging developments optimised for children, particularly educational events and anonymised dataset curation, and help to guide regulatory assessments.

Conclusion

Most healthcare professionals working in paediatric radiology have a positive outlook regarding usage of AI in their specialty and did not feel their jobs were at risk. Most welcomed the opportunity for further educational activities in this field, including a specialty focussed ESPR taskforce.

S5.4.4

E-PEER LEARNING: OUR MULTI-INSTITUTION EXPERIENCE

KATHLEEN Schenker¹, ANGIE Miller², CICERO Silva³, DOUGLAS Mooto⁴, SHAILEE Lala⁵, SARAH Milla⁶, JONATHAN Loewen⁶, MONICA Epelman⁷

¹ Department of Medical Imaging, Nemours/Alfred I duPont Hospital for Children, Wilmington, DE, USA

² Department of Pediatric Radiology, University of Colorado School of Medicine, Children's Hospital of Colorado, Aurora, CO, USA

³ Department of Radiology and Biomedical Imaging, Yale School of Medicine, New Haven, CT, USA

⁴ Department of Radiology, Connecticut Children's Medical Center, Hartford, CT, USA

⁵ Department of Radiology, New York University School of Medicine, New York, NY, USA

⁶ Division of Pediatric Radiology, Emory University School of Medicine, Children's Healthcare of Atlanta, Atlanta, GA, USA

⁷ Department of Radiology, Nemours Children's Hospital, Orlando, FL, USA

Background:

Recently there has been a shift in radiology away from a peer review model toward a peer learning model, focusing more on collaborative learning, creating an environment more accepting of medical errors and embracing learning opportunities. As stated in the 2015 Institute of Medicine report, organizations that embrace error as learning opportunities outperform those that do not.

Purpose:

To create an e-Peer Learning group to increase collaborative sharing of learning opportunities across institutions and assess the utility of the program among participants.

Materials and Methods:

The e-Peer Learning group consists of radiologists from 6 different pediatric radiology institutions. The representative members have exchanged

short presentations of 1-3 learning cases monthly since 11/2017, including missed, difficult, classic, or unusual diagnoses. The format is of the case and imaging, followed by a few important learning points. Cases are then shared more widely amongst all the radiologists at the participating institutions. We recently distributed a survey to participants for feedback about the program.

Results:

60 radiologists participated in the survey, representing each participating institution. Participants were asked a few questions on a scale of 1-5 (1 highest; 5 lowest). Regarding the educational value of the cases, 40 participants (67.8%) answered the highest educational value of 1, and another 13 (22%) gave a value of 2. Regarding how much new information was learned, 34 participants (56.67%) gave a rating of 1 (learned a lot) while another 18 (30%) gave a value of 2. 29 participants (48.33%) said the cases have changed their practice. Overall, 58/60 (96.67%) stated that they wish to continue receiving cases.

Conclusion:

Our e-Peer Learning group has successfully created a non-punitive, collaborative learning environment across multiple institutions. Our survey has shown that participants value the program and have learned new information that may potentially change clinical practice. We believe this model can be expanded or adapted to other groups.

S5.4.5

THE EVOLUTION OF A PEDIATRIC RADIOLOGY ELECTIVE: A SHIFT FROM READING-ROOM BASED INSTRUCTION TO A HYBRID MODEL OF LEARNING

MELISSA Hilmes¹, JACOB Ramsey², SUDHA Singh¹

¹ Vanderbilt University Medical Center, Nashville, Tennessee, USA

² Vanderbilt School of Medicine, Nashville, Tennessee, USA

Purpose:

At the height of the pandemic, there was a sudden need for distance learning. We successfully converted a reading room-based advanced elective in pediatric radiology into case-based modules that preserved our curriculum but allowed remote learning. It was a huge success, and the dynamic is now permanently shifted from traditional in-person, reading room-based teaching to a hybrid model. We describe the evolution of the course and our experiences.

Materials and Methods:

Asynchronous component: Case-based modules were created and grouped by modality: Each module references 5-7 cases with companion cases. Written didactic material and questions accompany each case. Students complete the modules at their pace over the 4-week course and complete weekly short essay questions to provide accountability and demonstrate understanding.

Synchronous learning took the form of weekly videoconferencing meetings or in-person sessions to review the materials and check on the learners' progress.

Results:

The distance learning modules were well-received and successful. Students enjoyed moving through the material at their own pace. Students became more comfortable in operating the PACS and found the essay questions useful in consolidating knowledge. The remote students performed similarly on the post-test to other groups. The elective scored perfectly on evaluations.

As some restrictions eased, the course has evolved to a hybrid experience, with the asynchronous learning modules at the center of the curriculum with supplemental time in the reading room and in-person didactic teaching. The reading room time helps to fill in gaps and provide "hands-on" portions of the curriculum. The synchronous didactics provide a forum for answering students questions rather than an old model of strict content delivery. This hybrid model did not negatively impact the student performance.

This hybrid model also accommodates pediatric residents better, as they have a more fragmented experience due to scheduling constraints.

Conclusions:

Our traditional reading room model of teaching has evolved. There has been a shift towards asynchronous learning and a "flipped-classroom" approach with the case-based modules that we developed. This sudden need for remote materials accelerated a change towards asynchronous learning and forced the teachers to be more open to explore new methods and bring them more in line with the needs and abilities of the new generation learners.

S6.2.1

2D SHEAR WAVE ELASTOGRAPHY IN STRICTURING CROHN'S DISEASE: CORRELATION WITH HISTOLOGY AND CONVENTIONAL US FINDINGS

NADEEN Abu Ata¹, JONATHAN R. Dillman^{1,2}, JONATHAN M. Rubin³, LAURA A. Johnson⁴, MARGARET Collins^{2,5}, LEE A. Denson^{2,6}, PETER D. Higgins⁴

¹ Cincinnati Children's Hospital Medical Center - Department of Radiology, Cincinnati, USA

² University of Cincinnati - College of Medicine, Cincinnati, USA

³ University of Michigan - Department of Radiology, Michigan, USA

⁴ University of Michigan - Division of Gastroenterology and Hepatology, Michigan, USA

⁵ Cincinnati Children's Hospital Medical Center - Division of Pathology, Cincinnati, USA

⁶ Cincinnati Children's Hospital Medical Center - Division of Gastroenterology and Hepatology, Cincinnati, USA

Purpose

To evaluate the associations between bowel wall stiffness, as measured by 2D ultrasound (US) shear wave elastography (SWE) and 1) conventional US findings of pediatric Crohn's disease (CD), and 2) correlative histology from surgically resected intestinal strictures.

Methods

Prospective research US exams (gray-scale, color Doppler, and 2D SWE) were performed in 18 pediatric patients with CD within 1 week of ileal resection (Acuson S3000; Siemens). Bowel wall shear wave speed (SWS) measurements were obtained from the area of stricturing without and with abdominal strain (0%, 10%, 20%) using a 9L4 transducer. Gray-scale findings, such as bowel wall thickness (mm), were documented; color Doppler signal in the bowel wall was scored 1-4 (0=no signal, 4=marked bowel wall and adjacent mesenteric signal). Transmural bowel wall tissue specimens were obtained from resected intestine corresponding to the imaged sites and were scored for fibrosis and increased smooth muscle, blinded to US findings. Spearman correlation was used to assess the relationships between SWS measurements and 1) conventional US findings of CD, and 2) histology scores. Mann-Whitney U test was used to compare continuous data between groups.

Results

Median age was 16.5 years (IQR: 14.8-18.0); 10/18 patients were female (56%). Overall mean bowel wall SWS at 0%, 10%, and 20% abdominal strain was 2.50, 2.68, and 2.91 m/s, respectively. There was no significant association between bowel wall SWS and conventional gray-scale US findings. However, bowel wall SWS decreased with increasing color Doppler signal ($p=0.0017$ at 0% abdominal strain). At histology, there were no significant correlations between bowel wall SWS and intestinal fibrosis ($p>0.05$). Bowel wall SWS was positively associated with muscularis propria thickening at all levels of abdominal strain ($\rho=0.56-0.72$, $p=0.002-0.03$).

Conclusion

Smooth muscle hyperplasia/hypertrophy, but not fibrosis is associated with increased bowel wall stiffness in stricturing pediatric small bowel CD. Increasing bowel wall color Doppler blood flow is associated with

decreasing SWS measurements.

S6.2.2

EFFECT OF BIOLOGIC THERAPY ON MESENTERIC BLOOD FLOW USING VELOCITY-ENCODED PHASE CONTRAST MRI IN NEWLY DIAGNOSED SMALL BOWEL CROHN'S DISEASE

NADEEN Abu Ata¹, JONATHAN R. Dillman^{1,2}, JEAN A. Tkach^{1,2}, DEEP B. Ghandi¹, LEE A. Denson^{2,3}

¹ Cincinnati Children's Hospital Medical Center - Department of Radiology, Cincinnati, USA

² University of Cincinnati - College of Medicine, Cincinnati, USA

³ Cincinnati Children's Hospital Medical Center - Division of Gastroenterology, Hepatology and Nutrition, Cincinnati, USA

Purpose

To assess changes in mesenteric blood flow (BF) using velocity-encoded phase contrast MRI (PCMRI) in newly diagnosed small bowel Crohn's disease (CD) patients treated with biologic (antiTNF) therapy.

Material and Methods

We prospectively performed research MRI exams in 15 healthy control subjects (mean age= 18 yr) and 14 pediatric patients (mean age=14 yr) with newly diagnosed small bowel CD treated with biologic therapy. Research MRI exams were performed at diagnosis, six weeks into treatment, and after six months in CD patients. PC-MRI (using standardized Velocity-Encoded parameters) was performed through the mesenteric root, at the level of the renal arteries. BF was measured in abdominal aorta (Ao), superior mesenteric artery (SMA), and superior mesenteric vein (SMV). Two radiologists independently reviewed anatomic images and provided simplified MARIA (sMARIA) scores for the most inflamed small bowel segment. The Mann-Whitney U test was used to compare BF measurements and sMARIA scores in CD patients and control subjects. Mixed models were used to evaluate changes in BF measurements and mean sMARIA scores over time in CD patients. Spearman correlation was used to assess relationship between BF measurements and mean sMARIA scores.

Results

SMV/Ao and SMA/Ao BF ratios in CD patients at baseline vs. control subjects were 0.32 vs 0.23 ($p=0.018$) and 0.44 vs 0.30 ($p=0.011$), respectively. At 6 weeks and 6 months, SMV/Ao BF decreased to 0.29 and 0.21 ($p=0.042$) and SMA/Ao BF decreased to 0.30 and 0.27 ($p=0.029$), respectively. Mean sMARIA score for both readers was 4.5 at baseline, 2.5 at 6 weeks, 2.0 at 6 months ($p=0.002$). There was moderate positive correlation between mean sMARIA scores and SMV/Ao ($\rho=0.49$; $p=0.0005$) and SMA/Ao ($\rho=0.37$; $p=0.011$)BF.

Conclusion

Mesenteric BF can be quantified in CD patients, decreases in response to biologic therapy, and is a potential novel biomarker of inflammation in small bowel CD.

S6.2.3

DISTINGUISHING TERMINAL ILEITIS FROM LYMPHOID NODULAR HYPERPLASIA IN PEDIATRIC CROHN DISEASE - DOES USE OF STANDARDIZED NOMENCLATURE HELP WHEN REPORTING MRE?

ABDULLAH Alshabanat¹, GHUFRAN Alhashmi², DENISE Castro³, JOSEPH Yang³, CATHARINE Walsh⁴, AFSANEH Amirabadi⁴, OSCAR Navarro⁴, JUAN Putra⁴, IRAM Siqqiqi⁴, MARY -LOUISE Greer⁴

¹ King Faisal Specialist Hospital and Research Center, Riyadh, SAUDI ARABIA

² King AbdulAziz University Hospital, Jeddah, SAUDI ARABIA

³ Kingston Health Sciences Centre/Queen's University, Kingston, CANADA

⁴ The Hospital for Sick Children/University of Toronto, Toronto, CANADA

BACKGROUND

Overlap in magnetic resonance enterography (MRE) features of mild inflammation of terminal ileum (TI) in pediatric Crohn disease (CD) and lymphoid nodular hyperplasia (LNH) can confound diagnosing inflammatory bowel disease and differentiating CD from ulcerative colitis, especially if only TI is affected. We applied MRE consensus guidelines for CD to TI to determine if specific imaging features could help distinguish CD from LNH.

METHODS AND MATERIAL

A single centre, ethics board-approved, retrospective study was performed in 66 patients < 18 years who had MRE and ileocolonoscopy with biopsy within 6 months. Radiology and pathology database searches by a medical student identified 3 groups of 22 patients each with TI defined on MRE as normal, LNH or CD. After randomization, blinded independent MRE review was performed by 2 readers (a pediatric radiologist and radiology fellow), discrepancies resolved by a 3rd pediatric radiologist. MRE enteric features included bowel wall thickening (BWT), length, T2-weighted (T2W) hyperintensity, enhancement, ulceration, symmetry, restricted diffusion (DWI) and stricture. Extra-enteric features were comb sign, fibrofatty proliferation (FFP), mesenteric T2W hyperintensity and enhancement, and penetrating disease. MRE consensus data was compared with histopathology, TI classified on review by a pathologist as normal (0), LNH only (1) or CD +/- LNH (2). Statistical analyses compared MRE TI enteric and extra-enteric features with these categories. $P < 0.05$ was considered statistically significant using the Kruskal-Wallis test for continuous and Fisher exact test for categorical variables.

RESULTS

Of 66 patients, mean age 13.4 (range 7-17) years at MRE, 30 (45.5%) were female. TI by histopathology was class 0 in 25 (37.9%), 1 in 13 (19.7%) and 2 in 28 (42.4%). TI BWT was statistically significantly increased in CD with increased severity compared with LNH and normal TI ($p=0.00012$). Wall T2W hyperintensity, hyperenhancement and DWI were also significantly increased in CD versus LNH and normal bowel ($p < 0.001$, $= 0.00021$, $= 0.001$), especially DWI referenced to lymph nodes ($p=0.00018$). Of extra-enteric features, only FFP was significantly associated with CD versus LNH or normal TI ($p=0.029$).

CONCLUSION

Using standardized nomenclature for MRE interpretation, enteric features (BWT, T2W hyperintensity and high DWI relative to lymph nodes) perform better than extra-enteric features in distinguishing CD from LNH in TI.

S6.2.4

EXPERIENCE WITH PEDIATRIC APPENDICITIS DURING THE COVID-19 PANDEMIC AT A REFERRAL PEDIATRIC HOSPITAL

ANDREW Sher, PAUL Guillerman, VICTOR Seghers, RIDA Salman, ANANTH Annapragada, MARLA Sammer
Texas Children's Hospital, Baylor College of Medicine, Houston, USA

Background: Although initially associated with severe acute respiratory syndrome, COVID-19 is increasingly recognized with extrapulmonary manifestations, including gastrointestinal. We report our experience with pediatric appendicitis during the COVID-19 pandemic.

Methods: Patients who underwent ultrasonography (US) for possible appendicitis since the local onset of the COVID-19 pandemic April 1, 2020 were identified and differences in positivity based on pathology and perforation based on ultrasound were compared to the same time periods in 2019 and 2018. For 2020, the proportion of appendicitis in patients undergoing US for possible appendicitis were compared for patients with (COVID+) or without (COVID-) a positive COVID test. COVID+ rates in patients with appendicitis were also compared to an institutional surveillance positivity rate. Fisher's exact test was used to test rate differences.

Results: In 2020, the proportion of appendicitis in patients who underwent appendiceal US was significantly higher for COVID+ (47/105 = 44.8%) compared to COVID- patients (678/2828 = 24.0%), $p < 0.0001$. Among children with appendicitis, 6.5% (47/725) were COVID+ compared to institutional COVID surveillance positivity rate of 3.4% (1082/31173), $p < 0.0001$.

The prevalence of appendicitis was significantly higher in 2020 (725/2933 = 24.7%) than either 2019 (735/2941 = 20.0%) or 2018 (680/3243 = 21.0%), both $p < 0.0001$, while the prevalence did not significantly differ between 2018 and 2019 ($p = 0.3548$). Perforation rates were not significantly different by year (2020: 26.7%, 2019: 26.7%; 2018 22.7%), $p = 0.59$. Mean ages were 11.1, 10.3, and 10.3 years (age ranges 0-18), and proportion female 53.1%, 51.3%, and 52.4% in 2020, 2019, and 2018.

Discussion: A higher proportion of appendiceal US exams positive for appendicitis among COVID+ patients, a higher COVID positivity rate in patients with appendicitis compared to the institutional surveillance rate, and a higher prevalence of appendicitis during the COVID-19 pandemic suggest that appendicitis is a possible manifestation of COVID-19 in children. However, a significant difference in perforation rate is not associated with COVID-19.

S6.2.5

RADIOGRAPHIC ASSESSMENT OF TRACTION-INDUCED ESOPHAGEAL GROWTH PATTERNS AND TRACTION-RELATED COMPLICATIONS OF THE FOKER PROCESS FOR THE TREATMENT OF LONG GAP ESOPHAGEAL ATRESIA IN CHILDREN

ALEXANDRA Foust¹, BENJAMIN Zendejas-Mummert², SOMALA MOHAMMED², JAY MEISNER², THOMAS HAMILTON², DAVID ZURAKOWSKI³, STEVEN STAFFA⁴, RUSSELL JENNINGS², MICHAEL CALLAHAN¹

¹ Boston Children's Hospital: Department of Radiology, Boston, USA

² Boston Children's Hospital: Department of Surgery, Boston, USA

³ Boston Children's Hospital: Department of Orthopedics, Boston, USA

⁴ Boston Children's Hospital: Department of Anesthesia Research, Boston, USA

Purpose:

Investigate the utility of chest radiographs (CXR) for assessing esophageal growth and traction related complications in long gap esophageal atresia (LGEA) patients undergoing the Foker process (traction-induced esophageal growth).

Materials and Methods:

43 infants with a diagnosis of LGEA, treated with the Foker process at a single institution over a 6-year period were retrospectively evaluated. Portable CXR obtained between placement of the esophageal segments on external traction (Foker I) and primary anastomosis (Foker II) were evaluated. Metallic clips (leading and trailer) mark the traction system and esophageal tip location respectively. The distance between the trailer clips (non-subject to direct traction) on the proximal and distal esophageal segments were measured as a surrogate for esophageal gap length and the distance between the leading clips (subjected to traction) and the

trailer clips were measured (leading-to trailer clip distance) for each esophageal segment to assess traction system/esophageal integrity.

Results:

There were 43 infants; 18 female (42%) and 23 male (58%) with a median age of 5 months (IQR: 3-6 months). Median number of days on traction was 14 days (IQR: 10-17 days) and the median starting esophageal gap length was 4.5 cm (IQR: 3.7-5.5 cm). Median number of CXR per patient was 11 (IQR: 8-13). Median daily esophageal growth rate was 2.2 mm/day (IQR: 0.8-4.2 mm) for both segments, or 1.1 mm per segment, and median cumulative growth during traction was 23.6 mm (IQR 14.8-32.0 mm), or 11.8 mm per segment. The leading-to trailer clip distance per esophageal segment was significantly greater in patients with traction system complications compared to those without ($p < 0.001$). Specifically, a daily change of greater than 12.3% resulted in a sensitivity of 85.7% and specificity of 92.4% (AUC 0.853 [95% CI 0.667-0.999]) for detection of a traction complication; while a cumulative change over the traction period threshold of greater than 30.1% resulted in a sensitivity of 84.6% and specificity of 84.7% (AUC 0.874 [95% CI 0.748-0.999]) in identifying a traction complication.

Conclusions:

Chest radiography can help assess rate of esophageal growth in patients with LGEA undergoing the Foker process. A sudden change in leading-to trailer clip distance of an esophageal segment across two sequential radiographs or a more gradual change over the traction period are sensitive and specific indicators of traction related complications.

S6.2.6

ACNES – A COMMONLY OVERLOOKED CAUSE OF CHRONIC ABDOMINAL PAIN IN CHILDREN. PRELIMINARY RESULTS

SVEN Weum¹, THOMAS Augdal¹, NIKLAS Stabell², LENE Nymo Trulsen², THORSTEN Köhler¹, KAREN Rosendahl¹

¹ University Hospital of North Norway, Dept. of Radiology, Tromsø, NORWAY

² University Hospital of North Norway, Dept. of Pediatrics, Tromsø, NORWAY

Purpose

Chronic abdominal pain is defined as persistent or recurrent episodes of abdominal pain lasting for more than three months. In the majority of cases, no somatic cause is identified. Studies have shown that up to 30% of hospitalized adults presenting with abdominal pain have pain from the abdominal wall and not from intra-abdominal organs, many of these patients have anterior cutaneous nerve entrapment syndrome (ACNES). The prevalence of ACNES among children with chronic abdominal pain is unknown.

Abdominal wall nerves are not visible on ultrasound, but their accompanying perforating vessels may be visualized with color Doppler. We aimed to 1) identify tender areas in the abdominal wall indicative of ACNES and 2) examine the correlation between these tender abdominal wall areas and perforating vessels as seen on color Doppler.

Materials and Methods

100 consecutive children, aged 6-17 years, referred to the pediatric outpatient clinic at the University Hospital of North Norway due to chronic abdominal pain will be recruited. Excluded are those with abdominal pain due to other disease such as inflammatory bowel disease or tumor. After having filled in a questionnaire addressing the nature and timing of pain, the patients will have a clinical examination by a senior pediatrician. A novel ACNES probability score (APS) will be used to estimate the relative probability of ACNES. Finally, all children will have a standardized abdominal ultrasound examination performed by an experienced pediatric radiologist. In case a tender point indicating ACNES is found, color Doppler will be used to evaluate whether or not there is a neurovascular

bundle at the same location. The study has been approved by the Regional Ethics Committee, and written informed consent will be given by all participants and/or their caregiver(s) as appropriate.

Results

At the time of abstract submission (March 2021), 26 children (18 female, mean age 11.5 years) have been included in the study. Eight patients had clinical findings indicative of ACNES. In all eight, color Doppler ultrasound showed a vessel perforating the anterior rectus fascia that corresponded to the tender area. Updated results will be presented during the meeting.

Conclusions

Preliminary results indicate that ACNES might be a more common cause of chronic abdominal pain in children and adolescents than previously believed. Potential clinical implications will be discussed.

S6.3.1

RATE AND SEVERITY OF PHYSICAL ABUSE IN HOSPITALISED CHILDREN DURING THE FIRST UK WIDE COVID-19 ENFORCED NATIONAL LOCKDOWN

MICHAEL Paddock¹, AMAKA C Offiah^{2,3}, HELEN Cliffe⁷, DANIEL JA Connolly³, ROBERT Dineen⁸, RACHEL Dixon⁹, HARRIET Edwards¹⁰, EMILY Evans¹¹, KATH Halliday⁸, KANDISE Jackson¹², CAREN Landes¹⁰, ADAM Oates¹¹, NEIL Stoodley¹³, STAVROS Stivaros^{4,5,6}

¹ Barnsley Hospital NHS Foundation Trust, Barnsley, UNITED KINGDOM

² Academic Unit of Child Health, University of Sheffield, Sheffield, UNITED KINGDOM

³ Sheffield Childrens NHS Foundation Trust, Sheffield, UNITED KINGDOM

⁴ Academic Unit of Paediatric Radiology, Royal Manchester Children's Hospital, Manchester, UNITED KINGDOM

⁵ Division of Informatics, Imaging, and Data Sciences, School of Health Sciences, Faculty of Biology, Medicine, and Health, Manchester, UNITED KINGDOM

⁶ The Geoffrey Jefferson Brain Research Centre, University of Manchester, Manchester Academic Health Science Centre, Manchester, UNITED KINGDOM

⁷ Leeds Teaching Hospitals NHS Trust, Leeds, UNITED KINGDOM

⁸ Nottingham University NHS Foundation Trust, Nottingham, UNITED KINGDOM

⁹ Manchester University NHS Foundation Trust, Manchester, UNITED KINGDOM

¹⁰ Alder Hey Childrens NHS Foundation Trust, Liverpool, UNITED KINGDOM

¹¹ Birmingham Womens and Childrens NHS Foundation Trust, Birmingham, UNITED KINGDOM

¹² Pennine Acute Hospitals NHS Trust, Oldham, UNITED KINGDOM

¹³ North Bristol NHS Trust, Bristol, UNITED KINGDOM

INTRODUCTION

The SARS-CoV-2 pandemic resulted in enforced national lockdowns in the UK and other countries. Published literature suggests that cases of abusive head trauma (AHT) increased by 1493% between 23 March and April 2020 during the first UK lockdown (March to July 2020). We sought to determine the absolute rates of presentation and positive imaging findings of cases of suspected physical abuse (SPA) and AHT during this first lockdown and to compare injury incidence and severity to pre-lockdown rates.

OBJECTIVES

To assess the incidence and severity of positive SPA and AHT investigations in children during the first national lockdown in England, UK.

METHODS

Multicentre retrospective study. A radiology system search of 8 participating centres in England for pre- and post-mortem SPA imaging investigations (skeletal survey and CT data) was performed between January 2018 and July 2020. Demographic data, number and site of fractures, presence of intracranial haemorrhage (ICH) and hypoxic ischaemic encephalopathy (HIE) were captured.

RESULTS

Across all participating centres, serving an estimated population of 15,695,126 million, 1587 skeletal surveys (SS) were performed: 1282 (81%) antemortem, 762 (48%) male and positive findings in 582 (37%). Mean patient age was 10 months (range 1 day–16 years, median 6 months).

There were 838 skeletal fractures in 491 children in the pre-lockdown cohort (1.7 fractures/child) compared to 120 fractures in 91 children (1.3 fractures/child) during lockdown. There was no significant difference between positive/negative SS rates between the March–June 2018 ($p=0.08$) and 2019 ($p=0.90$) periods compared to 2020. There was no difference between absolute ratio of pre-/post-mortem SS performed pre-lockdown compared to the lockdown period ($p=0.45$).

Regarding head injury, there was no difference in absolute numbers ($p=0.43$). The incidence and rates (when appropriate imaging was available) of skull fracture 30/244 (12%), ICH 28/220 (13%) and HIE 10/205 (5%) during lockdown were similar to pre-lockdown rates 142/1304 (11%), 116/1152 (10%) and 68/1089 (6%), respectively.

CONCLUSION

This multicentre study has shown no increase in absolute numbers of SS performed in children or in the ratios of pre and post-mortem assessments during the first lockdown period in England. There was no increase in the number of skeletal fractures or head injuries, and the severity of head injury, when present, was not significantly increased during the lockdown period.

S6.3.2

THE IMPACT OF COVID-19 ON NON-ACCIDENTAL INJURY IN AN IRISH TERTIARY REFERRAL CENTRE

CAOIMHE McDonnell¹, ANGELA Byrne²

¹ St James Hospital, Department of Diagnostic Imaging, Dublin, IRELAND

² Children's Health Ireland at Crumlin, Department of Radiology, Dublin, IRELAND

Purpose

The COVID-19 pandemic has had an unprecedented effect on the daily lives of citizens of many affected countries. The most significant change that many countries have experienced is the implementation of so-called “lockdowns,” leading to restrictions and modifications of citizens’ daily lives. Internationally, many countries that implemented significant COVID-19 restrictions, have experienced increased rates of reported cases of domestic violence among adults. The aim of this study was to examine the effects of these restrictions on children in an Irish setting, in order to evaluate any increased incidence of NAI since the pandemic began.

Materials and Methods

A retrospective search was performed for skeletal survey examinations carried out at our institution, a tertiary referral paediatric hospital, between the dates of 1st March and 30th September 2019. The indications for these studies were reviewed, and the number of surveys for suspected non-accidental injury was tallied. A search with the same inclusion and exclusion criteria was then performed for the same time period in 2020. The types of injuries on initial and follow up surveys was tabulated.

Results

The number of patients who underwent skeletal surveys for suspected NAI during the 2019 six month time period, was 10. The number of patients from the 2020 six month period was 21. This reflects a 110% increase in the number of patients undergoing skeletal survey for suspected NAI during the lockdown period.

Conclusion

Based on our review, the reported increase in domestic violence in the adult population appears to be mirrored by an increase in rates of presentations of paediatric patients with suspected NAI. This information is pertinent to radiologists and clinicians working with children to inform their diagnostic and clinical decision-making. Our findings should also prompt discussion regarding the need for resource redirection to help detect and indeed help prevent NAI during times of pandemic-related restrictions.

S6.3.3

FATAL NON-ACCIDENTAL INJURY IN SOUTH AFRICA: A GAUTENG HOSPITAL'S PERSPECTIVE ON THE INCIDENCE AND FRACTURE TYPES ON POST-MORTEM SKELETAL SURVEYS

ROBYN MERYL Wessels², HALVANI Moodley^{1,2}

¹ Charlotte Maxeke Johannesburg Academic Hospital, Johannesburg, SOUTH AFRICA

² University of the Witwatersrand, Johannesburg, SOUTH AFRICA

Background:

In its severest form, non-accidental injury (NAI) in children is fatal. South Africa has been reported to have double the global average of child homicides. Autopsy is the main investigation in fatal NAI with post-mortem skeletal surveys (PMSS) playing an adjunctive role. In South Africa, however, there is limited availability of PMSS due to resource constraints. Whilst fracture patterns associated with NAI in living patients have been established, this has not been investigated in PMSS in South Africa.

Objectives:

Determine the incidence and characteristics of fractures in suspected fatal NAI cases, the incidence of fractures according to high, moderate and low specificity fracture locations for NAI and evaluate fracture dating.

Methods:

A retrospective review of all consecutive PMSS done between 1 January 2012 to 3 December 2018 at Charlotte Maxeke Johannesburg Academic Hospital was conducted.

Results:

There were 73 PMSSs in total, 52/73 (71.2%) had inadequate views and 39/52 (75%) had incorrect positioning. 33/73 (45.2%) demonstrated fractures. No statistical significance in sex was found: 38 (52.1%) were male and 35 (47.9%) were female. The mean age of those that sustained at least one fracture was 28 months (SD: 21 months). A total of 115 fractures were sustained. The top five most common bones fractured were the ribs 37/115 (32.2%), skull 20/115 (17.4%), ulna 13/115 (11.3%), femur 13/115 (11.3%) and radius 11/115 (9.6%). High specificity fracture locations accounted for 40/144 (27.7%). 17/33 (51.5%) of cases demonstrated acute fractures, 16/33 (48.5%) healing fractures and 5/33 (15.2%) chronic fractures.

Conclusion:

Our study is the first on PMSS findings in South Africa. Fractures found in PMSS were similar to those in live skeletal surveys and predominantly in those under 24 months of age. PMSS in the South African setting is a valuable adjunct to autopsy in detecting occult fractures of the limbs, as these are not routinely dissected on autopsy. We recommend that PMSS be performed in suspected fatal NAI cases at least in children up to 24 months of age. In our resource limited setting, the ongoing education of radiographers regarding

imaging technique, adherence to imaging protocols and general radiologists and radiology registrars on interpretative skills for PMSS are vital to improve the medico legal investigation of these fatalities.

S6.3.4

SKELETAL SURVEY IN SUSPECTED CHILD ABUSE – THE GERMAN WAY

MARK BORN

University of Bonn, Department of Radiology, Bonn, GERMANY

In 2019 a new, fully evidence-based German guideline concerning all aspects of Child-abuse has been adopted, the so called ‚Kinderschutzleitlinie‘. It includes the proceedings recommended for imaging in suspected child abuse. An extensive research of literature has been performed and the preexisting international guidelines from the American College of Radiology, the Royal College of Radiologists (GB), and the Royal Australian and New Zealand College of Radiologists have been taken into account.

Although based on the same evidence (i.e. literature), the German Guideline commission has decided to modify the Skeletal Survey proposed by other guidelines, thus reducing the required radiation exposure considerably: Imaging of the spine (lateral view) and the pelvis is only performed if the other plain film views of the skeletal survey show at least one fracture. On the other hand oblique views of the thorax and a follow up survey after two weeks are mandatory only, if no fracture is found on the survey.

This presentation will explain the proposed proceedings and present the underlying evidence.

S6.3.5

VALIDATION OF DIFFUSION TENSOR IMAGING OF THE PHYSIS AND METAPHYSIS AS PREDICTOR OF CHILD GROWTH

DIEGO Jaramillo¹, PHUONG Dong¹, JIE CHEN Nguyen², SOGOL Mostoufi-Moab², MICHAEL Nguyen², ANDREW Moreau², CHRISTIAN Barrera³, SHIJIE Hong², JOSE Raya⁴

¹ Columbia University Medical Center, New York, USA

² Children's Hospital of Philadelphia, Philadelphia, USA

³ Massachusetts General Hospital, Boston, USA

⁴ New York University Medical Center, New York, USA

Background: Diffusion tensor imaging of the physis/ metaphysis (DTI-P/M) depicts physal columns and provides measures of tract volume that may predict growth.

Objective: To validate DTI-P/M as predictive biomarker of height velocity (1-year height change from MRI) and total height gain (height change from MRI until after growth cessation).

Methods: We analyzed distal femoral DTI-P/M in 160 children using a standard diffusion sequence (20 directions, b=600 s/mm²) and calculated tract volume, tract length, and fractional anisotropy. Children studied had measurements of height velocity (n=90), or total height gain (n=70, mean=34 months from DTI-P/M). We excluded children with height change < 0.5 cm, abnormal physes or inadequate imaging. In both groups, we used multilinear regression to assess the potential of DTI parameters to predict height velocity and total height gain. We compared DTI-P/M predictions to standard predictions based on bone age determinations.

Results: Larger tract volumes correlated with height gains one year after DTI-P/M (r=0.70) and with total height gain at skeletal maturity measured after cessation of growth (r=0.68) (P<0.01). Tract volume alone after controlling for age and sex accounted for over 50% of the

total variance in velocity height ($r^2=0.51$). A multilinear stepwise model algorithm identified tract volume as the strongest predictor for velocity height and total height gain. Optimal multilinear model significantly improved prediction of height velocity ($r^2=0.65$, root mean square error (RMSE)=1.76 cm) and of total height gain ($r^2=0.59$, RMSE=1.83 cm) compared to the standard method based on bone age (height velocity: $r^2=0.32$, RMSE=2.87 cm; total height gain: $r^2=0.42$, RMSE=4.97 cm).

Conclusion: Models using tract volume may overperform clinical standards in predicting height velocity and total height gain and may become a predictive biomarker of skeletal growth.

Bland-Altman Plots: Predicted and measured height velocity (left) and total height gain (right). Tract volume model (top) reduced error and bias compared to bone age model (bottom). boys: purple, girls: pink

S6.3.6

MR IMAGING OF PRIMARY LYMPHOMA OF BONE IN CHILDREN AND YOUNG ADULTS

PATRICK Duffy, KIRSTEN Ecklund
Boston Children's Hospital, Boston, USA

Purpose

Primary lymphoma of bone (PLB) is an uncommon non-Hodgkin lymphoma with rising incidence. We observed several MR features in pediatric PLB including epiphyseal location, infarct-like or osteomyelitis-type appearance, and multifocality. We set out to identify typical MR characteristics of PLB in children and young adults at diagnosis and following treatment.

Materials and Methods

A large children's hospital imaging database was used to identify 13 patients with MRI prior to biopsy-proven diagnosis of PLB. Two pediatric radiologists retrospectively reviewed MR images at presentation and after treatment for the following information: anatomic location, number of sites, location within bone (epiphyseal, metaphyseal, diaphyseal), margins on T1WI, soft tissue mass, T2WI appearance and enhancement pattern (homogeneous, heterogeneous, infarct-like), soft tissue edema, cortical disruption, and regional lymph nodes > 1cm short axis dimension. Discrepancies between the two readers were resolved by consensus.

Results
Of 13 patients, age range 6 – 25 years, median 15 years, 7 (54%) had multifocal disease, with >5 lesions in 4 (31%). Most common bone was the femur, 9 (69%), and 7 (54%) around the knee. 11 (85%) had at least 1 epiphyseal lesion; 9 (69%) metaphyseal, 6 (46%) diaphyseal. 9 (69%) showed T2WI infarct-like appearance; 7 of 8 (88%) with post-contrast imaging had infarct-like enhancement pattern. 8 (62%) had sharp T1 margins, 6 (46%) had cortical disruption, 10 (77%) of pts had surrounding soft tissue edema. Only 3 (23%) had soft tissue mass; only 4 (31%) had regional adenopathy. At follow-up (range 3–108 months, median 8 months), all had residual osseous abnormality with 7 (58%) maintaining an infarct-like appearance.

Conclusion

Our results in this largest series of children and young adults with PLB identified several frequent MR imaging features. Multifocality, epiphyseal involvement (especially about the knee), infarct-like enhancement pattern, sharp T1 margins, and surrounding soft tissue edema should raise suspicion for PBL. Awareness of these characteristics allows radiologists to suggest a diagnosis often not previously considered and one which influences biopsy planning. Following treatment, residual osseous abnormality is expected.

S6.4.1

CHARACTERIZATION OF RETROPLACENTAL CLEAR SPACE IN A MURINE MODEL OF PLACENTA ACCRETA SPECTRUM (PAS) USING CONTRAST-ENHANCED MRI

ANDREW Badachhape¹, LAXMAN Devkota², PRAJWAL Bhandari¹, MAYANK Srivastava³, POONAM Sarkar², VERGHESE George¹, ERIC Tanifum³, KARIN Fox⁴, KETAN Ghaghada³, CHANDRASEKHAR Yallampalli⁴, ANANTH Annappagada³

¹ Baylor College of Medicine - Department of Radiology, Houston, USA

² Baylor College of Medicine - Department of Pediatrics-Oncology, Houston, USA

³ Texas Children's Hospital - The Singleton Department of Pediatric Radiology, Houston, USA

⁴ Texas Children's Hospital - Department of Obstetrics and Gynecology, Houston, USA

Purpose: Placenta Accreta Spectrum (PAS) involves placental invasion of the myometrium and is responsible for severe maternal morbidity at delivery. Visualization of the retroplacental clear space (RPCS), is an indicator of normal placentation. However, the interface can be difficult to visualize with ultrasound and conventional magnetic resonance imaging (MRI). Previously, we demonstrated visualization of the RPCS with contrast-enhanced MRI (CE-MRI) using a high T1 relaxivity liposomal gadolinium nanoparticle contrast agent (liposomal-Gd) that does not cross the placental barrier. In this study, we demonstrate use of liposomal-Gd to identify disruption of the RPCS in a pregnant GAB3^{-/-} mouse model of PAS.

Materials and Methods: In vivo studies were performed at 16 days of gestation in pregnant GAB3^{-/-} mice that demonstrate placental invasion across the RPCS and GAB3^{+/+} controls. We performed CE-MRI on a 1T scanner using a T1-weighted 3D gradient-recalled echo sequence (100x100x600 μm^3 voxels). Post-contrast images were acquired following intravenous administration of liposomal-Gd (0.15 mmol Gd/kg). We also performed contrast-enhanced computed tomography (CE-CT) on a small animal micro-CT scanner (70 μm isotropic voxels). CE-CT was performed after intravenous administration of a liposomal-iodinated agent (1.1 g I/kg). MR images underwent blinded review to assess RPCS conspicuity (0 – completely obscured, 1 – partially obscured, 2 – not obscured). Post-mortem histological analysis of fetoplacental units (FPU) was performed for comparison.

Results: CE-MR and CE-CT images in GAB3^{-/-} mice demonstrated a heterogeneous and interrupted RPCS relative to GAB3^{+/+} counterparts. Blinded review demonstrated a significant difference ($p<0.05$) in the visibility of the RPCS in FPU of GAB3^{-/-} (28 FPU, 1.18 ± 0.54) and GAB3^{+/+} (20 FPU, 1.5 ± 0.5) mice. Histological analysis of FPU from GAB3^{-/-} mice confirmed placenta accreta as evidenced by a higher degree of vascularization and the invasion of placental trophoblast cells across the RPCS.

Conclusions: CE-MRI and CE-CT in a mouse model of PAS enabled visualization of placental invasion across the RPCS.

S6.4.2

PLACENTAL SURFACE HETEROGENEITY IN FETAL GROWTH RESTRICTION USING DIFFUSION WEIGHTED IMAGING: A FETAL MRI PILOT STUDY

MEYERS Mariana¹, DAVID Mirsky^{1,2,3}, CAMILLE Driver^{1,4}, JOHN Hobbins^{1,4}, ERIN Englund^{1,2,3}

¹ Children's Hospital Colorado, Aurora, USA

² University of Colorado School of Medicine, Aurora, USA

³ Department of Radiology, Aurora, USA

⁴ Department of Obstetrics and Gynecology, Aurora, USA

Purpose: to evaluate differences between maternal versus fetal placental surfaces in fetuses with growth restriction (FGR) (Fetal weight <10th percentile) compared to controls of (1) perfusion, assessed indirectly by 3T MRI apparent diffusion coefficient (ADC) and (2) relative signal intensity (SI) on heavily T2-weighted acquisitions.

Material and Methods: Retrospective, pilot study of 10 pregnancies with diagnosis of FGR (34± 2 weeks gestational age [GA]) compared to 10 controls (29± 4 weeks GA). All patients underwent axial 2D multi-slice DWI MRI of the placenta with b-values from 0–1000 s/mm². The placentas were divided into thirds: fetal, middle and maternal. Six region of interest (ROIs) were placed on each slice throughout the placenta in the ADC and T2W images, three per slice at the fetal and maternal surfaces respectively in both groups. The average ADC was computed for the maternal and fetal aspects of the placenta and compared by two-way ANOVA with post-hoc t-tests. The average T2W SI was determined for the fetal aspect and normalized by the maternal (average fetal SI/average maternal SI).

Results: There was significant difference between maternal and fetal ADC in the FGR group (1.71 vs 1.27 x10⁻³ mm²/s, p<0.0001), but not in controls (1.72 vs 1.79 x10⁻³ mm²/s, p=0.696). ADC on the fetal placenta side were significantly lower in the FGR compared to the controls (p= 0.0026). No difference was observed between the FGR and control groups in the maternal side of the placenta (p=0.782). The relative T2W SI was significantly lower in FGR group (0.48) compared to controls (0.92) (p<0.0001).

Conclusions: Our data suggest underlying physiological differences in the fetal versus maternal aspects of the placenta of fetuses with FGR. Reduced ADC signal at the fetal surface could suggest a reduction in perfusion while the reduced relative T2W SI could reflect reduced oxygen saturation or altered placental morphology. Further studies with larger population sample should follow.

S6.4.3

PLACENTAL VOLUME IN PREGNANT WOMEN WITH OPIOID USE: PRENATAL MRI ASSESSMENT

RACHEL Wise¹, BRANDON Brown¹, DAVID Haas², CHRISTINA Sparks³, SENTHILKUMAR Sadhasivam³, RUPA Radhakrishnan¹

¹ Indiana University School of Medicine Department of Radiology & Imaging Sciences, Indianapolis, USA

² Indiana University School of Medicine Department of Obstetrics & Gynecology, Indianapolis, USA

³ Indiana University School of Medicine Department of Anesthesia, Indianapolis, USA

Purpose: Opioid use is a growing public health concern with widespread impact on patients and their families. Opioid use in pregnant women is shown to be associated with lower infant birth weights. Placental volume changes in prior studies correlated with various maternal and fetal conditions. Given the integral role of the placenta in fetal growth, we aimed to identify differences between placental volumes in pregnant women with opioid use, and healthy pregnant women without drug use.

Methods & Materials: We prospectively recruited pregnant women with prenatal opioid use, including those on opioid maintenance therapy, and healthy pregnant women. All women underwent placenta/fetal MRI at 28–39 weeks gestation on a 3Tesla MR scanner. Placental volumes were measured by two blinded observers using a previously validated technique. We used multivariable linear regression to identify associations of placental volume with multiple maternal and fetal clinical factors. Significance threshold was set at P <0.05.

Results: 28 pregnant women (12 opioid-exposed) were included. Mean maternal age was 27.4 years in the opioid use group and 30.7 years in the control group. There was no significant difference (p=0.2) in mean gestational age at MRI between the opioid-exposed (34.1 weeks) and healthy (32.6 weeks) pregnancies. Placental volume was significantly associated with gestational age (p< 0.0001), polysubstance use (p=0.002), smoking (p=0.002), and fetal

sex (p=0.02). Placental volume was not associated with opioid use, maternal age, or education level. There was no significant association of placental volume with maternal weight or body mass index.

Conclusions: For pregnant mothers on opioid replacement therapy, there was no significant difference in placental volume when compared to healthy mothers. However, placental volume was significantly smaller in pregnant women who used multiple drugs, suggesting a potential influence of prenatal polysubstance use on fetal health. The impact of placental volume and function on fetal and neonatal outcomes is an important direction for future research.

S6.4.4

OUR INITIAL EXPERIENCE WITH A DEEP LEARNING RECONSTRUCTION ALGORITHM IN FETAL MRI

JANE Lyon¹, KARA Gill¹, SUSAN Rebsamen¹, R. MARC Lebel², TY A. Cashen³

¹ University of Wisconsin School of Medicine and Public Health, Department of Radiology, Madison, WI, USA

² GE Healthcare, MR Applications and Workflow, Calgary, CANADA

³ GE Healthcare, Magnetic Resonance, Madison, WI, USA

PURPOSE: Fetal MRI is an inherently signal starved examination due to the need for fast pulse sequences to overcome fetal motion. Our current Deep Learning Reconstruction (DLR) prototype software strives to improve signal to noise ratio (SNR) which we hypothesize should result in an improvement in lesion conspicuity, and ultimately diagnostic confidence.

TECHNIQUE: Our current DLR method comprises a deep convolutional residual encoder network (AIR Recon DL, GE) trained from a database of over 10,000 images to reconstruct images with high SNR and high spatial resolution. The tunable noise reduction factor was set to 75%.

Conventional fetal imaging was performed on 8 patients with T2 SSFSE(7) and FIESTA(1) pulse sequences, on either a 1.5T(6) or 3.0T(2) MRI scanner. Each case included clinical pathology. The DLR images were then subsequently generated from the raw MR data. Three board certified radiologists, (2 pediatric radiologists and 1 pediatric neuroradiologist), with combined experience of 49 years, independently compared chosen coronal, sagittal and axial sequences directly linked on PACS. The images were evaluated for perceived SNR, conspicuity of pathology, diagnostic confidence, and artifact reduction. Each DLR sequence was scored as “better, same or worse” compared to conventional imaging. The reviewers overall preference for the conventional v. DLR images was also assessed.

Although our institution is a GE test site, the reviewers have no commercial interest or conflicts and do not receive individual funding from GE. **RESULTS:** The 3 reviewers were in 100% agreement that the SNR of the DLR images was better. 17 of 24 times (71%), the conspicuity of the pathology in the DLR images was scored as “better.” 13 of 24 times (54%), the diagnostic confidence in the DLR images was scored as “better.” In 100% of the cases, the artifacts were scored as “same.” In every case, the DLR images were “preferred” over the conventional images.

SUMMARY: We have shown that our prototype Deep Learning Reconstruction (DLR) algorithm improves signal to noise, with resulting improvement in lesion conspicuity in 71% of cases. The diagnostic confidence was also scored better in 54% of cases. Although DLR also strives to visually decrease artifacts, we found that in this study any artifact present was perceived as similar from DLR to conventional. In summary, DLR is an exciting new tool with the potential to improve fetal imaging in the future.

S6.4.5

VIRTUAL AUTOPSY OF THE BRAIN USING POST-MORTEM MRI: IS IT HELPFUL?

NEETIKA Gupta, CLAUDIA Martinez-Rios, ELKA Miller, DINA El Demellawy, NICK Barrowman
CHEO, University of Ottawa, Ottawa, CANADA

Purpose: The role of conventional autopsy (CA) in post-mortem evaluation of the brain is undisputed but post-mortem magnetic resonance imaging (PMMRI) is less invasive and an acceptable alternative for the assessment of the post-mortem brain. The goal of this study is an attempt to evaluate the added value and limitations of PMMRI in assessing the brain when compared to antenatal magnetic resonance imaging (ANMRI) and CA. The study will evaluate qualitative and quantitative differences in brain PMMRI compared to ANMRI, for both solid and CSF-filled structures.

Materials and Methods: A retrospective, single-center study of fetuses who underwent ANMRI, PMMRI and CA from August 2010 to January 2020. A qualitative evaluation was done to assess the brain and PF abnormalities. Quantitative measurements of ventricles, supratentorial brain biometry and PF including the transcerebellar diameter, vermian length, brainstem thickness, maximum width of the cisterna magna, skull base angles, and PF volume. MRIs were evaluated by 2 pediatric neuro-radiologists and a pediatric radiology fellow.

Results: Twenty MRI exams were included. There was good congruence for qualitative evaluation between PMMRI, ANMRI and CA, with complete congruence in more than half of the fetuses. No incongruence was noted. Quantitative evaluation in PMMRI showed statistically significant enlargement for most of the PF structures compared to ANMRI and smaller CSF-filled spaces (p -value < 0.05).

Conclusion: Fetal PMMRI shows good congruence when compared to ANMRI and CA and is an acceptable imaging modality for the evaluation of brain and PF structures. Smaller CSF-filled spaces and enlargement of the brain are expected findings when evaluating PMMRI.

S6.4.6

OPTIMISATION OF HUMAN POST-MORTEM MICRO-CT SERVICE - IODINATION AND IMAGE QUALITY PREDICTORS

IAN Simcock, SUSAN Shelmerdine, DEAN Langan, NEIL Sebare, OWEN Arthurs

Great Ormond Street Hospital for Children and UCL/Institute of Child Health Biomedical Research Centre, London, UNITED KINGDOM

Purpose

Micro-CT is a non-invasive, high resolution imaging technique that can be used in human fetal post-mortem imaging to provide high diagnostic accuracy, typically by submerging the fetus within a solution of potassium tri-iodide (I₂KI), as a contrast agent. A range of fetal sizes can be imaged, but the optimal iodination staining duration, and relationship between satisfactory diagnostic image quality and fetal demographics are unknown. The aim of this study was to determine the effect of maceration and fetal size on image quality, and the relationship between patient weight and iodination time.

Method

In this single centre, prospective study, consecutive fetuses referred over a 3-year period for post-mortem micro-CT imaging were included. These were scanned on a Nikon micro-CT scanner (Tring, UK) following submersion within 2.5% Iodine solution to enhance tissue contrast. Single axial images through the brain and thorax were assessed independently for maceration and image quality (according to a Likert scale) by two paediatric radiologists. Simple and multivariable linear regression models were fitted for outcome variables, with demographics and maceration score considered as predictor variables. A subset of these fetuses was

utilised to determine the optimal immersion time for full iodination as determined by anatomy being visible throughout the fetus.

Results

258 fetal post-mortem micro-CT scans were evaluated (median fetal weight 41.7g (2.6-350g), mean gestational age 16 weeks (11-24 weeks). High image quality was observed in (497/516) 95.9% of the brain and thoracic images by the assessors.

The maceration score was the strongest positive indicator for poor image quality, with gestational weight being a weak negative predictor of image quality.

Increased median image quality scores were also observed in non-macerated head (9.5) and chest (9) images than in macerated head (8.5) and chest (8).

In a subset of 157/258 (60.1%) fetuses, we found a linear relationship between body weight and iodine solution immersion time which could be predicted using the formula: $\text{time(days)} = 0.03 \times \text{body weight(grams)} + 2.2$ ($R^2=0.64$).

Conclusion

Increased image quality scoring was observed in lower weight, non-macerated fetuses for micro-CT. We have identified key predictors and variables to help identify appropriate cases for referral, and the estimated iodine contrast submersion timing for a more efficient clinical post-mortem imaging service.

S7.1.1

MINIMALLY INVASIVE INTERVENTIONS UNDER ULTRASOUND NAVIGATION FOR ABDOMINAL ABSCESSES TREATMENT IN CHILDREN

AKIF Yusufov, ALEXEY Plyukhin

Tver State Medical University, Tver, RUSSIAN FEDERATION

Survey purpose. The goal was to improve the results of abdominal abscesses treatment in children with the help of minimally invasive technologies under the control of echography.

Materials and methods. The analysis of the results of treatment with the use of minimally invasive interventions of 25 children of 2 to 17 years age who were treated in the second surgical department of the Regional pediatric hospital of Tver in 2017-2021 with the diagnoses: appendicular infiltrate of the abdominal cavity in the stage of abscess formation (12) and abdominal cavity abscess (13).

Results. For the puncturing of abdominal abscesses, 18-20 G size needles were used, and 5-8 Fr size catheters were used for drainage. Fourteen children underwent therapeutic puncturing minimally invasive interventions, of which three of them underwent surgical puncturing of a pelvic abscess through the rectum under echography navigation. In ten patients, a therapeutic puncture of the abscess was performed once with lavage of the purulent cavity with antiseptic solutions and injection of a broad-spectrum antibiotic into the cavity. In 4 children therapeutic punctures were repeated. The method of minimally invasive percutaneous drainage under the control of ultrasonography was used in 11 patients. In 3 children with multiple abscesses of the abdominal cavity and pelvis both puncture method and percutaneous drainage method were used. The maximum number of abscesses of the abdominal cavity was in one child of 10 years old (8 units in total). The indications for therapeutic puncturing of abdominal abscesses were mainly 3: verified sonographic signs of an abscess (the presence of a capsule and heterogeneous content in it), acoustic access availability and a small volume of the abscess (from 1.5 to 25.0 ml). The method of percutaneous drainage under the control of ultrasonography was used in children with a larger abscess volume (more than 25.0 ml). Daily lavage of the abscess cavity with antiseptic solutions and injection of antibiotics have been done also. There were no complications during minimally invasive interventions. All children were discharged from the hospital with complete current recovery (out of them seven

patients were recommended for planned hospitalization for subsequent appendectomy).

Summary. Minimally invasive percutaneous methods of abdominal abscesses treatment in children under control of sonography has a low grade injury and high efficiency.

S7.1.2

IMAGING FEATURES OF SURGICAL AND PERCUTANEOUS CHOLECYSTOCHOLANGIOGRAPHY FOR SUSPECTED BILIARY ATRESIA

ABHAY Srinivasan¹, NAIF Alsaikhan¹, MICHAEL Acord¹, GANESH Krishnamurthy¹, FERNANDO Escobar¹, SETH Vatsky¹, MARIAN Gaballah¹, FIKADU Worede¹, RICHARD Bellah¹, ELIZABETH Rand², ANNE MARIE Cahill¹

¹ The Children's Hospital of Philadelphia - Department of Radiology, Philadelphia, USA

² The Children's Hospital of Philadelphia - Dept. of Gastroenterology, Hepatology, and Nutrition, Philadelphia, USA

BACKGROUND: Cholecystocholangiography (CCG) plays a crucial role in the diagnosis of biliary atresia (BA), in conjunction with liver biopsy that demonstrates cholestasis. A normal cholangiogram may exclude BA, but the cholangiographic patterns in BA have not been well described.

OBJECTIVE: We seek to evaluate patterns of BA on CCG, including the incidence of normal CCG, in patients with suspected BA.

METHODS: A retrospective review of imaging and clinical records of infants with suspected BA treated in our institution over the prior 10 years was performed, with imaging review performed independently by 2 radiologists. Definite diagnosis was determined by review of clinical records.

RESULTS: Sixty-five infants (30 female, mean age 67±33 d, range 9-201 d) with suspected BA underwent 67 CCG, 61 (91%) surgically and 6 (9%) percutaneously. Repeat CCG was performed in 2 patients.

Abnormal CCG patterns were: A, failed opacification (consistent with Kasai type IIb or III), N=6 (9%); B, wispy intra-hepatic ducts (consistent with Kasai type I), N=9 (13%); C, gallbladder with common bile duct (consistent with Kasai type IIa), N=19 (28%); D, gallbladder with or without cystic duct (consistent with Kasai type IIb or III), N=14 (21%). A normal CCG was seen in 19 patients (28%), and none of these patients had BA. The most common diagnoses in this group were neonatal hepatitis, parenteral nutrition cholestasis, and cystic fibrosis. Five of these CCG were performed percutaneously, therefore avoiding the need for laparotomy in 5 patients.

All patients with patterns A and B had BA, and 18/19 (95%) with C and 13/14 (93%) with D had BA. Both false-positive studies with patterns C and D were due to parenteral nutrition cholestasis.

CONCLUSION:

This is the largest series to date to evaluate patterns of BA on CCG. Pattern C, corresponding to atresia at the common hepatic duct (Kasai type IIa) was most common, followed by patterns consistent with types IIb and III.

There was a large proportion of normal CCG. Given that normal CCG showed a high negative predictive value, percutaneous technique may obviate laparotomy in selected patients.

S7.1.3

PERCUTANEOUS MANAGEMENT OF BENIGN BILIARY STRICTURES AFTER LIVER TRANSPLANTATION IN PEDIATRIC PATIENTS: A SINGLE-CENTER EXPERIENCE

LUDOVICO Dulcetta¹, PAOLO Marra², FRANCESCO SAVERI Carbone¹, CLAUDIO Sallemi², PIETRO ANDREA Bonaffini^{1,2}, SANDRO Sironi^{1,2}

¹ University of Milano-Bicocca, Monza, ITALY

² ASST Papa Giovanni XXIII Bergamo Hospital - Department of Radiology, Bergamo, ITALY

Liver transplantation (LT) is the standard of care for pediatric patients with end-stage liver disease and liver-based metabolic disorders either acute or chronic.

Complications of the biliary tract after LT are a common source of morbidity and mortality:

incidence of 10-45%. Benign biliary strictures (BBS) are the most common biliary complications after LT (40% of all biliary complications).

The purpose of this study is to assess the role of percutaneous transhepatic cholangiography (PTC), transluminal bilioplasty, and internal-external biliary drainage (IEBD) insertion for diagnosis confirmation and treatment of BBS in pediatric LT and to evaluate technical success and short-term clinical outcome.

Clinical, laboratory, imaging and procedural data of 52 pediatric patients (mean age 22.1 months; range 1-128; 28 males and 24 females), who underwent PTC after LT between 2009 and 2020 in a single center, were retrospectively reviewed.

Indication to PTC was clinical suspicious of BBS based on laboratory and liver biopsy data, regardless bile ducts dilation at pre-procedural non-invasive imaging.

122 PTCs were performed, with 2.3 procedures for each patient on average (range 1-8). Technical success of intrahepatic biliary catheterization was 99.2%; one failed catheterization was repeated successfully after 7 days.

In 108/121 cases (89.2%) ductal or biliodigestive anastomosis stenosis was found at PTC. In 95/108 cases (87.9%) stenosis was treated with transluminal bilioplasty and insertion of an IEBD at 1st attempt. In 10/108 the stenosis was managed in a second attempt. The remaining 3 cases failed all attempts of bilioplasty and underwent surgery.

In 13/121 cases without evident stenosis at PTC only an IEBD was placed.

In all cases, IEBD was maintained a mean of 31 ± 16 days.

Procedure-related complications were: 35 cholangitis, 4 bilomas, 3 sepsis and 1 septic shock.

Liver function tests (compared before, 7 days and 1 month after PTC) were available for 58 procedures.

Reduction in cholestasis was indicated by significantly improving in serum levels of γ -glutamyl transpeptidase ($p < .001$), total bilirubin ($p < .005$), direct bilirubin ($p < .05$) and alkaline phosphatase ($p < .05$).

In conclusion, the management of BBS after LT in pediatric patients may be insidious: PTC is a mini-invasive radiological procedure that should be considered before surgical management. In these cases, PTC with bilioplasty and IEBD is feasible, has low morbidity and improves cholestasis.

S7.1.4

DIFFICULT CENTRAL VENOUS PORT REMOVAL IN CHILDREN; ANALYSIS OF RISK FACTORS

FIKADU WOREDE Worede, ALIREZA Zandifar, MICHAEL Acord, SRINIVASAN Abhay, SETH Vatsky, FERNANDO Escobar, GANESH Krishnamurthy, ANNE MARIE Cahill
Children's Hospital of Philadelphia, Philadelphia, USA

Purpose

To determine risk factors for difficult port removal in a pediatric population with longstanding ports.

Methods

IRB exempt retrospective study of difficult port removals by interventional radiology in children from 1/1/2008 to 3/1/2021. Medical records were reviewed for; clinical history, port type and dwell time, additional interventions, procedure time, radiologic images for tip position. Analysis controls were randomly selected with the following inclusion criteria;

port dwell at least 6 months and radiographic images for tip position. Difficult removal was defined as failure to remove the port with normal traction, requiring additional intervention. Twenty-one difficult port removals were identified, (12M and 9F), median age at insertion and removal, 3.3 years (IQR: 2.19 – 6.20 years) and 7.25 years (IQR: 5.67 – 13.26 years) respectively. Control cohort number was 43, median age at port placement 5.9 years (IQR 3 – 13.5 years) and removal 7 years (IQR: 4.7 – 17.7 years).

Results.

Port material in case group was silicone in 18/21 and polyurethane in 3/21, and silicone in 34/43 and polyurethane in 9/43 in the control group. Most common port size was 6.5 Fr for case group (62 %, n=13/21) and control group (49 %, n=21/43). Removal interventions in case group included; extended pocket dissection, catheter guidewire and /or peel-away sheath insertion, venotomy dissection, catheter snaring. Kruskal-Wallis test revealed median difference between case group and control group in the following variables: age insertion (3.3 vs 5.9 year, $p = 0.03$), catheter dwell time (3.42 vs 1.2 year, $p < 0.001$), catheter tip position below carina (number of vertebral body levels) at time of removal (1.5 vs 2, $p = 0.016$). ROC analysis revealed catheter dwell for > 2.4 years predicted difficult removal with a sensitivity of 85.7 % and specificity of 93 %, $p < 0.001$. Fisher exact test revealed that the presence of calcification was associated with difficult port removal ($p = 0.009$). Procedure time was significantly higher in the case group (median duration, cases 68 minutes vs control 30 minutes, $p < 0.001$).

Conclusion

Port catheter placement at an early age and the presence of calcification could be associated with difficult port removal in pediatric patients. A port dwell time of > 2.4 years in our study predicted a more challenging port removal which may impact procedure planning.

S7.1.5

AN EMPIRICAL MODEL FOR COMPARING RADIATION DOSE IN PEDIATRIC PATIENTS UNDERGOING INTERVENTIONAL RADIOLOGY PROCEDURES UNDER C-ARM CONE BEAM CT VERSUS CONVENTIONAL CT

SAMUEL Brady^{1,2}, NICOLE Hilvert¹, JOHN Racadio^{1,2}

¹ Cincinnati Children's Hospital Medical Center, Cincinnati, Ohio, USA

² University of Cincinnati College of Medicine, Cincinnati, Ohio, USA

Purpose: To develop an empirical model comparing patient radiation dose in an interventional radiology (IR) procedure of the chest or abdomen using C-arm cone beam CT (CBCT) and fluoroscopy compared to conventional CT with or without CT fluoroscopy.

Method: Organ doses were measured using MOSFET dosimeters in a 5-year-old anthropomorphic phantom. Tomographic acquisitions (CBCT vs CT) and fluoroscopic series (conventional fluoroscopy vs CT fluoroscopy) were measured individually in the IR and CT suites. Tomographic series were acquired for craniocaudal scan coverages of 2.5, 7.5, 12.5, and 20 cm, and fluoroscopic series were acquired with coverages of 5, 24, and 75 cm for conventional fluoroscopy and 6, 12, and 24 mm for CT fluoroscopy. Organ doses were used to calculate effective dose per acquisition series.

Results: The relationship between patient dose [D (mSv)] and scan coverage [C (mm)] in the abdomen for a tomographic series is $D=0.51*\ln(C)-1.26$ and $D=0.30*\ln(C)-0.17$, and in the thorax is $D=0.07*\ln(C)+0.24$ and $D=0.36*\ln(C)+0.08$, for IR and CT, respectively. At smaller volume coverages (tighter craniocaudal collimation) effective doses for CBCT are up to 50% lower than similar CT coverages. Effective doses of CBCT and CT are comparable at full coverage. Dose rate [DR (mSv/min)] to scan coverage relationships for fluoroscopic series in the abdomen are $DR=0.09*\ln(C)+0.22$ and $DR=23.32*\ln(C)+27.44$ and thorax are $DR=0.04*\ln(C)+0.15$ and $DR=8.49*\ln(C)+13.98$, for IR and CT, respectively. CT fluoroscopy dose with similar volume coverage is 2-3

orders of magnitude greater than that of conventional fluoroscopy. All empirical relationships had coefficient of correlations > 0.98 .

Conclusion: We have developed an empirical model that will allow users to calculate tomographic and fluoroscopic patient doses in IR and CT for any patient volume coverage and time under fluoroscopy. Interventional radiologists can utilize this model to understand relative components of patient dose as they plan their procedures either in IR under CBCT or in a CT scanner under conventional CT.

S7.1.6

THE PEDIATRIC INTERVENTIONAL RADIOLOGY EXPERIENCE: PERSPECTIVE OF PATIENT FAMILIES

TIGIST Hailu, ABIGAIL Ginader, NICOLE Bodo, ALYSSA Sze, WILLIAM Corder, LYNN Thompson, FERNANDO Escobar, DORENE Balmer, RAYMOND Sze

Children's Hospital of Philadelphia, Philadelphia, USA

Purpose: Little is known about how families of children undergoing interventional radiology (IR) procedures experience their interactions with IR teams; therefore, we conducted a qualitative study to explore and learn from families experience with IR teams in order to educate pediatric IR staff and ultimately improve delivery of care.

Method: We conducted semi-structured interviews with 30 families of children (outpatient and inpatient) who recently underwent an interventional radiology procedure. Questions solicited information about their understanding of the procedures, their experiences with scheduling, and their pre- and post-procedure interactions with IR teams. We developed codes from important concepts in the data and revised codes based on team consensus. Four research assistants then applied codes to interview transcripts. The team reconvened to arrange codes into thematic categories that illustrated families experience with IR teams.

Result: Families identified a range of facilitators and barriers to overall positive experiences of family's experiences with IR staff. Facilitators included (a) taking a role of advocate for their child (b) receiving clear and useful education about the procedure and (c) the reputation of the hospital. Barriers to an overall positive experience with IR teams included (a) confusion about the location of the IR suite and (b) misalignment and uncertainty about what parent/guardian should do during the procedure time. Reported facilitators and barriers were not substantially different between families whose children were inpatient vs outpatient.

Conclusion: We found that families express a range of experiences with IR teams; while most reinforce existing, positive interactions there is room for improvement. Relatively simple steps to improve families' experience (e.g., signage) in addition to more complex communications education could advance the delivery of care by IR teams.

S7.2.1

ASSESSMENT OF HEPATIC ARTERY ANATOMY IN PEDIATRIC LIVER TRANSPLANT RECIPIENTS: MR ANGIOGRAPHY VERSUS CT ANGIOGRAPHY

MARTIJN Verhagen¹, RIKSTA Dijkers¹, RUBEN de Kleine², THOMAS Kwee¹, HUBERT van der Doef³, ROBBERT de Haas¹

¹ UMCG, Department of Radiology, Groningen, THE NETHERLANDS

² UMCG, Department of Hepatobiliary Surgery, Groningen, THE NETHERLANDS

³ UMCG, Department of Pediatric gastroenterology, Groningen, THE NETHERLANDS

Background:

During liver transplantation (LT) screening, children undergo computed tomography angiography (CTA) to determine hepatic artery anatomy. However, CTA imparts radiation, unlike magnetic resonance

angiography (MRA). The aim was to compare MRA to CTA in assessing hepatic artery anatomy in pediatric LT recipients.

Methods:

Twenty-one children (median age 8.9 years) who underwent both CTA and fast low angle shot 3D contrast enhanced (f3D-ce) MRA before LT were retrospectively included. Interreader variability between 2 radiologists, image quality, movement artifacts, and confidence scores, were used to compare MRA to CTA. Subgroup analyses for ages less than 6 years and 6 years or older were performed.

Results:

Interreader variability for MRA and CTA in children <6 years was comparable ($k=0.839$ and $k=0.757$, respectively), while in children 6 years or older CTA was superior to MRA ($k=1.000$ and $k=0.000$, respectively). Overall image quality and confidence scores of CTA were significantly higher compared to MRA at all ages (2.8/3 versus 2.3/3, $p=0.001$; and 2.9/3 versus 2.5/3, $p=0.003$, respectively). Movement artifacts were significantly lower in CTA compared to MRA in children 6 years or older (1.0/3 versus 1.7/3, $p=0.010$, respectively).

Conclusions:

CTA is preferred over f3D-ce MRA for the preoperative assessment of hepatic artery anatomy in children receiving LT, both at ages below 6 years and 6 years or older.

S7.2.2

ABDOMINAL ULTRASOUND FINDINGS IN PAEDIATRIC INFLAMMATORY MULTISYSTEM SYNDROME TEMPORALLY ASSOCIATED WITH COVID-19 (PIMS-TS)

SAIGEET Eleti, MYRIAM Guessoum, RIWA Meshaka, FERN Whittam, TOM Watson
Department of Paediatric Radiology - Great Ormond Street Hospital, London, UNITED KINGDOM

Purpose

PIMS-TS (also described as MIS-C) is a novel condition characterised by systemic immune-mediated inflammation temporally related to COVID-19 infection. Clinical presentation is non-specific and overlaps with several other inflammatory conditions including Kawasaki disease, toxic shock syndrome and sepsis.

Gastrointestinal symptoms appear to be a significant part of the symptomatology in the largest cohort papers on PIMS-TS. Several studies in a small number of patients have described abdominal imaging findings in PIMS-TS including ascites, bowel wall thickening and mesenteric lymphadenopathy. At our institution, all patients presenting with a clinical suspicion of PIMS-TS had an abdominal ultrasound to both assess for general features of sepsis and exclude alternative diagnoses.

We quantify the prevalence of abdominal US findings in our cohort of PIMS-TS at a large tertiary centre and assess its utility in this newly described disease.

Materials and methods

Retrospective review of all patients with a clinical suspicion of PIMS-TS who underwent an abdominal US study between April 2020 and January 2021. US findings were reviewed for patients diagnosed with PIMS-TS at initial presentation and follow up.

Results

129 abdominal US studies were performed in 82 patients with a diagnosis of PIMS-TS and 10 patients with alternative diagnoses.

88% of initial studies in PIMS-TS patients were abnormal. Ascites was the most common finding (63%) with periportal echogenicity, gall bladder debris, mesenteric inflammation, bowel wall thickening, echogenic kidneys and mesenteric nodes seen in decreasing frequency.

At follow-up, 50% of studies were abnormal and ascites was the most common finding.

In 10 patients with non-PIMS-TS diagnoses (including Kawasaki disease and bacterial septicaemia) similar non-specific findings were present. Appendicitis was identified in one patient.

Conclusion

Our study yielded a large number of non-specific abnormal findings in PIMS-TS and on limited follow-up, these features persisted in a significant proportion, but long-term data is unknown. In accordance with other studies, US should be the first line imaging study to assess for alternative diagnoses. Note the small number of appendicitis cases in our cohort despite very similar presenting features. Therefore, in non-specialist settings it is important to consider PIMS-TS in children presenting with abdominal pain and definitively image the appendix before surgery is considered.

S7.2.3

SPECTRUM OF IMAGING FINDINGS IN PAEDIATRIC MULTISYSTEM INFLAMMATORY SYNDROME – TEMPORALLY ASSOCIATED WITH SARS-COV-2 (PIMS-TS)

SHEMA Hameed¹, HEBA Elbaaly¹, CATRIONA Reid¹, RUI Santos¹, VINAY Shivamurthy², JAMES Wong³, HARAN Jogevaran¹

¹ Department of Children's Imaging, Evelina London Children's Hospital, London, UNITED KINGDOM

² Department of Paediatric Rheumatology, Evelina London Children's Hospital, London, UNITED KINGDOM

³ Department of Paediatric Cardiology, Evelina London Children's Hospital, London, UNITED KINGDOM

Purpose

Since April 2020, our tertiary paediatric hospital has experienced 2 waves of children presenting with a multi-system hyperinflammatory syndrome. Presentation included fever, headaches, abdominal symptoms, rash, and conjunctivitis. It is recognised that clinical and laboratory features can be similar to those of Kawasaki-disease shock or toxic-shock syndrome, although atypical and more severe. This presentation focuses on the spectrum of imaging findings in children with post COVID-19 inflammatory syndrome and postulates possible mechanisms for these findings.

Material and methods

A retrospective review of the clinical, laboratory and imaging findings of the first 35 children admitted to our institution, a tertiary paediatric hospital, meeting the case definition for PIMS-TS has been performed and published. Subsequent to this, a further 30 cases have presented, with imaging currently under review, making this the largest single-institution imaging assessment of this condition.

All imaging studies were initially reported by paediatric radiologists and for the purposes of this presentation, 2 paediatric radiologists have reviewed the imaging in consensus. A descriptive analysis is presented.

Results

Preliminary results from the first 35 cases show 54% of chest radiographs to be abnormal, with bronchial wall thickening, airspace opacification and pleural effusions to be the commonest abnormalities. Thoracic CT findings often correlated with the radiographic imaging. Three studies showed ground-glass changes, consolidation with an AP gradient and rounded consolidations. Cardiac CT showed 20% to have coronary artery aneurysms. Abdominal US was performed in 54% of children and was abnormal in all but 1, showing inflammatory changes within the right iliac fossa including lymphadenopathy, bowel wall thickening and expanded echogenic mesenteric fat, in addition to free-fluid. CT studies were performed infrequently and confirmed the above findings.

Conclusion

PIMS-TS is now a recognised late manifestation of prior exposure to SARS-CoV2 in children. Clinical presentation and disease severity can

be variable, including shock and myocardial injury. We will present a pattern of imaging findings including airway inflammation, rapidly progressive pulmonary oedema, coronary artery aneurysms and extensive abdominal inflammatory change within the right iliac fossa in order to aid radiological diagnosis.

S7.2.4

SPONTANEOUS EVOLUTION PATTERNS OF FOCAL CONGENITAL HEPATIC HEMANGIOMAS: A CASE SERIES OF 25 PATIENTS

CAROLINE Rutten¹, DELPHINE Ladarre², STÉPHANIE Franchi-Abella¹

¹ Department of Pediatric Radiology, Hôpital Bicêtre, Kremlin-Bicêtre, FRANCE

² Department of Pediatric Hepatology, Hôpital Bicêtre, Kremlin-Bicêtre, FRANCE

Background: Hepatic hemangiomas are the most common benign liver tumors of infancy. They are termed congenital if present fully grown at birth or infantile if they appear in the first weeks of life. Previous studies suggested that focal congenital hepatic hemangiomas (CHH) show an evolution that parallels their cutaneous counterparts, subdivided by pattern of involution, whether rapidly, partially, or non-involuting. However, in our experience, some focal CHH show postnatal growth, behaving like infantile forms.

Purpose: To analyze the spontaneous evolution of focal CHH with quantification of tumor volume changes over time; to find initial postnatal ultrasound (US) imaging biomarkers predictive of their evolution pattern. **Materials and methods:** A retrospective review of clinical and imaging data of children with focal CHH (prenatal diagnosis or age at diagnosis < 7 days and/or GLUT1-negative tumor) diagnosed between 2000 and 2018 was performed with analysis of tumor volume changes over time. Exclusion criteria were: treatment inducing a tumor volume change (hepatic artery embolization, propranolol or corticosteroids); follow-up less than 1 month or less than two US examinations. Volumetric analysis of CHH was based on US and cross-sectional imaging. Lesion volumes were estimated using the standard ellipsoid formula. We assumed a 35% margin of error for volume measurements.

Results: Twenty-five patients with CHH were included and followed up with serial imaging. Eight (32%) lesions showed postnatal growth before involuting, without signs of intralesional hemorrhage, as do infantile hemangiomas. The other 17 (68%) lesions exhibited a strict decrease in volume with age. Of these, 15 underwent complete involution and 2 underwent partial involution. No lesion could be categorized as NICH. The different evolution patterns of focal CHH showed overlapping imaging features. We found no initial US feature to be significantly associated with postnatal growth. However, three, almost identical, prenatally diagnosed, lesions composed of large cystic vascular spaces, without associated congenital portosystemic shunt resolved rapidly (complete regression < 7 months).

Conclusion: Focal CHH aren't the equivalent of cutaneous RICH, as some may increase in size before involuting and some may involute slowly. The different evolution patterns of focal CHH show overlapping imaging features.

S7.2.5

IMAGE QUALITY ASSESSMENT OF PEDIATRIC CHEST AND ABDOMEN CT BY DEEP LEARNING AND ITERATIVE IMAGING RECONSTRUCTION

HAESUNG Yoon, HYUN JI Lim, JISOO Kim, MI-JUNG Lee

Severance Hospital. Department of Radiology, Seoul, SOUTH KOREA

Purpose: To compare image quality of deep learning reconstruction (DLR) and iterative reconstruction (IR) on pediatric abdomen and chest computed tomography (CT).

Material and methods: This retrospective study included pediatric chest and abdomen CT from February 2020 to October 2020, performed in 51 patients (34 boys and 17 girls; age 1-18 years). Non-contrast chest CT (n=16), contrast enhanced chest CT (n=12), and contrast enhanced abdomen CT (n=23) were included. Standard 50% adaptive statistical iterative reconstruction V (50% ASIR-V) reconstruction was compared with 100% ASIR-V, DLR at medium and high strengths. Attenuation, noise, contrast to noise ratio (CNR), signal to noise (SNR) measurements were performed. Overall image quality, artifact and noise were subjectively assessed by two radiologists, blinded to examination details, using a four-point scale (superior, average, suboptimal, and unacceptable). The quantitative and qualitative parameters were compared using repeated measures ANOVA with Bonferroni correction and Wilcoxon signed-rank tests.

Results: DLR had better CNR and SNR than 50% ASIR-V in both pediatric chest and abdomen CT. When compared with ASIR-V 50%, high strength DLR was associated with noise reduction in non-contrast chest CT (33.0%), contrast enhanced chest CT (39.6%) and contrast enhanced abdomen CT (38.7%) with increased in CNR, 149.1%, 105.8% and 53.1% respectively. The subjective assessment of overall image quality and noise were also better on DLR images (p<0.001). However, there was no significant difference in artifacts between reconstruction methods.

Conclusion: Compared with 50% ASIR-V, DLR improved CT evaluation of pediatric chest and abdomen, with significant noise reduction. However, artifacts were not decreased with deep learning method, regardless of strength.

S7.2.6

SHEAR WAVE ELASTOGRAPHY EVALUATION OF LIVER, PANCREAS, SPLEEN, AND KIDNEYS IN PATIENTS WITH FMF AND AMYLOIDOSIS

ZUHAL Bayramoglu¹, ZEYNEP NUR Akyol Sari¹, OYA Koker², IBRAHIM Adaletli¹, RUKIYE Eker Omeroglu²

¹ Istanbul University, Istanbul Medical Faculty, Pediatric Radiology Department, Istanbul, TURKEY

² Istanbul University, Istanbul Medical Faculty, Pediatric Rheumatology Department, Istanbul, TURKEY

Rationale and Objectives

Amyloid deposits in a visceral organ can contribute to tissue stiffness that could be measured with shear wave elastography (SWE). We aimed to investigate changes in organ stiffness in conjunction with laboratory parameters in patients with Familial Mediterranean Fever (FMF) and amyloidosis.

Materials and Methods

This prospective study included 27 FMF patients, 11 patients with amyloidosis, and 54 age-matched healthy controls. Auxological parameters, medication history, and laboratory parameters were documented. Median shear wave elasticity values of the liver, spleen, both kidneys, and pancreas on SWE were compared between study and control groups. The mean/median values of laboratory parameters were compared between FMF and amyloidosis groups by the t-test or Mann-Whitney U test. Spearman's correlation analysis was performed to reveal the association of stiffness values with the laboratory parameters.

Results

The median liver, spleen, kidney, and pancreas elasticity values were significantly higher in the amyloidosis group compared to control subjects. The median renal stiffness values in the FMF group were significantly higher compared to control subjects. C-reactive protein (CRP),

erythrocyte sedimentation rate (ESR), and serum amyloid A (SAA) levels were significantly higher in the amyloidosis group compared to FMF patients. There were statistically significant positive correlations between the alanine transaminase levels with the liver stiffness ($p=0.038$, $r=0.36$); CRP ($p=0.001$, $r=0.56$), ESR ($p=0.001$, $r=0.61$), and SAA ($p=0.002$, $r=0.53$) levels with spleen stiffness; CRP ($p=0.006$, $r=0.48$) and ESR ($p=0.001$, $r=0.61$) levels with pancreas stiffness; and ESR ($p=0.004$, $r=0.51$) levels with the left kidney stiffness.

Conclusion

SWE would be a potential tool for noninvasive monitorisation of FMF and amyloidosis patients.

S7.3.1

MRI FINDINGS OF PROLIFERATIVE AND INFLAMMATORY SYNOVITIS IN THE KNEE IN CHILDREN: ARE THERE QUALITATIVE AND SEMI-QUANTITATIVE DIFFERENCES?

JIE C Nguyen^{1, 2}, ALYSSA Sze¹, ANDRESSA Guariento Alves¹, MICHAEL K Nguyen¹, ALEXANDRE Arkader^{2, 3}, DAVID M. Biko^{1, 2}

¹ Department of Radiology, Childrens Hospital of Philadelphia, Philadelphia, USA

² University of Pennsylvania School of Medicine, Philadelphia, Philadelphia, USA

³ Division of Orthopedic Surgery, Childrens Hospital of Philadelphia, Philadelphia, USA

INTRODUCTION: Synovium is responsible for the production of joint fluid, which lubricates and facilitates low-fraction loading and wear-resistant movement. In children, the most common causes for non-infectious synovial diseases are juvenile idiopathic arthritis (JIA), intra-articular tenosynovial giant cell tumor (TGCT), and primary synovial chondromatosis (PSC). While the underlying pathogenesis differs, inflammatory and proliferative synovitis can produce insidious and non-specific joint symptoms that can or preferentially involve the knee joint. **PURPOSE:** To characterize and compare the patterns of non-infectious synovitis in the knee on contrast-enhanced magnetic resonance imaging (MRI) in children with proliferative synovitis and JIA using qualitative and semi-quantitative scoring methods.

MATERIALS & METHODS: This retrospective study included children with intra-articular diffuse tenosynovial giant cell tumor, primary synovial chondromatosis, and JIA who underwent pre-procedure contrast-enhanced MRI of the knee between May 2008 and May 2020. Blinded to the diagnosis, 2 radiologists qualitatively characterized the synovium: susceptibility, effusion-synovitis complexity, Hoffa synovitis, and popliteus hiatus distention using non-contrast images; and effusion size, synovial pattern, and effusion-synovium distribution using contrast-enhanced images. Synovial thickness was measured at 11 predetermined intra-articular sub-regions and knee radiographs were also reviewed, when available. Fisher exact, Mann-Whitney U, and Student's t tests were used to compare values between diseases.

RESULTS: This study included 23 children (13 girls, 10 boys, mean age, 12.5 ± 2.9), 10 with proliferative synovitis (7 with TGCT; 3 with PSC) and 13 with JIA (all subtypes). Synovial susceptibility ($p=0.01$) and more severe Hoffa synovitis ($p=0.003$) were more common in children with proliferative synovitis than with JIA. Although the synovial hypertrophy scores were not significantly different between the groups ($p=0.17$), thicker synovium was more common with proliferative synovitis overall ($p<0.001$) and within suprapatellar, infrapatellar, medial parapatellar, intercondylar, medial and lateral perimeniscal sub-regions (p -range: $<0.001-0.03$) when compared to JIA.

CONCLUSION: Children with proliferative synovitis are significantly more likely to have synovial susceptibility, more severe Hoffa synovitis, and thicker synovium when compared to those with JIA.

S7.3.2

A SEMIQUANTITATIVE COLOR DOPPLER ULTRASOUND SCORING SYSTEM FOR EVALUATION OF SYNOVITIS IN JOINTS OF PATIENTS WITH BLOOD-INDUCED ARTHROPATHY

NINGNING Zhang¹, SHENG Yang², ANNE-FLEUR Zwagemaker³, AIHUA Huo¹, YING-JIA Li⁴, FANG Zhou⁴, PAMELA Hilliard⁵, SANDRA Squire⁶, VANESSA Bouskill⁷, ARUN Mohanta⁸, ALEX Zhou⁸, JOSE Jarrin⁸, RUNHUI Wu⁹, JING Sun¹⁰, BRIAN Luke¹¹, RAHIM Moineddin¹², CARINA Man⁸, VICTOR Blanchette⁷, YUN Peng¹, ANDREA Doria⁸

¹ Beijing Childrens Hospital - Department of Radiology, Toronto, CHINA

² Chengdu Women's and Childrens Central Hospital - Department of Ultrasound, Sichuan, CHINA

³ Amsterdam UMC - Department of Pediatric Hematology, Amsterdam, NETHERLANDS

⁴ Nanfang Hospital - Department of Radiology, Guangzhou, CHINA

⁵ The Hospital for Sick Children - Rehabilitation Service, Toronto, CANADA

⁶ St Paul Hospital, Providence Health Care -Service of Physiotherapy, Vancouver, CANADA

⁷ The Hospital for Sick Children - Hematology/Oncology, Toronto, CANADA

⁸ The Hospital for Sick Children - Diagnostic Imaging, Toronto, CANADA

⁹ Beijing Childrens Hospital - Hematology/Oncology Center, Beijing, CHINA

¹⁰ Nanfang Hospital - Department of Hematology, Guangzhou, CHINA

¹¹ Childrens Hospital of Eastern Ontario-Division of Haematology & Transfusion Medicine, Ottawa, CANADA

¹² University of Toronto-Division of Family & Community Medicine, Toronto, CANADA

Background: Due to the occurrence of subclinical joint bleeds in persons with hemophilia (PWH) and other bleeding disorders, early pathological synovial changes may go unrecognized leading to silent progressive arthropathy. Color Doppler holds potential for detection of synovial inflammation reactive to joint bleeds at an early stage by the time the joint can be saved from irreversible arthropathy.

Purpose: To explore the diagnostic value of color Doppler ultrasound in detecting synovitis in boys with bleeding disorders.

Materials and methods: Sixty boys with hemophilia and type 3 von Willebrand disease aged 5 to 18 years (median 12.3) were imaged by gray-scale and color Doppler ultrasound (US) in three centers (Beijing, $n=22$], Guangzhou, China [$n=12$] and Toronto, Canada. Twelve to 17 MHz linear-array transducers were employed using a standardized protocol. Images were independently reviewed by two radiologists blinded to clinical data using a subjective semi-quantitative scoring system (ranging from normal, to severe, grades 0-2) and objective measurements of synovial thickness and vascularity (count of color pixels) after a calibration session.

Results: Inter-reader reliability for using subjective vs objective color Doppler US methods for assessing synovial vascularity was excellent for the subjective method (intraclass correlation coefficient, ICC, 0.98-1.00) and moderate/lower range of substantial (ICC, 0.60-0.70) for the objective method. Agreement between degree of vascularity on color Doppler and extent of synovial hypertrophy on gray-scale US was overall poor for Canada data ($r=0.43$, $P=0.02$) and moderate for China data ($r=0.66$, $P<0.0001$). Correlations between degree of vascularity on color Doppler and synovial hypertrophy on gray-scale US, and clinical

constructs (number of lifetime study joint bleeds, interval from most recent study joint bleed, total Pettersson X-rays scores, total and itemized HJHS scores) for assessment of blood-induced arthropathy were all poor ($r=0.38-0.49$, $P<0.05$). Similarly, poor correlations were noted between color Doppler US and clinical constructs (Hemophilia Joint Health Score, $r=0.38$, $P=0.04$).

Conclusion: Color Doppler US is a valuable scoring method for evaluating reactive synovitis in joints of subjects with inherited bleeding disorders and holds potential for assessing post-bleed reactive synovitis once further information on its association with timing of the joint bleed becomes available in the literature.

S7.3.3

INTRA ARTICULAR INJECTIONS WITH PLATELET RICH PLASMA IN PATIENTS WITH JUVENILE OSTEOCHONDRITIS DISSECANCS OF THE KNEE: DOES IT HELP? A CLINICAL AND MR STUDY

MICHAEL Fadell^{1,2}, DAVID Howell^{3,4}, JILL Stein^{3,4}, MATTHEW Monson^{3,4}, KARI Hayes^{3,4}, KATHERINE Dahab^{3,4}

¹ Lucille Packard Children's Hospital, Palo alto, USA

² Stanford University, Palo Alto, USA

³ Children's Hospital Colorado, Aurora, USA

⁴ University of Colorado, Aurora, USA

Introduction:

Osteochondritis dissecans (OCD) is a painful condition characterized by osseous necrosis followed by re-ossification, and commonly occurs in adolescent knees. Lesions can be stable or unstable; treatment includes non weightbearing and surgery, respectively. As platelet rich plasma has been shown to promote healing, intra-articular injections may be an effective alternative to the current treatment for stable lesions and may improve symptoms, recovery time, or appearance on MRI.

Materials and Methods:

This was a prospective randomized controlled trial of stable knee OCD lesions. Lesions were scored on MRI utilizing the Dipaolo classification system, with a higher score correlating with increased severity. Associated marrow edema and subchondral cystic change was also assessed. Participants were randomly assigned to treatment or conservative therapy groups. The treatment group received three platelet rich plasma injections while the conservative therapy group did not. Pediatric International Knee Documentation Committee (Pedi-IKDC) and Knee Injury and Osteoarthritis Outcome Score (KOOS) scores were recorded at enrollment, 6 months, and 1 year. Knee MRI was obtained at enrollment and 6 months and scored by two Pediatric Radiologists. Clinical results were available from 12 participants and imaging was available from 9 participants.

Results:

Participants randomized to both groups were similar in age and gender distribution. IKDC and KOOS outcomes were not significantly different between groups. All participants were initially classified as DiPaola Stage I, while at the follow-up, 20% of the treatment group were classified as DiPaola Stage II compared to 0% of the conservative therapy group. Improvement in associated underlying marrow edema was similar between groups. Subchondral cystic changes improved in 20% vs 100% for the treatment and conservative therapy groups respectively.

Conclusion:

Though our small sample size may not have been sufficient to detect significant differences, intra-articular PRP injections demonstrated no significant improvement in clinical outcomes or the MR appearance of knee OCD when compared with conservative therapy.

S7.3.4

NORMAL SONOGRAPHIC APPEARANCE AND PITFALLS IN PEDIATRIC FINGER JOINTS

JESSE Sandberg, MAX Zalzman, SARAH Harris, ERIKA Rubesova
Lucile Packard Children's Hospital, Department of Pediatric Radiology,
Stanford University, Stanford, USA

Purpose: Recent developments in high resolution probes have allowed Ultrasound (US) to become an excellent diagnostic tool for evaluation of small joints such as pediatric hands. Inflammatory diseases in children such as Juvenile Idiopathic Arthritis usually manifest by synovial proliferation and joint effusion. At this time, there are however no normative data on the appearance of finger joint spaces in children. The purpose of this study is to assess the normal sonographic appearance of the finger joint in healthy children and describe any potential pitfalls.

Materials & Methods: IRB approved prospective study included children with no history of joint pathology. Sagittal grayscale US of the first three digits of the right hand was performed including volar images of the metacarpophalangeal (MCP) and proximal interphalangeal (PIP/IP) and dorsal images of the MCP joints. Subjective assessment of the joint recess was performed (Grade 0=not visualized, 1=visualized but not bulging, 2=bulging; subcategorized into A/B/C for fluid/synovial soft tissue (SST)/both, respectively). Anteroposterior depth measurement of joint fluid alone and the entire joint recess (fluid and SST combined) was performed. Incidental US findings, including but not limited to peritendinous fluid and erosions as well as imaging pitfalls were recorded. Children were asked questions regarding hand activity. All data analysis was conducted via consensus agreement between two diagnostic radiologists.

Results: A total of 22 children ranging between 4-17 years (mean 10.8±3.8 years) were included, total of 132 joints. No joint recess was visualized (grade=0) in 100 (76%) joints. The joint recess was visualized (Grade 1A-C) in 21 (16%) joints, and bulging (Grade 2A-C) in 8 (7%) joints (Table 1 for joint scoring and hand usage). 6 joints had measurable fluid (5%). Joint recess was not significantly more likely to be visualized in the MCP over the PIP/IP joints ($p=0.09$). Mean total joint recess depth was 0.7 ± 0.3 mm (range 0.1-1.3mm), joint fluid depth was 0.6 ± 0.4 mm (range 0.2-1.2mm). No incidental findings, including imaging of the dorsal aspects of the joint, were identified. Imaging pitfalls included anisotropy and prominent hypoechoic epiphyseal cartilage/perichondrium ($n=30$).

Conclusions: Finger joint recesses can occasionally be visualized in healthy children, while intraarticular fluid is rarely seen. Normal recess should not be misinterpreted as inflammatory change in the pediatric fingers.

S7.3.5

A CROSS SECTIONAL MAGNETIC RESONANCE IMAGING STUDY OF FACTORS INFLUENCING GROWTH PLATE CLOSURE IN ADOLESCENTS AND YOUNG ADULTS

OLA Kvist¹, ANA LUIZA Dallora², OLA Nilsson^{1,3}, PETER Anderberg^{2,4}, JOHAN Sanmartin Berglund², CARL-JOHAN Flodmark⁵, SANDRA Diaz^{1,6}

¹ Karolinska Institute, Department of Womens and Childrens Health, Stockholm, SWEDEN

² Blekinge Institute of Technology, Department of Health, Karlskrona, SWEDEN

³ Örebro University, School of Mecial Science, Örebro, SWEDEN

⁴ Skövde University, Department of Health, Skövde, SWEDEN

⁵ Lunds University, Department of Clinical Science, Lund, SWEDEN

⁶ Lunds University, Department of Radiology, Lund, SWEDEN

To assess growth plate fusion by MRI and evaluate its correlation with sex, age, pubertal development, physical activity and BMI.

Growth plates of radius, femur, proximal- and distal tibia and calcaneus in 958 healthy subjects aged 14.0–21.5 years old were examined using a 1.5T whole-body scanner and graded by two radiologists. Spearman's rank correlation coefficient was calculated to evaluate whether BMI, pubertal development or physical activity affected the maturity of the five growth plates. Logistic regression was performed to evaluate at what age growth plate closure was complete (stage 5). Stage 5 was the dependent variable and BMI, age and sex were the independent variables. Multiple logistic regressions were performed to calculate the odds ratio for each growth plate. Age and sex adjusted BMI was computed using the Swedish growth reference data and every individual was categorized as either normal- or overweight. Conditional logistic regression stratified for age and sex was performed to evaluate whether BMI affected the rate of maturity.

Complete growth plate fusion occurred in 75, 85, 97, 98, 98% and 90, 97, 95, 97, 98% (radius, femur, proximal- and distal tibia and calcaneus) in 17-year-old females and 19-year-old males, respectively. Complete fusion occurs approximately 2 years earlier in girls than boys. Pubertal development correlated with growth plate fusion score ($\rho=0.514-0.598$) but regular physical activity did not. BMI correlated with growth plate fusion ($\rho=0.186-0.384$). Stratified logistic regression showed increased odds ratio (OR F: 2.65–8.71; M: 1.71–4.03) for growth plate fusion of obese or overweight compared normal weight subjects. Inter-observer agreement was high ($\kappa=0.87-0.94$).

Implementation of MRI to determine the grade of growth plate fusion is feasible. Female growth plates are completely closed significantly earlier than male growth plates. Ordinary physical activity may not have significant effect on the maturation process. However, overweight does.

S7.3.6

DISRUPTION OF THE ZONE OF PROVISIONAL CALCIFICATION: AN MRI INDICATOR OF PHYSEAL STRESS INJURY OF THE PEDIATRIC KNEE

MARIA ALEJANDRA Bedoya¹, DIEGO Jaramillo², TAL Laor¹

¹ Boston Children's Hospital, Harvard Medical School, Boston, USA

² Morgan Stanley Children's Hospital, Columbia University, New York, USA

OBJECTIVE:

In athletic children with knee pain, it can be difficult to differentiate chronic physeal stress injury from an acute physeal disruption on MRI. Therefore, our aim is to identify MRI findings that can indicate a chronic physeal stress injury and differentiate it from an acute Salter Harris (SH) fracture of the pediatric knee.

MATERIALS AND METHODS:

Knee MRI examinations from 22 skeletally immature child athletes diagnosed with chronic physeal stress injury and 22 skeletally immature children with acute traumatic SH fractures were retrospectively reviewed by 3 pediatric radiologists with musculoskeletal expertise. Subject demographics, mechanism of injury and MRI characteristics (physeal thickening, abnormal physeal signal intensity (SI), disruption of the zone of provisional calcification (ZPC), disruption of the periosteum and perichondrium, pattern of bone marrow and soft tissue edema) in the two patient groups were compared using univariate and multivariate analyses.

RESULTS:

There were 28 chronic physeal stress injuries in the athlete group (median age 11.9yrs [8–15 yrs]) and 23 SH fractures in the acute injury group (median age

12.9yrs [5–16 yrs]). Mean time from clinical presentation to MRI was 36.2 weeks in the athlete group and 1.0 week in the SH fracture group. Physeal thickening was more common with chronic physeal stress (96% vs 78%, $p=0.04$). Increased physeal SI was more common in SH fractures (96%) ($p=0.04$), but it was seen in 75% of physeal stress injuries. ZPC discontinuity strongly suggested physeal stress injury compared to SH fractures (79% vs 30%, $p<0.01$). Periosteal or perichondrial elevation or rupture, and extra-articular soft tissue edema characterized acute SH fractures ($p<0.01$) and were rarely seen in stress injuries (<4%).

CONCLUSION:

Chronic physeal stress injuries of the knee show a significantly higher incidence of ZPC discontinuity or absence compared to SH fractures, reflecting alteration in the normal process of endochondral ossification. MRI features that strongly suggest SH fractures and are rarely present with chronic physeal stress injuries include periosteal or perichondrial injury, and extra-articular soft tissue edema.

S7.4.1

TWO-YEAR NEURODEVELOPMENTAL OUTCOMES OF HEALTHY FETUSES SCANNED AT 3 TESLA

FEDEL Machado Rivas¹, ANJALI Sathwani², JULIA Rohde³, CAITLIN K Rollins⁴, CAMILO Jaimes¹

¹ Boston Children's Hospital - Department of Radiology, Boston, USA

² Boston Children's Hospital - Department of Psychiatry, Boston, USA

³ Boston Children's Hospital - Department of Developmental Medicine, Boston, USA

⁴ Boston Children's Hospital - Department of Neurology, Boston, USA

Purpose:

To longitudinally evaluate the neurodevelopmental outcomes at 2 years of age of healthy fetuses that underwent 3T MRI

Materials and Methods:

This HIPAA-compliant, IRB-approved study analyzed a subset of children whose mothers enrolled as healthy volunteers in a longitudinal fetal brain MRI study. Criteria for inclusion were: a) normal pregnancy, b) maternal age 18–45 years, c) 3T MRI in 2nd trimester, d) completed neurodevelopmental testing. Imaging included T2-HASTE, SSFP, T2*, VIBE and DTI. We recorded maternal demographics, number of MRIs, and specific energy deposition (SED). Neurodevelopment was assessed at 18–24 months of age with the Bayley Scales of Infant and Toddler Development-III (BSID-III) and the Adaptive Behavior Assessment System-3 (ABAS-3). Cohort composite score means were compared to test norms (standardized composite score means = $100 \pm SD 15$) using a one-sample two-tailed Z-test. Test scores were evaluated as predictors of SED with a linear regression analysis.

Results:

29 children (17 male) had neurodevelopmental assessment at 23.9 ± 4.2 months of age. All subjects underwent a 2nd trimester MRI (mean gestational age (GA) 26.4 ± 3.1 weeks; mean SED 2138.5 ± 1250.2 J/Kg); 22 also underwent a 3rd trimester MRI (mean GA 37 ± 1.3 weeks, mean SED 1866.7 ± 985.1 J/Kg). Maternal age at birth was 33.2 ± 4.4 years, 86% of mothers identified as white, and 93% had at least partial college education. BSID-III Cognitive and Language composite scores and the ABAS-3 General Adaptive Composite were significantly higher than normative means at 105.9 ± 14 ($P=0.035$), 107 ± 17.4 ($P=0.006$), and 118.2 ± 2.8 ($P<0.001$), respectively. BSID-III Motor composite scores were not significantly different from the normative mean ($P=0.186$). We found no significant association between scores and SED exposure ($P>0.131$, all).

Conclusions:

Children who underwent fetal MRI at 3T have neurodevelopmental outcome at or above test norms and without dose-response relationship to SED.

S7.4.2

DIFFERENT PATTERNS OF VENTRICULAR DELINEATION IN SPINAL DYSRAPHISM BEFORE AND AFTER SURGERY

FREDERIC Guffens¹, M Ebner^{2,3}, L Fidon², J Deprest^{4,5}, P Demaerel¹, T Vercauteren^{2,3}, L De Catte⁵, S Dymarkowski¹, M Aertsen¹

¹ Department of Radiology, University Hospitals Leuven, Herestraat 49, 3000 Leuven, Belgium., Leuven, BELGIUM

² School of Biomedical Engineering & Imaging Sciences (BMEIS), Kings College London, UK, London, UNITED KINGDOM

³ Medical Physics and Biomedical Engineering, University College London, UK, London, UNITED KINGDOM

⁴ Elizabeth Garrett Anderson Institute for Womens Health, University College London, UK, London, UNITED KINGDOM

⁵ Department of Obstetrics and Gynaecology, University Hospitals and cluster Women and Child, Dept. Development and Rege, Leuven, BELGIUM

Objective: The purpose of this study is to (1) examine evolution in pre-operative and postoperative findings in ventricular size; (2) to correlate the ventricular size with the evolution in the lateral ventricle volume measured with a novel artificial intelligence based tool and (3) analyze the relation of the ventricular size with the ventricle delineation and grade of Chiari II malformation.

Methods: Retrospective review of fetal MRI-scans for open spinal defect (OSD) in a tertiary center in fetuses undergoing fetal surgery. Fetuses with preoperative, early postoperative (<7 days) and late postoperative MRI were included. The ventricular size and lining was analyzed as well as the evolution of the Chiari II malformation. 3D superresolution reconstruction (SRR) volumes were created using a python based tool performing motion correction and volumetric image reconstruction.

Results: 52 fetuses underwent fetal surgery for closure of OSD. Seventeen fetuses had all necessary images for this observational study. Mean GA prior to surgery was 24.5 w, at first MRI after surgery 25.9 w and 30.9 w at the late MRI. All had Chiari II malformation preoperatively and demonstrated some reversal at the last MRI ($p < 0.0001$). There was a significant increase in ventricle width between the preoperative and the late postoperative evaluation ($p = 0.0002$). Four patterns of ventricular lining were noted: normal, undulated, irregular or nodular. When moderate (9/51; 18%) or severe (21/51; 41%) ventriculomegaly was present, the undulated pattern was identified more often. The nodular pattern was seen in 1/11 fetuses with normal ventricles, 5/10 with mild ventriculomegaly, 2/9 with moderate ventriculomegaly and 5/21 with severe ventriculomegaly.

A strong correlation between atrial diameter and automatic volume segmentations was found. No significant correlation was found between the preoperative Chiari II grade and ventricular volume, nor between the pre- and postoperative evolution of Chiari II grade and ventricular volume.

Conclusion: Despite reversal of the Chiari II malformation there was a significant increase in ventricle size. 4 different patterns of ventricular lining were noted with the nodular type being identified most often late in pregnancy and more than half of them after surgery. A strong correlation between atrial diameter and volume was found. No significant correlation was found between the preoperative Chiari II grade and ventricular volume.

S7.4.3

CHANGES IN HINDBRAIN HERNIATION ON FETAL MRI PRIOR TO AND FOLLOWING PRENATAL REPAIR OF OPEN SPINAL DYSRAPHISM

SAAD Ranginwala, ROBIN Bowman, FEDERICO Scorletti, AIMEN Shaaba

Ann and Robert H. Lurie's Children's Hospital of Chicago, Chicago, USA

BACKGROUND AND PURPOSE:

As the practice of prenatal repair of myelomeningoceles becomes more commonplace, knowledge of the expected MR imaging findings has become increasingly important. Changes in hindbrain herniation have been previously assessed between fetal and postnatal MRI in patients, comparing differences between patients receiving prenatal and postnatal repair. Our aim was to examine neuroimaging findings such as hindbrain herniation and ventricular size in fetuses with open spinal dysraphism and to compare how these findings changed in fetuses undergoing prenatal repair between pre-surgical and post-surgical fetal MRIs.

MATERIALS AND METHODS:

Single-center retrospective analysis was performed on MRIs of fetuses with open spinal dysraphism who underwent prenatal repair and received both pre-surgical and post-surgical fetal MRI from March 2018 through March 2021. Fourteen fetuses were included. Images were reviewed by a board-certified pediatric radiologist with concentrated experience in fetal MRI. Descriptive analyses were performed to demonstrate the distribution of the imaging findings.

RESULTS:

Eleven of 14 fetuses (78.6%) fetuses had cerebellar ectopia (7 grade 3, 4 grade 2). After prenatal repair, 90.1% (10/11) had resolved cerebellar ectopia and 100% (11/11) had improved cerebellar ectopia on fetal MRI performed 35.2 ± 7.1 days post-repair. The degree of ventriculomegaly pre-repair (11.9 ± 2.6 mm) and post-repair (15.6 ± 5.3 mm) was not improved.

CONCLUSIONS:

In fetuses with open spinal dysraphism and Chiari II malformation that undergo prenatal repair with fetal MRI performed both prior to and after repair, most cases demonstrate resolution in cerebellar ectopia in utero after repair of spinal dysraphism.

S7.4.4

EVALUATION OF POSTERIOR FOSSA BIOMETRIC MEASUREMENTS ON FETAL MRI IN THE EVALUATION OF "DANDY-WALKER CONTINUUM"

USHA Nagaraj¹, BETH Kline-Fath¹, PAUL Horn¹, CHARU Venkatesan¹

¹ Cincinnati Children's Hospital Medical Center, Cincinnati, USA

² University of Cincinnati College of Medicine, Cincinnati, USA

Dandy Walker malformation (DWM), vermian hypoplasia (VH) and Blake pouch remnant (BP) are believed to represent a continuum of developmental anomalies and are common reasons for referral for fetal MRI. These terms, however, are not universally agreed upon and can be challenging to accurately distinguish from one another. Purpose: To determine whether posterior fossa biometric measurements on fetal MRI can be utilized to distinguish these three posterior fossa abnormalities. Materials/Methods: A single-center IRB approved retrospective analysis of all fetal MRI exams for malformations of the posterior fossa to include DWM, VH, and BP. Biometry data evaluated included measurements of the anterior to posterior (AP) pons, cranio-caudal (CC) and AP vermian, transverse cerebellar diameter (TCD), lateral ventricle size, tegmento-vermian (TVA) and posterior fossa angles (PFA). Measurements were compared with normal biometry and also between each subgroup. Results: 33 fetuses met criteria and were included in the study. 7 were designated DWM, 16 VH and 10 BP. TVA was significantly higher in DWM ($109.5 \pm 20.2^\circ$) when compared to VH ($52.13 \pm 18.8^\circ$) and BP ($32.1 \pm 17.9^\circ$) regardless of GA. PFA and lateral ventricle size were significantly higher in DWM at mean > 23.1 weeks GA compared to VH and BP. AP vermian and CC vermian were significantly smaller in

DWM when compared to VH and BP at mean > 23.1 weeks GA. Conclusion: Our data would support that DWM can be differentiated from VH and BP by increased elevation of the TVA, however other potential distinguishing biometric measurements are more helpful at > 23.1 weeks GA. The difficulty in distinguishing these entities from one another because they fall along the same spectrum of embryologic abnormalities makes precise morphologic and biometric descriptions important to allow for accurate prenatal counseling.

S7.4.5

SUPER RESOLUTION MR IMAGE RECONSTRUCTION IMPROVES IMAGE QUALITY AND DIAGNOSTIC CONFIDENCE IN FETUSES WITH BRAIN MALFORMATION

DIANNA Bardo, NICHOLAS Rubert, PATRICIA Comejo, JENNIFER Vaughn, LUIS Goncalves
Phoenix Children's Hospital, Phoenix, USA

Background: Fetal brain MRI is now a common imaging exam when a question of brain malformation or abnormality is suspected or diagnosed on prenatal ultrasound (US). Fetal structures are small and therefore challenging to image using MRI as spatial resolution is limited. Super resolution is a new technique for post-processing fetal MRI images. It is unknown if diagnostic accuracy and diagnostic confidence is improved using this technique.

Purpose: We sought to compare image quality, effects of image motion and diagnostic confidence in standard fetal brain MRI and super-resolution image reconstructed images produced from these standard fetal brain MRI images.

Methods: 19 fetuses with prenatal ultrasound (US) diagnosis of brain abnormality underwent brain MRI exams. Images of the brain were processed according to a previously published slice-to-volume recon algorithm, resulting in 38 total datasets.

In the recon algorithm, images are intensity corrected with the N4 algorithm, masked and cropped to the brain then registered manually. Scattered data approximation is used to create a guess at high-resolution volume & motion corrected using an interleaved rigid registration process (5 iterations) and high-resolution volume estimate is updated (20 iterations).

4 readers: individual, blind assessment of standard and super resolution images, graded on a Likert scale, image quality (very good/good/acceptable/poor/very poor), effects of image motion (none/minimal/moderate/ marked/severe) and diagnostic confidence (high/moderate/low/none). Diagnosis of brain abnormalities and specific comments regarding anatomy noted.

Statistical analysis: Wilcoxon matched pairs signed ranks test.

Results: 19 fetal patients, gestational age range 19 weeks/2days – 38 weeks/0 days.

Super resolution provided improved anatomical definition of normal anatomy & brain malformations. <FILE IMAGE=393_20210112164711.jpg>

Wilcoxon matched pairs signed ranks test showed all ratings improved by one point on the Likert scale for individual readers & combined data: image quality (p=0.0274), effects of image data (p=0.0002) & improved diagnostic confidence (p=0.0326).

Conclusion:

Super resolution image post-processing of fetal brain MRI images has potential for improving image quality and reducing effects of image motion, leading to increased confidence in making diagnoses

S7.4.6

WHAT IMAGING FEATURES DIFFERENTIATE LETHAL FROM NON-LETHAL PERINATALLY DIAGNOSED

OSTEOGENESIS IMPERFECTA? A SYSTEMATIC REVIEW WITH NARRATIVE SYNTHESIS

MOHAMED Hassan Mahmoud¹, MOHAMED Hassan Mahmoud⁵, CIARA McDonnell², CIARA McDonnell³, AMAKA C Offiah⁴, AMAKA C Offiah⁵

¹ Radiology Department, Ismailia, EGYPT

² Childrens Health Ireland, Temple St & Tallaght, Dublin, IRELAND

³ Trinity Research in Childhood Centre (TRICC), Paediatrics, Trinity College, The University of Dublin, Dublin, IRELAND

⁴ Department of Oncology & Metabolism, University of Sheffield, Sheffield, UNITED KINGDOM

⁵ Department of Radiology, Sheffield Children's NHS Foundation Trust, Sheffield, UNITED KINGDOM

Objective: To identify the perinatal diagnostic features that allow differentiation of lethal from non-lethal osteogenesis imperfecta.

Methods: A systematic review of studies published between 1st January 1980 and 15th July 2019 identified from the MEDLINE, Cochrane, Springer, and Google Scholar databases was undertaken using keywords [Antenatal] OR [Perinatal] OR [Neonatal] AND [Osteogenesis imperfecta] OR [Osteogenesis imperfecta type 2] OR [Osteogenesis imperfecta type 3] OR [Severe osteogenesis imperfecta] OR [Lethal osteogenesis imperfecta] AND [Radiology] AND [Ultrasound] AND [MRI] AND [CT]. Inclusion and exclusion criteria were applied. We assessed the studies' quality using the CASP tool for cohort studies and the "Methodological quality and synthesis of case series and case reports" tool for case reports. Data was extracted from each paper covering: gestational age, family history, diagnostic modality, diagnostic findings, post-natal diagnosis, type of osteogenesis imperfecta, and lethality.

Results: 854 publications were initially identified. Total publications after removal of duplicates were 763. After reviewing titles and abstracts, 700 papers were eliminated. Of the remaining 63 articles, 41 met the inclusion criteria, 30 were case reports, 11 were cohort studies. All 41 were included in the synthesis. Ultrasound was the primary diagnostic modality in 40 articles, followed by conventional fetography in 8, CT in 3, and MRI in 3 articles. The most frequently described antenatal features of lethal osteogenesis imperfecta (OI) described by the case reports include shortening and bowing of long bones, multiple fractures, reduced acoustic shadowing of bones, small chest circumference, and increased visualization of the intracranial content. The included cohort studies described the most frequent features linked to a lethal outcome as early shortening of long bones, multiple fractures, marked demineralization of fetal bones, and a small chest with decreased lung volumes.

Conclusion: Small lung volume (small chest) was the most frequently described feature linked to a lethal outcome in perinatal OI and not described in non-lethal OI. Typical OI findings (shortening and/or bowing of long bones, multiple fractures, demineralization of the skeleton) tend to be more severe and present at an earlier gestational age (as early as 13 gestational weeks) in lethal OI.

Keywords: systematic review; osteogenesis imperfecta; radiological diagnosis; lethal, perinatal.

S8.1.1

A COLLABORATIVE HYBRID OPERATING ROOM APPROACH TO PULMONARY NODULE LOCALIZATION AND RESECTION AS A TOOL FOR QUALITY IMPROVEMENT IN PEDIATRIC INTERVENTIONAL RADIOLOGY AND SURGERY

JOHN Racadio, ALEJANDRA Casar Berazaluze, NICOLE Hilvert, DANIEL von Allmen

Cincinnati Children's Hospital Medical Center, Departments of Radiology and Surgery, Cincinnati, OH, USA

Purpose:

CT-guided localization is an accepted method of pulmonary nodule identification that allows for VATS resection, avoiding thoracotomy. Traditionally, this involves marking in the radiology suite with transfer to the operating room (CT+OR) – requiring patient transportation under general anesthesia and re-positioning for thoracoscopy. Since February 2018, we have performed these procedures in a collaborative hybrid operating room (HOR) in an attempt to improve efficiency and patient safety. We sought to characterize the differences between these approaches.

Methods:

All cases performed in our HOR from February 2018 to August 2019 were retrospectively identified. Cases performed with CT+OR were selected in consecutive reverse chronological order for a 1:1 sampling. Descriptive statistics were obtained, and comparisons were made with t-tests.

Results:

A total of 26 cases were reviewed, 13 for each approach. Patients had similar age, diagnoses, and number of additional procedures performed. Time from localization to case start was shorter for HOR (17±12min vs 31±23min, $p=0.04$), representing the effect of patient transport time in CT+OR. Surgery time was shorter for HOR (103±35min vs 148±72min, $p=0.05$), signaling the burden of patient re-positioning in CT+OR. OR time was longer for HOR (272±72min vs 198±82min, $p=0.02$), an expected finding given that all portions of the intervention take place in this room. Anesthesia time was shorter for HOR (285±74min vs 318±94min, 0.17), a desired effect given the potential neurodevelopmental risks of anesthetic exposure in the pediatric population. There was no significant difference in patient charges.

Conclusion:

HOR is a promising alternative to the conventional CT+OR approach to pulmonary nodule localization and resection that minimizes surgery and anesthesia times while avoiding complications associated to patient transport (including potential marker dislodgment) without increasing patient charges. These differences are expected to become more pronounced as our HOR experience grows and we overcome the learning curve associated to the use of this new resource.

S8.1.2

SCLEROTHERAPY IN THE TREATMENT OF COMMON LYMPHATIC MALFORMATIONS “MYTH OR REALITY”: A 23 YEARS SINGLE CENTER EXPERIENCE

HEBA ELBAALY Elbaaly¹, JOSÉE Dubois¹, NIINA Kleiber², LOUISE Caouette-Laberge³, JEAN -NICOLAS Racicot¹, FRANÇOISE Rypens¹, JULIE Powell⁴

¹ Medical Imaging Department, CHU Sainte-Justine, Montréal, CANADA

² Pediatrics, CHU Sainte-Justine, Montréal, CANADA

³ Surgery Department, CHU Sainte-Justine, Montréal, CANADA

⁴ Dermatology Department, CHU Sainte-Justine, Montréal, CANADA

Purpose:

Lymphatic malformations (LM) have a significant aesthetic and functional impact. This study aims to review the intervention outcome in common LM in children.

Methods:

Retrospective review of LM referred to the Vascular Anomaly Clinic from 1996-2019. Patients with initial and end of treatment imaging were included. Patients awaiting sclerotherapy/post-treatment imaging, LM associated with overgrowth syndromes, intra-abdominal LM and complex lymphatic anomalies were excluded. Treatment outcome was classified into: >80% regression of initial size, 50-80%, 25-50%, <25%, spontaneous regression, asymptomatic followed-up.

Correlation between treatment outcome and multiple parameters (infection, haemorrhage, type of LM, localization, DeSerres Type for Head and Neck, sclerosant agent) was performed with one-way ANOVA.

Results:

505 patients were referred, 167 excluded. 338 LM (155F, 183M) classified into 177 H/N (DeSerres stage I (n=57), stage II (n=48), stage III (n=35), stage IV (n=4), stage V (n=9)), 71 trunk, 56 extremities, 34 multiple regions. 20 had infection, 39 haemorrhage. LM were classified on imaging into Type1: 100% of the cysts >1 cm (28.1%), type2a: 70% >1 cm (10.1%), type2b: 40-70% >1 cm (17.8%), type2c: 1-39% >1 cm (19.2%), type3: 100% <1 cm (24.9%). 166 had sclerotherapy alone, 32 had sclerotherapy following surgical recurrence, 54 had spontaneous regression, and 86 were asymptomatic. Doxycycline was used in 53% (105) of sclerotherapies. Side effects were infection (n=1), transitory neuropathy (n=1). Infection at presentation correlated with regression (p-value:0.06), haemorrhage did not. LM type correlated with %regression, >80%: type1 (39.6%), type2a (14.2%), type2b (19.8%), type2c (16.0%), type3 (10.4%) (p-value: 0.00), as did localization (p-value: 0.01), and DeSerres type (p-value: 0.03). Type1 is likely to regress spontaneously (48.1%, n=26), type3 to be asymptomatic (46.5% n=40). The sclerosant agent is not significantly correlated to %regression (p-value:0.79).

Conclusion:

Sclerotherapy is a safe and effective treatment modality. Symptomatology remains at the centre of the treatment decision. Initial imaging characteristics help predict treatment response.

S8.1.3

MESENTERICO-ILIAC CONGENITAL SHUNT A PARTICULAR FORM OF CONGENITAL PORTO-SYSTEMIC SHUNT: FROM PRENATAL DIAGNOSIS TO POST-NATAL MANAGEMENT

SOLÈNE Le Cam¹, ROMAIN Pommier¹, OLIVIER Meyrignac², CATHERINE Gareil³, CATHERINE Adamsbaum¹, STÉPHANIE Franchi Abella¹

¹ Pediatric radiology department, Bicetre Hospital APHP, Kremlin Bicetre, FRANCE

² Adult radiology department, Bicetre Hospital APHP, Kremlin Bicetre, FRANCE

³ Pediatric radiology department, Armand-Trousseau Hospital APHP, Paris, FRANCE

Congenital porto-systemic shunts (CPSS) are rare vascular malformations that expose to severe complications such as hepatic encephalopathy, hepatic tumors, cardio-pulmonary complications. Occlusion of CPSS have a significant benefit by reversing and/or preventing complications and hepatic portal deprivation. Mesenterico-iliac (MI) shunts are a particular form of extrahepatic CPSS poorly described in the literature. The aim of this work is to present cases of congenital MI shunts underlying the possibility of prenatal diagnosis and benefit of neonatal treatment.

Patients with mesenterico-iliac CPSS were included. Presentation at diagnosis, associated disorders, age at embolization and evolution were collected.

Among a series of 170 patients with CPSS, four patients presented with a communication between a large inferior mesenteric vein and one or the two internal iliac veins. Two patients had a prenatal diagnosis in a context of fetal anasarca in one; and fetal anemia related to alpha-thalassemia with cardiac insufficiency in the other. The two other patients were diagnosed at 6-month-old because of low limb edema for one and 14-year-old due to a preoperative abnormal coagulation test in a context of Proteus syndrome for the other. Hepatofugal portal flow was present in the intrahepatic and the main portal veins within the first hours of life in the two neonates who had a prenatal diagnosis. In the two older patients the main portal vein and the intrahepatic portal veins were very hypoplastic. Endovascular embolization was

performed in all: via the umbilical vein in the two neonates with prenatal diagnosis and via the jugular vein in the two others. Complete obstruction of the CPSS was obtained after a few days in 3 patients and obstruction is still partial in the most recent one. Restoration of normal portal anatomy with an hepatopetal flow was obtained in all. Signs revealing the CPSS resolved in the two patients with later diagnosis. Anasarca and cardiac failure resolved in the neonates. Follow-up (from 3 months to 10 years) showed no delayed complication of the procedure.

Mesenterico-iliac CPSS lead to severe hypoplasia of the main portal vein and portal deprivation. Prenatal diagnosis and neonatal embolization are possible and allow early restoration of the hepatic portal flow and prevention of further complications. Restoration of the hepatopetal portal flow is also possible later in life. Complications related to CPSS are reversible after closure

S8.1.4

MINIMALLY-INVASIVE, IMAGE-GUIDED TREATMENT OF FIBROADIPOSE VASCULAR ANOMALIES (FAVA): A SINGLE CENTER EXPERIENCE

VAZ Zavaletta¹, C. MATT Hawkins¹, RACHEL Swerdlin², ANNE Gill¹

¹ Children's Healthcare of Atlanta, Department of Radiology, Atlanta, USA

² Children's Healthcare of Atlanta, Vascular Anomalies Clinic, Atlanta, USA

Purpose:

Fibroadipose vascular anomaly (FAVA) is a recently described vascular malformation with few case series describing its clinical course. The purpose of this study is to describe the presentation, diagnostic work-up, and treatment outcomes of patients with FAVA from a single multidisciplinary vascular anomalies center and to validate previously published cohorts.

Methods:

IRB approved retrospective review identified 19 patients (age: 12 [8-21] years; 14 F/ 5 M) from 8/2018 - 9/2020 who presented with impaired mobility and pain. All patients were evaluated in the multidisciplinary vascular anomalies clinic and had pre-procedure MRIs.

Results:

Typical referring diagnosis was venous malformation (N=14). All patients lacked cutaneous findings and had pain, worsened by palpation. Locations of FAVA: calf (N=9), thigh (N=8), ankle (N=1), and paraspinal muscles (N=1). All calf lesions presented with flexion contractures. Thirteen patients received sotradecol sclerotherapy (2[1-7] treatments). After sclerotherapy, all patients demonstrated worsening pain or persistent symptoms. Due to either failure of sclerotherapy (N=13), atypical MRI findings (N=1), or high suspicion for FAVA at presentation (N=5), percutaneous core needle biopsy was performed; all biopsies were consistent with FAVA. Following biopsy-proven diagnosis of FAVA, all lesions were treated with cryoablation. Patients were followed clinically and 5 patients who experienced post procedure pain after cryoablation received an MRI. Clinical success, defined as symptomatic and/or functional improvement, was achieved in 17/19 (89%) patients; one patient recurred and one patient was lost to follow-up. Seven patients (7/19; 37%) had minor complications from cryoablation (transient skin injury=2, transient numbness=3, transient motor nerve injury = 2). There were no major complications.

Conclusion:

FAVA occurs more frequently in females and commonly presents with pain (exacerbated by palpation) and flexion contractures. Sclerotherapy alone is ineffective and commonly worsens symptoms. Core needle biopsy is useful in confirming the diagnosis and establish parent/patient expectations for outcomes. Cryoablation may be an effective therapy. These findings validate previously published cohorts.

S8.1.5

THE ROLE OF CT IN DIAGNOSIS AND PERCUTANEOUS TREATMENT PLANNING OF POST-PNEUMONIC PNEUMATOCELES IN INFANTS

ELISA Mercanzin¹, PIETRO ANDREA Bonaffini^{1,2}, ANTONINO Barletta², FRANCESCO Stanco^{1,2}, PAOLO Marra², SANDRO Sironi^{1,2}

¹ Milano-Bicocca University, Milan, ITALY

² Papa Giovanni XXIII Hospital, Bergamo, ITALY

PURPOSE

To underline the role of CT in assessing the main post-pneumonic pneumatocoles characteristics in infants, with the purpose of planning treatment.

METHODS AND MATERIALS

We retrospectively analyzed clinical records of a total of 5 infants (age < 1 year) with post-pneumonic pneumatocoles. These infants were treated with percutaneous drainage because of the persistence of the pneumatocoles or their symptoms. After standard chest X-Ray (CXR), patients underwent pre-treatment unenhanced chest CT scan to evaluate pneumatocoles' characteristics and assessment of those most suitable for drainage. All pneumatocoles were reviewed in terms of number, site, dimension, presence of septa, and relation with bronchial structures. The outcome of percutaneous treatment (US/CT guided drainage) was assessed by CXR and clinical parameters.

RESULTS

All 5 patients developed bacterial pneumonia (4 MRSA, 1 Pseudomonas) within the first year of life, complicated by pneumatocoles onset (single, 3 cases; multiple, 2 cases). Four patients (2 females) were premature and developed postnatal ARDS as a predisposing factor. CXR in all cases raised the suspicion of pneumatocoles. CT confirmed the diagnosis and allowed accurate characterization. The mean number of pneumatocoles per patient was 3.6 (range 1-8); the mean number of lobes involved was 2.2 (range 1-4). The mean dimension was 4.18 cm (range 2.4-6.5).

Septa were present in 4 cases and in 3 cases CT demonstrated the relation of pneumatocoles with the bronchial tree. In the cases of multiple or septated pneumatocoles, CT guided the choice of the components most suitable for drainage. Follow-up CXR confirmed complete regression of pneumatocoles in all cases.

CONCLUSION

CT has a complementary role to chest X-Ray in the pre-operative assessment of post-infectious pneumatocoles in infants, defining main imaging features and supporting treatment planning (US/CT-guided percutaneous drainage). Considered the good outcome provided, exposure to ionizing radiation of CT may be justified. CT-guided drainage is an efficient technique to treat pneumatocoles and to improve the prognosis of these infants.

S8.1.6

LYMPHATIC INTERVENTION FOR HEPATOPULMONARY CONNECTIONS IN CHILDREN WITH PLASTIC BRONCHITIS AND CHYLOTHORAX: INITIAL EXPERIENCE

FERNANDO Escobar¹, CATHERINE Tomasulo², ABHAY Srinivasan¹, GANESH Krishnamurthy¹, YOAV Dori², CHRISTOPHER Smith²

¹ Children's Hospital of Philadelphia, Department of Radiology, Philadelphia, USA

² Children's Hospital of Philadelphia, Division of Cardiology, Philadelphia, USA

Background

Plastic bronchitis (PB) and chylothorax (CTX) are complications of abnormal lymphatic flow via lymphatic channels to the lungs and pleural space. We describe our experience and approach for children who had lymphatic connections from the liver to the lung and underwent percutaneous lymphatic interventions.

Material and Methods

Retrospective review, including all patients who underwent lymphatic imaging and were found to have hepatopulmonary (HP) connections from 1/2016-3/2019. The intervention involved hepatic fluoroscopic lymphangiography followed by selective lymphatic network access and embolization of abnormal HP connections. Patient outcomes were recorded.

Results

HP connections were identified in 14 patients with a history of CTX (10/14) or PB (5/14) who underwent lymphatic imaging at the median age of 9.8 years (0.5-17 years). 4 patients had prior lymphatic procedures, but continued casts/CTX. 9 patients (64%) had congenital heart disease, including 7 (50%) with Fontan circulation and a median Fontan pressure of 17 mmHg (14-18 mmHg). 10 (71%) patients underwent lymphatic intervention for HP connections. Embolization of abnormal channels was performed with lipiodol (1/10) or TruFill glue (9/10). All targeted channels were successfully embolized. 1 patient had a second embolization for additional HP connections. 3 patients had additional non-HP lymphatic interventions.

Post-procedure complications included transient hypotension requiring dopamine (1/10), blood transfusion for anemia (2/10), and hemoperitoneum in a patient on ECMO with multisystem organ failure before intervention; care was withdrawn the next day. Non-targeted embolization occurred in 3 patients, resulting in a stroke in 1 patient. There was no intraprocedural mortality.

Excluding the fatalities, all patients had resolution or decrease in cast production and no CTX reaccumulation at median follow-up 93.5 days (7 days-3.6 years). 2 patients transferred to their home ICUs and the other six had a median ICU stay of 1.5 days (1-3 days) and a median hospital stay of 17.5 days (6-63 days).

Conclusion

HP connections are a rare cause of CTX and PB. This initial experience suggests the utility of assessment of hepatic lymphatics for guiding interventions. Lymphatic intervention for these connections is effective with the resolution of symptoms in all surviving patients. In patients with CTX or PB, if central lymphatic imaging does not show abnormalities, liver imaging should be performed

S8.2.1

EFFECT OF GADOLINIUM-BASED CONTRAST MEDIA ON THE DIAGNOSTIC PERFORMANCE OF MRI FOR SUSPECTED ACUTE APPENDICITIS

KUMAR Shashi, LAURA Cadogan, KELLYN Mahan, SARAH Bixby, MICHAEL Callahan
Boston Childrens Hospital, Boston, USA

Introduction: Magnetic resonance imaging (MRI) has replaced computed tomography as an adjunct to US when sonographic findings are indeterminate in the diagnosis of appendicitis. There are no prior studies comparing contrast enhanced (ceMRI) to non-contrast appendicitis MRI (ncMRI) or detailing the significance of an indeterminate MRI in the context of suspected acute appendicitis.

Purpose: Present our experiences for MRI appendicitis at a pediatric teaching hospital.

Material and methods: All patients referred for MRI for suspected appendicitis after US over a 40-month period (Jan 2017-Apr 2020) were included in the study. Patient demographics, white blood cell count (WBC), utilization of intravenous contrast (IVC), time of MRI, & radiologist focus (Body, MSK, Nighthawk) were recorded. MRIs were reported as positive, negative or equivocal at time of interpretation. Presence of perforation was noted. MRI interpretations were correlated with pathology findings & discharge diagnosis. Sensitivity (SN), specificity (SP), & accuracy (ACC) were calculated. Multivariate logistic regression was performed to determine odds of patient having appendicitis based on age, gender, WBC, time of exam, & the odds of IVC administration based on age, gender, WBC, exam time, radiologist focus, & presence of perforation.

Results: 625 MRI studies were performed over the study period. 210 patients received IVC. MRI was interpreted as positive in 130 (20.8%) patients, negative in 440 (70.4%) patients, & equivocal in 55 (8.8%) patients. SN, SP, & ACC of MRI for appendicitis was 90%, 91% & 91%, respectively. When MRI was equivocal, acute appendicitis was present 25% of the time (14/55). Male gender & higher WBC counts were associated with a diagnosis of appendicitis ($p < 0.001$). Odds of administering IVC significantly increased with an equivocal MRI diagnosis ($p < 0.0001$) & significantly decreased if the radiologist focus was Nighthawks ($p < 0.001$). Mean number of studies interpreted by Nighthawk, Body, & MSK radiologists over the study period were 67, 18, & 8 exams, respectively.

Conclusion: Equivocal MRI interpretation for appendicitis accounted for ~9% of all cases, & was the most significant factor associated with IVC. The majority of patients (75%) with an equivocal MRI did not have appendicitis. Nighthawks were less likely than other subspecialty groups to administer IVC regardless of exam time, suggesting that increased experience may allow additional confidence in interpreting ncMRI.

S8.2.2

THE IMPACT OF CONTRAST ENHANCED ULTRASOUND (CEUS) ASSESSMENT ON THE MANAGEMENT OF ABDOMINAL SOLID ORGAN INJURIES IN CHILDREN

TERRY Humphrey, HELEN Woodley
Leeds Childrens Hospital -Department of Radiology, Leeds, UNITED KINGDOM

Background

American Pediatric Surgical Association (APSA) guidance has been widely adopted for the management of solid organ injuries (SOI) in children. Their 2019 systematic review provides recommendations regarding length of hospital stay, activity restrictions, role of interventional radiology and follow up imaging.

Computed Tomography (CT) is the imaging gold standard for the initial assessment of solid organ trauma. In December 2015 we introduced the use of CEUS performed at least 5 days post trauma, to assess delayed pseudoaneurysm (PA) formation and the extent of organ injury in children presenting with SOI to our trauma centre.

Aim

To assess the impact of CEUS imaging on the management of children presenting with SOI to a trauma centre.

Method

The CEUS findings of all children examined consecutively between December 2015 and September 2019 were reviewed. The grade and organ of injury on presenting CT, incidence of PA detected with CEUS and further follow-up or interventions were recorded.

Results

Sixty children (41 boys) with a mean age of 10.9yrs (range 1-16yrs) presented for CEUS assessment. There were 28 liver, 24 splenic and 8 kidney injuries. The incidence of PA detected was 4/60 (6.6%). PA occurred in 2 splenic (grade 2 and 4 injuries), 1 liver (grade 5 injury) and 1 kidney (grade 3 injury). All 4 cases were asymptomatic, treated conservatively and resolved on follow-up CEUS performed 3-4 days later.

Conclusion

CEUS is a valuable non invasive way to follow up SOI. In line with the APSA review we found that children with PA who were asymptomatic could be treated conservatively and CEUS showed their resolution. Assessment of the extent of organ injury with CEUS helps inform decisions regarding returning to normal activities.

S8.2.3

CONTRAST-ENHANCED ULTRASOUND OF THE CHEST IN CHILDREN: ASSESSMENT OF ADDED DIAGNOSTIC VALUE

HALLEY Park¹, EDWARD Y. Lee¹, KUMAR Shashi¹, WENDY G. Kim¹, ABBEY J. Winant¹, GAIL MacCallum¹, DOMEN Plut², HARRIET J. Paltiel¹

¹ Boston Children's Hospital, Boston, USA

² Clinical Institute of Radiology, University Medical Centre Ljubljana, Ljubljana, SLOVENIA

PURPOSE: This retrospective study evaluated the added diagnostic value of contrast-enhanced ultrasound (CEUS) in pediatric chest abnormalities by comparing CEUS to findings obtained with conventional US.

MATERIALS AND METHODS: Nineteen children (10 male [52.6%], 9 female [47.4%]) ranging in age from 3 months to 17 years (mean age 9 years, 3 months +/- SD 5 years, 6 months) with a variety of suspected chest abnormalities underwent conventional grayscale and color Doppler US evaluation followed by CEUS between 1/2016 and 2/2020.

Indications included determining the presence of a chest mass in 9, assessment for lung necrosis in 7, differentiation of lung from air in 1, question of active bleeding in 1, and identifying a foreign body in 1. CEUS was performed after IV injection of 1-2 doses of sulfur hexafluoride microbubbles, 0.03mL/kg.

Studies were randomized and independently reviewed by two pediatric chest radiologists blinded to clinical information and prior imaging studies. Conventional US studies were interpreted first followed 2 weeks later by review of the CEUS studies to minimize reviewer bias. Interpretations of both studies were compared and the added diagnostic value was determined. Accuracy of diagnosis was based on patient clinical outcome. Interobserver agreement was evaluated with kappa statistics.

RESULTS: In 18/19 (95%) cases, CEUS provided additional diagnostic value, including verification of lung necrosis in 7 (36.8%), confirmation of a solid lung mass in 7 (36.8%), and identification of single cases of a mediastinal mass, extrathoracic mass, active bleeding, and differentiation of lung from air (21.1%). In one patient with possible esophageal foreign body CEUS provided no additional information (5.3%). Reviewers agreed in 18/19 cases, kappa = 0.9.

CONCLUSIONS: CEUS adds value in the diagnosis of chest abnormalities, particularly in identifying lung necrosis and solid lung masses. The results of this study support the promising role of CEUS as a non-invasive, radiation-free problem-solving imaging technique in children.

S8.2.4

EFFECT OF HYPERBILIRUBINEMIA ON THE EXCRETION OF HEPATOCYTE SPECIFIC CONTRAST IN CHILDREN UNDERGOING MAGNETIC RESONANCE CHOLANGIOGRAPHY

MICHAEL Acord¹, ANILAWAN Smithimedhin¹, RAMA Ayyala³, JANET Reid^{1,2}, SUDHA Anupindi^{1,2}

¹ Children's Hospital of Philadelphia, Philadelphia, USA

² University of Pennsylvania, Philadelphia, USA

³ Cincinnati Children's Hospital, Cincinnati, USA

Purpose: Magnetic resonance cholangiography (MRC) using hepatocyte specific contrast agents (HSCA) can be a useful, non-invasive means to evaluate the biliary system in pediatric patients. Often these patients present with hyperbilirubinemia and it is unknown how this may affect contrast excretion. The aim of this study was to identify a bilirubin value at which HSCA might be avoided.

Methods and Materials: This was a dual-center, retrospective cohort study of patients who underwent a hepatocyte specific contrast-enhanced MRC using gadoxetate disodium between June 2012 and September 2019. Imaging indication, total scan time, time at hepatobiliary phase (HBP) imaging, and total bilirubin levels were recorded. Patients that excreted contrast were compared to those that did not and T-test and linear regression were performed to assess the association with bilirubin levels and the lack of contrast excretion.

Results: 17 patients (8 female) with a mean age of 8.1 years (range: 1 month- 21 years) underwent 17 contrast-enhanced MRC during the study period. Indications included assessment for communication between the biliary tree and a hepatic cystic lesion (8, 47.1%), evaluation for biliary leak (5, 29.4%), or identification of functionally obstructive anastomotic stricture after liver transplant (4, 23.5%). After contrast administration, HBP was performed after a delay of <=20 minutes, (5, 29.4%), 21-60 minutes (10, 58.8%) or >60 minutes (2, 11.8%). In 6 patients (35.3%), contrast did not excrete into the biliary system at the conclusion of the study, all with bilirubin levels greater than 3 mg/dL. Bilirubin level was strongly associated with excretion of contrast (B=7.1, 95% CI=2.8-11.4, p=0.003) and patients who failed to excrete had a significantly higher bilirubin (7.9± 6.8 vs 0.8± 0.5 mg/dL, p=0.003).

Conclusion: In this dual-center study, patients with total bilirubin levels greater than 3 mg/dL failed to excrete contrast, suggesting a cut-off value for when HSCA might be avoided.

S8.2.5

THE CLINICAL USEFULNESS OF INTRAVENOUS CONTRAST-ENHANCED ULTRASONOGRAPHY IN CHILDREN: A SINGLE CENTRE EXPERIENCE

MARTIN Thaler, MOJCA Glusic, DAMJANA Kljucsek
University Childrens Hospital Ljubljana, Ljubljana, SLOVENIA

Purpose

The purpose of this study is to demonstrate the usefulness of intravenous contrast enhanced ultrasonography (CEUS) in clinical practice in children.

Material and methods

We performed a retrospective analysis how the results of CEUS influenced the further clinical management and selection of additional imaging. CEUS was considered as a) problem solving method, if we could make a final diagnosis, b) complementary, if the final diagnosis was not made, but important information was obtained that affects the further management, and c) non-diagnostic, when CEUS results had no impact on further management.

Results

We analysed 203 CEUS examinations in 157 children (67 boys, 90 girls), aged from 1 day to 18 years. Indications for CEUS were: 40 children with focal liver and 36 with kidney lesion, 7 spleen lesions, 14 abdominal or soft tissue tumor masses, 4 miscellaneous, and 50 evaluation of bowel wall perfusion. 107 children with 123 examinations were further analysed after excluding bowel CEUS which is considered as complementary method.

Overall 78.5% of all CEUS investigations proved to be a problem solving, 18.7 % were complementary, and only 2.8% were non-diagnostic. CEUS was problem solving in 84.5% of focal liver lesions and in 89.1% of kidney lesions. In evaluation of solid focal spleen lesions and abdominal and soft tissue masses CEUS was complementary method for more

than 50% of cases – better delineate perfusion of mass and its relation to surrounding tissue. Further imaging or biopsy was required. In 2.8% of cases CEUS was non-diagnostic.

Two children had minor transient side effects related to US contrast agent
Conclusions

CEUS has important clinical impact as problem solving and complementary method in 97.2% of all cases. It facilitates the characterization of focal lesions and evaluation of organ perfusion in children and helps to make a final diagnosis more quickly.

S8.2.6

INITIAL EXPERIENCE WITH CONTRAST-ENHANCED ULTRASOUND AS AN ADJUNCT TO CT FOR BLUNT ABDOMINAL TRAUMA IN CHILDREN WITH CONCERN FOR PHYSICAL ABUSE

M KATHERINE Henry¹, SUSAN J Back¹, AARON E Chen³, KASSA Darge¹, TENIOLA I Egbe⁴, LAURA Poznack¹, PHILIP V Scribano², SABAH Servaes¹, JOANNE N Wood²

¹ Department of Radiology, Children's Hospital of Philadelphia, Philadelphia, USA

² Division of General Pediatrics, Children's Hospital of Philadelphia, Philadelphia, USA

³ Division of Emergency Medicine, Children's Hospital of Philadelphia, Philadelphia, USA

⁴ Center for Pediatric Clinical Effectiveness, Children's Hospital of Philadelphia, Philadelphia, USA

Purpose: Intra-abdominal injuries from blunt trauma are rare in physically abused children, but can have important clinical and forensic implications. Contrast-enhanced computed tomography (CECT) of the abdomen and pelvis with intravenous contrast sometimes identifies findings of indeterminate significance. Due to the clinical and forensic importance of abdominal injuries, clarification of findings on CECT concerning for traumatic injury is critical. Our objective was to explore the added value of contrast-enhanced ultrasound (CEUS) in young children for whom there was concern for abuse. **Materials and Methods:** This is a retrospective study of children <8 years who underwent abdominal CEUS and CECT from 1/1/2015–10/18/2017 to evaluate for blunt abdominal injuries from suspected physical abuse. We described imaging findings of each modality to assess the role of CEUS in the evaluation of solid organ injury. The clinical team made the final determination regarding presence of solid organ injury.

Results: Eight subjects (0.2 – 5.8 years) underwent CEUS and CECT due to concern for physical abuse. In 7 of 8, CEUS was obtained following CECT to clarify CECT findings. In 6 of these 7 subjects, CEUS provided additional clarification regarding the presence/absence of traumatic solid organ injury. For 5 subjects in whom the CECT showed a questionable organ injury, CEUS was normal and therefore helped to exclude organ injury (specifically to the spleen, liver, and kidney). For 2 subjects, CEUS confirmed liver injuries seen on CECT. In one subject with a complex medical presentation, the CEUS confirmed the presence of the liver finding observed on CECT but did not clarify whether it was traumatic in origin.

Conclusions: Based on our initial experience, CEUS was useful in clarifying CECT findings of uncertain significance. Additional research comparing both modalities is needed to assess accuracy of CEUS and determine whether CEUS has a role as a radiation-free screening modality for intra-abdominal injuries in children with concern for abuse.

S8.3.1

NORMAL SPLEEN STIFFNESS VALUES IN HEALTHY CHILDREN BY SHEAR WAVE ELASTOGRAPHY AND

ASSOCIATIONS (WITH AGE, GENDER, AND SPLEEN SIZE)

ZUHAL Bayramoglu, ELIF HAZAL Karli, AYSE Ibis
 Istanbul University, Istanbul Medical Faculty, Radiology Department, Istanbul, TURKEY

Purpose

This study aims to define the normal elasticity and velocity values of the spleen with shear wave elastography (SWE) in healthy children and interpret associations with organ size and gender, age, body mass index (BMI) of the participants.

Methods

This prospective study included a total of 213 cases (male: 111; female:108), aged 0-17 years and each year of life included at least 15 participants. Age groups were created as preschool, school, and adolescent periods of 0–6 years (n =53), 7–12 years (n =104), and 13–17 years (n =56) along with pubertal status as prepubertal 3–10 years (n =122) and postpubertal 11–18 years (n = 91). The gender, age, height, body weight, and BMI were recorded as auxological data. Spleen length, splenic short-axis diameter, and spleen stiffness measurements were performed with a convex transducer (3.5–5 MHz) on the longitudinal plan. All patients underwent abdominal ultrasound examination to exclude liver pathology. Correlations and comparisons were performed for stiffness values among age groups. We used the Kolmogorov-Smirnov, Mann-Whitney U, Kruskal-Wallis, and Spearman's correlation tests for statistical purposes.

Results

Medians (Interquartile range) of age, height, and weight were 10 (6.75–13) years, 137 (120–156) cm, and 35 (22.5–49)kg. The median (Interquartile range) short and long axis dimensions for the spleen were measured as 40 (35-47) mm and 93 (82-104)mm. The median (Interquartile range) elasticity and velocity values for the spleen were measured as 15.1 (13.75-16.7) kPa and 2.18 (2.06-2.3) m/s. No significant differences were identified for stiffness values between gender and age groups. Splenic dimensions values presented positive correlations with age (r: 0.56, p: 0.001), height (r:0.59, p: 0.001), body weight (r: 0.62, p: 0.001). However, no significant correlation was found between splenic size and stiffness values.

The standardized values for spleen elasticity in healthy children are beneficial to differentiate the spleen involvement by various illnesses. Normal elasticity and velocity values were defined by SWE for each age group in children.

S8.3.2

CAN MRI DIFFERENTIATE HEPATIC HEMANGIOMA FROM OTHER LESIONS IN EARLY INFANCY?

DAN Halevy, BLAYNE Sayed, FURQAN Shaikh, SIMON Ling, IRAM Siddiqui, GOVIND Chavhan
 Hospital for Sick Children, Toronto, CANADA

Purpose: Confidant diagnosis of hepatic hemangioma on imaging avoids unnecessary biopsy in neonates and helps guide conservative management. Purpose of this study was to determine utility of MRI in differentiating liver hemangioma from other lesions in infants <100 days, and to determine frequency and association of MR imaging features with hepatic lesions.

Methods: MRI performed for liver lesions were retrospectively reviewed by 2 reviewers blinded to the diagnosis and clinical features. Features noted included size, signal intensity, pattern of enhancement, other characteristics of lesions and the best MRI diagnosis. In cases with multiple lesions, the largest lesion representing each different imaging feature/ diagnosis was included. Final diagnosis was assigned to each lesion based on pathology in available cases, and by corroborative standard of reference (CSOR) including overall clinical diagnosis, alpha fetoprotein (AFP) levels and stability or reduction in size of the lesion with minimum follow up period of 6 months.

Results: Of 30 infants (18 boys, 12 girls; average age- 42.2 days) included, 18 had solitary and 12 had multifocal lesions. Diagnoses in total 33 lesions (by

pathology in 8 and by CSOR in 25 with median follow up period of 29 months) included hemangiomas (23), hepatoblastoma (6), AVM (2) and one each of metastases and infarction. MRI diagnosis and final diagnosis matched in 94% lesions with almost perfect agreement ($\kappa=0.86$) for reader 1, and matched in 88% lesions with substantial agreement ($\kappa=0.71$) for reader 2. Inter-observer agreement for MRI diagnosis between two readers was substantial ($\kappa=0.62$). Sensitivity, specificity, PPV, NPV and accuracy of MRI in differentiating hemangioma from other lesions was 100%, 90%, 95%, 100% and 97% respectively. Centripetal (16/23) or flash (5/23) filling were only seen with hemangioma. There was no significant difference in AFP elevation ($p=0.08$), average size ($p=0.35$), multifocality ($p=0.38$) and intralesional hemorrhage ($p=1$) between hemangioma and hepatoblastoma. Washout was seen only with hepatoblastoma (1/6) and metastases (1/1). Both AVMs showed hypertrophied arteries, early draining veins and large network of vessels.

Conclusion: MRI reliably differentiates hepatic hemangioma from other lesions in early infancy and guides conservative management. Centripetal or flash filling on dynamic imaging and absence of washout are characteristic imaging features of hepatic hemangioma.

S8.3.3

DEVELOPMENT AND USE OF A SPIO NANOPARTICLES-BASED PHANTOM FOR VALIDATION AND DISSEMINATION OF NONINVASIVE MRI METHODS FOR EVALUATION OF LIVER IRON OVERLOAD

PETR Bulanov¹, EVELINA Nazarova¹, PETR Menshchikov^{1,2}, DMITRY Kupriyanov^{1,2}, GALINA Tereshchenko¹, GALINA Novichkova¹

¹ Dmitry Rogachev National Medical Research Center of Pediatric Hematology, Oncology and Immunology, Moscow, RUSSIAN FEDERATION

² Philips Healthcare, Moscow, RUSSIAN FEDERATION

Introduction

Liver iron overload is a common diagnosis in children with sickle cell disease etc. Assessment of iron overload by T2* MRI data is a promising noninvasive and safe technique. Earlier we carried out a study on the correlation of T2* values (ms) with LIC (mg/ml) values obtained from liver biopsy from children with varying degrees of liver iron overload. Thus, we obtained a formula for recalculation of T2* values into iron concentration in LIC [1]. However, this formula can be reliably used only with those MRIs on which it was obtained, because T2* values are very sensitive to various scanning parameters. This is a significant problem, because the construction of such a formula is complex and time-consuming process.

In order to make the use of our formula possible in other centers, we had the task of developing a method to standardize the obtaining of T2* values on various MRIs. The basis of this method was a MR-compatible phantom.

Materials and methods.

The phantom consisted of 28 test tubes, 50 ml each, with different solution concentrations of paramagnetic iron oxide nanoparticles. These nanoparticles were obtained by the Elmore chemical reaction. Solution with a high iron concentration was diluted to cover the entire range of T2* values corresponding to all liver iron overload grades [1].

To check the results for repeatability, the phantom was scanned throughout the year in 1-week increments on our MRIs: Philips Achieva 3T and Signa GE 1.5T.

We further verified reproducibility on other scanners (Research Institute of Emergency Pediatric Surgery and Traumatology, N.N. Priorov Scientific Research Institute of Traumatology and Orthopedics)

Results and discussion

As a result, the T2* values showed good repeatability on both our scanners. The phantom was stable throughout, indicating that it can be used for long time. On the other scanners tested we found statistical correspondence of values, so the T2* values obtained on them can be recalculated in LIC with the help of our formulas. In case of inconsistency of values next steps must be carried out:

- 1) calibration of scanning parameters and T2* mapping;
- 2) introducing additional calibration coefficients into the recalculation formula.

Thus, to be able to use formulas, it is enough to check the correspondence of T2* values using the phantom we created. If there are discrepancies, it is necessary to refine the scanning protocol up.

References

- 1) <https://doi.org/10.24287/1726-1708-2020-19-3-158-163>

S8.3.4

LIVER IRON QUANTIFICATION IN CHILDREN: COMPARISON OF MULTI-ECHO DIXON VIBE WITH T2* RELAXOMETRY

GEETIKA Khanna, SUDHIR Bhimaniya, ZHONGWEI Zhang
Washington University, St Louis, USA

Purpose:

MRI based liver iron quantification is the standard of care to guide chelation therapy in patients with iron overload. The purpose of our study was to evaluate the diagnostic accuracy of a vendor based technique (LiverLab) using Wood T2* relaxometry as the reference standard.

Materials and Methods:

This was a retrospective, HIPAA compliant, IRB approved study. The radiology information system was queried to identify all MRIs done for liver iron concentration (LIC) estimation between July 2015 - January 2020. All patient's had undergone T2* relaxometry on a 1.5T scanner. In addition, a multi-echo Dixon vibe was performed using the Siemens LiverLab technique. Two readers (fellow and attending radiologist) independently estimated liver R2* and T2* on the multi-echo Dixon vibe generated R2* and T2* maps. LIC estimated by Wood T2* relaxometry was used as the reference standard.

Inter-observer agreement was estimated by concordance correlation coefficient (CCC). Bland-Altman analysis was used for comparison of LIC by the 2 methods.

Results:

A total of 54 MRIs on 39 patients (23 females) were analyzed. Median patient age was 12 years (SD 5.27 years). LIC based on reference standard ranged 1.10-21.10 (median 6.80) mg/g dry weight of liver. The concordance between readers for R2* and T2* estimation using LiverLab was moderate [CCC 0.93 (0.88 – 0.96)] and substantial [CCC 0.99 (0.99 – 1.00)], respectively. Bland Altman analysis for both readers showed that all observations were clustered around the zero bias line if the LIC was less than 8mg/g dry. With increasing LIC there was a pattern of poor agreement with observations crossing the lower limits of agreement.

Conclusion:

LiverLab allows for good to excellent interobserver agreement in liver R2* and T2* estimation. LIC estimated by LiverLab has high accuracy only if liver iron is less than 8mg/g dry weight of liver.

S8.3.5

PROSPECTIVE STUDY OF QUANTITATIVE MRI IN CYSTIC FIBROSIS LIVER DISEASE: FEASIBILITY AND COMPARISON TO ULTRASOUND

TOWBIN Alexander¹, WEN Ye², SUIYUAN Huang², JEAN Molleston³, BOAZ Karmazyn⁴, PRAKASH Masand⁵, DANIEL Leung⁶, SAMUEL Chang⁷, MICHAEL Narkewicz⁸, ADINA Alazraki⁹, ALVIN Freeman¹⁰, RANDOLPH Otto¹¹, NICOLE Green¹², WIKROM Kamsakul¹³, IHAB Kamel¹⁴, JOHN Magee¹⁵, JOSEPH Palermo¹⁶

¹ Department of Radiology, Cincinnati Children's Hospital, Cincinnati, USA

² Department of Biostatistics, University of Michigan, Ann Arbor, USA

³ Pediatric Gastroenterology, Hepatology and Nutrition, Indiana University School of Medicine Riley Hospital for Children, Indianapolis, USA

⁴ Department of Pediatric Radiology, Riley Hospital for Children, Indianapolis, USA

⁵ Department of Radiology, Texas Children's Hospital, Houston, USA

⁶ Division of Gastroenterology, Hepatology and Nutrition, Texas Children's Hospital, Houston, USA

⁷ Department of Radiology, University of Colorado, Aurora, USA

⁸ Section of Pediatric Gastroenterology, Hepatology and Nutrition, Department of Pediatrics, University of Colorado SOM, Aurora, USA

⁹ Department of Radiology, Children's Hospital of Atlanta, Atlanta, USA

¹⁰ Division of Pediatric Gastroenterology, Hepatology and Nutrition, Emory University School of Medicine, Atlanta, USA

¹¹ Department of Radiology, Seattle Children's Hospital, Seattle, USA

¹² Division of Gastroenterology and Hepatology, Seattle Children's Hospital and University of Washington, Seattle, USA

¹³ Division of Gastroenterology and Hepatology, Johns Hopkins University School of Medicine, Baltimore, USA

¹⁴ Department of Radiology, Johns Hopkins University School of Medicine, Baltimore, USA

¹⁵ Department of Surgery, University of Michigan, Ann Arbor, USA

¹⁶ Division of Gastroenterology, Hepatology and Nutrition, Cincinnati Children's Hospital, Cincinnati, USA

PURPOSE: Cystic fibrosis liver disease (CFLD) is the third leading cause of death in cystic fibrosis (CF). Ongoing ultrasound (US) research performed as part of the PUSH study has shown that pediatric radiologists can identify a pattern of disease more likely to progress to advanced CFLD. However, reliably discriminating the pattern remains difficult. Quantitative MRI may provide an objective measure of CFLD. The purpose of this study was to determine if MR elastography (MRE) is feasible in children with CF and to determine how quantitative features compared to PUSH US.

METHODS: A prospective, multi-institutional trial was performed evaluating CF patients enrolled in PUSH. Participants underwent a standardized MRI. At central review, liver stiffness, fat fraction, liver volume, and spleen volume were obtained. Based on a priori determination, MRE was feasible if data could be obtained in > 90%. Participants were classified by their most recent consensus PUSH US grade as normal (NL), homogenous hyperechoic (HMG), heterogeneous (HTG), or nodular (NOD). Each MRI measure was compared among US grade groups using the Kruskal–Wallis test. A p-value <0.05 was significant.

RESULTS: 93 participants (51 girls [54.8%]; mean 15.6 years) were enrolled. There was no difference in the age or sex of participants between groups. MRE was feasible in 87 (93.5%). Non-feasible MRE was caused by motion (n=3), technical failure (n=2), and incomplete coverage (n=1). Livers classified as NOD had significantly higher liver stiffness (p <0.01) and spleen volume (p <0.05) compared to other groups. Those with an HMG pattern had significantly higher fat fraction (p <0.001) and their liver volumes trended larger (p range: 0.0046–0.062).

CONCLUSION: MRE is feasible in children with CF. Participants with a NOD liver had higher liver stiffness and larger spleen volumes supporting the US determination of advanced CFLD. Participants with an HMG liver had higher fat fractions and larger liver volumes supporting the diagnosis

of steatosis.

S8.3.6

PRE- AND POST-OPERATIVE SONOGRAPHIC ASSESSMENT OF PORTAL VEIN FLOW IN A PEDIATRIC COHORT AFTER TOTAL PANCREATECTOMY WITH ISLET CELL AUTO-TRANSPLANTATION

ADAM Yen¹, ANDREW Posselt², EMILY Perito³, MATTHEW Zapala¹

¹ University of California, San Francisco, Department of Radiology and Biomedical Imaging, San Francisco, USA

² University of California, San Francisco, Department of Surgery, Division of Transplant Surgery, San Francisco, USA

³ University of California, San Francisco, Department of Pediatrics, Division of Pediatric Gastroenterology, San Francisco, USA

Purpose: Compare pre- and post-operative flow within the main portal vein (MPV), right portal vein (RPV), and left portal vein (LPV) after total pancreatectomy with islet auto-transplantation (TPIAT) in a pediatric cohort.

Methods: Pediatric patients who underwent TPIAT from 2009 to 2020 at a tertiary pediatric hospital were identified. Flow velocities in the MPV, RPV, and LPV during the first two post-operative abdominal ultrasounds were measured and compared to velocities in pre-operative ultrasounds and in age-matched controls who underwent abdominal ultrasound for “pancreatitis”. Statistical analysis was performed using the student’s T-test.

Results: 21 pediatric patients (9:12 male:female; mean age 12.2 years) who underwent TPIAT were identified, 10 of whom had pre-operative ultrasounds and were included in the control group, for 42 total control patients (17:25 male:female; mean age 12.2 years). Mean flow velocities during the first ultrasound after TPIAT were significantly decreased compared to controls in the MPV (15.6+/-10.0 cm/s vs 25.6+/-6.2 cm/s, p<0.0001), RPV (13.3+/-7.9 cm/s vs 21.0+/-4.4 cm/s, p<0.0001), and LPV (8.9+/-8.4 vs 17.4+/-4.8 cm/s, p<0.0001). During the second post-operative ultrasound, velocities remained significantly decreased in the MPV (p<0.0001), RPV (p<0.0001), and LPV (p<0.0001). LPV flow decreased significantly more than MPV flow on the first (p=0.026) and second (p=0.0005) post-operative ultrasounds and RPV flow on the second ultrasound (p=0.004). One patient had thrombosed all portal veins on the first post-operative ultrasound, with MPV and RPV flow but not LPV flow restored on the second ultrasound. Three additional patients had thrombosed the LPV on the first and second post-operative ultrasounds. **Conclusion:** Velocities in the MPV, RPV, and LPV are significantly decreased in the immediate post-operative period after TPIAT, likely from a combination of post-operative edema and the desired result of islet cell embolization. The LPV appears to have the greatest decrease in velocity, with 19.0% of patients experiencing transient LPV thrombosis, possible due to inherent differences in flow dynamics.

S8.4.1

FEASIBILITY OF NON-GATED DYNAMIC FETAL CARDIAC MRI FOR IDENTIFICATION OF FETAL CARDIOVASCULAR ANATOMY

JULIA Geiger¹, RUTH Tuura², FRASER Callaghan², BARBARA Burkhardt³, KELLY Payette², ANDRAS Jakab², CHRISTIAN Kellenberger¹, EMANUELA Valsangiacomo³

¹ Imaging Department, Zurich, SWITZERLAND

² Center for MR research, Zurich, SWITZERLAND

³ Pediatric Cardiology, Zurich, SWITZERLAND

Purpose: To evaluate the feasibility of identifying the fetal cardiac and thoracic vascular structures with non-gated dynamic balanced steady-state free precession (SSFP) MRI sequences.

Material and Methods: We retrospectively assessed the visibility of cardiovascular anatomy in 66 fetuses without suspicion of congenital heart defect (mean gestational age (GA) 27+/-4, 21-38 weeks) in a consensus reading by an experienced paediatric cardiologist and radiologist. Non-gated dynamic SSFP sequences were acquired in three planes. An imaging score was defined by giving one point to each visualized structure. Basic diagnostics included the atria, ventricles, systemic veins, ventricular outflow tracts (RVOT/LVOT), aortic arch, descending aorta (DAO), ductus arteriosus and thymus (12pts); advanced diagnostics the atrioventricular (AV) valves, pulmonary arteries/veins, supraaortic arteries and trachea (21pts). Image quality was rated from 0 to 2. The influence of GA, field strength, placenta position, and maternal panniculus on image quality and score were tested.

Results: 34/32 scans were performed at 1.5/3T. Heart position, atria and ventricles were seen in 66 fetuses. Basic diagnosis was achieved in 60 (90%) cases, with visualization of the IVC/SVC in 65 (98%) / 63 (95%), RVOT in 62 (94%), LVOT in 61 (92%), aortic arch in 60 (91%), DAO in 64 (97%), ductus arteriosus in 59 (89%) and thymus in 50 (76%) fetuses. The AV valves were recognised in 55 (83%), pulmonary arteries in 35 (53%), at least one pulmonary vein in 46 (70%), supraaortic arteries in 42 (64%), and the trachea in 59 (89%) fetuses. The mean imaging score was 16.8+/-3.7. Maternal panniculus ($r = -0.3$; $p = 0.01$) and GA ($r = 0.6$; $p < 0.001$) correlated with imaging score. Image quality was better on 1.5T than 3T ($p = 0.04$) while the total score showed no significant difference.

Conclusions: Fetal heart MRI with non-gated SSFP sequences enables recognition of basic cardiovascular anatomy. Advanced diagnostics may be limited by thick maternal panniculus, lower GA and higher field strength.

S8.4.2

HIGH-RESOLUTION MORPHOLOGICAL AND FUNCTIONAL MR IMAGING OF THE FETAL HEART USING DOPPLER ULTRASOUND GATING: COMPARISON AND OPTIMIZATION ON A PULSE SEQUENCE ASPECT

ROLAND Cronenber¹, SHUO Zhang², BARBARA Ulm³, HENDRIK Kooijman-Kurfuerst², FABIAN Kording^{4, 5}, DANIELA Prayer¹, VANESSA Berger-Kulemann¹

¹ Dept Biomed Imaging, Division Neuroradiology and Musculoskeletal Radiology, Medical University of Vienna, Vienna, AUSTRIA

² Philips Healthcare, Hamburg, GERMANY

³ Dept Gynecology and Obstetrics, Division of Feto-Maternal Medicine, Medical University of Vienna, Vienna, AUSTRALIA

⁴ Dept Diagnostic and Interventional Radiology and Nuclear Medicine, University Hospital Hamburg-Eppendorf, Hamburg, GERMANY

⁵ Northh Medical GmbH, Hamburg, GERMANY

Purpose

MR imaging is considered a valuable diagnostic tool for studying cardiovascular structure and function in children and adults. However, simple, high-quality imaging of the fetal heart is challenging due to the lack of direct in-utero cardiac gating. We aimed to employ a recently introduced Doppler ultrasound (DUS) device combining and comparing different pulse sequences and to establish a standard acquisition method for high-resolution fetal cardiac MRI.

Materials and Methods

Three pregnant women underwent fetal MRI at 1.5T (Ingenia, Philips Healthcare) based on a previously diagnosed or suspected heart malformation in prenatal ultrasound. Two sequences based on multi-shot balanced turbo field echo in SSFP (bTFE) were investigated with 1) high spatial resolution 1.2x1.0x8-mm³ (temporal resolution 23-29 ms) and 2)

high temporal resolution 14 to 16 ms (1.6x1.4x8-mm³) for both breathhold (BH) and free breathing (FB), respectively. Cardiac gating signals were generated by a MR-compatible DUS device from fetal cardiac motion. Images were assessed visually according to general quality, artifacts, and visualization of the anatomical structures.

Results

All data were successfully acquired for multi-shot bTFE with retrospective DUS gating (gestational age 30 to 32 weeks, fetal cardiac frequency 150 to 180 bpm). Imaging times for BH scans were typically 7 to 12 s and 30 to 40 s for FB scan with multiple averaging (NSA=4) to mitigate gross motion without respiratory navigator. Different anatomical orientations including 4-chamber and short-axis cardiac views showed good image quality with excellent myocardium-to-blood contrast and clear fetal myocardial contractions in both sequence setups. No significant difference was found between BH and FB scans with maternal shallow and regular breathing.

Conclusions

High-resolution morphology and function of the fetal heart can be achieved with direct fetal cardiac gating from the DUS device in combination with commercially available pulse sequences. Preliminary experience in patients with free breathing may promise a wide clinical adoption for evaluation of congenital pathologies.

S8.4.3

FOUR-DIMENSIONAL FETAL CARDIAC MR IMAGING FOR FUNCTIONAL ASSESSMENT

NICHOLAS Rubert¹, JONATHAN D. Plasencia², DIANNA M.E. Bardo¹, CHRISTOPHER L. Lindblade², LUIS F. Goncalves¹

¹ Phoenix Children's Hospital -Department of Radiology, Phoenix, USA

² Phoenix Children's Hospital - Department of Cardiology, Phoenix, USA

Purpose:

To acquire objective functional measures derived from four-dimensional cardiac magnetic resonance (CMR) imaging.

Materials and Methods:

Three fetal CMR imaging studies have been performed with a 1.5T Philips Achieva scanner with further studies still ongoing. For each study, two-dimensional balanced retrospectively-gated Steady State Free Precession sequences were performed with between four and seven slice-select directions. Scan parameters for each sequence were as follows: 2.08x2.08x6.0 mm voxel size, slice overlap of 2 mm, and TE/TR 1.9/3.8 ms. Temporal frame rates between 84 and 94 ms were achieved with a kt-SENSE undersampling factor of 8. Raw data were exported from the scanner, retrospectively gated, and both anatomical images and velocity maps reconstructed, using the super-resolution algorithms developed in [1] and [2]. Isotropic spatial resolution of 1.25 mm and temporal resolution between 16.4 and 17.3 ms per frame were achieved, acquiring 25 uniformly spaced phases for a single RR interval.

Left (LV) and right (RV) ventricles were anatomically reconstructed in MIMICS (Materialise™). Outflow tract region-of-interests were generated to measure the localized blood velocity magnitudes.

Results:

Plots of the ventricular volumes and outflow tract blood velocity magnitudes are presented for a normal, hypoplastic left heart, and hypoplastic right heart at 34, 24, and 32-week gestational age, respectively.

The following ejection fractions/stroke volumes were found: Left ventricular LV – 33% / 1.5 ml, 35% / 0.1 ml, and 46% / 0.7 ml for the normal, HLHS, and HRHS heart. Right ventricular RV – 42% / 1.6 ml, 46% / 2.0 ml, and 39% / 0.2 ml for the normal, HLHS, and HRHS heart. Blood velocity magnitude curves show peak velocities of 38, 12, and 14 cm/s in the LVOT for the normal, HLHS, and HRHS heart. Blood velocity curves show peak velocities of 29 and 14 cm/s in the RVOT for the normal and HLHS heart. Due to the small size of the vessel diameter, a suitable region-of-interest in RVOT was not identifiable in the HRHS heart.

Conclusions:

Morphological and functional information about the fetal heart may be extracted from MRI. Fetal CMR imaging is especially promising for cases where ultrasound struggles due to factors like poor resolution from maternal obesity, oligohydramnios, or rib cage/spine shadowing in third trimester fetuses.

References:

- [1] van Amerom, J. F., et al (2019)
[2] Roberts, Thomas A., et al. (2020)

S8.4.4

LOCATION, LOCATION, LOCATION: THE REAL ESTATE OF FETAL LUNG LESIONS

EDWARD Oliver¹, RYNE Didier¹, SUZANNE DeBari¹, TERESA Victoria¹, SHELLY Soni², N. SCOTT Adzick², BEVERLY Coleman¹
¹ Children's Hospital of Philadelphia - Department of Radiology, Philadelphia, USA

² Children's Hospital of Philadelphia - Department of Surgery, Philadelphia, USA

Objectives: To assess the accuracy of prenatal ultrasound (US) and magnetic resonance imaging (MRI) in predicting lobar location of congenital lung lesions (e.g. CPAM, BPS), and the extent to which prenatal size and lobe affects accurate localization by both modalities.

Methods: Single center, retrospective IRB-approved searches of radiology and clinical databases were performed from 2008–19 for prenatally evaluated cases of suspected congenital lung lesions that underwent postnatal surgical resection. Only surgically confirmed intrapulmonary (i.e. intralobar) lung lesions were included for analysis as intrapulmonary lesions are assigned a location at surgery and extralobar lesions are not. Prenatal US and MRI imaging reports were reviewed for the predicted lobe and lesion size as determined by CVR. Prenatal localization was correlated with postnatal intraoperative location, and accuracy by each modality was correlated with baseline imaging size (CVR) and the specific lobe of origin.

Results: Of 513 solitary lung lesion cases with postnatal surgical confirmation, 455 were intrapulmonary lesions. All cases had baseline detailed fetal US and 81.3% (370/455) had corresponding fetal MRI. Median gestational age was 22.6 weeks (range, 16.4–38.3 weeks). Median baseline CVR was 0.62 (range, 0.03–4.8). Of 455 lesions, postnatal distribution was 38.2% left lower lobe, 35.2% right lower lobe, 13.4% left upper lobe, 7% right upper lobe, 2.4% right middle lobe, and 3.7% involving >1 lobe. Lobe of origin was reported in 92.3% (420/455) US reports and 74.9% (277/370) MRI studies. Both modalities demonstrated high accuracy in localizing the lobe of origin (US, 87.4% [K=0.82]; MRI, 90.6% [K=0.87]). By US and MRI, median CVR was higher for incorrectly localized lesions compared to correctly localized lesions (US: 0.93 vs 0.57, p<0.01; MRI: 0.82 vs 0.52, p=0.01). Accurate lobar localization was lowest for right middle lobe lesions (US, 33.3%; MRI 60%) and lesions involving >1 lobe (US, 0%; MRI, 20%). Accurate lobar localization for remaining lobes was 70–96% for US and 78.6–97.8% for MRI.

Conclusions: Prenatal US and MRI can have high accuracy in predicting lung lesion location, however, accuracy is inversely related to lesion size. Utilization of both modalities may be helpful when lesion localization is important for prenatal and/or neonatal management. Right middle lobe and multilobar lesions are uncommon but difficult to accurately localize prenatally by both US and MRI.

S8.4.5

EVOLUTION OF THE T1-WEIGHTED SIGNAL OF THE FETAL LIVER DURING PREGNANCY

MAX Zalzman, AURÉLIE D'hondt, JARRETT Rosenberg, SAFWAN Halabi, RICHARD Barth, ERIKA Rubesova

Lucille Packard Children's Hospital, Stanford University - Department of Pediatric Radiology, Stanford, USA

Objective: High T1 signal of the fetal liver compared to surrounding structures is believed to be related to extramedullary hematopoiesis. Pathology studies on animals reported a decline in fetal liver erythropoiesis during the third trimester. In this study we analyze the evolution of the T1 signal of the human fetal liver as a function of gestational age (GA), for indirect assessment of the erythropoietic liver function and its relationship to maternal hemoglobin levels.

Methods: This retrospective study included 327 fetuses, who underwent MRI for various indications from 20 to 39 gestational weeks. Signal intensity of the fetal liver was normalized to adjacent maternal psoas muscle. Liver-to-muscle signal intensity ratios (LMS) were measured on T1-weighted images as a function of GA. Linear regression analysis was used to evaluate the relationship between LMS and GA. In 219/327 patients, ratios were measured by two radiologists, Band-Altman plot was made for interobserver agreement. Hemoglobin levels were recorded among a subset of 40 patients with average LMS and among 6 outliers. **Results:** Average LMS was 1.52 with standard deviation of 0.58. Across GA, small but statistically significant increase of LMS was seen with a ratio increasing by 0.01009 per week, 95% CI: 0.01002-0.01017, p=0.17. The relationship between GA and LMS followed: $LMS = 0.013 GA + 1.1604$. High interobserver agreement between the two readers showed concordance correlation of 0.94. No significant difference in the presence of maternal anemia was found among outliers and patients with average LMS (p>0.7).

Conclusion: Although physiological studies on mammals showed a decreasing erythropoietic activity in fetal liver, our study shows a minimal increase of the T1 liver signal throughout the gestation. Although maternal anemia may have an effect on fetal erythropoiesis, we didn't find any clear correlation between liver T1 signal and hemoglobin levels. Further studies should investigate function and iron content such as T2* mapping in the fetal liver.

S8.4.6

PRENATAL MRI IN DIFFERENTIATING CYSTIC TERATOMAS AND VENOLYMPHATIC MALFORMATIONS OF THE FETAL NECK

SARA REIS Teixeira, CESAR A P F Alves, JUAN SEBASTIAN Martin-Saavedra, FABRICIO G Guimaraes, AVRUM Pollock, EDWARD Oliver, TERESA Victoria, LARISSA T Bilaniuk, TAMARA Feygin

Children's Hospital of Philadelphia, Philadelphia, USA

Purpose: To estimate most reliable prenatal magnetic resonance imaging (MRI) features to distinguish between fetal cystic teratoma (T) and venolymphatic malformation (VLM); to compare MRI with US in this scenario. **Methods & Materials:** Single institution retrospective IRB approved. Between 2009-2017, search through radiological database for fetal face and neck masses using keywords "neck", "venolymphatic malformation", "teratoma", "fetal". Inclusion criteria were cases with fetal neck mass of uncertain nature questioned to be T. Pediatric radiologists reviewed images for the following features: 1)morphology 2)distorsion of adjacent structures 3)tongue invasion 4)airway/upper GI compromise 5)polyhydramnios. Oropharyngeal swallowing phases were also assessed. **Results:** 43 fetuses met our inclusion criteria, 15(35%)T. Median gestational age at MRI was 24 weeks (IQR21-31). 15(100%)T were corrected

suggested by MRI, 12 out of 15(80%)T were suggested by US. Six cases were uncertain on MRI and US, 67% finally diagnosed as type 4 VLM. Sensitivity, specificity, and accuracy of MRI to diagnose T were 100%, 68%, and 79%, respectively. Distortion of adjacent structures, infiltration between spaces, airway/upper GI obstruction were the main imaging findings to distinguish between lesions ($p<.001-.01$). Additional features were levels within lesions (13.3%Tvs57.1%VLM), calcifications (100%Tvs57.1%VLM), displacement of midline structures(100%T vs 3.6%VLM). Polyhydramnios was more frequent in T($p=.012$). Impairment of the oropharyngeal swallowing phases was present in 15/15(100%) of T compared to 0 cases of VLM ($p<0.001$). Presence of blood, solid components, and chest invasiveness were not significantly different ($p.08-.48$), noting calcification were better seen on US. Conclusions: With high accuracy, the main prenatal MRI findings to distinguish T from VLM were distortion of adjacent structures, airway/upper GI obstruction, and infiltration between spaces. Combination of prenatal MRI and US has higher sensitivity and accuracy than each test alone. Highest rate of disagreement with final diagnosis was with cases of type 4 VLM. Both, T and VLM have significant variability of their imaging appearance, but different prognosis and perinatal management.

EDUCATIONAL AND SCIENTIFIC POSTER

Poster: EDU-001

BRITISH SOCIETY OF PAEDIATRIC RADIOLOGY ANNUAL MEETING (2020): THE TRANSITION FROM A VENUE-BASED TO A VIRTUAL CONFERENCE AND LESSONS LEARNED FOR THE FUTURE

NAGEENA Suleman, MARK Bishay, EMILY Evans, ULYA Malik, FATEMEH Hadian, WILLIAM Hedges, SANA Ali, HITEN Patel, MANIGANDAN Thyagarajan, ADAM Oates, SAMANTHA Low Birmingham Children's Hospital, Birmingham, UNITED KINGDOM
Summary

The British Society of Paediatric Radiology (BSPR) is a special interest group for paediatric radiologists and radiologists with combined adult and paediatric radiology interests. BSPR organises an annual 2-day meeting to stimulate discussion and provide a broad educational component to its members who are largely based in UK. In light of the global pandemic and the cancellation of the vast majority of venue-based meetings, this year's meeting moved to a purely virtual platform for the first time. We will describe this process and implications for future national and international conferences.

Learning objectives

In this interactive electronic poster, we describe the transition from a venue based to a purely virtual BSPR meeting, the effective use of social media and newer technologies such as Zoom and a web/app – based platform, incorporating a mixture of live and pre-recorded components. We will highlight the benefits and downsides of a solely virtual meeting, comparing our experience with previous annual BSPR meetings. We intend that this should inform others who are organising such conferences while the shadow of Covid-19 looms large, and beyond.

Purpose

To establish a sustainable model for future means of holding virtual Radiology meetings, which would be applicable to both small and large meeting groups.

Results

BSPR2020 received a greater number of abstract submissions and delegates than ever before and attracted speakers and delegates from further afield than previously. Analyses of speaker and overall meeting feedback was hugely favourable and demonstrated an improvement over previous meetings.

Conclusions

There are significant advantages to a virtual component at a scientific meeting and include, educational, financial and environmental aspects. We envisage a future where all conferences will be a combination of virtual and venue based, allowing greater geographical scope of both speakers and delegates.

Poster: EDU-002

“HOW TO REVIEW THE PAEDIATRIC RADIOLOGY ARTIFICIAL INTELLIGENCE EVIDENCE USING THE PICO/DATO METHOD”

BRENDAN Kelly¹, GABRIELLE Colleran², SIBOHAN Hoare², AONGHUS Lawlor³, RONAN Killeen¹

¹ St Vincents University Hospital, Dublin, IRELAND

² CHI @ Temple Street, Dublin, IRELAND

³ Insight @ UCD, Dublin, IRELAND

SUMMARY OF THE PRESENTATION

Brief introduction to Evidence Based Practise (EBP): Ask, Search, Appraise, Apply, Evaluate

Brief introduction to the advent of the application of artificial intelligence to radiology and the unique challenges it poses to EBP.

The PICO – DACO Model

How DACO compliments to the traditional PICO model to incorporate Data (both quality and quantity)

Algorithm (which model is used including ensemble models, “off the shelf” and custom models)

Comparison (human performance or other performance of another computer model)

Outcome (how outcome is measured – evaluation metric)

A Worked Example of EBRAI – Predicting Bone age in Children from wrist radiographs

EDUCATIONAL OBJECTIVES

Describe how the evidence-based practice (EBP) framework can be applied to the use of artificial intelligence in radiology Evidence Based Radiology Artificial Intelligence (EBRAI)

Introduction to the PICO DACO model - How Data Algorithm Comparison and Outcome compliment the traditional PICO model in EBRAI

Identify how EBRAI can be used as a starting point for the development and testing of in-house AI models

Identify how EBRAI can be used to evaluate commercial AI products

Poster: EDU-003

ADVANCED CARDIOVASCULAR COMPUTED TOMOGRAPHY (CT) IMAGING IN CHILDREN WITH CONGENITAL VARIANTS AND ANOMALIES OF THE AORTIC ARCH: FROM VOLUME RENDERING (VR) TO 3D MODELS AND 3D PRINTING

FLAVIO Zuccarino¹, MARÍA CLARA Escobar-Diaz², ALEX Perez², MARIA Navallas³, IGNACI Barber⁴, BOSCO ALEJANDRO Moscoso⁵, CONGIU Stefano⁵, JOSE MARIA Caffarena⁵, SALVATORE Marsico⁶, FREDY Prada², JUAN MANUEL Carretero², JOAN Sanchez de Toledo², JAVIER Mayol⁵, FERRAN Pifarre⁴, IRENE GOMEZ⁴, LAURA Acosta⁷, ARNAU Valls⁸, ENRIQUE LADERA⁴, JOSEP MUNUERA⁴

¹ Hospital Sant Joan de Deu, Department of Radiology and Hospital del Mar, Chief of Cardiothoracic Radiology, Barcelona, SPAIN

² Hospital Sant Joan de Deu, Department of Cardiology, Barcelona, SPAIN

³ Hospital 12 de Octubre, Department of Radiology, Madrid, SPAIN

⁴ Hospital Sant Joan de Deu, Department of Radiology, Barcelona, SPAIN

⁵ Hospital Sant Joan de Deu, Department of Cardiovascular Surgery, Barcelona, SPAIN

⁶ Hospital del Mar, Department of Radiology, Barcelona, SPAIN

⁷ Children's Hospital of Eastern Ontario, Department of Radiology, Ottawa, CANADA

⁸ Hospital Sant Joan de Deu, 3 D Printing Unit, Barcelona, SPAIN

Purpose

- To discuss the main indications for cardiovascular CT in newborns and children with congenital anomalies of the aortic arch (CAAA).
- To outline the key imaging findings of CT in CAAA, enhancing the usefulness of volume rendering (VR) and 3D models in differential diagnosis and the design of an optimal therapeutic approach.

Background

Echocardiography represents the first Imaging tool in the diagnostic process of CAAA. However, the morphology of the aortic arch and its relationship to other adjacent structures can be difficult or impossible to define. Consequently, CT has assumed a key role in the diagnosis of CAAA, allowing noninvasive visualization of aortic morphology, relationship between the aorta, the airways and the esophagus, and associated cardiac, thoracic or abdominal abnormalities.

Materials and methods.

In this work we review and organize the key imaging CT findings of different CAAA, focusing on 3D imaging reconstructions, as:

- Left-sided aortic arch anomalies.
- Left Aortic Arch with Aberrant Right Subclavian Artery with and without a Diverticulum of Kommerell
- Left Circumflex Aorta
- Right-sided aortic arch anomalies.
- Right Aortic Arch with Aberrant Left Subclavian Artery with and without a Retroesophageal Diverticulum
- Right Aortic Arch with Aberrant Brachiocephalic Artery
- Right Aortic Arch with Mirror Image Branching
- Right Aortic Arch with Isolation of the Left Subclavian Artery
- Right Circumflex Aorta
- Double aortic arch
- Cervical Aortic Arch
- Persistent Fifth Aortic Arch
- Interrupted Aortic Arch
- Aortic Arch Hypoplasia
- Coarctation
- Pseudocoarctation
- Gothic aortic arch

Conclusions

CT allows to define the complex aortic anatomy in patients with CAAA. 3D CT imaging techniques, such as VR and 3D models, enable to define the relationship of the aorta to the airways, esophagus, and other cardiovascular and thoracic structures, playing a pivotal role in CAAA diagnosis. Radiologists should be familiar with CT key imaging findings and with the advantages and limitations of these advanced techniques to establish an optimal diagnostic approach and therapeutic management.

Poster: EDU-004

CONGENITAL ABSENCE OF THE PERICARDIUM

BEVERLEY Newman

Stanford Childrens Hospital at Stanford University, Stanford, USA

Congenital absence of the pericardium is a very uncommon condition that may be focal, unilateral or bilateral but most frequently involves the left sided pericardium. The condition is typically asymptomatic and

discovered incidentally but may present with a variety of symptoms that mimic other intrathoracic pathology.

This poster will review and illustrate the presentation, diagnosis, imaging appearances and management of partial and complete absence of the pericardium. It is important to be aware of the distinctive imaging features as this is often the first time this diagnosis is considered. Prompt recognition can prevent further unnecessary evaluation

Poster: EDU-005

UNTWISTING ARTERIAL TORTUOSITY SYNDROME

GURDEEP MANN ¹, SANDRA Abusamaan ², SAAD Saeed ³

¹ Sidra Medicine - Department of Radiology, Doha, QATAR

² Hamad General Hospital - Clinical Imaging, Doha, QATAR

³ Sidra Medicine - Heart Center, Doha, QATAR

Purpose or Case Report: Arterial Tortuosity Syndrome (ATS) is a rare childhood-onset, congenital, autosomal recessive multisystem connective tissue disorder caused by mutations of the SLC2A10 gene. ATS is chiefly characterized by excessive tortuosity of the major arteries. Children present with a variable clinical spectrum of disease. Cardiovascular manifestations are related to elongation and twisting of the pulmonary arteries, the aorta, and its branches including the coronary arteries with complications due to stenosis or aneurysm formation. Thoracic associations comprise pectus deformities, hiatal and diaphragmatic hernias, and diaphragmatic entrancements. Skeletal manifestations include scoliosis, hypermobile joints, contractures, arachnodactyly, and cutis laxa. Rarely intestinal diverticula may be encountered.

Methods & Materials: We will present the multimodality imaging findings of ATS, focusing on the cross-sectional findings. We will highlight the key and typical imaging features of ATS by anatomical location. Our discussion will include descriptive features that will enable diagnosis.

Results: A structured approach should be used to evaluate the child with ATS; with particular attention paid to the pulmonary and systemic arteries, heart, thoracic cage, and diaphragms.

Conclusions: Familiarity with the imaging appearances of ATS will aid accurate characterization of this multisystem disorder and will assist in making a timely diagnosis and appropriate subspecialist referral and interventions.

Poster: EDU-006

SEGMENTAL ANALYSIS OF COMPLEX CONGENITAL HEART DISEASE: AN ODE TO CARDIAC IMAGING

NEETIKA Gupta ¹, LAURA Acosta-Izquierdo ¹, DEREK Wong ², JORGE Davila ¹

¹ Department of Medical Imaging, CHEO, University of Ottawa, Ottawa, CANADA

² Department of Pediatric Cardiology, CHEO, University of Ottawa, Ottawa, CANADA

Background:

The segmental approach for congenital heart disease was introduced by Van Praagh in 1960 and later an alternative classification system was developed by Anderson and colleagues known as Sequential segmental analysis. This system incorporates the fundamental of Van Praagh system and further emphasizes the importance of junctional variations and associated anomalies. The combined approach is widely applicable, flexible, and easy to understand allowing comprehensible communication between cardiologists and radiologists.

Educational Objectives:

1. Illustrate the relevant anatomy and connection of cardio-vascular structures critical for pre-operative reporting.
2. Demonstrate the precise role of cross-sectional imaging in accurately diagnosing and describing the complex congenital heart disease.

3. Convey and simplify major concepts of the Van Praagh and Anderson classification system to familiarize with the systemic approach.

Techniques:

1. Highlight the role of cross sectional imaging in assessing the cardiac anatomy, characterizing abnormal connections and extra cardiac anomalies to reach a final diagnosis.
2. Outline the key cardiac and extracardiac imaging findings of commonly encountered and rare complex congenital heart disease.
3. Discuss the step-by-step approach to evaluate complex congenital heart disease based on Van Praagh and Anderson Classification system.

Conclusion:

The purpose of this exhibit is to underscore the attention to systemic approach for imaging interpretation of complex congenital heart disease in a segment-by-segment fashion. This segmental approach shall significantly facilitate the detection and characterization of congenital heart disease among radiologists and cardiologists.

Poster: EDU-007

MOCK ENDOVASCULAR STENTING AND COMPUTED TOMOGRAPHY OF A DISTENSIBLE 3D MODEL FOR COMPLEX CONGENITAL HEART DISEASE

KENNETH Cheung¹, SIMA Zakani², JOHN Jacob², EIMEAR McGovern², MARTIN Hosking², JOHN Mawson¹, GORDON Culham¹

¹ Department of Radiology, University of British Columbia, Vancouver, CANADA

² Department of Paediatrics, University of British Columbia, Vancouver, CANADA

Background:

A 2 month old baby boy suffered from complex congenital heart malformation with right atrial isomerism, unbalanced atrioventricular septal defect, double outlet right ventricle, severe pulmonary stenosis and total anomalous pulmonary venous return draining into a retrocardiac confluence, vertical vein and to the left brachiocephalic vein.

Pulmonary venous congestion was present due to presence of stenosis at the pulmonary venous confluence and at the vertical vein.

Due to the complex anatomy and strategic location of the venous confluence and vertical vein, it was uncertain whether endovascular stenting for alleviation of the venous stenoses was technically feasible without subsequent compression of the adjacent structures, in particular the trachea and left main bronchus.

Methods:

A CT-based patient-specific 3D model was printed (Objet 260, Stratasys, Minnesota, USA) with flexible material (Tango Plus) for better understanding of the complex anatomy, and a trial stent placement was performed on the model. CT of the model with the stent in place was performed to assess the extent of anatomical distortion, as well to confirm that no significant airway compression was caused.

The findings reassured the interventionalist that stenting was feasible and safe, and a subsequent actual vascular stenting was performed with satisfactory improvement of the pulmonary venous flow.

Conclusion:

This case demonstrates the utility of 3D-printed models with distensible material for anatomical delineation of complex anatomy, and prediction of extent anatomical distortion after endovascular stent placement by CT of 3D model.

Poster: EDU-008

3D PRINTED CARDIAC MAGNETIC RESONANCE IMAGING TRAINING PHANTOM WITH RESPIRATORY SIMULATION

KENNETH Cheung¹, CAROL WING-KI Ng², MEI-YU Poon², WAI-SIU Kwok³, KA-HO Leung³, CHUI-KIN Lau³, FRANCIS Lee³, MADELEINE Lam³, TIFFANY Chung³, NAM-HUNG Chia³, ERIC So³, GEORGE Ng³, ELAINE Kan²

¹ University of British Columbia, Vancouver, CANADA

² Hong Kong Childrens Hospital, Hong Kong, HONG KONG

³ Queen Elizabeth Hospital, Hong Kong, HONG KONG

Background:

Cardiac magnetic resonance imaging (MRI) has become an indispensable tool for multifaceted assessment of various cardiac pathologies.

Due to the oblique orientation of cardiac structures, multiple oblique planes must be generated before standard cardiac planes can be derived. For volumetric imaging, dual gating with respiratory navigation and electrocardiogram triggering is required to minimize motion artifacts.

Training on real patients can be problematic as it incurs increased machine time as well as additional breath-hold maneuvers required by the patient. Problems are compounded in children due to frequent limited tolerance to prolonged scans.

As a result, a steep learning curve is encountered for beginners in cardiac imaging. Material and methods:

An open source 17 year old normal heart 3D model was modified to create a printable 3D model with normal anatomical alignment. Further refinement was performed with waterproofing and filling of the model with gadolinium doped water.

A gadolinium doped saline bottle was mounted onto a test lung of an MR compatible mechanical ventilator to simulate respiratory motion.

The chest wall, back muscles and upper limbs were simulated with wet blankets and normal saline bottles.

The entire phantom could be fitted into a plastic container for convenient handling and storage.

Heart beat simulation was performed on the MR scanner console.

Results:

The training phantom could simulate normal cardiac anatomy for prescription of standard cardiac planes. Simultaneous respiratory motion and heart beat simulation was feasible for setup of dual gating.

Conclusion:

A cardiac MRI training phantom was created for training of radiographers and radiologists in a realistic and stress-free environment, with the ability to provide training on scanning plane prescription and practice on dual gating for volumetric cardiac imaging.

Poster: EDU-009

DYNAMIC 4D AIRWAY CT: ACCOUNTING FOR VARIATIONS IN VENTILATION, POSITION, AND OTHER FACTORS IN INTERPRETATION AND OPTIMIZATION OF DIAGNOSTIC UTILITY

ELIZABETH Tang, ERIN Romberg, SARAH Menashe, FRANCISCO Perez, JEFFREY Otjen

Seattle Children's Hospital - Department of Radiology, Seattle, USA

CT with 4D cine airway imaging can non-invasively and dynamically characterize airways for various pathologies, such as airway caliber fluctuations in tracheobronchomalacia, airway compression by cardiovascular or other mediastinal structures, or airway constriction from anatomic anomalies like those associated with craniofacial syndromes. However, optimal interpretation of dynamic airway CT studies requires an understanding of the impact of extrinsic factors such as the presence of support apparatus (e.g., endotracheal tube, enteric tube), level of required respiratory support (e.g., positive end-expiratory pressure), and differences in positioning (e.g., with jaw thrust). We have performed more than 100 pediatric cases of dynamic airway CT under a variety of conditions, in patients who range from free-breathing to ventilator-dependent, and for a variety of pathologies. In this educational exhibit, we

will consider how to balance and tailor extrinsic factors when using dynamic CT for the guidance of airway management, in order to meet diagnostic considerations and supplement other cardiopulmonary investigations, including cases with bronchoscopic and surgical correlates.

Poster: EDU-010

RADIOLOGIC FINDINGS IN THE VITAMIN K DEFICIENT INFANT

EMILY Haas¹, ASHA Sarma¹, REKHA Krishnasarma¹, ALEXANDRA Borst², ELIZABETH Snyder¹

¹ Monroe Carell Jr. Children's Hospital at Vanderbilt Department of Pediatric Radiology, Nashville, TN, USA

² Monroe Carell Jr. Children's Hospital at Vanderbilt Department of Pediatric Hematology/Oncology, Nashville, TN, USA

Coagulopathy related to vitamin K deficiency represents an uncommon but potentially catastrophic condition in infants. Although rare in countries where prophylactic vitamin K is routinely administered, vitamin K deficiency in infants may occur in the setting of limited prenatal care, exposure to various maternal medications, hepatobiliary disorders, or refusal of postnatal intramuscular vitamin K. Early vitamin K deficiency bleeding (VKDB) occurs within the first 24 hours after birth, classic VKDB in the first week of life, and late VKDB between two weeks to three months of life. All have the potential to manifest as minor bruising and mucosal bleeding. Severe bleeding complications are more commonly associated with late VKDB. This may include spontaneous intracranial, gastrointestinal, or thymic hemorrhage. As clinical and imaging findings may overlap with those of non-accidental trauma, radiologists play an important role in the evaluation of these patients. Additionally, thymic hematomas may mimic anterior mediastinal masses and be mistaken for tumor. Consequently, VKDB is a crucial diagnosis for the radiologist to consider to help guide appropriate management and prevent potentially costly and unnecessary diagnostic testing.

The goals of this educational exhibit are to review various complications of VKDB, emphasize the importance of clinical history, and to illustrate imaging manifestations of VKDB utilizing multiple modalities (ultrasound, CT and MRI). Conditions that will be covered include: mediastinal hematoma due to thymic hemorrhage, hemothorax, as well as intraparenchymal, subdural, and subarachnoid intracranial hemorrhage.

Poster: EDU-011

CONGENITAL PERIPHERAL PULMONARY ARTERY ANOMALIES, SYNDROME ASSOCIATIONS - CT AND MR IMAGING

BEVERLEY Newman

Stanford Childrens Hospital at Stanford University, Stanford, USA

Peripheral pulmonary artery anomalies encompass right and left branch pulmonary arteries as well as intrapulmonary arteries. There are many different causes and associations with a spectrum from mild lesions without major clinical relevance to life threatening disease. Many different syndromes are strongly associated with these lesions. Imaging plays an important role in defining the site, extent and severity of pulmonary artery abnormality as well as helping in identifying underlying causes and providing a roadmap for surgical correction. CTA and MRA are key imaging modalities in evaluating these lesions.

This poster presentation will review the major syndromic associations of peripheral pulmonary artery anomalies and their imaging, including typical appearances, important associated findings and approach to management, where relevant. Anomalies covered will include ductus dependent

pulmonary arteries; truncus arteriosus; aortic origin of branch pulmonary artery; pulmonary sling, pulmonary hypoplasia/stenosis, pulmonary atresia and collaterals. Lesions illustrated will include Di George, CHARGE, VACTERL, heterotaxy, Scimitar, Elastin arteriopathy, Williams, Alagille and Noonan syndromes.

Poster: EDU-012

PEDIATRIC THORACIC MASSES: A PICTORIAL REVIEW

EVANGELOS Mourtos¹, EVA Penno¹, SANDRA Diaz Ruiz²

¹ Dept of Radiology, Akademiska University Hospital, Uppsala, SWEDEN

² Dept of Pediatric Radiology, New Karolinska University Hospital, Stockholm, SWEDEN

Purpose: Thoracic masses encompass a wide spectrum of pathology in the pediatric population ranging from simple cystic lesions to more complex benign or malignant tumors. Imaging with various radiologic studies has a pivotal role in the assessment of these lesions. The purpose of this educational exhibit is to familiarize radiologists with the imaging findings of masses in the pediatric chest.

Methods & Materials: A variety of cases representing a spectrum of pediatric thoracic lesions were collected at our institutions. We performed a retrospective review of the clinical presentation and imaging findings.

Results: The broad spectrum of lesions encountered in the pediatric chest will be illustrated using a case-based approach. The presented cases will be divided into three broad categories based upon presumed primary thoracic location: a)lung parenchyma/airways b)mediastinum c)chest wall/pleura.

Demographics, clinical presentation and further clinical evaluation will be discussed in each case.

Conclusion: Familiarity with the clinical presentation and the imaging appearance of the wide spectrum of pediatric chest masses is very important for correct diagnosis and subsequent optimal management.

Poster: EDU-013

HIGH-RESOLUTION COMPUTED TOMOGRAPHY IN CHILDHOOD INTERSTITIAL LUNG DISEASE: A HISTOLOGY-BASED APPROACH

LAURA Martelius¹, PÄRIA Miraftabi¹, JOUKO Lohi², TURKKA Kirjavainen³

¹ HUS Medical Imaging Center, Radiology, University of Helsinki and Helsinki University Hospital, Helsinki, FINLAND

² Department of Pathology, University of Helsinki and Helsinki University Hospital, Helsinki, FINLAND

³ Department of Pediatrics, Childrens Hospital, University of Helsinki and Helsinki University Hospital, Helsinki, FINLAND

Childhood interstitial lung diseases (chILD) form a heterogeneous group of rare disorders. In most cases, lung biopsy is necessary for a definitive diagnosis. The chILD classification describes histological patterns unique to infancy, both idiopathic and of known etiology, and lists etiologies of interstitial lung disease not specific to infancy. Children also present with histologic patterns included in the adult classification of idiopathic interstitial pneumonias (IIPs), but the clinical associations of these patterns may be different from adults. Additionally lung biopsies of children with chILD show histologic patterns, which present in adults, but are not included in the adult classification on IIPs. High-resolution computed tomography (HRCT) defines the presence, extent, and pattern of lung disease. Depending on the clinical situation, the HRCT pattern may be sufficient for a confident diagnosis, HRCT may suggest the diagnosis, or findings on HRCT may be non-specific.

This educational exhibit reviews the role of HRCT imaging in children with cHLD, and list clinical associations of histological patterns detected in pediatric lung biopsies (Table). The final presentation will also provide data on typical HRCT findings of the different histological patterns, and display both HRCT and histological images.

Poster: EDU-014

SARS-COV-2 INFECTION IN CHILDREN: REVIEW OF IMAGING FINDINGS

DIVYA Kishore¹, ASHISHKUMAR Parikh^{1,2}, ERICA Riedesel^{1,2}, EDWARD Richer^{1,2}

¹ Department of Radiology and Imaging Sciences, Emory University School of Medicine, Atlanta, USA

² Department of Radiology, Children's Healthcare of Atlanta, Atlanta, USA

1. Background/Purpose

a. The SARS-CoV-2 pandemic has been the dominant healthcare event of 2020. The common respiratory symptoms and imaging findings in adults with acute COVID-19 are now well known. However, less commonly discussed is how COVID-19 and the multisystem inflammatory syndrome in children (MIS-C) manifest in children. Multisystem inflammatory syndrome in children is thought to result from severe immune response to the virus resulting in clinically severe illness. MIS-C can present with a spectrum of symptoms throughout the body depending on affected organ systems, often mimicking other pathologies.

b. Literature summarizing manifestations of MIS-C in children is sparse and disparate across organ systems. In this presentation, we seek to outline the variety of imaging findings of MIS-C in children and to synthesize described findings throughout the body into a single, comprehensive source for practicing pediatric radiologists.

2. Content

a. Provide background on the incidence of COVID-19 and MIS-C in children.

b. Describe the pathophysiology of MIS-C in children.

c. Present cases of MIS-C from our institution, including imaging manifestations or lack thereof seen in multiple organ systems:

i. Pulmonary: Groundglass and patchy peripheral opacities, pleural effusions

ii. Gastrointestinal: Bowel thickening and hyperenhancement, mesenteric adenopathy, gallbladder wall thickening

iii. Cardiovascular: Myocarditis, coronary artery aneurysms

iv. Neurologic: In our experience, there were no abnormal neuroimaging findings seen in children with MIS-C.

d. Present pertinent differential diagnoses for these cases

3. Conclusions

a. Given that SARS-CoV-2 infection can mimic other pathologies, it is important for pediatric radiologists and clinicians to be aware of the wide variety of COVID-19 and MIS-C manifestations in children to facilitate appropriate diagnosis and to direct proper management of symptomatic patients.

Poster: EDU-015

LOW DOSE DYNAMIC CHEST CT FOR DETERMINATION OF OPTIMAL VENTILATION PEEP VALUES

HARUTYUN Haroyan, DARRAGH Brady, JANE Kim, NARENDRA Shet

Children's National Medical Center, Washington, DC, USA

Background

Patients with bronchopulmonary dysplasia (BPD) commonly develop tracheobronchomalacia which is associated with higher morbidity. Ventilatory support of patients with tracheobronchomalacia is complex. Pulmonologists need to establish appropriate amount of positive end-expiratory pressure (PEEP) setting on the ventilator. Inadequately low PEEP can result in airway collapse and higher PEEP values can result in barotrauma. PEEP values can be estimated based bronchoscopy or CT imaging.

Dynamic low dose limited chest CT scan is a non invasive method of determining optimal PEEP values.

Objective

1. Review pathophysiology and etiologies of tracheobronchomalacia

2. Describe importance of PEEP optimization for patients with BPD and methods to ways to determine optimal PEEP valuee

3. Introduce our institutional CT protocol for dynamic PEEP examination

4. Provide our approach to interpretation of the examination

5. Discuss radiation dose reduction techniques

6. Discuss organizational and technical difficulties associated with the examination

Methods:

Our experience is based on more than 30 dynamic cases we performed in conjunction with pulmonology.

Poster: EDU-016

CHEST X-RAY INTERPRETATION IN SEVERELY ILL NEWBORNS

ANA Forjaco¹, RITA Prata^{1,2}, JOÃO Dias¹, LÚCIA Fernandes¹

¹ Centro Hospitalar Universitário Lisboa Central, Lisbon, PORTUGAL

² Centro Hospitalar do Funchal, Funchal, PORTUGAL

Purpose:

There are several chest x-ray applications in the neonatal period, especially in the investigation of respiratory conditions and in the assessment of severely ill newborns. This poster intends to review the indications for the radiographic study of the chest in the neonatal period and show the specificities of chest x-ray interpretation in newborns.

Materials and Methods:

Bibliographical research in PubMed for terms such as 'neonatal chest x-ray', 'neonatal respiratory diseases' and 'neonatal intensive care. Revision and selection of content relevant to the theme. Selection of original images of studies performed in the neonatal intensive care unit of a level III university hospital.

Results:

The radiographic study of the chest in the neonatal period has four main applications: the assessment of the correct positioning of the support devices used in neonatal intensive care units; the etiological investigation of respiratory distress conditions in newborns; the monitoring of the progress of acute respiratory diseases and detection of acute and chronic complications resulting from the therapeutics aimed at those diseases. Several specific anatomical and physiological aspects in newborns compromise chest x-ray interpretation in this age group.

Conclusions:

The most frequent newborn chest x-ray applications are the initial investigation of the acute respiratory distress conditions and the assessment of the correct positioning of the support devices. Aspects such as uncooperativeness during inspiratory apnea and the presence of thymic shadow compromise chest x-ray interpretation in the neonatal period. Knowledge of these particularities is essential to use this important diagnostic method correctly.

This educational exhibit will highlight the normal imaging findings and complications of extensor spinae and paraspinal pain catheters encountered by the general pediatric radiologist on post-operative imaging.

Poster: EDU-017

Withdrawn

Poster: EDU-018

NON-NEOPLASTIC MEDIASTINAL MASSES IN PEDIATRICS

HIRAL Banker, PREET Sandhu

Le Bonheur Children's Hospital, University of Tennessee, Memphis, USA

Non-neoplastic mediastinal masses are uncommon in children. These lesions can be related to congenital conditions, trauma or post-surgical complications, benign enlargement of mediastinal structures, etc.

This presentation aims to describe various non-neoplastic pathologies that can present as or mimic mediastinal mass, in the pediatric age group. To describe and illustrate their appearance on various imaging modalities and describe the differentiating radiological features. An early and accurate diagnosis helps reduce patient morbidity or mortality, especially in life-threatening conditions. Correct diagnosis of these entities can also help in reducing unnecessary interventions.

Outline:

- Overview of mediastinal anatomy.
 - Describe various non-neoplastic entities that can present as a mediastinal mass in children
- Describe and elucidate imaging algorithm for workup of possible mediastinal mass in children.
- Describe the radiological appearance of nonneoplastic mediastinal masses and other mimickers in children with an emphasis on life-threatening conditions e.g. aortic aneurysm.

Poster: EDU-019

PULMONARY SEQUESTRATION, INITIAL SONOGRAPHIC APPROACH IN THE NEONATAL INTENSIVE CARE UNIT

LARISSA Andrade Defendi¹, RODRIGO Carneiro Marques², IRLINE Cordeiro de Macedo Pontes², YOSHINO Tamaki Sameshima²

¹ Universidade Federal de São Paulo, São Paulo, BRAZIL

² Hospital Isarelita Albert Einstein, São Paulo, BRAZIL

Background

Pulmonary sequestration is a rare congenital anomaly that represents 1-6% of all pulmonary malformations. It is characterized by a dysplastic lung tissue that lacks connection with the tracheobronchial tree and receives its blood supply from an abnormal systemic artery originating from the aorta. The primary role of imaging is to depict the aberrant vascular anatomy for accurate surgical planning in selected cases. Computed Tomography Angiography (CTA) remains the gold-standard for postnatal evaluation. Nonetheless, Doppler ultrasound (US) may help to identify the anomalous vascularization. It represents a safe, quick and radiation-free method for follow-up that may replace serial radiographs in asymptomatic infants.

Learning Objectives

1. Demonstrate the sonographic technique employed in the assessment of pulmonary sequestration;
2. Describe the sonographic features of pulmonary sequestration and correlate them with imaging findings from CTA.

Findings

Teaching cases from our Radiology Department will be used to elucidate the following topics:

1. Pulmonary sequestration: epidemiology and definition;
2. Exam technique in pulmonary ultrasound:
 - B-mode;

- Doppler ultrasound;

3. Pulmonary sequestration - imaging features:

- Main sonographic findings in the neonatal approach;
- Associated anomalies - what to look for in US and CT;
- CTA correlation.

Conclusion

US may be an important initial diagnostic method for assessing pulmonary sequestration in newborns, especially when CTA is not readily available. It is useful for follow-up and late management as well, avoiding multiple exposures to radiation. Nonetheless, further studies are required to include US as a definitive diagnostic method in scenarios of rare pulmonary conditions.

Poster: EDU-020

UNVEIL THE THYMUS SAIL

REEMA Agarwal¹, JOSHUA Wemmers², RACHEL Berkovich²

¹ SSM Saint Louis University Hospital - Department of Diagnostic Radiology, St. Louis, USA

² SSM Cardinal Glennon Hospital - Department of Pediatric Radiology, St. Louis, USA

The thymus is an organ in the anterior mediastinum involved in producing and developing T-cells in childhood. While thymic masses only account for 2% of childhood mediastinal masses, knowing the various appearances of the normal and abnormal thymus is imperative to the pediatric radiologist. Mistaking a normal thymus for a mediastinal mass may cause significant morbidity as well as unnecessary utilization of hospital resources.

The purpose of this educational exhibit is to review the various imaging appearances related to the thymus in a pediatric population. These include, but are not limited to, normal thymus, thymic aplasia, thymic hyperplasia, thymomas, thymic cysts, and thymic carcinomas. Additionally, we will present non-thymic related conditions, which may alter the appearance of the thymus at imaging, including pneumomediastinum and Langerhans Cell Histiocytosis. We will also review the various radiographic signs pertaining to the thymus, including the sail sign, wave sign, and notch sign, and what they represent anatomically.

The epidemiology, natural history, and diagnostic and management recommendations, including indications for MRI and biopsy/excision, pertaining to the various thymic pathologies will be reviewed.

After review of this presentation, the pediatric radiologist should be able to accurately identify normal versus abnormal thymus, formulate an appropriate differential, and be able to discuss further imaging and management strategies.

Poster: EDU-021

IMAGING OF MALIGNANT PEDIATRIC CHEST MASSES

KUMAR Shashi, STEPHAN Voss

Boston Childrens Hospital, Boston, USA

Purpose: Primary lung tumors in children are relatively rare, and in contrast to adults have a relatively broad histologic spectrum. The purpose of this educational exhibit is to present an overview of the most common primary pediatric lung tumors, with a focus on characteristic imaging features, including conventional radiographic and cross-sectional imaging features. In addition, the role of functional imaging in the assessment of primary pediatric lung tumors will also be presented.

Methods: A single institution 10-year retrospective record review was performed. A search of the radiology report database was used to identify representative cases of primary pediatric lung tumors, with an emphasis on cases in which a comprehensive imaging evaluation was performed and which provided characteristic imaging features for presentation in educational format. The focus was on primary pediatric lung tumors. Although examples of

primary mediastinal masses and metastatic disease will be shown for comparison, they were not specifically included in the database search.

Summary: Primary pediatric lung tumors are uncommon and have many overlapping clinical and imaging features. Knowledge of patient age, underlying predisposition syndromes, and functional imaging features may help narrow the differential. While metastases from other primary malignancies remain the most common type of malignant pediatric lung tumor, the examples presented in this educational exhibit highlight important differences between pulmonary metastatic disease and primary pediatric lung malignancies.

Poster: EDU-022

CHALLENGES WITH PEDIATRIC CENTRAL VENOUS CATHETER STUDIES: 10-YEAR EXPERIENCE AT A LARGE TERTIARY PEDIATRIC HOSPITAL

KUMAR Shashi, MICHAEL Callahan, ANDY Tsai
Boston Childrens Hospital - Department of Radiology, Boston, USA

Introduction: Central venous catheters (CVC) are commonly placed in individuals with either difficult peripheral venous access or patients with a need for prolonged intravenous medications and/or intravenous fluids. The most common complication of CVC is catheter obstruction, which can manifest as difficulty injecting fluids or withdrawing blood. A contrast-enhanced line study constitutes an important diagnostic tool to assess the functionality of a problematic CVC. However, there is a lack of standardization on how these studies should be performed. In addition, interpretation of these studies can be challenging.

Purpose: Illustrate the technical difficulties and diagnostic challenges associated with performing contrast-enhanced CVC studies.

Material and methods: Reports of central line studies performed on patients <21-years-old at a large tertiary-care children's hospital over a 10-year period (10/1/2010-9/30/2020) were reviewed. Select studies from our cohort were chosen to highlight variabilities in technique, variabilities in interpretation, and numerous pitfalls in interpretation.

Results: We identified 537 CVC studies from 391 children (average age = 9.3 years ± 5.8 years). Of the 537 studies, 34% had fibrin sheath or thrombus at the tip, 7% had fracture/leak along the catheter tubing, 10% had leak/malfunction at the port reservoir, and 1% had fracture/leak along the external tubing. In 48% of these studies, at least one of the above abnormal findings were identified. The average absorbed dose per study was 4.4 mGy. Review of selected studies showed limited standardization of technique and no clear consistency in diagnosis. Many pitfalls were unrecognized leading to management errors.

Conclusion: We highlight the practice patterns of CVC contrast-enhanced studies in our institution, drawing attention to some of the common difficulties and errors encountered. Revealing these problems and understanding the causative mechanism of the misdiagnoses can improve the diagnostic confidence and accuracy of the study. Furthermore, we advocate for a more rigorous and standardized approach in performing CVC contrast-enhanced studies including optimization of imaging parameters.

Poster: EDU-023

DEVELOPMENT AND IMPLEMENTATION OF A TRANSPARENT ORIGAMI FACE MASK FOR PATIENT AND FAMILY CENTERED CARE

MARIA Velez-Florez, ELIZABETH Silvestro, BRITTANY Bennett, ETHAN Larsen, ERIN Pohl, RAYMOND Sze
The Children's Hospital of Philadelphia, Philadelphia, USA

Summary of the presentation:

Wearing facemasks daily has become the new normal during the COVID-19 pandemic. Surgical masks being used during patient care block facial

expressions and visual cues, and interfere with communication. Emotions and non-verbal communication are conveyed and perceived through facial expression. Thus, using a facemask may interfere with communication and emotion recognition during the assessment of children, especially in individuals with autism. Furthermore, it abolishes communication strategies such as lip reading for deaf and hard of hearing patients/families. Our research team designed and tested (following the FDA and NIH guidelines) a transparent origami facemask that grants full-face visibility while maintain the breathability and protection of conventional surgical masks. It has also undergone usability testing, for word recognition, and comfort. The transparent origami facemask has been trialed in different Departments in our institution, including the Magnetoencephalography center. We aim to share our experience in developing and deploying the Transparent Origami Face Mask to improve communication and assessment of children.

Educational Objectives:

- Identify advantages and disadvantage of universal masking on interaction, communication, and expression.
- Learning about the application of problem-solving processes to develop and deployed device to support patient interaction.
- Learn to fold your own DIY origami folded transparent mask to implement into your own workflow.

Poster: EDU-024

PANCREATIC AND THYROID INTRAGLANDULAR FATTY TISSUE: PAY ATTENTION TO AVOID THE SONOGRAPHIC DIAGNOSTIC TRAP!

MARINA Vakaki ¹, RODANTHI Sfakiotaki ¹, ANNA Chountala ¹, DESPINA Pitsoulaki ¹, ELENI Koutrouveli ¹, IRENE Vraka ¹, GEORGE Daniel ², EKATERINI Haritou ¹, CHRYSOULA Koumanidou ¹
¹ P&A.Kyriakou' Children's Hospital, Athens, GREECE
² General Hospital of Thessaliniiki G. Gennimatas, Thessaloniki, GREECE

Ultrasound is the primary imaging method for the evaluation of the pediatric thyroid gland, whereas the pancreas is routinely examined during every abdominal pediatric ultrasound examination. Although two quite different organs from all aspects, which seem to have nothing in common, there is a noteworthy point. Small non-pathologic hyperechoic lesions may be detected either in the thyroid or in the pancreas, in any clinical scenario. They can be misdiagnosed as pathologic nodules/masses, even suspicious for malignancy, causing anxiety and leading to unnecessary further investigation.

The purpose of this educational exhibit is to a) present the sonographic characteristics of these hyperechoic nodules and b) familiarize pediatric radiologists with these non-pathologic thyroidal and pancreatic findings. To the best of our knowledge, there is sparse literature about these imaging findings in adults, whereas they have never been reported in children. The sonographic studies performed for the evaluation of the thyroid and pancreas at our tertiary referral Children's Hospital during a 12-year period were retrospectively reviewed. Representative cases were selected from our database to depict the characteristic appearance of thyroidal and pancreatic hyperechoic lesions. The sonographic key findings that we have noticed and led us to the appropriate diagnosis are highlighted. The ultrasound differential diagnosis is discussed. The 2- to 4-y sonographic follow-up of our cases is presented. These thyroidal and pancreatic hyperechoic lesions represent intraglandular invagination of perithyroidal or peripancreatic fatty tissue, but are usually misinterpreted as a thyroid nodule or pancreatic mass, respectively. Their embryologic and anatomic basis is analyzed.

Conclusions: Pediatric radiologists should have a comprehensive knowledge and understanding of the normal anatomy and embryology of the thyroid and pancreatic gland, in order to add the thyroid and pancreatic hyperechoic lesions caused by periglandular fat invagination, to the already known diagnostic pitfalls with no clinical significance.

Poster: EDU-025

A PICTORIAL REVIEW OF INJURIES CONSIDERED TO HAVE A HIGH SPECIFICITY FOR ABUSIVE INJURY IN CHILDREN

NAGEENA Suleman, SAMANTHA Low, ADAM Oates
Birmingham Children's Hospital, Birmingham, UNITED KINGDOM

Introduction;

One of the most challenging aspects of the radiological imaging of children is that related to matters of child protection and what constitutes an abusive injury. Clearly there is a fundamental importance to protect the most vulnerable in society, including children and the paediatric/neuro-radiologist may have an important role to play in this process. Moreover, there is a significant weight of responsibility on the shoulders of the expert radiologist in advising the authorities (e.g. police, social services and court process) on the likelihood that an injury is abusive. However this can be a very difficult question to address given the limitations of available experimental research, potentially unreliable nature of any witness statements and paucity of laboratory models.

Purpose;

To provide a pictorial review of imaging findings related to suspected physical abuse in children.

Materials and Methods;

A systematic assessment of cases of suspected physical abuse in our radiological practice at a large paediatric trauma unit. In light of the great difficulty in deciding what constitutes an abusive injury, we have restricted our assessments to those cases where there has been a perpetrator confession, or the presence of injuries involving multiple body parts or systems i.e. those that are highly improbable to come from a single accidental domestic traumatic event.

Results;

A large number of injuries will be described in both body and CNS systems and include extra-axial bleeding, parenchymal brain injury, spinal subdural bleeding, rib fractures, classic Metaphyseal Lesion (CML) fractures, isolated Subperiosteal New bone formation (SPNBF) and miscellaneous skull and long bone fractures.

Conclusions;

The radiologist may play a crucial role in the Court process related to the safeguarding of children. It is intended that this pictorial review will highlight practical imaging considerations that may help the radiologist guide the authorities as to what constitutes an abusive injury.

Poster: EDU-026

ADDITIVE MANUFACTURING (3D PRINTING) IN THE TIME OF A PANDEMIC: LESSONS, SUGGESTIONS, AND WHAT'S NEXT

ELIZABETH Silvestro¹, MARIA Velez-Florez¹, ETHAN Larsen¹,
MICHEAL Francavilla^{1,2}, RAYMOND Sze^{1,2}

¹ Childrens Hospital of Philadelphia, Philadelphia, USA

² Perelman School of Medicine at the University of Pennsylvania, Philadelphia, USA

Learning Objectives:

Describe the experiences and lessons learned from a radiology additive manufacturing/3d printing lab rapidly responding to a pandemic
Present suggestions to teams interested in starting or growing a Radiology Additive Manufacturing/3d Printing lab.

Contemplate the future of Radiology Additive Manufacturing/3d Printing lab following outcomes of the pandemic response and consider the challenges to balance innovation and regulation.

Purpose: The COVID-19 pandemic had a particular impact on healthcare and manufacturing. Many additive manufacturing (3D printing) labs around the world, many in Radiology Departments, focused all efforts to address urgent needs. Medical Printing and the maker community were uniquely positioned to stand up efforts to respond in areas such as personal protective equipment (PPE) and medical device replacements. This presentation shares the lessons learned in our lab, opens the discussion on how to start a lab, and challenges the audience to anticipate the field's future.

Lessons: We start with an overview of devices we developed, prioritization protocols, and deployment challenges while innovating and implementing changes in real-time. Key considerations included optimizing workflow, maintaining safety, leveraging collaboration, and balancing pandemic versus standard practice needs with a new prioritization tracking system.

Suggestion: We offer specific points to consider before jumping in and how to plan the growth of the lab-based on our experience. These include clarifying the mission of the lab-based on institutional needs, identification of team members with the requisite skill sets, and selecting the appropriate 3D printing technology.

What's Next: Finally, several points of consideration will be shared looking to the post-pandemic world. What is the best way to transition back to a new normal of practices and protocols without losing the current sense of innovation and responsiveness? What are future opportunities for medical 3D printing applications and shared networking?

Conclusions: The COVID-19 pandemic provided unprecedented challenges and opportunities for our 3D printing lab, transforming our mission, workflow, and collaboration network. We share these experiences in the spirit of the open-sourced maker community for those looking to take their first steps in the field of medical additive manufacturing.

Poster: EDU-027

CREATING A CASE-BASED ELECTRONIC TEACHING MODULE ON BASIC ABDOMINAL IMAGING

ALYSSA Schlotman¹, MELISSA Hilmes², SUDHA Singh²

¹ Vanderbilt University School of Medicine, Nashville, TN, USA

² Vanderbilt University Medical Center, Nashville, TN, USA

Purpose: Given that remote learning has become a necessity, we must incorporate creative approaches to teach pediatric radiology. We saw a need to create a novel case-based teaching module that introduces a simple approach to the abdominal radiograph. It would be used by medical students and pediatric residents for self-directed learning during the pediatric radiology elective.

Materials and Methods: The mnemonic 'gas, mass, stones, bones' is a simple approach to the abdominal radiograph. We used this mnemonic to guide the creation of a case-based teaching module using PowerPoint. Cases were organized in a uniform format starting with a clinical presentation, then asking the student to evaluate an abdominal radiograph using the above described method. Then follows an explanation of the additional imaging needed in the case and key clinical pearls about each diagnosis.

Results: After collecting appropriate cases, the new teaching module was successfully created. Pathologies included in the module are malrotation (abnormal bowel gas pattern), intussusception and liver mass (abnormal areas of mass effect), renal calculi and appendicitis (abnormal stones and calcification), and myelomeningocele (abnormal skeletal findings). By the end of the module, students should have an organized and systemic approach to analyzing abdominal radiographs, illustrated by key index example cases.

Conclusions: We successfully created an interactive curricular tool to be used in teaching learners in pediatric radiology a memorable method for

approaching abdominal radiographs. The module is particularly effective for remote learning settings and adds variety to the teaching materials for all radiology learners.

Poster: EDU-028

FETAL HEAD AND NECK PATHOLOGY ON 3-T MRI

MANUEL Patino ¹, FEDEL Machado Rivas ², JOHN Choi ², CAROLINE Robson ², CAMILO Jaimes ²

¹ Massachusetts General Hospital - Department of Radiology, Boston, USA

² Boston Children's Hospital - Department of Radiology, Boston, USA

Purpose:

The small size of fetal craniocervical structures, anatomical complexity, and fetal motion add to the considerable challenge in evaluating fetal patients with congenital anomalies. The multiplanar capabilities and soft tissue contrast of MRI contribute to adequate investigation of these abnormalities. Higher signal to noise ratio (SNR) and spatial resolution of MR imaging at 3-T is advantageous when characterizing fetal structural abnormalities. The purpose of this exhibit is to review cases of fetal head and neck pathology depicted on 3-T MRI and present correlations with prenatal ultrasound and postnatal imaging.

Objectives:

- Outline technical principles needed for adequate imaging and interpretation of the fetal head and neck at 3-T.
- Illustrate examples of common and rare head and neck congenital abnormalities, and present postnatal correlation.
- Discuss syndromic associations and differential diagnosis of these abnormalities.
- Summarize embryological considerations related to craniofacial malformations.

Materials and methods:

- We conducted a retrospective review of cases performed at our institution using 3-T MRI
- Correlation with prenatal ultrasound, postnatal imaging, direct inspection, and pathology was performed.

Results:

- We gathered cases with multimodal (ultrasonography/MRI) exams of abnormalities the fetal head and neck.
- Pathology illustrated includes abnormalities in the calvarium (craniosynostosis, encephaloceles), orbits (hypertelorism, hypotelorism, retinoblastoma), ears (external and internal ear malformations), maxilla (cleft lip and palate), mandible (micrognathia), oral cavity (epulis, foregut duplication cyst), and head and neck masses (teratoma, hemangioma, lymphatic malformation, and goiter).
- Associated syndromes and sequences include: CHARGE, Apert syndrome, Robin sequence, CLOVES, and CHAOS syndrome.

Conclusion:

Fetal MRI at 3T is useful in the evaluation of head and neck pathology. The information provided helps guide treatment decisions and family counseling.

Poster: EDU-029

AN UNUSUAL PRESENTATION OF PAEDIATRIC MYOFIBROMA (MYOPERICYTOMA): A CASE REPORT

TOBI Aderotimi, KATE Taylor-Robinson, ALEXANDRA Williams
Paediatric Radiology Department, Alder Hey Children's Hospital,
Liverpool, UNITED KINGDOM

Purpose:

Myofibromas (and myopericytoma) are part of a spectrum of benign pericytic smooth muscle (myoid cell) tumours. This often presents with a solitary lesion, or multifocal lesions +/- visceral involvement. We present an unusual case of multicentric myofibromas.

Patient information:

21-month-old female presented to hospital following an out of hospital ventricular fibrillation cardiac arrest. There was no relevant antenatal or postnatal history. Clinical examination was normal.

Imaging Findings:

On initial echocardiogram she was found to have a large cardiac mass involving the cardiac apex, as well as an intra-abdominal mass causing compression on the SVC. Further imaging with abdominal ultrasound, cardiac and abdominal MRI confirmed both masses. The cardiac lesion was a solid mass involving the interventricular septum with showed progressive peripheral enhancement and central hyperenhancement. The appearances were in keeping with a cardiac fibroma. The retroperitoneal intra-abdominal lesion was a solid heterogeneous mass on ultrasound, and homogeneously enhanced on MRI. The differing MR signal characteristics to the cardiac lesion were suggestive of a separate aetiology. Review of chest radiographs demonstrated multiple upper thoracic rib and vertebral anomalies, as well a high riding left scapula. A CT head study also demonstrated a large bregmatic wormian bone.

Diagnosis:

She underwent CT guided biopsy of the retroperitoneal mass with histology showing an atypical/cellular Myofibroma/Myopericytoma, likely SRF-RELA fusion variant.

Outcome:

She is being managed conservatively for both masses. Given the presence of multifocal myofibromas and skeletal dysplasia the patient is undergoing genetic testing, with a potential diagnosis of Gorlin syndrome as these findings can be a feature in this condition.

Poster: EDU-030

TYPICAL AND ATYPICAL FINDINGS OF DUPLEX KIDNEYS ON FETAL MRI

CAOILFHIONN Ní Leidhin ¹, MARIANA Meyers ², IAN Robinson ¹, GABRIELLE Colleran ¹

¹ Department of Radiology, The National Maternity Hospital, Holles Street, Dublin, IRELAND

² Department of Radiology, Children's Hospital Colorado, Aurora, Colorado, USA

Purpose:

This exhibit, through a pictorial review, illustrates the typical and atypical imaging findings of duplex kidneys on fetal MRI, along with postnatal correlation.

Materials and Methods:

Fetal renal anomalies represent approximately 20% of all congenital anomalies. Renal duplication is one of the most common congenital renal abnormalities, occurring in approximately 1% of neonates. It is defined by two separate pelvicalyceal systems/moieties. It can be complete, where two ureters enter the bladder or incomplete, where there is a bifid renal pelvis/ureter but only one ureter inserting into the bladder. Renal duplication can be associated with multiple complications, including ectopic ureteric insertion, ureterocolocele, obstruction, vesicoureteric reflux and/or infection. It is most commonly an isolated abnormality but can be associated with syndromes.

Results:

Increased use of antenatal US has resulted in increased detection of duplex kidneys. Antenatal detection of renal duplication allows for parental counseling, appropriate management of pregnancy/planning for delivery, early postnatal imaging and early postnatal intervention, where necessary.

Antenatal diagnosis of renal duplication may improve outcomes when compared with postnatal diagnosis.

While antenatal US is usually the first modality to infer renal duplication, fetal MRI is a useful adjunct in confirming the diagnosis, in better delineating anatomy, in identifying the level/cause of obstruction and in assessing the renal parenchyma.

This exhibit, through a comprehensive pictorial review, illustrates the typical and atypical imaging findings of duplex kidneys on fetal MRI and correlates fetal MRI with postnatal imaging. Representative cases illustrate simple uncomplicated duplex kidneys and those complicated by ectopic ureteric insertion, ureterocoele, hydroureteronephrosis and contralateral abnormalities.

Conclusion:

This exhibit illustrates the important role of fetal MRI in the detection and management of renal collecting system duplication and its potential complications.

Poster: EDU-031

AQUEDUCTAL STENOSIS: PRENATAL DIAGNOSIS AND POSTNATAL OUTCOME

MEGHAN McClure, EDWARD Yang, JUDY Estroff
Boston Children's Hospital, Boston, USA

Imaging diagnosis of aqueductal stenosis is often applied broadly and encompasses a wide range of pathologies, some of which are only uncovered on postnatal imaging and on post CSF diversion imaging. Frequently normalization of the size of the ventricles is not achieved after CSF diversion and neurologic abnormalities persist, despite procedural success. In this education exhibit, we present a large collection of cases of prenatally diagnosed aqueductal stenosis spanning a time period of a decade and correlate to postnatal imaging findings and neurologic outcomes. We will explore the different etiologies of aqueductal stenosis both in isolation and as a part of a spectrum of other neurologic and genetic abnormalities, correlating both prenatal and postnatal MR imaging. By the end of this educational exhibit, the learner will be able to describe the various pathologic causes of aqueductal stenosis, associated syndromes and genetic abnormalities, as well as the prenatal imaging findings that more accurately predict truly isolated aqueductal stenosis and better neurological outcomes, with an understanding that aqueduct stenosis is not encompassing diagnosis, but rather an imaging finding.

Poster: EDU-032

NEW LESSONS FROM MR IMAGING OF PLACENTA ACCRETA SPECTRUM: PRACTICAL INSIGHTS AND FUTURE PERSPECTIVES

IRINA Mashchenko, POLINA Kozlova, ELENA Semenova, EKATERINA Shelepova, OLGA Li, GENNADIY Trufanov
Almazov National Medical Research Centre, Saint Petersburg, RUSSIAN FEDERATION

Placenta previa and placenta accreta spectrum (PAS) disorders are pregnancy complications that can lead to major postpartum hemorrhage as a result of abnormal uteroplacental hypervascularization (AUH) and collateral vessel formation (CVF).

So, how can MR imaging of the placenta help save two lives?

“If you want to achieve excellence, you can get there today. As of this second, quit doing less-than-excellent work.” – Thomas J. Watson.

Learning objectives:

1) To demonstrate the importance of diagnostic MR imaging of the placenta in patients with PAS disorders

2) To illustrate the correlation between the placental imaging findings and the decision-making process in obstetrics

3) To describe the ways of current practice optimization and to look into the future of placental imaging.

Ultrasonography (US) remains the unique screening method used in placental imaging. However, MRI is believed to be most useful in cases where US findings are unclear or when the placenta has a posterior location. Therefore, the indications for MRI of the placenta includes:

- Clarification of the topography of the placenta and the area of the placental bed;
- Determination of the depth of the placental invasion and the location of areas of AUH;
- Assessment of CVF around the cervix and/or middle and lower uterine segments.

The structured MRI report shall describe:

- 1) Position and configuration of the placenta;
- 2) Evaluation of the placental morphology;
- 3) Assessment of the specifics of the placental bed and the adjacent myometrium;
- 4) Detailed description of the lower and middle uterine segments;
- 5) Evaluation of the presence of AUH areas and CVF.

The data are introduced into a special template that allows to predict the PAS grade and the risk of postpartum hemorrhage and can be used by a multidisciplinary team to ensure the patient-focused obstetric care.

The future of placental imaging appears exciting. Various techniques (including artificial intelligence technologies) are being currently developed to evaluate the specifics of placental perfusion, oxygenation, molecular transport and metabolism that might help future healthcare professionals make reasonable clinical decisions.

Take home messages

- 1) MRI of the placenta provides useful information about the severity and location of areas of AUH and CVF in patients with PAS disorders;
- 2) These MRI findings predetermine the surgical outcome and can help the decision making process when planning the patient management strategy.

Poster: EDU-033

TRANSLATION OF STANDARD CARDIOVASCULAR IMAGING TECHNIQUES TO THE FETAL HEART

BJÖRN Schönningel¹, MANUELA Tavares de Sousa², JIN Yamamura¹, JANINE Knapp¹, SHUO Zhang³, FABIAN Kording^{1,4}

¹ University Medical Center Hamburg-Eppendorf, Department of Diagnostic and Interventional Radiology and Nuclear Medicine, Hamburg, GERMANY

² University Medical Center Hamburg-Eppendorf, Department of Obstetrics and Fetal Medicine, Hamburg, GERMANY

³ Philips Healthcare, Hamburg, GERMANY

⁴ Northh Medical GmbH, Röntgenstraße 24, 22335, Hamburg, GERMANY

Summary of the presentation

We aim to provide a comprehensive overview on how to perform fetal cardiac MRI using standard cardiovascular MR sequences. A review of current available technologies will be given

List of educational objectives

- How to perform fetal CMR and to evaluate cardiac function and morphology using standard CMR sequences.

Purpose

Fetal cardiovascular MRI (CMR) can provide additional diagnostic information when echocardiography is inconclusive. The purpose is to review current available technologies for fetal CMR and to show how conventional CMR can be translated to the prenatal MRI examination of the fetal heart.

Materials and Methods

In total over 51 fetuses were examined at 1.5T and 3T. To evaluate the diagnostic performance of cardiac anatomy and function 31 fetuses were

examined using CINE SSFP sequences including fetuses with congenital heart defects (CHD). Peak flow velocities were measured in 12 fetuses in the aorta descendance using 2D phase-contrast angiography. Moreover, the feasibility of 4D PC-angiography was in 9 fetuses to access the hemodynamic in the great vessels.

Results

Dynamic CMR examination and evaluation of the aortic isthmus was possible. Fetuses with a normal heart could be differentiated from fetuses with CHD providing high spatial and temporal resolution for evaluation of the cardiac structure. PC-MR angiography in the AoD revealed typical arterial blood flow patterns with a significant correlation of peak velocities compared to Doppler Ultrasound. The thoracic aorta could be clearly visualized using 4D flow showing the blood flow in supra-aortic vessels as well as from the pulmonary artery into the aorta via the ductus arteriosus.

Conclusions

Cardiac gating and the use of adapted conventional CMR sequences allows the evaluation of cardiac anatomy and diagnosis of CHD as well as the quantification of blood flow. Fetal CMR may be useful as a second-line tool and may contribute more significantly to the diagnosis and planning of CHD in future.

Poster: EDU-034

FETAL CARDIAC MRI - PHYSICS AND TECHNOLOGY OF IMAGE ACQUISITION

DENZEL Cole², LUIS F. Goncalves¹, NICHOLAS Rubert¹, DIANNA M. E. Bardo¹

¹ Phoenix Children's Hospital - Department of Radiology, Phoenix, AZ, USA

² Larkin Community Hospital - Department of Radiology, South Miami, FL, USA

In this educational exhibit we present each of the following topics and supplement each point with technical illustrations and MRI images:

- Provide insights to the value of fetal cardiac MRI (FCMR)
- Used to visualize fetal cardiovascular anatomy and quantitative/qualitative analysis of cardiac function and blood flow
- Prenatal diagnosis of congenital heart disease (CHD)
- Especially of interest in patients who may have limited US/fetal echo evaluation
- Review basics of ECG-gating for cardiac MRI (CMR)
- Retrospective ECG-gating and ECG-triggering
- Temporal resolution
- Review CMR sequences
- Steady state free precession (SSFP)
- bright blood pool
- cardiovascular anatomy, quantitative/qualitative analysis of cardiac function
- Single shot-turbo spin echo (SS-TSE)
- dark blood pool
- anatomic definition
- T1, T2 tissue characterization
- Q-flow
- quantify blood flow, in plane, through plane, 4D
- Review k-space filling techniques and how to apply them to increase image acquisition speed for FCMR
- k-space filling: spatial frequencies are organized prior to image reconstruction
- FCMR imaging benefits from advanced k-space filling methods which underfill k-space and use interpolation or iterative image reconstruction - k-space filling methods:
- Cartesian techniques (centric, half-Fourier, partial-echo)
- Sensitivity encoding
- Compressed sensing

-kt undersampling

-Radial acquisition

Review the currently available MRI techniques and sequences for FCMR

-Pseudo ECG-gating

-Metric optimized gating

-Self-gated FCMR

-US-triggered FCMR

Each technique utilizes methods to extrapolate an estimation of the fetal HR and correlate it to acquired MR images in order to construct cine images of the appropriate point of the cardiac cycle.

Conclusions

FCMR can be complimentary to fetal echocardiography, especially for

-Clarification or confirmation of cardiac anatomy

-Particularly helpful when anatomy is obscured, distorted or displaced (oligohydramnios, maternal obesity, unfavorable fetal position during the fetal echocardiogram)

-Discovery of additional abnormalities and malformations

Poster: EDU-035

THE PERINATAL DIAGNOSIS OF THE BECKWITH-WIEDEMANN AND OTHER OVERGROWTH SYNDROMES: WHEN AND HOW TO DETECT

FRED Avni¹, CATHERINE Garel²

¹ Delta Hospital - Chirec, Brussels, BELGIUM

² Armand Trousseau - Hospital, Paris, FRANCE

The pre- and early postnatal suspicion of syndromic macrosomia (overgrowth syndromes) is important in order to provide all the needed information to the medical team (and to the parents)

and accordingly to adapt the management of the patients. It will also allow to tailor the follow-up taking into account the increased carcinologic risk associated with the syndromes.

The list of syndromes and associated genetic mutations is widening; still these syndromes are insufficiently diagnosed in the prenatal period or even in the early postnatal period. This might be related to the difficulties to recognize the anomalies before birth - for instance an hemihypertrophy. Furthermore, some anomalies will develop after birth only. An overlap between clinical and genetic aspects of several syndromes should also be underlined.

The purpose of this educational exhibit is to familiarize the readers with the most common overgrowth syndromes including:

- Beckwith-Wiedeman Syndrome
- Simpson-Golabi-Behmel syndrome
- Perlman syndrome
- Pallister-Killian syndrome
- Sotos syndrome

For each syndrome, the prevalence, the genetic mutations (when available) as well as the carcinologic risk will be detailed. The main focus will be put upon the perinatal imaging features (mostly demonstrated on US examinations, sometimes on MR imaging). The characteristic and less characteristic anomalies (or association of anomalies) will be illustrated. Features leading to specific diagnoses will be highlighted.

Some of the clinical or imaging aspects may lead to a wider range of differential diagnosis. This is particularly the case for hemihypertrophy that should raise the possibility of the more recently described PIK3CA mutations. This will be illustrated as well.

In conclusion, discovering a fetal or neonatal macrosomia opens to a wide panel of potential genetic syndromes (once maternal diabetes has been excluded). Perinatal imaging (mainly US has potentially an important role as some malformations and association of malformations can be detected in the neonatal period.

Poster: EDU-036

A LIGHT AT THE END OF THE TUNNEL- AN ILLUMINATION OF THE PEDIATRIC INGUINAL CANAL

ELLEN CHRISTINE Wallace, JEAN-MARC Gauguet, FARHANA R. Riaz, JULIA Rissmiller, AHMED M. Sobeih
University of Massachusetts & UMassMemorial Medical Center, Worcester, USA

Summary:

Describe normal anatomy and pathology of the inguinal canal, a soft tissue tunnel, present in boys and girls, by using anatomic, radiographic, ultrasonographic, fluoroscopic and CT images of normal and abnormal constituents of the inguinal canal. Common and unexpected contents will be featured. The pathologic relevance of these findings will be discussed.

Educational Objectives:

- 1). Review Anatomy and Contents: The inguinal canal is a tunnel through which structures pass from the pelvis to the perineum. The inferior epigastric artery differentiates direct from indirect herniae. It is lined by the aponeuroses of the external oblique, internal oblique, and transversus abdominis muscles. In both genders the ilioinguinal nerve and genital branch of the genitofemoral nerve are present. The spermatic cord is present in males whereas the round ligament is present in females.
- 2). Describe the Clinical Presentation of Conditions of the Inguinal Canal: Indirect hernias are most common in pediatrics, occurring when an intra-abdominal organ, or other abdominal content, descends through the inguinal canal. The patient usually develops swelling in the inguinoscrotal region in boys or inguinolabial region in girls. This bulge may appear with coughing, crying, straining or when upright. It may be accompanied by pain, discoloration and vomiting.
- 3). Highlight Imaging Techniques: Ultrasound is particularly useful, with a linear, high frequency transducer preferred. Available, dynamic techniques like compression, upright positioning, and the Valsalva maneuver, aid in the identification of a hernia. Plain radiography, contrast fluoroscopy and CT are also valuable techniques, especially with atypical presentations.
- 4). Illuminate Imaging Findings: Images of normal and abnormal inguinal canal content in both sexes: From the vas deferens and round ligament; hydrocele of the cord and fluid filled canal of Nuck; undescended testis and herniated ovary; ischemic testis and torsed ovary; herniated reducible, incarcerated and infarcted bowel and rare constituents including VP shunt tubing, both ovaries and even a uterus!

Poster: EDU-037

MAKING CONNECTIONS WITH TRACHEOESOPHAGEAL FISTULAS: SPECTRUM OF PRESENTATIONS AND TREATMENT COMPLICATIONS

GREGORY Vorona, LANDON Funicello, JASON Sulkowski, MADHURA Chitnavis, KATHRYN Jones, JACQUELINE Urbine
The Children's Hospital of Richmond at Virginia Commonwealth University, Richmond, USA

Purpose:

Esophageal atresia with and without tracheoesophageal fistula reflect a heterogeneous spectrum of abnormalities involving the esophagus and trachea, and it is imperative that radiologists who are involved in the care of children understand the vital contributions that imaging can make to management of patients with this condition before and after corrective surgery. The purpose of our electronic educational exhibit is to review these findings, with particular attention to the post-surgical complications that can occur including strictures, leaks,

gastroesophageal reflex, and problems with esophageal motility. We will also include a brief discussion of the current surgical approaches, and how imaging can play an important role in assisting the surgeons with their presurgical planning.

Methods & Materials:

A retrospective analysis of multimodality imaging in neonatal patients with congenital tracheoesophageal anomalies, who presented to a tertiary care children's hospital since 2010, is performed. Imaging and clinical history are correlated with surgical treatment and intraoperative pictures, where available, as well as the patient's clinical course.

Results:

Review of the variety of imaging presentations of tracheoesophageal anomalies is provided, utilizing radiographs and fluoroscopic evaluation. Various treatment-related complications are also discussed, including: anastomotic leak, stricture, pneumatocele, and surgical clip erosion.

Conclusions:

Esophageal atresia with and without tracheoesophageal fistula reflect a heterogeneous spectrum of abnormalities involving the esophagus and trachea, and it is imperative that radiologists who are involved in the care of children understand the vital contributions that imaging can make to management of patients with this condition before and after corrective surgery.

Poster: EDU-038

PICTORIAL REVIEW OF THE INGUINO-SCROTAL REGION IN CHILDREN: NORMAL ANATOMY AND PATHOLOGY

HARVEY Teo
KK Hospital, Singapore, SINGAPORE

Learning Objectives

To review the embryology and anatomy of the inguinal canal.
To familiarize the reader with the imaging findings of a wide spectrum of pathologies that may be encountered in the inguino-scrotal region in children.

Background

The inguinal canal is a passage that extends inferiorly and medially through the inferior part of the abdominal wall. The spermatic cord in males and the round ligament in females pass through the canal. The patent processus vaginalis (PV) is an embryonic developmental outpouching of the peritoneum that passes through the inguinal canal and usually closes by 2 months of age. Failure of closure results in an abnormal communication between the peritoneal cavity and the scrotum in males, and the labia majora in females. This may result in a number of conditions whose imaging findings will be shown in this poster. A patent processus vaginalis in females is known as the Canal of Nuck.

Imaging Findings

This poster will illustrate the anatomy of the inguinal canal. The imaging findings, with an emphasis on ultrasound, of a wide range of pathologies such as inguinal hernias containing incarcerated bowel, omentum, ovaries, uterus, the appendix and Meckel's diverticulum as well as pathologies such as testicular torsion, cryptorchidism and hydrocoele-communicating and non-communicating will be shown.

Conclusion

After reviewing this poster the reader will be familiar with the anatomy and embryology of the inguinal canal and as well as the imaging findings of pathologies that occur in this region in children.

Poster: EDU-039

IMAGING THE UMBILICUS AND ITS DISORDERS

HARVEY Teo
KK Hospital, Singapore, SINGAPORE

The umbilicus is a depression in the centre of the surface of the anterior abdominal wall that represents the site of attachment of the umbilical cord to the foetus. Umbilical disorders are common in children and can be classified into congenital and acquired anomalies.

Congenital anomalies are related to embryological remnants within the umbilicus such as the urachus, vitelline duct and round ligament of the liver. Urachal anomalies include the patent urachus, urachal cyst, umbilical-urachal cyst, vesico-urachal diverticulum. The commonest vitelline duct anomaly is the Meckel's diverticulum and recanalization of the umbilical vein situated within the round ligament of the liver is a common sign of portal hypertension.

Acquired anomalies often present as masses of the umbilicus and include omphaloceles, hernias, inflammation and primary and secondary neoplasms.

This poster will describe the anatomy, embryology and illustrate the multi-modality imaging features of these conditions.

After reviewing this poster, the reader will learn the embryology, anatomy, pathology and the use of imaging to diagnose these disorders.

Poster: EDU-040

WALKING THE FLANK: BULGING FLANKS-HELPFUL SIGNS ON ABDOMINAL RADIOGRAPHS IN THE DIAGNOSIS OF INTRABDOMINAL MASSES

DIANA Lopez-Garcia, JAYNE Seekins, HELEN Nadel, JESSE Sandberg
Stanford University, Palo Alto, USA

PURPOSE: To present a pictorial review of the importance of abdominal radiographs in diagnosing intrabdominal masses, as well as their mimickers, in the setting of abdominal pain or distention. Emphasis will be given on reviewing the signs of an intrabdominal mass on plain films. **MATERIAL AND METHODS:** A retrospective review of intrabdominal tumors and their mimics on abdominal radiographs was performed in a large tertiary children's hospital. A series of cases from newborns to older teenagers were collected.

RESULTS: The underutilized signs of an intrabdominal mass on abdominal radiograph are; displacement of bowel loops, effacement of the peritoneal fat stripe and lateral convexity or asymmetry of the abdominal wall musculature.

The list of cases include, but are not limited to: Wilms' Tumor, hepatoblastoma, neuroblastoma, teratoma, abdominal wall hernia, renal rhabdoid tumor as well as benign causes of flank bulging such as a hernia, ascites and prune belly syndrome.

CONCLUSIONS: The most common indication for an abdominal radiograph is abdominal pain or distention. In this setting, it is crucial to recognize signs of an intrabdominal mass, since an early diagnosis has a large impact in the prognosis of intrabdominal masses.

Poster: EDU-041

ROTATING 3D LIKE FLUOROSCOPIC TECHNIQUE USING AN OCTOSTOP AND A FIXED FLUOROSCOPY SYSTEM

MIKHAEL Sebaaly, TAKASHI SHAWN Sato, ROBERT Becker
University of Iowa Hospitals and Clinics, Department of Radiology, Iowa City, USA

Despite significant advances in cross sectional imaging, fluoroscopic gastrointestinal studies such as upper GI exams, esophagrams, small bowel follow throughs, and lower GI exam remain an essential part a pediatric practice. When examining the small and large bowel, it can be difficult to completely evaluate segments of bowel secondary to overlap and

positioning, particularly in infants. Using an Octostop immobilization device, we devised a method of getting rotating patients while acquiring fluoroscopic images to improve visualization and assessment of overlapping bowel. The purpose of this review was to determine the effectiveness of this technique in assessing malrotation without missing the timing of the contrast going to the ligament of Treitz and to better delineate the focus of perforation in case of leak.

Children less than 3 years of age undergoing a fluoroscopic guided gastrointestinal procedure (upper GI, esophagogram, small bowel follow through and lower GI) with octostop were the reviewed cases. We checked whether the octostop rotating images prevented us from missing the contrast as it was passing in the duodenum when the patient was rotated from right lateral decubitus position to supine. In addition, we checked if this technique was helpful in finding the focus of leak in cases of perforation.

We never missed the timing of contrast passing through the duodenum in an upper GI using this technique. In addition, the technique helped us identify the focus of contrast leak from the bowel in case of bowel perforation. Referring physicians, (particularly pediatric surgeons) liked the rotating images and expressed that it helps them with surgical planning.

Poster: EDU-042

BUBBLES OF THE NEONATAL ABDOMEN

MONICA Royero Arias
Servicios de Salud San Vicente Fundación, Medellín, COLOMBIA

Introduction:

Gastrointestinal pathologies in neonates constitute a set of congenital or acquired entities. A correct and timely diagnosis is essential to minimize morbidity and mortality in this population.

Conventional abdominal radiography has historically constituted, most of the time, the only study and the one that provides us with the best diagnostic approach in these alterations despite other innovative methods that emerged over time. However, on some occasions the help of ultrasound, fluoroscopic studies and even computed tomography or magnetic resonance imaging is required for difficult diagnoses.

On X-rays we can see the formation of gas bubbles when the air passes through the gastrointestinal tract at birth until it reaches the rectum 24 hours later. In the same way, pathological air bubbles can be seen and guide us to specific diagnoses.

It is recommended to take into account three steps in the radiological approach of neonates with gastrointestinal pathologies:

1. Rule out the presence of ominous signs such as pneumoperitoneum, intestinal pneumatosis (linear or cystic) or pneumoporta, because these children require urgent surgical evaluation.
2. Look for the classic signs such as: bubbles in the chest in cases of diaphragmatic hernias, a single bubble in pyloric atresia, a single bubble with distal gas in pyloric hypertrophy, double bubble in duodenal atresia, double bubble with distal gas in partial obstructions of the duodenum, triple bubble in jejunal atresia and soap bubbles in the lower right quadrant in meconium ileus.
3. Define if the pattern is consistent with upper or lower obstruction. In an upper intestinal obstruction only few intestinal air bubbles occupy the upper hemiabdomen, while in the lower obstruction there are many dilated upper intestinal loops (more than three).

Purpose: Describe the imaging findings of gastrointestinal pathologies in neonates for an adequate interpretation through a simple and didactic approach.

Materials and Methods: An interactive review will be presented with a series of cases with radiological studies where air bubbles in the abdomen were evidenced, from normal findings to gastrointestinal pathologies.

Conclusions: Abdominal radiographs are studies frequently performed in neonatal care units. The radiologist must be trained to differentiate between normal and pathological findings.

A three-step approach is recommended taking into account the air bubbles observed in the abdomen to make the correct diagnosis.

Poster: EDU-043

ADOLESCENT WITH MEDIAN ARCUATE LIGAMENT AND NUTCRACKER SYNDROMES

MONIQUE Riemann¹, CHRISTINE Markham
Phoenix Children's Hospital, Phoenix, USA

We present a case study of a 15 year old female with 4 weeks of periumbilical pain, nausea, vomiting and diarrhea. The patient was initially diagnosed with MALS and subsequently NCS.

MALS is a rare condition that predominantly affects females and is an often-overlooked cause of chronic functional abdominal pain. Its occurrence is due to the extrinsic compression of the median arcuate ligament of the diaphragm onto the proximal portion of the celiac artery. Compression of the celiac artery increases during expiration and can be a cause of painful mesenteric ischemia. Diagnostic criteria includes a PSV >200cm/sec and an EDV of >55cm/sec in the celiac artery on expiration and a deflection angle (DA) >50.

NCS is defined as the compression of the left renal vein as it courses between the aorta and superior mesenteric artery. It is a very rare condition and more prevalent in females. Diagnostic criteria includes a ratio of left renal vein diameter at the renal hilum and the aortomesenteric region of >4.7 and a peak systolic velocity >93cm/sec.

Our patient had a PSV 297cm/sec EDV 157cm/sec in her celiac artery on expiration. with a DA of 59. Her left renal vein revealed a ratio of 4.8 and PSV 131cm/sec.

Color Doppler sonography, due to its dynamic ability and lack of radiation, is an excellent tool that aids in the diagnosis of these uncommon conditions. Sonography of the abdomen should routinely include imaging of the celiac artery in patients with chronic abdominal pain, as MALS; although rare, can be the cause and assist in the diagnosis of this condition. In patients with LUQ pain and/or hematuria, the left renal vein should be interrogated with color and spectral Doppler to exclude NCS. To our knowledge there has been only one other reported case of a patient with both MALS and NCS.

Poster: EDU-044

IMAGING OF COLANGIOPATHIES IN CHILDREN

RITA Pina Prata, ANA Forjaco, ANA Nunes, EUGÉNIA Soares
Hospital Dona Estefânia, Centro Hospitalar Universitário Lisboa Central, Lisbon, PORTUGAL

Purpose:

(1) Get to know the most common biliary conditions in children by categorizing them as congenital, infectious, inflammatory or tumoral.
(2) Present a series of cases with emphasis on their imaging features and their differential diagnosis (both clinically and based on imaging findings).

(3) Correlate ultrasound and MRI findings of these patients and, when available, with prenatal diagnosis.

Materials and Methods:

We present a series of pediatric colangiopathies and illustrate them with schemes, ultrasound, CT and MRI examinations from our archive.

Results:

Congenital entities comprise biliary atresia which has to be corrected in the first months of life to prevent life-long hepatic complications making it crucial not to miss this diagnosis. Differential diagnosis of an abdominal

cystic lesion in the newborn's upper abdomen should consider choledochal cyst which also can present as obstructive hyperbilirubinemia in the newborn and is further classified according to Todani classification. Other congenital conditions include gallbladder agenesis and hypoplasia. Acquired conditions comprise obstructive colangiopathies which might have a multiplicity of causes such as calculous, infectious and inflammatory stenosis like in sclerosing cholangitis. Rare tumours such as rhabdomyosarcoma of the biliary tract is another entity that might present with a cholestatic clinical picture. Association of renal cysts and biliary ectasia should suggest a ciliopathy, like Caroli syndrome, which should be actively searched for. Normal imaging might also be a hint to a diagnosis like in inherited disorders such as progressive familial intrahepatic cholestasis whereas in Alagille syndrome, extra-hepatic ancillary findings, such as butterfly vertebra, are the hint to the diagnosis.

Conclusions:

Colangiopathies in children are increasingly imaged, particularly by cholangio-MRI making it crucial to know the clinical and imaging spectrum and signs that suggest each of these entities.

This is a case of a newborn with a cystic lesion on the common bile duct topography. Differential diagnosis between type 1 choledochal cyst and cystic biliary atresia, hints for their differentiation, companion case as well as the final diagnosis is provided.

Poster: EDU-045

Withdrawn

Poster: EDU-046

Withdrawn

Poster: EDU-047

PEDIATRIC RADIOLOGY ON-CALL PRIMER: WHAT NOT TO MISS IN KIDS

LEANN Linam, KIERY Braithwaite
Children's Healthcare of Atlanta, Atlanta, USA

Abstract: Pediatric diagnoses can be daunting to the radiology resident preparing to take call. This educational exhibit details diagnoses that are commonly seen in children who present to the emergency department radiology and tips and tricks on making the diagnosis.

Teaching Points:

- 1) Be able to recognize malrotation/midgut volvulus
- 2) Evaluation of ingested foreign bodies, and why this diagnosis is important
- 3) Evaluation of intussusception, including ileocolic and small bowel-small bowel
- 4) Recognize abnormalities in the neonate, including umbilical line abnormalities, necrotizing enterocolitis, and abnormally located air
- 5) Recognize injuries specific to child abuse and other trauma

Table of Contents:

- 1) Ingested foreign bodies
 - a. Button battery
 - b. Multiple magnets
- 2) Aspirated Foreign Body
- 3) Epiglottitis
- 4) Intussusception
- 5) Necrotizing Enterocolitis
- 6) Umbilical Lines
- 7) G-tubes gone wrong

- 8)Where is the Air?
- 9)Child abuse
- 10)SCFE/ hip avulsion injuries

Poster: EDU-048

PEDIATRIC FLUOROSCOPY 101

LEANN Linam, JONATHAN Loewen

Children's Healthcare of Atlanta, Atlanta, USA

Learning Objectives: The learner should be able to

- 1.Know basic fluoroscopy technique for multiple studies
- 2.Identify the abnormalities of the GI and GU system on fluoroscopy.

Table of Contents:

- 1.Upper GI
 - a.Technique
 - b.Abnormalities
 - i.Achalasia
 - ii.Tracheoesophageal fistula
 - iii.Hiatal hernia
 - iv.Gastroesophageal reflux
 - v.Hypertrophic pyloric stenosis
 - vi.Gastric volvulus
 - vii.Malrotation/midgut volvulus
 - viii.Duodenal web
- 2.Small Bowel Follow through
 - a.Technique
 - b.Abnormalities
 - i.Terminal ileitis
- 3.Enema
 - a.Technique
 - b.Abnormalities
 - i.Hirschprung's Disease
 - ii.Microcolon
 - iii.Small left colon syndrome
- 4.Voiding cystourethrogram
 - a.Technique
 - b.Abnormalities
 - i.Vesicoureteral reflux
 - ii.Ureterocele
 - iii.Posterior urethral valves
 - iv.Neurogenic bladder
 - v.Duplicated collecting system

Poster: EDU-049

MOVING BEYOND NONSPECIFIC BOWEL WALL THICKENING ON ULTRASOUND WITH PATHOLOGIC CORRELATION

IONE Limantoro, ANNA Lee, DANIEL Rosenbaum

BC Childrens Hospital and The University of British Columbia, Vancouver, CANADA

Purpose

Applications for ultrasound assessment of the bowel in children have been well-described. While a wide variety of entities can manifest with bowel wall thickening on ultrasound, less focus has been placed on patterns of bowel wall architectural change in specific disease states. Alterations to normal mural stratification, laminar predilection, loss of mucosal or serosal integrity, extent and symmetry of mural thickening, and changes in mural vascularity among other features can apprise the radiologist of likely differential considerations and potential complications. This pictorial essay will review the sonographic appearance of the normal bowel wall and the imaging manifestations of a variety of diseases that may derange normal bowel wall architecture, with illustrative pathologic correlation where appropriate.

Material/Methods

The goals of this educational exhibit will be to:

- 1.Review normal bowel wall architecture and appearances on ultrasound.
- 2.Highlight patterns of bowel wall architectural change across a variety of disease states, including congenital lesions, inflammatory bowel disease, infection, allergic and immune-mediated disorders, lymphatic disorders, vascular conditions, and neoplasms, as well as potential bowel disorder mimics.
- 3.Correlate sonographic findings with pathologic specimens in order to emphasize underlying pathophysiology.

Results

After reviewing the exhibit, the reader will be able to:

- 1.Identify 5 histologic layers of normal bowel wall that are visible on ultrasound.
- 2.Describe ≥ 3 changes to bowel wall architecture seen with inflammatory bowel disease.
- 3.List ≥ 3 categories of disease beyond “infectious or inflammatory” that may cause bowel wall thickening.

Conclusion

Although there exists significant overlap in sonographic findings among bowel disorders and pathognomonic features are relatively uncommon, a thorough understanding of normal and abnormal bowel wall architecture can inform differential considerations and guide appropriate management.

Poster: EDU-050

RECTOVESICULAR FISTULA: AN ODD PRESENTATION

LEAH Leonhardt, DOUGLAS Moote, SHANSHAN Bao

Hartford Hartford, Glastonbury, USA

We review a case of a 12-year-old boy who presents with urinary continence. Our patient has a 2-year history of metastatic desmoplastic small round cell tumor status post cytoreductive surgery and hyperthermic intraperitoneal chemotherapy. Patient reported no voluntary daytime urination for the past 4 days, did not feel the need to urinate, and nightly enuresis since symptoms began. Physical exam revealed mild discomfort in his lower abdomen. Initial imaging workup included a pelvic ultrasound, which demonstrated left-sided hydronephrosis and a thick-walled bladder containing only a small volume of debris-containing urine. The patient was hospitalized for a urinary tract infection. 10 days later without improvement, fluoroscopy cystogram was performed, which revealed a gas-filled bladder, followed by contrast infusion into the bladder with filling of the rectum and no contrast detected within the bladder. Diagnosis of a rectovesical fistula was made.

Poster: EDU-051

CONGENITAL AND INFANTILE HEPATIC HEMANGIOMAS: DIAGNOSTIC-THERAPEUTIC CHALLENGE

SAIDMAN Julia, UDAQUIOLA Julia, KREINDEL Tamara
Hospital Italiano de Buenos Aires, Caba, ARGENTINA

The International Society for the Study of Vascular Anomalies (ISSVA) classifies hemangiomas into congenital and infantile. The first of these develop in the prenatal period and correspond to the rapidly involving cutaneous hemangioma (RICH) liver form. The infantile hepatic hemangioma develops in the postnatal period, coexists with cutaneous hemangiomas and occurs in the multifocal and diffuse forms.

Most of them are asymptomatic and involute, representing an incidental finding in prenatal obstetric ultrasound (congenital hemangioma), or in screening tests in patients with multiple skin hemangiomas (infantile form). Anyway, a small percentage of the cases can be complicated with signs of high flow heart failure according to the growth peak of the hemangioma, as a consequence of porto-venous/arterio-venous shunts.

Within the complementary imaging methods, ultrasound in its grayscale and color doppler modes represents the study of the first line. More complex procedures such as Magnetic Resonance and Computed Tomography with intravenous contrast are reserved for a second instance, in case of diagnostic doubts, unusual presentations and/or complications. It is important to mention that hemangiomas have characteristic imaging findings at color doppler and enhancement pattern following intravenous contrast administration.

Although most of these tumors are benign and naturally involute, they require specialized follow-up and management by a multidisciplinary team. In this sense, different institutions have proposed standardized monitoring guidelines through laboratory tests and imaging methods

Most hepatic hemangiomas are amenable to conservative treatment and only a small minority of cases require medical treatment with propranolol, invasive or surgical approach.

In this review we discuss what liver hemangiomas look like with different imaging methods and their differential diagnoses

Educational objectives

- To review the different forms of presentation of hepatic hemangiomas, their different imaging characteristics and possible differential diagnoses

- Summary of recommendations for follow-up of congenital and infantile hepatic hemangiomas and their different therapeutic options

Poster: EDU-052

PAEDIATRIC VIDEOFLUOROSCOPIC SWALLOW STUDY (VFSS): A STEP-BY-STEP APPROACH

ANA Forjaco, ANA Rega, PEDRO Alves
Centro Hospitalar Universitário Lisboa Central, Lisbon, PORTUGAL

Purpose: Brief review of the Videofluoroscopic Swallow Study (VFSS) technique and the main specificities of its use in paediatrics, including the formulation of a step-by-step approach to this technique.

Materials and methods: Research of terms such as VFSS, oropharyngeal dysphagia and paediatrics in PubMed. Review of relevant articles. Selection of original sample images of VFSS in patients treated in a paediatric university hospital.

Results: Swallowing problems are seen in up to 25% of all children and may occur because of developmental disorders, neurological conditions, gastroesophageal reflux or anatomical anomalies. Physicians in charge of paediatric patients should be aware that malnutrition and respiratory diseases are frequently caused by unrecognized dysphagia and silent

aspiration. VFSS is a radiographic procedure that provides a dynamic view of the swallowing process. This process occurs in three main stages - oral, pharyngeal, and oesophageal - which have specific characteristics that must be recognized in the evaluation of a paediatric VFSS. The alteration of these phases results in different types of dysphagia, whose characteristics are typical of the children's underlying disease. The swallowing reflex and airway protection are among the most important aspects to be assessed in the study. Overall, an interdisciplinary team approach improves global assessment and therapy planning, based on clinical and imaging findings.

Conclusions: Swallowing difficulties can severely compromise pulmonary health and nutritional intake of paediatric patients. VFSS is the gold standard for the definitive evaluation of dysphagia in children. The success of this technique depends on the knowledge of the main phases of the swallowing process and the main specificities of the paediatric population.

Poster: EDU-053

POINT SHEAR WAVE ELASTOGRAPHY: ECOGRAPHIC TECHNIQUE AND PAEDIATRIC APPLICATIONS

ANA Forjaco
Centro Hospitalar Universitário Lisboa Central, Lisbon, PORTUGAL

Purpose: Review of the point shear wave elastography technique (p-SWE) and of the main specificities of its use in paediatrics, including the advantages, limitations and several applications of p-SWE in the paediatric population and the main reference values for each application.

Materials and methods: Research of terms such as p-shear wave elastography and paediatrics in PubMed. Review and selection of articles relevant to the study of elastographic technique applications in the paediatric age group. Selection of original sample images of elastographic studies in paediatric patients treated in a level III university hospital.

Results: Elastography assesses tissue elasticity in a non-invasive way, which becomes useful in diseases concomitant with fibrosis, hypercellularity or adipose tissue infiltration. The main application of p-SWE in the paediatric population is the assessment of liver fibrosis in inherited metabolic disorders or bile duct diseases. Organs such as the spleen, the pancreas, the thyroid and the muscle are also relevant targets for tissue changes susceptible to elastographic assessment. The implementation of normality standards in children depends on various characteristics inherent to this population, such as the variations that are associated with age and the ability to cooperate during the execution of the exam.

Conclusions: The p-SWE technique is useful when assessing liver, splenic, pancreatic, thyroid, and muscular rigidity in paediatrics. The success of these applications depends on the knowledge of the main specificities inherent to elastographic assessment and of the technique adaptation to this population.

Poster: EDU-054

MR IMAGING FINDINGS OF POST-OPERATIVE EVALUATION IN CHILDREN WITH ANORECTAL MALFORMATION

SALLY Emad-Eldin, OMAR Abdelaziz, MUSTAFA Gad
Cairo University Teaching Hospitals, Cairo, EGYPT

Anorectal malformations (ARM) are congenital anomalies of the anus and distal rectum, with associated genitourinary anomalies. Fecal incontinence and constipation are major postoperative problems in children after repair of ARM.

Because of its higher soft tissue contrast and multiplanar capabilities MRI is considered an essential imaging examination for post operative assessment of pelvic floor after repair of ARM.

Educational objectives:

- Describe the MR imaging technique.
- Assess MRI findings after repair of ARM and discuss the evaluation points:
 - * Position of neorectum.
 - * Measurement of anorectal angle.
 - * morphology and symmetry of the external anal sphincter.
 - * Presence of mesenteric fat interposition.
 - * Status of puborectalis sling and elevator and muscles.
 - * Post operative scar
- Discuss associated genitourinary anomalies.

Poster: EDU-055

LOST IN THE SPACE OF RETZIUS

PAULA dickson, KIERY Braithwaite, EDWARD Richer
Emory University/Department of Radiology, Atlanta, USA

Purpose: To review the anatomy of the Space of Retzius and to highlight the array of disorders that can occur in this space in the pediatric population. These disorders present as abdominal pain and might be missed or misdiagnosed without paying attention to this space and knowing the differential and differentiating factors of pathology that are found there.

Methods: Retrospective review of cases from 2007-2021 at Children's Healthcare of Atlanta involving pathology in the Space of Retzius.

Results: We present a series of patients age 3 – 18 years with a variety of pathologies in the Space of Retzius, imaged with ultrasound, CT, or MRI. Examples of infectious or inflammatory conditions include a 15 yo female with an infected urachal remnant and a 3 yo female undergoing evaluation for appendicitis found to have pubic osteomyelitis with abscess in the Space of Retzius. A case of traumatic extraperitoneal bladder rupture will be reviewed. A case of pelvic sarcoma illustrates the potential neoplastic conditions within the space. The review will utilize a case-based approach to highlight the relevant findings and review important anatomic landmarks.

Conclusion: Pathology in the Space of Retzius can easily be missed, particularly by ultrasound, and the various etiologies for abdominal pain in this space can be difficult to differentiate from each other. Awareness of these etiologies when scanning and interpreting the findings is essential for timely diagnosis.

Poster: EDU-056

ACUTE ABDOMEN IN NEONATES: IMAGING SPECTRUM AND CLASSIC FEATURES

ANKITA Chauhan, ANAND Raju, THOMAS Boulden, PREET Sandhu, HARRIS L. Cohen
University of Tennessee Health Science Center/Le Bonheur Children's Hospital, Memphis, USA

Purpose/Educational objectives:

1. To acquire a basic understanding of the normal bowel gas pattern in neonates and learn various acute abdominal conditions' radiographic appearances.

2. To be familiar with the characteristic imaging appearances and features of different disease processes leading to an acute abdomen in the neonatal age group.

3. To learn how to approach neonatal obstructions and perform appropriate imaging to ensure prompt diagnosis, especially for surgical emergencies.

Materials and Methods: We will be discussing the causes of high-level obstruction (such as esophageal atresia, duodenal atresia, jejunal atresia, malrotation, midgut volvulus) and low-level obstruction (including ileal atresia, left colon syndrome, Hirschsprung disease) as well as the acquired conditions that might lead to the acute abdomen in the neonates (for example, hypertrophic pyloric stenosis, necrotizing enterocolitis, intestinal perforation, ovarian torsion) and describe their salient imaging features. The primary focus will be on plain radiographs, ultrasound, and fluoroscopic examinations.

Results:

The surgical causes of acute abdomen in the neonates require an early and accurate diagnosis for timely intervention. Radiographic evaluation of the abdomen is the initial investigation of choice. Although neonates with classic radiographic findings of high intestinal obstruction, such as duodenal atresia, may directly undergo surgery without any additional imaging, an upper gastrointestinal series is typically performed for further evaluation. Similarly, an enema examination is used for further investigation of low intestinal obstruction in neonates.

Conclusion:

Acute abdominal condition in the neonatal age group usually presents with vomiting (bilious or projectile), abdominal distension, and constipation. The time of presentation of symptoms helps narrow down the differential diagnosis. It is crucial to adequately target the imaging techniques to ensure the correct diagnosis without unnecessary delay. This exhibit will discuss the congenital gastrointestinal obstructions and some acquired diseases responsible for an acute abdomen in the neonate.

Poster: EDU-057

ASSESSMENT OF ESOPHAGUS AND GASTROESOPHAGEAL JUNCTION IN THE PEDIATRIC AGE GROUP

ANKITA Chauhan, ANAND Raju, THOMAS Boulden, PREET Sandhu, HARRIS L. Cohen
University of Tennessee Health Science Center/Le Bonheur Children's Hospital, Memphis, USA

Purpose/Educational objectives:

1. Discuss the normal appearance and describe the congenital and acquired disease conditions involving the esophagus and gastroesophageal junction in the pediatric age group.

2. To illustrate the normal postsurgical appearances and discuss the complications.

3. To be familiar with the classic imaging appearance and provide an appropriate diagnosis when confronted with a child with esophageal disease.

Materials and Methods:

Fluoroscopy, combined with plain radiography, is a simple and cost-effective investigation to diagnose the functional and structural abnormalities of the esophagus. We will demonstrate an imaging spectrum of esophageal disorders in the pediatric population.

Results:

Many congenital and acquired lesions affect esophageal morphology and function. Our study emphasizes the use of fluoroscopy primarily to postulate key imaging points of esophageal disorders in children. Barium esophagram often remains the initial imaging study in pediatric patients with dysphagia, vomiting, and failure to thrive. Most radiologists consider it prudent to routinely assess the esophagus as an integral part of any

barium examination of the upper gastrointestinal tract. Our discussions will include but not be restricted to esophageal atresia, tracheoesophageal fistula, gastroesophageal reflux, achalasia, foreign body, hiatal hernia, and the postsurgical appearances. Knowledge of various imaging appearances would be useful for planning an appropriate management strategy for the child.

Conclusion:

Pediatric patients often present with dysphagia or feeding difficulties due to both congenital and acquired causes. Fluoroscopy is the primary imaging modality to assess the esophagus in children. We will review the imaging manifestations of various esophageal disorders encountered in children.

Poster: EDU-058

IMAGING SPECTRUM OF INGESTED FOREIGN BODY IN THE PEDIATRIC AGE GROUP: WHAT THE RADIOLOGISTS NEED TO KNOW

ANKITA Chauhan, ANAND Raju, THOMAS Boulden, PREET Sandhu, HARRIS L. Cohen
University of Tennessee Health Science Center/Le Bonheur Children's Hospital, Memphis, USA

Educational objectives:

1. To be familiar with imaging appearances of different kinds of ingested and aspirated foreign bodies in children and their clinical significance.
2. To understand the role imaging plays in the diagnosis and prompt identification of ingested foreign bodies to ensure appropriate treatment.
3. To help the trainees understand the appropriate imaging approach and recognize the classic radiographic signs of foreign-body aspiration and ingestion.

Materials and Methods: Children quite often present with complications related to foreign body ingestion, which, many a time, is an unwitnessed event. We will be discussing the imaging appearances of various commonly encountered ingested foreign bodies in the pediatric age group. Our discussion will include, but will not be restricted to, the ingestion of coin, button battery, magnet, foreign body aspiration, and different bezoar presentations in the pediatric age group.

Results: Imaging plays a vital role in diagnosing foreign body ingestion and associated complications in children, especially with unwitnessed ingestion events, and guides clinical management by helping determine the appropriate treatment. Features such as the type of foreign body ingested, the duration of ingestion, location, and associated complications, if any, help decide whether the ingested and aspirated foreign bodies need urgent removal or can be managed conservatively. Plain radiography is an essential modality in evaluating ingested or aspirated foreign bodies. In complicated cases, fluoroscopy and computed tomography help to provide additional but paramount information. All radiologists who interpret imaging examinations of children must be familiar with imaging characteristics of commonly ingested foreign bodies and understand their clinical significance.

Conclusion: When the event of foreign body ingestion is witnessed, diagnosis and management are usually not problematic. However, unwitnessed foreign bodies may present well after the occult initiating event with symptoms mimicking other conditions. Our educational exhibit reviews the imaging findings of foreign bodies in children, emphasizing the unsuspected or long-standing foreign bodies.

Poster: EDU-059

GASTRIC TRANSPOSITION FOR PAEDIATRIC OESOPHAGEAL REPLACEMENT SURGERY – A RADIOLOGICAL REVIEW

ANNE Carroll, JOE Curry, KIERAN McHugh
Great Ormond Street Hospital, London, UNITED KINGDOM

Purpose:

Gastric transposition, also known as gastric pull up, is a well-established surgical technique used for oesophageal replacement surgery. It involves mobilisation of the stomach into the thorax with a single anastomosis at the neck and can be safely performed minimally invasively.

The aim of this electronic educational exhibit is to demonstrate the radiological findings in paediatric patients who have undergone gastric transposition for oesophageal replacement surgery. We will illustrate the interesting post-operative appearances on plain radiography and fluoroscopy and highlight many of the associated complications that the radiologist should look out for.

Materials and Methods:

We reviewed the charts and imaging of 21 children who underwent gastric transposition and radiological follow-up at our centre between 2003 and 2020. Age range at time of surgery: 10 months to 8.5 years, (9 male, 12 female). The indication for surgery was oesophageal atresia in 14, oesophageal stricture of unknown aetiology in 1 and caustic injury in 6. Selected images demonstrate the expected post-operative appearances and commonly encountered complications of this surgical technique. The presentation will be in an interactive format to promote participant education and retention of learning.

Results:

The post-operative chest radiograph in a patient with gastric transposition demonstrates the presence of a trans-anastomotic tube (TAT) with the tip in the thorax. In the absence of adequate clinical information, this can be misinterpreted as an improperly sited nasogastric tube, prompting the radiologist to recommend that the tube be resited. Air within a gastric transposition can also be misinterpreted as a pneumomediastinum, when the surgical history has not been provided.

Examples of common complications that will be demonstrated include pneumonia, pneumothorax, pleural effusion, early anastomotic leak, anastomotic strictures, delayed gastric emptying, atonic stomach and herniation of bowel and mesentery into the chest (the latter can mimic a tumour).

Conclusion:

We will use an interactive pictorial review to educate participants about the expected post-operative radiological findings and common complications for this interesting and often complex cohort of patients who have undergone gastric transposition surgery for long gap oesophageal atresia or caustic injury.

Poster: EDU-060

THE SPLEEN IN THE CHILD

SANDRA bareno¹, LIZBET Perez¹⁻³, ISABEL Fuentealba¹⁻³

¹ Clinica Alemana De Santiago, Santiago, CHILE

² Hospital de La Florida, Santiago, CHILE

³ Hospital Dr. Luis Calvo Mackenna, Santiago, CHILE

Introduction:

The spleen parenchyma structure is unique and changes with age, and that reflects in its normal characteristics in the different imaging techniques.

Due to its embryology and functions, may be involved in various pathological processes, some primary and others as part of systemic diseases, and in some cases the findings on images of the spleen are indicative of specific diagnoses. US is the first imaging method recommended for the study of splenic pathology in children, and often the only one, however, we must know the usual characteristics of the spleen in the rest of the imaging techniques for an adequate interpretation of the findings

Objectives:

Describe the normal findings and manifestations of the main pathological processes of the spleen in pediatric age, in the different techniques of diagnostic images, with emphasis in ultrasound.

Discussion:

In ultrasound we can recognize the normal structure of the spleen, which varies with age, the ultrasound patterns of the parenchyma can be homogenous, micronodular and macronodular.

In MRI the intensity in T1 and T2 also changes with age. In contrasted CT, the heterogenous enhancement of the spleen is normal and its frequently present in children.

Congenital anomalies are related to the presence, number, location and relationships with other organs.

The size of the spleen changes with age, the diagnosis of splenomegaly in children can be based on the normal standard of the age and in the morphology that the spleen can adopt when it grows. The splenomegaly has multiple causes, infectious, congestive, immunological, inflammatory, storage disorders, lymphoproliferative and associated with systemic diseases.

Majority of the focal lesions in this age are benign and include cysts, lymphatic malformations, hemangiomas and hamartomas.

We must also know the manifestations of spleen injuries in closed abdominal trauma in the child.

In this review we will illustrate through a series of interactive cases, the normal characteristics and main pathologies of the spleen in the child.

Poster: EDU-061

THE CHILD'S SPLEEN

SANDRA Bareño, LIZBET Pérez, ISABEL Fuentealba
Clínica Alemana, Department of Radiology, Santiago, CHILE

Introduction:

The spleen parenchyma structure is unique and changes with age, and that reflects in its normal characteristics in the different imaging techniques.

Due to its embryology and functions, may be involved in various pathological processes, some primary and others as part of systemic diseases, and in some cases findings on images of the spleen are indicative of specific diagnoses.

US is the first imaging method recommended for the study of splenic pathology in children, and often the only one, however, we must know the usual characteristics of the spleen in the rest of imaging techniques for an adequate interpretation of the findings

Objectives:

Describe the normal findings and manifestations of the main pathological processes of the spleen in pediatric age, in different techniques of diagnostic images, with emphasis in ultrasound.

Discussion:

In ultrasound we can recognize the normal structure of the spleen, which varies with age, the ultrasound patterns of the parenchyma can be homogenous, micronodular and macronodular.

In MRI the intensity in T1 and T2 also changes with age. In contrasted CT, the heterogenous enhancement of the spleen is normal and its frequently present in children.

Congenital anomalies are related to the presence, number, location and relationships with other organs.

The spleen size changes with age, diagnosis of splenomegaly in children can be based on the normal standard of the age and in the morphology that the spleen can adopt when it grows. The splenomegaly has multiple causes, infectious, congestive, immunological, inflammatory, storage disorders, lymphoproliferative and associated with systemic diseases.

Majority of the focal lesions in this age are benign and include cysts, lymphatic malformations, hemangiomas and hamartomas.

We must also know the manifestations of spleen injuries in closed abdominal trauma in the child.

In this review we will illustrate through a series of interactive cases, the normal characteristics and main pathologies of the spleen in the child

Poster: EDU-062

IMAGING OF INGESTED FOREIGN BODIES AND THEIR COMPLICATIONS

HIRAL Banker, PREET Sandhu
Le Bonheur Children's Hospital, Memphis, USA

Foreign body ingestion is a common occurrence in children and may lead to significant morbidity and mortality. Imaging plays an important role in the identification of ingested foreign bodies (FB). Knowledge of appropriate imaging algorithms and familiarity with the appearance of different foreign bodies on various modalities is crucial for radiologists especially when clinical history is unavailable or trivial. Ingested FBs such as disk batteries and magnets can lead to life-threatening complications. Timely identification, documentation, immediate action, and treatment are extremely crucial in such cases. The purpose of this exhibit is to educate about commonly ingested FB in pediatrics with their appearance on different imaging modalities (e.g. US, X-ray, CT, MRI, fluoroscopy), identification of secondary signs, and associated complications.

Outline:

- Overview of most common ingested foreign bodies seen in pediatrics with an emphasis on life-threatening conditions.
- Demonstrate the appearance of various FBs on different modalities.
- Illustrate primary and secondary radiologic signs to suggest the presence of the ambiguous foreign body.
- Discuss and illustrate imaging findings and radiologic procedures that can help identify complications associated with foreign body ingestion.

Poster: EDU-063

CONGENITAL PORTOSYSTEMIC SHUNTS

EDUARDO Bandeira ¹, RITA Prata ², RITA Carneiro ², EUGÉNIA Soares ²

¹ Centro Hospitalar Lisboa Ocidental - Department of Radiology, Lisbon, PORTUGAL

² Centro Hospitalar Lisboa Central - Hospital D. Estefânia, Department of Radiology, Lisbon, PORTUGAL

Purpose

The purpose of this presentation is to demonstrate the imaging findings of various types of congenital portosystemic shunts and therefore allow for their recognition when characteristic features are present.

Materials and methods

Imaging features of these congenital malformations are presented and discussed, according to a review of the literature, and illustrated by cases from our institution.

Results

Congenital portosystemic shunts are rare developmental anomalies resulting in diversion of portal flow to the systemic circulation and have been divided into extra- and intrahepatic shunts.

Most often, the diagnosis is made primarily with Doppler ultrasonography. Computed tomographic angiography and magnetic resonance angiography may be used for further classification of the shunt and assessment of accompanying anomalies. Conventional angiography is necessary when results of the other tests disagree or are inconclusive.

Conclusions

Despite the rarity of congenital abnormal communications between the portal and systemic venous circulation, radiologists have to consider this diagnosis in children who present with nonspecific liver dysfunction. Familiarity with the characteristic features are useful for an early

diagnosis and to choose the best therapeutic approach.

Poster: EDU-064

A PICTORIAL REVIEW OF MALROTATION MIMICS IN PAEDIATRICS

SRIVIDYA Arya, SAIRA Haque
King's College Hospital NHS Trust, London, UNITED KINGDOM

Intestinal malrotation is a continuum of congenital anomalies due to lack of rotation or incomplete rotation of the fetal intestine around the superior mesenteric artery axis. The abnormal bowel fixation (by mesenteric bands) or absence of fixation of portions of the bowel increases the risk of bowel obstruction, acute or chronic volvulus, and bowel necrosis. The clinical presentation of patients with malrotation without, with intermittent, or with chronic volvulus can be problematic, with an important minority presenting late or having atypical or chronic symptoms, such as intermittent vomiting, abdominal pain, duodenal obstruction, or failure to thrive. The diagnosis is heavily reliant on imaging. Upper GI series remain the gold standard with the normal position of the duodenojejunal junction lateral to the left-sided pedicles of the vertebral body, at the level of the duodenal bulb on frontal views and posterior (retroperitoneal) on lateral views. However, a variety of conditions might influence the position of the duodeno-jejunal junction, potentially leading to a misdiagnosis of malrotation. Such conditions include improper technique, gastric over distension, splenomegaly, renal or retroperitoneal tumors, liver transplant, small bowel obstruction, the presence of properly or malpositioned enteric tubes, and scoliosis. All of these may cause the duodenojejunal junction to be displaced. We present a series of cases highlighting conditions that mimic malrotation without volvulus to increase the practicing radiologist awareness and help minimize interpretation errors. Is it malrotation? The variation in normal appearances of the duodenojejunal junction: Intestinal malrotation refers to incomplete bowel rotation that leads to an abnormal position of the duodenojejunal (DJ) junction and caecum. The occurrence of malrotation is reported to be 2.8 cases per 10,000 live births. It is a potentially serious surgical emergency and must be immediately diagnosed prior to the development of acute midgut volvulus, bowel ischaemia and midgut gangrene.

Poster: EDU-065

TRAUMATIC HANDLEBAR INJURIES IN CHILDREN

JOHN Adu, SAIF Sait, SAYANI Khara, SAIRA Haque
King's College Hospital, Department of Radiology, London, UNITED KINGDOM

Purpose:

Given the potential significant morbidity, it is imperative for radiologists to understand and recognize the imaging findings related to handlebar injuries in the paediatric population, which can often be subtle. Knowledge of the patient's history and recognition of the mechanism of handlebar-related injuries may aid in the early diagnosis of serious thoracoabdominal injuries.

The purpose of this educational exhibit is to familiarise the reader with the imaging findings and common patterns of injury related to handlebar trauma in children.

The exhibit will include CT, MRI and ERCP image findings in thoracoabdominal and limb soft tissue handlebar related trauma.

Materials and Methods:

A review of a prospectively maintained database of trauma patients aged 0-18 who either presented to our institution de novo, or were transferred to our institution for tertiary level care between 2010-2020 was undertaken. Patients whose mechanism of injury involved being struck by a

bicycle handlebar, or thrown from a bicycle were included. PACS and electronic clinical notes were reviewed.

Results:

Thoracic injury patterns included rib fractures, pneumothoraces, pulmonary lacerations and pulmonary contusions. Abdominal injury patterns included renal laceration, liver laceration pancreatic laceration, gastric laceration, small bowel haematoma and small bowel evisceration. Soft tissue injuries included deep thigh lacerations.

Conclusion:

Handlebar injuries may be subtle, are often underestimated, and can be overlooked. The radiologist plays an important role in the diagnosis and treatment of patients with handlebar injuries. Understanding of imaging findings and pattern of injury leads to appropriate AAST stratification, and consequently helps clinicians in deciding on surgical or conservative management. Given the significant potential morbidity related to handlebar trauma, it is crucial for every radiologist to be aware of the patterns of handlebar injuries for timely diagnosis and management.

Poster: EDU-066

ULTRASOUND IN DIAGNOSIS AND MONITORING OF PYELONEPHRITIS, AS THE ONLY IMAGING MODALITY IN CHILDREN

IRENE VraKa¹, MARINA Vakaki¹, RODANTHI Sfakiotaki¹, ELENI Koutrouveli¹, EKATERINI Haritou¹, ANNA Chountala¹, GEORGIOS Daniil², CHRYSOULA Koumanidou¹

¹ Children's Hospital of Athens P&A Kyriakou, Athens, GREECE

² General Hospital of Thessaloniki G. Gennimatas, Thessaloniki, GREECE

Purpose:

We advocate the role of ultrasound as the unique imaging tool in the diagnosis and follow-up of the evolution of pyelonephritis in the pediatric population.

Materials and methods:

There is vast experience in our department in diagnosing and recording the evolution stages and the extent of pyelonephritis only by the use of ultrasound in pyelonephritis, given the non-availability of cross-sectional imaging in our hospital. The advancing technology of the ultrasound equipment and especially the high resolution of the linear probes, along with the small body size of the pediatric population, contribute to the acquirement of highly detailed images of the infected kidneys.

Results:

There is a gradual change of the renal ultrasonographic image during the different stages of pyelonephritis.

The images received on an emergency basis by the children mostly presenting with fever and positive Giordano sign demonstrate a swollen kidney with diffuse nephromegaly, along with increased echogenicity of the renal parenchyma. Thickening of the renal pelvic wall is almost always present. Furthermore, some linear effusions and hyperemia of perinephric space may be detected.

While the infection advances, some hypoechoic foci appear, resulting in an evolving heterogeneity of the renal parenchyma. These lesions have decreased or even absent blood flow. During the next step of the disease, these lesions enlarge and extend towards the kidney's capsule, obtaining a triangle or band-like shape. If the antibiotic therapy is not appropriate for the pathogenic microorganism, the lesions advance and they become wedge-shaped, while they begin to liquefy. Thus, they result in renal abscess formation, with anechoic content and evident capsule, which separate them from the renal parenchyma. During all these stages, the corticomedullary differentiation may be lost or not.

When appropriate antibiotic therapy is applied, all these findings are gradually disappeared, while they may leave some scars on the renal parenchyma.

Conclusions:

Renal ultrasonography provides high-quality images in children, giving the necessary information to the point of being able to evaluate the response to treatment and guide the clinicians' decisions without the use of cross-sectional imaging.

Poster: EDU-067

MULTISYSTEM IMAGING FINDINGS OF HAEMOLYTIC URAEMIC SYNDROME IN CHILDREN: A PICTORIAL REVIEW

CAOILFHIONN Ní Leidhin¹, CAOIMHE Costigan², DERMOT Wildes², AILBHE McDermott¹, ATIF Awan², STEPHANIE Ryan¹, EILIS Twomey¹

¹ Department of Radiology, Children's Health Ireland at Temple Street, Dublin 2, IRELAND

² Department of Nephrology, Children's Health Ireland at Temple Street, Dublin 2, IRELAND

Purpose:

This exhibit, through a pictorial review of ultrasound (US), radiographic, computed tomography (CT) and magnetic resonance (MR) imaging, illustrates the multisystem imaging findings of haemolytic uraemic syndrome (HUS) in children.

Materials and Methods:

Our institution, Children's Health Ireland at Temple Street is the national paediatric haemodialysis and renal transplant unit. Between May 2005 and August 2018, 240 children with HUS were managed in our institution. Of those, 204 (85%) had Shiga toxin-producing *Escherichia coli* (STEC)-HUS. We retrospectively reviewed the imaging studies of these children.

Results:

Of 204 children with STEC-HUS managed in our institution during the above-outlined time period, 114 (55.9%) were girls. Mean age at admission was 4 years 4 months (± 3 years 5 months, min. 1 month, max. 15 years 5 months).

The most common imaging study performed was renal US, followed by chest radiography. The most common abnormalities on renal US were, in descending order: increased renal cortical echogenicity, increased corticomedullary differentiation and swollen/enlarged kidneys. The most common abdominal US abnormalities were ascites followed by bowel wall thickening/colitis/proctitis. The most common pathologies on chest radiograph were atelectasis/consolidation followed by findings suggesting fluid overload, i.e. increased interstitial markings, pulmonary oedema, pleural effusions and/or cardiomegaly. T2/FLAIR signal abnormality and reduced diffusivity were the most common intracranial MRI pathologies. There were two cases of catheter-associated thrombosis and one case of catheter-associated fungal septicaemia in patients undergoing plasma exchange.

Conclusion:

This exhibit, through a comprehensive pictorial review, illustrates the typical and atypical multisystem imaging findings of HUS in children. Representative images include increased renal cortical echogenicity and colitis on renal/abdominal US and acutely reduced white matter diffusivity on MRI brain. Radiology plays an important role in the management of this cohort of patients.

Poster: EDU-068

ECHOGENIC KIDNEYS IN NEONATES AND INFANTS: A PICTORIAL REVIEW

AILBHE McDermott, EOGHAN E. Laffan, ANGELA T. Byrne
Children's Health Ireland at Crumlin, Dublin, IRELAND

Learning objectives:

- To become familiar with the sonographic appearance of normal kidneys in neonates and infants.
- To review causes for echogenic kidneys in neonates and infants.
- To develop a diagnostic approach to echogenic kidneys in this paediatric population.

Background and purpose

Echogenic kidneys have a diverse aetiology ranging from a transient finding in the neonatal period to genetic disorders. This exhibit illustrates a broad range of aetiologies for this imaging feature through a pictorial review, and encourages the participant to develop a diagnostic approach for such cases.

Content

The sonographic appearance of the normal kidney in neonates and infants will be presented followed by an electronic pictorial review of echogenic kidney cases. The participant will be encouraged to develop a diagnostic approach by considering renal size for age (normal, large, small) and whether the process involves the cortex, medulla or both. This electronic exhibit will include cases of Tamm-Horsfall proteins in the neonate, polycystic kidney disease including autosomal recessive polycystic kidney disease (ARPKD) and hepatocyte nuclear factor (HNF) 1 β -associated kidney disease, diffuse pyelonephritis, glycogen storage disorders, Jeune syndrome, Angiotensin Receptor Blockers in utero, nephrocalcinosis, renal vein thrombosis, obstructive dysplasia, Trisomy 13, congenital nephrotic syndrome, Beckwith Wiedemann syndrome and Zellweger syndrome. Each case includes an overview of the diagnosis with sonographic images and a description of the sonographic features.

Conclusion

Through a comprehensive pictorial review this exhibit will help further educate the participant in recognising the sonographic appearance of echogenic kidneys in neonates and infants, and encourage the development of a systematic diagnostic approach to such cases.

Poster: EDU-069

THE USE OF MULTI-MODALITY IMAGING IN THE DIAGNOSIS OF CONGENITAL URACHAL ANOMALIES

NINA Mansoor¹, ERICA Makin², DEAN Huang¹, SAIRA Haque¹
¹ Department of Radiology, Kings College Hospital, London, UNITED KINGDOM

² Department of Paediatric Surgery, Kings College Hospital, London, UNITED KINGDOM

Urachal anomalies occur when there is partial or complete failure of obliteration of the urachus, which is a tubular embryologic structure arising from the allantois and urogenital sinus. It normally obliterates at the end of gestation or within the first few days of birth. Incomplete obliteration leads to anomalies including patent urachus, umbilico-urachal sinus, urachal cyst and vesico-urachal diverticulum. Failure of involution is most often characterised by persistent communication between the urinary bladder and the umbilicus, which can often be detected neonatally with umbilical urine leakage, and diagnosis can be confirmed with ultrasound. Whilst these anomalies are uncommon in adults, with a reported incidence of 1/5000 and usually asymptomatic, patients with urachal anomalies can present later in life with non-specific abdominal signs and symptoms. With increased use of cross-sectional imaging, there has also been an increase in detection of these anomalies. Thus, familiarity and recognition of imaging findings related to urachal anomalies are important in order to be able to establish the correct diagnosis, guide further management and avoid late complications, such as, infection and malignant transformation of the urachal remnant. Here we present a series highlighting the imaging appearances of urachal anomalies using ultrasound, fluoroscopy, computed tomography and magnetic resonance imaging.

Poster: EDU-070

WILMS OR NOT WILMS? A PICTORIAL REVIEW OF PEDIATRIC RENAL MASSES

ROHAN Biswas, AMI Gokli
Staten Island University Hospital, Staten Island, USA

Summary: The differential for pediatric solid renal masses has been dominated by Wilms tumor, which is the most common pediatric renal mass, accounting for 85% of pediatric renal masses. There are, however, a number of other renal masses with distinct imaging and clinical findings such as age at presentation that the pediatric radiologist should be aware of. Knowledge of these masses can lead to a specific diagnosis and can guide presurgical evaluation and prognosis discussions. There is some overlap in imaging and features of various renal masses, so we emphasize that correlation of findings with patient history is of paramount importance.

This pictorial review will illustrate and describe the imaging appearances, clinical manifestations, and tumor growth patterns of the more common masses arising from the pediatric kidney, i.e. path-proven masses that include mesoblastic nephroma, Wilms tumor, nephroblastomatosis, renal cell carcinoma, multilocular cystic renal tumor, clear cell sarcoma, rhabdoid tumor, angiomyolipoma, renal medullary carcinoma, and lymphoma. In addition to emphasizing distinguishing features between these masses, the purpose of this review is to increase radiologist's awareness of the ultrasound and cross-sectional appearances of common masses afflicting the pediatric urinary bladder other than Wilms tumor, in order to determine proper clinical management.

Educational Objectives:

Describe the most common pediatric renal masses, including Wilms tumor.

Recognize the imaging features of these masses and how to distinguish them using various modalities.

Correlate radiologic and clinical findings in pediatric renal masses and their presentations.

Poster: EDU-071

IMAGING INGUINO-SCROTAL ANOMALIES IN NEONATES (AND INFANTS) IN THE LIGHT OF THE EMBRYOLOGICAL DEVELOPMENT

FRED Avni¹, MARIE Cassart²

¹ Delta Hospital - CHIREC, Brussels, BELGIUM

² Iris-Sud Hospitals, Brussels, BELGIUM

The testis develop within the genital crests under appropriate hormonal stimulating effects around the 6th week of the embryological development. The various male genital structures (deferent ducts, seminal vesicles, rete testis ...and their inter-connections) will develop around the second month.

The testicular migration towards the scrotum occurs in three phases. First, the testes migrate within the abdominal wall – posterior wall first, anterior thereafter – behind the peritoneum. This phase takes place between the 10th and the 14th week. The second phase, during the fetal period, brings the testes at the inguinal canal opening. During the third phase, the testes migrate down to the scrotum, their final location. In this position, the testes remain in connection with the retro-peritoneum. The third phase can be followed thanks to obstetrical US. The testes can be demonstrated within the scrotum as early as the 24th weeks. Around 30 weeks gestation, in over 90% of fetuses, the testes can be demonstrated within the scrotum.

Requests for imaging the scrotum (mainly using US) is very common. The range of anomalies is quite wide but fortunately with a low rate of serious conditions.

The purpose of the educational exhibit is to illustrate various classical and less classical conditions in the neonates and infants. The aim being to focus on anomalies related to abnormal migration as well as on the «consequences» of the retroperitoneal location of the testes.

The approach will be based upon the clinical conditions leading to the requests of imaging and its input in establishing the diagnosis or differential diagnosis.

In neonates (or infants), there are mainly two clinical conditions necessitating imaging: empty scrotum or on the contrary swollen scrotum (uni- or bilateral).

– The differential diagnosis of empty scrotum includes

- Cryptorchidism and ectopic testis
- Testicular regression syndrome
- Anomalies of gender differentiation

– The differential of swollen scrotum includes

- Extratesticular origin anomalies
 - Hydrocele
 - Hernia
 - Hematoma
 - Infectious collections
 - Meconium periorchitis
 - Tumors
- Testicular origin anomalies
 - Orchi-epidymitis
 - Testicular torsion
 - Tumors

The sonographic features leading to a proper diagnosis will be highlighted

The importance of the evaluation of the entire abdomen will be underlined and illustrated.

The potential role of MRI will be discussed and illustrated as well.

Poster: EDU-072

WAGR IS WACK!

REEMA Agarwal¹, JOSHUA Wemmers², RACHEL Berkovich²

¹ SSM Saint Louis University Hospital - Department of Diagnostic Radiology, St. Louis, USA

² SSM Cardinal Glennon Hospital - Department of Pediatric Radiology, St. Louis, USA

WAGR syndrome is an extremely rare genetic syndrome that affects approximately 1 in 500,000 to 1 in 1 million children. It is caused by multiple microdeletions on chromosome 11, which is where the ocular development gene and Wilm's tumor gene are housed. Fluorescent in situ hybridization (FISH) is utilized to confirm the microdeletion. WAGR received its name due to the four primary illnesses/symptoms associated with it: Wilm's tumor, Aniridia, Genitourinary anomalies, and Retardation. The purpose of this educational exhibit is to initiate and support a movement to change the name of this syndrome to better represent accepted 21st century terminology.

In the early 2010s, we saw a drastic change in terminology in the medical world. In October 2010, Congress passed the "Rosa Law", adopting the term "intellectual disability". On September 3, 2013, the federal government replaced the term "mental retardation" to "intellectual disability" in its Listing of Impairments rules under the Social Security Act utilized to evaluate claims involving mental disorders in children and adults. The purpose of this change was to prevent misunderstandings about mental disorders and due to the negative connotations association with the term retardation.

WAGR is a pediatric population predominant syndrome. This educational exhibit will discuss that the stigma associated with the word “retardation” causes significant bias for these patients, socially and emotionally individualizing them due to its negative connotation. We will discuss how changing the name to WAGI (“I” representing “intellectual disability”) or WAGD (“D” representing “disability”) would allow the patient population to live their lives with pride, preventing unwanted bias towards them. Importantly, while maintaining the same professional understanding of the syndrome, we would be emotionally and socially supporting these vulnerable children.

Poster: EDU-073

A PICTORIAL REVIEW OF INTERVENTIONAL RADIOLOGY PROCEDURES IN PAEDIATRIC HEPATOBILIARY DISEASES

NASIM Tahir¹, ZAHRA Ramzan², OLIVER Johnson², ELLEN Collingwood¹

¹ Leeds Children's Hospital, Leeds, UNITED KINGDOM

² Leeds School of Medicine, Leeds, UNITED KINGDOM

Purpose: The focus of this educational exhibit is to present a pictorial review of the application of interventional radiology (IR) in the management of paediatric liver disorders. Although IR is widely practised in adults, paediatric IR is a relatively new speciality and the extent to which it is used varies throughout the world. When properly run, the service can be life changing and life saving for young patients.

Materials: Leeds Children's Hospital (LCH) is a 296 bed hospital and provides the full range of paediatric IR procedures expected of a large children's hospital. It is also one of three national children's hepatobiliary centres and performs approximately 20-25 liver transplants per year. Given the increased usage of split liver grafts and transplants being performed in smaller patients, paediatric IR plays a pivotal role in improving graft survival. It is also important in the diagnosis and management of other hepatobiliary disorders.

Results: Interventions can broadly be divided into vascular and non-vascular. Vascular interventions include angiography, angioplasty, stenting, embolisation of tumours and portosystemic shunts, and formation of transjugular intrahepatic portosystemic shunts (TIPSS). Non-vascular interventions include biopsies of native liver which can be performed percutaneously or via a transjugular approach. We also perform biopsies of transplant livers and liver tumours. Other procedures include drainage of collections and biliary interventions including percutaneous transhepatic cholangiography (PTC) and endoscopic retrograde cholangiopancreatography (ERCP).

Conclusion: This exhibit will provide a comprehensive pictorial review of radiologically guided interventions performed in paediatric hepatobiliary diseases as listed above. We will also provide some basic practical advice on indications and how we perform these.

Poster: EDU-074

ABNORMALITIES OF THE LYMPHATIC SYSTEM IN CHILDREN: IMAGE-GUIDED INTERVENTIONS

GALI Shapira-Zaltsberg¹, MICHAEL Temple², GOVIND Chavan², CHRISTOPHER Lam², MARY-LOUISE Greer², JOAO Amaral²

¹ CHEO, Ottawa, CANADA

² SickKids, Toronto, CANADA

Congenital or acquired abnormalities of the lymphatics system may cause chylous leaks into the pleural, peritoneal, and/or pericardial spaces, plastic bronchitis, and protein-losing enteropathy. Dynamic contrast-enhanced Magnetic Resonance Lymphangiogram

(DCMRL) has become the modality of choice for imaging of the central conducting lymphatic in children. Procedures such as drainage and dietary measures aim to reduce lymph production and collection to obtain local control. Despite being successful in some patients, these interventions require long periods of time to be effective and in some cases provide only transient improvement. Surgical interventions such as thoracic duct (TD) ligation, and TD bypass procedures may be curative, however, they are more invasive and they carry risks inherent to surgical procedures.

The aim of this educational exhibit is to summarize and illustrate the range of minimally invasive image-guided interventions used for the treatment of these pathologies, which may provide long-term symptomatic relief while avoiding the need for surgery.

Interventions will include lymphangiography with lipiodol or lymphangiography with lymphatic glue embolization for the treatment of lymphatic leakage, transhepatic lymphatic glue embolization for the treatment of protein-losing enteropathy, and lymphatic embolization of abnormal pulmonary lymphatic flow for treatment of plastic bronchitis.

Poster: EDU-075

A PICTORIAL REVIEW OF PROCEDURES IN PAEDIATRIC INTERVENTIONAL URORADIOLOGY

ELLEN Collingwood, NASIM Tahir

Leeds Teaching Hospitals NHS Trust, Leeds, UNITED KINGDOM

Purpose: This pictorial review aims to outline the range of paediatric interventional urology procedures. Broadly divided into vascular and non-vascular interventions, these minimally invasive procedures can be used to manage many presentations of conditions of the renal tract. In recent years there has been a focus on development of new techniques and refinement of procedures adopted from adult practice. Paediatric IR is a fast developing field, and in Leeds it is playing an increasingly significant role in the management of renal tract conditions due to its safety and efficacy, and its potential to decrease length of hospital stay.

Materials: The paediatric nephrology team at Leeds Children's Hospital provide a comprehensive range of tertiary paediatric nephrology services including dialysis and transplantation for patients from across the region. The paediatric surgical department is one of the most sub-specialised units in the UK and operates a dedicated paediatric urology service. A multidisciplinary approach involving urologists, nephrologists and interventional radiologists is central to the provision of paediatric urology services.

Results: Vascular interventions include embolisation, renal artery angioplasty/stenting and vascular access. Non-vascular interventions include renal biopsy, tumour biopsy, nephrostomy, percutaneous nephrolithotomy (PCNL), ureteric stent insertion, percutaneous peritoneal dialysis and suprapubic catheter placement, and radiofrequency ablation of renal cancers.

Conclusion: This pictorial review of paediatric urological procedures will outline the minimally invasive treatment options for many conditions affecting the renal tract, and provide an overview of how these are performed in our specialist centre.

Poster: EDU-076

A RADIOLOGIST'S GUIDE TO LYMPHATIC ANOMALIES IN PEDIATRIC PATIENTS

ELIZABETH Snyder¹, ALEXANDRA Borst², ASHA Sarma¹

¹ Monroe Carell Jr. Children's Hospital at Vanderbilt, Department of Pediatric Radiology, Nashville, TN, USA

² Monroe Carell Jr. Children's Hospital at Vanderbilt, Department of Pediatric Hematology and Oncology, Nashville, TN, USA

Lymphatic anomalies comprise a spectrum of disorders ranging from common localized micro- and macrocystic lymphatic malformations (LMs) to more rare complex disorders such as lymphatic anomaly (GLA), Kaposiform lymphangiomatosis (KLA), central conducting lymphatic anomaly (CCLA), and Gorham-Stout syndrome. Imaging diagnosis of cystic LMs is generally straightforward, although can be more difficult in uncommon locations (e.g. intra-abdominal or bone). Complex lymphatic anomalies, particularly those with multi-organ involvement organs or diffuse disease, may be more challenging to diagnose. Although complex lymphatic anomalies are rare, imaging plays an important role in their diagnosis and evaluation, and pediatric radiologists may be the first clinicians to suggest these diagnoses. Given the high morbidity associated with complex lymphatic anomalies, it is crucial for pediatric radiologists to be aware of the spectrum of these malformations and their typical imaging findings.

The aims of this educational exhibit are to review embryology of the lymphatic system and illustrate the characteristic imaging findings of lymphatic anomalies in fetal and postnatal cases, discuss multimodality imaging techniques used for evaluation of pediatric lymphatic disorders (including MR lymphangiography), as well as to highlight pearls and pitfalls in making these diagnoses. The viewer will also be familiarized with basic management considerations. Conditions covered include: macrocystic and microcystic lymphatic malformations in both common and less common locations; and complex lymphatic anomalies (including GLA, KLA, CCLA, and Gorham-Stout disease).

Poster: EDU-077

IMAGING REVIEW AND DISEASE FOLLOW UP OF CHRONIC NONBACTERIAL OSTEOMYELITIS WITH WHOLE BODY MRI

SHAWN Sato ¹, ALEKSANDER Lenert ², SEDAT Kandemirli ¹, MIKHAEL Sebaaly ¹, POLLY Ferguson ³

¹ University of Iowa Stead Family Children's Hospital, Division of Pediatric Radiology, Iowa City, USA

² University of Iowa Department of Internal Medicine, Iowa City, USA

³ University of Iowa Stead Family Children's Hospital, Division of Rheumatology, Allergy and Immunology, Iowa City, USA

Chronic nonbacterial osteomyelitis (CNO) or chronic recurrent multifocal osteomyelitis (CRMO) is a rare auto-inflammatory bone condition that can be diagnostically challenging due to the lack of specific clinical, imaging and laboratory findings. Timely diagnosis and appropriate treatment requires a high index of suspicion and a close working relationship between clinicians and radiologists. Whole body MRI is an integral tool for diagnosing and monitoring patients with CNO. In this presentation, we will review the typical imaging appearances of CNO/CRMO in various parts of the body using WBMRI imaging, disease course using longitudinal imaging, and suggest a fast whole body MRI protocol for screening and monitoring patients with CRMO.

Poster: EDU-078

INFLAMMATORY CONDITIONS OF THE PEDIATRIC HAND AND NON-INFLAMMATORY MIMICS

LEANNE Royle, THOMAS Mendes da Costa, DANIEL Rosenbaum
BC Childrens Hospital, Vancouver, CANADA

Purpose:

Hand complaints in children are common and can assume an outsized role in the perception and presentation of disease due to functional impairment, visual conspicuity, and susceptibility to structural damage. In the absence of trauma an underlying inflammatory condition may be suspected, however rheumatologic referral is frequently delayed due to assumptions of a mechanical, infectious, or neoplastic etiology. Alternatively, initial rheumatologic evaluation may be obtained for many non-inflammatory complaints. In this educational exhibit we aim to review the imaging appearances of common and uncommon inflammatory conditions affecting the pediatric hand as well as a variety of non-inflammatory mimics.

Materials/Methods:

The goals of this educational exhibit will be to:

- Provide a brief overview of technique in pediatric hand imaging.
- Review inflammatory conditions affecting the pediatric hand, including infectious, granulomatous, and drug-induced arthritis, as well as systemic connective tissue disorders, using juvenile idiopathic arthritis as a basis for comparison.

- Discuss a variety of non-inflammatory differential considerations, including congenital, vascular, neoplastic, and dysplastic conditions, highlighting areas of potential clinical and radiological overlap with inflammation.

Results:

After reviewing the exhibit, the reader will be able to:

- Expand the differential for inflammatory hand complaints beyond juvenile idiopathic arthritis.
- Differentiate inflammatory conditions from potential mimics based on the presence of clinical red flags and atypical or aggressive imaging features.

Conclusion:

A wide range of disorders can manifest as hand complaints in children. Recognition of overlapping and distinguishing features among inflammatory and non-inflammatory conditions should facilitate expeditious diagnosis and appropriate clinical referral.

Poster: EDU-079

SPECTRUM OF NORMAL FINDINGS, ANATOMIC VARIANTS AND PATHOLOGIC FINDINGS OF THE PAEDIATRIC STERNUM: A PICTORIAL REVIEW

ANDREAS Panayiotou, MARCELA De La Hoz Polo, SAIRA Haque
King's College Hospital, London, UNITED KINGDOM

Purpose:

Sternal abnormalities are an uncommon presentation in the paediatric population and can be caused by a variety of benign and malignant entities, as well as mimics from normal variants of the chest wall. Although there is overlap with processes affecting adults, many are unique to the paediatric population. Following clinical examination, radiography is usually the first type of imaging utilised, however, it has limited value in characterising many sternal processes therefore often patients will proceed to ultrasound or other cross-sectional imaging (CT/MRI) for further characterisation. An understanding of the normal anatomy is important but this can be challenging due to the varied appearances of age-related changes of the sternum.

Materials and Methods:

A pictorial review of normal findings, anatomical variants and pathology of the paediatric sternum. Emphasis will also be made on the normal anatomic appearance and age-related changes of the sternum on cross-sectional imaging.

Results:

A variety of abnormalities are described affecting the sternum including chest wall deformities, congenital vascular malformation, infarction, infection, tumours and trauma.

Conclusion:

A multidisciplinary and systematic approach to the assessment of the child including clinical history, physical examination and imaging findings is important to help the radiologist arrive at a differential diagnosis and potentially make a specific diagnosis, avoiding unnecessary invasive procedures such as biopsy or even surgery.

Poster: EDU-080

PRACTICAL APPROACH TO MRI OF THE TEMPOROMANDIBULAR JOINT IN JUVENILE IDIOPATHIC ARTHRITIS

MARIA NAVALLAS¹, EMILIO J INAREJOS², DAVID COCA¹, MARY-LOUISE GREER³, OSCAR M NAVARRO³

¹ Hospital 12 de Octubre, Madrid, SPAIN

² Hospital Sant Joan de Déu, Barcelona, SPAIN

³ Hospital for Sick Children, Toronto, CANADA

Educational objectives:

1. To discuss what is juvenile idiopathic arthritis and why the temporomandibular joint (TMJ) is so important in this disease
2. To review the role of different imaging modalities and the appropriate MRI technique for imaging the pediatric TMJ
3. To illustrate the imaging findings and score of TMJ arthritis

Summary of the presentation:

1. Juvenile idiopathic arthritis: definition, classification, etiology, importance of the TMJ
 2. Imaging tools: usefulness and pros and cons of different imaging techniques
 3. MRI: technique, protocol
 4. TMJ: anatomy, age-related changes, normal findings
 5. Manifestations of TMJ arthritis:
 - a. Acute inflammatory changes: joint effusion, bone marrow edema, bone marrow enhancement, synovial thickening, joint enhancement
 - b. Chronic changes: osseous deformity, condylar flattening, mandibular shortening, erosions, disc abnormalities, pannus, secondary osteoarthritis
 6. MRI scoring system for TMJ evaluation in juvenile idiopathic arthritis
- Conclusions:**

- Many patients with juvenile idiopathic arthritis have TMJ involvement at diagnosis
- Most of them are asymptomatic and have normal physical examination
- Increased risk of early damage of the mandibular growth center with long-term sequelae
- Growth disturbances of the mandible can be prevented or become less severe if juvenile idiopathic arthritis is treated well and promptly
- MRI is the technique of choice for diagnosis and management
- Images should be obtained soon after intravenous contrast administration
- Acute inflammatory findings: joint effusion, bone marrow edema and enhancement, and synovial thickening and enhancement
- Chronic changes: morphologic changes, bone erosions, disc abnormalities, pannus and secondary osteoarthritis

Poster: EDU-081

CHRONIC OSTEOMYELITIS OF LONG BONES: IMAGING PEARLS AND PITFALLS IN PEDIATRICS

LENA Naffaa¹, RIDA Salman², MARTY McGraw¹

¹ Nemours Children's hospital, Orlando, USA

² Texas Children's Hospital, Houston, USA

Chronic bacterial osteomyelitis is characterized by progressive inflammatory bone destruction and apposition of new bone most often caused by pyogenic bacteria. Clinical findings are non-specific, and serum inflammatory markers can be normal. Prompt diagnosis and treatment are essential. Left untreated, chronic infection can lead to high morbidity and mortality. Imaging's major role is to suggest the correct diagnosis, exclude other diagnoses that can mimic osteomyelitis, document extent of disease, and guide interventions such as image-guided biopsy or surgical debridement. Several conditions can mimic chronic osteomyelitis clinically and radiographically. The main differential diagnoses include an oncologic process, chronic nonbacterial or chronic recurrent multifocal osteomyelitis, bone infarct in sickle cell disease, osteoid osteoma, and stress reaction/fracture. The oncologic process to consider includes metastatic neuroblastoma and Langerhans cell histiocytosis in a child younger than five years or leukemia, Ewing sarcoma, and osteosarcoma in the older age group. However, these lesions can typically be excluded based on radiographs and magnetic resonance imaging findings. Therefore, radiologist familiarity with imaging findings and mimickers is essential. In this educational exhibit, we describe the imaging pearls and pitfalls of chronic bacterial osteomyelitis with discussion of the most common differential diagnoses.

Poster: EDU-082

NON-ACCIDENTAL TRAUMA AND ITS MIMICKERS: A PICTORAL EDUCATIONAL REVIEW

HANNAH Myers, AMI Gokli

Staten Island University Hospital, Staten Island, USA

Accurate diagnosis of non-accidental trauma (NAT) is an essential part of practicing pediatric radiology as it is a leading cause of mortality in young children. The Child Maltreatment Report from the U.S. Department of Health and Human Services estimates 1,770 children died of abuse and neglect in 2018. Radiologists are often the first clinical staff to detect physical findings of NAT and swift communication can prevent further injury or death. Unfortunately, due to conflicting literature, distinguishing fractures related to NAT from those caused by other medical conditions is a controversial topic. Despite this, pediatric radiologists are responsible for not only recognizing NAT but differentiating it from other pathologies. The purpose of this educational review is to describe and characterize specific imaging findings of NAT; review the differential diagnoses that must be considered; and discuss discrete differences between NAT and other possible diagnoses using a case-based comparison format. Multiple case examples will be used to depict the specific and sometimes subtle differences that can aid in this differentiation process. Case examples include rickets, metaphyseal dysplasia, osteogenesis imperfecta, pyknodysostosis, birth trauma, Menkes Disease, infantile cortical hyperostosis, and osteomyelitis.

The consequences of missing a case of NAT or unwarranted accusations against innocent parents or guardians are tremendous and should not be taken lightly. Full knowledge of NAT imaging findings and diseases that can present similarly is essential to provide adequate care as a pediatric radiologist.

Poster: EDU-083

A PICTORIAL REVIEW OF RADIOLOGICAL FINDINGS IN SUSPECTED PHYSICAL ABUSE IN CHILDREN

LAURA Marsland¹, SREENA Das², SAIRA Haque¹

¹ Department of Radiology, King's College Hospital, London, UNITED KINGDOM

² Department of Paediatrics, King's College Hospital, London, UNITED KINGDOM

Physical abuse is an important cause of morbidity and mortality in children. Incidence has increased during the COVID-19 pandemic, likely as a result of social isolation and financial uncertainty.

In the UK when physical abuse is suspected imaging is performed in accordance with guidelines. For children under two this includes a skeletal survey. Skeletal survey is performed on a case-by-case basis for older children. Specialist assessment of imaging requires comprehensive understanding of typical patterns of skeletal injury in physical abuse.

This retrospective review describes ten cases of suspected physical abuse in children occurring over a 5-year period. The objective is to outline typical skeletal abnormalities and patterns of injury that occur as a result of physical abuse. Cases include a spectrum of skeletal findings, ranging from complex, poly-traumatic injury to subtle, secondary signs of abuse. Imaging findings from initial and follow-up skeletal surveys are described and patterns of injury identified, correlated with clinical history. Follow-up and outcome is discussed.

Children were aged between six weeks and two years. All underwent imaging for suspected physical abuse prompted by various presenting circumstances. Fractures were identified on initial imaging for nine children. Five children had multiple fractures, of whom four had fractures of varying ages, suggesting repeated physical abuse. One child had an isolated skull fracture and two had isolated long bone fractures. For one child, skeletal survey showed no fracture but evidence of diffuse osteopenia, indicative of neglect. Lower limb fractures were most common (femur (5) and tibia/fibula (4)), but fractures sites included the skull (3), spine (1), humerus (2), radius/ulna (3) and ribs/clavicle (3). Follow-up skeletal survey identified previously unseen fractures in two cases.

Outcome was documented for nine children. Five were returned to the custody of their family with a comprehensive Child Protection Plan. Two were placed into foster care. In two cases, injuries were so severe as to result in death.

There are recognised clinical presentations and patterns of skeletal injury to support the diagnosis of physical abuse. Follow-up imaging is important, particularly when findings are inconclusive or there is a strong suspicion of occult injury.

This case series highlights the complexity and profound consequences of physical abuse in children, which extend beyond the physical.

Poster: EDU-084

IMAGING DURING THERAPY IN LATE PRESENTATION OF DEVELOPMENTAL DYSPLASIA OF THE HIP (DDH)

CRISTINA Hernández, IGNASI Barber
Hospital Sant Joan de Deu, Barcelona, SPAIN

Background: Magnetic resonance imaging (MRI) of the hips is being increasingly used to confirm hip reduction after surgery and spica-cast placement for developmental dysplasia of the hip (DDH). Anterior approach hip ultrasound (US) has also been used. Arthrography, plain films and CT should not be considered given the radiation burden.

Objective:

1. Pictorial and data review of a single institution experience using US and MRI in children undergoing closed hip reduction and spica-cast treatment.

2. Describe the utility of intraoperative MRI in directing the need for re-intervention.

Materials and methods: Retrospective review of all patients with late presentation of developmental dysplasia of the hip that were imaged during treatment in the last 10 years (2010–2020) using different imaging techniques (US, CT and MRI). In the last two years, we have included immediate intraoperative hip MRI. Data reviewed included image

technique, age, type of intervention performed, image findings, the need for re-intervention and the interval between interventions.

Results and discussion: Twenty-six patients were included. All patients were under one year old by the time of the first surgical intervention and were imaged using different imaging techniques (US, CT and MR). Eight patients were evaluated with contrast enhanced MRI. Seven patients were evaluated with the new intraoperative MRI protocol, and 5 of them (71%) needed re-intervention, with a success rate of the second surgery of 80%; just one of the patients required a third surgery.

Conclusion: Complete image evaluation of late presentation DDH during treatment is challenging. Intraoperative MR imaging is useful demonstrating results of surgical treatment. In addition, it has made possible to eliminate arthrography and CT reducing the radiation burden.

Poster: EDU-085

CREATION OF A NOVEL PEDIATRIC SPORTS MEDICINE IMAGING MODULE

HOLLY Harper ¹, GRANT MacKinnon ¹, YU Luo ^{1,2}, SUDHA Singh ^{1,2}, MELISSA Hilmes ^{1,2}

¹ Vanderbilt University School of Medicine, Nashville, USA

² Vanderbilt University Medical Center, Department of Radiology, Nashville, USA

Background: Currently, there is a paucity of dedicated teaching for musculoskeletal pathologies and imaging in the current Vanderbilt Medical School curriculum.

Purpose: Our purpose is to describe the creation of a novel case-based teaching module that brings together five common pediatric sports medicine cases. The cases fulfill a requirement for a portion of the pediatric radiology elective and are a useful resource in the remote learning setting.

Learning objectives:

- Recognize how common pediatric sports medicine conditions present based on history and physical exam

- Appreciate imaging modality selection in a diagnostic work-up

- Identify key structures on normal and abnormal radiographs, CT and MR examinations

Description: Learners on the pediatric radiology elective are asked to identify 50 common imaging findings during their elective as part of the scavenger hunt tool. In the remote setting, it became cumbersome to adequately cover some of the items without the ability to have in-person teaching. We identified five common musculoskeletal and pediatric sports medicine cases and created a cohesive remote, case-based teaching module. The module described the patients clinical background and presentation, physical exam and imaging findings. The scavenger hunt items included: discoid meniscus, tarsal coalition, osteochondral defects, and lipohemarthrosis. Entities included the above scavenger hunt items plus patellar fracture and dislocation and ACL tear. Anatomy of knee and foot was emphasized, as well as anatomy of the immature skeleton, like epiphysis, physis, and metaphysis. Additional questions to emphasize learning points were embedded within the module.

Outcomes: The newly created module was well received by learners on the elective. The module added variety into the curricular materials already in place.

Conclusion: Students successfully created an enduring curricular element that helps to spotlight common pediatric musculoskeletal conditions and sports medicine injuries that may not be addressed in other parts of medical school or pediatric residency. This module can be used in other settings like sports medicine teaching.

Poster: EDU-086

CONGENITAL TALIPES EQUINOVARUS: INITIAL AND LONG-TERM RADIOLOGICAL ASSESSMENT

ANA Forjaco, LÚCIA Fernandes, PEDRO Alves
Centro Hospitalar Universitário Lisboa Central, Lisbon, PORTUGAL

Purpose: Description of the techniques used in the radiological assessment of congenital talipes equinovarus, the morphological alterations found in the initial assessment of this deformity and the main findings in its long-term post-therapeutic assessment.

Materials and methods: Bibliographical research, review, and selection of the most relevant articles about radiological assessment of the deformity in talipes equinovarus. Selection of original sample images of radiological studies of patients with talipes equinovarus treated in a pediatric university hospital.

Results: The deformity in talipes equinovarus (also known as clubfoot) is the most common musculoskeletal congenital defect and affects up to 5% of live births. It courses with several morphological alterations related to muscle contractures, including an abnormally high plantar longitudinal arch (pes cavus), an unnatural adduction and inversion of the forefoot (pes varus) and an inability to dorsiflex the ankle (pes equinus). It is associated with countless skeletal dysplasias and syndromic conditions. The severity of this deformity is highly variable, from an almost normal foot to an extremely complex clubfoot. The radiological assessment starts with dorsoplantar and lateral radiographs of the foot in a standing position, if possible, to characterize the deformities and exclude associated bony anomalies. Computed tomography may be essential for further characterization. The main therapeutic options are nonoperative, including the Ponseti method, with serial manipulation and casting. The presence of associated lesions and the failure of conservative treatment are indications for surgical therapy, with tendon lengthening, osteotomies and soft tissues release. The post-therapeutic imaging assessment aims to evaluate the outcomes and exclude complications from these procedures. Common post-therapeutic complications include over- or under-correction, loss of stability of the tibiotarsal joint and talus osteonecrosis, which must be actively searched during imaging evaluation.

Conclusions: The radiological assessment of deformities in talipes equinovarus plays a complementary role in the initial characterisation and long-term assessment of this entity. The radiologist must know the alterations belonging to this deformity, the frequently associated anomalies and the characteristics of the main therapeutic interventions used in its correction.

Poster: EDU-087

CINEMATIC RENDERING IN PAEDIATRIC MUSCULOSKELETAL IMAGING

AISLING Fagan¹, OWEN Arthurs¹, NEIL Sebire², SUSAN Shelmerdine¹

¹ Great Ormond Street Hospital- Department of Radiology, London, UNITED KINGDOM

² Great Ormond Street Hospital- Department of Pathology, London, UNITED KINGDOM

Purpose: Cinematic rendering (CR) is a new technique in the post-processing of imaging studies. It allows for a more photorealistic reconstruction over volume rendering (VR) by using a complex light modelling algorithm, by including information from multiple light paths and predicted photon scattering patterns. Recent publications have demonstrated improved 'realism' and 'expressiveness' of CR over VR techniques in adult imaging, and CR has also been demonstrated to improve visualisation of musculoskeletal and vascular anatomy compared with conventional CT viewing. CR has also been shown to decrease time to comprehension of patient anatomy by surgeons. There is, however, a paucity of paediatric-specific imaging examples.

In this educational exhibit, we will provide an overview of the techniques used in CR and provide a brief review of the literature in this field. We will present a variety of congenital and acquired musculoskeletal pathologies in children, comparing both VR and CR reconstructions, and we will illustrate the cases in which CR reconstructions have been the most useful (e.g. multiple exostoses, Sprengel deformity). We will finally suggest the ways in which CR may be helpful in the future of paediatric musculoskeletal imaging— such as reaching a complex diagnosis, planning of surgery, and obtaining patient consent.

Poster: EDU-088

ULTRASOUND OF PEDIATRIC LUMPS AND BUMPS

RICHARD Bellah^{1,3}, JUAN S. Calle Toro¹, MOHAMED Elsingery¹, JAMES Treat^{2,3}

¹ Departments of Radiology, Childrens Hospital of Philadelphia, Philadelphia, USA

² Departments of Dermatology, Childrens Hospital of Philadelphia, Philadelphia, USA

³ Perelman School of Medicine, University of Pennsylvania, Philadelphia, USA

One of the most common referrals for ultrasound in pediatrics is for evaluation of superficial 'lumps and bumps' which can occur anywhere along the body. High-resolution US is a relatively simple, nonthreatening and noninvasive imaging technique, particularly well-suited for such evaluations, not only for obvious reasons of no radiation, but because the high-resolution US beam (linear high-resolution, with or without stand-off pads or water bath, with or without panoramic views) can more clearly evaluate cutaneous and subcutaneous lesions which may be difficult to fully characterize by other more expensive cross-sectional imaging studies.

The purpose of this interactive exhibit is to illustrate the US grayscale and Doppler appearances, and briefly describe relevant imaging/clinical features of several common and uncommon 'lumps and bumps' (~ 13 conditions altogether) that may be referred to the pediatric ultrasound division. Correlative plain film and/or cross-sectional imaging is provided in select cases.

By illustrating their characteristic, and sometimes variable US appearances, the examiner can hopefully provide '1 stop shopping' to the parents and referring clinician/s in the evaluation of such lesions.

Poster: EDU-089

MR IMAGING OF NON-TRAUMATIC NON-NEOPLASTIC PATHOLOGIES OF THE PEDIATRIC KNEE JOINT – A PICTORIAL REVIEW

MUDIT Arora, NARENDRA Shet, RAMON Sanchez
Children's National Hospital, Washington,DC, USA

Purpose: The knee joint is a common site of pain in the pediatric patient. While many patients present due to traumatic etiologies (in particular, sports injuries) as well as neoplastic etiologies, there is a wide variety of non-traumatic non-neoplastic causes for knee discomfort in children, including congenital/developmental, metabolic, nutritional, and infectious/inflammatory origins. Conventional radiographs play an important role and are the first line of imaging. Magnetic resonance imaging (MRI), however, is the imaging modality of choice when detailed evaluation of bone marrow, cartilage, growth plate (physeal) and soft tissue is required. MR evaluation in pediatric population is particularly challenging due to changes related to ossification, growth plate and marrow transformation involving the immature skeleton. In this review, we present a

variety of non-traumatic non-neoplastic causes of pediatric knee pathology.

Material and methods: A retrospective review of the institutional picture archiving and communication system (PACS) was performed using a departmental software solution (Montage; Nuance, Burlington, MA, USA). Cases from past 5 years were reviewed for inclusion in this educational review.

Results: In this pictorial review, we illustrate MRI findings of congenital/developmental, metabolic, nutritional, infective and inflammatory pathologies of the knee joint in children. Cases have been further categorized into limb deficiencies (tibial and fibular hemimelia), physal and epiphysal abnormalities (Blount's Disease, Trevor's disease and proximal femoral focal deficiency), meniscal and ligamentous abnormalities (discoid meniscus and congenital absence of anterior cruciate ligament), patellar developmental abnormalities (bipartite patella, patellar instability and recurrent dislocations), metabolic/nutritional disorders (Rickets, scurvy, and Gaucher's disease) and infectious/inflammatory pathologies (juvenile rheumatoid arthritis, hemophilic arthropathy, septic arthritis, osteomyelitis, and Brodie's abscess).

Conclusion: While traumatic and neoplastic etiologies for pediatric knee pain are frequently discussed, other causes should not be discounted, and MRI often demonstrates characteristic findings of these entities. This review highlights these pertinent considerations in order to provide framework of additional considerations for the interpreting radiologist.

Poster: EDU-090

ARTERIAL SPIN LABELLING (ASL) MRI IN PEDIATRIC HEAD AND NECK LESIONS WITH PATHOLOGICAL CORRELATION WHEN AVAILABLE

APARNA DEVI Yepuri, MATHEW Whitehead, JOSE Molto
Childrens National Medical Center, Washington, D.C., USA

Introduction:

Conventional MRI is the mainstay in diagnosing head and neck lesions with known various classic imaging features for tumors, vascular malformations, lymphatic malformations, inflammatory pathologies, cyst and abscess. In our institution we added ASL sequence to the routine MRI technique to assess the lesions further. As ASL is a noncontrast technique with short duration of scanning, which can determine the vascularity of the lesion without contrast administration.

Materials and Method:

Retrospectively we reviewed all radiology reports in Montage, a radiology data mining system of our institution. We collected around 50 cases with head neck lesions with various diagnosis including lymphatic malformations, venolymphatic malformations, venous malformations, Arteriovenous malformations (AVMs), inflammatory pathologies like acute sinusitis/cellulitis or abscess, cystic lesions and pediatric head and neck tumors including neuroblastoma, Juvenile nasopharyngeal angiofibroma, Juvenile trabecular ossifying fibroma and Ewing sarcoma etc.

Results:

We reviewed the cases in PACS to determine which lesions are hot and which lesions are cold on ASL. We also reviewed the charts to look for pathology and included when available. We also included required literature for each diagnosis for educational purpose.

Conclusion:

ASL MR imaging technique shows specific signal intensity in various head and neck lesions and can aid in diagnosis in addition to other MR sequences.

Poster: EDU-091

ON-CALL PRIMER FOR RESIDENTS: PEDIATRIC NEURORADIOLOGY

LILY Wolf¹, NUCHARIN Supakul²

¹ Indiana University School of Medicine, Indianapolis, USA

² Department of Radiology and Imaging Sciences, Indiana University School of Medicine, Indianapolis, USA

Teaching Points:

- List normal and variant sutures in pediatric skull that could be confused with fractures
- Discuss basic principle and characteristic imaging of intracranial hemorrhage and cerebral swelling
- Understand and be able to suggest a proper imaging technique and imaging workup algorithm during calls
- Recognize the characteristic imaging findings for the crucial diagnoses during calls including Non-Accidental Trauma (NAT), Benign Enlargement of Subarachnoid Spaces of Infancy (BESSI), Hypoxic Ischemic Encephalopathy (HIE)

Content Organization:

1. Introduction
2. List normal and variant sutures in pediatric skull
3. Discuss differences between sutures and fractures
4. Discuss basic principle and characteristic imaging of intracranial hemorrhage and cerebral swelling
5. Understand and be able to suggest a proper imaging technique and imaging workup algorithm during calls
6. Recognize characteristic imaging findings of:
 - Non-Accidental Trauma (NAT)
 - Benign Enlargement of Subarachnoid Spaces of Infancy (BESSI)
 - Hypoxic ischemic Encephalopathy (HIE)
7. Challenging cases
8. Summary

Conclusion:

1. Pediatric neuroimaging can be a challenge to radiology residents during call due to infrequently encountered in many institutions.
2. Understanding the pediatric brain anatomy, normal variation and pathology in preparation for taking call is important.
3. It is important to recognize crucial diagnoses, appropriate imaging workup, characteristic imaging findings to distinguish between normal anatomy, variation and life-threatening diagnosis.
4. This module helps to prepare radiology residents for call at institutions with pediatric patient populations and to close a radiology residency knowledge gap in pediatric emergency neuroimaging.

Poster: EDU-092

A MULTIMODALITY REVIEW OF NONTRAUMATIC PEDIATRIC INTRACEREBRAL HEMORRHAGE

GREGORY Vorona¹, MADHURA Chitnavis¹, LANDON Funicello¹, EWA Way¹, KATHARYN Jones¹, ERICA Poletto², JACQUELINE Urbine¹

¹ The Children's Hospital of Richmond at Virginia Commonwealth University, Richmond, USA

² St. Christopher's Hospital for Children, Philadelphia, USA

Purpose:

An otherwise healthy pediatric patient that presents with nontraumatic intracerebral hemorrhage can create significant diagnostic challenges if an underlying hemostatic disorder or structural brain lesion is not identified at the time of presentation. These challenges can delay the appropriate initial workup, treatment, and long-term care planning for this patient population. The purpose of our electronic educational exhibit is to conduct a brief review of the most common nontraumatic pediatric hemorrhagic brain lesions with illustrative

cases including arteriovenous malformations, cavernous malformations, aneurysms, and tumors. We will also briefly review some of the major genetic causes of pediatric intracerebral hemorrhage. Finally, we will offer a proposed succinct framework for the imaging workup of pediatric patients presenting with nontraumatic intracerebral hemorrhage.

Methods & Materials:

A retrospective analysis of multimodality imaging in pediatric patients with nontraumatic intracerebral hemorrhage, who presented to a tertiary care children's hospital since 2010, is performed. Multimodality imaging is correlated with pathology and surgical treatment as well as the patient's clinical course.

Results:

Review of the variety of imaging presentations of nontraumatic pediatric intracerebral hemorrhage is provided, utilizing CT and MRI.

Conclusions:

Although the majority of cases of nontraumatic pediatric intracerebral hemorrhage are caused by vascular malformations, it is imperative that the radiologist interpreting studies of these patients be aware of the breadth of potential causative etiologies.

Poster: EDU-093

IMAGING THE "PECULIAR" HEAD SHAPE

LOUKIA Tzarouchi, EVANGELIA Manopoulou, CHRISTINA Meleti, GEORGIOS Manganas, PANAGIOTIS Tagkalakis, SPYROS Yarmenitis, GEORGIA Papaioannou

Department of Pediatric Radiology, Mitera Children's Hospital, Athens, GREECE

Background: An abnormal skull shape during infancy may be the result of positional skull deformities, craniosynostosis or more complex craniofacial disorders.

Objectives: To review the normal appearance of the skull during the neonatal period and infancy and to discuss the optimal imaging methods for depicting abnormalities. Imaging approach in craniosynostosis includes ultrasonography, magnetic resonance imaging and computed tomography with 3-dimensional reconstruction and it is essential for the precise diagnosis, surgical planning, post-surgical evaluation and demonstration of coexisting anomalies in cases of complex cases. Typical radiologic findings of craniosynostosis (primary and secondary) are presented.

Poster: EDU-094

DEVELOPMENT AND MYELINATION OF THE FETAL AND POSTNATAL BRAIN, AN INTERACTIVE PICTORIAL REVIEW OF COMBINED MRI, ANATOMICAL AND HISTOPATHOLOGICAL ANALYSIS

RAMONA-ALEXANDRA Todea¹, FRIEDERIKE Prüfer², MARIOS-NIKOS Psychogios¹

¹ Department of Neuroradiology, Clinic of Radiology & Nuclear Medicine, University Hospital, Basel, SWITZERLAND

² Department of Pediatric Radiology, University Children's Hospital of Basel (UKBB), Basel, SWITZERLAND

Summary of the presentation: interactive, visual-oriented presentation of normal brain development and myelination in a chronological sequence from approximately 22GW (gestational weeks) until the postnatal age of 3 using MRI, anatomical and histopathological slices.

List of the educational objectives

After completing this presentation, participants will be able to:

1. Employ adapted MRI protocol to the stage of prenatal and postnatal development of the brain
2. Perform biometric measurements and to assess normal myelination and gyration patterns using reference slices for each developmental stage
3. Visual analyze and compare histopathological and anatomic slices at the same level and chronological stage of development

Purpose: To provide a fast tool for assessing the fetal and newborn brain development and myelination in a visually interactive PowerPoint presentation that can be easily retrieved on a condensed hospital day.

Material and methods:

We used prenatal and postnatal MRIs acquired in our institution during the last 3 years at 3T MAGNETOM Skyra Siemens scanner. The study protocol consisted of ultrafast T2w HASTE and T1w VIBE Cairpirinha sequences over the fetal brain and postnatal age-adapted T1w and T2w sequences.

We analyzed normal brain development from approximately 22 gestational weeks until birth and postnatal scans until the age of 3.

We provided reference slices and normal chronologic biometric measurements and patterns of gyration and myelination.

Additionally, we employed histopathologic and anatomic slices at the same level.

Results: chronologic presentation of brain development using combined MRI, histopathological and anatomical slices in the fetal and postnatal period until the age of 3.

Conclusions: Condensed and interactive information is of great help on charged days when the workload is mixed with the training of fellows and residents.

Histopathological and anatomical slices at the same level as MRI scans enhance the changes and eventually may help to track more details in the brain morphology change during development and myelination.

Poster: EDU-095

LOOKING INTO THE HARLEQUIN EYES: A PICTORIAL REVIEW OF CRANIOSYNOSTOSIS AND ITS MANAGEMENT

KENDALL Stevens, ROBYN Murphy
Atlantic Health System, Morristown, USA

Purpose: The focus of this educational exhibit is to present a pictorial review of the imaging of various types of craniosynostosis, their complications, management, and follow-up. A brief review of associated syndromes including primary and secondary etiologies with characteristic imaging findings will be included.

Methods: Craniosynostosis is a common pediatric condition wherein one or more of the cranial sutures prematurely fuse, causing altered calvarial shape. Broadly, fusion of the suture inhibits growth in the direction perpendicular to the suture. For instance, sagittal suture fusion causes dolichocephaly: a long, narrow calvarium. Conversely, fusion of the coronal sutures results in a short, wide calvarium known as brachycephaly. Fusions may be unilateral or bilateral, isolated or multiple, resulting in calvarial shapes that are a combination of types. Fusion of all sutures results in microcrania, causing either failure of brain growth or increased intracranial pressure.

Primary etiologies are most commonly related to mutations in fibroblast growth factor receptors. Numerous familial syndromes are associated with these mutations, including Pfeiffer, Apert, and Beare-Stevenson. Secondary craniosynostosis is related to systemic and metabolic conditions such as hyperthyroidism, hypercalcemia, vitamin D deficiency, and sickle cell disease.

Evaluation may begin with plain radiographs but the mainstay of imaging is CT scan with 3D surface-rendered reconstructions. Early identification is crucial as intervention should be performed during infancy to prevent deformity as well as other complications of increased intracranial pressure and growth failure. Management is surgical, involving excision of the fused suture and normalization of calvarial shape. Long-term follow up is required to monitor surgical outcome.

Results: We present a pictorial review of craniosynostosis cases with characteristic findings on multiple modalities and imaging findings of surgical management.

Conclusion/Learning Objectives:

Describe typical presentations and imaging findings of the cranosynostosis
 Review syndromes associated with cranosynostosis including primary synostoses and secondary synostoses
 Recognize potential complications of cranosynostosis
 Understand treatments and follow up of cranosynostosis.

Poster: EDU-096

CEREBROSPINAL FLUID SHUNT COMPLICATIONS IN CHILDREN: A PICTORIAL REVIEW

YOUCK JEN Siu Navarro, ERICA Poletto, ARCHANA Malik, ROBERT Koenigsberg
 St. Christopher's Hospital for Children, Philadelphia, USA

Introduction

Many pediatric patients with hydrocephalus are treated with cerebrospinal fluid (CSF) shunt. Ventriculoperitoneal (VP) shunting is most commonly used, due to fewer complications. In patients with VP shunt contraindications, the catheter can terminate in the pleural cavity, right atrium or gallbladder.

Yet shunt complications remain problematic, due to either extracranial outlet obstruction, extracranial shunt tubing disruption, or intracranial blockage. Shunt complication may be suspected by the clinical history and physical examination. A radiologic study is often performed to confirm the diagnosis or identify causes. It is important for the radiologist to recognize imaging findings of shunt malfunction, to enable prompt diagnosis and treatment.

Objectives

Describe the types of CSF shunts in the pediatric population.
 Demonstrate the multimodality approach to assess CSF shunt malfunction.
 Discuss the imaging findings in CSF shunt complications.

Methods

This is an educational review of children with suspected CSF shunt malfunction, who underwent imaging at St. Christopher's Hospital for Children. Studies that best exemplified the imaging findings were selected for presentation.

Results

The characteristic imaging findings of each CSF shunt complication are discussed on different imaging modalities. Unenhanced Computed Tomography (CT) and shunt radiographs are the most frequent initial studies in emergent settings. Magnetic Resonance Imaging (MRI) and occasionally abdominal ultrasound are utilized if infection or distal catheter tip obstruction is suspected. Limited/fast brain MRI, may replace head CT, depending on MRI availability.

The imaging examinations of children with identified CSF shunt malfunction were reviewed and classified as: mechanical failure, (including shunt discontinuity and migration), pseudocyst formation around the tip, over-shunting and infection.

Conclusion

Ventricular shunt malfunction in the pediatric population remains a common clinical problem in the treatment of hydrocephalus. As a radiologist it is important to understand various causes of shunt malfunction, imaging selection and key diagnostic findings, which allows for accurate diagnosis and treatment.

Poster: EDU-097

IMAGING OF OCULAR AND OPTIC NERVE TRAUMA IN CHILDREN

ADAM Hussain¹, ZISHAN Sheikh², PADMA Rao¹

¹ Royal Children's Hospital, Department of Medical Imaging, Melbourne, AUSTRALIA

² Birmingham Children's Hospital, Department of Radiology, Birmingham, UNITED KINGDOM

Background:

Trauma remains a leading cause for acquired blindness in children. Imaging plays a major role in suspected ocular trauma in the identification of possible globe rupture or laceration, assessing for an intra-ocular foreign body and evaluating for associated injuries to the optic nerve and bony orbit. In children, ocular injuries can be initially occult and the radiologist may be the first to identify clinically important injury. Computed tomography (CT) remains the most commonly used modality as it is widely available, gives excellent bony detail and allows for rapid acquisition of volumetric data. Magnetic resonance imaging (MRI) can be performed once a foreign body has been excluded on CT and is preferred for optic nerve visualisation. Ultrasound (US) has traditionally been less frequently utilised as an imaging tool in trauma. However, at our institution, ocular US under sterile conditions is performed on request to evaluate for choroidal or retinal detachment in cases where anterior segment haemorrhage precludes direct visual assessment.

Aim/Purpose: To review the imaging appearances of a spectrum of blunt and penetrating ocular injuries in children. To correlate CT and US findings, with particular respect to evaluating the posterior segment structures. To understand the spectrum of optic nerve injuries seen on CT and MRI.

Methods:

Reports from CT, US and MRI examinations performed in cases of orbital trauma imaged at a tertiary paediatric trauma and ophthalmology centre, between 2001-2020 were identified using a key word search on the local radiology information system (RIS). The imaging findings were then reviewed with correlation to ophthalmology assessment, surgical findings and clinical outcome on the electronic medical record (EMR). Appropriate images were then selected for presentation by the study authors.

Results:

A pictorial review of paediatric ocular injuries are presented, categorised anatomically by anterior segment, lens, posterior segment trauma and ocular foreign bodies. Optic nerve injuries ranging from optic nerve contusion, nerve sheath haematoma, extrinsic compression, stretching in traumatic proptosis and transection.

Conclusion:

Radiologists need to be aware of the varied appearances of ocular and optic nerve injuries in children. Whilst CT remains the prime modality in most cases, US provides better delineation of traumatic retinal or choroidal detachment.

Poster: EDU-098

NEUROIMAGING OF NEONATAL STROKE: CLASSIFICATION AND IMAGING FINDINGS

JACOPO Scaggiante, MILAD Yazdani, MANUEL Trevino, MARIA GISELE Matheus, MARIA VITTORIA Spampinato
 Medical University of South Carolina, Charleston, USA

Summary and Objectives:

A stroke occurring from 28 weeks of gestation to postnatal day 28 is widely defined as perinatal stroke. Arterial ischemic infarctions represent about 80% of perinatal cases, and occur in up to 1 over 3500 newborns, an incidence 6 times higher than in childhood. The remainder of perinatal strokes are caused by cerebral sinovenous thrombosis (CSVT) and intracerebral hemorrhage. Newborns with perinatal stroke present with seizures, acute encephalopathy, and altered mental status. Presumed perinatal strokes are also diagnosed later in life during the workup of a focal neurological deficit. Neuroimaging findings of perinatal stroke and stroke

mimickers vary among preterm and term neonates due to different degrees of brain maturation.

Our objectives are the following:

- Review of epidemiology and classification of perinatal stroke
- Review of brain maturation and mode of presentation
- Review of MR imaging protocol for neonatal stroke
- Case-based review of neuroimaging findings of neonatal stroke
- Review of neuroimaging mimickers of neonatal stroke

Purpose:

Our purpose is to provide a didactic review of perinatal stroke and stroke mimickers according to brain maturation and mode of stroke presentation.

Materials and Methods:

We will present perinatal stroke cases and mimickers from our teaching file. Our presentation will include stroke cases in preterm and term neonates, specifically cases of arterial ischemic infarct, CSVT, and intracranial hemorrhage, including subpial hemorrhage. We will also review imaging findings of stroke mimickers such as metabolic and infectious diseases, as well as imaging findings of hypoxic-ischemic brain injury, periventricular leukomalacia, germinal matrix hemorrhage. Cases will be accompanied by multiple-choice questions in an interactive format.

Results and Conclusion:

Imaging plays an important role in the diagnosis and management of perinatal stroke, and provides valuable information to rule out mimickers, such as metabolic diseases. It is important for radiology trainees to gain familiarity with perinatal stroke imaging findings in preterm and term neonates.

Poster: EDU-099

EYES ON ORBIT: A RADIOLOGICAL REVIEW OF THE MAIN PEDIATRIC ORBITAL LESIONS

ELEONORA Piccirilli¹, ALESSIA Carboni², ANTONIO Marrazzo², MASSIMO Caulo^{1, 3}, CARLO Gandolfo², PAOLO Tomà⁴, G. STEFANIA Colafati²

¹ University of Chieti - Department of Neuroscience, Imaging and Clinical Sciences, Chieti, ITALY

² IRCSS Bambino Gesù Children's Hospital - Department of Imaging, Neuroradiology Unit, Rome, ITALY

³ University of Chieti - ITAB, Institute of Advanced Biomedical Technologies, Chieti, ITALY

⁴ IRCSS Bambino Gesù Children's Hospital - Department of Imaging, Rome, ITALY

EDUCATIONAL OBJECTIVES

To illustrate the imaging features of orbital lesions in the pediatric population

INTRODUCTION

Although small, the orbit can be divided into different compartments and is made up of several structures deriving from four germ cell layers, thus accounting for the high variability of lesions encountered in this anatomical space, especially in children.

Implications of quoad vitam and quoad valetudinem prognosis make it mandatory to recognize them and to formulate a narrow list of differentials not only for pediatric neuroradiologists but also for general radiologists.

Multimodal imaging is therefore fundamental in the diagnostic work-up, allowing in the majority of cases - together with clinical presentation and epidemiological features - even the proper diagnosis.

DESCRIPTION

Orbital lesions in children differ from those of adults in terms of etiology, prognosis and clinical presentation. The lesions will be classified according to their etiology (vascular, neoplasms and malformations) and the main compartment affected (osseous, extra-conal, intra-conal, optic nerve-globe and multicompartmental) and are listed below: leukemias and lymphoproliferative diseases, metastases, retinoblastoma, vascular

tumors, vascular malformations, retinoblastoma, optic nerve gliomas, meningiomas, plexiform neurofibromas, rhabdomyosarcoma, Langerhans cells histiocytosis, epi/dermoids and fibrous dysplasia.

For each, the main imaging features are presented; the clinical features, physical examination and pathological characteristics are also touched upon.

CONCLUSIONS

Although small, the orbit is composed of several different anatomical structures coming from all germ cell layers. Due to this complex embryological development, the lesions in the pediatric orbit are numerous, oftentimes presenting with similar and overlapping clinical manifestations.

The difficulties in a bioptic approach and the detrimental effects of a late diagnosis make it mandatory to recognize these entities not only for the pediatric neuroradiologist.

Multimodal imaging is thus fundamental in guiding towards a correct diagnosis and a timely treatment.

BIBLIOGRAPHY

Chung EM, Smimiotopoulos JG, Specht CS, Schroeder JW, Cube R: From the archives of the AFIP: Pediatric orbit tumors and tumorlike lesions: nonosseous lesions of the extraocular orbit. *Radiographics* 2007, 27(6):1777-1799.

Castillo BV, Jr., Kaufman L: Pediatric tumors of the eye and orbit. *Pediatr Clin North Am* 2003, 50(1):149-172.

Poster: EDU-100

PAEDIATRIC CEREBRAL CAVERNOUS MALFORMATIONS

MICHAEL Paddock¹, SARAH Lanham², KANWAR Gill¹, SAURABH Sinha², DANIEL JA Connolly²

¹ Barnsley Hospital NHS Foundation Trust, Barnsley, UNITED KINGDOM

² Royal Hallamshire Hospital, Sheffield, UNITED KINGDOM

INTRODUCTION

This pictorial review of cases from a tertiary paediatric neurosciences centre explores the challenges of diagnosing paediatric cerebral cavernous malformations, their key imaging features and subsequent management options.

CLINICAL PRESENTATION

The presentation and clinical course of CCM is variable and up to 50% of cases are asymptomatic. The mean age in children at the time of diagnosis is 10 years of age. Children can present with focal seizures, intracranial haemorrhage (ICH) and focal neurological deficits (FNDs) without radiological evidence of recent haemorrhage. Familial cerebral cavernous malformation (FCCM) is responsible for one-third to one-half of multiple CCMs.

Vascular malformations, including CCMs, should be excluded in children who present with spontaneous ICH. The annual risk of haemorrhage in children with CCM is 1.6% per patient year climbing to 8% in symptomatic patients. ICH from CCMs are typically small and result in mild functional impairment. Risk factors for symptomatic haemorrhage include: brainstem location (accounting for 11-15% of CCMs in children), haemorrhagic clustering and associated DVA.

IMAGING FEATURES

CT findings in CCM are subtle and non-specific. MRI is the investigation of choice: key imaging features include the classic 'popcorn' dark haemosiderin ring on T2-weighted imaging, intrinsic high T1 signal from methaemoglobin, and susceptibility of iron within the haemosiderin which is exploited to increase lesion conspicuity.

Susceptibility weighted imaging is the most sensitive sequence in the detection of CCM due to haemosiderin 'blooming' artefact and should be performed in children undergoing MRI following acute ICH identified on CT imaging and those with seizure and/or FNDs.

MANAGEMENT

An individualised approach to patient management is advocated. Management options, including microsurgery and stereotactic radiosurgery (gamma knife), should be stratified on lesion location, symptom burden and history of haemorrhage. Frank discussions between patients and caregivers are encouraged to explore the risks of treatment, including the implications of genetic testing to the patient and their family unit.

CONCLUSION

CCM is an uncommon but important diagnosis in children which can be overlooked with standard imaging techniques. Understanding common presentations ensures patients have access to appropriate imaging and subsequent management.

Poster: EDU-101

IMPORTANCE OF FLEXION AND EXTENSION MRI IN HIRAYAMA DISEASE

ADEYINKA Owoyele

University of Pittsburgh Medical center, Pittsburgh, USA

Importance of flexion and extension MRI of cervical spine in diagnosis of Hirayama disease and differentiate from monomelic amyotrophy

Case Presentation: A 16-year-old male presented with one-year history of left-handed weakness and muscle atrophy. He was weightlifter and noticed pain when gripping the bar. On clinical examination the patient had tremor and weakness involving extensors of thumb (3/5), extensors of fingers (4/5), flexors of fingers (4/5) and triceps (4/5). An EMG obtained demonstrated anterior horn cell axonal neuropathy involving C7, C8 and T1 and concerning for monomelic amyotrophy versus Hirayama disease and an MRI obtained at outside institution demonstrated mild atrophy of spinal cord at C6-T1 levels. A repeat flexion and extension MRI demonstrated anterior displacement of posterior dura causing spinal cord compression, epidural venous plexus engorgement and laminodural space separation of 5.4mm on flexion views (Figure 1). There was increased T2 signal in left anterior horn cell at C6 level (Figure 2).

Discussion:

Hirayama disease occurs in young males and characterized by anterior horn cell degeneration and gliosis resulting in unilateral muscular atrophy. The hallmark of the disease is involvement of a single limb with lower motor neuron features. EMG can document anterior horn cell axonal neuropathy however MRI obtained in flexion and extension views are important for demonstration anterior displacement of posterior dura and cervical spinal cord compression which is reported in all patients (100%) with Hirayama disease (1). The laminodural space separation ranges from 3-9.8mm (1). Cervical spinal cord hyperintensity has been demonstrated in 35.6% of patients only (1). Post contrast T1 sequences demonstrates engorgement of dural venous plexus. Treatment is usually conservative with cervical collar to avoid cervical flexion.

Conclusion:

Flexion and extension MRI of cervical spine is indispensable to diagnose Hirayama disease by documenting anterior displacement of posterior dura resulting in cord compression and increased laminodural distance.

Poster: EDU-102

IMAGING OF PATHOLOGIES OF VISUAL PATHWAY

RAHUL Nikam¹, ASHRITH Kandula¹, SNIGDHA Puram¹, BEN Paudyal¹, XUYI Yue¹, SACHIN Kumbhar²

¹Nemours Alfred I. duPont Hospital for Children, Wilmington, USA

²Medical College of Wisconsin, Milwaukee, USA

Purpose:

The visual pathway consists of retina, optic nerves, optic chiasm, and retrochiasm structures such as optic tracts, lateral geniculate bodies, optic radiations, and visual cortex. In this exhibit, we will depict the normal anatomy of the visual pathway; and describe the imaging findings of various congenital and acquired pathologies of the visual pathway in pediatric population. We will put forth a segmentation-based approach to visual pathway pathologies, greatly aiding in diagnosis.

Materials and Methods:

The pathologies of the visual pathway can be divided into congenital, demyelinating, inflammatory, neoplastic, metabolic, and miscellaneous. The various pathologies covered in the exhibit include:

1. Congenital: Anophthalmia, Microphthalmia, Coloboma, Macrophthalmia, Retinal hamartoma, Optic nerve aplasia/hypoplasia, Septo-optic dysplasia, nondecussating retinal-fugal fiber syndrome (achiasma), congenital muscular dystrophies,
2. Demyelinating: Optic neuritis, multiple sclerosis, neuromyelitis optica, acute disseminated encephalomyelitis, progressive multifocal leukoencephalopathy
3. Inflammatory: Cat scratch disease, optic perineuritis, orbital pseudotumor, Neurosarcoidosis, Lyme disease,
4. Neoplastic: Retinoblastoma, Optic pathway gliomas (NF, and non-NF associated), optic nerve sheath meningioma
5. Metabolic: Globoid cell leukodystrophy (Krabbe disease)
6. Miscellaneous: Persistent hyperplastic primary vitreous (PHPV), Idiopathic intracranial hypertension, suprasellar masses such as craniopharyngioma, and germinoma.

Results/Conclusion:

The goal of this education exhibit is to use an image intensive PowerPoint presentation to familiarize the audience with the basic anatomy, and various pathologies of the visual pathway, and develop a segmentation-based approach to arrive at a diagnosis or a reasonable differential diagnoses.

Poster: EDU-103

PEDIATRIC CLINICAL MAGNETIC RESONANCE ELASTOGRAPHY OF THE BRAIN: A PRIMER FOR RADIOLOGISTS

RAHUL Nikam¹, GRACE McIlvain², VINAY Kandula¹, XUYI Yue¹, GURCHARANJEET Kaur¹, LAUREN Averill¹, ARABINDA Choudhary³, CURTIS Johnson²

¹Nemours Alfred I. duPont Hospital for Children, Wilmington, USA

²University of Delaware, Newark, USA

³University of Arkansas for Medical Sciences, Little Rock, USA

Purpose:

The aim of this exhibit is to use a graphical and image intensive PowerPoint presentation to familiarize the reader with the brief history, basic concepts, physics, hardware, imaging technique, and data analysis of magnetic resonance elastography (MRE) of the brain in pediatric population.

Materials and Methods:

Magnetic Resonance Elastography (MRE) is a novel technique evaluating the viscoelastic mechanical properties of the tissues, and can be used for probing brain structure in health and disease. MRE probes how tissue elements act and interact when mechanically forced, heightening the sensitivity to microstructural tissue integrity. Viscoelastic properties measured with MRE reflect critical information about the distribution and organization of neurons and axons, glial cells, and extracellular matrix. While MRE has been used to study the adult brain and neurodegenerative disorders, its application to pediatric populations has not been well established.

To introduce our topic, we will briefly discuss the history and basic concepts of MRE. Next, to serve as an overview, we will describe the physical principles underlying MRE including concepts of

viscoelasticity, complex shear modulus, stiffness, and damping ratio. In the second section, we will discuss technical aspects of implementing MRE for pediatric populations on clinical MRI scanners. This includes hardware considerations, shear wave generation, MRE acquisition strategies, and data analysis methodologies. Finally, we will illustrate several clinical examples of pediatric brain MRE from our institution, including tumors, neurofibromatosis, and tuberous sclerosis that all demonstrate altered tissue stiffness.

Conclusion:

After review of this exhibit, the audience will be well versed with concepts relevant to implementation, application, and interpretation of magnetic resonance elastography of the brain.

Poster: EDU-104

DEEP GRAY MATTER PATHOLOGIES: A PATTERN-BASED APPROACH. WHAT THE PEDIATRIC RADIOLOGIST NEEDS TO KNOW

SARAH Moum¹, MAURA Ryan¹, PAUL Caruso²

¹ Ann & Robert H. Lurie Children's Hospital of Chicago, Department of Medical Imaging, Chicago, USA

² Massachusetts General Hospital, Department of Radiology, Boston, USA

Purpose:

Signal abnormalities within the basal ganglia and thalamus are identified in several metabolic and genetic disorders, which tend to overlap clinically. MRI can help narrow the differential diagnosis as well as guide future testing and evaluation. We present a pattern-based approach to the MRI evaluation of these pathologies that can present in the pediatric population.

Materials and Methods:

Case examples on MR imaging were identified through clinical work and radiology report search engines. A comprehensive review of the current literature was also performed.

Results:

The basal ganglia require a large utilization of oxygen and glucose and are highly susceptible to toxic and metabolic insults. These structures often demonstrate signal abnormality in the setting of metabolic disorders and inborn errors of metabolism.

During early stages of disease, these pathologies can be subdivided based on (1) predominant involvement of the deep gray structures, (2) mixed involvement of both white matter and deep gray structures, and (3) predominant involvement of the white matter.

A pattern-based classification scheme and diagnostic algorithm using key MRI findings, including MR spectroscopy and other advanced imaging techniques, will be reviewed for a spectrum of deep gray matter pathologies focusing on metabolic and genetic syndromes. Clinical manifestations, genetic abnormalities, and syndromic associations will be described for each pathology. Alternative differential considerations and potential imaging pitfalls will also be presented.

Conclusions:

Metabolic and genetic disorders are not infrequently encountered in the pediatric population and commonly present a diagnostic challenge to clinicians. Multisequence MR imaging is fundamental to the evaluation of these patients with suspected metabolic disorders, leukodystrophies, and inborn errors of metabolism. A pattern-based imaging approach with MRI concentrating on deep gray matter features can be effective in clinical practice to help narrow differential considerations, suggest possible genetic associations, and precipitate diagnostic testing.

Poster: EDU-105

LAUGHING GAS: NOT SO SWEET SMELLING AFTER ALL "RAISING AWARENESS OF NITROUS OXIDE TOXICITY COMPLICATIONS AMONGST PAEDIATRIC RADIOLOGISTS"

FADI Maghrabia, LOUISE Hattingh

Bradford Teaching Hospitals, Bradford, UNITED KINGDOM

Introduction:

Nitrous oxide gas (N₂O) is a safe anaesthetic agent that can relieve pain and anxiety, and it is mainly used in dentistry and obstetrics. Nitrous oxide, also known as "laughing gas" or "hippy crack" is an odourless and colourless gas with a sweet taste. It is being increasingly used as a recreational drug among young adults for its relaxing and euphoric effects¹. During the COVID-19 pandemic lockdown period, the discarded N₂O canisters have become noticeably prevalent in the streets, and paediatric radiologists should be aware of the imaging findings in young patients presenting with myelopathic symptoms.

Case A: 19 years old presented with numbness and tingling of the forearm and the fourth and fifth fingers, in-coordination of upper and lower limbs.

Case B: 21 years old presented with lower back pain, saddle anaesthesia, and paraesthesia in the C8 and T11-L3 nerves distribution.

Radiological findings:

On the sagittal T2, note the contiguous high signal in the posterior spinal cord at cervicothoracic spine level. There is a symmetrical high signal in the dorsal columns on the axial T2 in both patients, giving an "inverted V-appearance".

Discussion:

- Both cases presented during the lockdown period with one of the patients admitting using 100 canisters of N₂O a day for about 6 weeks. The reason behind seeing more cases with N₂O toxicity during lockdown goes back to its cheap price which can be as cheap as 6-pound sterling for 10 canisters and the shocking fact that it can be easily ordered online with doorstep delivery service.

- One of the challenges we face is the possibility of the co-existent underlying cause of myelopathy alongside N₂O abuse. Other causes of myelopathy that should be investigated are pernicious anaemia, coeliac disease, copper deficiency and inflammatory myelitis.

Poster: EDU-106

COMPUTED TOMOGRAPHY FINDINGS AND INCIDENCE OF ROUND WINDOW ATRESIA IN CHILDREN AND ADOLESCENTS

TAKAO Kumazawa, HIROKO Hara, TAKAFUMI Ono, TAKASHI Koyama, SHINICHI Sato

Kurashiki Central Hospital, Kurashiki, JAPAN

Purpose:

There are many causes of hearing loss in children and adolescents, including otitis media, ossicular malformation, and inner ear anomaly. Round window atresia (RWA), initially reported by Scarpa in 1772, results in hearing loss. RWA is a rare abnormality and few papers have been reported. The purpose of this study was to describe the computed tomography (CT) findings and the incidence of RWA.

Materials and Methods:

The study population comprised 173 consecutive patients aged 25 or younger undergoing CT of the temporal bones in our hospital between January 2018 and December 2020. High resolution CT (HRCT) scans of the temporal bone were acquired using a scanner with 0.5 mm collimation, and coronal multiplanar reconstruction images of 0.5 mm thickness were generated. Diagnostic criteria included that the expected location of the round window niche was ossified, or closed by surrounding structures. The CT images were blindly evaluated by two board-certified

radiologists, and the CT findings of patients diagnosed with RWA were disclosed.

Results:

CT demonstrated that the round window niche was ossified in four cases. In one case, the round window was not ossified, however, closed by high jugular bulb. Therefore, the diagnosis of RWA was made in five, including three boys and two girls, age ranging six to twenty-two years (mean age was fourteen years).

Hearing test revealed mixed but predominantly conductive hearing loss with an air-bone-gap of 12–40dB, in four cases. Conductive hearing loss was reported in one case, referred by other hospital.

Incidence of RWA was 2.9 percent in this study. RWA was found only right side in four cases and only left side in one case. All cases with right RWA coexisted high jugular bulb on the same side. One of these cases was dehiscence of the jugular bulb. A case with left RWA didn't coexisted high jugular bulb. This case finally diagnosed as otosclerosis based on both CT images and the clinical course. All the five patients had no other obvious abnormalities of middle and inner ear.

Conclusions:

CT findings and incidence of RWA were presented. High jugular bulb was highly associated with RWA. Radiologists should know RWA causes hearing loss even though it is rare abnormality. Close attention should be paid to the morphology of the round window on temporal bone imaging especially performed for hearing loss.

Poster: EDU-107

NEUROIMAGING OF HMGCOA LYASE DEFICIENCY: CASE SERIES AND REVIEW OF LITERATURE

AMNA Kashgari¹, ABEER Al mehdar¹, PRASAD Hanagandi², MAJID Al Fadhel¹

¹ King Saud bin Abdelaziz University for Health Sciences, Riyadh, SAUDI ARABIA

² King Abdullah Specialized Children's Hospital, Riyadh, SAUDI ARABIA

Inborn error of metabolism is a wide spectrum disorder. Often, the rare entities can be a diagnostic imaging dilemma. In comparison to rest of the world, the middle east region and in particular Saudi Arabia has a high incidence of metabolic diseases with an approximate frequency of 1:635.

HMGCoA lyase (3-hydroxy-3-methylglutaryl coenzyme A lyase) is one such rare autosomal that we frequently encounter in this region. According to the updated literature, a meta-analysis study has revealed that there are approximately 200 cases worldwide. The imaging findings have been elaborated in approximately 60 cases and include isolated case reports or small cohorts of case series.

Deficiency of HMGCoA lyase results in impairment of leucine metabolism and ketogenesis.

The disease onset is usually during infantile period the laboratory results are suggestive for diagnosis.

Purpose:

Through this electronic educational exhibit we intend to highlight the neuroimaging spectrum of HMGCoA lyase deficiency.

Material and method:

We retrospectively analysed the brain MRI findings and evolution on follow up imaging in genetically confirmed HMGCoA lyase deficiency between (2014– 2020). Relevant information such as consanguinity, age of onset, sex, clinical presentation at onset and current neurologic outcome were included in our study.

Results:

MRI brain examination demonstrated a diverse spectrum ranging from diffuse and confluent white matter changes to involvement of the basal

ganglia with diffusion restriction. Abnormal spectral peaks were observed in cases where MRS OBTAINED.

We also observed a “tigroid pattern” in a chronic case that has not been previously reported.

Conclusion:

HMGCoA lyase is rare inborn error of metabolism with a diverse imaging spectrum. A unique feature of this small cohort is that we highlight neuro-radiology findings across different age groups and the disease evolution, especially on follow up imaging, that has not been clearly illustrated in the imaging literature.

Poster: EDU-108

A RADIOLOGIC PATHOLOGIC PICTORIAL REVIEW OF MEDULLOBLASTOMA SUBGROUPS BASED ON THE REVISED 2016 WHO CLASSIFICATION – AN IRISH PERSPECTIVE

JENNIFER Hennebray¹, SAEED Mamoun², SUSAN Singh¹, CONOR Fearon², JANE Cryan², ANGELA T. Byrne¹

¹ Radiology Department, Children's Health Ireland, Crumlin, Dublin, IRELAND

² Neuropathology Department, Beaumont Hospital, Dublin, IRELAND

Purpose

A revised classification of tumours of the central nervous system was published by the WHO in 2016, utilising an integrated phenotypic and genotypic approach to aid in the objective diagnosis of CNS tumours. The aim of this study was to retrospectively review all cases of diagnosed paediatric medulloblastoma in Ireland since 2016 and evaluate if MR imaging and pathology findings correlate with those described in the most recent literature. Characteristic MRI findings of each subtype are described with pictorial examples of each.

Material and Methods

This study is a multisite retrospective audit/review performed at the Irish National Paediatric Radiology Oncology department at Children's Health Ireland, Crumlin and the National Centre of Neurological Surgery and Pathology at Beaumont Hospital, Dublin. A retrospective search of all MRI Brain studies carried out from 2016–2020 was performed for cases of suspected medulloblastoma. Imaging characteristics were examined and correlation with biopsy results and molecular subtypes was performed.

Results

23 cases of biopsy proven medulloblastoma were found during this time period with classic pictorial examples of each imaging and pathology type demonstrated in this exhibit. Restricted diffusivity was noted within all medulloblastomas and the majority enhanced on post contrast imaging apart from Group 4 subtype. Tumour location at the cerebellopontine angle/cerebellar peduncle was observed to be the most defining feature of WNT activated medulloblastoma which were all extra-parenchymal and attached either to the surface of the brainstem or cerebellum in our series. An intracerebellar location was observed in all cases of SHH activated medulloblastomas. The majority of group 3 and 4 medulloblastomas had a vermian location.

Conclusion

The specific imaging features of molecular sub-types of medulloblastomas described in the literature to date were observed in the majority of Irish cases diagnosed since 2016. Excellent diagnostic accuracy and radiologic-pathologic correlation was observed in this pictorial review with examples of the classic imaging and pathology provided.

Poster: EDU-109

TO LEAVE OR NOT TO LEAVE ALONE – IMAGING APPROACH TO PETROUS APEX LESIONS IN CHILDREN

NEETIKA Gupta¹, SHIVAPRAKASH Hiremath², SANTANU Chakraborty², CLAUDIA Martinez Rios¹, ELKA Miller¹

¹ Department of Medical Imaging, Childrens Hospital of Eastern Ontario, University of Ottawa, Ottawa, CANADA

² Department of Medical Imaging, The Ottawa Hospital, University of Ottawa, Ottawa, CANADA

Background:

The petrous apex is involved in a wide range of pathological conditions due to its precarious location and close relationship to major neurovascular structures. Clinical presentations of petrous apex lesions are quite variable and frequently depend on the structures involved and age at presentation. We intend to depict the imaging approach based on anatomical structure of origin of the petrous apex lesions.

Educational Objectives:

1. Illustrate the relevant anatomy of petrous apex and surrounding critical neurovascular structures.
2. Discuss various lesions commonly affecting the petrous apex in paediatric population.
3. Demonstrate the precise role of cross-sectional imaging modalities in diagnosis of the petrous apex lesions.
4. Propose a diagnostic algorithm based on imaging findings to aid in presurgical diagnosis and facilitate appropriate management.

Technique:

1. Comprehensive discussion of the pediatric petrous apex lesions including benign and malignant entities.
2. Describe the typical imaging findings of common petrous apex lesions in the pediatric population.
3. Provide a simplified imaging approach to the pediatric petrous apex lesions based on imaging features that may help to narrow the differential diagnoses of petrous apex lesions in children.

In this educational exhibit, we propose to classify the pediatric petrous apex lesions based on the imaging appearance on cross-sectional imaging (CT and MRI). They are divided into nonexpansile, expansile non-destructive and expansile destructive lesions. Nonexpansile lesions are do not touch lesions that include asymmetric pneumatization, trapped fluid, prominent arachnoid granulation and aberrant internal carotid artery. Commonly encountered non-destructive expansile lesions are cholesterol granuloma, cholesteatoma, cephalocele, fibrous dysplasia and rarely mucoceles. The expansile destructive lesions of petrous apex in pediatric age group are langerhans cell histiocytosis, metastasis, rhabdomyosarcoma and osteomyelitis.

Conclusion:

An organized imaging approach to the myriad of petrous apex pathologies with understanding of the critical anatomy of the petrous apex help in appropriate presurgical diagnosis and facilitate adequate management in the pediatric population.

Poster: EDU-110

NEUROIMAGING FINDINGS IN MAPLE SYRUP URINE DISEASE-EXPERIENCE IN A TERTIARY REFERRAL CENTRE

MARY LOUISE Gargan¹, SIOBHAN O'Sullivan², INA Knerr³, STEPHANIE Ryan¹

¹ Department of Paediatric Radiology, Children's Health Ireland (CHI) at Temple Street, Dublin, IRELAND

² Department of Paediatrics, Royal Belfast Hospital for Sick Children, Belfast, UNITED KINGDOM

³ National Centre for Inherited Metabolic Disorders, Children's Health Ireland (CHI) at Temple Street, Dublin, IRELAND

Purpose

Maple syrup urine disease (MSUD) is an inborn disorder of branched-chain amino acid metabolism and can provoke encephalopathy. The purpose of this exhibit is to present the spectrum of both acute and chronic neuroimaging findings in MSUD.

Materials and Methods

All patients who were diagnosed with MSUD by newborn screening in the Republic of Ireland since 1972 were identified. Two patients were diagnosed at two and eight weeks of age in their home countries. Patients who had neuroimaging were included in our case series (with consent/ethics approval).

Results

Neuroimaging was available for ten patients (five male and five female) with MSUD.

In five of these patients, initial neuroimaging was performed in the neonatal period. On MRI, abnormalities including restricted diffusion were seen in the brainstem and cerebellum as well as the internal capsules and corticospinal tracts. A broad peak at 0.9ppm was seen on MR spectroscopy. In three of these babies, MRI abnormalities resolved on follow up imaging.

In the remaining five patients, imaging was performed in early or late childhood and in adulthood. In one baby at 8 months, marked cerebellar atrophy was seen. In another at 18 months, MRI showed abnormal high T2 signal in the crura of the midbrain. One child had an abnormal MRI at 2 ½ years but normal subsequent imaging. One adult patient had diffuse brain atrophy and another had a normal MRI brain.

Conclusion

In our case series, a wide spectrum of imaging findings is presented with both acute and chronic findings. Neuroimaging is most likely to be abnormal during an acute neonatal presentation when MRI shows a characteristic combination of abnormal diffusivity due to intramyelinic oedema in myelinated tracts and abnormal signal with normal diffusivity due to vasogenic oedema in unmyelinated white matter. Unlike the reduced diffusivity associated with acute ischaemia, the intramyelinic oedema seen on MRI in our patients with MSUD resolved completely or nearly completely with a full recovery clinically. Therefore, prognostication in the early stages of MSUD based on MRI may be difficult, with initially very dramatic MRI abnormalities potentially resolving if there is a good biochemical and clinical response to disease-specific emergency treatment.

Acknowledgement: We wish to acknowledge all the staff involved in patient care and thank Temple Street Foundation for financial support.

Poster: EDU-111

PEDIATRIC NON-TRAUMATIC INTRACRANIAL HEMORRHAGE: WHAT RADIOLOGIST NEED TO LOOK FOR?

ALESSIA Carboni¹, ANTONIO Marrazzo¹, EMMA Gangemi², IOAN PAUL Voicu³, MARIA LUISA D'Andrea⁴, ANDREA Carai⁵, ANGELA Mastronuzzi⁶, CARLO Gandolfo¹, PAOLO Tomà⁴, G. STEFANIA Colafati¹

¹ Neuroradiology Unit, Department of Imaging, Bambino Gesù Children's Hospital, IRCCS, Rome, ITALY

² Departmental Faculty of Medicine and Surgery, Center for Integrated Research, University Campus Bio-Medico of Rome, Rome, ITALY

³ Department of Imaging, G. Mazzini Hospital, Teramo, ITALY

⁴ Department of Imaging, Bambino Gesù Children's Hospital, IRCCS, Rome, ITALY

⁵ Neurosurgery Unit, Department of Neuroscience and Neurorehabilitation, Bambino Gesù Children's Hospital, IRCCS, Rome, ITALY

⁶ Department of Pediatric Haematology/Oncology, Cell and Gene Therapy, Bambino Gesù Children's Hospital, IRCCS, Rome, ITALY

EDUCATIONAL OBJECTIVES

•to illustrate imaging findings of different causes of pediatric non-traumatic intracranial hemorrhage from our case studies.

•to provide some elements that can address the radiologist in the causative differential diagnosis.

INTRODUCTION

Non-traumatic intracranial hemorrhage (NTIH) is a rare event in the pediatric age and it represents a disabling and potential fatal event. Owing to the rarity of this entity and its potentially fatal course, it poses a diagnostic as well as therapeutic challenge to physicians in the current era. Clinical presentation is sudden and commonly non-specific with headache and other signs of acute intracranial hypertension variably associated to focal neurological signs. Neuroimaging has a predominant role in the workup and it's crucial to exclude intracranial vascular malformations and to identify indirect signs of intracranial hypertension, which may require immediate surgical treatment.

DESCRIPTION

In the pediatric population, haemorrhagic strokes are frequently associated with vascular lesions such as arteriovenous malformations, arteriovenous fistulas, cavernous malformations and aneurysms. Coagulopathies, leukemia, congenital or immune mediated thrombocytopenias represent others causes of pediatric non-traumatic hemorrhages. Cross-sectional imaging is readily available in most Centers and allows efficiently managing these patients in the hyper-acute phase. Computed Tomography (CT) shows bleeding characteristics but differential diagnosis is not always obvious. Magnetic Resonance Imaging (MRI) and/or MR-angiography of the brain should be obtained to identify rare causes of hemorrhages, such as intracranial tumours, infection, cerebral vasculitis, moya moya disease, illicit drug abuse.

CONCLUSIONS

Non-traumatic intracranial hemorrhage in childhood can present with a broad spectrum of underlying conditions, typical of this developmental age. When confronted with nontraumatic pediatric intracranial hemorrhage in an emergency setting, radiologists should be aware of possible causes and typical associated imaging features. In this paper, CT, MRI and DSA imaging features of nontraumatic intracranial hemorrhage associated to different etiologies have been described. We provide an overview of the possible causes of pediatric NTIH and the different imaging findings based on the experience of our Center, in order to help the radiologist to familiarize with these conditions.

Poster: EDU-112

ORBITAL LESIONS IN PEDIATRICS- A RADIOLOGIST'S PRIMER

HIRAL Banker, PREET Sandhu
Le Bonheur Children's Hospital, University of Tennessee, Memphis, USA

Orbit is comprised of many structures including the optic nerve, globe, muscles, and retro-orbital fat. A wide range of pathologies can be seen affecting the orbit. The spectrum of orbital lesions in children differs from that of adults. Certain tumors such as rhabdomyosarcoma and vascular anomalies are more common in pediatrics and have characteristic imaging appearance. Recognition of key features of various pathologies help make the correct diagnosis and facilitate appropriate management.

Purpose:

- Overview of CT & MRI anatomy of orbit.
- Describe the imaging appearance of various orbital lesions on different modalities such as USG, CT scan & MRI.
- Explain key radiological differentiating features of pediatric orbital lesions including congenital conditions, infection, neoplasm, trauma, and vascular anomalies.
- Review uncommon orbital lesions with case illustration, e.g. orbital toxocariasis.

Poster: EDU-113

ANOMALIES OF THE CORPUS CALLOSUM: AN MR ANALYSIS OF THE SPECTRUM OF ASSOCIATED MALFORMATIONS

MEENA Anamika

Lady Harding Medical College, New Delhi, INDIA

Objective: To analyze the structural brain anomalies associated with abnormalities of the corpus callosum.

Materials and Methods: Brain MR images of pediatric patients from our institution were retrospectively evaluated for the type and severity of corpus callosum anomalies and the presence and type of other structural abnormalities

Results: Of 6 cases that were reviewed, 4 patients had agenesis of the corpus callosum (ACC), while 2 had hypogenesis of the corpus callosum (HCC). Of the overall cases, almost all had colpocephaly and showed reduced white matter volume outside the commissures, two had malformations of cortical development (heterotopia), almost all patients had Probst bundles, which were more common in patients with ACC than in those with HCC. One case had interhemispheric cyst, One case had dandy walker malformation association and an another case had colloid cyst.

Conclusion: Most cases of ACC and HCC were associated with complex telencephalic, rhombencephalic malformations. Reduced cerebral hemispheric white matter volume and malformations of cortical development were seen in the patients, suggesting that many commissural anomalies are part of an overall cerebral dysgenesis. ACC and HCC appear to lie along a dysgenetic spectrum.

Poster: EDU-114

NEONATAL THYROID IMAGING DOESN'T HAVE TO BE A PAIN IN THE NECK!

AISLING Fagan, SIMON Clifford, FERN Whittam, DAVID Garbera, SAI Elegiti, MARINA Easty, LORENZO BIASSONI
Great Ormond Street Hospital- Department of Radiology, London, UNITED KINGDOM

Neonatal hypothyroidism is an important cause of morbidity and mortality worldwide. It affects approximately 1/3500 children in the UK. Abnormal development of the thyroid gland accounts for 85% of cases, with dysmorphogenesis causing the remaining 15%. Although it is usually detected at birth via a 'heel prick' test, it is important to radiologically evaluate the presence and location of thyroid tissue, in order to guide management. Prompt thyroid hormone replacement is essential in order to preserve growth and neurological potential. There are also a number of transient causes of hypothyroidism which are important to keep in mind (e.g. maternal thyroid antibodies, iodine deficiency).

In this talk we will:

- Review the pathogenesis of hypothyroidism and the causes which affect neonates
- Review the scintigraphic imaging used in the investigation of hypothyroidism and the techniques used in preparation and acquisition
- Review the normal ultrasound appearance of the neonatal thyroid, and corresponding important ultrasound findings seen in hypothyroidism
- Provide clinical case examples to highlight the key learning points
- Give examples of rare presentations e.g. triple ectopic thyroid tissue
- Provide imaging examples of the perchlorate discharge test (and its use in the diagnosis of Pendred syndrome)

- Provide a brief overview of other syndromes that are associated with congenital hypothyroidism (and the genetic implications of these).

Poster: EDU-115

HYBRID ONCOLOGIC IMAGING IN PAEDIATRIC RADIOLOGY: ADVANTAGES OF I123 MIBG SPECT/CT IN NEUROBLASTOMA

SIMON Clifford, SAIGEET Eleti, AISLING Fagan, THOMAS Davies, FERN Whittam, DAVID Garbera, MARINA Easty, LORENZO Biassoni
Great Ormond Street Hospital, London, UNITED KINGDOM

Purpose:

I123 mIBG SPECT/CT is commonly performed for evaluation and monitoring of neuroblastoma. This educational exhibit will outline the numerous advantages of using SPECT/CT. Multiple imaging examples from our institution are provided to illustrate the benefits of SPECT/CT in paediatric oncology.

Materials and Methods:

The technique of performing I123 mIBG SPECT/CT imaging is explained. Using multiple imaging examples, the benefits of using SPECT/CT are described, in an interactive format, encouraging viewer participation. The benefits of using SPECT/CT include improved anatomical localisation, which can help in identifying both the primary lesion and metastatic lesions in soft tissues and nodes. SPECT/CT can help locate metastases in bone and determine their specific location. Non mIBG avid lesions may also be identified on the CT component, for example as a lesion with calcification. A contrast enhanced CT component of the mIBG SPECT/CT can be performed, meaning that a separate CT examination is not required, which can be helpful during both staging and follow up imaging. The SPECT/CT can be reformatted so it can be fused with other modalities such as MRI. The SPECT/CT improves certainty when reporting and can reduce the reporting of false positives, such as brown fat. SPECT/CT allows calculation of SUV max. Scoring systems (SIOPE/Curie) can be determined using SPECT/CT. Recent advances in SPECT/CT may facilitate further research. The aforementioned are just some of the benefits of SPECT/CT which will be described.

Results

The benefits of SPECT/CT will be explained, with relevant imaging examples provided. These imaging examples will encourage the reader to perform and report SPECT/CT. For those who already report SPECT/CT, the provided interesting examples should improve their reporting accuracy.

Conclusion:

After reading and interacting with this clearly laid out presentation explaining the many benefits of SPECT/CT imaging in neuroblastoma, with multiple examples, the viewer will gain an increased understanding and appreciation of this valuable imaging technique.

Poster: EDU-116

BENIGN VERSUS MALIGNANT? UNUSUAL VASCULAR MASSES IN CHILDREN

LILLIAN Lai¹, TAKMAN Mack², JOSEPH Miller¹

¹ Children's Hospital Los Angeles, Los Angeles, USA

² Naval Medical Center, San Diego, USA

Hemangiomas are common benign masses in children that can mimic malignancies, particularly their aggressive varieties. Conversely, vascular malignancies can also be confused with hemangiomas. The purpose of the exhibit is to expose radiologists to challenging unusual cases of vascular masses in children to help radiologists improve diagnostic accuracy when facing similar cases.

The exhibit will be in quiz format. Key differential diagnostic points will be highlighted for each case discussion. Cases will include: Aggressive

spine hemangioma versus sarcoma; posterior mediastinal hemangioma versus neuroblastoma; multifocal hepatic hemangiomas versus abscesses or metastases; hepatic hemangioma versus embryonal rhabdomyosarcoma; intra-parotid hemangioma versus parotitis; soft tissue hemangioma versus kaposiform hemangioendothelioma, angiosarcoma, hemangiopericytoma, and sarcomas.

Poster: EDU-117

IMAGING OF PAEDIATRIC VENO-OCCLUSIVE DISEASE

AISLING Fagan, FERN Whittam, QUYNH Tran, FARIBA Williams, DAVID Garbera, TOM Davies, KIERAN McHugh, TOM Watson
Great Ormond Street Hospital- Department of Radiology, London, UNITED KINGDOM

Veno-occlusive disease (also called sinusoidal obstruction syndrome) is an early complication of bone marrow transplant (BMT), usually occurring in the first 3 weeks. It has been reported to affect up to 50% of those transplanted for haematological malignancies. It is also seen following chemotherapy in the treatment of solid malignancies.

VOD usually presents with jaundice, painful hepatomegaly and ascites or pleural effusions.

It is important to have a low threshold for performing liver ultrasound in children following BMT or chemotherapy.

There are several indicative ultrasonographic findings, including: hepatosplenomegaly, thickening of the gallbladder wall, ascites, increased diameter of the portal vein, and decreased diameter of the hepatic veins. Doppler findings include reduced (<10cm/s) or reversed flow within the portal veins, increased resistive index of the hepatic artery (>0.75), and monophasic flow within the hepatic veins.

In this exhibit, we will

- Discuss the pathogenesis of VOD, and the criteria required to make a clinical diagnosis.
- Demonstrate imaging of VOD and illustrate the findings with a number of case examples.
- Provide an overview of the medical and interventional management of these cases, including thoraco/abdominocentesis and TIPS (transjugular intrahepatic portosystemic shunt).
- Outline how to differentiate VOD from other important differential diagnoses, particularly those that affect a similar cohort of children (e.g. Budd Chiari, graft vs host disease, portal vein thrombosis).

Poster: SCI-001

PEDIATRIC BODY COMPOSITION: REFERENCE VALUES FOR L3 MUSCLE AND FAT AREAS USING AUTOMATIC SEGMENTATION

ATIA Samim¹, SUZANNE Spijkers¹, PIM Moeskops^{1,3}, ANNEMIEKE S. Littooi^{1,2}, BOB D. de Vos^{3,4}, WOUTER B. Veldhuis^{1,3}, PIM A. de Jong¹, HANNEKE M. van Santen^{1,2}, RUTGER A. J. Nijelstein^{1,2}

¹ University Medical Centre Utrecht, Utrecht, THE NETHERLANDS

² Princess Máxima Centre for Pediatric Oncology, Utrecht, THE NETHERLANDS

³ Quantib-U B.V., Utrecht, THE NETHERLANDS

⁴ Amsterdam University Medical Centers, Amsterdam, THE NETHERLANDS

Background: Body composition, in particular muscle and fat distribution, can be an important predictor of various health outcomes. In order to identify children with an aberrant body composition, data on the normal variation in body composition throughout childhood are necessary.

Objective: To establish age- and sex-dependent reference values for muscle and fat areas in children on computed tomography (CT).

Methods: Children ages 1–17 years who underwent abdominal CT at the emergency department between 2002–2019 were retrospectively identified. Muscle areas (total, psoas, paraspinal, abdominal wall; cm²) and fat areas (total, subcutaneous and visceral; cm²) were measured at the level of the third lumbar vertebra (L3) with an automated segmentation tool. A subset of 52 scans were also manually segmented. CT examinations were excluded in case of abnormal anatomy, post-traumatic changes or incorrect CT segmentations. Age- and sex-specific reference values (median with interquartile range) and quantile regression curves were provided. Student t-tests were performed to compare sexes.

Results: CT images of 493 children (66% boys) were included. Intraclass correlation coefficient between manually- and automatically-segmented areas was excellent (>0.98). Fat accumulation increased in children from the age of 7–8 years. Median total fat area increased from 37 to 129 cm² in boys and 35 to 227 cm² in girls. Muscle area was comparable for both sexes until the age of thirteen, whereafter boys developed relatively more muscle tissue when compared to girls. Total muscle area increased from 38 to 174 cm² in boys and 34 to 127 cm² in girls. Boys had significantly higher visceral-to-subcutaneous fat ratios and girls higher total fat-to-muscle ratio.

Conclusion: This study provides reference values for L3 level muscle and fat areas during childhood. This will aid the identification of children with aberrant body composition, the evaluation of its prognostic impact and ultimately the implementation of adequate interventions.

Poster: SCI-002

WRONG EXAM, WRONG PATIENT: REPORTING AND TRACKING OF ERRORS AND NEAR MISSES IN GENERAL PEDIATRIC RADIOLOGY

LYNNE Ruess, REBECCA Shaffer, LAUREN Mack, JULEE Eing, TAMARA Viggiano, RAJESH Krishnamurthy
Nationwide Children's Hospital, Columbus, USA

Background: Any radiography of the wrong site or wrong patient is a serious radiation safety event. Our technologists use 2 patient identifiers and perform a time out to verify orders. When errors occur, technologists report safety events via an enterprise wide confidential reporting system (CSSTARS) and submit a form to the radiation safety officer. Near misses, or 'good catches,' are reported via an electronic departmental reporting system called Ongoing Professional Evaluation (O.P.E.N.). These entries are shared in the department daily huddle and monthly newsletters.

Purpose: To compare general radiography exam safety error and near miss rates at a large multi-site pediatric radiology department.

Methods: CSSTARS and O.P.E.N. entries regarding general radiography exams from January 1, 2019 to September 30, 2020 were identified and reviewed along with radiation safety event forms from January - September 2020.

Results: There were 230,992 general radiography exams during the study period with 67 (0.03%) CSSTARS reported safety events. The most common errors were wrong exam performed (20, 30%) and incorrect orders for which imaging proceeded and another exam was required after it was recognized (18, 27%). Other errors included wrong side (right/left) imaged despite correct order (11, 16%), wrong patient (6, 9%) and incorrect dose 3 (4%). Radiation safety forms were completed for all CSSTARS reported events in 2020. There were 75 (0.03%) 'good catches' reported via O.P.E.N. during the study period. Most (74, 99%)

were incorrect orders related to either wrong body part (54, 73%) or wrong side (right/left) (20, 27%) with 1 (1%) potential wrong patient exam averted.

Conclusion: 'Good catches' which avert radiation safety events were reported more often than radiation safety imaging errors, although both are uncommon at our institution. We believe regular reporting of 'good catches' serve as a reminder to good practice. Technologists create duplicate reports for each safety event, suggesting system redundancy that could be combined.

Poster: SCI-003

IMPLEMENTING ACADEMIC PRODUCTIVITY OF RESEARCH USING MACHINE LEARNING IN A SYSTEM DYNAMICS MODEL

ANDREA Doria¹, AFSANEH Amirabadi¹, OLGA Pinto¹, SAHAR Hashmi²

¹ The Hospital for Sick Children, Toronto, CANADA

² MIT, Cambridge, USA

Background: Production of knowledge is one of the hallmarks of the mission of academic institutions. Research productivity (expressed both in terms of quantity, number of papers published in scientific journals per year and quality) is an output of production of knowledge. Nevertheless, in many radiology departments research productivity generated by trainees and staff is suboptimal compared to that of other clinical specialties. For example, in Radiology only approximately 30% of abstracts presented in scientific meetings are published in journals, which causes financial losses for funding invested in research by radiology departments.

Purpose: To demonstrate causes of problems (bottlenecks) for suboptimal completion rate of research projects conducted by trainees and staff of departments of radiology (from the pipeline of idea generation to acceptance of manuscript in a scientific journal) so that we can increase the completion rate by 40% (from 30% to 70%) in relation to the current acceptance rate of abstracts in scientific meetings using a system dynamics model.

Methods & Materials: Observational data (literature review estimates) was used to build a system dynamics model incorporating machine learning as a quality improvement tool. System dynamics is a simulation approach to help us understand nonlinear behaviour of complex systems over time using stocks, flows, internal feedback loops, and time delays. In this study we mapped out the process of fellows (stocks) coming to a radiology department and publishing papers.

Results: We discuss current interventions (research meetings with supervisor, research design day, course) used in the process and propose additional interventions (mentorship, hiring research staff, offering research awards and seed funding with a priori advertisements to stimulate engagement, promoting annual research retreats, establishing a research board to increase research production) based on results of sensitivity analyses. Our results show how machine learning techniques can leverage interventions that show promise for improving research productivity in a radiology department.

Conclusions: Additional interventions taking advantage of machine learning techniques in research programs of radiology can break up vicious cycles (balancing feedback loops) of conduct of research by trainees and staff, innovating processes and improving research productivity.

Poster: SCI-004

SYNTHESIZING CONTRAST ENHANCEMENT FROM NON-CONTRAST CHEST COMPUTED TOMOGRAPHY USING A GENERATIVE ADVERSARIAL NETWORK

YEON JIN Cho, JAE WON Choi, SEUL BI Lee, SEUNGHYUN Lee, YOUNG HUN Choi, JUNG-EUN Cheon, WOO SUN Kim
Seoul National University Hospital, Seoul, SOUTH KOREA

Objectives: This study aimed to propose and evaluate a deep learning approach using GAN for synthesizing CECT images from non-contrast chest CT images.

Materials and Methods: We collected three separate CT data sets, the development set from Hospital #1 for the training and tuning, and test sets from Hospital #2 for the technical validation. For the development set, we obtained paired virtual non-contrast (VNC) and CECT data in December 2019 at Hospital #1 on a single CT scanner. For test sets, we acquired paired NCCT and CECT data which is thoracic CT angiography between NCCT and CECT scans, taken on various CT scanners between February 2020 and April 2020 at Hospital #2. We adopted a three-dimensional implementation of the pix2pix mod to train a generative adversarial network (GAN). We employed the peak signal-to-noise ratio (PSNR), multiscale structural similarity index measurement (MS-SSIM), and learned perceptual image patch similarity metric (LPIPS) to perform an objective image quality assessment on the sCECT images in the tuning set and test set

Results: The sCECT images showed significant improvements compared with the NCCT in all quantitative image quality metrics in both the tuning set and test set. In the tuning set, the sCECT images showed higher PSNR (25.96 ± 0.98 vs 18.95 ± 1.66 , $P < 0.001$), higher MS-SSIM (0.97 ± 0.01 vs 0.90 ± 0.03 , $P < 0.001$), and lower LPIPS (0.04 ± 0.01 vs 0.09 ± 0.02 , $P < 0.001$) than the NCCT. Similarly, in test set, the sCECT images showed higher PSNR (17.37 ± 1.70 vs 16.00 ± 1.75 , $P < 0.001$), higher MS-SSIM (0.81 ± 0.08 vs 0.79 ± 0.08 , $P < 0.001$), and lower LPIPS (0.15 ± 0.04 vs 0.16 ± 0.04 , $P < 0.001$) than the NCCT

Conclusions: we implemented a deep learning model for generating synthetic contrast enhancement from non-contrast chest CT images. The proposed model demonstrated good quantitative performance and promising results that suggest that it may provide additional clinically useful information without any added risks of radiation or intravenous contrast injection to the patients.

Poster: SCI-005

EVALUATION OF USEFULNESS OF REAL-TIME, DEEP LEARNING BASED DENOISING TECHNIQUE INTEGRATED INTO PACS : IMAGE QUALITY AND USER PREFERENCE

YEON JIN Cho, DAE HEE Kim, SEUL BI Lee, SEUNGHYUN Lee, YOUNGHUN Choi, JUNG-EUN Cheon, WOO SUN Kim, JONG-HYO Kim
Seoul National University Hospital, Seoul, SOUTH KOREA

Objectives

To evaluate the usefulness of real-time, deep learning (DL) based denoising technique by comparing it with conventional filtered back projection (FBP) images and iterative reconstruction (IR) images.

Materials and Methods

From January 2016 to July 2019, children under 18 year of age who underwent abdomen CT with available FBP and IR images were enrolled in this study. Nine invited radiologists reviewed images for qualitative assessment. The overall image quality of three different reconstructed CT images was evaluated with using a 5-point Likert scale. Reviewers denoted the most preferred denoising level and edge blending level in lesion assessment. To compare the image quality of each reconstructed image and to evaluate differences in the preferred denoising and edge blending level among reviewers, Kruskal-Wallis test was performed followed by Wilcoxon signed rank test. For quantitative image analysis, single radiologist drew region of interests on targeted organs at each reconstruction method in the same image level. ROIs were drawn on liver, pancreas, and

spleen respectively in pediatric abdomen CT and signal to noise ratio (SNR) was calculated for each reconstructed images.

Results

The overall image quality of DL-based reconstruction images was superior to that of FBP images (4.28 vs. 3.33; $p < 0.001$) and inferior to that of vendor-provided IR images (4.28 vs. 4.48; $p < 0.001$). In preferred denoising and edge blending level among reviewers, each reader had his or her own preference for pediatric abdomen CT ($p < 0.001$). In quantitative analysis, DL-based reconstructed images showed significant higher SNR than FBP images and IR images in the liver (10.4, 11.4 and 14.1; $p < 0.001$), pancreas (9.4, 10.4 and 12.9; $p < 0.001$) and spleen (11.1, 12.2 and 15.2, respectively; $p < 0.001$).

Conclusions

The DL-based reconstruction images had superior image quality to FBP images and comparable to IR images. The real time, DL-based denoising had advantage of being able to adjust image quality to the individual's preference over vendor provided IR images.

Poster: SCI-006

IMAGE GENTLY FAMILY FRIENDLY CAMPAIGN: REDUCING CHILDHOOD RADIATION EXPOSURE THROUGH AN INNOVATIVE EDUCATION MODULE

SAMUEL Brady¹, ALEX J. Towbin¹, DONALD Frush², AMI Gokli³, KRISTEN Hood-Watson⁴, DINA Kurzweil⁵, GRACE Mitchell³, MOELLE Molter⁵, DANA R. Nguyen⁵, EMILEE Palmer⁶, CHRISTOPHER W. Bunt⁴

¹ Cincinnati Children's Hospital, Cincinnati, USA

² Stanford healthcare, San Jose, USA

³ ImageGently, Durham, USA

⁴ Medical University of South Carolina, Charleston, USA

⁵ Uniformed Services University, Bethesda, USA

⁶ OhioHealth, Westerville, USA

Purpose: The purpose of the ImageGently Family Friendly Campaign is to develop an educational tool to teach third year medical students the basics of radiation risk during their Family Medicine clerkship. The campaign aims to equip students with knowledge and communication skills to help advocate for change within their healthcare team and use shared decision making to guide appropriate image selection.

Method: A multidisciplinary team met for two years to devise a curriculum for an online learning module. The team authored four individual lessons, which include: the basics of radiation safety and risk reduction, clinical decision support and critical appraisal of scientific literature, using motivational interviewing to advocate for change within a healthcare team, and shared decision making to enable communication with families. The online module was designed jointly with ImageGently and the ACR. The final product will reside on the ACR's learning management system; however, each medical school will be given the option of hosting the module themselves.

Results: The final version runs approximately 45 minutes in length and engages the student through animation, dialogue selection, live action videos, and critical appraisal of the ACR Appropriateness Criteria. Medical students are provided the basics in layperson terms, and practice critical thinking skills related to imaging radiation use. With the script complete, the educational module is currently in production, with a goal to implement in medical schools by spring 2021.

Conclusion: The ImageGently Family Friendly campaign has created an innovative online educational tool, using radiation protection as a framework, to teach medical students a broad range of concepts that they can use in their future medical practice, regardless of specialty. Equipping non-radiology trained physicians with the knowledge and tools to accurately discuss imaging radiation use and its benefits and risk will improve patient and parent cooperation during radiologic imaging, and lessen their

fear and anxiety associated with imaging radiation.

Poster: SCI-007

DEVELOPMENT OF AN IMAGING BASED INTEGRATED SIMULATOR PROGRAM (ISP) TO PROVIDE A MEANS FOR ON-GOING PEDIATRIC RESIDENT COMPETENCY ASSESSMENT AND DETERMINATION OF ABILITY TO PROVIDE INDEPENDENT CALL

DENISE A Castro¹, JOSEPH Yang², TIN Li¹, SALEHA Munawar¹, AMY Acker¹, DON Soboleski¹

¹ Queen's University, Kingston, CANADA

² Memorial University, St. John's, CANADA

PURPOSE: To develop a process allowing for assessment of pediatric resident competence in imaging interpretation and subsequent patient management utilizing an ISP.

MM: The collaborative funded project between radiology and pediatrics required multiple steps illustrated in the flowchart. Step 1 involved the IT department which anonymized imaging studies after their placement into junior and senior folders on our PACS. Step 2 required audits of the ER/in-patient population to determine the types and distribution of imaging cases. A survey of residency programs and society guidelines identified resources utilized to guide resident expected knowledge base. A list of diagnoses that involve significant imaging studies was formulated. Step 3 - Two pediatricians then assigned a designation of junior or senior folder to each diagnosis based on whether there was an expectation for the resident to be competent in the image interpretation and patient management to allow for independent call. Step 4 - After a pilot study a formal test of residents utilizing the junior ISP folder was performed. Each resident generated a report on each of 10 selected cases.

RESULTS: The post-pilot study survey identified the speech recognition system as a barrier and the residents were directed to write their responses to each case in the formal testing. A total of 16 of the 19 pediatric residents completed the 10 cases. The over-all grading demonstrated no significant difference between juniors and seniors. Specific cases where there was poor overall grading included diagnoses of non-accidental abuse (presenting with irritability and decreased leg movement) and Wilms tumor (presenting decreased appetite and low grade fever). On analysis, there was no significant correlation with resident OSCE scores. **CONCLUSION:** The ISP allows for standardized assessment of resident knowledge helping identify gaps in knowledge base and can aid in the determination of competence to perform independent on-call. Present pediatric OSCEs may not be adequately evaluating competence in imaging interpretation.

Poster: SCI-008

TECHNICAL ASPECTS OF HOME PACS: A SPR AND SCORCH SURVEY

MATTHEW Seghers¹, MARLA Sammer², SID Jadhav², ANDREW Trout³, LISA States⁴, ADINA Alazraki⁵, ANDREW Sher², VICTOR Seghers²

¹ Dell Medical School, University of Texas, Austin, USA

² Texas Children's Hospital, Houston, USA

³ Cincinnati Children's Hospital, Cincinnati, USA

⁴ Children's Hospital of Philadelphia, Philadelphia, USA

⁵ Children's Healthcare of Atlanta, Atlanta, USA

The COVID-19 pandemic highlighted the need for pediatric radiologists to be able to work from home to support stay home, work safe orders while ensuring institutional and patient access to their subspecialty

imaging expertise. To date, little has been published regarding technical aspects of home PACS within pediatric radiology departments. Collaborators from four children's hospitals in North America who utilize home PACS released a Society of Pediatric Radiology survey to the members of the SCORCH committee, comprising Chairs of Pediatric Radiology departments. Questions comprising technical aspects of Home PACS including hardware, software, internet connectivity configurations, availability of Home PACS for trainees, geographic rules for where Home PACS could be installed, and communication methods when working from home were included. Questions also focused on experience during the COVID-19 pandemic, as well as predictions for how many at-home assignments could persist once the pandemic is over. There were 50 respondents representing multi-sized pediatric radiology departments ranging from <5 to >40 faculty. 94% provided home PACS to faculty, 49% of which came from departmental funds, 45% hospital funds, 4% professional funds, and 2% self-pay. The majority of departments (54%) offer identical Home PACS relative to in-hospital systems. However, a sizeable minority offered varying configurations with different number/type of monitors or CPU. 96% of department faculty utilize a virtual private network when connecting to their institutional network. Only 11% of departments offered an institutional-issued phone for faculty use when working from home with 89% utilizing a personal cell phone/landline when communicating. Interestingly, 21% of respondents created an "internal" 5-digit institutional phone number for each home PACS to streamline communication. Although 94% of respondents reported 0-20% of non-procedural rotations were worked from home prior to the COVID-19 pandemic, based on the experience gained there is greater willingness to consider more at-home assignments moving forward. Once it is safe to work in the hospital again, 42% predicted 1-20% of assignments could be worked from home, 35% predicted 21-40% of assignments, and 13% predicted 41-60% of assignments. Responses to this survey can guide others in the technical specifications of Home PACS and offer insight into the future of working from home arrangements within pediatric radiology.

Poster: SCI-009

WORKING FROM HOME IN RESPONSE TO THE COVID-19 PANDEMIC: AN SPR MEMBERSHIP SURVEY

MATTHEW Seghers⁵, MARLA Sammer¹, SID Jadhav¹, ANDREW Trout², LISA States³, ADINA Alazraki⁴, ANDREW Sher¹, VICTOR Seghers¹

¹ Texas Children's Hospital, Houston, USA

² Cincinnati Children's Hospital, Cincinnati, USA

³ Children's Hospital of Philadelphia, Philadelphia, USA

⁴ Children's Healthcare of Atlanta, Atlanta, USA

⁵ University of Texas, Dell Medical School, Austin, USA

In response to the global COVID-19 pandemic radiology departments needed to utilize existing or rapidly deployed home PACS to facilitate physical distancing and guarantee radiological expertise despite stay home, work safe orders. In addition to clinical workflows, educational training and research were impacted. Despite possibilities of improved work-life balance, wellness, and shorter commuting times, there are concerns regarding working-from-home long-term including maintaining emotional engagement of faculty and preventing commoditization of pediatric imaging services. Collaborators from four children's hospitals in North America with experience with home PACS released a Society of Pediatric Radiology sponsored survey in January 2021 with questions organized by clinical workflows, non-clinical activities (education, research, virtual meeting participation), and emotional engagement. The survey was structured to enable comparison of predicted effect of working from home from those stating they did not have home PACS and actual effect from those who had existing home PACS and experience working from home. There were 255 respondents of whom 207 (81%) had home

PACS versus 48 (19%) who did not. Based on experience from March 2020–December 2020, 79% of respondents with home PACS felt that up to 60% of non-procedural clinical rotations could be performed from home once the COVID-19 pandemic is over. The majority of those with home PACS expressed no differences in their feeling of professional accomplishment, ability to communicate with referring providers, research productivity, diagnostic accuracy, cognitive ability, and ability to participate in meetings when working from home versus in-hospital. They felt more clinically productive but had decreased ability to teach trainees and decreased emotional engagement when working from home versus in-hospital. Those without home PACS had lower predicted satisfaction if able to work from home relative to those with home PACS (weighted average of 6 versus 8.3 on 10-point scale) and lower predicted feelings of professional accomplishment (weighted average 3.5 versus 5 on 10-point scale) if working from home. Those without home PACS also predicted decreased ability to perform research or engage during meetings if working from home relative to those with home PACS who expressed no change. Responses to this survey can offer insight into the future of working from home arrangements within pediatric radiology.

Poster: SCI-010

ANALYSIS OF RADIOLOGY QIS INFRASTRUCTURE RESPONSE TO THE COVID PANDEMIC: LESSONS FOR THE FUTURE

ELLEN Chung, LYNNE Ruess, MARGARITA Chmil, TAMARA Viggiano, RAJESH Krishnamurthy
Nationwide Children's Hospital, Columbus, USA

Background: We analyzed the response of our QIS infrastructure during the early months of the COVID-19 pandemic to learn lessons for planning future infrastructure needs.

Methods: Our department uses a 3-pronged approach to QIS raw data accrual: 1) Departmental Huddle for daily operational and personnel issues 2) an informatics solution embedded within the RIS called Ongoing Professional Evaluation (OPEN) to capture encounter-specific QI data 3) an enterprise-wide reporting system for safety/near miss events (CSSTARS). We reviewed huddle, OPEN and CSSTARS entries and leadership meeting notes from February–July 2020 and analyzed the impact that COVID related entries had on new and revised policies for this period.

Results:

There were 858 daily huddle entries; 245 (29%) were COVID-19 related, primarily about PPE shortages (54, 22%), clarifications of policy/protocol changes and implementation (46, 19%), and volume concerns after reinitiating elective services (30, 12%). There were 793 OPEN entries; 94 (12%) were COVID-19 related, most commonly about delay of care (31, 33%), inconsistencies in safe practices (17, 18%), and COVID-19 testing approaches (11, 12%). There was 1 CSSTARS related to COVID-19. Eighty leadership meetings occurred between March–July, resulting in new or revised policies regarding personnel safety, patient triage, testing/screening patients, COVID modality workflows, personnel furloughs/cohorting, PPE conservation, service/staffing reduction, and return of service. A custom calculator allowed for input of region-specific incidence/prevalence of COVID-19, hospital census, and hospital resource utilization to determine resource PPE demand, availability, and potential shortfall daily. Five new policies and 34 new processes/workflows were created in response to COVID. 36 COVID related newsletter summaries were written, with the top 3 related to PPE use (27/87, 31%), disinfection (8/87, 9%), and COVID-testing (6/87, 7%).

Conclusion: Our 3-pronged QIS infrastructure responded nimbly to routine and emergent needs during the COVID-19 pandemic, providing a rich data source for in-depth meaningful analysis and policy changes, with impact on work flow and outcomes.

Poster: SCI-011

TRAINING A PEDIATRIC RADIOLOGIST MUST LOOK BEYOND CONVENTIONAL METRICS TO FOCUS ON DEVELOPMENT OF HEALTHY PROFESSIONAL IDENTITY

SUSAN Hamman¹, PETER Loper², JANET R. Reid³

¹ University of Michigan, Ann Arbor, USA

² University of South Carolina, Columbia, USA

³ University of Pennsylvania, Philadelphia, USA

Purpose

Our trainees' development of professional identity is influenced by intermingling effects of personal experiences, medical education process, and others' perceptions of us. It's a process beyond acquiring knowledge and extends to "ways of being and relating in professional contexts". Developing a unique and autonomous professional identity requires the intersection of personal professional identities. One's personal identity can be tied to gender identity, age, race/ethnicity, or primary language. We aim to drill down on the intersectionality of personal and professional development and identify methods to foster healthy development of professional identity in our trainees.

Materials and Methods:

Semi-structured interviews were conducted with radiologists identified as having personal and social challenges to healthy development of personal identity. Interview questions focused on self-concept and perception from others within the interviewees' sphere of influence. Demographic data included questions addressing privilege, bias, and potential adversity faced during the formative years.

Results:

Five semi-structured interviews were conducted with radiologists on non-traditional paths. Candidates were chosen to represent an array of challenges: gender, sexual orientation, ethnicity, religion, socioeconomic status, and age. All interviewees learned during training that the most important metrics to ensure success in the field related to the number of published manuscripts, the value and number of external grants, and number of invitations to present lectures and research. None identified professional identity development as a focus of their fellowship training. Qualitative methods involved coding interview transcripts using grounded theory leading to key themes identifying potential roadblocks to the development of professional identity including gender expectations, lack of connection with a mentor or sponsor, feeling of lacking a voice, etc (as given in Table 1).

Conclusion:

It is time to design our radiology training to include healthy development of professional identity. This requires a concerted effort to embrace the intersectionality of traditional metrics for academic achievement, as well as elements that define the personal self.

Poster: SCI-012

SOCIETY FOR PEDIATRIC RADIOLOGY FELLOWSHIP SURVEY - A FOCUS ON WHAT'S BEHIND OUR CAREER CHOICE

SYED Hussaini, MARIA Velez-Florez, JANET Reid
Children's Hospital of Philadelphia, Philadelphia, USA

Purpose

Pediatric radiology residency training varies greatly between institutions. Our purpose was to identify training factors that attract candidates to pediatric radiology in order to inform a revised curriculum that best showcases pediatric radiology regardless of institution.

Materials and Methods

Mixed methods prospective design was employed. An anonymized on-line questionnaire was distributed to members of the Society for Pediatric Radiology through the Education Committee. Multiple choice and free text questions assessed when and why participants developed interest in pediatric radiology and focused on time points before and during radiology residency. The survey was open for one month with a reminder at 2 weeks. Free text responses underwent thematic analysis.

Results

275 total completed surveys were received (26% response rate). Most respondents entered pediatric radiology fellowship immediately following radiology residency (83%) and were at least 5 years into practice (74%). A common theme among those interested in pediatric radiology before radiology residency was preceding exposure/interest in pediatric medicine. Most of those not interested in pediatric radiology expressed unfamiliarity with the sub-specialty. 56% rotated in radiology at a free-standing children's hospital. Most rotated less than 3 weeks in pediatric radiology in their first year of residency. 81% developed an interest in pediatric radiology during radiology residency, 68% within their first 2 years. 65% stated their residency experience significantly increased their interest in pediatric radiology. Common themes that attracted current SPR members were an interest in pediatric pathology, relationships with referring clinicians, and a mentor in the field.

Conclusions

Pediatric radiology is a sub-specialty that is under-recognized with misconceptions about its complexity. Most gain interest in pediatric radiology in the first 2 years of residency. Based on these observations we propose curriculum change to grow the specialty's pipeline such as encouraging earlier rotations through pediatric radiology. Rotation at a free-standing children's hospital may not be as influential in attracting residents to the sub-specialty.

Poster: SCI-013

PATIENT FEEDBACK IN PEDIATRIC RADIOLOGY - A PERFORMANCE ANALYSIS

MICHAEL GEORG Grasser, ERICH Sorantin, JANA Lacekova, ARIANE Hemmelmayr
Division of Pediatric Radiology, Department of Radiology, Medical University of Graz, Graz, AUSTRIA

Purpose of learning objective

The aim of the study was to create a performance analysis in a pediatric radiology academic unit in Austria by analyzing patient satisfaction surveys, which were conducted from 2014 to 2020 in a regular manner.

Methods and Materials

All pediatric referrals, respectively their adult representatives, were asked to complete a questionnaire consisting of 10 questions in a monthly manner. Seven of these were closed questions rated by a scale from 1 (best) to 4 (worst). Furthermore, patients were asked about their experience regarding the waiting time and to what extent they were informed about the procedure itself and the radiation exposure. Another closed question evaluated, if this unit would be recommended to others. The last four were free text questions to collect personal recommendations and feedback.

Results

In the observation period a total of 297,058 examinations were performed and 3,917 completed questionnaires were collected, which represents a response rate of 1.32%. The overall rating for the scaled multiple choice questions was 1.21.

95.2% of the respondents claimed to be sufficiently informed about the procedure and radiation exposure as well as 98.2% of them would recommend the facility to others. The waiting time before the examination was described either as short, appropriate or acceptable by 97.5% of all patients.

Conclusion

The well-being of a child is essential for the quality of pediatric imaging. The pediatric radiology team has examined all influencing factors, such as environment, procedure information and waiting time. Moreover, team dedication is an important factor. Apart from medical and technical aspects, it has been shown that in pediatric radiology high satisfaction of patient or adult representatives can be achieved through careful management and monitoring tools.

Limitations

The perception of an examination can vary between pediatric patients and adults. Therefore, the answers to our questions might differ based on who completed the questionnaire.

Poster: SCI-014

TWO-DIMENSIONAL (2D) SHAPE-FEATURES CAN QUANTIFY THE SEVERITY OF LIVER DISEASE IN CHILDREN WITH AUTOSOMAL RECESSIVE POLYCYSTIC KIDNEY DISEASE (ARPKD) ASSOCIATED CONGENITAL HEPATIC FIBROSIS (CHF)

ADARSH Ghosh, SURAJ Serai, SHYAM Sunder B Venkatakrishna, MOHINI Dutt, ERUM Hartung
Children's Hospital of Philadelphia, Philadelphia, USA

Purpose: the use of MR elastography for follow up of hepatic fibrosis in patients of ARPKD is limited by availability and costs. Changes in liver shape, volume and nodularity has been evaluated as predictors of fibrosis. The morphological changes in congenital hepatic fibrosis (CHF), is however, different from cirrhosis. CHF demonstrates hypertrophy of segment II, III and IV vis-a-vis atrophy seen in cirrhosis. We evaluate the correlation of segment IV/ II and III 2D shape-based features with magnetic resonance elastography (MRE)-derived liver stiffness and portal hypertension (pHTN) in children with ARPKD-associated congenital hepatic fibrosis.

Methods: In a prospective IRB-approved study, 14 children with ARPKD (mean - SD= 13.8 +- 5.8 years) and 14 healthy controls (mean + - SD = 13.7 +- 3.9 years) underwent liver MRE. To quantify the hypertrophy and change in shape of segment IV/ II and III, a 2D region of interest (ROI) outlining the liver at the level of the abdominal aorta was drawn on sagittal T2w images. Eight shape features (perimeter, major axis length, maximum diameter, perimeter to surface ratio (PSR), elongation, sphericity, minor axis length, and mesh surface) describing the ROI were calculated. Spearman's correlation was calculated between shape features and MRE-derived liver stiffness (kPa) (n = 28). Shape features were compared between participants having ARPKD with pHTN (splenomegaly and thrombocytopenia), (n = 4) and without pHTN (n = 8), using the Mann Whitney-U test.

Results: In ARPKD participants and healthy controls, all eight shape features, except elongation, showed moderate to strong correlation with liver stiffness (kPa); the perimeter surface ratio had the strongest correlation ($\rho = -0.75$, $p < 0.001$). In ROC analysis, PSR had an area under the ROC curve (AUC) of 1.0 (95% CI: 0.88 to 1.00) in identifying ARPKD participants with liver stiffness > 2.9 kPa, the cut off used for fibrosis in children. Individuals with pHTN had a lower median PSR (mean+- SD = 0.05 ± 0.01) than those without (0.07 ± 0.01 ; $p = 0.027$) with an AUC of 0.91 (95% CI: 0.60 to 0.99) in differentiating the participants with and without pHTN.

Conclusion: Hypertrophy of segment II, III and IV is a known feature of CHF. Shape-based quantification of the extent of segmental hypertrophy shows potential as non-invasive biomarkers of liver fibrosis and portal hypertension in children with ARPKD.

Poster: SCI-015

PREDICTORS OF PEDIATRIC RADIOLOGY EXAM ORDER AND COMPLETION DURING THE COVID-19 PANDEMIC

SEBASTIAN Gallo-Bernal, FEDEL Machado-Ricas, DANIEL Briggs, OLEG Pinykh, MICHAEL S. Gee
Massachusetts General Hospital, Department of Pediatric Radiology, Boston, USA

Purpose: we aimed to evaluate the impact of the COVID-19 pandemic on the type of pediatric imaging exams ordered as well as the likelihood of exam completion.

Materials: A single academic tertiary care pediatric center database was queried to identify pediatric (<18 years) imaging exam orders from 9/15/19-3/15/20 (pre-COVID), and from 5/01/20-9/1/20 (COVID-19 period). Exam completion rate was recorded and classified according to a) age (neonatal, infant, early childhood, late childhood, and adolescents); b) modality (fluoroscopy, MRI, radiography, nuclear medicine, ultrasound, or CT); c) indication (fever/infectious, trauma, non-trauma pain, oncologic, congenital/developmental); and d) need for anesthesia/ sedation. Exam distribution and predictors associated with exam completion were analyzed using a multivariate logistic regression.

Results: 16,629 exam orders corresponding to 9,043 pediatric patients were analyzed (15,424 baseline period; 1,205 COVID-19 period). Exam orders during the pandemic were associated with younger patient age, with a significant increase in infant (47.32%, $P<0.001$) and early childhood patients (30.46%, $P<0.001$), and a lower proportion of adolescents (-14.93%, $P<0.001$). An increase in the proportion of CT (32.59%, $P<0.001$) and ultrasound orders (33.18%, $P<0.001$), and decreased radiography orders (-12.55%, $P<0.001$) was also noted. Orders for exams due to oncologic (37.18%, $P<0.001$) and congenital/developmental disorders (51.50%, $P<0.001$) had a proportional increase, while a lower proportion for non-traumatic pain exam orders (-16.06%, $P<0.001$) was seen. The proportion of orders for studies under anesthesia doubled (118.07%, $P<0.001$) versus the baseline period. Regarding exam completion likelihood, neonatal exam orders in the baseline (OR 0.457) were less likely to be completed ($P<0.001$) than in the pandemic period (OR 1.960). MRI orders in the baseline period (OR 0.261) were less likely to be completed ($P=0.049$) than in the pandemic period (OR 0.502). In contrast, fluoroscopy orders in the baseline period (OR 0.524) were more likely to be completed ($P=0.011$) than in the pandemic period (OR 0.095).

Conclusions: This analysis identifies a distinct shift in radiology exam order distribution during the COVID-19 pandemic and identifies a sub-set of exams that are more resilient to cancellation. This analysis proposes a framework of pediatric radiology resource allocation for future pandemics and other times of acute resource limitation.

Poster: SCI-016

EVALUATION OF INTER-READER REPRODUCIBILITY FOR DETECTION AND LABELING OF PEDIATRIC RIB FRACTURES ON RADIOGRAPHS

GAURAV Gadgeel¹, JONATHAN Burkow¹, FRANCISCO Perez², JOSEPH Junewick³, ANDREW Zbojniec³, JEFFREY Otjen², ADAM Alessio¹

¹ Michigan State University- Department of Computational Mathematics, Science, and Engineering, East Lansing, USA

² Seattle Children's- Department of Radiology, Seattle, USA

³ Spectrum Health- Department of Radiology, Grand Rapids, USA

Background: Child abuse is a serious problem in the USA with rib fractures being a common injury. Rib fractures can be challenging to detect on pediatric chest radiographs, with estimates suggesting that up to 40% of fractures are missed. There is limited knowledge about the inter-reader reproducibility for rib fracture interpretation. Furthermore, we are developing automated, machine-learned methods for fracture detection. In

order to gauge performance of these methods, we must understand radiologist performance for this same detection task.

Methods: In an IRB-approved study, 195 fracture-present pediatric chest radiographs were included. These images contained predominately male patients (64% male) with a distribution of ages (median, mean+/-std [range]: 0.5, 1.1 +/- 1.9 [0 – 18] years of age) reflective of patients who present with rib fractures at a pediatric hospital. Four board-certified pediatric radiologists independently labeled with rectangular regions of interests the margins of fractures in each image without knowledge of fracture presence or location. Each image was evaluated by two separate radiologists. We analyzed the detection reproducibility between readers with the free-response kappa, a measure of agreement beyond chance when only positive findings are reported.

Results: Readers detected a median of 4.0 rib fractures per image (Read 1: IQR: 2 to 7) (Read 2 IQR: 2 to 6). ROIs were deemed in agreement when they shared at least a 30% intersection over union. Of the ROIs that were in agreement, the average percent overlap between labels was 79%, indicative of similar interpretations of the fracture size. Treating the first read as a reference, the sensitivity of the second read was 0.76 with an accuracy of 0.62. The free-response kappa of the readers was 0.76.

Conclusions: While the accuracy of the second reader compared to the first for individual fracture detection was modest, the free-response kappa of 0.76 reveals a high level of agreement. Unlike conventional Cohen's kappa scores for inter-reader agreement used for whole image classification, a free response kappa value greater than 0.5 is considered a substantial agreement for the task of detecting multiple locations of pathology. This work suggests that while rib fracture detection is challenging, radiologists mostly agree on location, size, and number of fractures. Thus, this suggests that radiologist labeling can provide a valid reference to develop machine learned models.

Poster: SCI-017

DO THE “EYES HAVE IT”? “SEEING“ PEDIATRIC CT PERFORMANCE IMPROVEMENT OPPORTUNITIES THROUGH AN AUTOMATED QUALITY AND RADIATION DOSE TOOL

DONALD Frush¹, JAYNE Seekins², AIPING Ding¹, PREET Patel³, ARMISTEAD Sapp¹, EHSAN Samei¹

¹ Duke University Medical Center, Durham, USA

² Lucile Packard Children's Hospital at Stanford, Palo Alto, USA

³ Duke University School of Medicine, Durham, USA

Purpose: As generalized CT performance is assessed almost entirely through dose, with occasional observer review, the purpose was to implement an automated CT quality (noise) and dose metric tool at a 361 bed academic women's and children's hospital.

Methods: A proprietary tool that automatically assesses each CT exam for quality using a validated recon kernel specific global noise paradigm, a localizer-derived effective diameter (E.diam), and customary DICOM dose metrics (CTDIvol/DLP) was implemented without any necessary adjustments in conventional existing IT platforms. Data were reviewed for a 1 yr period ending 3/15/21. Global noise value and CTDIvol were displayed relative to 25, 50 and 75% determined from the total protocol data spread with outliers using a dose deviation index (DDI): CTDIvol actual - CTDIvol expected (pooled data)/CTDIvol expected. Outliers were defined by <-0.8 or >0.8 .

Results: For the 2155 pediatric CT examinations - all but 38 on the primary a CT scanner (Siemens Flash) - 92 total protocols were mapped. The most common body and brain exams were chest Flash $<55\text{kg}$ ($n=375$; 17.4%) and head CT 6-18yr ($n=144$; 6.7%). Protocols with occurrence $<3\%$ were mapped to “other” ($n=770$; 34.5%). Additional % curves (e.g. 5, 95%) can be customized. There were 364/2155 (1.7%) outliers distributed as: daily QI: 47.5%; chest/cardiac 19%; chest abdpelvis 13.2%; neuro 10.4%; intervention 8.8%; abdpelvis 1.1%. The neuro and chest/cardiac outliers when adjusted for

total occurrence were 2.1% (8/374) and 6.9% (10/144) of the protocol total, respectively. As an example of cross referencing, a chest Flash <55kg exam with a high outlier (CTDIvol 4.55 mGy; expected appx 1.9 mGy), had global noise between 75 and 95% and not low noise as predicted and therefore not necessarily warranting further investigation.

Conclusions: A vendor-generic, practice-configurable and easily implemented tool supplies customary metrics of radiation exposure with an additional benefit of individual examination quality. This tool affords more efficient identification of protocols with more outliers using both traditional % curves for CTDIvol ranges and customizable outlier thresholds (e.g. DDI) and more appropriate focus on exam outliers for both dose and quality. This automated tool provides advanced and more representative opportunities for assessment of and improvement in pediatric CT performance.

Poster: SCI-018

TOWARDS IMPLEMENTATION OF UNSUPERVISED LESION DETECTION OF PEDIATRIC CANCER WITH WHOLE BODY MRI SCREENING BY INCORPORATION OF 3D CONTEXT

SAYALI Joshi¹, ALEX Chang¹, ABHISHEK Moturu¹, VINITH Suriyakumar¹, NIPAPORN Tewattanarat², LISA States³, SURAJ Serai³, ANNA Goldenberg¹, ANDREA Doria⁴

¹ The Hospital for Sick Children - Research Institute, Toronto, CANADA

² Srinagarind Hospital - Radiology Department, Khon Kaen, THAILAND

³ Childrens Hospital of Philadelphia - Radiology Department, Philadelphia, USA

⁴ The Hospital for Sick Children - Diagnostic Imaging, Toronto, CANADA

Background: To perform anomaly detection for pediatric wbMRIs is more challenging than for other settings due to difficulties in registration and images involving multiple body regions. While previous generative modelling approaches successfully perform anomaly detection by learning the distribution of healthy 2D image slices, they process such slices independently and ignore the fact that they are correlated, all being sampled from a 3D volume.

Purpose: To develop an AI technique that help detection of cancer lesions as early as possible. We propose using conditional variational autoencoders to model the distribution of noncancerous patients and doing out-of-distribution detection to highlight anomalous cases, i.e. those with cancer in pediatric whole-body MRI (wbMRI).

Methods: We tested the efficacy of the proposed method on a dataset of coronal STIR whole-body MRI provided by a tertiary Children's Hospital containing 535 noncancerous images (22 to 45 slices each for a total of 18012 slices) and 27 annotated images with at least one lesion. Images are preprocessed with histograms. We incorporated the 3D context and processing whole-body MRI volumes to distinguishing anomalies from their benign counterparts. We introduced a multi-channel sliding window generative model to perform lesion detection in wbMRI. We evaluated model performance with the Area Under the PrecisionRecall Curve (AUPRC) and DICE coefficients.

Results: Our proposed method significantly outperformed processing individual images in isolation and our ablations clearly show the importance of 3D reasoning. Processing multiple consecutive slices of 3D volumes significantly improved unsupervised anomaly detection.

Conditioning on patient meta-features can lead to substantial improvements in anomaly detection as observed by a 0.062 increase in AUPRC performance and a 0.047 increase in DICE.

Concerning the inclusion of additional patient specific features in the model we observed that the model benefits from the inclusion of patient's sex (0.061 AUPRC improvement) but including age and weight worsen the model performance.

Conclusion: We were able to successfully perform unsupervised anomaly detection for pediatric wbMRIs using conditional variational autoencoders, 3D context and processing whole-body MRI volumes.

This method holds potential to facilitate the detection of true-positive cancers in patients with cancer predisposition disorders undergoing screening protocols with wbMRI.

Poster: SCI-019

RIB FRACTURE DETECTION IN PEDIATRIC RADIOGRAPHS VIA DEEP CONVOLUTIONAL NEURAL NETWORKS

JONATHAN Burkow¹, GREGORY Holste¹, FRANCISCO Perez², JOSEPH Junewick³, ANDY Zbojniec³, JAMIE Frost³, ERIN Romberg², SARAH Manashe², JEFFREY Otjen², ADAM Alessio¹

¹ Michigan State University - Departments of CMSE and BME, East Lansing, USA

² Seattle Children's Hospital - Department of Radiology, Seattle, USA

³ Spectrum Health - Advanced Radiology Services, Grand Rapids, USA

Purpose:

Detecting rib fractures in pediatric radiographs is a time-consuming process requiring meticulous analysis of images from trained radiologists. Previous studies suggest that radiologists can miss up to two-thirds of rib fractures on chest x-rays. Reliably identifying unsuspected rib fractures is particularly important in infants and young children because it can be a sign of child abuse. Detection methods based on deep convolutional neural networks (CNNs) have the potential to augment the capabilities of radiologists, providing guidance on regions of the image that warrant additional scrutiny.

Materials and Methods:

A dataset of over 500 fracture-present radiographs from Seattle Children's Hospital was curated and processed. Board-certified pediatric radiologists annotated rib fractures using a rectangular region of interest tool on each image to use as ground truth for training the deep CNN. During processing, each image is sent through a U-Net segmentation model previously trained on thoracic cavity regions to crop the thoracic cavity. We use an implementation of the RetinaNet architecture using a ResNet152 backbone pre-trained on ImageNet.

Results:

The dataset was split into training, validation, and test sets of 376, 75, and 51 images, respectively. The test set of 51 patients contained a total of 244 fractures. After training for 100 epochs, the RetinaNet model correctly identified 159 fractures on the test set using a 50% confidence threshold, achieving an accuracy of 0.49, sensitivity of 0.64, and precision of 0.68. Of the 159 accurately identified fractures, the predicted boxes from the model on average covered 80.4% of their corresponding ground truth boxes.

Conclusions:

Preliminary results show that there is promise for the implementation of deep CNNs for augmenting pediatric rib fracture detection. Efforts are ongoing to enrich the diversity in the data sets and improve performance of the detection model.

Poster: SCI-020

ESTABLISHING A WHOLE BODY MRI REPOSITORY FOR CHRONIC NON-BACTERIAL OSTEOMYELITIS (CNO)

MARIAM AL-Dajani¹, KAREN Alexander², OLGA Carpio¹, AMIE Robinson², MICHAEL Gee³, GOVIND Chavhan¹, SHERWIN Chan², MARY-LOUISE Greer¹

¹ The Hospital for Sick Children, University of Toronto, Toronto, CANADA

² Children's Mercy Hospital, University of Missouri-Kansas City, Kansas City, USA

³ Massachusetts General Hospital, Harvard Medical School, Boston, USA

Background:

Small patient populations can limit evaluation of pediatric diseases. Conventional multicentre studies permit larger patient cohorts to be assessed but are confined by initial study parameters and varied access to source data. Technological advances in recent years have enabled large volumes of data to be rapidly transferred, stored and retrieved leading to creation of centralized imaging repositories now used by healthcare networks. The purpose of this study is to assess the feasibility of creating a multicentre pediatric imaging research repository (PIRR).

Objectives:

To identify processes required to establish a PIRR using Whole-Body Magnetic Resonance Imaging (WBMRI) in Chronic Non-bacterial Osteomyelitis (CNO).

Methods and material:

A pediatric patient population likely to benefit from multicentre, longitudinal analysis was selected as a pilot cohort to guide larger PIRR development. A working group identified institutions for housing and/or populating the PIRR. A study proposal and manual of operations were created, data variables defined following literature review. Operational steps, staffing and software needs were recorded.

Results:

Patients < 18 years undergoing WBMRI for suspected or confirmed CNO were identified as a suitable cohort for a PIRR, to facilitate WBMRI protocol standardization and development of image-based grading of disease severity. One institution was identified to house the PIRR, 3 to contribute data. Four core areas were identified as central to the PIRR:

1. Ethics review board (ERB) approval and institutional data-sharing agreements
2. Access to a centralized data collection platform
3. Consensus on data collection items and definitions
4. Institutionally-approved image de-identification and upload software

Barriers included single versus multi-institutional ERB approval and data-sharing agreements. Defining and refining data collection items required close collaboration to capture site-specific variations in patient chart terminology and MRI acquisition parameters. Training streamlined data entry and image upload of 110 patients to date. PIRR data analysis and WBMRI review capabilities will be assessed in the next phase.

Conclusion:

Creation of an international PIRR is feasible although initially time and resource intensive. Guidelines for different institutional requirements can facilitate inclusion of more sites, building larger patient cohorts and enhancing multicentre research in pediatric radiology.

Poster: SCI-021

PERFORMANCE OF DEEP LEARNING MODEL USING ENSEMBLE METHOD FOR PEDIATRIC BONE AGE ASSESSMENT

KRISHNA PANDU Wicaksono¹, IDO NARPATI Bramantya², MOHAMAD YANUAR Amal²

¹ Department of Radiology, Kyoto University, Kyoto, JAPAN

² Department of Radiology, University of Indonesia, Jakarta, INDONESIA

Objective:

To evaluate a deep learning model's accuracy using the ensemble method in assessing pediatric bone age.

Materials/methods:

We used a publicly available dataset provided by the Radiological Society of North America (RSNA) comprised of 12,611 hand x-ray images as training data and 1,425 validation images. Each was labeled with gender and bone age. We developed a model based on three Keras models: InceptionV3, Xception, and InceptionResNetV2. Images were preprocessed to 500x500 resolution without changing the anatomical aspect ratio. Gender inputted as a binary, and its tensor was concatenated to the last convolutional layer's output of each base model. Each base

model output then ensemble using a weighted average approach. The model was trained for 50 epochs using Adam optimizer and mean absolute error (MAE) as metrics. We used 200 hand x-ray images from the RSNA test dataset to evaluate model accuracy. Twenty-four images were randomly chosen and evaluated blindly by two pediatric radiologists. Accuracy of the model and the radiologist's assessment were compared. Results:

Our ensemble model yielded an MAE of 4.18 months, markedly improved from the individual base model's MAE of 4.78, 4.90, and 5.15 months (InceptionV3, Xception, and InceptionResNetV2, respectively). Almost 98% of model predictions were within a 1-year range to the reference. On 24 subset images, our model can predict the bone age with 4.40 months MAE, exceeding the radiologist performance of 7.60 months MAE.

Conclusions:

Using the ensemble method, a deep learning model demonstrated state-of-the-art accuracy in performing bone age assessment, even exceeding radiologist performance.

Poster: SCI-022

PREFERENCE MATRIX ANALYSIS OF OUTSIDE IMAGING WORKFLOW

MARLA Sammer, NILESH Desai, VICTOR Seghers, THIERRY Huisman, ANDREW Sher

Texas Children's Hospital, Baylor College of Medicine, Houston, USA

Purpose: To share our experience at a quaternary care pediatric academic center in using a formal decision making process to shape outside imaging workflow. Formal decision-making processes such as preference matrices can provide objectivity for departmental operational decisions. The preference matrix is useful in decisions involving multiple criteria that cannot be evaluated with a single value metric.

Methods & Materials: Alternative scenarios for outside imaging were outlined to assess the performance of the outside imaging workflow. Alternatives were defined for sequential decision categories: Storage Type, Storage Length, Exam Disposition, Type of Report, and Report Disposition. Options were scored according to 5 performance criteria: mitigation of patient harm, operations compatibility, investment requirement, accessibility, and potential for increased market share. Prior to scoring the options, weights were assigned to each criterion based on perceived importance. The highest scored alternative of each decision category informed the options for the next step.

Results: Itemized weights and scores are provided in Figure 1 with highest possible score of 100, summarized as follows. Storage type: CD's in file room: 19.0, Upload studies onto PACS 85.0. Storage length: Same length as local studies 83.5, Limited time 41.0. Exam disposition: Available for reference only 51.0, Available with second interpretation only 58.0, Available either for reference or second interpretation 83.0. Report type: Limited response to initial report 51.5, Comprehensive report to same standards as local reports 73.5. Report disposition: Unbilled reports, 66.5, Billed reports 83.0.

Conclusions: Our outside imaging workflow preference matrix analysis suggests the preferred workflow is storing outside studies on PACS for the same length of time as locally performed studies. Studies may be stored for reference or a formal interpretation, which if performed would be reported and billed similarly to locally performed exams. Our experience in using the decision-making process shared here can inform other pediatric hospitals in their outside imaging workflow decisions.

Poster: SCI-023

COMPARISON OF FERUMOXYTOL CONTRAST-ENHANCED MAGNETIC RESONANCE ANGIOGRAPHY WITH CONVENTIONAL CONTRAST ENHANCED CTA IN

CONGENITAL CARDIOVASCULAR DISEASE

ERIC Morgan, RAMKUMAR Krishnamurthy, ERIC Diaz, RAJESH Krishnamurthy
Nationwide Children's Hospital, Columbus, USA

Since its clinical availability in 2009, there has been increasing use of ferumoxytol as a blood pool contrast agent in contrast-enhanced magnetic resonance angiography (CEMRA). In our institution, we have actively engaged in the utilization of ferumoxytol in CEMRA imaging of congenital cardiovascular disease, and, in some cases, have chosen to utilize CEMRA with ferumoxytol in addition to conventional contrast enhanced CTA. In this educational exhibit, we present several cases with both CTA images and CEMRA images obtained from the same patients, highlighting key differences in the appearance and visibility of the evaluated pathologies.

Poster: SCI-024

RIGHT CIRCUMFLEX AORTA AND AORTIC COARCTATION IN AN INFANT: A CASE REPORT

LAURA Acosta-Izquierdo¹, MARIA CLARA Escobar-Diaz², FLAVIO Zuccarino³

¹ Medical Imaging, CHEO, University of Ottawa, Ottawa, CANADA

² Department of Cardiology, Hospital Sant Joan de Deu, Barcelona, SPAIN

³ Department of Radiology, Hospital Sant Joan de Deu and Hospital del Mar, Chief of Cardiothoracic Radiology, Barcelona, SPAIN

Purpose/Background:

Right aortic arch anomalies are rare in the general population, with an unusual association with aortic coarctation. This case demonstrates an infrequent cause of a vascular ring in a child with right circumflex aortic arch and aortic coarctation and highlights the importance of presurgical imaging for better assessment and operative planning.

Educational objectives:

To briefly review the embryology of the aortic arch.

Demonstrate the relevant features of the right aortic arc anomalies.

Illustrate a paediatric case of right circumflex aortic arch with aortic coarctation.

Conclusion:

Although the right circumflex aorta with an aortic arch coarctation is a rare anomaly, it is essential to recognize it in a timely fashion, look for other vascular and cardiac associations due to the multisystemic complications that can arise from the vascular ring. Understanding the embryology and depicting the anatomy in cross-sectional imaging for an accurate diagnosis guides the management and helps the surgeons for optimal surgical repair if needed.

Poster: SCI-025

KAWASAKI DISEASE AND PAEDIATRIC INFLAMMATORY MULTISYSTEM SYNDROME: TEMPORALLY ASSOCIATED WITH SARS-COV-2 (PIMS-TS) – RARE CAUSES OF PAEDIATRIC CORONARY ARTERY ANEURYSMS: TWO CASE REPORTS USING CTCA

DIVYA Vaid¹, REEM Bedir¹, SUMIT Karia¹, YING HUI Chee², JUDITH Babar¹, MARIA TA Wetscherek¹

¹ Department of Radiology, Cambridge University Hospitals NHS Foundation Trust, Cambridge, UNITED KINGDOM

² Department of Paediatric Medicine, Cambridge University Hospitals NHS Foundation Trust, Cambridge, UNITED KINGDOM

Coronary artery aneurysms (CAA) are rare in the paediatric population. A well-known cause is Kawasaki's disease (KD), a vasculitis of unknown aetiology involving medium-sized arteries and affecting mainly children

<5 years old. Recently CAA have also been demonstrated in a new entity – Paediatric Multisystem Inflammatory Syndrome: Temporally associated with SARS-CoV-2 (PIMS-TS). This has emerged in mainly older children with prior exposure to SARS-CoV-2 with Kawasaki-like disease spectrum.

We describe two cases of KD and PIMS-TS focusing on distinct patterns of aneurysmal coronary arteries on Computed Tomography Coronary Angiography (CTCA).

Case 1: A 13-year-old boy who presented in infancy with features typical of KD, defined by the American Heart Association and was noted to have giant RCA and LAD CAA. He developed myocardial infarction aged 4 years which prompted bypass-grafting and long-term aspirin therapy. Surveillance scans with CTCA and MRI were performed.

Case 2: A 17-year-old girl, transferred to the paediatric ICU of our hospital with one week history of fever, headache, joint pains and intermittent abdominal pain. She had red conjunctivae on examination with tachycardia and tachypnoea. The inflammatory markers, troponin/NT-proBNP and D-dimer were significantly elevated; negative RT-PCR and positive SARS-CoV-2 antibody on admission. She was diagnosed with PIMS-TS based on the Royal College of Paediatric and Child Health Criteria. Echocardiogram and CTCA were performed during admission.

Case 1 displayed calcified giant aneurysms of the RCA measuring 16mm and LAD measuring 10mm with normal ostia and interposing segments between the aneurysms. The LIMA and RIMA bypass-grafts to distal LAD and RCA respectively were patent. Enlarged bilateral hilar and mediastinal lymph nodes measuring up to 2cm were also noted, which have remained stable for following 3 years on CT and MRI.

Case 2 showed uniformly dilated right and left coronary arteries in keeping with coronary artery ectasia (Z score for LMS 2.6, LAD 3.7, LCX 3.1 and RCA 2.6; normal <2). The LMS ostium was ectatic at 6mm. No focal aneurysms were seen and the distal segments were spared.

The novel condition described in children called PIMS-TS shows overlap in clinical features and manifestations with other inflammatory disorders such as KD. Cardiac involvement with aneurysmal coronary arteries is described in both diseases, but there is a distinction in the pattern of involvement as shown in our cases.

Poster: SCI-026

ROLE OF ULTRA HIGH PITCH FAST CT ANGIOGRAPHY IN IMAGING POST-OPERATIVE CONGENITAL HEART DISEASE

SIDDHI Chawla, RENGARAJAN Rajagopal, TARUNA Yadav, PUSHPINDER Khara

All India Institute of Medical Sciences, Jodhpur, INDIA

PURPOSE: With advancement in surgical techniques and increased survival of children operated for congenital heart disease (CHD), cross sectional imaging plays a central role in follow up and for early detection of complications. With the advent of dual source CT, faster table speeds have been achieved resulting in lower temporal resolution. We evaluated the diagnostic ability of ultra high pitch prospective ECG gated fast CT scanning technique for morphological evaluation of children with operated CHD, presenting with recurrent or worsening symptoms.

METHODS: This was a retrospective study of 35 children with operated CHD (post modified Blalock Taussig shunt, Glenn shunt, ASD closure etc) aged between 4 months and 10 years. All scans were acquired with mild intravenous sedation or without sedation. Intravenous iodinated contrast (1 – 1.5ml/kg) was injected using 22/24G cannula with a half dose chaser. Data acquisition was by an ultrahigh pitch ECG gated fast prospective scan at 40% RR interval, followed by a non-ECG gated ultrahigh pitch fast scan (Siemens Flash, Germany). The scans were interpreted by two radiologists, blinded to the acquisition techniques. For subjective

evaluation, interobserver agreement was calculated using Kappa scores with discrepancies resolved by consensus.

RESULTS: For the morphological evaluation of the post-operative status, the interobserver agreement was excellent. The complications which were seen in children after modified Blalock Taussig shunt were thrombosis, shunt occlusion, shunt seromas and aneurysmal degeneration. In children with Glenn shunt, shunt thrombosis was seen in one fifth of patients, with normal shunt morphology in rest of the patients. Children with Fontan failure had large aorto-pulmonary collaterals and veno-venous collaterals as a cause for failure.

CONCLUSION: In conclusion, ultra high pitch fast CT scanning is a quick and safe imaging technique with lower radiation dose for imaging children with operated congenital heart disease.

Poster: SCI-027

COMPARISON OF FERUMOXYTOL ENHANCED 4D FLOW TECHNIQUE VS TRADITIONAL 2D IMAGING CARDIAC MRI STUDY ACQUISITION TIMES IN PEDIATRIC PATIENTS

ERIC Morgan, RAMKUMAR Krishnamurthy, ERIC Diaz, RAJESH Krishnamurthy
Nationwide Children's Hospital, Columbus, USA

Background: One of the prevailing limitations of pediatric cardiac MRI (CMRI) is the length of time required to complete a diagnostic study. Newly developed imaging methods, including 4D flow imaging, show promise in reducing image acquisition times while maintaining diagnostic image quality. Here, we compare conventional 2D and 4D imaging results and image acquisition times in the same patients.

Methods: 7 pediatric patients with various indications undergoing CMRI were imaged with both traditional 2D imaging techniques and with a 4D flow sequence with ferumoxytol as a blood pool contrast agent. Total acquisition times for the 2D and 4D flow sequences were recorded. Traditional 2D sequences obtained included: short axis, 2 chamber, 3 chamber, 4 chamber, and phase contrast (PC) imaging of the ascending aorta, superior vena cava, descending aorta (all three obtained from a single "3-Vessel plane"), and main pulmonary artery and branch pulmonary arteries. The same 4 views and PC data were derived off-line from the single 4D Flow contrast enhanced sequence. Results from 2D and 4D flow data were internally validated, and the study length times were compared. Data are expressed as Average \pm SEM. **Results:** There were no significant differences in diagnostic data derived from the 4D flow images when compared to 2D images. The total acquisition time for all 2D sequences combined averaged 16.8 \pm 0.2 minutes, while the average acquisition time for the 4D flow sequence was 7.4 \pm 0.2 minutes ($p < 0.005$). **Conclusions:** 4D Flow imaging with ferumoxytol allows for significantly shortened CMRI imaging times in the pediatric population while providing data equivalent to that of 2D imaging. These findings are of key importance as they may allow for imaging of patients who cannot tolerate long scan times and may reduce or even possibly eliminate the need for anesthesia in some patients.

Poster: SCI-028

CONTRAST PROTOCOL OPTIMISATION IN FONTAN CIRCULATION COMPUTED TOMOGRAPHY PULMONARY ANGIOGRAPHY

LUCY Boyle, MARK Hamilton, CARINA Brolund-Napier, SOPHIE Watson
Bristol Royal Infirmary and Bristol Heart Institute, Bristol, UNITED KINGDOM

A fontan circulation is the result of several stages of surgical procedures to palliate a functional single ventricular congenital cardiac system. It diverts systemic venous return directly to the pulmonary arteries, allowing the single

ventricle to supply the systemic arteries. The resulting anatomy includes a conduit system, bypassing what would conventionally be the right ventricle. These patients are at increased risk of thrombosis due to altered flow mechanics and the presence of foreign graft/stent material. The ability to obtain optimum angiographic imaging of these patients is therefore paramount. However, the fontan circulation presents challenges in contrast enhanced imaging due to the altered cardiovascular physiology.

We present a retrospective cohort of computed tomography pulmonary angiogram (CTPA) studies in patients with fontan circulation using a contrast protocol devised using magnetic resonance imaging time resolved angiography by Duerden et. al (Journal of Cardiovascular Computed Tomography, 2020). This study aims to assess the adequacy of the contrast protocol with a view to optimise imaging of these patients with complex cardiovascular anatomy.

The proposed contrast and computed tomography (CT) scan protocol comprised scanning at a low kV (e.g. 80kV), with a contrast strength per kg body weight of > 800 mg/kg and a scan delay of 70 seconds following the contrast bolus.

Demographic, contrast and scan data were collected and CT attenuation measured in multiple vascular a background tissues. Initial analysis of the studies compared the contrast dose per kg body weight to the attenuation in the fontan conduit and left pulmonary artery.

Results revealed increased attenuation in the conduit and pulmonary artery with increased contrast dose/kg at all contrast delay timings and specifically at a delay of 70-80 seconds. Attenuation values in the target regions in the scans using the above protocol were > 250 HU.

250 HU is considered adequate, diagnostic opacification in standard CTPA studies. Using this protocol, this standard was obtained in the complex circulatory anatomy of the fontan circulation. Initial assessment of the protocol supports its use in this specific group of patients.

Poster: SCI-029

INFRACARDIAC TYPE TOTAL ANOMALOUS PULMONARY VENOUS RETURN: CASE REPORT OF THE RARE CONGENITAL CARDIAC ANOMALY

ZUHAL Bayramoglu, EZGI Kara, ESHGIN Sahibli, SEÇKIN Çobanoğlu
Istanbul University, Istanbul Medical Faculty, Radiology Department, Istanbul, TURKEY

Total anomalous pulmonary venous return (TAPVR) is a rare congenital heart anomaly in which all pulmonary veins fail to drain into the left atrium. We describe a case of infracardiac type TAPVR, diagnosed with computed tomography angiography findings.

TAPVR is a cyanotic congenital heart anomaly in which all four pulmonary veins do not connect normally to the left atrium. TAPVR is divided into different types depending on how and where the pulmonary veins flow to the heart. The less common infracardiac type accounts for 13 to 24% of cases. TAPVR can be misdiagnosed as respiratory distress syndrome or persistent fetal circulation.

A full-term female newborn, obtained by C-section, developed progressive central cyanosis with respiratory distress during the early hours of life. On physical examination, the patient appeared dyspneic, cyanotic, and presented poor peripheral perfusion. On auscultation, she had a regular cardiac rhythm and a generalized constant heart murmur. A chest x-ray was performed, but it was not diagnostic for lung or heart disease. A computed tomography angiography was ordered and it showed an infracardiac total anomalous venous return with drainage to the left branch of the vena porta. There was a long segment confluent vein between the confluence of the pulmonary veins and the left portal vein. Hypoplastic ascending aorta and the aortic arc were observed. Also, a patent ductus arteriosus was confirmed. The patient was taken to surgical repair. TAPVR is a rare congenital cardiac anomaly. An interatrial communication with an atrial septal defect or patent foramen ovale is required for survival. To

achieve early diagnosis, computed tomography angiography has a crucial role. TAPVR treatment is important for a successful outcome.

Poster: SCI-030

DUAL-ENERGY CT EVALUATION OF PEDIATRIC THORACIC DISORDERS: CLINICAL APPLICATIONS WITH EMPHASIS ON UP-TO-DATE PRACTICAL TECHNIQUES AND ADDED DIAGNOSTIC VALUE

PATRICK Tivnan¹, ABBEY J. Winant², DOMEN Plut³, EDWARD Y. Lee²

¹ Department of Radiology, Boston Medical Center, Boston, USA

² Department of Radiology, Boston Children's Hospital, Boston, USA

³ Clinical Institute of Radiology, University Medical Centre, Ljubljana, SLOVENIA

Purpose: Dual energy CT (DECT) is a cutting edge CT technology which utilizes simultaneous or sequential CT scanning performed with multiple energy levels. Scanning at different energy levels allows for calculation of different tissue attenuation. DECT technology has important implications for pediatric imaging because it has the potential to eliminate the need for multiphase CT scanning, substantially reducing radiation dose. In addition, lung perfusion mapping, soft tissue vascularity assessment, and metallic artifact reduction capabilities are other potential benefits of DECT. This educational exhibit presents practical clinical applications of DECT for evaluating pediatric thoracic disorders, with an emphasis on up-to-date imaging technique and added diagnostic value.

Material and Methods: Our educational exhibit provides an up-to-date summary of the currently available evidence of the practical role of DECT in pediatric thoracic imaging. In addition, our exhibit reviews the currently available types of DECT, focusing on salient differences and unique advantages. Lastly, our presentation discusses the types of image sets that can be generated with DECT technology, with an emphasis on added diagnostic value in specific clinical scenarios.

Results: This practical summary of the pearls and pitfalls of DECT in pediatric thoracic imaging aims to provide fundamental knowledge to practicing radiologists for employing this new CT technique for enhanced pediatric patient care. Up-to-date information regarding the three distinct DECT technologies currently existing on the market is presented to improve radiologists' understanding of this new CT technique. Improved understanding of DECT and its unique capabilities to optimize evaluation of various pediatric thoracic disorders is essential information for practicing radiologists to provide optimal pediatric patient care.

Conclusion: DECT technology has important benefits that can be especially valuable for pediatric thoracic imaging. Clear understanding of up-to-date DECT imaging techniques as well as its practical clinical applications, including the potential to reduce CT radiation dose and added diagnostic value, has great potential for enhancing pediatric patient care.

Poster: SCI-031

INVESTIGATING CONGENITAL LUNG LESIONS IN INFANTS; AUDIT OF CT PROTOCOL AND DOSE

LEANNE Royle, ZONAH Khumalo, GORDON Culham
B.C. Children's, Vancouver, CANADA

Purpose: To review adequacy of CT chests at B.C. Children's when investigating for congenital lung lesions in infants and compare the

radiation doses of these studies to diagnostic reference range suggested by Strauss et al 2017.

Materials and Methods: 23 CT chests performed at B.C. Children's from December 2019 to November 2020 to investigate for congenital lung lesions. The details of the scan, contrast usage and radiation dose were collated and compared to the DRLs. The diagnostic quality of the images were assessed by 3 staff radiologists and a fellow.

Results: All CT chests were considered adequate quality, however there was a variation in the radiation doses and contrast usage.

Conclusion: We suggest a guideline for CT chest in infants under 2 years old when investigating for congenital lung lesions, to use contrast and radiation efficiently and obtain diagnostic images using as low a dose as possible.

Poster: SCI-032

HIGH-RESOLUTION CT FINDINGS IN CHILDREN WITH NON-SPECIFIC INTERSTITIAL PNEUMONIA

PÄRIA Miraftebi¹, LAURA Martelius¹, JOUKO Lohi², TURKKA Kirjavainen³

¹ HUS Medical Imaging Center, Radiology, University of Helsinki and Helsinki University Hospital, Helsinki, FINLAND

² Department of Pathology, University of Helsinki and Helsinki University Hospital, Helsinki, FINLAND

³ Department of Pediatrics, Childrens Hospital, University of Helsinki and Helsinki University Hospital, Helsinki, FINLAND

Purpose

In children, non-specific interstitial pneumonia (NSIP) is rare. It associates with genetic disorders of surfactant metabolism, viral pneumonitis, hypersensitivity pneumonitis, and collagen vascular diseases. In adults, high-resolution computed tomography (HRCT) images may suggest the diagnosis in the right clinical setting. This report describes the HRCT findings of NSIP in children.

Material and methods

A multidisciplinary team (a pediatric radiologist, a pediatric pulmonologist, and a pediatric pathologist) reviewed consecutive patients aged under 18 years with a history of diagnostic lung biopsy and lung HRCT between January 2004 and January 2020. There were eight patients with NSIP histology. The presence of a HRCT pattern suggestive of NSIP, as described in adults, was noted: 1) presence of bilateral ground-glass opacities with predominance in lower lobes and subpleural area, 2) varying degree of additional reticulation, 3) traction bronchiectasis, 4) consolidation and 5) honeycombing.

Results

NSIP was idiopathic in one patient. Five patients had collagen vascular disease, and two had the immune-related systemic disease. On HRCT, all patients showed bilateral disease with ground glass opacities. Additional findings included cysts and focal crazy paving. Four patients (50%) showed a HRCT pattern suggestive of NSIP.

Conclusions

NSIP in children is clinically and radiologically heterogeneous. The HRCT pattern suggestive of NSIP appears similar to adults in children with collagen vascular disease.

Poster: SCI-033

CONGENITAL THORACIC ABNORMALITIES: INTERESTING CASES FROM A TERTIARY PAEDIATRIC CENTRE

JONATHAN Bevan, LINDA Stephens
Royal Manchester Children's Hospital, Manchester, UNITED KINGDOM

Introduction:

With advances in imaging techniques we are increasingly able to provide our patients and their clinical teams with a more detailed visual representation of congenital structural abnormalities of the thorax. The radiology department plays a critical role in guiding medical and surgical management of these often complex conditions using a multimodality approach, providing timely and precise diagnoses and delivering accurate anatomical information. This is particularly important when patients present with severe respiratory distress where decision making is extremely time critical.

Method:

We present a collection of rare and complex congenital abnormalities from a tertiary paediatric hospital that illustrate the diverse range of pathology that can affect the thoracic cavity and its contents. The cases include complex abnormalities of the lungs and airways including oesophageal bronchus, horseshoe lung and complex tracheo-oesophageal abnormalities. Other interesting cases include bilateral Morgagni hernia, a rarely seen entity. We include a range of modalities and provide details on imaging technique as well as key learning points from each case. Where possible we have included three-dimension reconstructions to illustrate the pertinent features of each condition as well provide surgical correlation and clinical outcomes.

Aim:

This review of complex congenital thoracic abnormalities will illustrate the breadth of pathology that can occur in the thorax and raise awareness of the more complex and rarely seen abnormalities where radiologists can have a significant impact on the management and outcome of these often seriously ill children.

Poster: SCI-034

ASSESSMENT OF LUNG DENSITY IN PEDIATRIC PATIENTS USING ZERO ECHO-TIME AND ULTRASHORT ECHO-TIME SEQUENCES

KONSTANTINOS Zeimpekis¹, CHRISTIAN Kellenberger², JULIA Geiger²

¹ Department of Nuclear Medicine, University Hospital Zurich, Zurich, SWITZERLAND

² Department of Diagnostic Imaging, University Children's Hospital Zurich, Zurich, SWITZERLAND

³ Children's Research Center, University Children's Hospital Zurich, Zurich, SWITZERLAND

Purpose:

The aim of this study was to evaluate the performance of ultrashort echo-time (UTE) and zero echo-time (ZTE) sequences for quantification of lung density in correlation with age in pediatric patients.

Methods and Materials

17 controls and 9 patients with cystic fibrosis were included in this retrospective study (median age 4.7 years, age range 15 days to 17 years). The 3D UTE Cones (Cones) and the 4D ZTE MRI sequences were used to capture the fast decaying T2* lung signal. Scans were acquired with a 32 channel cardiac coil. Parameters used for Cones: (TR/TE 3.7/0.032ms, resolution 0.88mm, slice thickness 2mm) while for ZTE: (TR/TE 294/0.016Ms, resolution 1mm, slice thickness 1.5mm). The lung signal was assessed in Signal Intensities (SI) extracted from lung segmentation (OSIRIX MD, Pixmeo Sarl 2020). For assessment of the anterior-to-posterior pulmonary gradient, regions-of-interest (ROIs) were placed in the anterior, middle and posterior areas of both lungs without including high-intensity vessels. The background SI was calculated as the average of 4 ROIs. Lung-to-background ratio (LBR) analysis was performed for both cohorts. The Spearman rank test was used to show the correlation between LBR and increasing age of the patients. The two-tailed Wilcoxon rank sum test and the Mann-Whitney U test were used to compare statistical significances between sequences and cohorts respectively ($p < .05$).

Results

We did not find a significant difference between LBR of control using Cones and ZTE. Both sequences revealed an age-dependency of LBR with a high negative correlation for Cones ($R_s = -0.77$) and ZTE ($R_s = -0.82$). LBR values of CF patients were not significantly different in both sequences. In addition, no significant difference was shown between the two cohorts for both Cones and ZTE.

The anteroposterior gradient was more prominent with ZTE compared to Cones. ZTE exhibited 12% higher posterior signal ($R_2 = 0.94$) while Cones 9.4% ($R_2 = 0.97$). This however could be explained by the fact that the anterior ROIs in ZTE were generally with higher noise than in Cones and produced less average signal.

Conclusion

The lung-to-background ratio analysis showed that ZTE sequence is able to measure signal intensity similarly to Cones. Both sequences reveal an age- and gravity-dependency of LBR. These findings can be used for further evaluation of both MRI sequences to establish a possible reference for implementation in lung pathologies.

Poster: SCI-035

RADIOGRAPHIC SEQUEL OF A NEWBORN DIED BY COVID-19 INFECTION

IRENE Vraka¹, RODANTHI Sfakiotaki¹, CHRISTINA Zouridaki¹, ELENI Koutrouveli¹, ANNA Chountala¹, MARINA Vakaki¹, GEORGIOS Daniil², EKATERINI Haritou¹, CHRYSOULA Koumanidou¹

¹ Children's Hospital of Athens P&A Kyriakou, Athens, GREECE

² General Hospital of Thessaloniki G. Gennimatas, Thessaloniki, GREECE

Purpose:

We record the radiological progress of COVID-19 infection in a newborn who died of the disease since this outcome is very rare so far.

Case description:

The infant came up with a fever and respiratory distress on the 15th day of life, which was the second day of clinically apparent symptoms. The boy had a positive COVID-19 test, thus he remained for five days in a COVID-19 isolation ward, without the need for intubation. During the 21st day of life, he was transferred to the intensive care unit (ICU) of our hospital, due to his continuously worsening respiratory ability, and he was intubated. Although all existing therapeutic tools were used, the disease progression was not able to be reversed. Unfortunately, the infant died on the 38th day of life.

A series of chest radiographs during the hospitalization of the infant in the ICU depicts the advance of the disease and its complications. The first radiograph demonstrated hyperventilation of the lungs, extended areas with ground-glass opacities on both lungs, most evident to the medial parts of the lung basis, as well as a radio-opaque area on the periphery of the upper lobe of the right lung. Three days later, a diffuse and subtle reticular pattern was added to the radiological image of both lungs, along with peribronchial wall thickening, predominated in the perihilar regions. The increasing predominance of the latest findings and the gradual effacement of the lung opacities followed the previous days, while on the ninth day of hospitalization in the ICU, a reticulonodular pattern was settled, with increased radio-opacity in the perihilar regions. The next day the first pneumothorax appeared on the right hemithorax, while the following days the reticulonodular pattern was increasingly even more evident. Some new pneumothorax events were depicted on both sides, the last day before the infant's death.

Conclusion:

Fatal COVID-19 infection in children and especially in newborns is hopefully a very rare event, but it is also important to be recorded radiologically, adding some important information about the nature of the disease and helping to its better treatment in the future.

Poster: SCI-036

IMAGE QUALITY OF DSCT WITH HIGH-PITCH SPIRAL SCAN MODE (TURBO FLASH SPIRAL MODE) WITH OR WITHOUT GENERAL ANESTHESIA: CTA EVALUATION OF CONGENITAL THORACIC DISORDERS IN INFANTS AND YOUNG CHILDREN

PATRICK Tivnan¹, ABBEY J Winant², PATRICK R Johnston², KATHERINE Smith², GAIL MacCallum², EDWARD Y. Lee²

¹ Department of Radiology, Boston Medical Center, Boston, USA

² Department of Radiology, Boston Children's Hospital, Boston, USA

Purpose: To compare the image quality of thoracic computed tomography angiography (tCTA) studies performed for evaluation of congenital thoracic disorders (CTD) in children with general anesthesia (GA) and without GA using dual source computed tomography (DSCT) with turbo flash spiral mode (TFSM).

Material and Methods: All children (age < 6 years) who underwent tCTA studies from 01/2018-10/2020 for suspected CTD were categorized into two groups: with and without GA. All tCTA were performed on a DSCT (Somatom Force, Siemens, Munich Germany) using TFSM (scan speed of 737 mm/s, 0.25s rotation, pitch 3.2, 66 ms temporal resolution per image). Two pediatric radiologists independently evaluated presence and degree of motion artifact (MA) within 3 lung zones (upper, mid, and lower). Degree of MA was graded on a 0-3 scale (0, none; 1, mild; 2, moderate, and 3, severe). Logistic models adjusted for age and gender and linear models were used to compare the odds of and mean score of the degree of MA. Interobserver agreement between reviewers was evaluated with kappa statistics.

Results: 73 patients were identified (43 male (59%), mean age 1.4 years), 31 patients (42%) without GA and 42 patients (58%) with GA. The presence of MA was higher for the group without GA in all lung zones, but this was significant only in the upper lung zone (odds ratio = 20, $p = 0.043$). A similar finding applied to the degree of MA, for which the difference of mean scores in the upper lung zone was 0.28 ($p=0.011$). Inter-reviewer agreement for detecting MA was high in all lung zones ($K > 0.88$, lower 95% confidence bound > 0.81).

Conclusion: MA was significantly higher in the upper lung zone without GA using DSCT with TFSM. Stabilization in the upper chest should be considered when performing tCTA with DSCT with TFSM without GA in infants and young children for evaluating CTD.

Poster: SCI-037

AN X-RAY SCORE TO DESCRIBE EVOLVING BRONCHOPULMONARY DYSPLASIA (BPD) IN PRETERM BABOONS

JULIA Schönfeld¹, MARIUS Möbius^{1,2}, STEVEN Seidner³, DONALD McCurnin³, CYNTHIA Blanco³, SHAMIMUNISA Mustafa³, ISABEL Fürbötter-Behnert¹, LEONHARD Menschner¹, BERNARD Thebaud^{4,5,6}, MARIO Rüdiger^{1,2}, GABRIELE Hahn⁷

¹ Neonatology and Pediatric Critical Care Medicine, Department of Pediatrics, University Hospital and Medical Faculty, TU, Dresden, GERMANY

² Good Manufacturing Practice, Center for Regenerative Therapies, Technische Universität, Dresden, GERMANY

³ Neonatology, Department of Pediatrics, University of Texas Health Science Center, San Antonio, USA

⁴ Regenerative Medicine Program, Ottawa Hospital Research Institute, Ottawa, CANADA

⁵ Neonatology, Department of Pediatrics, Childrens Hospital of Eastern Ontario and CHEO Research Institute, Ottawa, CANADA

⁶ Department of Cellular and Molecular Medicine, University of Ottawa, Ottawa, CANADA

⁷ Division of Pediatric Radiology, University Hospital and Medical Faculty, TU, Dresden, GERMANY

After preterm birth, the immature lung undergoes morphological and functional changes often resulting in alveolar and capillary hypoplasia, termed 'new' BPD. Estimating those changes is still challenging in a clinical context due to a lack of an appropriate surrogate. We therefore hypothesized, that a quantitative x-ray score indicates lung function and histologic changes.

Preterm baboons (n=13, mean gestational age 126 days (term= 185 days), mean birth weight 369g) were intubated, got surfactant and mechanical ventilation. Baboons received intensive care treatment for 14 days. Daily chest X-rays were done, oxygenation (OI) and ventilation (VI) indices were calculated for every 24h. Lung morphology was evaluated postmortem by design-based stereology. Chest X-rays were evaluated by a non-interpreting, objectified scheme including the criteria lung haziness and visibility of limits of heart and diaphragm. Based on that an x-ray score was established from 0 (= normal findings) to 30 (= white lung). Rank correlation coefficient was used to validate the score.

The study shows a high correlation between OI and x-ray score with $r=0.62$ (95%-CI [0,52 – 0,7], $t=10,4$, $p<0,05$) and VI and x-ray score with $r=0.63$ (95%-CI [0,53 – 0,71], $t=10,6$, $p<0,05$). Heteroscedasticity with a statistical significant increase of dispersion in values > 23 in x-ray score for both, VI and OI was seen, which was indicating potential limitations of the score in high values. A correlation of histology and the score of the final x-ray showed a high effect with functional/ ventilated parenchyma $r = -0,64$ (95%-CI [0,1 – 0,89], $t= -2,6$, $p<0,05$) and nonfunctional/ not ventilated tissue $r = 0,75$ (95%-CI [0,31 – 0,93], $t= 3,6$, $p<0,05$). Regarding the development of x-ray score over time, a typical radiographic course including characteristic maxima was described.

In this study, an x-ray score was developed to objectively measure changes in BPD. In comparison to former trials, that already showed correlations between x-ray findings and clinical severity, for the first time a correlation to functional and morphological parameters was shown and a typical radiographic sequence of evolving 'new' BPD was described. Further studies should test its potential in clinical settings and research on evolving BPD since our data suggest individual and also typical patterns.

Poster: SCI-038

TENSION GASTROTHORAX MASQUERADING AS TENSION PNEUMOTHORAX IN A CHILD

PRADEEP RAJ Regmi¹, ISHA Amatya²

¹ Hospital for Advanced Medicine and Surgery (HAMS), Kathmandu, NEPAL

² Kathmandu Medical College (KMC), Kathmandu, NEPAL

INTRODUCTION

Tension gastrothorax is a rare and emergency condition a child can present in the emergency department. It develops when a stomach herniates into the thorax through the diaphragmatic defect causing a mediastinal shift towards the contralateral side of herniation. It is commonly misdiagnosed as pneumothorax leading to wrong management. We are presenting a case of a 10-year-old female child presented in our emergency department with left-sided chest pain and shortness of breath for 6 hours duration.

FINDINGS

Chest X-ray revealed a large air cavity almost occupying the left hemithorax. The outline of the left hemidiaphragm is not clearly delineated. Fundic gas was not seen. After CT chest with oral contrast, the stomach was seen herniating through the oesophageal hiatus and distended with trapped air causing passive atelectasis of the left lung. The contralateral mediastinal shift was seen.

EDUCATIONAL OBJECTIVES

The importance of this case is recognizing the difference from tension pneumothorax in emergency settings which can lead to further morbidity and mortality. Poorly defined left hemidiaphragm, absence of fundic gas, apical compression of the lung are the differentiating points in favour of gastrothorax in chest X-Ray from pneumothorax. In pneumothorax, the hemidiaphragm appears well delineated and depressed with a clear costophrenic angle and fundic gas is visible and the lung is collapsed centrally towards the hilum.

CONCLUSION

Tension gastrothorax is a rare and emergent condition in a child with a good prognosis if managed properly in acute settings. If the distension of the stomach is large enough to cause the mediastinal shift, the child could land up in obstructive shock and cardiac arrest. Therefore, diagnosing a case with gastrothorax and differentiating it from pneumothorax is very important. For this, a pediatric radiologist could play a vital role in diagnosis which leads to proper management.

Keywords: Gastrothorax, child, pneumothorax, X-Ray, CT

Poster: SCI-039

RALE RADIOGRAPHIC SCORING IN PEDIATRIC ACUTE RESPIRATORY DISEASE SYNDROME (PARDS)

MARIA Raissaki¹, EVANGELIA Vassalou¹, IOANNA Mpatziou², GEORGE Briassoulis², STAVROULA Iliá²

¹ University Hospital of Heraklion, School of Medicine, Department of Radiology, Heraklion, GREECE

² University Hospital of Heraklion, School of Medicine, Pediatric Intensive Care Unit, Heraklion, GREECE

Background and purpose: Following the 2015 Pediatric Acute Lung Injury Consensus Conference (PALICC), broadened radiographic requirements for the definition of PARDS [any new infiltrate(s)], and the concept of “at-risk of PARDS”, were introduced. Radiographic Assessment of Lung Edema (RALE) score (0 to 48) has been extensively used in adults. We aimed to review radiological findings in children with and at-risk of PARDS, and investigate associations between RALE score, clinical, laboratory findings and outcome.

Materials and methods: Fifty children (23 males, 27 females), aged 3.5 years (IQR, 1.5-9) with PARDS (n=26, group 1) or “at-risk of PARDS (n=24, group 2), admitted to the Pediatric Intensive Care Unit (PICU) between 2009-2019 were enrolled. Clinical, laboratory, radiographic data were collected on admission day (D1), on day PARDS/at-risk of PARDS criteria were fulfilled (D-PARDS), and on “oxygenation” worst day (WD) (worse lung mechanics/gas exchange, respiratory support). A total of 81 radiographs (43 on D1, 13 at D-PARDS, 25 at WD), were evaluated and graded according to the RALE score.

Results: Co-existing radiographic findings included alveolar opacities in 57 radiographs (70%), interstitial infiltrates in 36 (44%) atelectasis in 26 (32%), hypoinflation in 37 (46%), hyperinflation in 19 (24%), effusions in 11 (14%), pneumothorax/air leaks in 7 (9%), and did not differ significantly between the 2 groups.

RALE score at D1 was independently associated with length of PICU stay, mechanical ventilation days ($p=0.029$ and $p=0.027$, respectively), while WD RALE score correlated with clinical severity indices PELOD and PRISM upon admission ($p=0.004$ and $p=0.026$, respectively). RALE scores at D1, D-ARDS and WD did not differ significantly among patient groups.

Conclusions: Radiographs of children with PARDS or at-risk of PARDS, may exhibit parenchymal abnormalities of various extent with/out pleural disease and altered lung volumes. RALE scoring in PARDS is associated with severity of illness and may be used for disease stratification and prognosis.

Poster: SCI-040

HRCT FINDINGS IN CHILDREN WITH CHRONIC SUPPURATIVE LUNG DISEASE (CSLD) AND P. AERUGINOSA COLONIZATION

SPYRIDON Proutzos¹, OLYMPIA Sardeli², DAFNI Moriki², ANGELIKI Galani¹, ORNELLA Moschovaki Zeiger², KONSTANTINOS Douros², EFTHYMIA Alexopoulou¹

¹ University General Hospital Attikon - 2nd Radiology Department, Athens, GREECE

² University General Hospital Attikon - Pediatric Allergiology Unit, Athens, GREECE

Chronic suppurative lung disease (CSLD) falls under the spectrum of pediatric suppurative lung disorders, along with protracted bacterial bronchitis (PBB) and bronchiectasis, and is defined as a syndrome with clinical symptoms suggestive of bronchiectasis, although lacking the characteristic radiological features. This study aimed to compare pulmonary High-Resolution CT (HRCT) findings in children having Chronic Suppurative Lung Disease (CSLD) with *Pseudomonas Aeruginosa* colonization in sputum cultures to children having CSLD with other types of bacteria colonization. This retrospective study included thirty-four children (14 females, 20 males) with a median age of 7 years. Patients were divided into two groups; the first group included twelve children with CSLD and *P. aeruginosa* in their sputum cultures (Group #1), whereas the second group consisted of twenty-two children in which their sputum cultures came back with other bacteria such as Gram (-), *Streptococcus*, *S. aureus* or *Candida* spp (Group #2). All patients were symptomatic during the time of their examination and had completed the first round of treatment regimes. Children with known cystic fibrosis were excluded from the study. The modified Bhalla scoring system was used to evaluate the imaging findings of each examination of the patients' groups. Group #1 patients showed an overall higher modified Bhalla score compared to Group #2 patients (p -value =0.0051). Group #1 demonstrated having more bronchiectasis, which extends to more bronchopulmonary segments than Group #2 patients (p value=0.0004 and p value=0.0009 respectively). No significant difference was observed between the two groups neither in the development of collapsed parenchyma or consolidations nor in the appearance of a mosaic pattern of attenuation of the lung parenchyma (p value= 0.4203 respectively). More studies are needed to be carried out in order to further validate the results.

Poster: SCI-041

GRAVES' DISEASE AND THYMIC HYPERPLASIA IN PEDIATRIC PATIENTS

SAELIN Oh

Anam Hospital, Korea University College of Medicine, Seoul, SOUTH KOREA

Graves' disease is an autoimmune disorder characterized by thyroid enlargement and hyperthyroidism. Thymic hyperplasia is a known feature of Graves' disease in adults, but is rarely reported in children. We present three patients with Graves' disease and relatively rapid resolution of thymic enlargement after successful treatment of their hyperthyroidism.

Three patients (one male and 2 females, age range 11-17 years) with thyrotoxicosis secondary to Graves' disease and marked thymic enlargement were seen at our institution during a 1-year period. All cases went through computed tomography and revealed a homogenous anterior mediastinal mass with no invasion into the surrounding tissue. Treatment of Graves' thyrotoxicosis resulted in a spontaneous shrinkage of the mediastinal mass.

Considering the diagnosis of Graves' disease for a child with an anterior mediastinal mass and without the typical physical findings of

autoimmune hyperthyroidism (goiter, exophthalmos) may prevent unnecessary diagnostic studies and their associated financial and emotional costs.

Poster: SCI-042

FREQUENCY OF CHEST RADIOGRAPHIC FINDINGS IN PEDIATRIC COVID-19 POSITIVE PATIENTS

JOSE FRANCISCO Molto Garcia ¹, JONATHAN Zember ¹, RAMON Sanchez ¹, KARUN Sharma ¹, GUSTAVO Nino ², RYAN Kahanowitch ², HECTOR Aguilar ², XILEI Xu Chen ², JERED Weinstock ², CARLOS Tor Diez ³, MARIUS GEORGE Linguraru ³

¹ Department of Pediatric Radiology, Children's National Hospital, Washington, District of Columbia, USA

² Division of Pediatric Pulmonary and Sleep Medicine, Children's National Hospital, Washington, District of Columbia, USA

³ Institute for Pediatric Surgical Innovation, Children's National Hospital, Washington, District of Columbia, USA

PURPOSE: To establish the frequency of hyperinflation, peribronchial markings and lung opacities in pediatric patients with COVID-19.

MATERIALS AND METHODS: Chest radiograph (CXR) of 83 COVID-19 positive patients (0-18 years) between March and June 2020 were retrospectively reviewed. Only the first radiograph of each patient (at manifestation of COVID symptoms) was assessed, and follow-ups were excluded. Three pediatric radiologists reviewed the first CXR and assessed hyperinflation, peribronchial markings and lung opacities.

RESULTS: 40 females and 43 males were included (ranging from 16 days to 17 years and 11 months). Distribution by age group showed that 22 (27%) were between 0-2 years, 27 (33%) between 2-10 years and 34 (41%) between 10-18 years. Normal CXR was the most common finding reported (45%) in the general population, followed by peribronchial markings, lung opacities (27%) and hyperinflation (10%). Normal CXR was depicted in 50% (0-2 years), 37% (2-10 years) and 48% (10-18 years). Peribronchial markings in 36% (0-2 years), 69% (2-10 years) and 44% (10-18 years). Lung opacities in 11% (0-2 years), 33% (2-10 years) and 31% (10-18 years). Hyperinflation in 23% (0-2 years), 9% (2-10 years) and 2% (10-18 years).

CONCLUSION: Our preliminary results suggest that COVID-19 infection in young children between 0 and 2 years of age does not typically result in lung hyperinflation, which is more typical to cases of viral bronchiolitis. This is one biomarker that CXR could play a role in the differential diagnosis between viral bronchiolitis and COVID-19 infection in young children.

Poster: SCI-043

LUNG DENSITY ASSESSMENT OF PULMONARY DISEASE IN CYSTIC FIBROSIS WITH COMPUTED TOMOGRAPHY SCANS

ISABELLA Liu ¹, GOUTHAM Mylavarapu ³, RAOUF Amin ³, ROBERT Fleck ²

¹ University of Cincinnati College of Medicine, Cincinnati, USA

² Cincinnati Children's Hospital Medical Center - Department of Radiology, Cincinnati, USA

³ Cincinnati Children's Hospital Medical Center - Division of Pulmonary Medicine, Cincinnati, USA

Purpose: Structural lung abnormalities in children with cystic fibrosis (CF) are observed on CT scans even in asymptomatic patients. This visual assessment is often subjective and not reproducible. Lung density

assessment with CT can measure regions of low attenuation and quantify the degree of parenchymal tissue abnormality. The objective of this study was to compare measures of lung densitometry in pediatric CF patients and their age-matched controls. We hypothesized that total lung volume and lung volume in the low-density range (< -920 HU) would be greater in CF patients compared to children with normal lungs.

Materials and Methods: Non-contrast, high-resolution CT chest scans from patients with varying degrees of CF disease severity and controls were included. Disease severity was based on FEV1% predicted: normal (> 100%), mild (80-100%), moderate (60-80%) and severe (< 60%). Control studies were obtained through query of the Radiology Information System from January 1, 2015 to December 31, 2019 for children with solid tumors who had CT scans pre-treatment. Control exclusion criteria: 1) acute/chronic respiratory disease, 2) congenital disorder/syndrome, 3) prior surgery violating the chest wall. Controls also had a CT scan within 1 year of diagnosis of malignancy, normal findings on impression, and secondary vetting by radiologist as normal study. Semi-automatic three-dimensional lung segmentation was performed using Vitrea CT Lung Density Analysis software. Lung density measurements of total lung volume, low-density (-1024 to -920 HU), medium-density (-920 to -720 HU), and high-density (-720 to 0 HU) volumes were compared with a Mann-Whitney U test.

Results: 57 CF patients (14 normal, 15 mild, 11 moderate, 17 severe; 14.7 ± 4.1 years) and 80 controls (14.5 ± 3.1 years) were included in this study. CF patients had significantly greater total lung volume normalized to body surface area (p=0.005), high-density volume (612.4 ± 306.4 ml vs 468.9 ± 211.9 ml, p = 0.002), and low-density volume index (10.7 ± 13.0 vs 6.9 ± 10.6, p = 0.049) compared to the controls. Severe CF patients also had significantly greater total lung volume normalized to body surface area (p = 0.006), high-density volume (709.8 ml ± 378.6 ml, p = 0.004), and low density volume index (16.9 ± 16.5 vs 10.7 ± 13.0, p = 0.004) compared to controls.

Conclusions: Lung density analysis may be useful in assessing disease severity in pediatric CF or as a component of automated scoring.

Poster: SCI-044

TRAUMATIC PNEUMATOCELE IN NONACCIDENTAL TRAUMA

MICHAEL CHIGOZIR Lewis, SHEENA Saleem
Children's Hospital of Michigan, Detroit, USA

Our case focuses on the course of a 2-month-old male who arrived at our facility with injuries that raised the suspicion of nonaccidental trauma. Imaging revealed fractures of the posterior ribs and an unusual loculated paraspinal lucencies. Given the injuries and provided history, a differential diagnosis of loculated pneumothorax and traumatic pneumatocele was considered. It is important for the pediatric radiologist to be aware of this etiology in the setting of nonaccidental trauma. Traumatic pneumatoceles have been described in significant trauma in motor vehicle accidents but the pediatric radiologist should be aware that it may occur in the setting of child abuse. This case report will briefly discuss imaging features, etiology, symptom presentation and a literature review of traumatic pneumatoceles with the goal of informing/reinforcing the knowledge of the existence of this etiology so it will be considered in the differential diagnosis.

Poster: SCI-045

ENDOTRACHEAL AND INTRAOSSEOUS VASCULAR LINE PLACEMENTS IN PEDIATRIC EMERGENCY CARE: A REVIEW BASED UPON POSTMORTEM COMPUTED TOMOGRAPHY

PATRICIA Harty, EMILY Gripp, MATTHEW Dina, SHARON Gould, H. THEODORE Harcke

Nemours Children's Health, Alfred. I. duPont Hospital for Children, Wilmington, USA

Purpose:

To evaluate emergency intervention endotracheal tube (ETT) and intraosseous intravenous (IO-IV) placement in a group of non-surviving children who underwent postmortem imaging with computed tomography (PMCT). Prehospital tube placement by emergency medical system (EMS) first responders was compared with placement by hospital emergency room (ER) personnel. Effect of age and needle length was considered.

Methods and Materials:

PMCT scans are performed prior to autopsy with all support devices in place. Retrospective review of 139 consecutive studies showed 84 ETT and 55 IO-IVs placed under emergency conditions. When possible, group was divided into prehospital or ER placement. The children were grouped by age. ETT placement was categorized by location and IO-IV placement by location and needle length.

Results:

ETT position was determined to be good, borderline (at carina level), or bronchial in 74/84 cases (88%). Esophageal placement was found in 10/84 (12%). Esophageal placement occurred more frequently (8/41) in infants younger than 6 months, whereas it occurred in 2/43 children age 6 months or older ($p < .05$, Fisher's exact test). It was determined whether ETT was placed prehospital or in the ER in 61 cases. Esophageal placement occurred twice in each location. When esophageal and bronchial placement across all age groups was combined (prehospital 16/35, ER 8/26), there was no significant difference between locations.

Placement of IO-IV (medullary, cortex, perforation, outside bone) was evaluated in 40/84 cases (total of 55 needles). Needle lengths of 15mm and 25mm were used. Successful IO-IV placement of 15mm needles was 25/37 (67.6%) and of 25mm needles was 9/18 (50%). By age, needle placements in infants younger than 6 months succeeded in 20/39 (51.3%). Successful placement in children 6 months or older was 14/16 (87.5%) ($p < .05$, Fisher's exact test). No significant difference in placement success was seen between prehospital and in the ER.

Conclusion:

Emergency intervention in infants younger than 6 months produced more problematic placement of both ETT and IO-IVs than in older infants and children. Use of 25mm IO-IV needles in infants younger than 6 months is more likely to fail. Fewer successful placements of both ETT and IO-IV lines occurred in both the prehospital and ER settings in infants younger than 6 months. PMCT can be useful in studying medical intervention to improve patient outcomes through education of EMS and ER personnel.

Poster: SCI-046

REVIEW OF INTER-CENTRE VARIATION BETWEEN UK PAEDIATRIC CYSTIC FIBROSIS CENTRES IN THEIR APPROACH TO ANNUAL ASSESSMENT A DONNELLY, A REID AND A PATERSON ROYAL BELFAST HOSPITAL FOR SICK CHILDREN BELF

AUSTIN Donnelly, ANNIE Paterson, ALISTAIR Reid
Royal Belfast Hospital for Sick Children, Belfast, UNITED KINGDOM

Background:

UK guidelines (2017) call for a multi-disciplinary annual review (AR) of Cystic Fibrosis (CF) patients including: clinical, dietary, pharmacological, psychological, laboratory, radiological, physiotherapy and social work assessments.

When carried out during a single hospital visit, it is time consuming for all concerned and arduous for many children.

Anecdotal evidence suggests significant variation in AR in different UK centres. Our aim was to collect data to confirm/refute such evidence, and

use it as a basis to reduce inter-centre variation, facilitating easier comparison of interventions/outcomes and streamline AR visits for children.

Methods

A questionnaire was sent to the clinical leads of the 27 UK paediatric centres.

Basic demographic questions were asked alongside binary questions about the inclusion/exclusion of AR components per NICE guidelines. More open ended questions focused on additional laboratory tests and scoring of radiological images plus how information is used to direct patient care.

Results

All respondents carried out AR of paediatric CF patients.

80% of centres include a meeting with a physician. Measurement of growth metrics, enzyme use, evaluation of nebuliser use and routine bloodwork were universally recorded. There was widespread variation in other blood work, and the inclusion of pharmacy and psychology review.

All respondents included some form of radiology review. 95% include a PA CXR, with 10% performing a lateral view also. Only 45% centres routinely score CXRs: Northern score in 40%, modified Crispin Norman plus Schwachman score in 5%, and all 3 of these systems in 5%. 15% monitor bone age.

95% use abdominal US. Portal vein diameter measurement and Doppler studies are not always obtained.

Scoring is used mainly to share information with families.

Conclusions

NICE advocate a structured AR of paediatric CF patients in the UK. There is variability between centres, particularly with respect to the role of radiology. Consensus over components of AR would help reduce workload of professionals and improve patient experience.

Poster: SCI-047

UNUSUAL LESION OF THE MEDIASTINUM: LANGERHANS CELL HISTIOCYTOSIS

ZUHAL Bayramoglu, ELIF HAZAL Karli, EZGI Kara
Istanbul University, Istanbul Medical Faculty, Radiology Department, Istanbul, TURKEY

Introduction

Langerhans cell histiocytosis (LCH) is characterized by infiltration of monocytic cell and large histiocytes (Langerhans cells) in various tissues and organs. In LCH, pathological cells reveal strongly positive for CD1a and S-100 protein positivity in the immunohistochemical analyses.

It can involve various organs, but mostly LCH presents as the unifocal disease typically involves bone in older children and adults. Lymph nodes, skin, and lungs are the other common sites. We present an unusual presentation of LCH originating from the mediastinum.

Case Report

An 11-year-old female patient presented with dyspnea and hemoptysis. In bronchoscopy, there was a lesion compressing the right main bronchus. The lesion was biopsied but came out as inconclusive. Contrast-enhanced thorax CT was performed. There was a 3.5 cm spherical-shaped central cystic lesion in the right paratracheal region extending to the carina. The lesion was compressing the right main bronchus, narrowing the airway. Also, multiple spheric lymph nodes with no fatty hilum were detected. The patient underwent cranioplasty and postoperative pathology came out as Langerhans cell histiocytic infiltration and proliferation. No post-operative treatment is needed and bronchoscopy seems normal after 1 year from the surgery.

Discussion

The etiology and pathogenesis of LCH remain unknown.

According to the involvement, LCH is divided into three groups. Localized (unifocal) form comprises 70% of LCH cases, confined to

single bone or fewer bones. Multifocal unisystem form is seen in approximately 20% of cases and affects bones and reticuloendothelial system (ie, the liver, spleen, lymph nodes, skin). Eosinophilic granuloma, histiocytosis X, Letterer-Siwe, and Hand Schuller Christian disease were the names used for the forms of LCH, and these names are disregarded. Any part of the body can be affected by LCH and the clinical presentation will vary from the involvement and extent of the disease. Diagnosis is made with clinical features, histopathology, immunohistochemistry, and radiological imaging.

Lymph node involvement is usually accompanied in pediatric patients with known systemic disease, however primary lymph node involvement can be seen. Cervical chain lymph nodes are usually affected. When solitary node involvement is seen in the mediastinum, the differential of lymphoma, thymoma, teratoma, and other mediastinal masses should be considered.

Poster: SCI-048

CALCIFYING FIBROUS PSEUDOTUMOR OF THE MEDIASTINUM: A RARE CASE REPORT

ZUHAL Bayramoglu, EZGI Kara, ELIF HAZAL Karli, ARAZ Gafarli
Istanbul University, Istanbul Medical Faculty, Radiology Department,
Istanbul, TURKEY

Calcifying fibrous pseudotumors (CFPTs) are rare, benign fibroblastic tumors of the soft tissues that affect dominantly children and young adults, and most usually occur in the extremities. We present a case of CFPT in the pleura which is an unusual location.

Pseudotumors are benign lesions of the lung, pleura, and soft tissue that may occur as a result of previous inflammation. CFPTs have histologically similar properties to other inflammatory pseudotumors. Also, CFPTs characteristically have extensive psammomatous calcification.

A 17-year-old female patient was referred to our hospital for further evaluation for recurrent chest pain. Physical examination and routine laboratory tests were within normal limits. A pleural mass blunting the costodiaphragmatic sinus was detected on chest radiography. Contrast-enhanced chest computed tomography showed a solitary pleural mass with lobulated contours and well defined margins of heterogeneous attenuation (75 HU) due to internal calcifications. The calcifications were in punctate and interrupted curvilinear form. Surrounding lung parenchyma was normal and no hilar or mediastinal adenopathy was depicted. She refused resection and the mass was followed-up with radiological examinations. The mass was of similar size and internal content after 1-year follow-up duration.

CFPTs usually occur in the first three decades of life and grow slowly. CFPTs of pleura are rare lesions that typically occur as solitary calcified pleural masses in young adults. The differential diagnosis include calcified hemothorax or empyema, and pleural plaques due to asbestos exposure. Askin tumor and metastatic disease to the pleura. In conclusion, although CFPT of pleura is uncommon, keeping in mind its characteristic radiologic appearance especially in young adults may helpful noninvasive diagnosis.

Poster: SCI-049

ECTOPIC THYROID AND THYMUS TISSUE AT THE SUBMANDIBULAR REGION IN A PRE-SCHOOL MALE PATIENT

ZUHAL Bayramoglu, SINAN Seyrek, ARAZ Gafarli, EZGI Kara
Istanbul University, Istanbul Medical Faculty, Radiology Department,
Istanbul, TURKEY

A 6-year-old male patient applied to our department to be examined for hypothyroidism. The patient was receiving regular thyroid hormone replacement therapy from birth. In the ultrasonographic evaluation of the neck, we found that the left thyroid lobe was in the usual location, but the right thyroid lobe was located ectopically adjacent to the right submandibular gland. In addition, in the right anterior cervical compartment, adjacent to the ectopic thyroid tissue, presenting echogenicity equal to the mediastinal thymus containing punctate echogenicity compatible with aberrant cervical ectopic thymus tissue was observed.

Ectopic thymus tissue can often be encountered mediolaterally in the anterior cervical region of the neck. In addition, ectopic tissue can be seen with intrathyroidal thymic inclusions. However, the presence of aberrant ectopic thymus and thyroid tissue within the context of undescended tissue is not a common entity. In this case, we aimed to show the ectopic thymus and ectopic thyroid tissue in the same ultrasound image in the submandibular area.

Doppler Us examinations and elastographic examinations contribute to distinguishing ectopic aberrant tissues of the thymus and thyroid. Thyroid tissue is stiffer and more hypervascular than thymus tissue even it is located ectopically.

Poster: SCI-050

DISSEMINATED HYDATID CYST DISEASE

ZUHAL Bayramoglu, RANA GUNOZ Comert
Istanbul University, Istanbul Medical Faculty, Radiology Department,
Istanbul, TURKEY

The 9-years-old male patient was referred for urinary incontinence and underweight abdominal ultrasound examination. There were thick-walled multiple anechoic hepatic and splenic cysts on ultrasound. Additionally, there were multiple fluid-filled cysts in the bilateral lung parenchyma in some demonstrating air-fluid level on chest X-ray. Laboratory examinations revealed elevated white blood cell count and sedimentation rate. As Turkey is endemic for cyst hydatid disease and imaging findings were compatible with disseminated cyst hydatid disease the patient received medical treatment. Follow-up examination showed size reduction in the cysts and none of the required surgical resection.

Disseminated cyst hydatid disease is a very extreme entity even in endemic countries. Additionally, multiple cystic lesions were detected incidentally and no respiratory symptoms were depicted in this case although some of the cysts were complicated. Constitutional and atypical symptoms should be evaluated carefully in terms of infectious diseases in endemic countries.

Poster: SCI-051

RESPONSE OF THE MEDIASTINAL INFLAMMATORY PSEUDOTUMOR TO THE MEDICAL TREATMENT

ZUHAL Bayramoglu, HAZAL ELIF Karli
Istanbul University, Istanbul Medical Faculty, Radiology Department,
Istanbul, TURKEY

Inflammatory pseudotumor (IP) is a term used to describe benign mass-forming lesions characterized by myofibroblastic proliferation. Clinical and imaging findings can mimic malignancy due to its aggressive appearance. Primary involvement of the mediastinum is extremely rare. There are reported cases of spontaneous regression of IPT, sometimes long-term antibiotic and steroid treatment can yield the tumor regression which may reflect the inflammatory nature of the tumor.

This case involved a 9-year-old boy who had symptoms of dyspnea and right-sided chest pain. Chest X-ray showed mediastinal enlargement and

right-sided pleural effusion (Fig). Thorax CT revealed a 4-cm, central necrotic heterogeneous round hypodense mass in the right paratracheal space extending to the paravertebral region. High-density pleural effusion of the right hemithorax accompanying atelectasis in some areas was depicted. 20 ml of hemorrhagic fluid collected by thoracentesis. Chemical, microbiological cultural, and cytological analyses were not significant. PET-CT showed high FDG (fluorodeoxyglucose) uptake (SUVmax:25.1). There was no pathological FDG affinity throughout the body.

CT guided biopsy-confirmed benign spindle cell infiltration with mesenchymal origin accompanying necrosis compatible with inflammatory pseudotumor. The patient underwent corticosteroids and antibiotic treatment. Contrast-enhanced MRI 1.5 months after the initial diagnosis revealed low intensity on T1 weighted images and heterogeneous signal intensity on T2 weighted images with peripheral dominant, heterogeneous enhancement. An approximate %50 decrease in the tumor size is detected compared to the previous CT scan. The patient has been followed over the 24 months with mediastinal MRI and a 1.5 cm residual lesion remains the same as previous studies.

Imaging characteristics of IP in non-specific but due to the fibrous nature some common features are described. On CT, lesions commonly appear as heterogeneous attenuation and can be iso to hypodense relative to the muscle on unenhanced images. In the contrast-enhanced images, relative low enhancement is seen in the arterial phase followed by a gradual increase in the delayed phase.

On MRI, these lesions are commonly hypointense relative to muscle on T1 weighted images. On T2 weighted images intensity may vary depending on the dominance of inflammation and fibrosis. Diffusion-weighted imaging (DWI) can show alteration with the inflammation and cellularity.

Poster: SCI-052

RADIOLOGICAL FINDINGS OF PULMONARY CHRONIC GRANULOMATOUS DISEASE IN AN ADOLESCENT MALE PATIENT

ZUHAL Bayramoglu, RANA GUNOZ Comert
Istanbul University, Istanbul Medical Faculty, Radiology Department,
Istanbul, TURKEY

Objective: Chronic granulomatous disease (CGD) is an immunodeficiency characterized by an inability to eliminate catalase-positive infectious agents due to the NADPH oxidase deficiency in phagocytic cells.

The inflammation cascade does not limit, resulting in histopathologically exaggerated granuloma formation.¹

The most common manifestation of the disease is pulmonary recurrent bacterial and fungal infections², and often consolidation or nodules (lobar pneumonia/bronchopneumonia), cavitation, bronchiectasis, empyema, mediastinal lymphadenopathy are detected. Because of the multisystemic findings, radiologists should be familiar with the presentation spectrum of this disease in the evaluation of complications.

Case: A 17-year-old male patient was diagnosed with pneumonia with complaints of malaise, fever, cough, and sweating. He had pancreatitis and cholecystectomy in his 4th year of life and was hospitalized for pneumonia. PA chest radiography showed increased opacity in the right upper lobe and reticulonodular opacities in the upper and middle zones of the right hemithorax. In thorax CT examination, lobar consolidation in the right upper lobe apical and posterior segments, surrounding ground-glass opacity, accompanying centrilobular nodular opacities, and the cavitating nodule was detected in the superior segment of the right lower lobe. Besides, mediastinal lymphadenopathies were detected, being more prominent in the right lower paratracheal region. In the abdominal ultrasound, hepatomegaly and lymphadenopathy adjacent to the liver hilum were detected. One month after anti-biotherapy, a chest X-ray revealed right upper lobe opacity, and thorax CT showed partial regression of the

consolidated lobar pneumonia in the right upper lobe and sequelae of thick-walled cystic bronchiectasis. Genetic tests were also performed for the autoimmune lymphoproliferative syndrome (ALPS), and it was negative. In the control imaging performed 4 months later consolidation regresses in the right upper lobe but here thick-walled post-infectious cystic bronchiectasis and interstitial thickening centrilobular dispersed ground-glass nodules and cavitating nodule in the left upper lobe lingular segment. A positive NBT test revealed a chronic granulomatous disease. *Aspergillus fumigatus* growth was detected in the sputum culture and then antifungal treatment was administered to the patient.

Poster: SCI-053

CLASSIFICATION OF PEDIATRIC CYSTIC AND CAVITATORY LESION IN LUNG USING COMPUTED TOMOGRAPHY AND ULTRASONOGRAPHY

SHRAMANA Bagchi
Indira Gandhi Institute of Child Health, Bengaluru, INDIA

INTRODUCTION

A prospective study demonstrating imaging features of 50 patients in the first decade of their life (infants and children < 10 years), for the evaluation of cystic or cavitary lung lesion.

As imaging plays an important role in accurate early diagnosis and the optimal treatment, therefore an approach based on the most sensitive and least invasive imaging modality holds a paramount importance.

We correlated the conventional radiographs, the computed tomography and USG findings of the most common cystic and cavitary lung lesions in infants and children.

OBJECTIVES

To define the characteristics of a pulmonary cyst and to establish the differences with other lesions that can simulate it.

To describe the semiology of different diseases that manifest with cystic and pseudocystic pulmonary lesions.

To know the main clinical data that will help us to reach the correct diagnosis.

OUTCOME MEASUREMENT

There are recognizable radio-pathologic patterns of lung parenchymal abnormalities that help us in characterizing the various causes of cystic and cavitary lung lesions in the pediatric population. Chest radiograph being the most useful and inexpensive examination is always a part of the primary examination of children with for cavitary and cystic lung lesions. USG being the next best modality which is not only non-invasive and inexpensive but also is not associated with harmful effects of the radiation. Though CT has an ionising radiation exposure, it is the best tool for the evaluation of paediatric lung

HRCT and especially MDCT are substantially more sensitive techniques than conventional radiography for the detection of structural changes and assessing the pattern of affection of the different cystic lung diseases.

Though imaging plays an essential role in the evaluation of cavitary and cystic lung diseases, the need of the hour is to consider the clinical, functional and analytical aspects to establish the final diagnosis.

Poster: SCI-054

THE DIAGNOSTIC PERFORMANCE OF CHEST COMPUTED TOMOGRAPHY IN THE DETECTION OF RIB FRACTURES IN CHILDREN INVESTIGATED FOR SUSPECTED PHYSICAL ABUSE: A SYSTEMATIC REVIEW AND META-ANALYSIS

NASSER Alzahrani^{1, 2}, ANNMARIE Jeanes³, MICHAEL Paddock^{2, 4}, FARAG Shuweihdi⁵, AMAKA C Offiah^{2, 6}

¹ Diagnostic Radiology Department, College of Applied Medical Sciences, King Abdulaziz University, Jeddah, SAUDI ARABIA

² Academic Unit of Child Health, Department of Oncology and Metabolism, University of Sheffield, Sheffield, UNITED KINGDOM

³ Department of Paediatric Radiology, Leeds Children's Hospital, Leeds Teaching Hospitals NHS Trust, Leeds, UNITED KINGDOM

⁴ Medical Imaging Department, Barnsley Hospital NHS Foundation Trust, Barnsley, UNITED KINGDOM

⁵ Leeds Institute of Health Sciences, University of Leeds, Leeds, UNITED KINGDOM

⁶ Radiology Department, Sheffield Children's NHS Foundation Trust, Sheffield, UNITED KINGDOM

Objectives

To assess the diagnostic performance of chest CT in the detection of rib fractures in children investigated for suspected physical abuse (SPA).

Methods

Medline, Web of Science and Cochrane databases were searched from January 1980 to April 2020. The QUADAS-2 tool was used to assess the quality of the eligible English-only studies following which a formal narrative synthesis was constructed. Studies reporting true positive, false positive, true negative, and false negative results were included in the meta-analysis. Overall sensitivity and specificity of chest CT for rib fracture detection were calculated, irrespective of fracture location, and were pooled using a univariate random-effects meta-analysis. The diagnostic accuracy of specific locations along the rib arc (anterior, lateral or posterior) was assessed separately.

Results

Of 242 identified studies, 4 met the inclusion criteria. Of these, 2 were included in the meta-analysis. Chest CT identified 142 rib fractures compared to 79 detected by initial skeletal survey chest radiographs in live children with SPA. Post-mortem CT (PMCT) has low sensitivity (34%) but high specificity (99%) in the detection of rib fractures when compared to the autopsy reference standard. PMCT has low sensitivity (45%, 21% and 42%) but high specificity (99%, 97% and 99%) at anterior, lateral and posterior rib locations, respectively.

Conclusions

Chest CT detects more rib fractures than initial skeletal survey chest radiographs in live children with SPA. PMCT has low sensitivity but high specificity for detecting rib fractures in children investigated for SPA.

Poster: SCI-055

CONTRAST-ENHANCED ULTRASOUND (CEUS) IN PEDIATRIC RADIOLOGY: WHERE WE ARE AND WHERE WE GO?

LUCA Basso ¹, FIAMMETTA Sertorio ¹, ELENA Arkhangelskaya ¹, FRANCESCA Rizzo ¹, ELISABETTA Vignale ¹, FRANCESCO Pasetti ¹, NICOLA Stagnaro ¹, MARTA Pongiglione ¹, MAURA Valle ¹, FRANCESCA Magnaguagno ¹, ELENA Aleo ¹, VALENTINA Prono ¹, ANNA Marzoli ¹, FRANCESCA Nardi ¹, LORENZO Anfigeno ², SILVIA Pamparino ², MARTINA Fiannacca ², SARA Perissi ², MARCELLO Carlucci ³, STEFANO Avanzini ³, MICHELA Wong ³, LUCA Pio ³, GIROLAMO Mattioli ³, GIORGIO Piaggio ⁴, MARIALUDOVICA Degl'Innocenti ⁴, GIAN MARCO Ghiggeri ⁴, EMANUELA Piccotti ⁵, ANDREA Moscatelli ⁶, MARIA BEATRICE Damasio ¹

¹ IRCCS Istituto Giannina Gaslini - Radiology Department, Genova, ITALY

² University of Genoa - Health Science Department (DISSAL), Genova, ITALY

³ IRCCS Istituto Giannina Gaslini - Surgery Department, Genova, ITALY

⁴ IRCCS Istituto Giannina Gaslini - Nephrology Department, Genova, ITALY

⁵ IRCCS Istituto Giannina Gaslini - Emergency Department, Genova, ITALY

⁶ IRCCS Istituto Giannina Gaslini - Intensive Care Unit (ICU), Genova, ITALY

Summary of the presentation

- Physical Principles of Contrast-enhanced Ultrasound (CEUS)
- Safety-profile of contrast media used in CEUS
- Acquisition technique of CEUS
- Indications and off-label application of CEUS in pediatric population
- Case series

List of educational objectives

- To explain the safety of intravenous application of UCAs
- To mention current indications of UCAs in child
- To discuss indications and limits of intravenous application of UCAs in different radiological settings in pediatric population (i.e. characterization of focal organ lesion, blunt abdominal trauma, pyelonephritis, vasculitis, etc.)
- To make Radiologists aware of the advantages of CEUS in diagnosis and follow-up in different radiological settings in children being a radiation-free and repeatable imaging technique.

Purpose

The aim of this educational exhibit is to describe the current indications of UCAs in children and discuss their potential and possible future applications for intravenous administration.

Materials and Methods

We report a case series of different applications of UCAs in pediatric population:

I. Contrast-enhanced Voiding Urosonography (CEVUS) for Vesicoureteral Reflux (VUR) through endocavitary administration

II. Intravenous administration for:

- a. Characterization of focal organs lesions
- b. Blunt abdominal trauma
- c. Pyelonephritis
- d. Vascular pathologies (i.e. vasculitis)
- e. Inflammatory Bowel Disease (IBD) assessment
- f. Testicular lesions

Results

In pediatric field, CEUS is largely used for the diagnosis of VUR. However, it showed great potential if implemented for evaluation of focal organ lesions allowing differential diagnosis between benign and malignant lesions, without radiation exposure and with great advantages for longitudinal follow-up programs. In low-energy blunt abdominal trauma, it can identify isolated solid abdominal organ injuries, avoiding Computed Tomography and radiation exposure when it may not be fully or at least initially justified. Moreover, its safety-profile opens the door to different potential applications in children, for example in IBD and vasculitis, that are still a field of investigation.

Conclusions

Although in Europe intravenous UCAs administration in children is still off-label, several recent studies on a large population demonstrated that this imaging radiation-free technique is extremely safe, with low risk and a small number of reported adverse reactions and its use should be encouraged as an adjuvant tool in pediatric radiology.

Poster: SCI-056

WHEN LIFE DOES NOT GIVE YOU LEMONS...

JESSA M. Tunacao, JOHANNA Monsalve, JOYE Wang, FARZANA Nuruzzaman

Stony Brook Medicine, Stony Brook, USA

OBJECTIVES

1. Know risk factors for scurvy in children

2. Know MRI findings of scurvy may mimic chronic nonbacterial osteomyelitis (CNO)

7-year-old female with autism presents with new onset difficulty walking. 11 days ago, she reportedly had an unwitnessed fall, causing a limp which progressed to inability to bear weight and needing to drag herself in a seated position to move. Besides bruises along both thighs, negative review of systems.

Physical exam: Underweight nonverbal child in no acute distress. Bilateral knees with reduced range of motion beyond 90° flexion, with no active synovitis. Normal muscle strength/tone. Gait limited due to pain. Skin with linear tender ecchymosis on lateral thighs.

Labs: elevated ESR (43mm/hr), normal CBC.

She was admitted for further evaluation.

Differential diagnoses: non-accidental trauma, spinal mass, juvenile arthritis, and chronic nonbacterial osteomyelitis (CNO).

Skeletal survey and lumbar spine MRI normal. MRI bilateral lower extremities showed symmetric bone marrow low T1 and high T2 signal in the distal femoral and proximal tibial metadiaphyses with contrast enhancement with radiological impression of CNO.

Infectious and rheumatic studies normal. Complete diet history revealed patient ate only cheese sticks prompting further labs. Serum vitamin C levels returned as <5 µmol/L [normal: 23–114µmol/L]. Percutaneous gastric tube was placed for nutrition in addition to vitamin C supplementation. Within 1 week, patient regained the ability to ambulate with full range of motion and resolution of pain. No recurrence of symptoms, no need for anti-inflammatory drugs, and normal vitamin C levels upon follow-up with pediatric rheumatology, indicated a final diagnosis of scurvy.

Thus, MRI findings of symmetric T1 hypointensity and T2 hyperintensity and enhancement in metadiaphyses of long bones can suggest both scurvy and CNO. Clinical follow-up is key to differentiate these conditions as the latter requires anti-inflammatories to prevent long-term complications. Children with autism may have limited diets, predisposing them to nutritional deficiencies. Diet history can aid physicians towards diagnosis of scurvy when MRI findings are uncertain.

A. Normal bilateral lower extremity X-rays

B. Skin exam

C. Sagittal PD WI demonstrate symmetric bilateral bone marrow metaphyseal edema

D. Coronal T1 FS WI with contrast demonstrate bilateral symmetric metaphyseal and juxta-cortical enhancement

Poster: SCI-057

DETECTION OF SOFT TISSUE FOREIGN BODIES IN CHILDREN USING ULTRASONOGRAPHY

ALEXANDER Sheeka, RICHARD Jenkins, STACEY Castle, SUFI Sadigh

Imperial College Healthcare, London, UNITED KINGDOM

Summary:

Retained foreign bodies are a significant cause of morbidity in patients following traumatic injury. Complications include infection, poor wound healing, pain, and damage to underlying structures. In certain cases foreign bodies can travel significant distances from the site of initial injury. Children are at particularly high risk of foreign body retention following injury as some studies have suggested that foreign body sensation in children does not have good correlation with foreign body presence as is seen in adults.

In a recent case at our institution, a young child sustained a glass injury and to the right obturator region resulting in a retained 3cm shard of glass in the more proximal groin. The foreign body was

diagnosed using ultrasound nine months after the presenting injury. On surgical exploration a transected right spermatic cord was identified.

This is an educational poster to demonstrate the imaging characteristics of foreign bodies on ultrasound and the inter-operator reliability of ultrasound in detecting various foreign bodies in a phantom.

Educational Objectives:

To demonstrate the appearances of soft tissue foreign bodies on ultrasound and the reliability of using ultrasound to assess soft tissue injuries in children.

Materials and Method:

An ultrasound phantom containing foreign bodies of different sizes and type including metal, wood, and the major types of commercial glass. Radiologists and sonographers of differing grade are tested on their ability to detect the different materials using ultrasound.

Results:

Ultrasound images of foreign bodies in the phantom. In vivo ultrasound images of a retained foreign body in a child. Detection rates of each foreign body in the phantom, subdivided based on type of material and grade of assessor.

Conclusion:

Diagnostic imaging is useful in the assessment of children with suspected soft tissue foreign bodies. The most common imaging method for foreign bodies is plain radiograph; however, ultrasound is a recognized yet underused assessment method which is non-ionizing and has the added benefit of aiding in surgical planning and the assessment of adjacent neurovascular structures.

Poster: SCI-058

THE PEDIATRIC OVERNIGHT CALL CONUNDRUM: OPTIMIZING EXPERTISE AND DECREASING BURNOUT

MICHAEL Frazier, CHRISTINA Cinelli, JENNIFER Talmadge
Maine Medical Center, Portland, USA

Summary:

There is a noticeable trend for subspecialty staffing in radiology, particularly in the setting of overnight fluoroscopy call coverage. At our institution, a tertiary care level one trauma center and a referral center for pediatrics, the hospital administration requested pediatric subspecialty coverage, however we only have 3–4 pediatric fellowship trained attendings. To try to satisfy this request, we developed a yearlong pilot program to train a small cohort of non-pediatric radiologists who would help cover this call pool. As part of this process, we created a call curriculum, provided hands on training, performed interval assessments of comfort, performance, and satisfaction with the program, and implemented a peer learning process for this call cohort. Overall, the experience was positive for the group and the hospital. We are continuing for another year with this same call paradigm incorporating changes in response to feedback we received from radiologists and surgeons.

Educational Objectives:

-Illustrate a practical approach of covering emergent pediatric fluoroscopy overnight call in a private practice setting with a small cohort of non-peds fellowship trained radiologists to help cover with fellowship trained radiologists.

-To create a curriculum to help train up the radiologists without peds subspecialty training.

-To assess the pilot project with a focus on quality and safety.

-Incorporate Peer Learning in the evaluation and continuing education for pediatric overnight call.

Materials and Methods:

Our pediatric radiologists created guides for indications, diagnostic criteria, and technical aspects of overnight cases. A pre-call

knowledge assessment quiz was created. The volume, type of exams, hours on pager and in house were tracked. Surveys were conducted mid-year and at 12-months to evaluate the call-pool experience. Surgeon feedback was solicited. A total of 9 radiologists participated in this call pool.

Results:

25 total after hours cases were performed. Of the 9 radiologists, 78% reported feeling comfortable with the technical aspects of pediatric fluoroscopy. 100% found the training content helpful, and 78% were satisfied with new call paradigm. Volvulus/malrotation and intussusception were the most problematic cases for the non-pediatric radiologists. Of the 5 pediatric surgeons, all were in favor of the new cohort design. 5/25 cases received constructive criticism from surgeons. No adverse patient outcomes were reported.

Poster: SCI-059

PLUNGING RANULA IN CHILDREN: DIAGNOSIS BY CROSS-SECTIONAL IMAGING

DIKSHA Diksha, PAREEKSHITH Bhat
Kasturba Medical College, Mangalore, INDIA

A plunging ranula is a rare mucous fluid collection that develops after the rupture of sublingual gland mucocele and its extension into the submandibular space posteriorly. Plunging ranulas are rarely encountered in children under 10 years of age and hence, quite often tend to be misdiagnosed, inevitably leading to incorrect treatment. This case report presents a seven-year-old male child who presented with a blue, translucent swelling in the floor of the mouth. Clinically, it was suspected to be simple ranula. But, magnetic resonance imaging revealed the true extent of the lesion and its relationship to the surrounding structures and the characteristic signs led to the correct diagnosis of plunging ranula. Marsupialization was performed and the histopathological examination of mucosal lining of ranula turned out to be consistent with the diagnosis.

PURPOSE: MRI of plunging ranula is rarely reported in the literature. But, it, indeed, facilitates us to reach the appropriate diagnosis and plan the treatment of the suspected ranula, accordingly.

Poster: SCI-060

OPTIMIZING UTILIZATION OF ULTRASOUND, MRI, AND PLAIN FILM USE IN PEDIATRIC SICKLE CELL PATIENTS

WILLIAM NOLAN DI Dickson¹, CYNTHIA Hanemann¹, GERARD Ballanco¹, SARAH Long¹, CAROL Becker³, MARIA-GISELA Mercado-Deane²

¹ Tulane University School of Medicine Department of Radiology, New Orleans, LA, New Orleans, USA

² River City Imaging Associates, San Antonio, TX, San Antonio, USA

³ LSU School of Medicine Department of Radiology, New Orleans, LA, New Orleans, USA

Purpose

To examine the use of ultrasound, MRI, and plain films in the evaluation of pediatric sickle cell complications to limit radiation exposure, and to serve as a review of radiologic pathophysiology as it pertains to pediatric sickle cell.

Background

Efforts have been made to reduce radiation in pediatric patients¹. On average pediatric sickle cell patients will have completed 26.7 radiographic tests by age 18; six percent have over 3 CT scans, which may be associated with an increased risk of cancer². These patients are living longer due to treatment advances—it is imperative to reduce radiation to prevent future complications^{3,4}.

Objectives

To provide examples of modalities used to minimize radiation exposure among pediatric sickle cell patients, to provide imaging examples of the varying pediatric sickle cell manifestations, and to review the radiologic anatomy of children as it pertains to sickle cell.

Methods

Abdominal ultrasound can be used to evaluate spleen size (auto-infarction), to search for cholelithiasis or cholecystitis, to assess renal size and echogenicity for chronic disease, or to localize extramedullary hematopoiesis in the spleen, liver or adrenals. Ultrasound images will be included with comparison CT to support that interrogation of the abdomen via ultrasound is an adjuvant, comparable or superior to CT. MRI is used for the diagnosis of stroke, Moyamoya, and musculoskeletal ailments like avascular necrosis of bone or infarct. Judicious use of CT has a role, appropriate when pulmonary embolus is suspected. Indications for use of Dual Energy CT in the symptomatic Sickle Cell patient will be reviewed. Plain radiographs are the imaging of choice for diagnosis and follow up for pneumonia and acute chest syndrome. Imaging will be arranged in a format with blank arrows, asking the viewer to identify pathology.

Conclusion

There is an important role for ultrasound and MRI in the care of pediatric sickle cell patients. CT should be used judiciously when other modalities are inadequate.

1.<https://www.imagegently.org/>

2.Gilyard, SN. Archer-Arroyo K, Milla, SS., Hamlin, SA., Herr, KD. “Imaging Sickle Cell Disease in the Emergent Setting” Electronic presentation at the meeting of the American Society of Emergency Radiology, Scottsdale, AZ, September 11–14, 2019.

3.<https://www.cdc.gov/ncbddd/sicklecell/treatments.html>

4.Lin EC. Radiation risk from medical imaging. *Mayo Clin Proc.* 2010;85(12):1142-1146. doi:10.4065/mcp.2010.0260.

Poster: SCI-061

HANDS-ON ULTRASOUND TRAINING FOR RADIOLOGY RESIDENTS: THE IMPACT OF AN ULTRASOUND SCANNING CURRICULUM

MARIA Velez-Florez¹, SHAUNA Dougherty¹, MICHELLE Retrouvey¹, HAILU Tigist¹, ABIGAIL Ginader¹, NICOLE Bodo¹, JANET Reid¹, AMI Gokli²

¹ The Children's Hospital of Philadelphia, Philadelphia, USA

² Staten Island University Hospital, Staten Island, New York, USA

Purpose: A radiologist's competency in performing ultrasound (US) is crucial. In the USA, increasing demands and limited hours in residency programs have led to prioritizing the training of ultrasound technologists over radiologist trainees. Moreover, other specialties are actively integrating US scanning into their programs. Most radiology residents do not feel confident performing US examinations on their own. The purpose of this study is to evaluate the impact of implementing an abdominal US scanning rotation and virtual course as it pertains to radiology residents' ability and confidence in performing US.

Materials and methods: 65 radiology residents on a pediatric radiology rotation were divided into control (A N=39) and intervention groups (B N=26). Both groups completed a pre-and post-survey regarding confidence in scanning ability, and pre-and post-skills assessment test. Residents in both groups were asked to perform an abdominal US on a volunteer with scanning skills being evaluated concurrently by an expert technologist. In the intervention group, participants were enrolled in a 1-week hands-on pediatric abdominal US scanning rotation with an abdominal US e-course (composed of audio/video demonstrations). At

completion, they were given a “perception questionnaire” regarding their thoughts about the course and scanning rotation. Trainee performance in each group was evaluated by comparing the pre- and post-test results using paired-T tests, and effect size [ES] with Cohen’s d.

Results: The pre-confidence and pre-skill performance was comparable in both groups. Confidence in scanning ability significantly improved in both groups, with a greater ES in group B (B $d=1.5$ [large ES] $p<0.001$; A $d=0.47$ [small ES] $p=0.001$). Although both groups demonstrated skill improvement, a greater ES was observed in group B than A (B $d=1.77$ [large ES] $p<0.001$; A $d=0.47$ [small ES] $p=0.005$). Overall, group B residents expressed that the US rotation and virtual course was helpful for developing US skills.

Conclusion: Obtaining optimal US images is a learned and practiced skill. Although participating in a general pediatric radiology rotation may familiarize residents with US scanning and increase their confidence/skills, a dedicated scanning rotation paired with an US e-course has greater impact in improving resident’s confidence and skills.

Poster: SCI-062

THE IMPACT OF INTEGRATING RADIOLOGY DIDACTICS IN CLERKSHIP CURRICULA

GRANT MacKinnon¹, TRAVIS Crook^{1,2}, MELISSA Hilmes^{1,2}

¹ Vanderbilt University School of Medicine, Nashville, USA

² Vanderbilt University Medical Center, Nashville, USA

Background: The majority of US medical schools do not require a radiology rotation for graduation, and consequently the introduction to radiology may be fragmented. Integration of radiology didactics in clerkships may provide students an early exposure to the field. Our goal was to evaluate the impact of radiology lectures on medical student perspectives on radiology.

Methods & Materials: Radiology lectures were developed for pediatric and internal medicine second-year clerkships. The pediatric lecture focused on important radiological findings potentially covered on the NBME exam, whereas the internal medicine lecture provided a systematic approach to interpreting chest radiographs. The online recorded lectures were made available one week prior to a mandatory group discussion and case review. Students were provided an optional REDCap survey before and after the lectures for quantitative assessment. Data was analyzed by T-test, with pairing of responses when possible.

Results: The lectures were provided to 23 students in the pediatric clerkship and 15 students in the internal medicine clerkship. The combined response rate for both surveys was 57.9% (44/76). Of the responses, 26 were pre-lecture, 18 were post-lecture, and 16 students completed both the pre- and post-lecture surveys. Results demonstrate the lectures improved medical student comfort in speaking to a radiologist about imaging ($p < .001$) and identifying “do not miss” diagnoses ($p < .0001$). In addition, there was an increase in satisfaction of radiology education in medical school ($p < .002$). There was no significant increase in student perspective on the importance of radiology to future practice, importance of radiologists on clinical care, and interest in a career in radiology.

Conclusions: The integration of radiology lectures into clerkship didactics is feasible and benefits medical students by increasing comfort in identifying important diagnoses and discussing imaging with a radiologist. Medical students have a high perceived importance of radiologists as members of the health care team.

Poster: SCI-063

PRESENTATION TO PUBLICATION REVISITED: TRENDS IN PUBLICATION RATE OF ORAL PRESENTATIONS FROM ESPR, SPR, AND IPR

HARSIMRAN Laidlow-Singh¹, RIWA Meshaka², OWEN JOHN Arthurs², SUSAN CHENG Shelmerdine²

¹ Department of Imaging, The Royal London Hospital, London, UNITED KINGDOM

² Department of Radiology, Great Ormond Street Hospital for Children, London, UNITED KINGDOM

Purpose:

Publication of research presented at international conferences allows for these to reach a wider audience, and provides the evidence basis for future academic work and change in practice. Nevertheless, a previous publication found that <50% of work presented at paediatric radiology conferences from 2010-2012 reached publication status. Our aim was to determine whether there has been any change in the presentation to publication rate from more recent conferences, and how this could be improved.

Materials and Methods:

A retrospective review of oral presentation abstracts over 3 years of conferences (ESPR, SPR and IPR 2014-16) was undertaken, and subsequent publication within PubMed cited journals in 2020 were recorded. Multiparametric data extracted for each abstract included: the presence of subsequent publication, originating institution, institution type, recipient journal, study sample size. Results tabulated and analysed in Excel and SPSS.

Results:

The oral abstract to publication rate was 45.8% (318/694), and not statistically significantly different to ESPR, IPR and SPR from 2010-2012 ($p=0.1443$, >0.05). The mean time from conference to publication was 18 months (range -30 to +73 months). Academic-affiliated, tertiary care institutions and USA-based teams continue to contribute the largest proportions of presented data (95.4%, 71.5% and 66.9% respectively). The rate of international collaboration in published studies has fallen from 6.3% previously to 3.2% (22/694).

Conclusions:

Approximately half of all oral presentations reviewed resulted in a peer-reviewed publication. This rate has not changed significantly over 4 years. International collaboration should be encouraged and barriers to publication from non-academic centres explored to help better represent their work.

Poster: SCI-064

IMPACT OF COVID-19 PANDEMIC ON MRI OPERATIONS AND ACCESS: A DICOM-HEADER DATA ANALYTICS APPROACH

SAMANTHA Harrington¹, CAMILO Jaimes^{2,3}, CAROLINE Robson^{2,3}, SARAH Bixby^{2,3}, FEDEL Machado-Rivas^{2,3}, SIMON Warfield², RICHARD Robertson^{2,3}, BENOIT Scherrer⁴

¹ Massachusetts General Hospital, Boston, USA

² Boston Children’s Hospital, Boston, USA

³ Harvard Medical School, Boston, USA

⁴ Quantivly, Cambridge, USA

Materials and methods: IRB approved and HIPAA compliant study. Retrospective analysis of single pediatric center data from 1/1/2019-10/31/2020. Metrics were extracted using the Quantivly platform, a unified metadata layer that extracts, cleans and harmonizes metadata from DICOM images providing previously unattainable metrics (e.g: exam duration, number of acquisitions, efficiency [gradient time/exam duration]). We analyzed number of MRIs/week, organ system (body, neuro, MSK, fetal, ventricular check[VC]), scan duration (<30 min, 30-45 min,

45–60 min, >60 min), efficiency, number of acquisitions, duration of each, and age (<5 yr, 5–10 yr, 10–15 yr, >15 yr). We compared these parameters before lockdown (Stage-1)(3/23/2020), during lockdown (Stage-2)(3/23/2020–5/18/2020), and after phase I of reopening (Stage-3)(5/18/2020–10/31/2020).

Results: We analyzed 32876 MRI exams over 96 weeks. Average MRIs per week in Stages 1, 2, and 3, were 362, 137, and 358. ANOVA showed significantly less exams during Stage-2 ($P<0.05$). Absolute number of all studies significantly decreased ($P<0.05$) between stage-1 and 2, except for fetal; percentage decrease in MSK (from 27.2 to 15.1%) ($P<0.05$) and increase in VC (from 7.2 to 12.4%) ($P<0.05$) were significant. Percentages were not significantly different between stage-1 and 3. In stage-2 there was a significant increase in percentage of children <5 years (from 19.2 to 29.1%) and decrease in >15 years (from 42.1 to 35.7%) ($P<0.05$, both). Although there was no difference in efficiency between stage-1 (0.53) and -2 (0.52), efficiency did increase significantly in stage-3 (0.55) relative to stage-2 ($P<0.05$). The average number of acquisitions per MRI was significantly higher ($P<0.01$) during stage-2 (11.5) vs. stage-1 and -3 (10.6, both).

Conclusions: Impact of legislation and social distancing for CoVID-19 varied with organ-system and age. During lockdown, decrease in volume was most severe for MSK, while fetal and VC maintained similar numbers and thus represented a higher percentage of the studies performed. Demographics also changed, with mean age of patients being lower.

Poster: SCI-065

FELLOW-DRIVEN VIRTUAL EDUCATION DURING A PANDEMIC: A PILOT PROJECT

ALEXANDER El-Ali¹, AMY Mehollin-Ray², ERIC Crotty³, ARNOLD CARLSON Merrow³, JANET Reid⁴, AMI Gokli⁵

¹ New York Univeristy, New York City, USA

² Texas Children's Hospital, Houston, USA

³ Cincinnati Children's Hospital Medical Center, Cincinnati, USA

⁴ Children's Hospital of Philadelphia, Philadelphia, USA

⁵ Staten Island University Hospital | Northwell Health, New York City, USA

Background: The pandemic has upended graduate medical education of every specialty and there is continued need for measures to improve trainee education, particularly in radiology.

Objective: We evaluated an educational intervention tailored to advanced-level radiology trainees (fellows and residents) whose education was abruptly interrupted due to the pandemic.

Methods: Six-step model for curriculum design was utilized to create an educational intervention specifically for fellowship-level learners whose educational programs were interrupted by the pandemic. A mixed-methods assessment was undertaken including baseline and post-intervention survey data. Primary outcome was learner attitude towards virtual learning. Secondary outcomes were (1) session participation numbers and (2) instructor attitude toward virtual learning.

Results: Quantitative needs assessment was obtained from 373 individuals at 191 separate institutions in 47 different countries. Most respondents were trainees, $n = 199$ (53%). Learning preferences varied by international status (USA vs non-USA) regarding presentation style and top-3 subject selections ($p<0.05$). Based on the needs assessment, a virtual curriculum via interactive web-based lectures was devised. 386 post-session feedback responses were obtained (response rate: 36%). Participants indicated that instructors were able to engage learners in a virtual-lecture format, “Strongly Agree” Post-Intervention: 88% vs Pre-Intervention: 62%, $P<0.01$. All instructors indicated that they “Strongly Agree” that virtual learning activities can meet an important educational need and that virtual learning events can serve as an important learning tool to fellowship-level learners.

Conclusions: We characterized learning preferences of a cohort of international radiology learners. Our intervention was associated with improved attitudes toward virtual learning regardless of geographic location. These results suggest that alternative educational platforms may allow us to add new practices into our pedagogical armamentarium.

Poster: SCI-066

INTRODUCING AND INTEGRATING MINDFULNESS WITHIN THE RADIOLOGY RESIDENCY EDUCATION

RITA Sico, AMISHA Shah, ERICA Kar
UPMC Children's Hospital, Pittsburgh, USA

Purpose:

Physician burnout is increasing in prevalence. Personal resilience is an essential component of individual wellness which decreases burnout. Mindfulness is a proven effective technique for this purpose. The Accreditation Council for Graduate Medical Education (ACGME) requires all residency and fellowship programs to address well-being more directly and comprehensively with the goal of developing a competent, caring, and resilient physician. The objective of our study is to assess the feasibility of introducing mindfulness to our radiology trainees during educational conferences.

Methods:

During pediatric radiology rotations at UPMC Children's Hospital of Pittsburgh, mindfulness sessions were incorporated into two case conference periods. The first session of mindfulness was a 20-minute PowerPoint presentation introducing the technique of mindfulness and the scientific rationale behind it. The second session was approximately 10 minutes of mindfulness meditation. Both sessions were conducted by the same pediatric radiologist and followed by a routine pediatric radiology case conference. Following both sessions, the radiology residents were sent a 10-question survey using the Likert scale. Surveys were collected over a period of approximately four months.

Results:

Out of a total of 14 respondents, 78% attended both sessions. Out of all participants 75% agreed or strongly agreed that they enjoyed the mindfulness session, and that presenting mindfulness during the case conference did not detract from their learning of either subject. 58% either agreed or strongly agreed that they would enjoy more wellness-related topics in this type of integrated format. 75% of respondents recognized the scientific rationale behind mindfulness as presented in the first session. 90% recognized breathing as an essential element of mindfulness meditation, and 75% reported that they were able to focus on their breathing for at least some time during meditation. 64% reported that they will seek out more wellness resources to enhance stress reduction. 75% strongly agreed or agreed that the wellness program offered through the residency program is enhanced by the incorporation of mindfulness sessions, and that mindfulness practices will help them decrease stress.

Conclusion:

Mindfulness can be integrated into resident education programs effectively.

Poster: SCI-067

USELESS AND LIMITS OF POST MORTEM COMPUTER TOMOGRAPHY (PMCT) IN A CASE OF INFANT MURDER IN A PRETERM

ILARIA Viola¹, GIUSEPPE Lo Re¹, GIOVANNI De Lisi², MICHELE Santoro³, EMILIANO Maresi², SERGIO Salerno¹

¹ Dipartimento di Diagnostica per Immagini, Policlinico Università di Palermo, Palermo, ITALY

² U.O di Diagnostica Autoptica Policlinico Università di Palermo, Palermo, ITALY

³ Policlinico Gemelli Università Cattolica del Sacro Cuore, Roma, Roma, ITALY

One of the most frequent and important medico-legal question is whether a fetus, in case of suspected neonaticide, was born alive or not. The certainty of the viability of the product of conception at birth could be obtained both from the autopsy examination which highlighted the floating of the lungs in water (docimasic test) both from the histological examination.

Unfortunately, there is no “universal consensus” on the use of the hydrostatic test for the diagnosis of live birth versus stillborn. The use of post mortem CT (PMCT) can substantially add to forensic examinations.

The present case-report examines the usefulness of postmortem computed tomography (PMCT) in the detection of live birth signs and it compares the results with the autoptoc examination. A newborn was thrown out the window after delivery. The pregnant mother has hidden the pregnancy. PMCT showed multiple fractures of the skull with degeneration of cerebral parenchyma, clavicle fracture and pulmonary distress confirming that the baby has breath for some times. While autoptoc examination showed greater diagnostic accuracy to identify proof of live birth on the heart and to study cerebral parenchyma confirming that the baby born alive but deceased when thrown out the window. In conclusion, both PMCT and autoptoc examination showed widespread ventilation phenomena with complete aeration of the lungs, indicating the potential role of PMCT as a non-invasive tool in addition to autopsy procedures to differentiate between stillbirths and live births.

Poster: SCI-068

UTILIZATION OF POSTMORTEM IMAGING IN NORTH AMERICA

MARY Harty, SHARON Gould, LAUREN Ayers, H THEODORE Harcke
Nemours/AI DuPont Hospital for Children, Wilmington, USA

Purpose:

Autopsies, an important tool in helping to bring closure to the families of the deceased as well as contributing to the body of medical knowledge, have become uncommon procedures except when required by statute. Postmortem Imaging (PMI) has stepped in to fill the void left by the decline in the number of conventional autopsies. PMI is widely accepted in Europe, Asia and Oceania but there has been a delay in acceptance in North America. Our objective is to determine the utilization of PMI and define the current barriers to PMI with the goal of expanding the role of PMI in the USA and Canada. Materials and Methods:

A survey using the Survey Monkey® platform was distributed in April 2021 to the active SPR membership, consisting of approximately 2000 members. Survey results will be evaluated in May 2021. The survey included a series of questions requesting specific information on the use of PMI: imaging modalities, PMI readers and subspecialists, methods of communication, relationship with Medical Examiner/Coroner, correlation with autopsy, reimbursement, and barriers to implementation of PMI. Results:

Findings from the survey will be presented. We will test hypotheses generated from two preliminary surveys that (1) the majority of imaging facilities performing PMI utilize radiographs; (2) dedicated children’s hospitals providing CT and MRI are an exception; (3) PMI is primarily interpreted by radiologists with neuroradiologists providing additional expertise as needed; (4) there is a paucity of formal relationships with Medical Examiners; (5) infrequent formal correlation with conventional autopsies occurs. We also expect to confirm that little reimbursement is available for PMI performed in the USA. Conclusion:

Anticipated survey results will define the current status of PMI throughout the North American pediatric radiology community and reveal

existing obstacles to implementation of PMI. The results will be used to develop practice guidelines for prenatal and pediatric PMI that will be shared with the radiology and pediatric communities.

Poster: SCI-069

THE PANDEMIC'S EFFECT ON RESIDENT PEDIATRIC RADIOLOGY EDUCATION AS MEASURED BY INDEPENDENT CALL PERFORMANCE

LYNN Della Grotta, GEORGE Koberlein
Wake Forest Baptist Health, Winston Salem, USA

Purpose:

The COVID 19 pandemic has caused unprecedented changes in the workflow of academic radiology departments. These changes have been due to multiple factors from changes in case volume due to the temporary suspension of nonessential surgeries and appointments, to changes in delivery of teaching due to social distancing. It is still unclear how these changes have impacted the career development and performance of radiology residents. The purpose of this study is to assess the impact of the pandemic on radiology resident imaging volumes as it applies to pediatric studies and assess the impact on performance measured by number of reports changed during independent call.

Materials and Methods:

Change in volume of studies and in number of changed reports was assessed during defined pre-pandemic and intra-pandemic time periods for pediatric studies (age less than 18). Change was assessed by absolute difference per resident and percent difference. Attention was paid to the first and second year radiology residents as this is when new call responsibilities are added for Wake Forest radiology residents. Results:

Comparing pre-pandemic to intra-pandemic, there was a change of 53 less studies per first year radiology resident and 57 less studies per second year radiology resident within the 6 months leading up to starting their new independent call responsibilities with a percent decrease of 9% and 11% respectively. For change of reports, there were 2 less change of reports per first year radiology resident during the pandemic compared to pre and 1 less per second year resident, with a percent decrease of 96% and 78% respectively.

Conclusion:

While there was a decrease in number of studies read by residents as they prepared for independent call during the pandemic, there was, interestingly, also a decrease in the number of change of reports during pandemic times compared to pre-pandemic. Our leading hypothesis for these results relates to volume demand during independent call. During the pandemic, total volume of studies read during independent call was decreased, with volume decreased by 47% for first years and by 39% for second years. The decrease in error during the pandemic may highlight that decreased workload and thus increased time per study contributes to increased accuracy.

Poster: SCI-070

CONGENITAL IMMATURE TERATOMA OF THE THYROID: A MULTIMODAL IMAGING APPROACH

JOSE MARIA Ulloa-Gonzalez ¹, ABRAHAM Reynoso-Topete ¹, MONICA HASSEL Gomez-Sahagun ², EVA MARIA Alba-Garcia ², GONZALO Ramos-Rubio ³, CLAUDIA Mendoza-Cerpa ³

¹ Instituto Mexicano del Seguro Social UMAE HE CMNO - Departamento Radiologia, Guadalajara, MEXICO

² Instituto Mexicano del Seguro Social UMAE HGO CMNO - Departamento Medicina Materno Fetal, Guadalajara, MEXICO

³ Instituto Mexicano del Seguro Social UMAE HE CMNO - Departamento Patología, Guadalajara, MEXICO

INTRODUCTION

Congenital neoplasms appear in 1.7-13.5 cases per 100,000 live births,1 they are considered congenital when detected in-utero or the first 3 months of life; they are comprised of all three germ cell layers and can differentiate in components from every organ in the body 3.

Cervical teratoma represents between 1 and 5% of all children teratomas. Thyroid teratoma is rarer with 40 reports in the literature, 28 of them from a 75-year long series. 3

We present a case of congenital thyroid teratoma diagnosed in-utero. The mass size caused airway compression leading to the product death. Autopsy confirmed the diagnosis of immature teratoma.

FINDINGS

A 24-year-old patient was referred to our institution due to a fetal cervical mass diagnosed on routine ultrasonography. Sonography demonstrated a complex cystic mass with a solid component, vascular flow at Doppler interrogation; an MRI scan showed findings consistent with a complex loculated mass compromising the cervical region, causing apparent obstruction of the trachea and esophagus, concomitant polyhydramnios was evident. In consent with fetal medicine, otolaryngology and neonatology departments the case was evaluated. Cesarean section was performed a week later, upon birth orotracheal intubation and tracheostomy were attempted but given the close relation to the carina results where unfavorable. Post-mortem CT scan and x-rays showed a cervical mass displacing the mandible, compressing the trachea, and passing the thoracic operculum. Autopsy reported a congenital benign immature thyroid teratoma.

CONCLUSION

Congenital tumors are uncommon conditions; modern imaging techniques allow us to detect this entities in-utero and provide a presumptive diagnosis for histologic type based on characteristics, location and associated findings such as amniotic fluid disturbances while allowing a better understanding of the fetus condition to plan for the best moment for pregnancy interruption and interventions for the newborn.

BIBLIOGRAPHY

- 1.Chapman, M., et al. Congenital Oral Masses: An Anatomic Approach to Diagnosis. *Radiographics* 2019; 39:1143-1160.
- 2.Alamo, L., Beck-Popovic, M., Gudinchet, F., Meuli, R. Congenital tumors: imaging whe life just begins. *Insights Imaging* 2011;2:297-308.
- 3.Redlinger, W., Lack, E., Robson, C., Rahbar, R., Nose, V. Primary Thyroid Teratomas in Children A Report of 11 Cases With a Proposal of Criteria for Their Diagnosis. *Am J Surg Pathol* 2005;29:700-706.

Poster: SCI-071

FETAL THROMBOSIS OF THE TORCULAR HEROPHILI

STEPHANIE Spieth ¹, CHRISTOPH Meissner ¹, MATEJ Komár ², RALF-THORSTEN Hoffmann ¹, GABRIELE Hahn ¹

¹ Department of Diagnostic and Interventional Radiology, University Hospital Carl Gustav Carus Dresden, Dresden, GERMANY

² Department of Gynecology and Obstetrics, University Hospital Carl Gustav Carus Dresden, Dresden, GERMANY

Summary

Fetal thrombosis of the intracranial confluence of sinuses (torcular herophili) is a rare disease. Usually it is detected in ultrasound (US) and confirmed in magnetic resonance imaging (MRI). Published cases reveal mostly good outcomes. Follow-up imaging is required for prognostic evaluation and patient guidance. We describe a case with incomplete resolution of thrombosis in pre- and postnatal imaging in a baby without clinical abnormalities.

Educational objectives

To describe the diagnostic value of imaging in the prenatal diagnosis and management of thrombosis of the torcular herophili.

Material and Methods

We present a male patient with a large intracranial posterior mass in routine US at 20 weeks of gestation. To confirm suspicious thrombosis of the torcular herophili and monitor the course of the disease four antenatal 1.5 Tesla MRI scans using multiplanar T2w sequences were performed in monthly intervals, followed by transfontanellar US as well as multisequence MRI at birth.

Results

Prenatal US showed an intracranial posterior midline and hypoechoic lesion with hyperechoic centre. Fetal MRI revealed an extraaxial mass in the region of the torcular herophili of low intermediate signal with a central hypointense structure corresponding to massive dural sinus dilatation with thrombosis and extension into the superior sagittal, straight and transversal sinuses. There was mass effect on the occipital lobes and cerebellar hemispheres. At no point there were signs of brain parenchymal injury or ventriculomegaly. After interdisciplinary counselling the parents decided to continue pregnancy. Follow up-imaging initially showed growing dural sinus dilatation, followed by progressive decrease of ectasia and mass effect in the subsequent exams. Postpartum imaging of the term born baby without neurologic disorders revealed residual thrombosis of the torcular herophili, straight and transversal sinuses as well as hypoplasia of the left cerebellar hemisphere and frontotemporal cortex.

Conclusion

Fetal thrombosis of the torcular herophili has a good outcome in 85% of cases. Partial or complete thrombus resolution, absence of brain parenchymal injury and arteriovenous shunt indicate a favourable outcome. Poor prognostic factors are deep thrombosis, large persistent mass effect, ventriculomegaly, ischemic brain damage or cardiac failure. Because prognosis can only be determined over time, outcome evaluation requires periodic prenatal imaging including US and MRI.

Poster: SCI-072

PRENATAL IMAGING OF CONGENITAL EPULIS

CHRISTOPH Meissner ¹, STEPHANIE Spieth ¹, CHAHIT Birdir ², GABRIELE Hahn ¹, RALF-THORSTEN Hoffmann ¹

¹ Department of Radiology University Hospital, Dresden, GERMANY

² Department of Obstetrics and Gynecology University Hospital, Dresden, GERMANY

Summary

Congenital epulis, also known as Gingival granular cell or Neumann’s tumor is a rare tumor of the oral cavity. It was first described in 1871 by Neumann. In the majority of cases it occurs at the anterior ridge of the maxilla, less often at the mandible. It is a solitary tumor with only some reported cases of multiple tumors. It is not associated with other congenital abnormalities and the teeth are not affected. Etiology is unknown, some prefer a “hormone theory” because of a clear female predominance (10:1). In histology epulis consists of large cells with eosinophilic cytoplasm, no capsula and an atrophic stratified squamous epithelium cover. Size varies between 1 mm and 8 cm. Depending on the size of the tumor epulis can cause feeding and airway problems. Prenatal imaging enables to detect the tumor and to exclude differential diagnoses like hemangioma or teratoma. It also helps for planning the delivery (vaginal versus cesarian section) and postnatal therapy. Treatment is surgery. These tumors are benign and do not tend to local recurrence, no malignant transformation is described. Therefore no follow up is needed. Ultrasound is the first line imaging, fetal MRI helps to confirm diagnosis and excludes differentials.

Educational impact

To be aware of the extremely rare diagnosis of epulis and to help differentiate it from more common congenital oral cavity tumors like heman-gioma or teratoma.

Material and Methods

A 36 year old III. gravida, II. para in gestation week 36+3 (female fetus) came to our institution with the suspicion of an oral or cervical tumor. We performed ultrasound and fetal MRI (3T, body array, three dimensional T2 HASTE and T1w sequences).

Results

Ultrasound could not reliably locate the tumor to the oral or cervical compartment. Subsequently fetal magnetic resonance imaging (MRI) was performed, which showed a T1-/ T2-muscleisointens exophytic tumor arising from the oral cavity. We diagnosed congenital epulis. Cesarean section was performed in gestation week 37+0 without complications. At day 1 oral surgery was done. Histology confirmed our diagnosis.

Conclusion

Epulis is a rare congenital benign oral cavity tumor arising from the alveolar ridge of the mandible or maxilla. Prenatal ultrasound and MRI can detect and differentiate fetal oral masses and help to plan delivery and postnatal therapy.

Poster: SCI-073

RETROSPECTIVE MOTION CORRECTION IN FETAL MRI: HOW TO IMAGE A MOVING TARGET

FEDEL Machado Rivas, CLEMENTE Velasco-Annis, ONUR Afacan, SIMON K. Warfield, ALI Gholipour, CAMILO Jaimes
Boston Children's Hospital - Department of Radiology, Boston, USA

Background:

Motion remains a major challenge in fetal MRI. Clinical exams are constrained to the use of ultra-fast sequences (e.g.: single-shot FSE, bSSFP, VIBE), sacrificing tissue contrast and spatial resolution. This limitation also extends to research, as it precludes utilization of many advanced/quantitative pulse-sequences and introduces bias. Retrospective motion correction techniques have emerged as safe and effective tools to mitigate the deleterious effects of motion; however, their implementation remains limited to a few hospitals/groups. A growing body of techniques allows to compensate for rigid and non-rigid motion in structural MRI and motion in DTI.

Objectives:

- 1)To review methods of retrospective motion correction for structural fetal MRI
- 2)Illustrate scientific and clinical applications of motion corrected fetal structural MRI
- 3)Highlight recent development in motion correction: fetal body MRI and fetal brain DTI.

Approach:

- 1)Graphically present the conceptual basis of retrospective motion correction for fetal brain MRI using a slice-to-volume registration (SVR) technique.
- 2)Present publicly available spatiotemporal atlases of fetal brain development with existing anatomic labels and illustrate potential applications.
- 3)Review of clinical cases processed with SVR technique: malformations (Polymicrogyria, inferior vermian hypoplasia, rhombencephalosynapsis, holoprosencephaly, band heterotopia); Syndromes (Tuberous sclerosis, charge); vascular (vein of Galen).
- 4)Illustrate reconstruction of fetal body MRI for improved visualization and measurement of visceral organs.
- 5)Review motion-tracked SVR for fetal DTI and show application in tractography.

Conclusion:

Retrospective motion correction results in substantial improvements in image quality in fetal MRI that can facilitate clinical evaluation of cases and enable quantitative research techniques.

Poster: SCI-074

CASE REPORT OF ZELLWEGER SYNDROME DIAGNOSED BY FETAL MRI

JOANA Diaz¹, MATSUMOTO Larry², KUCERA Jennifer²

¹ University of South, Tampa, USA

² Johns Hopkins All Children's Hospital, St. Petersburg, USA

Zellweger Syndrome (ZS) is a rare peroxisomal disorder also referred to as cerebrohepatorenal syndrome. The estimated incidence is approximately 1 in 50,000 to 1 in 75,000 with a dismal prognosis and average lifespan of approximately 1 year. As the name implies, it involves the central nervous system, the liver and the kidneys. The most common prenatal ultrasound features include fetal hypokinesia, renal hyperechogenicity, and cerebral ventricular enlargement; however, the imaging findings on fetal MRI have been only rarely illustrated.

We present a case of a 36-year-old pregnant female without significant past medical history. Prenatal screening ultrasound at 19.5 weeks demonstrated hyperechoic kidneys. Initial amniocentesis was negative. Follow-up ultrasounds demonstrated dilated lateral ventricles at 34 weeks at which point a syndromic diagnosis was suggested, and the patient was referred for fetal MRI. The fetal MRI demonstrated ventriculomegaly, white matter signal abnormality, focal pachygyria, numerous cortically based renal cysts and subjective decreased fetal motion suggesting a potential diagnosis of Zellweger syndrome. A repeat amniocentesis sent for specific PEX-1 analysis, and ultimately autopsy, confirmed the diagnosis of Zellweger syndrome. In addition to serial ultrasound and fetal MRI images, we will also present postmortem histopathologic correlates for the imaging findings.

Our case highlights the pivotal role fetal MRI can play in potentially devastating diagnoses. It is important for pediatric radiologists to be familiar with the imaging features of Zellweger syndrome on fetal MRI to better facilitate prenatal counseling and guide appropriate clinical management.

Poster: SCI-075

FETAL MR IMAGING OF CRANIOPAGUS

KRITI Gwal, GARRICK Biddle, ARZU Ozturk, OSAMA Raslan, JENNIFER Chang

University of California Davis Health, Sacramento, USA

Purpose:

To review the fetal MR imaging for craniopagus and to emphasize the important points to mention for postnatal and surgical planning

Objectives:

- 1.Important points to emphasize for fetal MRI evaluation of conjoined twins, in particular craniopagus
- 2.Pictorial review of the findings and eventual postnatal correlates, in addition to postnatal imaging

Materials and Methods:

A retrospective case review evaluated the fetal MRI scans performed on the twins. Axial, sagittal, and coronal views of the fetal brains were performed. Additional sequences including echo-planar imaging (EPI) were performed for further evaluation of the dural venous sinuses.

Evaluation of the fetal MRI for classification as complete or partial craniopagus was accomplished, in addition to evaluation of the conjoined twins for fusion of different levels of cranium, vasculature, and brain parenchyma.

Results:

Partial craniopagus was demonstrated in the conjoined twins showing abnormal fistulous connection of the transverse sinus of one twin to the other twin's sagittal sinus. The imaging depicted the herniation of the parietal lobe of one twin partially extending

into the cranium of the other twin. No fusion of the brain parenchyma was demonstrated.

Conclusions:

With fetal MRI, we were able to diagnose the abnormality, in addition to providing important information regarding the conjoined twins for prenatal and treatment planning.

Poster: SCI-076

DURAL SINUS MALFORMATION: A CASE SERIES WITH A FOCUS ON FETAL IMAGING

THOMAS RICHARD VerHage¹, JAVIER Quintana^{1,2}, JENNIFER Kucera^{1,2}

¹ University of South Florida, Tampa, USA

² Johns Hopkins All Children's Hospital, St. Petersburg, USA

Dural sinus malformation (DSM) is a rare entity consisting of an abnormally dilated dural venous sinus. Most commonly, DSMs are located posterior to the cerebellar vermis involving the torcular herophili with extension into adjacent sinuses; however, they may also be positioned laterally involving the jugular bulb.

While the exact etiology of DSM is unknown, a popular hypothesis involves persistent ballooning of the affected dural sinuses. From four to seven months of gestation, dural sinuses undergo physiologic ballooning and gradually resolve by one year of age. It is hypothesized that patients with DSM lack this regression after seven months of gestation and instead experience disorganized development resulting in abnormally dilated dural sinuses. Another hypothesis includes beginning with an arteriovenous fistula which may eventually progress into a DSM. The most common natural history of DSM is eventual thrombosis, which has a controversial effect on the prognosis of DSMs. Although some authors believe thrombus formation may compromise normal cerebral venous drainage, other authors believe thrombus formation may actually be a favorable prognostic factor because it represents the beginning of involution and the healing process of a DSM.

This pictorial review will illustrate three cases of DSM from our institution, including brief patient histories and images from prenatal ultrasound, fetal magnetic resonance imaging (MRI) and postnatal MRI. The imaging findings unique to DSM will be discussed. The current literature on DSM will be reviewed including the prognosis and management.

Although DSM is rare, it is essential for radiologists to be able to differentiate this entity from other fetal intracranial lesions, as early diagnosis can help management with potentially significant prognostic implications.

Poster: SCI-077

ASSESSMENT OF MEDIASTINAL SHIFT ANGLE IN CONGENITAL PULMONARY AIRWAY MALFORMATION: A NEW FETAL MRI INDICATOR OF CONGENITAL LUNG DISEASE

JUN Tsukamoto¹, OSAMU Miyazaki¹, YUKI Saito¹, SAHO Irahara¹, REIKO Okamoto¹, MIKIKO Miyasaka¹, YOSHIYUKI Tsutsumi¹, YUSHI Ito², HARUHIKO Sago², YUTAKA Kanamori³, YOSHIKO Hayashida⁴, TAKATOSHI Aoki⁴, SHUNSUKE Nosaka¹

¹ National Center for Child Health and Development-Department of Radiology, Tokyo, JAPAN

² National Center for Child Health and Development-Center for Maternal-Fetal, Neonatal and Reproductive Medicine, Tokyo, JAPAN

³ National Center for Child Health and Development-Department of Surgical Specialties, Tokyo, JAPAN

⁴ University of Occupational and Environmental Health-Department of Radiology, Kitakyushu, JAPAN

The objectives of this research are to establish the mediastinal shift angle (MSA) as a new index of the severity of CPAM on fetal MRI, to compare the MSA between CPAM patients and the control group (normal fetus) for both hemithoraces, and to evaluate the correlation between the MSA and CPAM volume ratio (CVR).

Objectives:

The aims of this research were to establish what is the normal range for the mediastinal shift angle (MSA) on fetal MRI in a control group, to evaluate the MSA of fetuses with congenital pulmonary airway malformation (CPAM) and to compare the MSA with an established index, and to assess how MR image characteristics and the MSA vary.

Materials and Methods:

To establish the normal range, as a control group, we measured the MSA bilaterally in 125 fetuses without any lung abnormality. Subsequently, measurement of the MSA was carried out in 32 fetuses who received a retrospective pathological diagnosis of CPAM. We conducted a statistical comparison of the MSA results in CPAM patients with the normal range for both hemithoraces. Also, using fetal ultrasound and MRI, a comparison between MSA with the CPAM volume ratio (CVR) was carried out, as this is a known common index of CPAM.

Results:

In the right hemithorax, the mean value for a normal MSA was 19.1° (range, 10.9°–34.5°), and in the left hemithorax it was 26.2° (13.4°–38.4°). With CPAM on the left, the MSA (mean, 39.5°, range, 17.4°–61.4°) is larger than that seen in right-sided CPAM (mean, 36.9°, range, 25.2°–51°). There was a positive statistical correlation between the MSA and the CVR as determined by ultrasound (right: $r = 0.76$, left: $r = 0.61$) and MRI (right: $r = 0.81$, left: $r = 0.61$). Statistical analysis (student t test) revealed a significant difference in normal-MSA as compared to CPAM-MSA bilaterally ($p < .0001$).

Conclusion:

The MSA in CPAM correlates well with the CVR and will be a useful tool for evaluating the severity of CPAM during the fetal period.

Poster: SCI-078

INVESTIGATION OF MRI CRITERIA DETERMINING THE RISK OF MAJOR POSTPARTUM HEMORRHAGE IN PATIENTS WITH PLACENTA ACCRETA SPECTRUM AND PLACENTA PREVIA

ELENA Semenova, POLINA Kozlova, IRINA Mashchenko, ELENA Vyshedkevich, GENNADIY Trufanov

Almazov National Medical Research Centre, Saint-Peterburg, RUSSIAN FEDERATION

Background

MRI of the placenta provides important supplementary information in patients with placenta accreta spectrum (PAS) disorders and placenta previa (PP).

Goal of the study

The goal of the study was to evaluate the MRI criteria determining the risk of severe (>1,000 mL) postpartum hemorrhage (PPH) in patients with PAS and PP.

Materials and methods

We analyzed outpatient and inpatient medical records and the findings of MRI of the placenta in 46 pregnant women with PP and PAS diagnosed based on sonographic data who were followed up at our center from December 2019 to December 2020. The average age of patients at the time of MRI was 35.6 ± 4.7 years (range: 26–45 years), and the gestational age was 31.2 ± 4.0 weeks (range: 19–37 weeks). MRI was performed using a 1.5 T MRI scanner. The investigations were conducted in three

orthogonal projections using T1-weighted and T2-weighted images with and without fat suppression.

Results

MRI findings were compared with the results of histopathological examination of the placenta and the blood loss following surgical delivery. 14/46 patients (30%) were found to have PAS1/placenta accreta; 16/46 (35%) - PAS2/placenta increta; 16/46 (35%) – PAS3/placenta percreta. Placenta previa was diagnosed in all patients. Abnormal uterine hypervascularization (AUH) was observed in all (100%) patients and included retroplacental, intramural or subserous AUH with the retroplacental AUH being the most frequent (43/46 cases; 93%). Subserous AUH was observed in 21/46 (65%) cases and was an important sign of borderline increta/percreta invasion. Abnormal collateral vessel formation (CVF) in the paracervical and/or periuterine regions was observed in 30/46 (65%) patients. The most important risk factors of major PPH included extended area of placental attachment (3 segments or more) in combination with AUH and abnormal CVF.

Conclusions

MRI of the placenta plays an important role in planning of surgical delivery in patients with PAS and placenta previa as it allows to evaluate the exact segmental location of the placenta and the degree of its abnormal invasion into the myometrium and the parametrium.

Our data demonstrate that there is a direct correlation between the MRI findings and maternal blood loss following a cesarean section.

A combination of collateral vessel formation in the periuterine or paracervical adipose tissue with the areas of abnormal uterine hypervascularization is associated with the highest risk of major PPH.

Poster: SCI-079

THREE FOETUSES WITH MOLAR TOOTH SIGN IN MRI

DARIA Dziechcinska-Poletek

Resonica Diagnostic Imaging Centre, MR Unit in Ruda Slaska, Ruda Slaska, POLAND

The molar tooth sign visible on an axial CT or MR scan is formed by parallel alignment of thickened and elongated superior cerebellar peduncles with a deep interpeduncular fossa between them. It is accompanied by hypoplastic or absent vermis. Initially it was considered pathognomonic for Joubert syndrome but is now known to occur in other diseases. In this report three cases of prenatal diagnosis of this abnormality. Pregnant patients were examined on a 1.5 Tesla scanner in 34/30/31 weeks of pregnancy. First patient was referred to foetal MRI because of suspected agenesis of the corpus callosum, the other two with suspected Blake pouch cyst. In the first case ACC was confirmed with molar tooth sign, hypoplastic vermis and small occipital meningocele as additional abnormalities, all of which were also demonstrated in the postnatal brain MRI. On the basis of clinical examination orofacioidigital syndrome was suspected. In the second case there was no history of genetic diseases in the family, whereas in the third case there was Joubert syndrome diagnosed in an older sibling.

Poster: SCI-080

THREE MRI CASES OF FOETUSES WITH SEVERE VENTRICULOMEGALY AND DIENCEPHALIC-MESENCEPHALIC JUNCTION DYSPLASIA

DARIA Dziechcinska-Poletek

Resonica Diagnostic Imaging Centre, MR Unit in Ruda Slaska, Ruda Slaska, POLAND

This is to report three cases of foetuses referred to fetal MRI because of severe ventriculomegaly with suspected agenesis of corpus callosum. Pregnant patients were examined on a 1.5 Tesla scanner in 24/30/30 weeks of pregnancy. Foetal MRI confirmed severe supratentorial ventriculomegaly with dysgenesis of the corpus callosum. Moreover, features of the diencephalic-mesencephalic junction dysplasia were visualised - fusion of the hypothalamus and midbrain, a ventral midbrain cleft (butterfly sign), anteriorly positioned interthalamic adhesion together with a small kinking of the cervicomedullary junction. Non-visualization of the cerebral aqueduct was also a feature noted in all three cases. Cerebellum (including vermis) was normal sized for gestational age. As all three foetuses were male with adducted thumbs, what favoured diagnosis of LICAM gene mutation. Available pre- and post-natal genetic and clinical data was also reviewed.

Poster: SCI-081

MRI CONTRIBUTION TO THE PRENATAL DIAGNOSIS OF THE MOST FREQUENT CONGENITAL VASCULAR ANOMALIES: LYMPHATIC MALFORMATIONS AND CONGENITAL HEMANGIOMAS

LAURENCE Crivelli ¹, ANNE-ÉLODIE Millischer ², PASCALE Sonigo ², DAVID Grévent ², SYLVIANE Hanquinet ³, YVAN Vial ¹, LEONOR Alamo ¹

¹ Centre Hospitalier Universitaire Vaudois, Lausanne, SWITZERLAND

² Hôpital Universitaire Necker - Enfants malades, Paris, FRANCE

³ Hôpitaux Universitaires de Genève, Genève, SWITZERLAND

Background: Screening ultrasound (US) has increased the detection of congenital vascular anomalies in utero. Complementary Magnetic resonance imaging (MRI) may improve the diagnosis, but its real utility is still not well established.

Objectives: 1.- To describe the imaging findings on prenatal US and MRI of the most frequent congenital vascular anomalies: lymphatic malformations and congenital hemangiomas; 2.- To assess the accuracy of prenatal US and MRI exams for diagnosis and 3.- To evaluate the relevance of the additional information obtained by complementary fetal MRI.

Materials and methods: All postnatal confirmed congenital vascular anomalies detected in the last 10 years at 3 University Hospitals were retrospectively identified. The prenatal diagnosis was compared with the final diagnosis for both methods and the clinical relevance of additional MRI information was evaluated. A second MRI in advanced pregnancy was performed in fetuses with lesions in a sensible anatomical location and the clinical relevance of the additional information evaluated.

Results: Twenty-four patients were included in the study - 20 lymphatic malformations and 4 hemangiomas. MRI slightly improved the diagnosis of lymphatic malformation- 85% vs 80% at US, especially for abdominal located lesions. Both methods had a low identification rate (25%) for tumors. Late performed MRI in 5 fetuses with lymphatic malformation allowed optimized management at birth.

Conclusion: MRI improves the diagnosis of congenital lymphatic malformations whereas hemangiomas remain difficult to identify in utero. The main role of MRI is to provide high-defined anatomical data to guide management at birth.

Poster: SCI-082

3D PRINTED TRAINING SIMULATION FOR PEDIATRIC UPPER GI FLUOROSCOPY

JACOB Wallace, KAMRAN Ali, DEBBIE Desilet-Dobbs, CHARLES Mcguire, ADAM Zarchan

University of Kansas - Wichita, Wichita, USA

Learning GI tract fluoroscopic exams is often a challenging component of resident education. Knowledge of normal anatomy in different planes, hand-eye coordination and specific timing add to the difficulty in performing a high quality exam. This is combined with the need to obtain the necessary images with the least radiation exposure (ALARA).

In order to approach this problem, a low cost and reusable simulator model was fashioned to practice pediatric upper GI exams as well as observe differences in residents as years in training progress. Inexpensive gastrografin was used for intraluminal contrast.

Two stomach models were created using CAD software. The models were fashioned to mimic the appearance of distal esophageal, gastric and duodenal anatomy. One model simulated normal anatomy, mimicking appropriate positioning of the ligament of treitz with the duodenum crossing midline. The other model simulated malrotation with the duodenum not crossing midline. An off-the-shelf hollow doll with internal tubing was used to house the stomach models and was connected using watertight adhesive.

During a training session, residents were sent to the fluoroscopy room and told to perform an Upper GI exam for the purpose of ruling out malrotation based on their current level of expertise. The fluoroscopy time and DAP were calculated for each resident, as well as the choice of contrast and overall impression as either normal or malrotated.

The results showed differences in resident fluoroscopy time and familiarity with the equipment as residents advance in training.

Limitations to this project include the inability to fully replicate the pediatric upper GI exam with a moving patient. Peristalsis is also not simulated, however the model was designed to utilize gravity to achieve movement of contrast.

Future work on this projects and ones like it include expanding this to other organs such as the colon.

Poster: SCI-083

THE MECKEL'S DIVERTICULUM AND ITS COMPLICATIONS - PICTORIAL REVIEW OF IMAGING FINDINGS

TIMOTHY SHAO ERN Tan, HARVEY EU LEONG Teo
Department of Diagnostic and Interventional Imaging, KK Women's and Children's Hospital, Singapore, SINGAPORE

PURPOSE:

To familiarise with the anatomy, embryology and pathology as well as the multi-modality imaging features of Meckel's Diverticulum (MD).

BACKGROUND/METHODS:

The MD results from failure of closure of the omphalomesenteric duct and is the commonest congenital abnormality of the gastrointestinal tract, present in about 2% of the general population. They are located on the anti-mesenteric border of the ileum and may contain ectopic gastric or pancreatic tissue. Most cases of MD are asymptomatic and incidentally discovered. Symptoms often develop in children due to complications such as gastrointestinal bleeding, bowel obstruction, perforation and inflammation.

RESULTS:

A wide range of multimodality imaging is used in diagnosing MD and its complications. In children, ultrasound is often the first-line imaging modality used for evaluating abdominal pain. Non-specific mesenteric inflammation may be seen. In uncomplicated cases, the MD is often indistinguishable from normal small bowel and may be

seen as a blind-ending fluid-filled structure in continuity with small bowel on high resolution sonography.

Conventional radiography and small bowel fluoroscopic studies are of limited value in diagnosis, but can be useful in demonstrating features of bowel obstruction and/or free intraperitoneal air which may warrant further cross-sectional imaging evaluation such as CT/MRI. Scintigraphy with ^{99m}Tc-Na-pertechnetate is sensitive in diagnosing MD, particularly those containing ectopic gastric or pancreatic tissue.

CONCLUSION:

Pre-operative diagnosis is challenging as presenting symptoms are often non-specific and may mimic other pathologies. Knowledge of clinical and radiological features of MD may aid in early and accurate diagnosis.

Poster: SCI-084

WITHDRAWN

Poster: SCI-085

COLORECTAL DUPLICATION: A RARE CASE WITH RADIOLOGICAL AND SURGICAL CORRELATION

LUKE DANIEL Metelo-Liquito ^{1,2}, HALVANI Moodley ^{1,2}, THESHNI Govender ^{1,2}, ELLEN MARY Mapunda ^{1,2}

¹ Charlotte Maxeke Johannesburg Academic Hospital, Johannesburg, SOUTH AFRICA

² University of the Witwatersrand, Johannesburg, SOUTH AFRICA

Purpose:

Colorectal duplications are the rarest type of alimentary tract duplications (7-20%). They are per definition part of the intestinal tract, have a smooth muscle wall, and mucosal lining. The usual presentation is younger than 2 years of age due to complications. We present a rare case of a young girl with a rectosigmoid tubular duplication.

Case Presentation:

An otherwise healthy one-year old female presented with an index episode of complete rectal prolapse and diarrhoea. Her parents described protrusion of rectal mucosa with straining and defecation from the age of six months. The child had no history of constipation, incontinence, rectal bleeding, or discomfort. Examination revealed rectal mucosa, partially prolapsing on the right. The prolapsed mucosa was easily reducible. Initial abdominal and pelvic ultrasound revealed no pelvic masses and a normal genitourinary system. A subsequent MRI pelvis demonstrated two parallel pelvic structures with rectal morphology. A CT abdomen and pelvis demonstrated bifurcation of the proximal sigmoid colon into two rectosigmoid segments, completely separated along their length, with both terminating in a common anal canal. There were no associated genito-urinary or vertebral anomalies. The patient was treated surgically via stapled fenestration (EndoGIA 80 mm) of the double anorectal canal.

Conclusion:

Colorectal duplications are rare and clinically occult which poses a challenge for the paediatric surgeon for diagnosis and management. Imaging therefore has a critical role in making the diagnosis, assessing for other associated genitourinary and vertebral anomalies and classifying the type of duplication.

Poster: SCI-086

IMAGING "TWISTS" IN VOLVULUS AROUND MECKEL'S DIVERTICULUM – A CASE SERIES INCLUDING US, CT AND MRI WITH DWI

IONE Limantoro¹, ARASH Eftekhari², SONIA Butterworth¹, DANIEL Rosenbaum¹, HEATHER Bray¹

¹ BC Childrens Hospital and The University of British Columbia, Vancouver, CANADA

² Surrey Memorial Hospital, Surrey, CANADA

Purpose

Meckel's diverticulum is the most common congenital anomaly of the small bowel. The majority of patients with Meckel's diverticulum remain asymptomatic during their lifetime. When symptomatic, patients with Meckel's diverticulum may present with rectal bleeding or abdominal pain caused by obstruction, intussusception, perforation, or inflammation. In the acute setting, symptoms may mimic acute appendicitis or Crohn's disease and diagnosis is challenging.

Bowel obstruction and ischemia caused by volvulus around a Meckel's diverticulum/band is often not considered or diagnosed preoperatively with the etiology of the bowel obstruction only becoming apparent at surgery. In this poster, we present the imaging findings of a series of three cases of volvulus around Meckel's diverticulum with imaging findings at MRI with DWI, US and CT leading to correct pre-operative diagnosis.

The goals of this educational exhibit poster are to:

1. Review embryology of Meckel's diverticulum and etiology of volvulus around Meckel's diverticulum
2. Review imaging findings of volvulus around Meckel's diverticulum on multiple imaging modalities including radiographs, MRI with DWI, US and CT
3. Emphasize importance of considering volvulus around Meckel's band in children presenting with bowel obstruction, especially when initial imaging investigation does not demonstrate common etiology such as intussusception or complicated appendicitis

Conclusions

Volvulus around a Meckel's diverticulum should be included in the differential diagnosis in children presenting with acute abdominal pain and small bowel obstruction. Ultrasound is often the first choice cross-sectional imaging examination in these children. If initial imaging shows small bowel obstruction without obvious cause, such as appendicitis or intussusception, volvulus secondary to Meckel's diverticulum should be considered. Knowledge of the cross-sectional imaging findings of volvulus around a Meckel's diverticulum facilitates pre-operative diagnosis, which may in turn lead to earlier surgical treatment and decreased bowel ischemia.

Poster: SCI-087

NEW SONOGRAPHIC SIGNS IN NEONATES WITH NECROTIZING ENTEROCOLITIS

CATALINA Le Cacheux, ALAN Daneman, AGOSTINO Pierro, CHRISTOPHER Tomlinson, RICARDO Faingold
The Hospital For Sick Children, Toronto, CANADA

Background:

Many published reports have highlighted the sonographic findings that are valuable for the diagnosis and follow-up of neonates suspected of or known to have necrotizing enterocolitis (NEC). We have recently observed previously unreported sonographic findings that are useful for diagnosis and follow-up of neonates with NEC and appear to be useful in predicting outcome.

Objective:

To illustrate four new sonographic findings in neonates with NEC and to determine whether they are useful for predicting outcome.

Materials and Methods:

We review the clinical, sonographic, and surgical findings in a large series of neonates with NEC in order to document the frequency of the presence of four new sonographic findings. We also determine whether these signs are useful for predicting outcome. The four signs include (1) Thickening and hyperemia of the mesentery, (2) Poor definition of the bowel wall, (3) Thickening, hyperechogenicity, and fluid tracking in the abdominal wall, and (4) Hyperechogenicity of bowel content.

Findings:

Neonates with more severe NEC have varying degrees of thickening, increased echogenicity, and hyperemia of the mesentery which can be visualized between loops of bowel particularly when some ascites is present. In more severely affected bowel, the outer margins of the bowel wall become indistinct due to edema and inflammation making separation of adjacent loops difficult or impossible on sonographic images. The abdominal wall develops edema and inflammation in more severely affected neonates and this manifests as increased thickness, hyperechogenicity of the wall, and eventually fluid tracking in the tissue plains of the abdominal wall. In more severely affected neonates the intraluminal content of the bowel becomes hyperechoic as a result of intraluminal hemorrhage, shedding of the necrotic components of the bowel wall into the lumen, and eventually some calcification. These signs appear to be useful for predicting outcome and are thus useful in guiding management.

Conclusion:

All four of the sonographic signs described are more frequently seen in neonates with more severe NEC. These findings illustrate that an attempt should be made to document the presence or absence of all four signs on all sonograms of the abdomen in neonates

Poster: SCI-088

THE SPECTRUM OF IMAGING FINDINGS IN PIMS-TS (MIS-C) PRESENTING AS AN ACUTE ABDOMEN TO A TERTIARY PAEDIATRIC HOSPITAL

HARSIMRAN Laidlow-Singh, CHARLOTTE A. Roberts, JONATHAN Colledge, ANOUSHKA Ljutikov
Department of Imaging, The Royal London Hospital, London, UNITED KINGDOM

Purpose: PIMS-TS (MIS-C) is a novel diagnosis thought to relate to the worldwide COVID-19 pandemic and documented in children following acute SARS-CoV-2 infection. This multisystem disorder commonly involves abdominal symptoms at the time of presentation. Patients are often referred for imaging to investigate for an alternative initial clinical diagnosis. We demonstrate a sample of the wide gamut of imaging appearances.

Materials and Methods: The range of imaging findings and modalities utilised in a series of paediatric patients presenting with acute abdominal pain to a tertiary paediatric hospital with a final multi-disciplinary diagnosis of PIMS-TS are presented.

Results: 11 patients met the selection criteria (age range 5-17 years, 8 male:3 female). The most common indication for imaging was to investigate for acute appendicitis, mentioned in 8/11 referrals. Only 2 specifically mentioned PIMS-TS at the time of initial imaging. The most common imaging appearance is mesenteric lymphadenopathy, with or without appendiceal enlargement (seen in 5/11). However, a wide range of findings was seen amongst individuals, including one case presenting unusually with inflammatory change in the small bowel, gallbladder wall, and epididymis on both sides, and another case with transient alterations to hepatic echogenicity.

Conclusions: PIMS-TS (MIS-C) may present as an acute abdomen. Imaging findings are varied, although a significant number of cases in our cohort demonstrate mesenteric lymphadenopathy. A multi-disciplinary approach with consideration of clinical, biochemical, and immunological factors in addition to diagnostic imaging is required to diagnose PIMS-TS confidently. However, as it presents non-specifically, radiologists may play a crucial role in recognising the possibility of the diagnosis - especially if there are inflammatory intra-abdominal findings on imaging in the correct wider clinical context. The local prevalence of COVID-19 should be noted in considering the pre-test probability of PIMS-TS (MIS-C).

Poster: SCI-089

PAEDIATRIC SPLENIC LESIONS – A CASE SERIES FROM A BUSY LONDON HOSPITAL

RICHARD Jenkins, STACEY Castle, ALEX Sheeka, AFSHIN Alavi
Imperial NHS, London, UNITED KINGDOM

Summary

Focal splenic lesions are a relatively uncommon paediatric presentation and can present a daunting challenge. Splenic pathology can be classified as traumatic, congenital, inflammatory, haematological, infective or malignant. Focal splenic lesions may be investigated using ultrasound, CT, MRI and nuclear medicine techniques. This poster will explore focal splenic lesions through a series of interesting cases encountered at our centre over recent years.

Purpose

This poster will set out a system to investigate and classify splenic lesions.

Materials and Methods

The poster will use multiple cases with selected images to discuss the following:

- Splenic cysts are the most common focal lesion in the paediatric spleen. These may be acquired or congenital. Previous trauma and hydatid infection are more common causes of acquired cysts.
- Abscess is a relatively rare presentation in the immunocompetent child but is more often seen in the immunocompromised population. A septated hypoechoic lesion is seen on ultrasound. Cross sectional imaging shows an enhancing rim.
- Lymphoma represents the most common solid splenic malignancy in children. This may present as diffuse splenomegaly or focal lesions. Focal lesions are commonly hypoechoic and hypoattenuating.
- Splenic haemangiomas may be solitary or present as multiple lesions. Imaging appearances can be varied with enhancement from the periphery inwards being the most common finding.
- Sarcoidosis is a multisystem disease which rarely shows focal splenic manifestations. However, the diagnosis should be considered in atypical focal splenic lesions.

Conclusion

Over the case series we will explore a range of splenic lesions. The appearance across a range of modalities will be discussed. We hope this will serve as a useful refresher on the tricky nature of this topic and promote discussion amongst colleagues.

References

- Hilmes, M. A., & Strouse, P. J. (2007). The Pediatric Spleen. *Seminars in Ultrasound, CT and MRI*, 28(1), 3–11. doi:10.1053/j.sult.2006.10.003
- Elsayes, K. M., Narra, V. R., Mukundan, G., Lewis, J. S., Menias, C. O., & Heiken, J. P. (2005). MR Imaging of the Spleen: Spectrum of Abnormalities. *RadioGraphics*, 25(4), 967–982.

Paterson, A., Frush, D. P., Donnelly, L. F., Foss, J. N., O'Hara, S. M., & Bisset, G. S. (1999). A Pattern-oriented Approach to Splenic Imaging in Infants and Children. *RadioGraphics*, 19(6), 1465–1485.

Poster: SCI-090

PANCREATIC PSEUDOPAPILLARY TUMOR: A CASE REPORT

MADÉLINNE Granados Macías, ANGIE Becerra Cervantes, JESUS Maldonado Rayas
Nucleo Diagnostico Avanzado, Tijuana, MEXICO

Background: The Pseudopapillary tumor of the Pancreas or Franz's Tumor, is an uncommon primary tumor of the pancreas, few cases are reported worldwide (about 1-3% of exocrine tumors of the pancreas), it has been described predominantly in young women. It is slow-growing with unspecific clinical manifestations. Shows pathological properties of solid and cystic components, imaging diagnosis is mainly by Tomography and the treatment is surgical resection and it usually has a favorable prognosis.

Case: We present here the case of a 6-year-old female patient who underwent clinically abdominal pain, nausea, vomiting, and conjunctival jaundice, an abdominal tomography is performed presenting an undetermined origin solid lesion of the head of the pancreas, subsequently, an MRI was performed confirming the findings, denoting an 8x8mm tumor of the head of the pancreas. She underwent surgery achieving complete resection of the tumor and her final diagnosis was Pseudopapillary Tumor of the Pancreas. One year after her surgery, she is asymptomatic and clinically healthy.

Poster: SCI-091

UNUSUAL CYSTIC LESIONS IN THE PEDIATRIC ABDOMEN AND PELVIS: HOW COMMON IS UNCOMMON

ALJOHARAH Aljabr, GALI Shapira, NAGWA Wilson
Children hospital of eastern Ontario, ottawa, CANADA
Unusual Cystic lesions in the pediatric abdomen and pelvis: How common is uncommon.
Aljoharah Aljabr MD, Gali Shapira Zaltsberg MD, Nagwa Wilson MD, PhD.

ABSTRACT

Although abdominal cystic lesions are common in the pediatric population, a large variety of unusual lesions can also be encountered. In addition, some common lesions may have an unusual presentation. In making the diagnosis, it is essential to recognize the site of origin of the lesion (although can be challenging, particularly in very large lesions), and its characteristics on different imaging modalities.

The objectives of this educational poster are:

- To present the imaging features of some unusual abdominal and pelvic cystic lesions in the pediatric population and their prevalence.
- To review the best imaging modalities for the evaluation of these lesions
- To present a reasonable differential diagnosis and probable management Pathologies will be categorized according to the organ of origin and will include:

- Liver - Hydatid cyst, cystic metastases of known Wilms tumor, Iatrogenic hepatic hematoma in a neonate, cystic mesenchymal hamartoma, and focal Caroli disease
- Spleen - Splenic cyst
- Adrenal gland - Neurofibromatosis Type 1 with adrenal neuroblastoma
- Renal - perinephric urinoma caused by congenital obstruction of the urinary tract
- Mesenteric and Retroperitoneal - Mature cystic teratoma, retroperitoneal lymphatic malformations, meconium pseudocyst, and peritoneal cerebrospinal fluid (CSF pseudocysts)
- Bowel - Enteric duplication cyst as a leading point for ileoileal intussusception
- Miscellaneous - Scimitar sacrum, urachal leiomyoma, and auto-amputated ovary

Uncommon abdominal and pelvic cystic lesions can be symptomatic or incidental findings in pediatric patients. Imaging evaluation can provide precise information regarding their origin, appearance, size, and mass effect on adjacent abdominal structures. This information is crucial for early and correct diagnosis, which, in turn, can lead to optimal patient management.

Poster: SCI-092

THE ASSESSMENT OF MRE IN PAEDIATRIC PATIENTS WITH CLINICAL SYMPTOMS SUGGESTING CROHN'S DISEASE

MONIKA Zbroja¹, MARYLA Kuczynska³, WERONIKA Cyranka¹, KAROLINA Siejka², MALGORZATA Nowakowska², MAGDALENA Grzegorzczak², MONIKA Piekarska², AGNIESZKA Brodzisz⁴, MAGDALENA Wozniak⁴

¹ Students Scientific Society at the Department of Pediatric Radiology, Lublin, POLAND

² Students Scientific Society at the Department of Interventional Radiology and Neuroradiology, Lublin, POLAND

³ Department of Interventional Radiology and Neuroradiology, Lublin, POLAND

⁴ Department of Pediatric Radiology, Lublin, POLAND

Purpose: Crohn's disease (CD) is a chronic inflammatory bowel disease. A characteristic feature of inflammatory changes is their focal or segmental nature. Up to 20-30% of patients present first symptoms during childhood or adolescence. Active inflammation can manifest as mural thickening, edema, ulcerations, abscesses or fistulas. In case of any CD suspicion, magnetic resonance enterography (MRE) is usually used to represent all of these manifestations. The aim of the study was to assess MRE in paediatric patients with clinical symptoms suggesting Crohn's disease. **Materials and Methods:** The study included 23 children (10 boys, 13 girls) with suspicion of CD due to presented symptoms. Cramping, abdominal pain was noticed in 23 children, diarrhea in 5 patients. 5 individuals were constantly exhausted and experienced loss of appetite. Fever was confirmed very rare. 6 children developed bleeding within the gastrointestinal system. Each patient then underwent MR enterography using a 1.5T scanner, according to a local study protocol, which showed classical image of CD. The diagnosis was then confirmed by endoscopic examination and histopathologically.

Results: All MRE findings were associated with small bowel inflammation. All patients showed asymmetric ileal wall thickening and edema. Edematous ileocecal valve was visible in 10 patients. In 9 cases reactive lymphadenopathy was detected (lymph nodes 10 mm in short axis). In 5 patients small intestine fistulas were found, whereas abscess was

observed in another 5 patients, in 2 between intestinal loops and in 3 perianally. In contrast-enhanced images, a vivid enhancement of the affected bowel section was revealed in all patients and in 12 children inflammatory infiltration of peri-intestinal fat was depicted.

Conclusion: MRE shows high sensitivity and specificity in detecting inflammatory lesions in the small intestine in case of Crohn's disease. In correlation with clinical symptoms, it's a reliable tool in diagnosis, monitoring of the disease activity and assessment of potential complications.

Poster: SCI-093

A REVIEW OF THE SPECTRUM OF INCIDENTAL FOCAL LIVER LESIONS REFERRED TO A TERTIARY REFERRAL PAEDIATRIC HEPATOBILIARY UNIT

HELEN Woodley, OMAR Nasher², TERRY Humphrey¹, NAVED Alizai², MICHAEL Dawrant²

¹ Paediatric Radiology, Leeds Children's Hospital, Leeds, UNITED KINGDOM

² Paediatric Surgery, Leeds Children's Hospital, Leeds, UNITED KINGDOM

Background:

Incidental focal liver lesions (FLL) are defined as 'unexpected abnormalities found in patients without relevant symptoms' and are well documented in the adult literature with algorithms developed for their management. Due to the increased access to imaging, incidental FLL are increasingly encountered in the paediatric population. It is stated that 2/3 of paediatric liver tumours are malignant but there are few scientific papers in the literature describing the incidence and spectrum of incidental FLL in children.

Aim:

To review the spectrum and incidence of incidental FLL presenting to a paediatric tertiary referral paediatric hepatobiliary centre.

Method:

The clinical details and presentation of all children referred to a paediatric hepatobiliary tertiary referral centre with FLL between July 2012 and July 2019 were reviewed. The imaging findings, histology where available and final diagnosis of all incidental FLL's was documented.

Results:

43 children (22 females) age range 1 month to 15 years were referred with incidentally detected FLL's. All lesions were detected on ultrasound. 4 malignant lesions; 1 hepatocellular carcinoma and 3 hepatoblastoma were diagnosed. The spectrum of benign lesions was focal nodular hyperplasia 9, congenital or infantile haemangioma 13, liver cyst 9, cystic mesenchymal hamartoma 2, adenoma 2, focal fat 3 and TPNoma 1.

Discussion:

In concordance with adult literature this study demonstrated the majority of incidental FLL were benign in contrast to traditionally quoted incidence of paediatric liver tumours. However, 4/43 (9.3%) of lesions were malignant. Whilst unnecessary investigation and biopsy should be avoided, all incidental FLL require appropriate referral and may require further imaging and biopsy. Imaging algorithms for the investigation of paediatric FLL should be developed in line with adult practice.

Poster: SCI-094

DIAGNOSTIC EFFICIENCY OF ULTRASOUND FOR INTESTINAL MALROTATION IN INFANTS: EXPERIENCE FROM A TERTIARY CHILDREN'S HOSPITAL

MAKHETHE Vuma¹, LUIS OCTAVIO Tierradentro-García¹, REBECCA Dennis¹, ASEF Khwaja¹, ALIREZA Zandifar¹, KASSA Darge¹, SUDHA Anupindi¹, THANE A. Blinman², MISUN Hwang¹

¹ Department of Radiology, Children's Hospital of Philadelphia, Philadelphia, USA

² Department of Surgery, Children's Hospital of Philadelphia. Perelman School of Medicine, University of Pennsylvania, Philadelphia, USA

Purpose: Intestinal malrotation (IM), caused by abnormal embryologic rotation, is frequently diagnosed in infants. Presence of IM does not necessarily constitute an emergency, but complications such as midgut volvulus (MV) may arise. Upper gastrointestinal (UGI) series is considered the diagnostic gold standard for suspected cases of IM, to the exclusion of ultrasound (US). In this study, we aim to determine the diagnostic performance of US versus UGI series to diagnose IM in cases with surgical confirmation.

Methods: We evaluated 43 children (age range 0-48 days) with clinical suspicion of IM who underwent US, UGI series, and surgery at our institution over a 10-year period. Two pediatric radiologists evaluated the images to determine the presence of IM on US and UGI series (present/absent/equivocal). The diagnostic criteria used for IM was the presence of expected superior mesenteric vein (SMV) and artery (SMA) location, with the SMV to the right of SMA on Color Doppler US; not all cases in this retrospective study were evaluable for retroperitoneal duodenal and cecum location. A third pediatric radiologist evaluated the discrepant responses. We calculated sensitivity (Sen), specificity (Spe), positive predictive value (PPV), and negative predictive value (NPV) of US and UGI fluoroscopy versus surgery. Inter-rater reliability (IRR) was calculated using inter-class correlation coefficient (95% CI).

Results: The cohort comprised 25 (58.1%) males and 18 (41.9%) females (mean age 16.5 days \pm standard error 2.5). Interpretation labeled as equivocal on US (n=3) and UGI (n=19) were excluded from analysis. Based on IM findings at surgery, UGI series had 100% Sen, 73.3% Spe, 69.2% PPV, and 100% NPV. US had 88.9% Sen, 86.4% Spe, 84.2% PPV, and 90.5% NPV. Fourteen cases presented MV concurrently with IM. IRR for UGI was 0.81 (0.63-0.90), $p < 0.001$; for US it was 0.96 (0.92-0.98), $p < 0.001$.

Conclusion: In our cohort, we found that while UGI has higher sensitivity and negative predictive value than US, US has higher specificity and positive predictive value than UGI in diagnosing IM. US had higher inter-rater reliability than UGI. Note that this retrospective analysis utilized the SMA/SMV relationship only for IM diagnosis on US, yet showed the complementary role of US in the evaluation of IM. Future research integrating the retroperitoneal duodenum and cecum locations on US in comparison to UGI in terms of diagnostic accuracy for IM evaluation is much needed.

Poster: SCI-095

DIAGNOSING MIDGUT VOLVULUS IN INFANTS

LUIS OCTAVIO Tierradentro-García¹, REBECCA Dennis¹, ASEF Khwaja¹, MAKHETHE Vuma¹, ALIREZA Zandifar¹, KASSA Darge¹, SUDHA Anupindi¹, THANE A. Blinman², MISUN Hwang¹

¹ Department of Radiology, Children's Hospital of Philadelphia, Philadelphia, USA

² Department of Surgery, Children's Hospital of Philadelphia. Perelman School of Medicine, University of Pennsylvania, Philadelphia, USA

Purpose: Midgut volvulus (MV) is an abdominal emergency that requires prompt surgery. It is commonly seen in the first few months of life. Although upper gastrointestinal (UGI) series is considered the

diagnostic gold standard, its limitations include radiation, resources and staff, cost, and non-portability. Ultrasound (US) is a non-invasive, portable and low-cost modality that can be used as an alternative and/or complementary to UGI series in most clinical settings. In this study, we aim to evaluate the accuracy of US compared to UGI series for diagnosis of MV in comparison to the reference standard operative results of positive or negative MV.

Methods: Our study included 43 infants with clinical suspicion of MV who underwent both US and UGI and who had surgical/operative reports for confirmation of imaging findings at our institution from July 2010 to November 2020. Studies with insufficient images for diagnostic evaluation (e.g. limited static images available) were discarded. MV was considered if -on Color Doppler US- swirling appearance (superior mesenteric vein swirling around superior mesenteric artery) was present. Two pediatric radiologists evaluated the images to determine the presence of MV in US and UGI series (present/absent/equivocal). A third pediatric radiologist evaluated the discrepant responses. We calculated sensitivity (Sen), specificity (Spe), positive predictive value (PPV) and negative predictive value (NPV) to evaluate the diagnostic accuracy of US and UGI series versus surgery. Inter-rater reliability (IRR) was calculated using intraclass correlation coefficient (95% confidence interval). Quantitative data are reported as mean \pm standard error.

Results: The study cohort included 25 males and 18 females (mean age 16.5 \pm 2.5 days). Studies interpreted as equivocal for MV in US (n=3) and UGI (n=21) were discarded from the final analysis. Based on MV findings at surgery, UGI series had 80% Sen, 94% Spe, 80% PPV, and 94% NPV. On the other hand, US had 100% Sen, 92.3% Spe, 87.5% PPV and 100% NPV. IRR for UGI series was 0.77 (0.54-0.88), $p < 0.001$; for US it was 0.88 (0.78-0.94), $p < 0.001$.

Conclusion: In this study, US showed a higher sensitivity and negative predictive value than UGI for diagnosing MV. US also showed higher positive predictive value and comparable specificity than UGI. US demonstrated higher inter-rater reliability than UGI. Our results demonstrate that US can serve as a useful screening tool for suspected cases of MV.

Poster: SCI-096

MAKING INTUSSUSCEPTION REDUCTIONS EASIER: USE OF MEDICAL AIR IN LIEU OF MANUAL PUMP IPR 2021

ELIZABETH Snyder, MARTA Hernanz-Schulman, SUMIT Pruthi Monroe Carell Jr. Children's Hospital at Vanderbilt, Nashville, USA

Purpose: Pneumatic reduction of ileocolic intussusception is commonly performed with manual insufflators. Operating a hand-held device and maintaining constant reduction pressure, controlling the fluoroscope and monitoring the procedure can be challenging. Our aim in this IRB-approved retrospective study was to describe and evaluate the use of medical air in intussusception reduction.

Materials/Methods: In 2018 we began using medical air for fluoroscopic intussusception reduction. The device connects tubing from the wall medical air outlet through a valve system, including a pressure gauge, to the rectal tube. We retrospectively reviewed all reductions over 6-years: 2015-2018 using the manual insufflator and 2018-2021 using medical air. We compared time to reduction as documented on image timestamps, maintenance of pressure head, success and complication rates. First attempts and delayed attempts were analyzed separately. Demographic data were obtained from the medical record. A survey of attending radiologists and fluoro technologists was performed to evaluate preference between methods, ease of use and setup, perceived duration of procedure and perceived difference in success rates. Data were analyzed using independent t-test and chi-squared tests

Results There were 182 first reduction attempts in 164 unique patients; 18 episodes on same patients were remote in time and not part of the same event. The manual insufflator was used in 95 attempts; the wall air in 88. There was no difference in procedure duration (8:23 for insufflation, 8:22 for wall air, $p=0.99$) with a tendency to improved success rate for wall air, without statistical significance (67.4% for insufflation and 75.2% for wall air, $p=.08$). There was one instance of bowel perforation in the insufflation group; none in the wall air group. A steady pressure could be maintained on wall air reductions, while pressure in the manual method was highly variable. All survey respondents preferred the wall air method and reported it easier to use. Most (93%) perceived that the wall air method was a faster procedure.

Conclusion Hospital wall air can be used to successfully reduce intussusceptions without incurring time burden or loss of effectiveness. The method allows for less fluctuant pressure with additional perceived efficiency in not having to rotate the pump operator during prolonged reductions. Our data show that this procedure is not only feasible but also highly successful in the clinical setting

Poster: SCI-097

LIMITED RANGE CT FOR RADIATION REDUCTION IN CHILDREN WITH SUSPECTED APPENDICITIS

VANESSA Rameh¹, FARAH Abi Zeid¹, CHRISTEL Tamer², HALA Khasawneh³, LARA Nassar¹, LAMYA Ann Atweh¹

¹ American University of Beirut Medical Center, Beirut, LEBANON

² Memorial Sloan Kettering Cancer Center, New York, USA

³ Mayo Clinic, Rochester, USA

Purpose:

Imaging plays a major role in the diagnosis of acute appendicitis. Ultrasound is considered the imaging modality of choice followed by CT according to the ACR appropriateness criteria.

However, ultrasound for appendicitis is operator dependent and not all institutions have the expertise to perform it. Therefore, CT is the preferred exam at many institutions because of its availability, high accuracy, and ability to provide alternative diagnoses. However, CT is not desirable due to the associated radiation dose.

Our objective is to evaluate the position of the appendix with respect to identifiable anatomic landmarks and to determine whether cranio-caudal coverage can be reduced in attempt to lower radiation dose, while maintaining diagnostic accuracy for appendicitis and alternative diagnoses.

Material and Methods:

A retrospective review of all patients below the age of 18 who underwent a CT of the abdomen and pelvis for acute abdominal pain in our institution between January 2007 and August 2017 was performed. The superior and inferior anatomic landmark of the appendix was recorded for all CT examinations. The minimum cranio-caudal length capturing all appendices was determined (L1-superior acetabular rim). In addition, a smaller scan length was determined based on inclusion of most of the appendices in the dataset (L3-S3). The dose length products (DLP) were then calculated and the percentage of radiation dose reduction between limited and full ranges were calculated.

Results:

Appendicitis was diagnosed in 111 (28%) CT exams conducted on 394 patients (M:F 215:179; age range: 5-18 years). Alternative diagnoses were found in 39% of patients and 13% of patients had incidental findings. A scan length from inferior L1 to the superior acetabular rim captured all appendices. This resulted in a reduction of DLP by 58%. 91.5% of the alternative diagnoses were seen in this limited range. Limiting the cranio-caudal scan length from L3 to S3 allows visualization of 97% of the appendices, with however a larger dose reduction of 72%. 75% of the alternative diagnoses were seen on this range.

Conclusion:

Limiting the cranio-caudal coverage on CT examinations based on a model of the anatomic distribution of appendices permits a substantial reduction of radiation dose in children while preserving its diagnostic accuracy.

Poster: SCI-098

UTILIZATION OF ABDOMINAL ULTRASOUND AND MOST COMMON SONOGRAPHIC FEATURES OF ACUTE PANCREATITIS IN PEDIATRIC PATIENTS

RUPESH Patel¹, MAISAM Abu-El-Haija², JAIMIE Nathan³, TOM Lin², DAVID Vitale², ALEXANDER Nasr⁴, ANDREW Trout¹

¹ Cincinnati Children's Hospital Medical Center - Department of Radiology and Medical Imaging, Cincinnati, OH, USA

² Cincinnati Children's Hospital Medical Center - Department of Pediatric Gastroenterology, Cincinnati, OH, USA

³ Cincinnati Children's Hospital Medical Center - Department of Surgery, Cincinnati, OH, USA

⁴ Cincinnati Children's Hospital Medical Center - Department of General Pediatrics, Cincinnati, OH, USA

Purpose:

Pancreatic ductal dilation has been reported as the most common sonographic feature of acute pancreatitis (AP) in children, but it's uncommonly seen in our experience. The purpose of our study was to report sonographic findings of AP in a large cohort of pediatric & young adult patients at the initial AP attack.

Materials & Methods:

Institutional review board approval was obtained for retrospective review of imaging of 192 patients with AP, who were prospectively enrolled in a registry between May 2013 - July 2020. All patients met INSPPIRE criteria for AP. Two reviewers (R1, R2) independently reviewed the first ultrasound obtained within two weeks of the first AP attack. Frequencies of findings are reported as counts & percentages. Duct dilation was classified per the criteria of Chao et al. (J.Ult.Med 2000).

Results:

163 (84.9%) patients (mean age 12.5±5.3 years, 88 male) had an abdominal ultrasound within two weeks of AP diagnosis. Peripancreatic edema was most commonly reported finding for both reviewers, (65% R1, 53% R2). Pancreatic hyperechogenicity relative to liver was reported in 58% (79/136) & 49% (67/134) of ultrasounds by R1 & R2 respectively. The pancreatic duct was visible in 33% (45/136) and 34% (46/138) of ultrasounds by R1 and R2 respectively and was dilated in only 11% (15/136) and 14% (19/136) of patients. Mean pancreatic duct diameter was 0.2 ±0.12 cm (R1) and 0.22 ± 0.13 cm (R2).

Findings of chronic pancreatitis (CP) were present at first attack in 11% (15/136) & 9% (12/136) of patients according to R1 and R2. Pancreatic calcifications were not documented by either reviewer.

Conclusion:

A dilated pancreatic duct is not the most common finding of AP in children despite existing literature to this effect. Peripancreatic edema & increased (relative to liver) pancreatic parenchymal echogenicity are more common findings. Nearly 10% of children may have findings of CP at the initial AP attack.

Poster: SCI-099

IMAGING EVALUATION FOR G-TUBE COMPLICATIONS IN THE PEDIATRIC ED: FLUOROSCOPY VS TWO-VIEW RADIOGRAPHS

SAKURA Noda¹, MURAT ALP Oztek², HASSAN Aboughalia², JEFFREY Otjen¹

¹ Seattle Children's Hospital/University of Washington Department of Radiology, Seattle, USA

² University of Washington Department of Radiology, Seattle, USA

Purpose

As malpositioned percutaneous gastrostomy tubes (G-tubes) can cause sepsis and death, correct position must be confirmed for malfunctioning or newly replaced gastric tubes. This study compares two-view abdominal radiographs with contrast injection (DX) to fluoroscopy (FL) after assessment or bedside replacement of malfunctioning G-tubes in the paediatric emergency department (ED).

Methods

We retrospectively identified FL and DX G-tube studies performed in our paediatric ED between 11/7/2009 and 2/21/2020 by code review. We reviewed radiology reports and electronic medical records (EMR) for imaging and clinical information including our gold standard for true G-tube complication, which was EMR documentation of additional G-tube evaluation or management within 72 hours following G-tube study. Descriptive statistics, Mann-Whitney U test, and Fisher's Exact test were performed.

Results

Of 83 patients, 73 (88%) were studied by FL and 10 (12%) were studied by DX. The FL group had a statistically significantly longer ED length of stay compared to the DX group (4.8 vs 3.5 hours, $p = 0.04$). There were no differences in age, sex, G-tube tract age, recent G-tube trauma, vital signs, difficulty replacing G-tube, or rate of missed true G-tube complication between groups.

Eight (11.0%) FL and 1 (10%) DX cases were positive for complication by imaging, including peritoneal contrast extravasation.

Six (8.2%) FL and 1 (10%) DX cases without imaging evidence of G-tube complication had a true G-tube complication within 72 hours following G-tube study.

There were no statistically significant differences in clinical presentation between patients with and without true G-tube complication.

Conclusion

Most G-tube studies were performed fluoroscopically. Although no clinical differences were identified between fluoroscopy and radiograph groups, ED length of stay was longer for patients who were studied by fluoroscopy. G-tube complications including peritoneal contrast extravasation were identified by both modalities. Neither modality identified all true G-tube complications.

Poster: SCI-100

WHERE'S THE APPENDIX? CONTRIBUTING FACTORS FOR VISUALISATION OF THE APPENDIX ON ULTRASOUND IN THE PAEDIATRIC POPULATION

LAN Nguyen, KATHLEEN O'Brien, BOSCO Wu, ROSS O'Neil
The Canberra Hospital, Canberra, AUSTRALIA

Background

Appendicitis is a common cause of abdominal pain requiring surgery in the paediatric population. Clinical diagnosis is often difficult and ultrasound is commonly utilised as the initial imaging modality. Ultrasound accuracy in diagnosing appendicitis is largely dependent on the visualisation of the appendix.

Objective

To determine the accuracy of ultrasound in diagnosing appendicitis and the factors contributing to its visualisation rates in the paediatric population at a non-dedicated paediatric hospital in Australia.

Materials and methods

A single institution retrospective cohort study of all ultrasounds performed on children less than 16 years of age for clinically suspected acute appendicitis in a 12-month period was conducted. The imaging and histopathology data of 249 studies were collated and analysed.

Results

The appendix visualisation rate was 27.3%. The accuracy of ultrasound in diagnosing acute appendicitis was 94.8% with seven false positive cases and six false negative cases. The sensitivity and specificity was 85.4% and 96.6% respectively; the positive predictive value and negative predictive value was 83.3% and 97.1% respectively.

Conclusion

The reasons for reduced ultrasound appendix visualisation rates in the paediatric population were not related to patient weight/body habitus, ultrasound machine, scanning duration or the time of day the study was performed.

Further training of general sonographers to gain paediatric experience may improve ultrasound appendix visualisation rates and its diagnostic performance.

Poster: SCI-101

ATTENUATION COEFFICIENT MEASUREMENT USING HIGH FREQUENCY TRANSDUCER FOR SMALL CHILDREN

HYUN JI Lim¹, HAESUNG Yoon¹, MI-JUNG Lee¹, KAMIYAMA Naohisa², TAKUMA Oguri²

¹ Department of Radiology and Research Institute of Radiological Science, Severance Hospital, Seoul, SOUTH KOREA

² Ultrasound General Imaging, GE Healthcare, Tokyo, JAPAN

Purpose: Nonalcoholic fatty liver disease is increasing in children and non-invasive diagnosis is needed even for small children. Fatty liver estimation is now available by some ultrasound scanners, but it was mainly for adults with larger liver. We evaluated measurement feasibility and normal range of ultrasound-guided attenuation parameter (UGAP) using conventional and higher frequency transducer in children.

Materials and Methods: This prospective study included all consecutive children who underwent abdomen ultrasonography from July to October 2020. We excluded children with hepatobiliary lesion or abnormal laboratory findings. Attenuation coefficients (ACs) of liver were measured using both 1-6 MHz (AC1-6) and 2-9 MHz (AC2-9) probes. UGAP algorithm for AC2-9 was newly developed for the paediatric use. After normality test using Shapiro-Wilk test, Mann-Whitney U test for group comparison and Spearman for correlation analysis were performed, and the cut-off values of ACs for diagnosing fatty liver were obtained from reference intervals.

Results: In 43 children (M:F = 25:18; 0–17 years; median 5 years), the measurement success rate was 100% for AC2-9, but only 23% (10/43) for AC1-6 with only possible in children with more than 9 cm depth of liver. The range of AC2-9 was 0.420-0.631 dB/cm/MHz with median value of 0.530 dB/cm/MHz. The AC2-9 were in normal distribution and the reference interval was 0.632 dB/cm/MHz (confidence interval 0.608-0.656 dB/cm/MHz). The AC2-9 showed no significant difference between sex and no correlation with age or body size.

Conclusions: Measurements of ACs are feasible in small children using high frequency transducer. We suggest a cut-off value of a 0.632 dB/cm/MHz for diagnosing fatty liver in children regardless of sex, age or body size.

Poster: SCI-102

THE SIGNIFICANCE OF INTRAMURAL AND INTRALUMINAL CALCIFICATION OF THE INTESTINE ON SONOGRAPHY IN NEONATES WITH CONGENITAL INTESTINAL OBSTRUCTION

CATALINA Le Cacheux¹, ALAN Daneman¹, GINA Nirulla¹, CLAUDIA Martínez-Rios², HAIYING Chen¹

¹ The Hospital for Sick Children, Toronto, CANADA

² Childrens Hospital of Eastern Ontario, Ottawa, CANADA

Background:

In neonates with congenital intestinal obstruction, calcification in the abdomen most commonly occurs in the peritoneum as meconium peritonitis or in a meconium pseudocyst. Much less commonly calcification may occur in the wall (intramural {IM}) and/or lumen (intraluminal {IL}) of the intestine. To the best of our knowledge, no study has reported the appearances and significance of IL and IM calcification on sonography (US) in neonates with congenital intestinal obstruction.

Objective: Firstly, to illustrate the US appearances of IM and IL calcification in neonates with congenital intestinal obstruction. Secondly, to determine whether these US findings obviate the need for contrast examinations of the gastrointestinal tract and are predictive of the need for surgery.

Materials and methods: Retrospective analysis of the clinical, imaging, surgical and histological findings in neonates with congenital intestinal obstruction in whom IM +/- IL calcification was recognized on US in the period 2019-2020.

Results: During this period, eight neonates (5M:3F) with congenital intestinal obstruction had IM and/or IL calcification recognized on postnatal US. All presented with symptoms on the first day of life. In 5 (62.5%) the diagnosis was made on prenatally US. None had an antenatal infection and one had cystic fibrosis (11%).

IM calcification was recognized as increased echogenicity of the wall of the intestine and IL calcification as increased echogenicity of intraluminal content. On US, IM calcification was recognized in all 8, IL calcifications in 5 and peritoneal calcifications in 2.

Only four (50%) had Contrast exams of the GI tract (colon in 4 and UGI series in 1 of these). Only 1 of the colon exams depicted the site but not cause of the obstruction. The other exams did not depict the site or cause of obstruction.

All 8 underwent surgery. Surgical findings included: ileal atresia in 6 (2 with associated segmental volvulus) and jejunal atresia with apple peel deformity in 1. The final patient had a meconium pseudocyst communicating directly with a previously perforated loop of intestine.

Conclusion: Recognition of the presence of IM +/- IL calcification on US in neonates with congenital intestinal obstruction obviates the need for additional contrast examinations of the GI tract as these exams did not add diagnostic information. US documentation of the presence of IM and IL calcification predicts the need for surgery.

Poster: SCI-103

ATTENUATION COEFFICIENT MEASUREMENT USING HIGH FREQUENCY TRANSDUCER FOR CHILDREN WITH FATTY LIVER

JISOO Kim¹, HAESUNG Yoon¹, HONG Koh², NAOHISA Kamiyama³, TAKUMA Oguri³, MI-JUNG Lee¹

¹ Department of Radiology and Research Institute of Radiological Science, Severance Hospital, Yonsei University, Seoul, SOUTH KOREA

² Department of Pediatrics, Severance Children's Hospital, Yonsei University College of Medicine, Seoul, SOUTH KOREA

³ Ultrasound General Imaging, GE Healthcare, Hino, Tokyo, JAPAN

Purpose: Nonalcoholic fatty liver disease is increasing in children and non-invasive diagnosis is needed even for small children. Fatty liver estimation is now available by some ultrasound scanners, but it was mainly for adults with large liver. We evaluated the ultrasound-guided attenuation parameter (UGAP) for diagnosing fatty liver in children using high frequency transducer with a new algorithm for pediatrics.

Materials and Methods: This prospective study included all consecutive children who underwent abdomen ultrasonography from July to October 2020. We excluded children with hepatobiliary lesion other than fatty liver. Attenuation coefficients (ACs) of liver were measured using both 1-6 MHz (AC1-6) and 2-9 MHz (AC2-9) probes. UGAP algorithm for AC2-9 was newly developed for the pediatric use. The ACs were compared with the proton density fat fraction (PDFF) on MRI and controlled attenuation parameter (CAP) on transient elastography, if available. The diagnostic performance of ACs for steatosis grades as determined by PDFF were also evaluated.

Results: In 30 children (M:F = 23:7; 8–18 years; median 11.5 years), the measurement success rate was 100% for AC2-9 and 87% (26/30) for AC1-6. The range was 14.4-36.3 kg/m² for body mass index (BMI), 0.610-0.878 dB/cm/MHz for AC1-6, 0.499-0.954 dB/cm/MHz for AC2-9, 2-58% for PDFF and 256-363 dB/m for CAP. The PDFF showed positive correlations with AC2-9 ($\rho=0.500$, $p=0.005$) and AC1-6 ($\rho=0.465$, $p=0.017$), but not with BMI ($\rho=-0.132$, $p=0.486$) or CAP ($\rho=0.160$, $p=0.456$). The steatosis grades were S0 in four, S1 in two, S2 in one, and S3 in 23. The AC2-9 cut-off value of 0.600 dB/cm/MHz demonstrated 92.3% sensitivity and 100% specificity for diagnosing S0 and 100% sensitivity and 85.7% specificity for diagnosing S3.

Conclusions: Measurements of ACs are feasible in children using high frequency transducer. The AC2-9 showed positive correlation with PDFF and good diagnostic performance for grading hepatic steatosis.

Poster: SCI-104

TITLE: ESTABLISHMENT OF LOCAL DIAGNOSTIC REFERENCE LEVELS OF PEDIATRIC ABDOMINOPELVIC AND CHEST CT EXAMINATIONS BASED ON BODY WEIGHT AND SIZE IN SOUTH KOREA

JAE-YEON Hwang¹, YOUNG HUN Choi², HEE MANG Yoon³, YOUNG JIN Ryu⁴, HYUN JOO Shin⁵, HYUN GI Kim⁶, SO MI Lee⁷, SUN KYUNG You⁸, JI EUN Park⁹

¹ Department of Radiology, Research Institute for Convergence of Biomedical Science and Technology, Pusan National University, Yangsan, SOUTH KOREA

² Department of Radiology, Seoul National University Hospital, Seoul National University College of Medicine, Seoul, SOUTH KOREA

³ Department of Radiology and Research Institute of Radiology, University of Ulsan College of Medicine, Asan Medical Center, Seoul, SOUTH KOREA

⁴ Department of Radiology, Seoul National University Bundang Hospital, Seoul National University College of Medicine, Seongnam, SOUTH KOREA

⁵ Department of Radiology and Research Institute of Radiological Science, Severance Childrens Hospital, Yonsei University, Seoul, SOUTH KOREA

⁶ Department of Radiology, Eunpyeong St. Marys Hospital, College of Medicine, The Catholic University of Korea, Seoul, SOUTH KOREA

⁷ Department of radiology, Kyungpook National University Hospital, School of Medicine, Kyungpook National University, Daegu, SOUTH KOREA

⁸ Department of Radiology, Chungnam National University Hospital, Chungnam National University College of Medicine, Daejeon, SOUTH KOREA

⁹ Department of Radiology, Ajou University Hospital, School of Medicine, Ajou University, Suwon, Suwon, SOUTH KOREA

Purposes

The purpose of this study were; 1) measure radiation dose of pediatric abdominopelvic and chest CT examinations from several university hospitals in South Korea; 2) establish local DRL by grouping of patient by body weight and size.

Materials and methods

Total 2494 CT examinations (1625 examinations for abdominopelvic CT and 869 CT for chest CT) performed between January 2017 to December 2017 from seven university hospital in South Korea were analyzed by using an automated dose management software. DRLs were calculated with grouping of patients by body weight and effective diameter. DRLs were set at the 75th percentile of distribution of typical values of each institution.

Results

DRLs (CTDI_{vol}) were 1.4, 2.2, 2.7, 4.0 and 4.7 mGy in abdominopelvic CT and 1.2, 1.5, 2.3, 3.7, 5.8 mGy in chest CT for body weight of 5 kg, 15 kg, 30 kg, 50 kg, and 80 kg. DRLs (SSDE) were 4.1, 5.0, 5.7, 7.1, 7.2 mGy in abdominopelvic CT and 2.8, 4.6, 4.3, 5.3, and 7.5 mGy in chest CT for effective diameter of <13 cm, 14–16 cm, 17–20 cm, 21–24 cm, and >24 cm. SSDE was greater than CTDI_{vol} in all age groups. Overall, local DRL was lower than previously conducted dose survey and other countries.

Conclusion

Our study set local DRL in pediatric abdominopelvic and chest CT examinations in weight and body size. Further study with more facilities and CT examinations is needed to be addressed to development of national DRL and update of current DRL.

Poster: SCI-105

UTILITY OF COMPUTED TOMOGRAPHY FOR EVALUATION OF SMALL BOWEL ROTATION

NATHAN Hull¹, JEFFREY de St Jeor², LARRY Binkovitz¹, AMY Kolbe¹, PAUL Thacker¹, KRISTEN Thomas¹, SHANNON Zingula¹, MATTHEW Thorpe¹

¹ Mayo Clinic Department of Radiology, Rochester, USA

² Mayo Clinic Alix School of Medicine, Rochester, USA

INTRODUCTION: The standard of practice to assess for small bowel malrotation is a contrast fluoroscopic upper gastrointestinal (UGI) exam. With advances in computed tomography (CT) with both rapid acquisition and lower doses, we investigated if CT could be used to evaluate the position and course of the duodenum in infants and very young children. **METHODS:** A retrospective review was performed from 2013–2017 of all abdominal CTs performed on children ages 0–2. CTs were reviewed by board-certified and subspecialty trained pediatric radiologists to assess if the course and position of the duodenum could be determined on CT. Confidence in visualization was recorded on a modified Likert scale (1=not confident, 2=somewhat confident, 3=moderately confident, 4=very confident). Inter-reader reliability was also assessed. **RESULTS:** 202 CT scans in 155 unique patients were reviewed. The duodenal course could be seen in 86% (95% CI 80–90%) of cases. The mean confidence score in visualizing the course of the duodenum was 3.2. A linear mixed regression model was used to predict confidence in visualizing the course of the duodenum. IV contrast improved confidence by 1.02 points (SE 0.59). Reviewers describing a scan as motion limited, CT dose limited, artifact limited or having altered anatomy reduced confidence by 1.45 (0.22), 0.97 (0.28), 1.34 (0.30) and 1.06 (0.41) respectively; a collapsed duodenum was the most common limiting factor identified (30% of cases), reducing confidence by 1.45 (0.11; all $p < 0.01$). Oral contrast did not improve confidence and did not interact with or prevent duodenal collapse from reducing confidence. 20 randomly selected cases were reviewed by all reviewing pediatric radiologists. Inter-rater reliability for confidence in identifying the course of the duodenum, measured on a 1–4 Likert scale, was 0.52 (95% CI 0.33–0.72), using a two-way random effects, agreement, single unit type intra-class correlation coefficient ($p < 0.01$) BMI, CTDI and DLP did not predict confidence identifying the course of the duodenum. **CONCLUSION:** The course of the duodenum can be seen in a high percentage of CT exams in very young children with a moderately high confidence level. The most

important factor for increasing confidence in identifying the duodenal course was the use of IV contrast; the most limiting factor was under-distension of the duodenum.

Poster: SCI-106

SENSITIVITY OF CONTRAST-ENHANCED ULTRASOUND VERSUS CT IN DETECTION OF SOLID ORGAN INJURIES FROM BLUNT ABDOMINAL TRAUMA IN YOUNG CHILDREN

M KATHERINE Henry¹, JOANNE N Wood², AARON E Chen², KASSA Darge¹, TENIOLA Egbe³, MOHAMED Elsingery¹, VICTOR Ho-Fung¹, SUMMER Kaplan¹, JENNY Y Kloss⁴, MICHAEL L Nance⁴, PHILIP V Scribano², SUSAN J Back¹

¹ Department of Radiology, Children's Hospital of Philadelphia, Philadelphia, USA

² Department of Pediatrics, Children's Hospital of Philadelphia, Philadelphia, USA

³ Center for Pediatric Clinical Effectiveness, Children's Hospital of Philadelphia, Philadelphia, USA

⁴ Department of Surgery, Children's Hospital of Philadelphia, Philadelphia, USA

Purpose: Intra-abdominal injuries from blunt trauma are rare in physically abused children but have important clinical and forensic implications. With contrast-enhanced CT (CECT) as the gold standard modality, clinicians must weigh the risks of radiation with risk of missed abdominal injury. Contrast-enhanced ultrasound (CEUS) is a radiation-free modality for blunt abdominal trauma, but less is known about its performance in young children. Our objective was to compare the sensitivity and specificity of CEUS with CECT in detection of solid organ injuries in young children.

Materials and Methods: We performed a prospective pilot clinical trial of children <8 years who all underwent CECT due to trauma (accidental or abusive) from 05/2018–09/2020. Subjects additionally underwent either a research CEUS with blinded image acquisition within 72 hours of CECT or CEUS as part of clinical care. Two blinded pairs of radiologists reviewed CEUS, and CECTs. CECT was used as the gold standard. We calculated sensitivity and specificity of CEUS in detection of solid organ injury at the level of the patient and total solid organs.

Results: Twelve of 13 subjects had evaluable CEUS (median age 2.6 years [range 3 months–6.9 years]). The Child Protection Team consulted in 6 (50%). CECT identified 4 liver, 1 pancreatic, 1 splenic, 0 adrenal, and 1 kidney injuries. Compared to CECT, CEUS was 66.7% sensitive and 83.3% specific for any solid organ injury at the level of the patient (N=12). Among all solid organs imaged (N=84), CEUS was 71.4% sensitive and 98.7% specific. The precision of sensitivity estimates are limited with only 7 injured organs in 6 subjects.

Conclusions: We demonstrated feasibility of performing clinical trial of CEUS in a young patient population including victims of physical abuse. Further research on larger populations, with both positive and negative CECTs, is needed to further assess the role of CEUS in the imaging evaluation of young trauma victims.

Poster: SCI-107

ASSESSING THE VALUE OF A COMBINED MR ENTEROGRAPHY-PERIANAL MRI PROTOCOL IN THE EVALUATION OF SMALL BOWEL AND PERIANAL DISEASE IN PEDIATRIC CROHN'S DISEASE PATIENTS

SAMANTHA Harrington, GARY Wang, KATHERINE Nimkin, MICHAEL Gee

Massachusetts General Hospital, Boston, USA

Purpose: MR enterography (MRE) and pelvic perianal MRI are the gold standard imaging studies for evaluating Crohn's disease involvement. The purpose of this study was to assess the value of a combined MRE-perianal MRI protocol in the pediatric population to evaluate both small bowel and perianal disease in the same visit.

Materials and Methods: This IRB-approved, retrospective study assessed combined MRE-perianal fistula protocols in the pediatric population (age < 19 years) at a tertiary hospital from 2012–2020. The combined MRE-perianal fistula protocol consisted of a standard MRE protocol with the addition of dedicated small pelvis field-of-view axial and coronal fat-suppressed fluid-sensitive sequences. Patient demographics (age and gender), length of exam and exam value were assessed. Two fellowship-trained pediatric radiologists determined clinical value of the exam. Student's t test was used to assess differences in MR exam scan times, with P-values < 0.05 considered significant.

Results: A total of 51 scans for 45 patients met criteria for this study. No exams were terminated prematurely. The mean time for the combined MRE-perianal fistula study was 59 + 19 minutes. For patients undergoing separate MRE and fistula exams, the mean time for MRE was 39 ± 8 minutes and for perianal MRI was 48 minutes ± 8, with aggregate time for the separate exams of 87+ 12 minutes. The combined protocol was associated with a 32% time savings, which was statistically significant (P<0.001, Student's t test). Small FOV images were found to improve disease characterization in 80% (41/ 51), with 49% (25/51) providing better delineation of perianal disease, 14% (7/51) detecting disease not seen on MRE alone and 18% (9/51) increasing confidence that no perianal disease was seen.

Conclusion: Combined MRE-perianal MRI protocol is well-tolerated in pediatric Crohn's disease patients and improves evaluation of perianal disease compared to MRE alone, while decreasing MR time compared to separate MRE and perianal MRIs.

Poster: SCI-108

UTILIZATION OF EOS IMAGING FOR EVALUATION OF BOWEL MANAGEMENT AND RADIATION DOSE REDUCTION

KRITI Gwal¹, REBECCA Stein-Wexler¹, PAYAM Saadai²

¹ University of California Davis Health, Department of Radiology, Sacramento, USA

² University of California Davis Health, Department of Pediatric Surgery, Sacramento, USA

Purpose:

To assess the radiation dose of the EOS(TM) imaging system compared with conventional digital or computed radiography (DR/CR) for a single radiograph of the abdomen and pelvis obtained to evaluate stool burden.

Materials and Methods:

Following IRB approval, we retrospectively identified 56 patients in our Bowel Management Program who were being treated for chronic constipation and who had abdominal/pelvic radiographs to evaluate stool burden obtained with the EOS imaging system between 07/01/2017–05/30/2018. 17 were excluded because they had not also had DR/CR of the abdomen and pelvis at some point during that time period. We then compared the dose area product (DAP) for the radiographs obtained with the EOS imaging system with the DAP for radiographs performed on the same patients with DR/CR. Comparison of the doses was performed with calculation of difference, percent dose reduction, and paired t test.

Results:

The percent reduction in DAP ranged from 94.5% to 17.9%. The mean dose with the EOSTM imaging system showed an overall decrease in dose by 82% when compared to mean DR/CR DAP (p=0.005).

Conclusions:

An abdominal/pelvic radiograph with short exposure time performed by the EOS imaging system may provide a way to decrease DAP compared to DR/CR in patients having radiographs to evaluate stool burden in bowel management programs.

Poster: SCI-109

DIAGNOSTIC PERFORMANCE OF ULTRASOUND HEPATORENAL INDEX AS A QUANTITATIVE MEASURE OF PEDIATRIC FATTY LIVER DISEASE AND COMPARISON TO FIVE HUMAN RADIOLOGISTS

MICHAEL Frankland¹, JONATHAN Dillman², CHRISTOPHER Anton², BRIAN Coley², MICHAEL Nasser², SARA O'Hara², YINAN Li², ANDREW Trout²

¹ University of Cincinnati College of Medicine, Cincinnati, USA

² Cincinnati Children's Hospital Medical Center, Cincinnati, USA

Non-alcoholic fatty liver disease (NAFLD) is the most common pediatric chronic liver disease in the developed world. The purpose of this study was to evaluate the diagnostic performance of quantitative measurement of liver echogenicity (hepatorenal index [HRI]) for NAFLD in a pediatric cohort and compare it to the diagnostic performance of pediatric radiologists.

Pediatric patients (<18 years-old) that underwent abdominal US and MRI with liver proton density fat fraction (PDFF) within 3 months (July 2015–April 2020) were identified (n=69). Using ImageJ, small circular regions of interest (ROI) and large freehand ROIs were drawn in the liver and right kidney on single longitudinal and transverse images to measure echogenicity (arbitrary units). Four HRIs (liver:kidney) were subsequently calculated; liver histogram features also were calculated. Five pediatric radiologists, blinded to MRI PDFF and US HRI measurements, also indicated the presence/absence of hepatic steatosis. Pearson correlations (r) assessed associations and receiver operating characteristic (ROC) curve analyses evaluated diagnostic performance. Multivariable logistic regression was used to further assess relationships.

Mean (SD) patient age was 11.6 (4.7) years; 27 (36.2%) patients were female. Mean MRI PDFF was 12.5% (13.1%). There were significant, positive correlations between all four US HRI methods and MRI PDFF (r=0.51–0.61); longitudinal freehand ROIs exhibited the strongest correlation (r=0.61; p<0.0001). ROC AUCs for prediction of >6% liver PDFF with the four US HRI methods ranged from 0.74–0.80. Longitudinal, freehand ROI HRI had moderate diagnostic performance (AUC=0.80, p<0.0001), with an optimal cut-off value >1.75 (sensitivity=70.6%, specificity=77.1%). ROC AUCs for five pediatric radiologists ranged from 0.90–0.96 (mean sensitivity=88.3%, mean specificity=94.8%). Significant multivariable predictors of PDFF >6% included HRI (p=0.002; OR=34.2), BMI-percentile (p=0.005; OR=1.06), and liver gray-scale echogenicity standard deviation (p=0.02; OR=0.79) (ROC AUC= 0.92).

Quantitative US HRI positively correlates with MRI PDFF and has moderate diagnostic performance for detecting liver fat. The addition of BMI-percentile and gray-scale echogenicity standard deviation improves diagnostic performance.

Poster: SCI-110

FREQUENCY OF DUODENAL ANATOMICAL VARIANTS IN NEONATAL AND PEDIATRIC UPPER GASTROINTESTINAL TRACT SERIES (UGI) AND THE INFLUENCE OF EXAM QUALITY ON DIAGNOSTIC REPORTING

MOHAMED Elsingerly, JUAN S. Calle Toro, REBECCA Dennis, DAPHINE Grassi, HANSEL Otero, SAVVAS Andronikou

The Children's Hospital of Philadelphia, Department of Radiology, Philadelphia, USA

Purpose: Despite being current standard for visualizing duodenal anatomy in clinical diagnosis, challenging procedural aspects, often out of the control of radiologists, can affect UGI exam quality. Poor awareness of the frequency and appearances of normal duodenal anatomical variants may also contribute to misdiagnosis of malrotation, posing risk of unnecessary surgery. Our goal is to map the frequency of duodenal variants and determine if quality of UGI plays a role in misdiagnosis.

Methods: Retrospective review of UGI exams in children aged 0-18 years from January to December 2018. Exams were considered diagnostic if the duodenojejunal (DJ) flexure was located. For diagnostic exams, quality of the exam was determined based on continuity of duodenal visualization, number of bolus passes required, and patient positioning. Duodenal anatomy was categorized as normal (C-shaped loop with DJ flexure lateral to left pedicle of L1 vertebrae, at height of first duodenal part (D1)), normal variant (redundant/inverted), or abnormal (malrotated/nonrotated).

Results: UGI exams of 100 patients (66 males /34 females) were reviewed. Mean age was 5.2 months \pm 6.2 SD.

In our review, 90 exams were considered diagnostic. 38/90 exams (42%) were of 'high quality'—duodenum was visualized continuously up to DJ flexure, on 1st pass bolus and without any patient rotation. 52/90 exams (58%) were of 'low quality'—DJ flexure was visualized but in 12 exams not on 1st pass bolus, in 23 exams, the duodenum was visible intermittently, in 9 exams were associated with patient rotation and, in 31 exams, patient rotation assessment was not technically possible. 10 exams were considered non-diagnostic. In total only 38% of the exams were considered diagnostic and of high quality.

Of the 90 diagnostic exams, duodenal anatomy was normal in 69/90 (77%), normal variant in 18/90 (20%) and abnormal in 3/90 (3%) exams. Original reports considered 99 exams as diagnostic—where duodenum was normal in 91 (92%), normal variant in 3 (3%), and abnormal in 5 (5%) exams—and 1 exam as non-diagnostic. The 2 additional cases originally reported as abnormal, were considered normal variants on our review, and the exams were of 'low quality'.

Conclusion

Discrepancy in frequency of normal variants (18% vs.3%) and non-diagnostic exams (10 vs.1) between our review and the original reports respectively, questions performing radiologists' objectivity and poses a risk of misdiagnosis of an abnormal duodenum (3% vs.5%).

Poster: SCI-111

FACTORS AFFECTING THE SUCCESS OF AIR ENEMA REDUCTION OF INTUSSUSCEPTION IN CHILDREN. WHAT STARTING PRESSURE?

HEBA ELBAALY Elbaaly, MARIE-CLAUDE Miron, RAMY El Jalbout, AMÉLIE Damphousse, CHANTALE Lapierre, JOSÉE Dubois Medical Imaging Department, CHU Sainte-Justine, Montréal, CANADA

Purpose:

Evaluate the success rate and the predicting factors of air enema intussusception reduction (AIR) in children. Assess the optimal pressure to use.

Methods:

Retrospective review of AIR from 2017- 2020. All patients with ultrasound confirmed intussusception were included. AIR is done with a pressured air delivery reduction device and an inflated rectal balloon for seal. The sex, age, presentation, duration of symptoms (DOS), type of intussusception, ultrasound findings, AIR attempts, pressure, delayed repeated attempts, presence of pathological lead point (PLP), fluoroscopic time and radiation dose were collected. Correlation between AIR and multiple parameters was performed with Fisher's exact test. The

composite AIR reduction rate (RR) is calculated as: (total reduced cases/ (attempted cases- surgical cases for PLP))x100.

Results:

115 (79M, 36F) had confirmed intussusception. 114 underwent AIR, 1 spontaneously reduced. Mean age 22.45M. 87% had DOS <48 hours. 73.9% had acute episodes of crampy abdominal pain. 20% had rectal bleed. 71.1% (n=81) were reduced in the first attempt 80 mmHg (n=20), 90 (n=48), 100 (n=9), 120 (n=4), and 83.3% (n=95) after 3 attempts. Delayed repeated reduction (n=8, 2 failed) RR is 88.6% (n=101). No perforation occurred. 13 underwent surgery. 9 had PLP (7 Meckel's diverticulum, 1 mucoviscidosis, 1 cecal duplication cyst), 4 did not (2 cecal ulceration).

AIR reduction is associated with Ileocolic (90.5%), ileo-ileo-colic (4.2%), ileo-colo-colic (3.2%) colo-colic (1.1%) p-value 0.008; absence (86.3%), vs. presence of bowel wall edema + intussusciens fluid + small bowel obstruction (13.7%) on ultrasound p-value 0.000; DOS< 48 hrs (90.5%) p-value 0.014; absence of PLP (91.4%) p-value 0.000. The mean pressure 93.1mmHg correlated with reduction (p-value 0.000) without increase in fluoroscopy time (Mode 0.35 min) or radiation (0.2 mGy).

Conclusion:

AIR composite reduction rate is 96.2%. 90 mmHg appears sufficient for successful AIR provided it is continuously maintained. DOS>48 hours, severity on US, PLP are adversely associated with AIR.

Poster: SCI-112

IS ORAL CONTRAST BENEFICIAL FOR VISUALIZATION OF THE APPENDIX IN LOW-WEIGHT CHILDREN?

GALI Shapira-Zalstberg ¹, MARIA FERNANDA Dien Esquivel ¹, NICHOLAS Mitsakakis ², ELKA Miller ¹

¹ CHEO-University of Ottawa, Ottawa, CANADA

² CHEO Research Institute, Ottawa, CANADA

Purpose: It has been shown that CT with oral contrast does not improve the diagnostic accuracy of acute appendicitis in pediatric patients, however, the cohorts were not stratified by weight or BMI. The purpose of this study is to retrospectively assess the benefit of oral contrast administration before CT to identify the appendix in younger children in the lower weight quartile (< 25%).

Materials and Methods: This retrospective study comprised 83 pediatric patients (2-10 years) in lower weight quartile (<25%) who have had IV contrast-enhanced CT of the abdomen and pelvis, 30 of which with oral contrast, and 53 without oral contrast. Patients with prior history of appendectomy, large abdominal mass displacing the bowel loops, or oral contrast that has not reached the cecum were excluded. A pediatric radiologist and pediatric radiology fellow independently assessed whether the appendix was visualized or not. In case of discrepancy, a second pediatric radiologist was the 'tie-breaker'. Inter-rater agreement was determined for each group. Fisher exact test was used to compare the visibility of the appendix between the 2 groups.

Results: There was 100% interrater agreement in the group with oral contrast, compared to 77.4% agreement in the group without oral contrast, yielding a significant difference (p=0.003). There was no significant difference in the visualization of the appendix between the group with oral contrast (86.6%) and without (84.9%).

Conclusions: There is no significant difference in the visualization of the appendix using CT with or without oral contrast including in low-weight pediatric patients. The study confirms that oral contrast-CT should not be routinely used for the indication of appendicitis in this population.

Poster: SCI-113

REFERENCE RANGES OF AGE-BASED LIVER, SPLEEN, PANCREAS AND KIDNEY SIZE IN CHILDREN IN CONJUNCTION WITH WAIST CIRCUMFERENCE

ZUHAL Bayramoglu, HAKAN Ayyildiz, BERKE Ersoy
Istanbul University, Istanbul Medical Faculty, Pediatric Radiology
Department, ISTANBUL, TURKEY

We aimed to provide a nomogram of solid intraabdominal organ size by age for Turkish children on contrast-enhanced abdominal computed tomography images in conjunction with waist circumference (WC). 800 pediatric patients (468 male; mean age: 8.68±5.2 years, 332 female; mean age: 9.12±5.04) previously underwent abdominal computed tomography examinations were enrolled. The transverse diameter of the liver and lengths of both liver lobes, the thickness of the pancreas from the head, corpus, and tail, width and length of the spleen, and both anteroposterior diameters and lengths of kidneys were measured. Descriptive statistics of the data were expressed as mean, standard deviation, and percentiles. Differences in mean diameters among ages were compared with the ANOVA test. Pearson correlation analysis and regression equations were assessed to depict the association of size with age and WC parameters. There have been statistically significant positive correlations of all measured size parameters with age ($p < 0.001$; $r: 0.53-0.83$) and WC ($p < 0.001$; $r: 0.53-0.83$). WC was significantly correlated with age ($p < 0.001$, $r: 0.77$). We documented 5th, 50th, 90th, and 95th percentiles of solid organ diameters for each age. Age (years) dependant regression equations for lengths (mm) of the liver ($3.64 \times \text{age} + 80.681$), spleen ($3.07 \times \text{age} + 63.47$), the left kidney ($2.89 \times \text{age} + 63.65$), and the right kidney ($2.76 \times \text{age} + 62$) have been calculated. There were no statistically significant differences among the mean ratios of the right liver lobe to the right kidney (1.56 ± 0.26), left to the right kidney (1.03 ± 0.09), and spleen to the left kidney lengths (1 ± 0.2) ($p < 0.4$) by age groups. The right to left liver lobe length ratio was 1.9 ± 0.37 without significant differences among age and gender groups ($p < 0.18$). Age (years) dependant regression equation for WC (mm) was depicted as " $22 \times \text{age} + 408$ ". WC (mm) dependant organ length (mm) estimations by regression equations have been found as: " $0.11 \times \text{WC} + 45$ " for right liver lobe, " $0.1 \times \text{WC} + 30$ " for spleen, " $0.09 \times \text{WC} + 35$ " for the left kidney and " $0.085 \times \text{WC} + 35$ " for the right kidney. Spleen length (SL; mm) dependant right liver lobe length ($0.96 \times \text{SL} + 48$) and left kidney length ($0.6 \times \text{SL} + 34$) were also depicted. Left kidney length (LL; mm) dependant spleen length ($0.97 \times \text{LL} + 3.78$) and the right kidney length (RL) dependant right liver lobe length ($1.14 \times \text{RL} + 14.48$) were calculated by regression equations. Age and WC would be reliable parameters to predict reference ranges for organ diameters.

Poster: SCI-114

ABDOMINAL IMAGING FINDINGS OF BASIDILOBOMYCOSIS IN CHILDREN

ABEER ALMEHDAR, NESREEN ABOUROKBAH, HETAF ALSRHAN
KING SAUD BIN ABDULAZIZ UNIVERSITY FOR HEALTH SCIENCES, JEDDAH, SAUDI ARABIA

Basidiobolomycosis is a rare fungal infection caused by *Basidiobolus ranarum* and is commonly found in the tropical areas. The fungus commonly affects the skin and subcutaneous tissues of immunocompetent adults and children. Gastrointestinal basidiobolomycosis (GIB) is uncommon with only few cases reported, most were from Saudi Arabia, Iran and the USA. Radiologic findings share similarities with abdominal malignancies, IBD and tuberculosis.

To our knowledge, there are no published studies describing the imaging findings of GIB in children.

Purpose

To describe the abdominal imaging findings in pediatric patients with gastrointestinal Basidiobolomycosis infection.

Methods

A retrospective review performed on all pathology proven GIB cases in pediatric patients who had abdominal imaging studies. Two radiologists aware of the diagnosis reviewed the imaging findings and had a consensus. Additional information was obtained from the medical records

Results

Out of the 12 GIB cases, 10 were male and 2 were female and the median age was 4.2 years. All cases had imaging studies (8 abdominal radiographs, 6 abdominal ultrasounds, 12 CT scans). Opacity and displacement of bowel gases were the most reported finding (87.5%) on the abdominal radiographs. Large Heterogeneous mass with bowel wall involvement was present in all ultrasound cases. All cases demonstrated large/ infiltrative mass with heterogeneous enhancement on the CT scan with mesenteric (100%) and retroperitoneal extension (91.7%). Bowel wall involvement was present in all cases with aneurysmal dilatation in 83.3% of the cases. Cecum, ascending colon and distal small bowel were the most affected bowel segments. All cases were associated with enlarged mesenteric and retroperitoneal lymph nodes with fat stranding, peritoneal enhancement and ascites.

Conclusion

An infiltrative abdominal mass involving the right colon and distal small bowel, mesenteric and retroperitoneal infiltration and lymph nodes enlargement are the most common imaging findings of GIB. Familiarity with the imaging findings is important to avoid misdiagnosis, unnecessary surgery or delay in management

Poster: SCI-115

CONGENITAL VITELLINE BAND CAUSING INTESTINAL OBSTRUCTION IN A 15 YEAR OLD BOY - A DIAGNOSTIC CHALLENGE FOR HIGH-FREQUENCY SONOGRAPHY

ELENI Koutrouveli¹, RODANTHI Sfakiotaki¹, IRENE Vraka¹, MARINA Vakaki¹, GEORGIOS Daniil², ANNA Chountala¹, CHRYSOULA Koumanidou¹

¹ Children's Hospital of Athens P&A Kyriakou, Athens, GREECE

² General Hospital of Thessaloniki G. Gennimatas, Thessaloniki, GREECE

PURPOSE:

To highlight the feasibility of ultrasound in the pre-operative diagnosis of congenital vitelline band complicated with small bowel obstruction.

MATERIALS & METHODS:

A 15-year old boy, with no prior surgical history, presented with acute abdominal pain, abdominal distention and vomiting. Physical examination and blood tests were normal.

Plain X-ray showed evidence of small bowel obstruction, with grossly distended small bowel loops and absent rectal gas.

Ultrasound revealed fluid distended aperistaltic bowel loops and a distinct ring-like lesion in the right lower quadrant, with smooth margins and hyperechoic boundary, including strangulated small intestine. It was surrounded by hyperechoic mesentery. Clinical and ultrasonographic findings led to the suspicion of congenital vitelline band. An urgent laparotomy was performed.

RESULTS:

A thick, soft tissue band extending from the terminal ileum to the umbilicus was found, with small bowel loops twisting around the band, forming a volvulus. The identified congenital vitelline band was resected and obstruction was relieved.

CONCLUSION:

High frequency ultrasound being non-radioactive, performed in real-time and repeatedly when necessary and producing high-quality images can actually be an effective modality in the pre-operative imaging diagnosis of the congenital vitelline band in cases of intestinal obstruction.

Poster: SCI-116

SPATIAL ENTROPY OF THE LIVER IN SICKLE CELL DISEASE PEDIATRIC PATIENTS: A HIGHER SPATIAL RESOLUTION SURROGATE TO T2*-BASED LIC MEASURES

PATRICK Tivnan¹, RYAN McNaughton², HERNAN Jara¹, ILSE Castro-Aragon¹

¹ Department of Radiology, Boston Medical Center, Boston, USA

² Department of Mechanical Engineering, Boston University, Boston, USA

Purpose: Iron monitoring can be important in sickle cell (SCD) patients as iron overload can develop from chronic transfusions. To this end, we evaluated the utility of MR spatial entropy mapping as an alternative method to standard T2* correlation with liver iron concentration (LIC) levels for quantifying hepatic iron accumulation.

Material and Methods: Any MRI of the abdomen with reference T2* iron quantification sequences and T2w-sshTSE in SCD patients >21 years old were gathered retrospectively from 01/01/2010-10/01/2020. The reference iron quantification technique used in this work is based on T2* mapping followed by LIC mapping according to the phenomenological equation of Sirlin Reeder (2010): $LIC = -0.63 + 26.7/T2^*$. Spatial entropy mapping was performed with a DICOM compatible algorithm written in Python. As part of this algorithm, the amount of local structural information was measured pixelwise on images of the single-shot T2-weighted turbo spin echo (T2w-sshTSE). Three region of interest (ROI) measurements were taken in spatial locations with minimal liver vasculature. Linear regression analysis was performed to assess correlation between reference LIC and spatial entropy.

Results: 16 MRIs were gathered from 8 patients (4 had follow up MRIs). The cohort was 50% (4/8) female, 8/8 HgSS, with an average of 10.7 (range 3 to 18) years old at time of scan. LIC levels ranged from 0.8 to 21 (average 7.6) mg Fe/g of dry weight liver. Average spatial entropy of the three ROI measurements ranged from 4278.6 to 5160.8 (average 4805.7) kBytes. Scatterplots of the spatial entropy versus LIC demonstrated a statistically significant negative correlation ($R^2=0.263$, $P=0.042$).

Conclusion: In this small cohort, spatial entropy measures of the liver have strong correlation to liver iron quantification levels in SCD patients. As these analyses can be performed based of T2 single shot turbo spin, this data suggests these analyses can function as a surrogate sequence in the calculation of LIC.

Poster: SCI-117

FOLLOW-UP ULTRASONOGRAPHIC FINDINGS AMONG CHILDREN WITH UNCOMPLICATED, ACUTE APPENDICITIS, MANAGED CONSERVATIVELY

RODICA Stackievicz^{1,2}, ROTEM Milner¹, HASAN Haskiya¹, MYRIAM Werner^{1,2}, SHMUEL Arnon^{3,2}, ZVI Steiner^{4,2}

¹ Department of Radiology, Meir Medical Center, Kfar Sava, ISRAEL

² Sackler Faculty of Medicine, Tel Aviv University, Tel Aviv, ISRAEL

³ Department of Neonatology, Meir Medical Center, Kfar Sava, ISRAEL

⁴ Department of Pediatric Surgery, Meir Medical Center, Kfar Sava, ISRAEL

Background and Objective:

Ultrasound (US) is an accurate tool for diagnosing pediatric acute appendicitis (AA). The conservative treatment for uncomplicated AA is feasible and safe in children, sparing the need for surgery. However, US to follow children with AA managed non-operatively has not been evaluated. This study describes the sonographic appearance of the appendix at follow-up US and tries to identify signs predictive of recurrent AA (RAA).

Methods:

Clinical records and US data of all children diagnosed with uncomplicated AA, treated conservatively in our institute 2015-2019 who underwent follow-up US were recorded. US signs included appendiceal diameter, fat infiltration, enlarged lymph nodes, and free fluid in the abdomen. Clinical follow-up was matched to US findings.

Results:

Among 835 children with uncomplicated AA treated conservatively, 204 had follow-up US. At 3 months follow-up, 29 (14.2%) had RAA and 175 (85.8%) had uneventful follow-up (non-RAA). In 17/29 (58.6%) RAA cases, US depicted an abnormal diameter of appendix, compared with 39/175 (22.3%) in non-RAA ($p=0.0004$). Twenty-six children (7 from the RAA group and 19 from the non-RAA group) with an abnormally large appendix at first follow-up US continued to be followed for another 3–6 months. At the end of this period, the sonographic appearance of the appendix remained abnormal in 5/7 cases from the RAA group (71.4%) and converted to normal in 15/19 (78.9%) cases from the non-RAA group ($p=0.016$). RAA was treated surgically in 23 and non-operatively in 6. Enlarged appendix at follow-up US also positively correlated with the need for surgery ($p=0.0009$).

Conclusions:

An enlarged appendix was detected more frequently in children who later developed RAA. The results of this study support the hypothesis that US can be useful in predicting RAA in patients treated conservatively for uncomplicated AA. As this is the first study to report these findings, additional, larger studies are needed to establish guidelines.

Poster: SCI-118

SONOGRAPHIC FINDINGS OF COMPLICATED AMYAND'S HERNIA IN A NEONATE. A SCROTAL ABSCESS WITH A RARE CAUSE THAT WE SHOULD BE AWARE OF

RODANTHI Sfakiotaki¹, IRENE Vraka¹, ANNA Chountala¹, MARINA Vakaki¹, ELENI Koutrouveli¹, GEORGIOS Daniil², CHRYSOULA Koumanidou¹

¹ Children's Hospital of Athens P&A Kyriakou, Athens, GREECE

² General Hospital of Thessaloniki G.Gennimatas, Thessaloniki, GREECE

Purpose: Amyand's hernia (AH) is an uncommon form of inguinal hernia. It represents <1% of all hernias and its complication with appendicitis is still rarer with 0, 1-0, 13% being reported. When the contained appendix is inflamed it can mimic testicular inflammation or torsion. Preoperative diagnosis can be difficult due to its rarity and the majority of cases are revealed on the operation. We present the sonographic features of this rare condition, its mimics; discuss the different stages of Amyand's hernia and the possible pathogenetic mechanisms.

Materials and methods: We present the sonographic findings in a neonate with complicated AH who presented atypically with a tender inguinoscrotal hernia. The neonate was relatively active, continued to feed well and had bowel movements despite ongoing appendicitis.

Results: His abdominal examination was normal. Local examination revealed a firm right irreducible inguinoscrotal swelling with mild tenderness of the overlying skin and the right testis was not palpable separately. Ultrasound examination showed the right testis in the scrotum with obvious internal blood flow. The testis was surrounded by a heterogenous area representing a scrotal abscess with inflammatory fat and tissues extending into the inguinal canal

Conclusion: Prompt diagnosis is mandatory because timely operative intervention reduces both mortality and morbidity. Pediatric radiologists should keep this rare condition in the list of differential diagnoses while evaluating a patient with inguinoscrotal swelling. Sonographic findings can confirm the presence of blood supply of the testis and indicate the urgency of surgical intervention.

Poster: SCI-119

CAN SONOGRAPHIC ABDOMINAL FINDINGS COMPLETE THE CRITERIA FOR THE DIAGNOSIS OF MIS-C? A NON-SPECIFIC IMAGE THAT DEVELOPS INTO A PATTERN

RODANTHI Sfakiotaki¹, IRENE Vraka¹, ANNA Chountala¹, ELENI Koutrouveli¹, MARINA Vakaki¹, GEORGIOS Daniil², CHRISTINA Zouridaki¹, CHRYSOULA Koumanidou¹

¹ Children's Hospital of Athens P&A Kyriakou, Athens, GREECE

² General Hospital of Thessaloniki G.Gennimatas, Thessaloniki, GREECE

PURPOSE: In recent months, a multisystem hyperinflammatory condition (MIS-C) has emerged in children in association with prior exposure or infection to COVID-19. The purpose of our presentation is to present a pattern of abdominal sonographic findings that we observed in the children that experience this life-threatening hyperinflammatory condition. **Materials and Methods:** Two patients 8 and 9 years old respectively presented to the emergency department with fever and clinical symptoms mimicking acute appendicitis. Clinical examination revealed acute abdominal pain, rash and conjunctivitis, while their clinical status rapidly deteriorated to warrant management in the pediatric intensive care unit. Abdominal ultrasound was requested to exclude acute surgical abdominal pathology.

Results: Abdominal ultrasound showed inflammatory changes localized in the right iliac fossa that shared common sonographic features in both patients. High-frequency images revealed enlarged hypoechoic lymph nodes (short axis larger than 1,3cm), hyperechoic thickened mesenteric fat, bowel wall thickening (cecum and terminal ileum), appendix without signs of inflammation, and ascites with internal echoes. Both of them met the case definition for MIS-C. They developed severe myocardial dysfunction and one of them required extracorporeal membrane oxygenation (ECMO).

Conclusions: Our findings are consistent with the reported cases worldwide. The sonographic findings in the right iliac fossa in a child with acute abdominal pain, fever, rash and conjunctivitis should raise the suspicion of the clinician for this life-threatening condition. Since the pandemic is ongoing, we may include more cases for our presentation.

Poster: SCI-120

NON-INVASIVE BIOMARKERS OF NAFLD IN ASYMPTOMATIC SCHOOL-AGED VOLUNTEERS

MARIA Raissaki¹, STAVROS Charalambous¹, GEORGIOS Kalaitzakis¹, MARINA Vafeiadi², KATERINA Margetaki², THEANO Roumeliotaki², NIKOS Stratakis³, LEDA Chatzi³, THOMAS G Maris¹

¹ Department of Radiology University Hospital, School of Medicine, University of Crete, Heraklion, GREECE

² Department of Social Medicine, School of Medicine, University of Crete, Heraklion, GREECE

³ Department of Preventive Medicine, Keck School of Medicine, University of Southern California, Los Angeles, CA, USA

Background and Purpose: Nonalcoholic fatty liver disease (NAFLD) has been increasingly diagnosed in asymptomatic children. Our aim was to

develop and validate a non-invasive tool for liver fat estimation and to assess indices for the presence of liver steatosis in school-aged volunteers utilizing Magnetic Resonance Imaging (MRI).

Methods: Following informed consent, children from the Rhea cohort underwent clinical and MRI tests in a 1.5T Siemens MAGNETOM Vision/Sonata system. MRI sequences included T2-w TSE, MECSE (Multi-echo Dixon), T1-weighted fast low angle GRE through the liver, and HASTE at the level of L4-L5 intervertebral disc. Data were post processed using an in-house tool (QMRI Utilities-X) and by the validated HepaFat-Scan® approach, to calculate the mean %liver fat fraction. Pre-liver, subcutaneous, visceral fat and area of body fat were measured. Liver steatosis was categorized into four groups: normal(0-5%), mild(5.1-10%), moderate(10.1-20%) and heavy(>20%), according to mean %liver fat fraction values.

Results: Overall 69 children, 42(60.9%) males, participated, at the age of 10-11 years, with BMI 21.2±4.0 kg/m². Liver fat fraction was 3.6±7.5%. Liver steatosis was detected in 10 children (14.5%), among whom heavy steatosis in 3 (4.4%). QMRI Utilities-X showed great reliability compared to HepaFat-Scan® (ICC=0.982 and 0.944 for %liver fat and steatosis, respectively). Steatosis was mostly identified in males (21.4% among boys, 3.7% among girls, p=0.041). Body fat area, body fat thickness, visceral fat and pre-liver fat thicknesses were positively correlated with steatosis: 147.9±92.0cm², 3.5±0.9cm, 1.8±1.0cm and 1±0.3cm in healthy, vs 326.0±88.1cm², 4.9±2.3cm, 3.3±0.8cm and 1.4±0.3cm, in children with steatosis, respectively (all p<0.001). Steatosis was more prevalent among overweight/obese children (3.6%, 11.1% and 42.9% in children with normal weight, overweight and obesity, respectively, p=0.002). Steatosis was positively correlated with height, weight, waist and hip circumference, serum triglycerides and ALT levels.

Conclusions: The proposed MRI protocol with the aid of the inhouse software can be used to identify NAFLD in up to 6% of school-aged asymptomatic children while simple linear and area measurements of body and visceral fat, together with clinical and laboratory indices can be used as non-invasive biomarkers for the presence of liver steatosis.

Poster: SCI-121

REDUCING RADIOGRAPHS AFTER CROSS-SECTIONAL IMAGING IN PEDIATRIC TRAUMA TO REDUCE RADIATION EXPOSURE

JONATHAN Phuong, JENA Fujimoto, SAMUEL Yap, REBECCA Stein-Wexler

University of California, Davis, Sacramento, USA

Numerous radiographs and cross-sectional imaging studies are often performed after pediatric trauma. However, in our experience, many of the radiographs performed after cross-sectional imaging rarely add any new clinically significant finding. The purpose of this study is to evaluate the relationship between time after cross-sectional imaging and the frequency that these radiographs show clinically significant findings. In this single level-one trauma and tertiary care center retrospective analysis, all radiographs performed after cross-sectional imaging of the abdominopelvic region from October 1st, 2016 to October 31st 2018 were evaluated for new clinically significant findings. Time between the cross-sectional imaging and radiographs were recorded. This came out to 81 patients and 104 total radiographs. Out of the 104 radiographs, only 2 (2%) demonstrated clinically significant findings not seen on the prior cross-sectional imaging. These occurred at 35 minutes and 3 hours and 32 minutes after cross-sectional imaging. The other 102 (98%) radiographs did not show any additional clinically significant findings. These data show how rarely these radiographs demonstrate new significant findings regardless of time after cross-sectional imaging. Given the minimal clinical impact of these radiographs and the increased sensitivity of the pediatric patients to radiation, limiting these radiographs would reduce unnecessary exposure to

radiation as well as align with the principles of Image Gently and ALARA. Thus, we recommend being more judicious when ordering radiographs after cross-sectional imaging of the adominopelvic region in pediatric trauma.

Poster: SCI-122

SHOULD POSTNATAL ULTRASOUND BE PERFORMED WHEN ISOLATED ECHOGENIC BOWEL HAS BEEN REPORTED ON THE ANTENATAL ULTRASOUND?

MICHAEL Paddock¹, GEORGE Beattie¹, DANIEL Froste¹, AMAKA C Offiah², RICHARD Nicholl³

¹ Barnsley Hospital NHS Foundation Trust, Barnsley, UNITED KINGDOM

² Sheffield Children's NHS Foundation Trust, Sheffield, UNITED KINGDOM

³ Northwick Park Hospital, Harrow, UNITED KINGDOM

PubMed and Medline databases on NHS Evidence and Web of Science were searched which returned 8 studies; forward citation retrieved 1 further study.

Fetal echogenic bowel (FEB) is the subjective 'bright' appearance of the fetal bowel on antenatal ultrasound (US). The reported FEB incidence in 2nd trimester pregnancy is 0.2-1.8%. The clinical significance of FEB remains contentious: it is thought to be isolated in up to 70% cases and a normal finding in the 3rd trimester representing fetal meconium. Reported associations include intra-amniotic haemorrhage, meconium peritonitis, intrauterine (IU) CMV infection, trisomy 21/aneuploidy, cystic fibrosis, IUGR and IU demise.

Visualisation of fetal bowel on US may be limited by operator experience and the presence of overlying gas. Falsely increased bowel echogenicity can result from the use of a high frequency transducer, particularly when an 8 MHz, rather than 5 MHz transducer, is used. Other US markers (concurrent dilated bowel) and associated abnormalities (resulting in an increased risk of adverse neonatal outcome) should be actively sought when

FEB is detected.

Good postnatal outcomes are reported: when FEB is isolated (fetuses had uneventful pregnancies with no pathological abnormalities postpartum); if resolution or decrease in FEB echogenicity on serial US; regardless of trimester in which FEB is detected. Isolated, and US resolution of, FEB are the strongest prognostic factors for an uneventful neonatal outcome. Isolated FEB will typically resolve before birth with no adverse postnatal outcomes (neonates will be clinically well and asymptomatic). It has also been reported that FEB has no association with neonatal outcome and should no longer be used in antenatal US reporting.

When additional US findings are present, clinical and imaging follow-up will be dictated by other antenatal investigations, postnatal symptoms and clinical assessment. Neonates who have adverse postnatal outcomes e.g., meconium ileus or bowel obstruction, will be symptomatic and require surgical assessment. In this setting, postnatal sonography rarely adds any further diagnostic information.

Isolated FEB is a benign sonographic finding which carries a favourable prognosis. There is no role for postnatal sonography in clinically well, asymptomatic neonates in whom isolated fetal echogenic bowel has been detected antenatally, particularly when FEB resolves during pregnancy.

Poster: SCI-123

AN OBSERVATION OF UPPER GI CONTRAST STUDIES IN 3 IRISH PAEDIATRIC HOSPITALS DURING THE COVID-19

PANDEMIC IN IRELAND

AILBHE McDermott¹, CAOILFHIONN Ni Leidhin¹, AILBHE Tarrant², ANGELA T. Byrne³, STEPHANIE Ryan², GABRIELLE Colleran⁴

¹ Children's Health Ireland at Temple Street, Dublin, IRELAND

² Children's Health Ireland at Temple Street and The Rotunda Hospital, Dublin, IRELAND

³ Children's Health Ireland at Crumlin, Dublin, IRELAND

⁴ Children's Health Ireland at Temple Street and The National Maternity Hospital, Dublin, IRELAND

Introduction

Intestinal malrotation is the abnormal positioning of the bowel within the peritoneal cavity due to abnormal gut rotation during embryogenesis. Malrotation predisposes to midgut volvulus. Up to 75% of symptomatic malrotation cases occur in neonates. An upper gastrointestinal (GI) contrast study is the examination of choice to evaluate suspected malrotation. The COVID-19 pandemic reached Ireland at the end of February 2020 with restrictive measures being implemented from 12th March beginning with the closure of schools, colleges and childcare facilities followed by a nationally enforced 'lockdown', which eased in phases the most significant of which commenced on 29th June 2020.

The birth rate, malrotation incidence and subsequent referral rate for upper GI contrast studies should have been unaffected during this first wave of the COVID-19 pandemic (1). The aim of this study was to evaluate rate of referral for upper GI contrast studies to rule out malrotation across three Dublin paediatric hospitals during the first wave of the COVID-19 pandemic in Ireland, and compare against the preceding year.

Methods

All upper GI contrast studies performed across three paediatric hospitals in Dublin, Ireland, between 12th March and 29th June 2019 and 2020 were identified. The indication for referral was reviewed and neonatal studies were identified. Patient and study demographics were retrieved and analysed.

Results

There were 145 upper GI contrast studies performed between 12th March and 29th June 2019, while 90 were carried out during the same period in 2020. Sixteen (13 male, 3 female) neonates underwent studies during this timeframe in 2019 and 10 (3 male, 7 female) in 2020. All babies were less than 15 days old (mean 3.6 days). Bilious vomiting was the indication for the study in 19 babies (19/26, 73%). The upper GI contrast study of one baby was positive for malrotation and volvulus (1/26, 4%, performed in 2019).

Conclusion

Referral rates for upper GI contrast studies in neonates for investigation of malrotation were reduced during the first wave of the COVID-19 pandemic in Ireland compared to the same time period in the preceding year, despite a stable birth rate. This may reflect a higher threshold for referral by neonatologists.

References

1. The impact of the COVID-19 pandemic on maternity services: A review of maternal and neonatal outcomes before, during and after the pandemic. S McDonnell et al, Eur J Obstet Gynaecol Reprod Biol, Oct 2020.

Poster: SCI-124

WITHDRAWN

Poster: SCI-125

DETERMINING ACUTE APPENDICITIS IN PEDIATRIC PATIENTS: COMPARING RISK PREDICTABILITY AMONG CLINICAL ASSESSMENT SCORES AND DIAGNOSTIC IMAGING

DONALD Lee

Staten Island University Hospital, Staten Island, USA

Purpose

Acute appendicitis (AA) is a common etiology of abdominal pain, with a highest occurrence in the second decade of life. Complications include perforated appendix, which can lead to abscess formation or peritonitis; hence early intervention with surgical appendectomy is crucial. Several clinical prediction scores have been developed to aid in assessing pediatric appendicitis. One study comparing four prediction scores found that the appendicitis inflammatory response score and pediatric appendicitis risk calculator showed higher specificity and positive predictive value compared to the pediatric appendicitis score (PAS) and Alvarado score. However, most clinical prediction scores do not take into account radiologic testing. One study showed that combining ultrasound (US) with the pediatric appendicitis score can increase specificity for distinguishing complicated vs uncomplicated appendicitis. Another study compared the diagnostic performance of PAS, US, and low dose CT and found that CT remains the most accurate diagnostic tool for AA, but that PAS and US can be used in conjunction to decrease the use of CT in some cases. This single institutional study will seek to provide a more comprehensive review by comparing the diagnostic performance of multiple clinical risk assessment scores and multiple imaging modalities to each other in order to determine which method provides the strongest risk indicator of acute appendicitis in pediatric patients.

Materials/Methods

Retrospective chart review of pediatric patients with surgically and histopathologically diagnosed acute appendicitis. Clinical data including physical exam, laboratory results, and radiology reports will be obtained. We plan to study and compare the pediatric appendicitis score, the appendicitis inflammatory response score, the pediatric appendicitis laboratory score, CT of the abdomen/pelvis, and ultrasounds evaluating the appendix.

Results

This study is still in the process of data collection.

Significance/Conclusion

This single institutional review will compare multiple clinical risk assessment scores and imaging modalities to determine which method provides the strongest risk indicator of acute appendicitis in pediatric patients.

Poster: SCI-126

MAGNET INGESTION IN THE PAEDIATRIC POPULATION – OUR EXPERIENCE IN ALDER HEY CHILDREN’S HOSPITAL AHMED Khoujali², ALMUZAMEL Khair¹, CAREN Landes¹

¹Radiology Department, Alder Hey Children’s NHS Foundation Trust, Liverpool, UNITED KINGDOM

²Kettering General Hospital NHS Foundation Trust, Liverpool, UNITED KINGDOM

Background:

Foreign body ingestion in children is a common presentation in the emergency department. Magnet ingestion has risen rapidly in the last 20 years

with the earliest reports of complications in the UK dating back to 2002. The alarming increase in magnet ingestion in children may be explained by the marketing of small, rare earth neodymium magnets sold together in the shape of colourful cube of magnets which have been advertised as a desk toy or stress reliever for adults. Due to the appealing appearance of these magnets, they are often seen to appear like sweets to younger children and are accidentally ingested. In teenagers, accidental ingestion occurs following attempts at displaying fake piercings or fake dental braces, but teenagers are also ingesting these magnets as a form of deliberate self-harm. Although the ingestion of a single magnet carries some risk, ingestion of multiple bears a more harmful one. This is due to the force of attraction of two or more magnets across adjacent bowel walls. This leads to significant pressure necrosis and eventually perforation, fistula formation or bowel obstruction.

Objectives:

- 1.To identify the number of patients that underwent imaging following magnet ingestion
- 2.To calculate the number of radiographs performed secondary to this
- 3.To identify the number of patients that required surgical intervention
- 4.To identify any patterns associated with magnetic ingestion

Methodology:

Retrospective study, data collected from 08/01/2019 to 20/01/2021

Patients were identified by searching for the key word “magnet” in the clinical history within all imaging requests on CRIS. Studies that were not related to magnet ingestion were excluded – for example orthopaedic studies.

Results:

57 patients were identified, 32 girls and 25 boys. Within the early to mid-teenage years, it is more common in females. The majority of the patients had between 2–4 x-rays following admission with suspected magnet ingestion. 5 patient required lifesaving surgical intervention within 2–4 days after admission.

Conclusion:

Magnet ingestion in the paediatric population may be considered as a serious epidemic. Throughout the recent years there has been a significant increase in the number of admissions secondary to accidental magnet ingestion. Our study aims to highlight the life-threatening complications associated with this, as well as the exposure to radiation that too carries a lifelong risk of stochastic effects.

Poster: SCI-127

RECTOURETHRAL FISTULA IN ANORECTAL MALFORMATIONS: AN AUSTRALIAN PERSPECTIVE ON PREVALENCE AND DETECTION ON MEDICAL IMAGING

TIMOTHY JAMES Jeffery, RICHARD Warne

Perth Childrens Hospital, Perth, AUSTRALIA

Introduction:

Anorectal malformations (ARMs) are important diverse clinical entities which are commonly associated with further congenital anomalies. The presence of an underlying fistulous tract is common, with rectourethral fistulae frequently occurring in male patients. The identification of such a fistulous tract has vital surgical and prognostic implications.

Despite this, no studies have accurately established the prevalence of rectourethral fistulae in male patients with ARMs. Furthermore, the relative accuracy of different modalities in detection is relatively unexplored in the literature. As a result, no clear guidelines are in place to guide

clinicians in undertaking pre-operative imaging for ARMs prior to definitive surgical repair.

Methods:

34 male patients with surgically confirmed ARMs were reviewed between May 2013 to July 2020 at the sole tertiary paediatrics hospital in Western Australia. All performed Micturating Cystourethrograms (MCUGs), Pelvic MRIs and Distal Colostography radiology reports were reviewed for the presence of an underlying rectourethral fistula and additional abnormalities.

Results:

Of the 34 identified cases, 13 cases had surgically proven rectourethral fistulae. This equates to a prevalence of 38%

MRI was the most common investigation, with 25 studies performed and 11 positive cases. MCUGs were frequently undertaken, with 23 studies and 9 positive cases. Distal colostography was least commonly performed, with 16 studies and only 4 positive cases. One surgically proven case of a recto-urethral fistula was radiographically occult.

Conclusions:

Recto-urethral fistulae in the setting of ARMs are common in our Western Australian population with a prevalence of 38%. MCUG and MRI pelvis are effective methods in detecting recto-urethral fistulae, with few cases identified on distal colostography alone. Additional significant findings such as vesiculoureteral reflux can also be identified.

As a result, we advocate that pre-operative evaluation with both MCUG and MRI pelvis should be considered in all male patients with ARMs. However, cases can be radiographically occult, and therefore pre-operative imaging cannot definitively exclude a fistulous tract

Poster: SCI-128

DIAGNOSTIC ACCURACY OF INCREASED LIVER ECHOGENICITY AS A MARKER FOR STEATOSIS IN CHILDHOOD OBESITY

ERIC Graham, MONIQUE Riemann, SMITA Bailey
Phoenix Children's Hospital, Phoenix, USA

Purpose

Liver ultrasound is typically the initial imaging technique of choice in the pediatric patient with obesity and concern for fatty liver disease. While increased liver echogenicity is often associated with hepatic steatosis, this finding can be subjective. We undertook a review of obese patients who had both liver ultrasound and liver MRI fat fraction calculation to determine the accuracy of liver ultrasound echogenicity in diagnosing steatosis in this at-risk population.

Materials and Methods

A total of 85 obese pediatric patients (ages 6-17 years, BMI \geq 95%) underwent ultrasound and MRI of the liver between May 2017 and August 2020. IRB approval was obtained. Four patients were excluded due to missing images. 56.8% were male. 86.4% were of Hispanic descent. Seventy-seven patients underwent ultrasound elastography as part of their examination. Liver echogenicity characterization was performed by two pediatric radiologists and an experienced sonographer.

Results

- 62 obese patients (76.5%) with MRI fat fraction greater than 5%, defined as steatosis
- 23.5% of obese patients did not have steatosis
- 65 patients (80.2%) with echogenic liver on ultrasound
- Liver Fat percentage weakly correlated with increased echogenicity (Spearman coefficient $r=0.30$, $p=0.038$) and with abnormal elastography ($r=0.27$, $p<0.001$)
- Steatosis at the 5% fat fraction level was not significantly associated with increased echogenicity ($r=0.08$, $p=0.236$)

•AST and ALT levels were moderately predictive of fat percentage ($r=0.49$ and $r=0.59$, $p<0.001$)

•Predictive value of increased echogenicity for steatosis:

o5% fat fraction: sensitivity 85.4%, specificity 36.8%, PPV 81.5%, NPV 43.8%, accuracy 74.1%

o10% fat fraction: sensitivity 94.1%, specificity 29.8%, PPV 49.2%, NPV 87.5%, accuracy 56.8%

o20% fat fraction: sensitivity 100%, specificity 24.2%, PPV 23.1%, NPV 100%, accuracy 38.3%

Conclusions

Increased liver echogenicity has limited accuracy for hepatic steatosis in the obese pediatric population. 23.5% of obese patients did not have increased fat percentage by MRI. These data suggest risk of both over- and under-diagnosis of hepatic steatosis using grayscale ultrasound.

Poster: SCI-129

AUTOIMMUNE PANCREATITIS IN PEDIATRIC GROUP

BERRIN demir¹, SUKRIYE Yilmaz¹, BIRSEL Sen Akova¹, CEYDA TUNA Kirsaclioglu², ZARIFE Kuloglu², SUAT Fitoz¹

¹ Ankara University Department of Pediatric Radiology, Ankara, TURKEY

² Ankara University Department of Pediatric Gastroenterology, Ankara, TURKEY

Autoimmune pancreatitis (AIP) is a rare disease and there has been increasing recognition in pediatric age group. We aimed to present characteristic and uncommon imaging findings of AIP in pediatric patients.

CASE 1

A 14-year-old boy presented with epigastric pain and nausea for 4 weeks. Serum levels of amylase, lipase and C reactive protein (CRP) were increased. The level of IgG4 antibodies was within normal range. Contrast-enhanced computed tomography (CT) demonstrated pancreatic enlargement and increased enhancement of the head. Main pancreatic duct was narrowed in the head and dilated in its distal course. MR imaging showed a diffusion restriction in the head. Endoscopic retrograde cholangiopancreatography (ERCP) was planned to rule out malignancy and showed focal pancreatitis findings. 3-month follow-up imaging revealed significant resolution of the findings.

CASE 2

A 9-year-old previously healthy girl presented with nausea, abdominal pain and anorexia for 2 weeks. Liver function tests were increased. The level of IgG4 antibodies was in normal range but IgG1 antibodies level was high. Ultrasonography showed diffuse edematous thickening of the pancreas. Dynamic MR imaging revealed diffusely heterogeneous, enlarged pancreas with loss of the cobblestone architecture of the pancreatic surface. The findings were consistent with autoimmune pancreatitis.

CASE 3

A 13-year-old boy with autoimmune sclerosing cholangitis presented with abdominal pain. MR imaging of abdomen showed thickening of the pancreatic tail and T1 hypo-, T2 hyperintense signal changes. The serum level of IgG4 antibodies was found in upper limit of normal range, IgG1 and IgG3 antibodies levels were increased. Based on imaging and laboratory findings IgG4 associated pancreatitis was considered. On follow-up, MR imaging findings of the pancreas were normal.

RESULT: Imaging plays important role in the diagnosis of IgG4 associated pancreatitis in children. Awareness of imaging findings are very important, because the biopsy is not recommended and not the first step procedure in children and laboratory tests can be negative.

CONCLUSIONS: The diagnoses of AIP in pediatric groups are usually made with the combination of clinic findings and imaging features. It is important in differentiating AIP from other chronic pancreatitis, because the corticosteroids are the primary choice of therapy in AIP.

Poster: SCI-130

INTER-RADIOLOGIST VARIABILITY IN REPORTING SONOGRAPHIC MEASUREMENTS OF THE PEDIATRIC LIVER: A CONUNDRUM OF HEPATOMEGALY PROPORTIONS

POURIA Koushesh¹, JOSEPH Cao², CORY Pfeifer²

¹ Texas Tech University Paul L Foster School of Medicine, El Paso, USA, El Paso, USA

² University of Texas Southwestern - Department of Radiology, Dallas, USA, Dallas, USA

Purpose

Hepatomegaly is a common early presenting symptom of liver disease and pediatric radiologists are often asked to comment on liver size in reference to a set of published standards regardless of interobserver variability, limited acoustic windows, and anatomic variants. The implications of diagnosing hepatomegaly including unnecessary consults, follow up scans, and even biopsy, which result in pediatric radiologists adjusting their practice creating confusion for referring clinicians.

Materials, Methods, and Procedures

This study examined the practice of fellowship trained pediatric radiologists in a tertiary pediatric referral hospital. Imaging studies over a 10-year period with clinically suspected hepatomegaly were reviewed. Reports were examined for presence or absence of hepatomegaly and quantitative liver length measurements. Additional descriptors were tracked including steatosis and suspected Riedel lobe.

Results

187 ultrasound reports issued by 15 radiologists were reviewed. There was high degree of inconsistency when reporting liver lengths between radiologists with individual reporting rates of 0% to 50%. The concordance rate of hepatomegaly on ultrasound with clinical exam was 50%. Within the positive studies of hepatomegaly, only 22% of studies reported quantitative liver size measurements. Only 7% of studies reported a possible Riedel lobe.

Conclusion

The use of craniocaudal liver measurements in assessing hepatomegaly was not uniform between radiologists. When used, available reference standards have significant limitations given the patient populations from which they are derived. An additional limitation of the reference population was the body mass index, which is strongly correlated to organ size. Despite these limitations, referring clinicians routinely request measurements of liver size on ultrasound. The high level of discordance between clinical and imaging findings along with limitations of existing reference standards raises questions regarding the efficacy and utility of reporting hepatomegaly considering potential complications and costs of further testing, imaging, and even biopsy. Alternative approaches for this work up are varied and require additional lines of research.

Poster: SCI-131

PRIMARY ADRENAL SCHWANNOMA

ZUHAL Bayramoglu, ELIF HAZAL Karli

Istanbul University, Istanbul Medical Faculty, Radiology Department, Istanbul, TURKEY

Schwannoma is a benign tumor composed of neoplastic neural crest cells. Primary adrenal schwannoma is extremely uncommon usually detected incidentally. We report a case of a right adrenal schwannoma discovered in a 13-year-old boy during an examination of right flank pain. The patient was found to have a hypoechoic right adrenal mass of 7.2 cm on abdominal ultrasonography. A dynamic contrast-enhanced MRI of the abdomen revealed low signal intensity on T1 images and heterogeneous signal intensity with cystic components on T2 images. It demonstrated heterogeneous but gradually increased enhancement. The metabolic evaluation was unremarkable. No retroperitoneal lymphadenopathy was present. A standard transperitoneal laparoscopic adrenalectomy was performed. Pathologic evaluation showed the tumor composed of schwannian cells and demonstrated positive S-100 and vimentin staining, which corresponded to a benign nerve sheath tumor. Visceral schwannomas are rare and usually discovered incidentally. Retroperitoneal schwannomas comprise only 1-3 % of all schwannomas. These tumors do not produce steroids or catecholamines. Most of the patients are asymptomatic that can cause delayed diagnosis, a significant size of the tumor is usually seen.

On both CT and MRI, the imaging characteristics are non-specific. Schwannomas of the retroperitoneum are well-circumscribed round masses that may show septa and cystic change. (5) Mild heterogeneous enhancement on arterial phase and gradual enhancement during portal venous phase is considered as the enhancement characteristics. (6) On MRI, low signal intensity on T1 weighted images and heterogeneous high signal intensity on T2 weighted images is usually encountered.

The differential diagnosis of adrenal schwannomas includes adenoma, neuroblastoma, ganglioneuroma, ganglioneuroblastoma, adrenocortical carcinoma, metastasis, pheochromocytoma, and adrenal myelolipoma. MRI can be helpful in the differential because adrenal adenoma and adrenal myelolipoma have fat content. (7)

Surgical excision is generally considered for a non-functional adrenal mass larger than 4 cm.

Preoperative diagnosis of adrenal schwannomas remains challenging due to non-specific imaging and clinical findings. MRI sometimes can provide further benefit during differential diagnosis. A definitive diagnosis can only be made by histological and immunohistochemical evaluations.

Poster: SCI-132

UNUSUAL IMAGING PRESENTATION OF WOLMAN DISEASE

GHUFRAN Alhashmi^{1,2}, TAGHREED Shuaib^{3,4}, SHATHA Albokhari^{3,5}, RAYAN Ahyad^{1,2}

¹ King Abdulaziz University, College of Medicine, Department of Radiology, Jeddah, SAUDI ARABIA

² King Abdulaziz University Hospital, Department of Radiology, Jeddah, SAUDI ARABIA

³ King Abdulaziz University, College of Medicine, Department of Pediatrics, Jeddah, SAUDI ARABIA

⁴ King Abdulaziz University Hospital, Department of Medical Genetics, Jeddah, SAUDI ARABIA

⁵ King Abdulaziz University Hospital, Division of General Pediatrics, Department of Pediatrics, Jeddah, SAUDI ARABIA

Introduction:

Wolman disease is an autosomal recessive disorder of fat metabolism due to deficiency of lysosomal acid lipase, resulting in intracellular accumulation of cholesteryl esters and triglycerides. It is well known to radiologists by the enlarged calcified adrenals. We report a case of previously undiagnosed Wolman disease that presented with an unusual appearance of the mesentery in the absence of radiographically visible adrenal calcifications.

Case presentation:

A 34-day-old African boy, product of consanguineous marriage, admitted with recurrent vomiting and progressive abdominal distension and investigated for bowel obstruction. An abdomen radiograph showed gaseous distention of the bowel. The upper and lower GI studies were normal, apart from an unusual small bowel loops distribution, located mostly in the left upper quadrant. Ultrasound revealed: 1- diffusely hyperechoic lobulated mesentery with few scattered tiny hyperechoic foci & mild internal vascularity, without mesenteric vessels narrowing, 2- right adrenal cystic lesion with debris and no vascularity, 3- enlarged hypoechoic left adrenal gland with a small hyperechoic shadowing focus and 4- hepatosplenomegaly. On CT, the mesentery was mildly displacing the bowel and contained few small ill-defined soft tissue density regions. No mesenteric or adrenal calcifications. On MRI, there were multiple well-defined small round/oval fat-containing lesions throughout the mesentery surrounded by mild mesenteric edema. The right adrenal cystic lesion decreased in size and was non-enhancing, most likely a hematoma. The differential diagnosis of the mesenteric abnormality was between fat-containing tumor or malformation and fat metabolism disorder. The metabolic diseases team was then consulted; Wolman disease was highly suspected and later confirmed by low lysosomal acid lipase activity. The patient received supportive care and dietary modifications; however, enzyme replacement therapy could not be initiated due to eligibility issues. The patient developed hemophagocytic lymphohistiocytosis & sepsis. He progressively deteriorated & later passed away from multiorgan failure.

Conclusion:

In the absence of radiographically visible adrenal calcifications, mesenteric lymph node fat deposition, adrenal enlargement, and hepatosplenomegaly can be the presenting imaging findings of Wolman disease. Radiologists' awareness of this presentation can help guide appropriate subspecialty referral & early intervention.

Poster: SCI-133

IMAGING APPROACH TO SUSPECTED FOREIGN BODY INGESTION IN CHILDREN

OLUSEYI Adesalu¹, SAYANI Khara¹, ERICA Makin², OMOWUNMI Akindolie³, FIRAS Sa'adedin⁴, ANDREAS Panayiotou¹, SAIRA Haque¹

¹ King's College Hospital Department of Radiology, London, UNITED KINGDOM

² King's College Hospital Department of Paediatric Surgery, London, UNITED KINGDOM

³ King's College Hospital Department of Paediatrics, London, UNITED KINGDOM

⁴ King's College Hospital Department of Emergency Medicine, London, UNITED KINGDOM

Purpose

To examine cases of paediatric foreign body ingestion at a tertiary paediatric centre, with a focus on the radiological investigations, and to identify trends in follow-up imaging and management.

Materials and Methods

Cases were collected from the imaging and surgical database over a 10-year period (2010-2020). Inclusion criteria were children under the age of 16 with a radio-opaque foreign body demonstrated on imaging. Patient demographics, imaging modality, findings and clinical management were analysed.

Results

75 patient attendances were identified with a median age 4 years (5 months-15 years). There was an almost equal occurrence in males and females, n=32:43 respectively. The commonest ingested foreign bodies were coins (45%,n=34), magnets (19%,n=14), nails/bolts (9%,n=7) and button batteries (5%,n=4).

The majority of patients had some form of follow-up imaging (55%,n=41), with a total of 81 follow-up studies being performed. The median number of studies per patient was 1, with a range of 7. The most common follow-up study was abdominal x-ray (65%,n=53), followed by chest x-ray (26%,n=21) and ultrasound scan (5%,n=4). One patient required CT abdomen due to persistent abdominal pain following ingestion of a plastic spoon. The median time interval between time of initial study and the first follow-up study was 7 hours, with a range of 171 hours.

20 (n=27%) patients required one or more surgical interventions. There were 17 oesophago-gastro-duodenoscopies (OGD) and 4 patients required laparoscopy/laparotomy to retrieve magnets or button batteries from intestines. One patient sustained 3 bowel perforations due to erosion from magnets.

Conclusions

The majority of patients who had ingested foreign bodies were managed conservatively and the foreign body passed without intervention. Initial radiographic imaging was able to define the size, structure and location of the foreign body, which aided subsequent management. It may be possible to reduce the number of follow-up studies based on the nature of the foreign body and natural history.

Poster: SCI-134

OVARIAN TORSIONS IN CHILDREN

CLARISSA Valle¹, PIETRO ANDREA Bonaffini^{1,3}, FRANCESCO Lacanna², ELVIRA Zaranko², DAVIDE Dalla Rosa², MAURIZIO Cheli², SANDRO Sironi^{1,3}

¹ Department of Diagnostic Radiology, ASST Papa Giovanni XXIII, Piazza OMS 1, 24127, Bergamo, ITALY

² Department of Pediatric Surgery, ASST Papa Giovanni XXIII, Piazza OMS 1, 24127, Bergamo, ITALY

³ Post-Graduate School of Diagnostic Radiology, University of Milano-Bicocca, Monza, ITALY

Purpose

To highlight the clinical presentation of ovarian torsions in children and to review main imaging features on ultrasound (US) and magnetic resonance imaging (MRI).

The educational objectives are to:

- learn how to suspect an ovarian torsion among main differentials
 - recognize twisted ovary presentation on US
 - explore a feasible MRI protocol and relative features in ovarian torsions
- Materials and Methods

Mia is a 4-year-old girl who presented to the Emergency Department (ER) of our Institution because of the onset of an abdominal pain with constipation, treated with an enema and discharged. After two days symptoms recurred, with vomiting. Mia presented again to the ER. Fever and diarrhea appeared afterwards, and a soft mass was palpable in the right pelvis. Mia's laboratory tests included: white blood cells (WBC) 23030/mm³; C-reactive protein (CRP) 24 mg/dL, lactate dehydrogenase (LDH) 315 U/L. An US was performed.

Results

US findings demonstrated a well-defined hyperechoic mass, measuring 56x48x55 mm in the right posterior pelvis. A few little anechoic rounded

areas were noted as displaced peripherally in the mass. No Doppler signal, both arterial and venous, was detectable within the mass. MRI examination subsequently performed under controlled anesthesia revealed a markedly enlarged left ovary dislocated in the right pelvis. Follicles were eccentrically displaced and contained some hemorrhagic declining components. The left tuba, congested, had a whirling twisted course. Ovarian vascularization was absent both at the cortical and medullary levels. The adnexal swelling thus shaped compressed and anteriorly displaced the bladder. Right ovary (located supero-posteriorly) and uterus were regular.

The subsequent urgent exploratory laparoscopy confirmed the normal appearance of the right adnexa. The left tuba turned out to be doubly twisted. The right pelvic mass was mobilized and, once derotated, highlighted the completed necrotic torsion of the left ovary. A left salpingo-oophorectomy was performed.

Conclusions

Ovarian torsion in children is an uncommon cause of acute abdominal pain that requires a prompt diagnosis and an early surgical management to prevent adnexal damages. However, the clinical presentation may be tricky, mimicking other more common differentials, such as acute appendicitis. The close synergy between pediatricians, pediatric surgeons and pediatric radiologists in the ER ensures the best approach to the abdominal urgency of these patients.

Poster: SCI-135

PELVIC PAIN IN FEMALE CHILDREN AND ADOLESCENTS: NOT JUST APPENDICITIS

GEORGIA Papaioannou, EVAGGELIA Manopoulou, LOUKIA Tzarouchi, CHRISTINA Meleti, GEORGIOS Manganas, PANAGIOTIS Tagalakis, SPYROS Yarmentitis
Department of Pediatric Radiology Mitera Children's Hospital, Athens, GREECE

OBJECTIVES: To illustrate the imaging findings, common and rare, in female children and adolescents referred to pediatric radiology department for pelvic pain.

CONTENTS: Entities presented include appendicitis and relevant complications, mesenteric lymphadenitis, bowel intussusception, ovarian pathologies (cysts, tumors, and torsion), congenital müllerian duct anomalies, inflammatory bowel lesions and other neoplastic lesions. Initial imaging approach includes ultrasound of the abdomen in the majority of the cases and cross-sectional imaging, preferably MRI of the pelvis, in complex or inconclusive cases.

TEACHING MESSAGE: In female children and adolescents with pelvic pain, differential diagnosis should not only include the common and rare intestinal abnormalities but it should also rule-out genital and bony pelvic pathologies; imaging algorithm should be adjusted accordingly.

Poster: SCI-136

THE IMAGING APPEARANCE OF RARE-EARTH NEODYMIUM MAGNETS

MICHAEL Coker, MORGAN McBee
Medical University of South Carolina, Charleston, USA

Purpose:

To investigate and characterize the imaging appearance of rare-earth neodymium magnets utilizing ultrasound, radiograph, and computed tomography imaging modalities.

Educational Objectives:

1. Describe rare-earth magnets, their history, and how they are relevant to the pediatric population.
2. Provide examples of imaging appearance of neodymium magnets on ultrasound, radiographs, and CT.
3. Emphasize the potential risks, complications, and morbidity associated with neodymium magnets.

Materials and Methods:

We first report the patient presentation and unusual appearance on ultrasound of neodymium magnets that had been transurethrally inserted into the bladder. Subsequently, we sought to perform a radiologic analysis by imaging the magnets utilizing ultrasonography, radiography, and dual-energy computed tomography (CT). We then compare our experimentally acquired imaging findings with those of the patient whom presented with visceral intra-luminal localized magnets.

Results:

The magnets demonstrate strong attractive force to conglomerate into an irregularly contoured structure. On ultrasonography, the magnets exhibited extensive comet tail artifact, mirroring, and twinkling artifact seen with color Doppler. On radiographic and CT imaging, the magnets portrayed the expected imaging appearance of hyperdense objects with beam hardening artifact.

Conclusion:

While they were not sold between 2012 and 2017 in the United State for safety concerns, they are once again available for sale. Recognizing and understanding the imaging appearance of neodymium magnets could help in the identification of the atypical appearance of these magnets as a foreign body utilizing various imaging modalities.

Poster: SCI-137

A CASE OF SERTOLI-LEYDIG CELL TUMOR WITH INTRA-ABDOMINAL RECURRENCE IN A PATIENT WITH A DICER1 GENE MUTATION

SANA Basseri, DENISE A. Castro, DON Soboleski
Queen's University, Kingston Health Sciences Centre, Department of Diagnostic Imaging, Kingston, CANADA

Learning objectives:

- 1) To describe a case of DICER1 syndrome
- 2) To illustrate imaging characteristics of cystic nephroma and Sertoli-Leydig cell tumor with heterologous elements

Case:

A 14-year-old female presented to the emergency department with right lower quadrant pain. Her past medical history was significant for a cystic nephroma with left-sided nephrectomy at 1 year of age. Initial ultrasound imaging revealed a large adnexal mass, prompting further evaluation with MRI which demonstrated an ovarian mass with inhomogenous signal intensity, regions of enhancement and restricted diffusion, and areas of low T2 signal intensity reflecting possible fibrous components. Findings were suggestive of a Sertoli-Leydig cell tumor (SLCT) with heterologous component. The possibility of a DICER1 gene mutation was considered given the history of a cystic nephroma, which was later confirmed with genetic testing.

The patient underwent a salpingo-oophorectomy and histopathology showed a poorly differentiated SLCT with heterologous elements. Chemotherapy was initially declined, however three months later imaging revealed multiple new intra-abdominal masses which demonstrated similar MR signal characteristics as the original tumor. The patient underwent surgical debulking and adjuvant chemotherapy was initiated. Pathology confirmed recurrent intraperitoneal SLCT with extensive

heterologous component. A few months later there was a second recurrence requiring extensive surgical debulking.

Discussion:

DICER1 syndrome is a familial tumor predisposition syndrome with increased risk of developing pleuropulmonary blastoma, multinodular goiter and thyroid cancer, cystic nephroma, ovarian tumors (most commonly SLCT), embryonal rhabdomyosarcoma of the cervix, and less commonly brain and other tumors. Therefore, it is important to consider DICER1 syndrome in a patient who presents with these tumor types. The DICER1 gene mutation is most often inherited in an autosomal dominant pattern, however de novo mutations can occur. Due to variable penetrance, not all individuals with a DICER1 gene mutation develop tumors. Here we describe a case of DICER1 syndrome and illustrate the imaging findings of cystic nephroma and SLCT. This case also highlights the role of the radiologist in recognizing DICER1 syndrome and the importance of similar imaging protocols on follow up studies to help with recognition of disease recurrence/metastasis.

Poster: SCI-138

ROLE OF RI OF INTRA-RENAL ARTERIES IN CONGENITAL HYDRONEPHROSIS

SHRAMANA Bagchi, VINODH D

Indira Gandhi Institute of Child Health, Bangalore, INDIA

STUDY: A cross-sectional study of fifty infants and children (<5 years) with congenital hydronephrosis were enrolled using consecutive sampling.

Congenital hydronephrosis may present with a variety of symptoms - the pediatrician may be able to feel a swelling in the region of the kidney (under the anterior angle of the ribs or in the back).

Decreased bouts of micturition and lumbar swelling that occurs later in the kidney area or UTI are also other possible symptoms of this problem. Ultrasonography to assess the degree of hydronephrosis in the infants was performed.

Doppler ultrasonography of both kidneys for assessment of the mean resistive index of the intra - renal arteries was performed for both obstructive and non-obstructive hydronephrosis, and also for the normal kidneys. RESULTS:

There were many causes for obstructive hydronephrosis , most common being the pelviurethric junction obstruction (>50%) followed by an equal picture in posterior urethral valve (27 %) and Urinary tract infections (23%) .

Vesicoureteral reflux was the main cause for non-obstructive hydronephrosis, The resistive index for non-hydronephrotic kidneys was in the range of 0.621 - 0.689 for nonobstructive hydronephrotic ones was 0.621 and obstructive ones was 0.780 The mean resistive index difference between the obstructive and non-obstructive hydronephrosis was statistically significant (P-<0.001).

CONCLUSION: The above study determined that the mean renal arterial resistive index was significantly higher in obstructive hydronephrotic kidneys than non-obstructive hydronephrotic kidneys.

This diagnostic parameter can be widely used as a valuable tool for diagnosis . On follow-up serial scans and re-assessments after intervention there has been a decrease in the mean resistive index of the intra - renal arteries of the obstructive hydronephrotic kidneys

Poster: SCI-139

OVARIAN CYSTIC LESIONS IN FEMALE PEDIATRIC POPULATION: LOCAL TERTIARY CENTER EXPERIENCE

AZZA Yosuph, AMNA Kashgari, AMIN Alzahrani

King Abdullah Specialist Children Hospital, Riyadh, SAUDI ARABIA
Background and objective: Ovarian masses are a rare entity in the pediatric population.

We present our experience with 74 patients with pelvic cystic lesions, to assess the natural history of ovarian lesions in the pediatric population. Study and Methods: This retrospective observational analysis was performed on 74 female patients under the age of 14 years with pelvic cystic lesions who were diagnosed and managed at our institute between January 2015 and October 2020. The cases were reviewed retrospectively and analyzed based on the age at presentation, presenting symptoms, clinical assessment, radiological findings, tumor marker, management, and follow-up. We excluded the female patients of 14 years and older as well as the patients with small follicular cysts. The antenatal diagnosis, lump, and abdominal/pelvic pain were the most clinical indication for further investigation.

Results: Sixteen patients underwent complete surgical excision of the pelvic cystic lesions, 9 of them through a laparoscopic approach while 7 experienced laparotomy exploration. The histopathology results include mature cystic teratoma, serous cystadenoma, seromucinous cystadenoma, immature cystic teratoma, and mucinous cystadenocarcinoma. The two later diagnoses were required chemotherapy. On the other hand, 7 (43%) simple ovarian cyst / follicular cysts were confirmed by tissue diagnosis, 1 turned to be a vaginal cyst and another was a case of tubo-ovarian abscess. The Alpha-fetoprotein (AFP) was the tumor marker tested in 13 (17.5%) patients and 5 turned to be positive.

Nevertheless, the most common radiological findings were hemorrhagic cysts with or without internal septations (78.3%), other diagnoses such as hemato/hydrocolpus, enteric duplication cyst, and lymphangioma were suspected.

Serial laboratory and imaging follow-ups were obtained in those patients. Conclusion: Giving the rarity and however the importance of the ovarian masses in the pediatric age group, early detection, and proper management through a multidisciplinary team will play a major role in decreasing the risk of complication and improving the long-term outcome.

Poster: SCI-140

THE MORE WE BECOME FAMILIAR WITH THE NUTCRACKER SYNDROME, THE MORE WE ADD SONOGRAPHIC DIAGNOSTIC CLUES

MARINA Vakaki, ANNA Chountala, ELENI Koutrouveli, RODANTHI Sfakiotaki, IRENE Vraka, DESPINA Pitsoulaki, EKATERINI Haritou, CHRISTINA Zouridaki, CHRISOULA Koumanidou
Children Hospital P and A.Kyriakou Radiology Department, Athens, GREECE

Purpose: to present the usefulness of Doppler ultrasound (US), with its technical considerations in the challenging diagnosis of Nutcracker syndrome (NCS).

Materials and Methods: During a 5-year-period 19 children and adolescents (12 girls and 7 boys; age range 6-16 y) were diagnosed with NCS in our Ultrasound Department. The US examination was performed due to micro-/macroscopic hematuria (n=8), proteinuria (n=7) or both (n=4). Both kidneys were evaluated with gray-scale US and the anteroposterior diameter and peak velocities (PV) of the left renal vein (LRV) were measured at the renal hilar and the aortomesenteric (AM) portion. The ratios of the diameter and PV between the 2 sites were calculated (cut-off value of >4.7 for both ratios, according to published studies). The AM angle was measured (cut-off of <250). The LRV PV and AM angle were also measured in the erect position.

Results: In all our patients, the NCS diagnosis was based on the above established US criteria. However, we ascertained that US examination in the erect position is crucial because in 5 cases, the LRV PV was

significantly higher and the AM angle decreased at the erect position, obviously associated with the orthostatic proteinuria of these patients. Furthermore, we noticed that the NCS findings subsided in 2 adolescents when they gained weight. We also mention that the compression by the transducer, especially during a deep breath may cause additional compression of the LRV. 5 cases of posterior NCS were revealed (due to retroaortic LRV course). In another case, there were 2 LRVs with an AM and a retroaortic course respectively.

Conclusions: The NCS diagnostic algorithm and imaging criteria are not so far well established. Many cases of unexplained hematuria and proteinuria remain undiagnosed without the appropriate US technique. LRV diameter and PV and AM angle should be evaluated in the erect position as well, at least in doubtful NCS cases.

Poster: SCI-141

CORRELATION OF ECHOGENICITY OF THE RENAL MEDULLA TO RENAL FUNCTION TESTS IN CHILDREN WITH SICKLE CELL DISEASE

PATRICK Tivnan¹, BINDU N. Setty¹, AMY Sobota², ILSE Castro-Aragon¹

¹ Department of Radiology, Boston Medical Center, Boston, USA

² Department of Pediatrics, Boston Medical Center, Boston, USA

Purpose: Evaluate whether the observation of an echogenic renal medulla (RM) in pediatric patients with sickle cell disease (SCD) had any correlation to renal function tests (RFT).

Material and Methods: In this IRB approved retrospective study, we identified pediatric patients (<22 years old) with SCD (HbSS or HgSC) who had sonographic imaging of the kidneys between 01/2010-09/2020. Of this cohort, any patients who had a random urine microalbumin (MA) and serum creatinine tests within 1 year of this ultrasound were selected for retrospective image review of the kidneys by two experienced pediatric radiologists. RFT and treatment data were also collected closest to the time of the ultrasound. eGFR was calculated using the bedside Schwartz equation. The sonographic appearance of the RM was evaluated in relation to the renal cortex and columns of Bertin, with medullary echogenicity categorized as either hypoechoic/normal, mild/moderately increased, or severely increased. Chi-squared test was performed between medullary echogenicity and increased MA levels (>30 mg ab/g cr).

Results: 32 patients (20/32 (63%) female), ranging between 7-21 (average 13.5) years old with SCD (HbSS 24/32 (75%), HgSC 8/32 (25%) matched our inclusion criteria. Average time between ultrasound and eGFR was 31 days and MA levels was 159 days. 18/32 (56%) were on oral hydroxyurea and 7/32 (22%) were undergoing chronic transfusions at the time of the ultrasound. All patients demonstrated an echogenic RM, with it being mildly or moderately increased in 29/32 (91%) and severely in 3/32 (9%). 31/32 of these patients had normal eGFR (>80 eGFR) and 6 /32 (19%) had elevated MA levels (>30 mg alb/g cr). 3/3 with severe echogenicity had normal MA levels. There was no significant correlation between degree of echogenicity and increased MA levels ($p = 0.04$).

Conclusion: Increased echogenicity of the RM is a common finding in children with SCD and the presence of this finding did not correlate with abnormal RFT.

Poster: SCI-142

COMPARISON STUDY OF REAL-TIME CONTRAST-ENHANCED VOIDING ULTRASONOGRAPHY WITH DMSA

RENAL SCAN IN CHILDREN

SAELIN Oh¹, JI YOUNG Ha²

¹ Korea University Anam Hospital, Seoul, SOUTH KOREA

² Gyeongsang National University Changwon Hospital, Changwon, SOUTH KOREA

Objective: To investigate the diagnostic performance of contrast-enhanced voiding ultrasonography (CeVUS) for detection of intrarenal reflux (IRR) compared with acute 99mTc 2, 3-dimercaptosuccinic acid (DMSA) renal scan in pediatric patients.

Materials and Methods: Thirty eight kidneys in 19 patients (15 males and 4 females, age range 0-10 years, median age 6 months) who underwent CeVUS and acute DMSA renal scan for recurrent UTI or pyelonephritis were included. Results of CeVUS including the grade of vesicoureteral reflux (VUR), the presence of intrarenal reflux (IRR), and the location of IRR were analyzed by experienced pediatric radiologist comparing with acute DMSA renal scan.

Result: There were seven patients (7 males, age range 4-15 months) with total 9 cases of VUR (5 left and 4 right). All cases with VUR showed high grade VUR (3 grade III and 6 grade IV). Among the cases, 7 cases demonstrated IRR and 8 cases showed photon defects on acute DMSA renal scan, and the location of IRR in each kidney was various (3 upper pole, 4 multifocal). Among 38 cases, 37 cases showed concordant results about VUR grade and a single case showed discordant (false negative) result. The sensitivity, specificity, positive predictive value, negative predictive value, and accuracy of CeVUS were 87.5, 100, 100, 96.8 and 97.4%, respectively.

Conclusion: CeVUS and acute DMSA renal scans showed a high correspondence in detecting IRR, implying CeVUS might replace acute DMSA renal scan. Therefore, utilizing CeVUS can avoid radiation exposure and determine the management plan, as well.

Poster: SCI-143

NOVEL USE OF CONTRAST-ENHANCED MAGNETIC RESONANCE MICTURATING CYSTOURETHROGRAM IN DEPICTING ANO-URETHRAL FISTULA IN A PEDIATRIC PATIENT

CAROL Ng, YU HIN Lam, CHRIS KWOK CHUN Wong, YEE LING ELAINE Kan, MEI YU Poon

Hong Kong Children's Hospital - Department of Radiology, Hong Kong, HONG KONG

Purpose:

To illustrate the novel application of TWIST sequence in dynamic imaging of the urinary tract

Background:

Fluoroscopy has traditionally been the gold-standard in showing bladder-urethral abnormalities. It has the inherent disadvantages of radiation exposure, contrast use, catheterization and overlapping structures.

MRI has advantages of no radiation, superior soft tissue resolution and multiplanar imaging. With the advent of time-resolved MR fluoroscopy and MRA sequences, there is increasing use of dynamic imaging of the urinary tract using these techniques in adults. However there is limited report of use of these techniques in imaging the bladder-urethral structures in the pediatric population even though there is increasing use of MR voiding cystourethrography to diagnose vesicoureteral reflux in the upper tract. We describe a case where we successfully use the TWIST sequence to demonstrate an ano-urethral fistula.

Introduction

A 15-year-old boy has had recurrent epididymo-orchitis. Prior ultrasound of the urinary tract was unrevealing. MCUG showed irregularity at the prostatic urethra and cystoscopy found an anourethral fistula. The fistula

was depicted best with MRI during micturition when the bladder was filled with gadolinium contrast using the TWIST sequence.

Materials and Methods:

The MR micturating cystourethrogram was done with patient's cooperation. Gadolinium-based contrast was administered IV at a dose of 0.1mmol/kg. 40 phase-dynamic TWIST scan of the pelvis was done with a body coil, the boy was asked to urinate into a plastic urinal after the first dynamic phase with whole k-space matrix filling. Scanning parameters: 1.5T MRI Scanner (MAGNETOM Aera, Siemens Healthcare), 3D GRE sagittal plane, FOV 220mm, Resolution 1.14 x 1.14 x 1.33mm, TR 2.61ms, TE 0.92ms, Flip angle 27, bandwidth 610. Acquisition time 3min56 seconds. Temporal resolution 2.33sec. TWIST view sharing central region A 15%, peripheral sampling density B 20%.

Results:

The TWIST sequence showed a linear tract arising from the midline of the posterior prostatic urethra, with an opening at 12 o'clock of the anus. It was easier to perceive on this dynamic contrast sequence compared with the static MRI sequences and MCUG.

Conclusions:

TWIST is traditionally used as a MR angiography sequence. This case illustrates a novel application in dynamic micturition imaging. It is superior to MCUG in depicting the ano-urethral fistula.

Poster: SCI-144

INTEROBSERVER AGREEMENT IN DIAGNOSTIC IMAGING IN EVALUATION OF CONGENITAL FEMALE GENITAL TRACT ANOMALIES USING ESHRE/ESGE CLASSIFICATION

FAIZAH MOHD ZAKI MOHD ZAKI¹, WOUI KEE Chiam¹, NUR AZURAH Abdul Ghani², SURAYA Abd Aziz¹, ERICA Wong Yee Hing¹, MARJMIN Osman³, DAYANG ANITA Aziz³

¹ Department of Radiology, UKM Medical Center, Kuala Lumpur, MALAYSIA

² Department of Obstetric & Gynaecology, UKM Medical Center, Kuala Lumpur, MALAYSIA

³ Pediatric Surgery Unit, Department of Surgery, UKM Medical Center, Kuala Lumpur, MALAYSIA

Objectives: To assess the interobserver agreement in imaging findings of congenital female genital tract anomalies based on ESHRE/ESGE classification.

Material and Methods: This was a retrospective study which all patient who has been diagnosed with congenital female genital tract anomalies which had MRI done to evaluate female organs with surgical procedure performed in a university hospital involving a period of 10 years (from 1st January 2009 until 31st December 2019). A total of 28 patients were included. All radiology images were interpreted based on ESHRE/ESGE classification by a radiologist (>5 years experiences) and a radiology resident who were blinded from operative finding and diagnosis. The operative findings were documented based on local institutional template. The MRI findings between radiologist and resident were compared using kappa statistic. The discrepancy between interobserver report and operative findings were also analysed and described.

Results: There was good kappa agreement between MRI findings on uterine anomalies by radiologist and radiology resident. (kappa= 0.73) (95% CI, 0.55–0.91). However, there was only fair agreement on cervix (kappa= 0.59) (95% CI, 0.36–0.82) and vaginal anomalies (kappa= 0.55) (95% CI, 0.33–0.75). Disagreement in all categories was seen in 4 out of 28 patients. There was fair agreement between the radiological diagnosis and final operative diagnosis in all three categories: Uterine anomalies (kappa= 0.49) (95% CI, 0.30–0.69), cervix anomalies (kappa= 0.55) (95% CI, 0.30–0.80), and vagina anomalies (kappa= 0.45) (95% CI, 0.20–0.69). There were 9 out of 26 patients (35%) show discrepancy in at least 2 categories.

Conclusion: Reporting the congenital female genital tract anomalies using ESHRE/ESGE classification is reproducible with good

interobserver agreement of different level of training. The cause of disagreement especially between radiological diagnosis and intra-operative findings is mainly due to lack of standard integrated classification between gynaecologist, surgeon and radiologist. Thus, proper MRI acquisition and standard imaging reporting template such as using ESHRE/ESGE classification are strongly recommended to allow good agreement between gynaecologist, surgeon and radiologist.

Poster: SCI-145

IMAGING FINDINGS IN 46 XY DISORDERS OF SEXUAL DEVELOPMENT

EVELYN Lankester^{1,2}, HEATHER Bray^{1,2}, LYDIA Bajno^{1,2}

¹ University OF British Columbia (UBC), Department of Radiology, Vancouver, CANADA

² British Columbia Children's Hospital (BCCH), Department of Radiology, Vancouver, CANADA

The disorders of sexual development (DSD) are complex and heterogeneous disorders characterized by a discordance between the chromosomal, gonadal and phenotypic sex of an individual.

Imaging studies play a pivotal role in the diagnosis and management of these conditions. Ultrasound is the first and often most valuable imaging modality in the investigation of a patient with DSD.

This educational exhibit focuses on the spectrum of imaging findings in the subgroup of children and adolescents with DSD and 46XY karyotype. The 46 XY disorders of sexual development (46 XY DSD) are characterized by a range of under-virilised male to female-appearing external genitalia, and internal genital organs that range from complete absence of müllerian structures to apparent well-developed müllerian structures.

This exhibit discusses the chromosomal and hormonal pathways leading to normal sexual development in 46XY individuals and categorizes etiologies of 46XY DSD by stage at which normal development is interrupted: 1) testicular differentiation, 2) defect in testosterone biosynthesis or impaired action, 3) failure of action of anti-müllerian chromone. The relevant clinical findings are discussed. The spectrum of imaging findings in children and adolescents with 46XY on ultrasound, genitography and MRI are illustrated, with discussion of those imaging findings typical of various types of 46XY DSD, allowing accurate diagnosis when possible.

Currently, the underlying genetic anomaly is found in only about 50% of individuals with 46XY DSD. Management decisions in individuals found to have 46XY DSD, including gender of rearing in neonates presenting with ambiguous genitalia, are complex and require a multi-disciplinary team of specialists working with affected families. Accurate depiction of internal gonadal and müllerian structures by imaging studies is crucial to these difficult management decisions.

The goals of this educational exhibit poster are to:

1. Review embryology and physiology of normal sexual development and of the disorders associated with 46XY DSD.
2. Illustrate common imaging findings in children with 46XY DSD, and discuss key imaging features in each 46XY DSD etiologic category.
3. Create a better understanding of the imaging findings in 46XY DSD, leading to improved and optimized diagnosis and management of these complex entities.

Poster: SCI-146

VIABILITY OF CONTRAST ENHANCED VOIDING UROSONOGRAPHY AS AN ALTERNATIVE TO FLUOROSCOPY FOR URODYNAMICS

NICOLE Kapral, REZA Daugherty

University of Virginia, Charlottesville, USA

Purpose: The purpose of our manuscript is to determine the feasibility of performing contrast enhanced voiding urosonography (CeVUS) during urodynamic studies in place of fluoroscopy, in order to better serve our patients and uphold ALARA principles.

Materials and Methods: The study was approved by the University of Virginia institutional review board (IRB) for enrollment of 25 subjects under the age of 18 years. All patients had a history of prior urodynamic study with fluoroscopy (standard urodynamics). Grayscale sonographic imaging of the kidneys and bladder was obtained initially for documenting renal anatomy and urinary tract dilation. After retrograde administration of 1% ultrasound contrast (Lumason) into the bladder via pump, continuous imaging of the kidneys and bladder was performed.

Results: The microbubble ultrasound contrast agent was compatible with the urodynamic equipment. Destruction of the bubbles by a mechanical pump was a potential complication not encountered during our study. Clinic scheduling and time logistics of the ultrasound urodynamics was comparable to the standard examination. All 25 patients underwent CeVUS during their routine urodynamic study and diagnostic quality images were obtained with satisfactory urodynamic EMG and pressure measurements.

Conclusion: Destruction of the bubbles by a mechanical pump was a potential limitation in using contrast ultrasound to replace fluoroscopy. This complication was not encountered during our study. CeVUS has been successfully implemented during urodynamic studies without logistical, technical, or patient complications. Ultrasound is radiation free, an important factor in the pediatric imaging, especially for patients undergoing multiple exams each year. CeVUS has the extra advantage of real-time imaging, which may be more sensitive to subtle or intermittent reflux. Our study has demonstrated that CeVUS is a reasonable alternative to standard fluoroscopy during urodynamic imaging, and pending further controlled comparisons between the modalities, offers a potential replacement imaging modality free of radiation.

Poster: SCI-147

DYNAMIC CONTRAST ENHANCED ULTRASOUND (DYN-CEUS) FOR ANALYZING OVARIAN MASSES IN CHILDREN AND ADOLESCENTS

KATJA GLUTIG Glutig, PAUL CHRISTIAN Krüger, MATTHIAS Waginger, HANS-JOACHIM Mentzel
Section of Pediatric Radiology, Institute of Diagnostic and Interventional Radiology, Jena University Hospital, Jena, GERMANY

Problem

Ovarian masses are not easy to differentiate in transabdominal ultrasound in children. In case of adnexal torsion, it is difficult to distinguish additional neoplasia from congestion-induced enlargement. MRI may be performed presurgical for an extended assessment. Dynamic contrast enhanced ultrasound (dyn-CEUS) appears to be a useful alternative despite off-label use. We present three cases in which the dyn-CEUS was used to further characterize an ovarian mass.

Introduction

Neoplasms of the ovaries in children and adolescents are rare diseases. Non-specific abdominal pain is the most common clinical symptom in these cases. An ovarian cyst that has bled, endometriosis, torsion of the adnexa or a conglomerate tumor following perforated appendicitis can be the reason. Mature teratomas are the most common benign neoplasms and germ cell tumors are the most common malignancy. A malignant mass has to be suspected in cystic lesions larger than 8 to 10 cm which contain solid parts.

Transabdominal ultrasound (US) is the imaging method of first choice for assessing. Dyn-CEUS may be a well-tolerated diagnostic method in pediatric patients. It can be performed quickly and easily. But up to now

there is very limited information for the usage of dyn-CEUS in children with ovarian masses.

Cases

We examined a 16 year old girl with a mature teratoma, a 10 year old girl with an immature teratoma and a seven year old girl with adnextorsion and ovarian cysts. See attached figures.

Conclusion

Quantitative analysis of dyn-CEUS with relative peak enhancement (PE), relative rise time (RT), relative time to peak (TTP) and relative wash in area under the curve (WiAUC) showed significant differences in the three cases. Dynamic CEUS can increase diagnostic accuracy and analyze the clinical characteristics of ovarian masses in children and adolescents very well.

Poster: SCI-148

UTERINE ADENOMYOSIS IN AN ADOLESCENT GIRL

ZUHAL Bayramoglu, EZGI Kara, RANA GUNOZ Comert, HAZAL ELIF Karli
Istanbul University, Istanbul Medical Faculty, Radiology Department, Istanbul, TURKEY

17 years old female patient was presented with prolonged uterine bleeding. She has no medical history of a predisposition to bleeding. Laboratory examinations revealed normal levels of platelet count and prothrombin time. The adolescent gynecology examination was unremarkable. Pelvic ultrasound examination demonstrated uterine mural expansion with increased local patchy echogenicity. A pelvic MRI was requested. Sagittal planT2 weighted image shows local T2 hypointensity in the fundus and corpus anterior Wall isointense with the endometrium. Relatively lower contrast enhancement compared to the myometrium was depicted on postcontrast MRI sequences. No other adnexal or pelvic pathology was found and the final diagnosis was uterine adenomyosis in an adolescent girl. There has been no previous surgical intervention or known ovarian cyst.

Adenomyosis may affect large portions of the uterus typically the posterior wall. The sensitivity and specificity of transabdominal ultrasound are variable, 32-63% and 95-97%, respectively. Classically, adenomyosis commonly affects multiparous women of reproductive age. Adenomyosis is seen with higher frequency in women with a history of uterine surgical procedures. Adenomyosis is relatively rare in postmenopausal women and children. We demonstrated MR imaging features of uterine adenomyosis in an adolescent girl.

Poster: SCI-149

LENGTH OF BOWEL REST DOES NOT PREDICT RISK FOR GASTROJEJUNOSTOMY RELATED INTUSSUSCEPTION RECURRENCE

FIKADU WOREDE Worede, MOHAMED Elsingerly, ANNE MARIE Cahill, MICHAEL Acord
Children's Hospital of Philadelphia, Philadelphia, USA

Purpose: Gastrojejunostomy (GJ) tube related intussusception entails tube removal and bowel rest. In patients dependent on jejunal access, hospital admission and initiation of parenteral nutrition may also be required. The aim of this study was to identify the length of bowel rest associated with decreased risk of GJ-tube related intussusception recurrence.

Material and Methods: A 10-year retrospective study identified 61 GJ-related intussusceptions in 57 patients treated with variable discretionary bowel rest prior to tube replacement. Comparison was made between two cohorts, intussusception recurrence, defined as reoccurring within 30 days,

and non-recurrence. Days of bowel rest and change in tube type and/or length at replacement were assessed for risk of recurrence. Patients were excluded if a GJ tube was not replaced or replaced >2 weeks later (n=20).

Results: 41 episodes of intussusception were included, with a median age of 3.1 (IQR, 1.7–5.1) years and weight of 12 (IQR, 9.7–15.1) kg. Of those diagnosed as an outpatient, 23/25 (92%) prompted hospital admission, 2/25 (8%) were managed as outpatients. 13/41 (31.7%) required central access for parenteral nutrition. Resolution was confirmed by ultrasound in 32/41 (78.0%), performed after a median of 2 days, and by fluoroscopy in 9/41 (22%) at the time of replacement. There were 10 recurrences (24.4%) with no difference in days of bowel rest compared to those that did not recur (5 vs 5.5 days, p=0.66). No difference in recurrence with less than 3 days of bowel rest compared to greater than 3 days (3/14 (21.4%) vs 7/27 (25.9%), p=1.00). Altering the tube was not associated with odds of recurrence (OR=0.82, 95% CI=0.2–3.4, p=0.79).

Conclusion: In this single center study, duration of bowel rest after GJ-tube related intussusception was not associated with recurrence risk, suggesting that less than 72 hours may be sufficient prior to tube replacement. This finding has the potential to decrease the length of hospital stay.

Poster: SCI-150

PRESURGICAL ENDOVASCULAR EMBOLIZATION OF GIANT PEDIATRIC MENINGIOMA: CASE REPORT

ANDREA PAOLA González Rodríguez¹, MARCO ANTONIO Díaz Montoya², GEORGINA Gómez Gallardo³, GIL Badallo Rivas³, CARLOS HUMBERTO González Rodríguez⁴

¹ Centro Médico Nacional de Occidente. Department of Diagnostic Radiology, Guadalajara, MEXICO

² Centro Médico Nacional de Occidente. Department of Neurosurgery, Guadalajara, MEXICO

³ Centro Médico Nacional de Occidente. Department of Pediatric Radiology, Guadalajara, MEXICO

⁴ Centro Médico Nacional de Occidente. Department of Neurology, Guadalajara, MEXICO

EDUCATIONAL OBJETIVES:

- Present a case of a pediatric patient who presented with giant meningioma.
- Analyze technical aspects, benefits and complications of endovascular preoperative embolization of meningiomas
- Review the characteristics that make meningioma most likely to benefit from embolization.

ABSTRACT

Meningiomas occur most commonly in the fifth decade of life, accounting for approximately 15–20% of primary intracranial tumors. Intracranial meningiomas in children and adolescents are rare tumors. In most large series, the incidence of meningiomas before the age of 16 years ranges from 0.4 to 4.6% of all primary brain tumors in this age group. Meningiomas in children have been considered by some to be more aggressive than their adult counterparts. The large and giant skull base meningiomas are challenging lesions. We present a case of a child, male 14 years old presented with a month history of headache and recent bilateral papilledema and diplopia. CT brain revealed a large (96 mm) right sphenoid wing well defined extra axial, Dural-based mass lesion and adjacent skull erosion. The patient underwent craniotomy, but a massive hemorrhage made the resection impossible. The posterior angio CT of the brain revealed a hypervascular tumor and showed intense contrast enhancement, The angiography revealed a dominant ECA endovascular supply, and an embolization with onyx 19 was decided, subsequent surgery was performed three days later. The mass was totally removed. Microscopic examination of the specimen revealed a meningotheelial meningioma. The follow-up of the patient at eleven months did not show neurological sequelae.

Poster: SCI-151

LARGE PORTAL VENOUS PSEUDOANEURYSM IN A PEDIATRIC LIVER TRANSPLANT PATIENT WITH SUCCESSFUL CLOSURE USING A BALLOON EXPANDABLE COVERED STENT

MAX American¹, JONATHAN Jo², JESSE Courtier², MATTHEW Zapala², K. PALLAV Kolli², RACHELLE Durand^{1,2}

¹ UCSF Benioff Children's Hospital Oakland - Department of Radiology, Oakland, USA

² UCSF Benioff Children's Hospital San Francisco - Department of Radiology, San Francisco, USA

Introduction

Portal venous pseudoaneurysms are rare, accounting for less than 1% in the population, and have presented as a spontaneous or incidental finding, secondary to iatrogenic intervention, and in liver transplant settings. Even fewer has been reported in the pediatric population. Although pediatric liver transplants are at risk for portal venous stenosis, the development of a portal venous pseudoaneurysm is rare and has not been specifically reported. We present a case of a 3-year-old boy found to have a portal venous pseudoaneurysm successfully treated with a balloon expandable stent.

Case Presentation

A 3-year-old boy with biliary atresia and congenital ASD underwent liver transplant at 6 months of age, complicated by hepatic artery thrombosis requiring urgent re-transplantation at age 7 months. After a complicated course of perihepatic abscess and hemoperitoneum, high grade portal vein stenosis was found and successfully treated with balloon venoplasty at age 10 months. On routine surveillance, he was found to have elevated liver enzymes, with ultrasound and MR abdomen evaluation demonstrating recurrent portal vein stenosis and a large extrahepatic portal venous pseudoaneurysm, approximately 3 cm size. The patient was referred to Interventional Radiology for angiography and possible intervention. Direct transhepatic and transsplenic portal access was performed for complete portography, demonstrating severe stenosis at the main portal vein with a large downstream extrahepatic portal venous pseudoaneurysm. Following venoplasty, portomesenteric stenting was performed using an 8mm balloon expandable covered stent to exclude the pseudoaneurysm.

Educational Objectives

- Recognize portal venous pseudoaneurysms as a rare entity
- Understand the complications of pediatric liver transplant patients
- Treatment considerations of portal venous interventions in pediatric patients

Conclusion

Portal venous pseudoaneurysms are extremely rare and can occur in pediatric liver transplant recipients who face a variety of complex complications. Newer balloon expandable stents with the capability for over-dilation can be a useful tool in treating pediatric patients.

Poster: SCI-152

IMAGING AND MANAGEMENT OF PAEDIATRIC ARTERIOVENOUS MALFORMATION – AN INTERVENTIONAL RADIOLOGICAL PERSPECTIVE

RAJAN Aggarwal, MUTHUSUBRAMANIAN Rajasekaran, SALIL Pandey, SURESH A

Vydehi institute of Medical Sciences and Research Centre, Department of Radio Diagnosis, Bangalore, INDIA

BACKGROUND:

-Arteriovenous malformations show a wide variety of clinical and radiologic manifestations. AVMs are fast-flow vascular malformations, consisting of anomalous capillary beds between the arterial and venous system, thus causing shunting of blood. Fast-flow vascular malformations usually become evident during childhood and puberty.

-Being in the facial region these malformations may have cosmetic issues also along with pain and discomfort.

-AVMs present a therapeutic challenge because of their haemodynamic characteristics and their modality of growth. Surgical resection is often associated with extensive blood loss and an incomplete resection frequently leads to re-growth of the tumour to sizes that are often larger than its original size.

-Recent developments in the design of microcatheters and distal navigation techniques have facilitated the catheterization of feeding arteries close to the nidus. Interventional radiology may deliver primary treatment such as staged sclerotherapy and embolization for malformations that are poor candidates for primary surgical resection with lesser complications and better cosmetic outcome.

Clinical Scenario & Endovascular Management:

-We present a case of 11-year-old male patient with left facial swelling and pain since 5 years who underwent colour doppler ultrasonography & CT angiogram and diagnosed to be a case of arteriovenous malformation of the left cheek.

-Patient was further subjected to diagnostic catheter angiography and the drainage pattern of the veins into the bilateral cavernous & inferior petrosal sinuses and the supply from the contralateral (Right) internal maxillary artery was demonstrated.

-Patient was managed by glue embolization of the malformation in our department and was discharged within 2 days of treatment with no complications.

Conclusion:

-Our objective is to understand and carefully evaluate the role of imaging in narrowing down to definitive diagnosis and endovascular management of such lesions in the paediatric population.

-The clinical course and patient prognosis depend on the sites of manifestations. Familiarity with the clinical and radiologic findings in various organs is crucial in diagnosis and treatment.

-In view of the paediatric age group interventional radiology provides a better outcome cosmetically, with fewer complications and reducing the duration of treatment significantly as compared to surgery.

Poster: SCI-153

PERCUTANEOUS CRYOABLATION FOR THE TREATMENT OF PRIMARY AND RECURRENT PEDIATRIC AND ADOLESCENT CHONDROBLASTOMA

KARIM VIRANI Virani, ANNE Gill, CLIFFORD MATTHEW Hawkins

Department of Radiology and Imaging Sciences, Emory University School of Medicine, Atlanta, USA

Image-guided percutaneous cryoablation of bone tumors offers a favorable safety profile and recovery time compared to open surgical techniques. Chondroblastoma is a rare cartilaginous tumor (2% of all benign bone tumors) afflicting individuals in the second to third decades of life, involving predominantly the epiphyses of long bones. Historically, surgery has been first-line therapy, involving localized bone curettage with grafting, and is commonly associated with recurrence and/or arthropathy secondary to cartilage or growth plate injury. Limited published literature exists on the use of percutaneous cryoablation of chondroblastoma. This study is intended to evaluate the clinical efficacy, technical feasibility, and safety profile of percutaneous cryoablation of chondroblastoma in pediatric and adolescent patients at a single institution.

All patients with chondroblastoma treated with percutaneous cryoablation between May 2014 through September 2020 were identified via retrospective chart review. Five patients were identified (mean age = 14 years). Lesion locations included proximal tibia (n=3), proximal humerus (n=1), and calcaneus (n=1). Average diameter of treated lesions was 1.4 cm (range: 0.9 to 1.6). All lesions were pathologically proven. Two patients were previously treated via surgery prior to secondary treatment with cryoablation. Three patients had cryoablation as their primary treatment. Mean follow-up was 18.1 months (range: 1.7 - 33.1). Four of five patients had resolution of pain post cryoablation, either complete (3/5) or marked reduction (1/5), with no evidence of local recurrence. The fifth patient was lost to follow-up. There were no major complications. There was 1 minor complication in a patient who suffered an ipsilateral lower leg stress fracture, 3 months post cryoablation, distal from the ablation site after resuming normal activity. No patients suffered cartilaginous injury or limb-length discrepancy secondary to growth-plate injury.

This exploratory report suggests percutaneous cryoablation may be a clinically efficacious primary and secondary treatment option for pediatric and adolescent chondroblastoma, with a favorable safety profile. Further study is warranted.

Poster: SCI-154

WHEN CROHN'S COMES TO RADIOLOGIST: VALUE OF MRE AND US IN CHILDREN

MONIKA Piekarska ¹, MARYLA Kuczynska ¹, MALGORZATA Nowakowska ¹, KAROLINA Siejka ¹, MAGDALENA Grzegorzczak ¹, MONIKA Zbroja ¹, WERONIKA Cyranka ¹, AGNIESZKA Brodzisz ², MAGDALENA MARIA Wozniak ²

¹ Department of Interventional Radiology and Neuroradiology Lublin, Lublin, POLAND

² Department of Pediatric Radiology Lublin, Lublin, POLAND

Introduction: Crohn's disease is classified as chronic inflammatory bowel disease. The incidence of it in Europe ranges from 1 to almost 11.4 per 100,000 population per year. Ultrasound and magnetic resonance enterography examinations play an important role in imaging diagnostics of inflammatory bowel lesions. They allow for recognising and monitoring changes during therapy as well as assessing complications such as fistula or abscess.

Materials and Methods: 36 children were included in the study: 16 boys and 20 girls with an active phase of Crohn's disease. Each patient underwent intestinal ultrasound examination with a high frequency 7-12 Mhz linear probe and MRE with intravenous administration of a contrast agent.

Results: All patients showed a significant correlation between ultrasound and MRE. In the US examination all children had thickened, low echogenic wall showing varying degrees of vascular flow signals. Additionally, in 8 patients Bauhin' valve edema was visible. In 16 children, inflammatory infiltration of the periintestinal fat around the affected segment of the intestine was found. In all patients a mesenteric lymphadenopathy in the short axis of 10-15mm was visible. MRE confirmed the presence of the confirmed ideal lesions and Bauhin' valve edema in all 36 children. In addition, in 4 patients small intestine fistulas were found whereas abscess was observed in another 4 patients. In contrast-enhanced images, a vivid enhancement of the affected bowel section was revealed and in 10 children inflammatory reactions of periintestinal fat was demonstrated.

Conclusion: US and MRE are reliable tools in diagnosis of enteric inflammatory disease of the small intestine, evaluation of disease activity and assessment of potential complications. They are complementary elements in diagnostics of Crohn's disease.

Poster: SCI-155

PERCUTANEOUS, IMAGE-GUIDED TREATMENT OF ANEURYSMAL BONE CYSTS (ABCs): IS THERE A SUPERIOR TREATMENT OPTION?

C. MATTHEW Hawkins, ANNE Gill

Children's Healthcare of Atlanta, Emory University School of Medicine, Atlanta, USA

Purpose:

Doxycycline sclerotherapy (DS) is a well-described therapy for ABCs. Its osteoblastic-inductive properties and inhibition of osteoclasts promote sclerosis of the tumor. Recently, cryoablation has been shown to have favorable osteoinductive properties that promote normal bone remodeling. Comparatively, little is known about osteoinductive properties of heat-based ablation. The purpose of this study is to compare clinical and imaging outcomes of DS versus ablation in treatment of pediatric ABCs.

Materials/Methods:

Pediatric patients with ABC who underwent image-guided treatment from 2014-2020 at a single institution were retrospectively evaluated. Doxycycline was delivered as a foam (200mg in 5mL sterile H₂O+5mL 25% albumin+10mL air). Cryoablation sessions included 2 10-minute freeze cycles & 2 5-minute thaw cycles. Cross-sectional imaging and IR clinic follow-up were scheduled at 3, 6, and 12 months post-procedure.

Results:

21 patients (11F, 10M; avg age=13.5 yrs; range: 7-18) with ABC underwent 41 procedures (mean=2; range: 1-6). Patients were treated with: DS alone (N=5), cryoablation alone (N=4), cryoablation+DS (N=10), MW ablation (N=1), MW+DS (N=1). Patients with DS alone required an average of 3 (range: 1-6) procedures to attain adequate sclerosis. Patients that had ablation required an average of 1.6 (range: 1-4) treatments. Technical success = 100%. Clinical success (increased sclerosis, decreased size) = 95% (19/20); 1 patient required surgical resection after cryoablation+DS failure). 1 patient was lost to follow-up. Mean clinical follow-up = 21.8 mos (range: 1.2-68.3). Mean cross-sectional imaging follow-up = 16.1 mos (range: 0-38.9). Cross-sectional imaging for patients treated via ablation demonstrated more normal appearing osseous remodeling, as compared to disorganized, thickened sclerosis following DS. 15/17 (88.2%) patients that presented with pain had resolution of pain at their 1 month follow-up visit. There were 2 major complications (4.9%; 2/41). 1 patient suffered transient lower extremity paralysis. 1 suffered a posterior circulation stroke following DS of a C4 vertebral body ABC and has since recovered entirely.

Conclusion:

DS and percutaneous ablation are efficacious treatment options for ABC, however ablation may be able to successfully treat ABC with fewer procedures. Based on the excellent osteoinductive properties of cryoablation, further research in its treatment of ABC is warranted.

Poster: SCI-156

TISSUE SAMPLING IN CHILDREN – THE “PATH” LESS TRAVELLED

MARIAN Gaballah¹, GANESH Krishnamurthy^{1,2}, MICHAEL Acord^{1,2}, FERNANDO Escobar^{1,2}, ABHAY Srinivasan^{1,2}, SETH Vatsky^{1,2}

¹ Children's Hospital of Philadelphia, Philadelphia, USA

² University of Pennsylvania, Perelman School of Medicine, Philadelphia, USA

Purpose: To present a series of innovative and adaptive techniques for route creation for lesional biopsy.

Materials and Methods: This series includes 15 biopsies in 15 children, median age 6.5 yrs, (IQR 2.2-16.3yrs) and median weight of 26.8 kg (IQR 14.7-56.7 kg).

Results: Biopsies were performed via the following approaches; percutaneous (n=12), endovascular (n=2), or intracavitary (n=1) (i.e. intravesicular via cystoscope). Percutaneous approaches included transiliopsoas (n=1), transperineal (n=1), trans-gluteal (n=1), trans-costal (n=1), sub-xiphoid (n=1), and with adjunctive use of protective pleural fluid (n=2) or hydrodissection to create a safe route for access (n=2).

Intra-vascular routes: liver dome (transcaval, n=1), tumor extension via the hepatic vein into right atrium (transjugular, n=1); intracavitary route: bladder wall (US guided transjugular needle via cystoscope, n=1); percutaneous routes: bladder base (transperineal, n=1), prostate (transgluteal, n=1), mediastinal (trans-costal, n=1), presacral (trans-iliopsoas, n=1), mesentery and retroperitoneal (hydrodissection, n=2), mediastinal and right upper lobe (protective pleural fluid, n=2), an iliac lytic lesion requiring transosseous bone biopsy cannula access followed by the coaxial insertion of an automated cutting needle through cannula (n=1), sternal marrow lesion (sub-xiphoid, n=1). Additional interesting lesion locations biopsied percutaneously included bowel wall mass (n=1) and upper cervical vertebral body mass (n=1). The trans-cystoscopic biopsy using a modified trans-jugular needle approach was performed after a negative urologic biopsy.

Imaging guidance consisted of ultrasound (n=8), CT (n=2), US and CT (n=1), US and fluoroscopy (n=2), cone beam CT with navigation (n=1), and transthoracic echocardiography with fluoroscopy in one patient.

Diagnostic success, defined as a tissue diagnosis was 100%. Diagnoses included focal necrosis/inflammation (n=2); reactive lymphoid tissue (n=1), infection (n=1), Ewing's sarcoma (n=1), neuroblastoma (n=2), hepatoblastoma (n=1), Langerhan's cell histiocytosis (n=1), lymphoma (n=2), chordoma (n=1), rhabdomyosarcoma (n=2), inflammatory myofibroblastic tumor (n=1).

No immediate or post procedure complications occurred.

Conclusion: Tissue sampling in children may require unique routes or adjunctive techniques to facilitate safe and feasible tissue acquisition.

Poster: SCI-157

INTRA-ABDOMINAL LYMPHATIC MALFORMATION MANAGEMENT IN LIGHT OF THE UPDATED INTERNATIONAL SOCIETY FOR THE STUDY OF VASCULAR ANOMALIES

HEBA ELBAALY Elbaaly¹, NELSON Piché², FRANÇOISE Rypens¹, NIINA Kleiber³, CHANTALE Lapierre¹, JOSÉE Dubois¹

¹ Medical Imaging Department, CHU Sainte-Justine, Montréal, CANADA

² Surgery Department, CHU Sainte-Justine, Montréal, CANADA

³ Pediatrics Department, CHU Sainte-Justine, Montréal, CANADA

Background:

The International Society for the Study of Vascular Anomalies (ISSVA) classification distinguishes between common lymphatic malformations and complex lymphatic anomalies. These entities have overlapping features but differing responses to treatment. Surgery has been the mainstream treatment in intra-abdominal lymphatic malformation, with variable reported success in the literature.

Objective:

The aim of this study was to review the outcome of different treatments for intra-abdominal lymphatic malformations in children.

Materials and methods:

We retrospectively reviewed all intra-abdominal lymphatic malformations from 1999 to 2019 in children treated by the surgical team or followed in the vascular anomalies clinic of our institution. Children were classified into one of three groups: group A, isolated intra-abdominal lymphatic malformation; group B, common lymphatic

malformation in continuity with other regions; or group C, intra-abdominal involvement as part of a complex lymphatic anomaly or associated syndrome.

Results:

Fifty intra-abdominal lymphatic malformations were diagnosed; five of these were excluded. In group A (n=28), the treatment was surgical resection (n=26) or sclerosing treatment (n=1), with one case of spontaneous regression; no recurrence was observed in 25 patients. In group B (n=7), three patients had partial resection and all had recurrence; four had sclerotherapy alone with good response. In group C (n=10), therapeutic options included surgery, sclerosing treatment and pharmacotherapy, with variable outcomes.

Conclusion:

The management of intra-abdominal malformations requires a team approach. Sclerotherapy is successful in treating macrocystic lymphatic malformation. Surgery is successful in treating isolated intra-abdominal common lymphatic malformation, albeit at times at the cost of intestinal resection, which could be avoided by combining surgery with preoperative sclerotherapy. With surgery, there is often limited resectability, and therefore recurrence in intra-abdominal lymphatic malformations that are part of complex lymphatic anomalies associated with syndromes, or in common lymphatic malformations in continuity with other regions. Sclerotherapy is an effective modality in these instances along with pharmacotherapy.

Poster: SCI-158

COVID-19 AND MIS-C, A YEAR IN REVIEW: GLOBAL CONTRIBUTIONS OF INTERVENTIONAL RADIOLOGY TO THE CARE OF PEDIATRIC PATIENTS

TINA Sankhla, MORGAN Whitmore, MOHAMMED Loya, JAY Shah
Emory University, Department of Radiology and Imaging Sciences, Atlanta, USA

Educational Objectives:

1. Demographic, clinical and radiographic findings of the SARS-CoV2 virus (COVID-19).
2. General demographic, clinical and radiographic findings of Multisystem Inflammatory Syndrome in Children (MIS-C)
3. Supportive interventions performed within the Adult IR department.
4. Supportive interventions performed within the Pediatric IR department.
5. Novel procedures, algorithms and clinical roles managed by IR

Purpose:

Following discovery of novel SARS-CoV-2 in Wuhan, China in December 2019, the subsequent spread of severe respiratory and inflammatory symptoms has changed the way we live our lives and in turn deliver healthcare. With rapid rise to pandemic status, and hospitals in cities around the world rapidly surpassing capacity, physicians and health care workers across disciplines were tasked with providing supportive care, optimizing limited inpatient/ICU occupancy, and mitigating mortality of COVID-19 and MIS-C patients.

1. Anesthesia/Sedation Trends
 - a. Trend to minimally invasive alternatives preferred due to droplet and anesthesia risk (Cholecystostomy vs Cholecystectomy)
2. Central Venous Catheter Placement
3. Pleural Drainage
4. IVC Filter Placement

5. Thrombolysis/Thrombectomy
6. Novel Uses of IR

Conclusions:

Internationally, interventional radiologists played a unique and important role in the service of COVID-19 and MIS-C patients. Innately minimally invasive approach, ability to perform procedures without general anesthesia, and flexibility to offer procedures at the bedside, cements IRs role as a critical service line in the unique clinical setting created by this global pandemic. Reflection on the early and continuous contributions by IR to the care of patients with COVID-19 and MIS-C will help to inform innovation in caring for future emergencies.

Poster: SCI-159

LOWER EXTREMITY DEEP VEIN THROMBOSIS CATHETER-DIRECTED THROMBOLYSIS IN PEDIATRIC PATIENTS: SINGLE-CENTER EXPERIENCE

JONATHON Weber, NATHAN Fagan, MANISH Patel
Cincinnati Children's Hospital Medical Center - Department of Radiology, Cincinnati, USA

PURPOSE

Report experience using catheter-directed thrombolysis (CDT) to treat patients with lower extremity (LE) deep vein thrombosis (DVT).

M&M

IRB-approved retrospective review of clinical and imaging databases was performed for every patient who underwent LE DVT CDT. Risk factors, procedural success, and complications were reviewed. Outcomes assessed include procedure durability, development of post-thrombotic syndrome, and anticoagulation status.

RESULTS

52 patients, 21 males and 27 females, ranging from 3 to 21 years-old, were identified. 59 total CDT sessions performed from July 2008 to June 2020. Thrombosis was identified on the left during 40 sessions, right during 16, and bilaterally during 3. Extent of thrombus was isolated to the lower extremity in 7 sessions, iliofemoral in 32, iliac vessels in 2, and extending from the LE to the IVC in 18.

Of the 51 patients with documentation of risk factors, 50 had identifiable risk factors. These included 12 with a genetic thrombophilia, 4 with OCP use, 3 with a diagnosis of cancer, 4 with recent surgery or immobility, 1 catheter associated, 4 with May-Thurner syndrome, 1 with an atretic IVC, and 1 with increased inflammatory state (Crohn's disease flare). 19 patients had some combination of above risk factors.

All patients were treated with pharmacomechanical thrombectomy. Angiographic success was established in 53 sessions. Angiographic success was not established in 6 sessions due to thrombus chronicity or IVC atresia. Recurrence of thrombus in the same segment recurred after 9 sessions in 8 patients. 5 of these patients were successfully retreated with CDT, one of whom was retreated twice. Iliofemoral stents were placed in 3 patients. There were no major complications.

14 patients discontinued anticoagulation after CDT. 41 patients had documentation for post-thrombotic syndrome; 15 had PTS ranging from mild to moderate.

CONCLUSION

CDT is safe and effective for pediatric patients with LE DVT. CDT may provide an avenue for discontinuing anticoagulation in select patients.

Poster: SCI-160

FUSION OF INTRAPROCEDURAL CONE BEAM CT AND PRE-PROCEDURAL MRI IMAGES FOR THE EVALUATION OF

COMPLETENESS OF KNEE JOINT VENOUS MALFORMATION EMBOLIZATION

ELENA Violari, JOHN Cieslak, VICTORIA Young, MATTHEW Lungren, AVNESH Thakor, SHELLIE Josephs
Stanford, Lucile Packard Children's Hospital, Palo Alto, USA

Purpose:

Immediate surgical excision following glue embolization is a well-established treatment for intra-articular venous malformations of the knee. Given the complex anatomy of intra-articular venous malformations, intraprocedural assessment of completeness of embolization remains a hurdle limiting technical success. Here we present a new method for intraprocedural assessment of completeness of embolization.

Methods:

Percutaneous sclerotherapy of an intra-articular venous malformation of the knee was performed using ultrasound and fluoroscopic guidance. A 3:7 mixture of nBCA glue:lipiodol was injected into the malformation using fluoroscopic visualization to ensure that there was no filling of the deep venous system. Intraprocedural contrast enhanced cone beam CT was performed after the initial embolization. While the patient was still on the table, cone beam CT images were fused with pre-procedural T1W post contrast MRI images. The fused images were then evaluated for areas of matched enhancement within the venous malformation, with matched enhancement representing areas of incomplete embolization. This data was then used to guide subsequent injections to ensure completeness of embolization prior to surgical excision.

Results:

Two female patients (age 11 and 14) with intrarticular venous malformations of the knee underwent pre-operative glue embolization followed by surgical excision with orthopedic surgery, using the aforementioned technique (n = 2). Technical success was defined as complete embolization of the excised lesion, as determined intraoperatively by the orthopedic surgeon. Complete embolization of the targeted lesion was achieved prior to operative excision in both cases (technical success rate = 100%). Clinical success was 100% as defined by improvement of patient's symptomatology and no recurrence on imaging up to 6 month follow-up visits.

Conclusion:

Fusion of intraprocedural post-embolization cone beam CT and pre-procedural MRI images is a novel technique which allows for identification of areas of incomplete embolization of intraarticular venous malformations. This technique may improve technical and clinical success rates, potentially reducing costs and procedural-related morbidity by reducing the need for subsequent interventions.

Poster: SCI-161

ATTEMPTED PLUG EMBOLISATION OF A CONGENITAL PORTOSYSTEMIC SHUNT WITH SUBSEQUENT EMBOLISATION INTO THE PULMONARY ARTERY AND SUCCESSFUL ENDOVASCULAR SNARE RETRIEVAL

NASIM Tahir, ELLEN Collingwood, JAI Patel
Leeds Children's Hospital, Leeds, UNITED KINGDOM

Congenital portosystemic shunts (CPSS) are abnormal connections between the portal and systemic circulations. The risk of hyperammoniaemia, portopulmonary syndrome, pulmonary hypertension and focal nodular hyperplasia means that if spontaneous closure does not occur shunt closure is recommended. We present a case of a 14-year-old with an intrahepatic CPSS which was closed using a plug device. The plug then embolized to the right pulmonary artery but was successfully retrieved endovascularly. The patient was referred to our centre following local investigations for premature adrenarche which included abdominal ultrasound that incidentally showed abnormal portal venous anatomy. MRI confirmed this

finding demonstrating drainage of the main portal vein into the right atrium via a large shunt. There was absence of the right and the left main portal vein branches.

The patient was closely monitored for symptoms for a number of years and eventually it was decided to attempt endovascular embolization of the shunt. This was performed via a right internal jugular approach. A balloon occlusion test was initially performed which showed no significant rise in portal pressure. An 18mm Cera vascular plug was then deployed in good position and remained in a stable position over a ten minute period. As expected, shunt occlusion did not occur immediately.

The following day an ultrasound was performed to check for shunt patency and the position of the plug. This showed that the shunt remained patent and the occlusion device could not be visualised. A chest x-ray was subsequently performed which demonstrated that the plug had embolized into the right pulmonary artery. The patient was asymptomatic. She subsequently returned to theatre and the plug was successfully retrieved using an endovascular snare without further complication. Since the shunt remains patent, further MDT discussion will be undertaken to decide whether a repeat endovascular procedure using a different plug or an open surgical procedure should be performed.

Poster: SCI-162

ADDED VALUE OF CONTRAST ENHANCED ULTRASOUND (CEUS) IN THE DIAGNOSIS OF SPLENIC ARTERY PSEUDOANEURYSM

PETER Slak, DOMEN Plut
Department of Pediatric Radiology, Clinical Radiology Institute, University Medical Centre, Ljubljana, SLOVENIA

Introduction

Post-traumatic splenic artery pseudoaneurysm (SAP) is an infrequent complication of blunt abdominal trauma. It may potentially lead to a life-threatening bleeding.

In the last years, contrast-enhanced ultrasound (CEUS) proved to be a reliable alternative to contrast enhanced computed tomography (CECT) in the follow-up of splenic and hepatic injuries. It is especially recommended for use in paediatric patients because of the lack of radiation.

Case presentation

A 13-year-old boy was admitted to our hospital after a bicycle accident. Ultrasound (US) performed in emergency room revealed laceration of the spleen and massive haematoperitoneum. Emergency median laparotomy was performed. Two tears in the splenic capsule were found and treated with surgical haemostasis. Child's recovery was clinically uneventful.

On day 6 after the trauma, a follow-up US was performed. Colour doppler ultrasound (CDU) revealed an intraparenchymal SAP, which measured 10 mm in size. Conservative approach to the management of SAP was chosen. CEUS was performed on day 8. CEUS demonstrated not only one, but two SAPs. On B-mode examination the second, smaller (6 mm), SAP was not detectable, due to the heterogeneity of injured splenic parenchyma. On day 9, a CECT was performed. CECT confirmed two SAPs; the larger of which has spontaneously thrombosed. On CDU on days 12 and 13, no signs of SAP were visible. CEUS was repeated on day 14 and demonstrated the small SAP. Conservative management was continued. The follow-up CDU on day 27 demonstrated the small SAP, the same on day 48. On day 83, the SAP was not visible by CDU anymore. CEUS was again performed and confirmed that the second SAP spontaneously thrombosed.

Conclusion

CEUS is a useful tool in follow-up of splenic trauma and provides additional information to CDU, comparable to CECT.

Conservative management of posttraumatic SAP can lead to spontaneous closure several weeks after trauma.

Poster: SCI-163

THE CLINICAL USEFULNESS OF THE DYNAMIC-CONTRAST MR LYMPHANGIOGRAPHY: INITIAL EXPERIENCE FOR THE ASSESSMENT OF NON-TRAUMATIC LYMPHATIC ANOMALY

LEE Seunghyun, HUR Saebeom, YEON JIN Cho, YOUNG HUN Choi, SEUL BI Lee, JUNG-EUN Cheon, WOO SUN Kim
Seoul National University Children's Hospital, Seoul, SOUTH KOREA

Purpose: To evaluate the clinical usefulness of the dynamic contrast-enhanced magnetic resonance lymphangiography (DCE-MRL) in non-traumatic lymphatic anomaly patients.

Methods: From January 2017 to December 2019, we performed 32 DCE-MRL examinations for 20 patients with non-traumatic congenital lymphatic anomaly (13 males and 7 females; median age 19.0 years). We obtained dynamic T1-weighted volumetric interpolated breath-hold examination 3D gradient images in the coronal plane during 1 minute after the MR contrast material injection via bilateral inguinal lymph nodes. We repeated ten images to three times and reconstructed maximum intensity projection to evaluate the lymphatic anomaly. We divided three categories according to the extent of abnormal lymphatic involvement and assessed both the imaging and treatment success.

Results: There were seven patients of the anomaly above the cisterna chyli (4 cases of chylothorax and 3 of chylopericardium), six patients below the cisterna chyli (3 of protein-losing enteropathy, 1 of chylous ascites, 1 of chylous urine, and 1 of leg edema), and seven patients of both of anomalies (4 of the mainly chylothorax and 3 of mainly chylous ascites). The DCE-MRL could show successful pre-treatment planning regarding both of the thoracic duct anomaly and collateral channels in all of the lymphatic anomaly above the cisterna chyli, and we successfully treated via embolization except the 8-month old baby (85.7%, 6/7 cases). In terms of the lymphatic anomaly below cisterna chyli, DCE-MRL could not show all abnormalities (33.3%, 2/6 cases). If the lymphatic anomaly involves both sides of cisterna chyli, we could visualize the lymphatic anomaly using DCE-MRL, but they received drug treatment due to unable to demonstrate any lymphatic leakage nor reflux abnormal point.

Conclusion: DCE-MRL can lead to help in management in all patients, continuation of conservative treatment, and intervention treatment in the lymphatic anomaly above cisterna chyli.

It is meaningful to accumulate clinical experience centered on DCE-MRL findings in a situation where the congenital lymphatic anomaly is rare, expression patterns are diverse, and classification systems are not uniform.

Poster: SCI-164

CONE-BEAM COMPUTED TOMOGRAPHY GUIDANCE FOR PEDIATRIC BONE BIOPSIES

LAVI Nissim, SCOTT Willard, RICHARD Towbin, DAVID Aria
Phoenix Children's Hospital, Phoenix, USA MINOR OUTLYING ISLANDS

Purpose: To demonstrate feasibility of pediatric bone biopsies using cone-beam CT as an alternative to traditional CT guidance.

Materials and Methods:

A retrospective review of cone-beam CT bone biopsies performed at a single institution. Data was analyzed for 46 attempted bone biopsies from time period of January 2016 through May 2020 using XperCT cone-beam CT (Philips).

Results:

46 Bone biopsies were performed at our institution from the 53-month time period of January 2016 through May 2020, using XperCT cone-beam CT (Philips). 40 biopsies were attempted on focal lesions (mean greatest diameter 1.7 cm) and 6 biopsies were attempted on regional osseous abnormalities. The mean patient age was 11.7 years. Biopsies were technically successful in 91.3% (42/46). The mean number of cores obtained was 2.1. The procedures were performed with mean (median) exposures as follows: fluoroscopy time of 3.7 min (3.0 min) for 46 procedures; DAP of 28872 mGycm² (22790) and air kerma skin dose of 132.6 mGy (104.3) recorded in 39 of the 46 procedures. Biopsies were diagnostic in 93.5% (43/46) and non-diagnostic in 6.5% (3/46). There were no immediate post-procedure complications of bleeding or tissue injury. There was one delayed complication of wound infection (2.1%).

Conclusion:

Cone-beam CT-guided bone biopsies may be performed with accuracy in the pediatric population and with low procedural-related risk.

Poster: SCI-165

SINGLE-CENTER, RETROSPECTIVE STUDY OF OUTCOMES IN PEDIATRIC HEREDITARY HEMORRHAGIC TELANGIECTASIA PATIENTS FOLLOWING PULMONARY ARTERIOVENOUS MALFORMATION EMBOLIZATION

VIET Le¹, NATHAN Fagan¹, ADRIENNE Hammill¹, KATIE Wusik¹, ROSS Ristagno², MANISH Patel¹

¹ Cincinnati Children's Hospital Medical Center, Cincinnati, USA

² University of Cincinnati, Cincinnati, USA

Purpose: Hereditary Hemorrhagic Telangiectasia (HHT) is a genetic disorder resulting in mucosal and skin telangiectasias and brain, lung, and liver arteriovenous malformations (AVMs). Patients present with recurrent nosebleeds with increased risk for stroke and intracranial hemorrhage. Clinical presentation, imaging findings pre- and post-embolization, and procedural findings from pulmonary arteriovenous malformation (PAVM) embolization are described. **Materials and Methods:** IRB approved retrospective chart and imaging review was performed of pediatric patients with HHT who underwent PAVM embolization from 2010-2020 at a tertiary care pediatric hospital. **Results:** 13 HHT pediatric patients with 22 PAVMs (median age at embolization 11 years, range 2-21 years) identified. 12 of 13 patients had genetic mutations. Before embolization, skin telangiectasias were in 10 patients (77%), shortness of breath or fatigue in 6 patients (46%), nosebleeds in 12 patients (92%), and headaches/migraines in 11 patients (85%). No patients suffered stroke or intracranial hemorrhage during this period; two patients had remote strokes before intervention. Before embolization, the average size of the PAVM nidus was 11 mm (range 2-29 mm) with an average feeding vessel size of 3 mm (range 1-5 mm). When possible, the PAVM sac was embolized, in addition to the feeding artery, with 0.018 detachable coils. All but one patient had a pre-embolization bubble echo study. Six-month follow up bubble echo studies were performed on all but the most recent patients. In all patients where pre-procedural bubble echo were appropriately graded, stable to improved bubble echo results were seen after embolization. No recanalization of embolized PAVM was noted on follow up. **Conclusion:** Pulmonary AVM embolization can be safely performed in pediatric patients. Our study did not demonstrate recanalization of the PAVM after embolization of the sac and its feeding vessel; although, some of our patients had limited follow up. **Objectives:** To identify clinical manifestations of HHT in pediatric patients and evaluate the role of PAVM embolization.

Poster: SCI-166

FEASIBILITY OF INTERVENTIONAL CARDIAC MRI AT 3T

RAMKUMAR Krishnamurthy¹, RAJESH Krishnamurthy¹, RANDOLPH Setser², KAN Hor³, JOHN Kelly³, CHRISTOPHER Breuer⁴, HIMANSHU Bhat², AIMEE Armstrong³

¹ Nationwide Children's Hospital - Radiology, Columbus, USA

² Siemens Healthineers - Advanced Therapies, Erlangen, GERMANY

³ Nationwide Children's Hospital - The Heart Center, Columbus, USA

⁴ Nationwide Children's Hospital - Surgery, Columbus, USA

Interventional cardiac magnetic resonance (iCMR) in pediatrics is currently performed in 1.5T machines due to its higher safety profile, and lesser frequency of artifacts, while diagnostic CMR at 3T does have some advantages. In this study, we document our experiences in using a 3T scanner in performing iCMR in a large animal model.

Methods:

In this IACUC approved study, 3T Siemens scanners (SkyraTM and PrismaTM) were connected to prototype software (Monte-Carlo) which enables real time, interactive image positioning and guidance. An InVivoTM patient entertainment was used for communication and display of images inside scanner room. In-room field sterility was ensured, and intra-cardiac pressure monitoring was performed.

In 4 sheep, diagnostic cardiac MRI images were initially obtained, followed by the right heart catheterization. For image guidance during the intervention, balanced SSFP and GRE sequence real-time sequences were tested. Three sheep had no contrast injected, while one had ferumoxytol (3mg/kg). Acquisition parameters were: SSFP: TR = 3 ms, TE = 1.5 ms, flip = 50 degrees, GRAPPA acceleration = 2; bandwidth = 500 Hz/px; frame rate = around 12 fps. GRE: TR = 4.5 ms, TE = 2.2 ms, flip = 15 degrees, GRAPPA acceleration = 2; bandwidth = 800 Hz/px (1800 Hz/px with ferumoxytol); frame rate = around 9 fps (15 fps at high bandwidth).

A balloon wedge catheter was advanced under real time MR guidance without a guidewire into the right ventricle and positioned in the pulmonary artery (PA). PA pressure was measured.

Results:

1. In all studies, the GRE sequence performed better.
2. CO₂ and gadolinium filled balloons were both visible.
3. Ferumoxytol enhancement helped with faster dynamics (15 fps).
4. The deeper bore length of 3T scanner (compared to 1.5T) is ergonomically challenging for the interventionalist.

Conclusion: iCMR is feasible at 3T using a Monte-CarloTM system in real time to visualize the balloon to guide catheter manipulation. Ferumoxytol enhancement might aid improved temporal resolution.

Poster: SCI-167

ASSESSMENT OF THE SUPERIOR MESENTERIC ARTERY ANGLE IN THE PEDIATRIC GROUP ON COMPUTED TOMOGRAPHY (CT) SCAN: VALUES IN DIFFERENT AGE GROUPS, GENDER AND (BODY MASS INDEX) BMI CATEGORIES

SHAIMA ALEID, ASRAR AlZaher
King Fahad Specialist Hospital, Dammam, SAUDI ARABIA

Objective: to find the normal range of the SMA angle and its relationship with different BMI categories, age group and gender type in pediatric population.

Methods: we retrospectively measured SMA angle in 287 pediatric chest/abdominal CT (110 females and 177 males) with unremarkable upper abdomen and absent gastrointestinal symptoms. The subjects were 3 months to 204 months old. Relationships of the SMA angle with sex,

age, body weight and height were investigated. Suggested limits of normal angles were defined.

Result: mean SMA angle was 46.2±24.9 degree (range 8–125 degree). Dimensions of the measured angles were not statistically different in females and males. SMA angle measurements showed the best correlation with age, body weight, height and BMI. Mean, minimum and maximum values; fifth and 95th percentile values; standard deviations and suggested limits of normal angle values were given.

Conclusion: determination of pathological changes in size of the SMA angle necessitates knowing the normal range in pediatric group. Age, height and BMI should be considered the best criteria to correlate with SMA angle.

Keywords: Superior mesenteric artery, Body mass index and Computed tomography.

Poster: SCI-168

PEDIATRIC PALEORADIOLOGY: WHAT IT IS AND WHY WE SHOULD GET INVOLVED

KATHERINE Van Schaik¹, ANDY Tsai², MARIA Liston³

¹ Beth Israel Deaconess Medical Center/Harvard Medical School, Boston, USA

² Boston Children's Hospital/Harvard Medical School, Boston, USA

³ University of Waterloo, Waterloo, CANADA

INTRODUCTION

Paleoradiology is the application of clinical radiology technologies to the study of human remains from past populations. As imaging technologies have advanced, anthropologists have eagerly applied these technologies to mummies and excavated skeletons. However, the ad hoc application of clinical radiology techniques occurs without standardized protocols, and image interpretation only rarely happens with the assistance of a radiologist. These challenges are especially problematic for pediatric remains.

TEACHING MESSAGE

A literature review focusing on 3 major bioarchaeology journals yielded 116 studies since 1980 that used plain film radiography, CT, MRI, or mammography to assess pediatric remains recovered from bioarchaeological contexts. Sixteen papers used CTs to examine 33 mummies that ranged in age from a 15-week-old fetus to a 16-year-old child. Another 100 studies used mostly plain film radiography to evaluate non-mummified remains. Pathologies identified included: genetic dwarfism, osteogenesis imperfecta, congenital syphilis, tuberculosis, juvenile arthritis, rickets, scurvy, leukemia, and suspected abuse. Imaging (mostly dental) was used to assess age-at-death. Although imaging played a significant role in assessment of these remains, a radiologist was listed as a co-author in only 5% of the papers that examined non-mummified remains. Imaging parameters and equipment were rarely published.

Of interest for this educational paper, anthropological literature has acknowledged that assessment of forensic/bioarchaeological imaging is inadequate without interpretation by an individual with radiological training. As paleoradiological techniques have great potential to provide information about rare and delicate pediatric human remains, it is important that clear protocols be developed and followed to ensure consistent and information-rich imaging.

CONCLUSION

The field of pediatric paleoradiology is under-developed because of (1) greater variation in findings relative to adults, (2) paucity of pediatric remains, (3) lack of standardized techniques, and (4) lack of radiologist involvement in image interpretation. This educational paper will describe the history of pediatric paleoradiology, discuss the findings that can be identified in the paleoradiographic assessment of pediatric remains, and provide multi-modality protocols regarding the acquisition and interpretation of images obtained of pediatric remains excavated from archaeological contexts.

Poster: SCI-169

A PICTORIAL REVIEW OF PAEDIATRIC SOFT TISSUE LESIONS

ALEXANDER Sheeka, RICHARD Jenkins, STACEY Castle, MAY-AI Seah, JOANNA Danin
Imperial College Healthcare, London, UNITED KINGDOM

Summary:

Soft tissue lesions are common in children with the vast majority of benign etiology. Prompt and accurate diagnosis is necessary in order to provide parental reassurance, or refer for further imaging and intervention as necessary. This is an educational poster to demonstrate the imaging characteristics of various paediatric soft tissue lesions on ultrasound, CT, and MRI.

Educational Objectives:

To simplify the diagnosis and classification of paediatric soft tissue lesions. This is often an area that junior radiology trainees find daunting.

Materials and Method:

Paediatric patients referred for assessment of soft tissue lesions at our centre were assessed with various imaging modalities. Imaging findings were correlated with patient history and final histological diagnosis if biopsy/resection was performed.

Results:

Images of various benign and malignant soft tissue lesions including:

- Hemangioma
- Arteriovenous/lymphatic malformations
- Lipoma
- Breast buds.
- Dermoid/epidermoid cysts
- Lymph node abnormalities (lymphadenitis and lymphoma).
- Sarcoma
- Pilomatricoma
- Histiocytoma

Conclusion:

Many paediatric soft tissue lesions have characteristic appearances on ultrasound, CT, and MRI. Ultrasound is an effective first-line method of distinguishing soft tissue lesions. Depending on initial appearances, cross-sectional studies can be performed for further assessment in cases of uncertainty or to aid in surgical planning.

Poster: SCI-170

WHAT SKELETAL IMAGING MODALITY IS BEST FOR ASSESSING BONE HEALTH IN CHILDREN AND YOUNG ADULTS? SYSTEMATIC REVIEW AND META-ANALYSIS

HEBA SALEH SHALO Shalof¹, PAUL Dimitri^{1,2}, FARAG Shuweihdi³, AMAKA Offiah^{1,4}

¹ Academic Unit of Child Health, Department of Oncology and Metabolism, University of Sheffield, Damer Street Building, Sheffield, UNITED KINGDOM

² Department of Paediatric Endocrinology, Sheffield Childrens NHS Foundation Trust, Western Bank, Sheffield, UNITED KINGDOM

³ Leeds Institute of Health Sciences, University of Leeds, Leeds, UNITED KINGDOM

⁴ Radiology Department, Sheffield Childrens NHS Foundation Trust, Western Bank, Sheffield, UNITED KINGDOM

Skeletal imaging techniques have become clinically valuable methods for measuring bone mineral density in children and young adults. Dual-energy X-ray absorptiometry (DXA) is the current reference standard for evaluating bone density, as recommended by the International Society for Clinical Densitometry (ISCD). Various bone imaging

modalities, such as quantitative ultrasound (QUS), peripheral quantitative computed tomography (pQCT), high-resolution peripheral quantitative computed tomography (HR-pQCT), magnetic resonance imaging (MRI), and digital X-ray radiogrammetry (DXR) have been developed to further quantify bone health in children. The purpose of this review, with meta-analysis, was to systematically research the literature to compare the various imaging methods and identify the best modality for evaluating bone status in healthy and unhealthy populations (up to 18years).

Methods A systematic computerised search of Medline, PubMed, and Web of Science databases was conducted to identify relevant papers published between 1st January 1990 and 1st December 2019. In this review, clinical studies comparing imaging modalities with DXA were chosen according to the inclusion criteria. The risk of bias and quality of articles was assessed using the Quality Assessment Tool for Diagnostic Accuracy Studies (QUADAS-2). The meta-analysis to estimate the overall correlation was performed using a Fisher Z transformation of the correlation coefficient. Additionally, overall diagnostic accuracy measures of different imaging methods compared with DXA were calculated. Publication bias was tested using Funnel plots.

Results The initial search strategy identified 13,412 papers, 29 of which matched the inclusion and exclusion criteria. Of these, twenty-two papers were included in the meta-analysis. DXA was compared to QUS in 17 papers; to DXR in 7 papers and to pQCT in 4 papers. A single paper compared DXA, DXR, and pQCT. The meta-analysis demonstrated that the strongest correlation was between DXR and DXA, with a coefficient of 0.71, while the correlation coefficients between QUS and DXA, and pQCT and DXA were 0.57 for both modalities.

We conclude that no imaging modality can provide a full evaluation of bone health in children and young adults. Compared to QUS and pQCT, DXR achieved the strongest relationship with DXA. There may be potential to use DXR (BHI) as a reliable method for evaluating bone health and as a predictor of fractures in children and young adults.

Poster: SCI-171

PEDIATRIC ANTERIOR CRUCIATE LIGAMENT: TEARS AND REPAIRS

WILLIAM WATKINS Pryor¹, VICTOR Ho-Fung², SOSAMMA Methratta¹, J. TODD Lawrence², NANCY Chauvin¹

¹ Penn State Health, Hershey, USA

² Children's Hospital of Philadelphia, Philadelphia, USA

Purpose:

The anterior cruciate ligament (ACL) is a vital structure in the knee that provides stability and helps to prevent secondary knee injury in active individuals. There has been an increased incidence of ACL injuries in skeletally immature children due to increased participation in youth sports, sports intensity and early sports specialization. In addition, year-round training and longer practice sessions are common in today's youth athletic programs. For active children, conservative treatment of ACL tears has been shown to result in meniscal and cartilage injury, recurrent knee instability and premature osteoarthritis. For these reasons, surgical procedures are recommended in active children to restore functional knee stability and reduce the risk of secondary injury. This exhibit will provide the general pediatric radiologist with a practical approach to evaluate the ACL on MRI as well as review the imaging appearance of various surgical techniques utilized to reconstruct torn ligaments.

Material and Methods:

We will review the normal appearance of the ACL on MRI as well as the spectrum of ACL injuries in children. Using multiple modalities, we will show intraoperative and post-operative imaging of various surgical techniques, including the "physeal respecting", "transphyseal", "extraphyseal", and "all epiphyseal" approaches to reconstruct torn ACLs. Potential complications specific to each approach will be

discussed. In addition, imaging features of interest to the orthopedic surgeon will be highlighted.

Results:

There are several approaches to reconstruct torn ACLs in children. Operative approach depends on the degree of skeletal maturity and surgeon preference. Preoperative and post-operative imaging is crucial to diagnosing knee injuries as well as guiding management and return-to-play.

Conclusions:

Pediatric radiologists should be familiar with the imaging appearance of the ACL as well as various surgical approaches used to reconstruct torn ACLs in children in order to accurately diagnose injuries, assess graft integrity or other post-operative complications.

Poster: SCI-172

IMAGING OF THE LIMPING CHILD

GEORGIA Papaioannou, LOUKIA Tzarouchi, CHRISTINA Meleti, PANAGIOTIS Tagalakakis, GEORGIOS Manganas, EVAGGELIA Manopoulou, SPYROS Yarmentitis
Department of Pediatric Radiology Mitera Children's Hospital, Athens, GREECE

OBJECTIVES: To illustrate the imaging algorithm and findings, common and rare, in different age groups of children with limp.

CONTENTS: The limping child is primarily investigated clinically through medical history, physical examination and laboratory tests, if necessary. In presence of localized prolonged pain and/or systematic symptoms, imaging investigation is indicated. According to the clinical evaluation, initial imaging includes plain film of either the symptomatic joint or the lower extremities, with extra views, such as frog view of the hips or lateral view of the joints. In suspicion of joint effusion, ultrasound of the joint is substantial to confirm synovitis and set the suspicion of complex effusion. In the latter scenario, especially when laboratory tests suggest infection or systematic disease, further imaging is indicated: MRI of the affected joint or whole-body imaging, according to availability (Whole-body MRI or bone scintigraphy). Entities presented include common cases of limp in preschool children (toddler's fracture, transient synovitis, septic arthritis, osteomyelitis), in school children (Perthes disease, slipped capital femoral epiphysis, osteomyelitis, stress-fractures in young athletes), systematic disease causing limp (lymphoproliferative disease, juvenile idiopathic arthritis, chronic non-bacterial osteomyelitis, metastatic neuroblastoma) but also pathology distant to the lower extremities (spondylodiscitis, spinal tumors).

TEACHING MESSAGE: The imaging algorithm of limping child is approached; imaging findings of different entities with different modalities are presented.

Poster: SCI-173

IT'S NOT ALWAYS A SUPRACONDYLAR FRACTURE!

ELAINE O'Boyle, ANNIE Paterson
Royal Belfast Hospital for Sick Children, Belfast, UNITED KINGDOM

Learning Objectives:

1. To review the normal radiographic anatomy of the developing elbow.
2. To use developmental anatomy and a systematic approach to correctly describe bony injuries.

3. To demonstrate a comprehensive range of paediatric elbow fractures.

Background:

Acute paediatric elbow injuries are a very common reason for emergency department attendance in children of all ages.

Radiographs of the developing elbow with its many ossification centres can be difficult to interpret, and often cause consternation for both trainees and experienced radiologists.

Elbow injuries account for up to 15% of all paediatric fractures with potential acute and long term complications including: neurovascular injury, non- or mal-union and subsequent functional impairment. It is important to make a correct, prompt anatomical diagnosis to aid orthopaedic management and to give an optimal outcome for the patient.

Imaging Findings:

We review the developmental bony anatomy of the elbow joint, specifically revising the appearance of the ossification centres through childhood. We illustrate a systematic approach to reporting the paediatric elbow radiographs following trauma. We present a comprehensive spectrum of cases from a dedicated paediatric Emergency Department depicting the type of fractures and dislocations seen in children relative to patient age and injury mechanism.

Conclusion:

Radiographic imaging and its accurate interpretation play a huge part in the correct management of elbow injuries in children.

Poster: SCI-174

STRUCTURED REPORTING OF SCOLIOSIS IN PEDIATRIC PATIENTS WITH IMAGING OF POST SURGICAL FIXATION HARDWARE AND COMPLICATIONS

DONALD Lee
Staten Island University Hospital, Staten Island, USA

Purpose/Objectives:

This is an educational review regarding scoliosis in pediatric patients as well as spinal fixation hardware and complications following corrective surgery. Following this review, the radiologist will be able to achieve the following:

- Describe scoliosis on imaging of pediatric patients and accurately report relevant information to the pediatric orthopedic surgeon.
- Describe normal spinal fixation hardware placement and alignment on imaging.
- Describe various surgical approaches and associated complications.
- Describe normal post-surgical imaging findings following placement of prosthetics.
- Describe spinal hardware complications and associated imaging findings, including nuclear studies.

Summary:

The planned presentation will progress as follows:

- Epidemiology and pathophysiology of scoliosis.
- Various spinal hardware including plate-and-rod hardware and posterior fusion devices, and how they are expected to be positioned.
- Normal radiographs/intraoperative fluoroscopic images/CT/MR images of spinal fixation hardware. Parts of hardware will be identified, as well as other fixation substrates used such as cement.
- Normal expected post-surgical changes on imaging.
- Various complications related to spine hardware and how they appear on various imaging modalities including CT/MR/nuclear studies not limited to infection, prosthetic and peri-prosthetic fractures, hardware loosening, and hardware misplacement.

-Discussion of various surgical approaches such as oblique lumbar interbody fusion (OLIF), extreme lateral approach, or direct lateral approach and associated complications with each approach.

-The medical and/or surgical management of aforementioned hardware complications.

Conclusion:

Practicing radiologists will be able to describe scoliosis on imaging and have a framework for structural reporting of scoliosis for the pediatric orthopedic surgeon. Radiologists will be able to identify spinal fixation hardware on imaging and recognize normal positioning of prosthetics. Radiologists will be able to identify normal postsurgical findings and recognize complications associated with spinal hardware.

Poster: SCI-175

CONGENITAL SYPHILIS- A CASE STUDY

RICHARD Jenkins, STACEY Castle, AFSHIN Alavi, ERIN Butterworth
Imperial NHS Trust, London, UNITED KINGDOM

Summary

Congenital syphilis is an uncommon presentation in the UK. Symptomatic neonates may present with premature birth, pneumonia, poor feeding, and skeletal abnormalities. The characteristic skeletal appearances were described by Rasool et al as periostitis, osteitis and metaphyseal changes.

Due to the relative rarity of presentation in UK hospitals the findings are no longer easily recognisable to the radiology trainee. This poster presents a case study in an infant with typical imaging features.

Educational Objectives

The poster aims to educate the radiology trainee in the typical appearances of congenital syphilis. It will also discuss the wider clinical considerations for this presentation.

Materials

An 8 week old infant presented to the Emergency department with a swollen tender right wrist. Initial imaging demonstrated a pathological radial fracture with distal metaphyseal lucency and periostitis. The clinical team suspected underlying metabolic or infective pathology.

Upon further imaging there was widespread periosteal reaction in all limbs, pathological radial fracture and metaphyseal lucencies. On careful inspection Wimberger's sign was present in the tibial metaphyses. Ultrasound demonstrated mild hepaosplenomegaly. Congenital syphilis was confirmed by the clinical team.

Conclusion

This poster will present classic congenital syphilis imaging findings from this case study across radiograph, ultrasound and MRI imaging. It will include post treatment appearances.

References

Rasool, M. N., and S. Govender. 'The skeletal manifestations of congenital syphilis. A review of 197 cases.' *The Journal of bone and joint surgery*. British volume 71, no. 5 (1989): 752-755.

Cooper, Joshua M., and Pablo J. Sánchez. 'Congenital syphilis.' In *Seminars in perinatology*, vol. 42, no. 3, pp. 176-184. WB Saunders, 2018.

Brion, L. P., M. Manuli, B. Rai, M. J. Kresch, H. Pavlov, and J. Glaser. 'Long-bone radiographic abnormalities as a sign of active congenital syphilis in asymptomatic newborns.' *Pediatrics* 88, no. 5 (1991): 1037-1040.

Poster: SCI-176

AUTOMATIC DETECTION OF SLIPPED CAPITAL FEMORAL EPIPHYSIS ON PEDIATRIC PELVIC RADIOGRAPHS USING MACHINE LEARNING

ANDREW Champion¹, AUDREY Ha³, BAO Do^{1,4}, CHARLES Fang^{1,4}, KEVIN Shea^{1,2}, MICHAEL Fadell^{1,2}

¹ Stanford University School of Medicine, Palo Alto, USA

² Lucille Packard Children's Hospital, Palo Alto, USA

³ Menlo-Atherton High School, Menlo Park, USA

⁴ VA Palo Alto Healthcare System, Palo Alto, USA

Introduction

Slipped capital femoral epiphysis (SCFE) is the most common hip abnormality in adolescence. In patients with suspected SCFE, initial evaluation is performed with frontal and frog leg lateral pelvic radiographs, as the frog leg view increases sensitivity. However, frequently symptoms are nonspecific leading to initial evaluation with frontal view only. Evaluation by single view can lead to subtle cases being missed. We therefore propose a system to automatically evaluate frontal pelvic radiographs for subtle SCFE cases.

Materials and Methods

We collected 503 de-identified pediatric pelvic radiographs and graded each hip (1006) as normal, subtle SCFE, or severe SCFE. The system consists of 2 modules. Module 1 detects severe SCFE by using an object detection neural network to detect and classify the lateral margin of the femoral physis as severe VS non-severe (normal or subtle). Module 1 was tested on 121 abnormal pelvic cases. Module 2 is an image classification neural network that distinguishes non-severe inputs from module 1 and classifies them as normal or subtle SCFE. Frog leg views served as gold standard for subtle cases.

Results

Module 1 analyzed 121 pelvic radiographs and classified 54 hips as severe and 188 as non-severe. Of the 54 classified as severe, 5 were normal; false positive rate 2.1% and accuracy 97.9%. Module 2 analyzed 104 non-severe hips and correctly classified 90/90 as normal and 13/14 as subtle SCFE; sensitivity 92.7% and overall accuracy 99% (103/104).

Conclusion

Our research holds promise for A.I. based evaluation of SCFE, potentially enabling expert level detection of subtle SCFE while requiring only single AP pelvic radiographs. However, further work is needed to improve generalizability and study clinical impact.

Poster: SCI-177

A CASE OF LATE DIAGNOSIS OF X-LINKED HYPOPHOSPHATEMIC RICKETS

DENISE A. Castro¹, ALÉXIA A. Cabral², CECÍLIA P. Silva², ISABELA R. P. Giesta², MICHELINE A. R. Souza³

¹ Kingston Health Science Centre, Queen's University, Kingston, CANADA

² Centro Universitário de Volta Redonda UNIFOA, Volta Redonda, BRAZIL

³ Instituto de Puericultura e Pediatria Martagão Gesteira IPPMG, Rio de Janeiro, BRAZIL

Summary of Presentation:

X-linked hypophosphatemic rickets (XLHR) is a multisystemic disorder that manifest in children once they start standing. Untreated, it will lead to severe handicap. Disease awareness helps early diagnosis improving health outcomes.

Educational Objectives:

- Review the radiological findings of XLHR.

- Stress the importance of early diagnosis and treatment for improved skeletal deformities and height outcomes.

Case Report:

Two-year-old female presented with genu varum, growth delay, pectus carinatum and asymmetric scaphocephalic skull shape. The only abnormal laboratory test was elevated serum alkaline phosphatase.

Radiographs demonstrated bulbous enlargement of costochondral junctions (rachitic rosary), frontal bossing with increased convolutional markings, growth plate widening with splaying, cupping and fraying of the metaphysis around wrists and knees and proximal femurs. The child was treated with oral vitamin D with a provisional diagnosis of vitamin D deficiency rickets. She was lost to follow up and returned 3 years later with more pronounced bony deformities on exam, having interrupted treatment during that period. She was then referred to a pediatric endocrinologist, with genetic analysis revealing a heterozygous mutation in the PHEX gene and the diagnosis of XLHR. She has been treated with oral phosphate for the past 3 months, has demonstrated some degree of bony metaphyseal healing and resolution of the rachitic rosary on follow up radiographs and a z-score of -1.76 to -1.59 SD for height since the first presentation.

Discussion:

X-linked hypophosphatasia is the prototype disorder of renal phosphate wasting and the most common form of heritable rickets.

Patients present when they start standing/walking with bowed legs and short stature. XLHR is often misdiagnosed for vitamin D deficiency rickets. It's imperative these patients are seen in an adequate center where diagnostic tools are available.

Early diagnosis and treatment, as well as patient compliance, can lead to better outcomes in linear growth, final height, bone mass accrual and fewer bone deformities.

Poster: SCI-178

T2 RELAXATION TIME CHANGES IN DISTAL FEMORAL CONDYLAR CARTILAGE IN CHILDREN WITH DISCOID MENISCUS

HAESUNG Yoon, JISOO Kim, HYUN JI Lim, MI-JUNG Lee
Severance Hospital, Department of Radiology, Seoul, SOUTH KOREA

Purpose: To investigate microstructural changes in distal femoral condylar cartilage by T2 relaxation time mapping in children with discoid meniscus. **Material and methods:** We retrospectively reviewed knee MRI with sagittal T2 maps of distal femoral condylar cartilage (FCC). Regions of interest were selected and T2 relaxation time profiles were generated for both medial and lateral FCC. FCC was measured in both weight bearing and non-weight bearing portions. Wilcoxon signed rank test was used to test within individuals.

Results: There were 79 patients (2-20 years) including 52 patients with lateral discoid meniscus, without difference in age between both groups. There was difference in lateral FCC in weight bearing and non-weight bearing portions in discoid group (median, 47.5 vs 52.6; $p=0.002$). Also weight bearing lateral FCC demonstrated lower T2 relaxation time compared to medial FCC in discoid group (median, 47.5 vs 51.7; $p = 0.014$). There was no difference in T2 relaxation time in normal group between weight bearing medial and lateral FCC and between non-weight bearing medial and lateral FCC.

Conclusion:

T2 relaxation time difference in weight bearing lateral femoral condyle cartilage in discoid meniscus patients suggests the possibility of microstructure changes in these patients.

Poster: SCI-179

IMAGING OF NON-ACCIDENTAL TRAUMA DURING THE BEGINNING OF THE 2020 NOVEL CORONAVIRUS PANDEMIC

SUSAN Taylor¹, ERICA Riedesel^{1, 2}, JONATHAN Loewen^{1, 2}, EDWARD Richer^{1, 2}

¹ Department of Radiology and Imaging Sciences, Emory University School of Medicine, Atlanta, USA

² Department of Radiology, Children's Healthcare of Atlanta, Atlanta, USA

Purpose: The 2020 novel coronavirus pandemic has greatly disrupted normal life throughout the world, including the USA. Drastic changes to limit the spread of infection, including social distancing, shelter-in-place orders, and cessation of in-person classes, have caused societal stress and uncertainty. These changes as well as limited social interactions outside of the family unit have the potential to place children at higher risk for non-accidental trauma (NAT). In this study, we evaluated if there were increased rates of NAT and if children presented with more serious or advanced injuries on skeletal surveys during the pandemic.

Materials and Methods: A retrospective, single institution study was performed. The radiology information system was queried for all skeletal surveys performed between March 1 – September 1 for the years 2017 – 2020. This period was chosen as the duration of most restrictive stay-at-home orders and social isolation during the beginning of the pandemic in the USA. Surveys performed for reasons other than non-accidental trauma were excluded. The radiology reports were then searched for the following: positive findings, more than 1 fracture, healing fractures, and fractures highly specific for NAT.

Results: There was a progressive increase in the number of skeletal surveys performed for suspected NAT from 2017 – 2020; however, there was also a statistically significant progressive decrease in positive surveys over the same time period. Additionally, indicators more suspicious for NAT, including high specificity fractures for NAT (11.9% vs 11.4%, $p = 0.825$), multiple fractures (17.5% vs 19.0%, $p = 0.581$), and healing fractures on initial skeletal survey (7.7% vs 8.9%, $p = 0.593$), were not significantly different in 2020 compared to prior years.

Conclusions: The incidence of non-accidental trauma, including more specific indicators of non-accidental trauma, did not significantly change during the initial 6 month period of the 2020 novel coronavirus pandemic for patients presenting for imaging evaluation.

Poster: SCI-180

MRI OF THE FOOT: A STEP TOWARDS DEFINING THE EARLY IMAGING FINDINGS IN JUVENILE IDIOPATHIC ARTHRITIS

CATRIONA Reid¹, CLAIRE Lloyd¹, NICK Wilkinson², SHEMA Hameed¹

¹ Department of Radiology, Evelina London Children's Hospital, London, UNITED KINGDOM

² Department of Rheumatology, Evelina London Children's Hospital, London, UNITED KINGDOM

Purpose

Juvenile idiopathic arthritis (JIA) of the foot is difficult to assess clinically, however can lead to significant morbidity if left untreated. Literature on specific MRI findings of the foot is sparse, and in subtle early disease, interpretation of findings can be challenging. The purpose of our study is to compare the MRI findings of children with known JIA with a selective control group of children who have had an MRI of the foot for other indications, in order to elucidate specific findings that can aid the radiologist in making a definite diagnosis of inflammatory arthropathy.

Materials and Methods

Children were assigned to two cohorts: those with JIA and those without. Two paediatric radiologists with a subspecialty interest in musculoskeletal imaging retrospectively reviewed MRI imaging of the foot in children, blinded to the final diagnosis. Demographic data and clinical details were obtained from the electronic patient notes in collaboration with a paediatric rheumatologist. MRI findings of joint effusions (measurements obtained of the deepest recess in all planes available), bone marrow oedema, erosions, synovial hypertrophy and tenosynovitis were recorded. A comparative analysis of the two groups was undertaken.

Results/ Conclusion

Data will be presented on 60 children who have undergone imaging of the foot, 30 of whom have a diagnosis of JIA and 30 without inflammatory arthritis. We will summarise the percentage of patients in each group with MRI criteria as detailed above, with particular emphasis on the amount of joint fluid and enhancement, as well as correlation with clinical findings. We will conclude by highlighting the most commonly encountered signs and patterns encountered on MRI in children with JIA of the foot.

Poster: SCI-181

WHOLE BODY POST-MORTEM COMPUTED TOMOGRAPHY VERSUS SKELETAL SURVEY IN THE DETECTION OF FRACTURES IN SUSPECTED CASES OF FATAL NON-ACCIDENTAL INJURY

DANIEL NICHOLAS Prince^{2,4}, HALVANI Moodley^{1,4}, JEANINE Vellema^{3,4}

¹ Charlotte Maxeke Johannesburg Academic Hospital, Johannesburg, SOUTH AFRICA

² Chris Hani Baragwanath Academic Hospital, Johannesburg, SOUTH AFRICA

³ Gauteng Department of Health, Johannesburg, SOUTH AFRICA

⁴ University of the Witwatersrand, Johannesburg, SOUTH AFRICA

Background:

The use of post mortem skeletal surveys (PMSS) and post mortem CT (PMCT) in first world countries has been explored. Despite the highest rates of child abuse being accounted for by the World Health Organization's African region, there is a paucity of research on the role and validation of post mortem imaging for NAI. No studies have been conducted on paediatric PMCT in South Africa.

Objectives:

Compare the fracture detection rates of PMCT and PMSS in suspected cases of fatal NAI, determine the incidence and fracture types, specificity for fracture locations for NAI and fracture dating. Determine the average study time of PMCT and PMSS.

Methods:

A prospective study of consecutive PMCTs from 1 August 2019 to 31 July 2020 at Charlotte Maxeke Johannesburg Academic Hospital was performed. All decedents first underwent a whole body PMCT (64 or 128 slice Philips CT scanner) and then whole body PMSS on digital radiography units. A paediatric radiologist, blinded to all details except age and sex, reviewed the PMSSs first and a month later all PMCTs.

Results:

A total of 20 decedents were included: 9 males (45%) and 11 females (55%). The ages ranged from 3 months to 10 years (median age = 24 months). Fractures were detected in 7/20 (35%) decedents. Five had fractures on both modalities: 2 cranial fractures and 1 fracture each of the humerus, radius and ulna. One decedent had a tibial metaphyseal corner fracture detected only on PMSS, another had a mandibular fracture, pubic ramus and iliac crest fractures detected solely on PMCT. There was no statistically significant difference in the number of fractures detected in all regions on both modalities, in the specificity of fracture locations for NAI or fracture dating. The PMCT acquisition time (median time 4.758 minutes; SD 1.486) was significantly faster than PMSS (median time 27.633 minutes; SD 11.944) [$p < 0.0001$].

Conclusion:

We describe the first use of paediatric PMCT in South Africa in investigating suspected fatal NAI and compared it to PMSS findings. Whilst there was no statistically significant difference in the number of fractures detected in all regions, PMCT proved useful in detecting the complexity of skull fractures and uncommon fractures of the facial and pelvic bones, occult on PMSS. PMCT is acquired faster with increased radiographer

compliance and satisfaction. Larger multicentre prospective studies are required in our resource - limited setting.

Poster: SCI-182

ARE LATERAL RADIOGRAPHS OF JOINTS HELPFUL IN THE SUSPECTED PHYSICAL ABUSE SKELETAL SURVEY?

RIWA Meshaka, SUSAN Shelmerdine, OWEN Arthurs
Great Ormond Street Hospital for Children NHS Trust, London, UNITED KINGDOM

Purpose

The latest UK Royal College of Radiologists (RCR) guidance (2017) for imaging suspected physical abuse (SPA) recommends the addition of lateral coned radiographs of joints to detect subtle metaphyseal fractures, despite limited published evidence for this addition. Our aim was to determine the additional yield of lateral views in appendicular fractures.

Method

A 1.5 year retrospective, single centre review of our imaging database was conducted for primary skeletal surveys undertaken for suspected physical abuse in children < 2years of age. The authorised reports were reviewed, and a re-review of the images was performed for fractures. Where a fracture was identified, frontal and lateral views were re-assessed by an independent observer.

Results

In total, 76 skeletal surveys were performed in 71 patients, with a mean age of 2 months. There were a total of 19 fractures in 9 individuals (3 cases of multiple fractures): 6 distal tibia, 5 distal radius, 2 distal femur, 2 distal ulna, 1 proximal tibia, 1 proximal humerus, 1 metatarsal and 1 proximal finger phalanx.

All 19 fractures were visible on the frontal view, of which 18/19 (94.7%) were also visible on the lateral view. Only one distal tibial fracture was not visible on the lateral view. The lateral view did not identify any fractures not captured by the frontal projection.

Conclusions

In our small cohort, all fractures could be seen on the frontal view. The lateral views may have been useful in adding to diagnostic certainty at the time of reporting, but did not lead to additional fracture detection. Multicentre, larger scale studies are required across a range of different fracture types for further evaluation.

Poster: SCI-183

WHAT IS THE EFFECT OF SELECTIVE ULTRASOUND SCREENING ON THE INCIDENCE OF LATE PRESENTATION OF DEVELOPMENTAL HIP DYSPLASIA?

LENE BJERKE Laborie¹, KAREN Rosendahl², AMIRA Dhouib³, PAOLO Simoni⁴, PAOLO Tomà⁵, AMAKA C. Offiah⁶

¹ Haukeland University Hospital, Department of Radiology, and HelseVest, Bergen, NORWAY

² University Hospital of North Norway, Department of Radiology, and the Arctic University of Norway, Tromsø, NORWAY

³ Réseau hospitalier Neuchâtelois, Neuchâtel, SWITZERLAND

⁴ Hôpital universitaire des enfants Reine Fabiola- Université Libre de Bruxelles, Bruxelles, BELGIUM

⁵ Ospedale Pediatrico Bambino Gesù, Rome, ITALY

⁶ University of Sheffield, Department of Oncology & Metabolism, Sheffield Children's NHS Foundation Trust, Sheffield, UNITED KINGDOM

Purpose: Different screening strategies for developmental dysplasia of the hip (DDH) exist. Despite screening efforts, cases of late presentation

continue to occur, often necessitating surgery. This systematic review and meta-analysis will assess the effect of newborn selective ultrasound screening for DDH on the incidence of late presentation, complications and surgery in infants and children, compared to only clinical and to universal ultrasound strategies.

M&M: We performed a systematic search across Medline and EMBASE databases, between January 1950 and February 2021. Search terms included hip dislocation, congenital; developmental dysplasia of the hip; developmental hip dysplasia; neonatal screening; newborn screening; mass screening; late presentation; early diagnosis; late sequelae; delayed diagnosis and undiagnosed diseases. A consensus-based evaluation of abstracts led to retrieval of relevant full text, original articles or systematic reviews in English only. These were assessed according to agreed eligibility criteria, and their reference lists reviewed to identify additional eligible publications. Following final consensus on included publications, data will be extracted, analysed and reported as per PRISMA and Prospero (CRD42021241957) guidelines.

Results: The initial search yielded 213 abstracts (Medline = 85, EMBASE = 128), of which 36 were duplicates. Of the 177 unique abstracts, 154 were excluded. We performed a consensus review of the 23 full text articles retrieved and of 12 additional full text articles identified. Data from the 21 eligible publications will be extracted and results of this systematic review and meta-analysis presented at IPR 2021. Although data extraction has not yet commenced, the variable nature of selective ultrasound screening strategies is already apparent. Reasons for the variability relate to eligibility criteria/risk factors for DDH, age at time of screening, prevalence of DDH in a given area, and experience of those performing clinical hip exams and/or hip ultrasound. There is also variation in the definition of late.

Conclusions: Variability in selective screening strategies and inconsistent definition of late cases is challenging. It is hoped that results of this systematic review and meta-analysis will allow both the recommendation of consistent definitions and the identification of the screening strategy most likely to reduce the prevalence of late presentation of DDH and its complications.

Poster: SCI-184

COMPARISON OF RELIABILITY OF MAGNETIC RESONANCE IMAGING USING CARTILAGE AND T1-WEIGHTED SEQUENCES IN THE ASSESSMENT OF THE CLOSURE OF THE GROWTH PLATES AT THE KNEE

OLA Kvist¹, ANA LUIZA Dallora², PETER Anderberg^{2,3}, OLA Nilsson^{1,4}, JOHAN Sanmartin Berglund², CARL-JOHAN Flodmark⁵, SANDRA Diaz^{1,6}

¹ Karolinska Institute, Department of Womens and Childrens Health, Stockholm, SWEDEN

² Blekinge Institute of Technology, Department of Health, Karlskrona, SWEDEN

³ Skövde University, Department of Health, Skövde, SWEDEN

⁴ Örebro University, School of Medical Science, Örebro, SWEDEN

⁵ Lunds University, Department of Clinical Science, Lund, SWEDEN

⁶ Lunds University, Department of Radiology, Lund, SWEDEN

To determine the state of growth plate closure of the knee in healthy adolescents and young adults and compare the reliability of staging using cartilage sequences and T1-weighted (T1W) sequence between pediatric and general radiologists.

A prospective, cross-sectional study of MRI of the knee with cartilage and T1W sequences was performed in 395 male and female healthy adolescents and young adults (14.0-21.5 yo) The examinations were performed on a 1.5-T MR scanner with dedicated knee coils. The femoral and tibial growth plates were assessed using a five-stage scale by two pediatric and two general radiologists. Intraclass correlation coefficient (ICC) was used to measure inter- and intra-observer reliability. Two-way random effects

model was chosen for the random selection of the study population and to generalize the reliability of the results to raters with the same experience. A mean value of 2 raters was used to assess the population, hence a “mean of k-raters” of 2. Absolute agreement of the ratings between the two observers was used. Cohen’s kappa coefficient (κ) was used to evaluate intra- and inter-observer agreement for T1W and cartilage sequences separately. Intraclass correlation was overall excellent. The inter- and intra-observer agreement for pediatric radiologists on T1W was 82% ($\kappa=0.73$) and 77% ($\kappa=0.65$) for the femur and 90% ($\kappa=0.82$) and 87% ($\kappa=0.75$) for the tibia. The agreement for general radiologists on T1W was 69% ($\kappa=0.56$) for the femur and 56% ($\kappa=0.34$) for the tibia. The inter- and intra-observer agreement for cartilage sequences was 93% ($\kappa=0.86$) and 89% ($\kappa=0.79$) for the femur and 95% ($\kappa=0.90$) and 91% ($\kappa=0.81$) for the tibia. The observership agreement for cartilage sequences was only calculated for pediatric radiologists.

Cartilage sequences are superior to T1W when assessing the growth plate and should be part of standardized MRI protocol and pediatric radiology experience is preferable.

Poster: SCI-185

MYOSONOGRAPHIC PATTERNS IN INFANTILE AND JUVENILE ONSET POMPE DISEASE

JULIAN Jürgens¹, RIEKE Meister¹, KATHARINA von Cossel², NICOLE Muschol², LUDWIG von Rohden³, JOCHEN Herrmann¹

¹ University Medical Center Hamburg-Eppendorf - Department of Pediatric Radiology, Hamburg, GERMANY

² University Medical Center Hamburg-Eppendorf - Department of Pediatrics, Hamburg, GERMANY

³ University Hospital Magdeburg - Clinic for Radiology and Nuclear Medicine, Magdeburg, GERMANY

Objectives

Pompe disease is a rare form of lysosomal storage disease with either infantile onset (IOPD) or late onset disease (LOPD). LOPD can be divided in juvenile and adult form. Lack of acid alpha-glucosidase results in intracellular accumulation of glycogen in muscle tissue. This leads to progressive decay of muscle cells. Myosonography is an established tool for screening and characterization of changes in skeletal muscle architecture. In the adult form of LOPD, characteristic sonographic changes have been described. The aim of this exploratory study was the identification of typical myosonographic patterns in children.

Methods & Materials

All pediatric patients with genetically established form of Pompe disease who had a standardized myosonographic examination between 08/2018-07/2019 were retrospectively assessed. Of 10 children identified during the study period 4 had IOPD (median age 44.5months, range 7-109) and 6 patients LOPD (median age 134months, range 44-297). Only one case with LOPD (44months) was clinically asymptomatic. Myosonography was performed on the front of the upper thigh in both legs, back of the lower right leg and upper right arm using a commercially available ultrasound system (Logiq E9, ML6-15 probe, GE Healthcare, Chicago, Illinois, USA). The obtained images were reviewed for recurring texture abnormalities by two musculoskeletal radiologists with experience in myosonography. The spectrum of changes was compared to the clinical presentation.

Results

All symptomatic patients (9/9 patients) showed changes in all examined muscle groups. Noted were increased muscle echogenicity with positive Pfeiffer-signs (apparent difference in echogenicity of gastrocnemius muscle vs. soleus muscle) and altered muscle architecture with inhomogeneity and recurring thick lamellas. Lower degree changes were also found in the clinical asymptomatic child with LOPD.

Conclusion

Children with Pompe disease are characterized by a myopathic pattern on myosonography, which can be already noted in cases with early onset IOPD and asymptomatic early presenters with LOPD. Further longitudinal examinations are needed in order to test if the method can be used to monitor the treatment effect of enzyme therapy.

Poster: SCI-186

YIELD OF POST-MORTEM SKELETAL SURVEYS IN INFANTS PRESENTING WITH SUDDEN UNEXPECTED DEATH

M KATHERINE Henry¹, TENIOLA I Egbe², SAVVAS Andronikou¹, PHILIP V Scribano³, SABAH Servaes¹, AMMIE White¹, JOANNE N Wood³

¹ Department of Radiology, Children's Hospital of Philadelphia, Philadelphia, USA

² Center for Pediatric Clinical Effectiveness, Children's Hospital of Philadelphia, Philadelphia, USA

³ Department of Pediatrics, Children's Hospital of Philadelphia, Philadelphia, USA

Purpose: In cases of sudden unexpected infant death (SUID), physical abuse should be considered and post-mortem imaging with skeletal survey (PM-SS) to detect abusive fractures is recommended. Little is known about the performance practices and yield of SS in SUID. Our objectives were to describe the population of infants who present to an urban emergency department (ED) with SUID and to report PM-SS performance and yield.

Materials and methods: We performed a retrospective study of infants <12 months with SUID who presented to an urban pediatric emergency department between 2007-2019. Infants with complex chronic conditions and out of hospital births were excluded. Medical records were reviewed to abstract clinical information, medical examiner (ME) referrals, and PM-SS performance. PM-SSs were reviewed by radiologists blinded to clinical history. Descriptive statistics were performed.

Results: Of 81 infants identified, 6 had complex congenital heart disease and 2 presented following out of hospital births. Of the remaining 73 infants included, 41 (56.2%) were male, 61 (83.6%) were publicly insured, median age was 2.4 months. Thirteen (17.8%) were premature, and 45 (61.6%) had concern for unsafe sleep environment. One infant (1.4%) had a nonspecific posterior thigh abrasion. No other external signs of trauma were documented. Medical providers performed cardiopulmonary resuscitation (CPR) in 71 (97.3%). PM-SSs were performed in all 73 infants (100%). Definite and/or possible fractures were identified in 6 (8.2%) PM-SSs. Four (5.5%) PM-SSs had definite fractures, including rib fracture(s) in 4 PM-SSs and an additional femur classic metaphyseal lesion (CML) in 1 PM-SS. Four (5.5%) PM-SSs had findings that included possible fracture(s), with possible rib fracture(s) in 4 PM-SSs and a possible femoral CML in 1 PM-SS. All 73 infants (100%) were referred to the ME.

Conclusion: PM-SS revealed fractures suggestive of trauma or highlighted possible fractures for further ME evaluation. Larger multicenter studies are needed to further evaluate PM-SS yield and other modalities.

Poster: SCI-187

CHILD ABUSE IMAGING AND FINDINGS IN THE TIME OF COVID

M KATHERINE Henry, JOANNE N Wood, COLLEEN E Bennett, BARBARA H. Chaiyachati, TENIOLA I Egbe, HANSEL Otero
Children's Hospital of Philadelphia, Philadelphia, USA

Purpose: The COVID-19 pandemic has placed profound stresses on families, which may increase the risk of child abuse. Simultaneously, decreased exposure to mandated reporters including medical providers raises concern that many cases of abuse may go undetected. Rates and yield of radiographic imaging performed to evaluate for suspected abuse injuries provide one perspective from which to monitor abuse. Our objectives were to compare the rate and yield of imaging to evaluate for abusive injuries prior to and during the COVID pandemic and to assess differences in injury severity. We hypothesized that during COVID, fewer children would undergo imaging for suspected abuse, but that imaging yield and severity would increase.

Materials and Methods: We retrospectively studied children <2 years undergoing skeletal surveys (SS) to evaluate for suspected abuse during the periods 3/15/2019-10/15/2019 (nonCOVID) and 3/15/2020-10/15/2020 (COVID) at a tertiary children's hospital. We abstracted imaging performed and injuries identified. Severe injuries were defined as requiring intensive care, intubation, having abnormal mental status, or resulting in death. We determined differences during time periods by chi-squared tests.

Results: We identified a 22% decrease in SS performance during COVID (N=161 nonCOVID versus 125 COVID). There were no changes in SS yield for clinically occult fractures (6.8% nonCOVID vs 6.4% COVID; P=0.9) or percent severe presentations (28.0% nonCOVID vs 24.8% COVID; P=0.6). The percent of children with head imaging performed (CT or MRI) was constant (63.4% nonCOVID vs 63.2% COVID; P=0.9) as was the yield for intracranial hemorrhage (41.2% nonCOVID vs 30.4% COVID; P=0.1). CPS involvement decreased during COVID (64.0% nonCOVID vs 50.4% COVID; P=0.02).

Conclusions: Though limited by statistical power, our results suggest that despite decreases in evaluations for abuse, SS yield for occult injury, severity of presentation, and head imaging yield did not change during COVID. Multi-center research is needed to further understand the pandemic's impact on abuse rates and severity.

Poster: SCI-188

Withdrawn

Poster: SCI-189

Withdrawn

Poster: SCI-190

FEASIBILITY OF ASSESSING SYSTEMIC OXALOSIS BY MRI

MARK BORN¹, ALOIS Sprinkart¹, GUIDO Kukuk¹, JÜRGEN Gieseke², BERND Hoppe³

¹ University of Bonn, Department of Radiology, Bonn, GERMANY

² Philips Healthcare, Hamburg, GERMANY

³ University of Bonn, Department of Pediatrics, Bonn, GERMANY

Introduction: Primary Hyperoxaluria (PH) is a rare inherited metabolic disease. Due to the deficiency of a specific hepatic enzyme, oxalate is produced in high amounts and excreted renally. As the level of oxalate in the plasma exceeds its solubility, in the course of the disease renal stones and nephrocalcinosis develop in parallel to a decreasing renal function. Finally

oxalate-deposition in different tissues as bone, heart or retina will occur, which is called systemic oxalosis.

The progress of the disease is however very variable, even in the same family, affected members can have a very different course of the disease. As there is no reliable and validated test to measure the amount of oxalate deposition in the body, except for instance bone biopsy, we tried to visualise bony oxalate deposition by MRI.

Methods: Using a highly resolved GE-sequence at 3 T (inplane resolution: 0,2 mm, FOV 140mm; matrix: 768 pixel, TE 11,5 ms, TR 35,4 ms) we examined the trabecular structure of the proximal tibia (r/t- 16 channel knee coil) in 9 healthy volunteers (Fig 1) and 31 patients with PH Type I in different stages. In severely affected patients the trabecular structure was hardly detectable, the intertrabecular spaces became strongly hypodense (Fig 2). The trabecular structure was rated using a 4-point scale (1 normal, 2 unclear, 3 mild changes, 4 severe changes) by two radiologists in a blinded way.

Results: Radiologist 1: volunteers (n=9) normal (scale 1) n= 8, pathologic (scale 3 or 4) n= 1; patients (n=31) normal n=13, pathologic n=15.

Radiologist 2: volunteers – normal n= 5, pathologic n= 1; patients – normal n=7, pathologic n=14.

Conclusion: The results are promising. Images show significant changes in severely affected patients. Just one false positive volunteer.

Poster: SCI-191

RELIABILITY OF CONE BEAM CT IN THE ASSESSMENT OF DESTRUCTIVE CHANGE OF THE TEMPOROMANDIBULAR JOINT IN PATIENTS WITH JUVENILE IDIOPATHIC ARTHRITIS (JIA)

THOMAS A. Augdal¹, OSKAR W. Angenete^{2,3}, MATS Säll³, KAREN Rosendahl^{1,4}, XIEQI Shi⁵

¹ UiT The Arctic University of Norway, Department of Clinical Medicine, Tromsø, NORWAY

² Norwegian University of Science and Technology, Faculty of Medicine, Department of Circulation and Medical imaging, Trondheim, NORWAY

³ St. Olav Hospital HF, Trondheim University Hospital, Department of Radiology and Nuclear Medicine, Trondheim, NORWAY

⁴ University Hospital of North Norway, Section of Paediatric Radiology, Tromsø, NORWAY

⁵ University of Bergen, Faculty of Medicine and Dentistry, Department of Clinical Dentistry, Bergen, NORWAY

Purpose

The temporomandibular joints (TMJs) are involved in the majority of children with JIA, however, accurate imaging markers for TMJ disease are sparse. We aimed to examine the agreement within- and between observers in the assessment of cone beam computed tomography (CBCT) features indicative of destructive change.

Material and methods

A subset of 84/228 CBCT examinations were identified from a longitudinal multicenter study (NorJIA), in order to define a novel scoring system. Volume reorientation and grading were carefully discussed and standardised prior to independent scoring (TAA, OWA, XQS) of the variables, masked for all information except study ID. TAA repeated the measurements after an interval of minimum three weeks. The fossa and the condyle were scored for irregularities and changes of shape with and without division into regions.

Intra- and interobserver agreement was analysed using kappa statistics. A kappa coefficient of <0 was considered poor, 0-0.20 slight, 0.21-0.40 fair, 0.41-0.60 moderate, 0.61-0.80 substantial and 0.81-1.00 almost perfect. Results are given for the right TMJ. The study was approved by the

Regional Ethics Committee, and written informed consent was obtained from each participant and/or caregiver.

Results

Temporal fossa: For 3 regions the intra-observer agreement was slight to moderate for irregularities (k=0.13-0.47) and fair to moderate for shape (k=0.31-0.56), while the corresponding inter-observer agreement was -0.04-0.18 and 0.20-0.58. The non-regional agreement was substantial for irregularities (k=0.66) and shape (k=0.77) within observers, moderate (k=0.55) for irregularities and substantial (k=0.65) for shape between observers.

Mandibular condyle: For irregularities, both the intra- and inter-observer agreement was slight to fair, with kappa values of 0.17-0.32 and 0.05-0.39, respectively, for 5 different regions. For shape, the corresponding figures were 0.14-0.60 and 0.10-0.52. The non-regional intra-observer agreement was substantial (k=0.77) for irregularities and almost perfect (k=0.82) for shape, while the corresponding interobserver agreement was 0.70 and 0.76.

Conclusions

We have shown that irregularities and flattening of the fossa and condyle are precise markers when assessed without attributing regions. Regional markers were not precise.

Poster: SCI-192

CBCT-BASED MEASUREMENTS OF THE TEMPOROMANDIBULAR JOINT IN PATIENTS WITH JUVENILE IDIOPATHIC ARTHRITIS (JIA)

THOMAS A. Augdal¹, OSKAR W. Angenete^{2,3}, MATS Säll³, KAREN Rosendahl^{1,4}, XIEQI Shi⁵

¹ UiT The Arctic University of Norway, Department of Clinical Medicine, Tromsø, NORWAY

² Norwegian University of Science and Technology, Faculty of Medicine, Department of Circulation and Medical imaging, Trondheim, NORWAY

³ St. Olav Hospital HF, Trondheim University Hospital, Department of Radiology and Nuclear Medicine, Trondheim, NORWAY

⁴ University Hospital of North Norway, Section of Paediatric Radiology, Tromsø, NORWAY

⁵ University of Bergen, Faculty of Medicine and Dentistry, Department of Clinical Dentistry, Bergen, NORWAY

Purpose

The temporomandibular joints (TMJs) are involved in the majority of children with JIA, however, accurate imaging markers for TMJ disease are sparse. We aimed to examine the precision (intra- and interobserver variability) of various measurements of the TMJ on cone-beam computed tomography (CBCT).

Material and methods

A subset of 84/228 CBCT examinations were identified from a longitudinal multicenter study (NorJIA), in order to define a novel scoring system. Volume reorientation and measurement points were carefully discussed and standardised prior to independent scoring (TAA, OWA, XQS) masked for all information except study ID. TAA repeated the measurements after an interval of minimum three weeks. As advised by Bland and Altman we calculated mean difference and standard deviation of the differences to establish 95% limits of agreement (LOA). The limit for clinically acceptable variability was set at 15% of the sample mean. Results are given for the right TMJ and with ramus corrected volume reorientation unless stated otherwise. The study was approved by the Regional Ethics Committee, and written informed consent was obtained from each participant and/or caregiver.

Results

Bland-Altman plots of differences within and between observers showed constant variance across the range of mean values. The limits of agreement (intra-

and interobserver) were wider than clinically acceptable for measurements of condyle length axial corrected (2.4 mm and 3.0–3.6 mm), fossa length axial corrected (4.0 mm and 5.3–7.2 mm), fossa length (4.3 mm and 4.8–5.5 mm), fossa depth method 1 axial corrected (1.8 mm and 1.7–4.6 mm), fossa depth method 1 (1.5 mm and 1.6–2.5 mm), fossa depth method 2 (2.0 mm and 2.8 mm), fossa-eminence inclination angle method 1 axial corrected (14.3° and 18.5–25.2°), fossa-eminence inclination angle method 1 (11.6° and 16.2–17.4°) and fossa-eminence inclination method 2 (26.3° and 24.3°).

Measurement of the condyle width axial corrected (mesio-lateral diameter) was borderline with intraobserver LOA of 2.4 mm (14.4%, right) and 3.2 mm (19.1%, left), and corresponding interobserver values 2.2–4.0 mm (13.6–24.0%).

Conclusion

We have shown that measurements of the fossa-eminence inclination angle, fossa depth, fossa length and condyle length are imprecise.

Poster: SCI-193

DIAGNOSTIC ACCURACY OF 3D ULTRASOUND AND ARTIFICIAL INTELLIGENCE FOR DETECTION OF PEDIATRIC WRIST INJURIES

JACK Zhang, NAVEENJYOTE Boora, SARAH Melendez, ABHILASH Rakkunedeth Hareendranath, JACOB Jaremkov
University of Alberta Faculty of Medicine and Dentistry - Department of Radiology and Diagnostic Imaging, Edmonton, CANADA

Background: Wrist trauma is common in children, and they typically receive x-ray imaging for diagnosis and treatment planning. However, many children do not have fractures and are unnecessarily exposed to radiation, and radiography often requires time-consuming transfer to a different department. Ultrasound can be performed at bedside with a handheld probe, detecting fractures as cortical disruption. Modern tools including three-dimensional ultrasound (3DUS) and artificial intelligence (AI) have not yet been applied to this task. We aim to assess 1) feasibility, reliability, and accuracy of 3DUS for detection of pediatric wrist fractures and 2) examine the accuracy of AI-aided detection of fractures from 3DUS sweeps.

Methods: Children (age 0 – 17 years) presenting to an emergency department with unilateral upper extremity injury to the wrist region were scanned on both affected and unaffected limb. Radiographs of the symptomatic limb were also obtained for gold-standard diagnosis. Ultrasound scans were read by three individuals to determine reliability. AI interpretation was evaluated as a fourth reader and compared against human readers. Scans were separated into 21 training and 36 testing images; the key frames were labelled. Several CNNs with different parameters were trained and the best 3 were included in the final classifier.

Results: 30 participants were enrolled resulting in scans from 55 wrists, 2 were excluded due to incorrect labelling. The median reader achieved a sensitivity of 1.00 and specificity of 0.90. Individual readers achieved a moderate to high interrater reliability (ICC=0.536 to 0.602). Two cases had subtle fractures identified on ultrasound and visible only in hindsight on x-ray, while 3 cases had ultrasound findings considered false-positive due to artifacts.

AI interpretation was indistinguishable from human interpretation, with all fractures detected in the test set of 36 images (sensitivity = 1.0). Similar to the human interpretation, the AI approach also had 3 false positives most likely due to image artifacts.

Conclusion: 3D ultrasound is accurate for diagnosis of wrist fractures in children and can be performed reliably. The high sensitivity suggests ultrasound may be able to rule out fractures in the emergency department and reduce number of radiographs taken. Automated AI interpretation of 3DUS was as accurate as human readers.

Poster: SCI-194

A CASE SERIES; IMAGING FINDINGS OF CHRONIC RECURRENT MULTIFOCAL OSTEOMYELITIS

SÜKRIYE Yilmaz¹, BIRSEL Sen Akova¹, BERRIN Demir¹, BIRSIN Özcakar², PINAR ÖZGE Avar², SUAT Fitoz¹

¹ Ankara University Department of Pediatric Radiology, Ankara, TURKEY

² Ankara University Department of Pediatric Rheumatology, Ankara, TURKEY

Chronic recurrent multifocal osteomyelitis (CRMO) is primarily a disorder of children and adolescents characterized by multifocal bone pain secondary to sterile osseous inflammation. CRMO should be considered as an exclusion diagnosis in cases of subacute and chronic multifocal osteomyelitis. Radiologists should be well aware of the characteristic radiological appearances and distribution of the disease. Typical involvement sites are metaphyses of the long bones and medial parts of the clavicle and axial skeleton with pelvic bones. We aimed to describe the imaging findings of 23 patients followed up in our unit and diagnosed with CRMO.

Materials and Methods: A total of 59 magnetic resonance imaging (MRI) examinations of 23 patients with CRMO were retrospectively evaluated. Eight of them were whole body MRI. MR imaging findings at initial diagnosis and during follow-up period were recorded. Also the initial location of the disease and distribution of the symptoms with accompanying clinical conditions were examined.

Results: Patients usually had pain in more than one area at the time of first admission to the hospital. Knee and hip were the most commonly affected locations. Mean age at diagnosis was 8.5 years. As a co-existing disease, one patient had Crohn disease and Familial Mediterranean fever (FMF), one patient diagnosed as FMF and three patients had widespread skin rashes. The most common referred examination was sacroiliac joint MRI and the most common imaging finding was sacroiliitis. Vertebral involvement accompanied in 9 patients. Only two patients had clavicle involvement. Accompanying soft tissue changes included as joint effusion in two patients and synovitis in three patients.

Conclusions:

CRMO is a diagnosis of exclusion and tentative approach and teamwork among pediatric rheumatologist, orthopedic surgeon, radiologist, and pathologist is needed. Well-known associations are skin lesions, auto-inflammatory disorders and inflammatory bowel disease, especially Crohn disease.

In cases with metaphyseal involvement it is difficult to differentiate from hematogenous osteomyelitis. However, clavicular involvement is more diagnostic for the CRMO. Although higher frequencies up to 30% are reported in the literature only two of our 23 patients (9%) had clavicle involvement. We also observed mild synovitis and joint effusion which is not studied previous reports.

Poster: SCI-195

LONG TERM SEQUELAE OF CHRONIC NONBACTERIAL OSTEOMYELITIS

SHAWN Sato¹, ALEKSANDER Lenert², SEDAT Kandemirli¹, MIKHAEL Sebaaly¹, POLLY Ferguson³

¹ University of Iowa Stead Family Children's Hospital, Division of Pediatric Radiology, Iowa City, USA

² University of Iowa, Department of Internal Medicine, Iowa City, USA

³ University of Iowa Stead Family Children's Hospital, Division of Rheumatology, Allergy and Immunology, Iowa City, USA

Purpose: Chronic nonbacterial osteomyelitis (CNO) or chronic recurrent multifocal osteomyelitis (CRMO) is a rare auto-inflammatory condition characterized non specific bone pain and with a waxing and waning course. Because of the nonspecific clinical and radiologic findings seen in this disease, reaching a correct diagnosis can be a long process. We review the long term sequelae of CNO as well as the rates of development of long term damage in these patients.

Methods and Materials: Institutional review board approved this retrospective HIPAA compliant study; informed consent was waived. Whole body MRIs for patients with CNO were reviewed from April 2014 through April 2020.

Results: A total of 312 whole body MRIs were evaluated from 106 children and young adults (35 male, 71 female). Patients had an average of 1.7 years of follow up (max 5.1 years) with an average of 2.9 whole body MRIs (max 9). During the course of follow up, 42 (39.6%) patients developed damage which was defined as hyperostosis (24 patients, 12.2 %), physeal bars (3 patients, 7.1%) or fractures (19, 9.7%).

Conclusion: Since CNO is a rare, difficult to diagnose disease, patients often experience significant delays between onset of symptoms and diagnosis. We identify that a significant portion of patients with CNO develop long term damage, reinforcing the importance of familiarity with this disease process and timely diagnosis and treatment to try and mitigate long term sequelae.

Poster: SCI-196

SPONTANEOUS CORRECTION OF CONGENITAL ANTEROLATERAL TIBIAL BOWING ASSOCIATED WITH POLYDACTYLY: A CASE REPORT

YOUNG JIN Ryu, JI YOUNG Kim

Seoul National University Bundang Hospital, Seongnam, SOUTH KOREA

Congenital anterolateral tibial bowing is commonly associated with neurofibromatosis type 1 (NF-1), which usually leads to recurrent fractures and is considered a precursor to congenital pseudoarthrosis of the tibia. However, when a child presents with combined ipsilateral polydactyly of the hallux, the congenital anterolateral bowing of the tibia had a favorable prognosis with spontaneous correction of the bowing. Thus, pediatric radiologists need to recognize that the congenital anterolateral tibial bowing associated with polydactyly is a rare and distinct disease entity that should be differentiated with NF-1.

A 2-week-old boy visited our hospital due to congenital deformity of left lower leg and polydactyly of the hallux. His lower leg radiographs showed anterolateral bowing in the middle third of the left tibia with a normal left fibula. Radiographs of his left foot demonstrated duplication of the first distal phalanx with varus deformity. The patient revisited our hospital at the age of 6 months to undergo a correction operation of polydactyly. Plain radiographs of his left tibia revealed spontaneous partial correction of anterior and lateral bowing. Radiographs obtained at the age of 1 year showed the complete correction of the bowing in the sagittal plane and advanced partial correction in the frontal plane. The patient was followed up until the age of 20 years, and there was no evidence of the bowing recurrence and pathologic fracture.

Congenital anterolateral tibial bowing and polydactyly is a distinct entity diagnosed clinically on physical and radiographic findings. Congenital anterolateral tibial bowing and polydactyly show a favorable prognosis with a spontaneous correction of the bowing. Congenital anterolateral

tibial bowing and polydactyly should not be confused with NF1. It is unnecessary to wear protective leg braces or perform examinations and familial counseling for NF-1.

Poster: SCI-197

TO CT OR NOT TO CT? IMAGING STRATEGY IN BLUNT PAEDIATRIC TRAUMA

SPARSH Prasher, JOSHUA Taylor, SRIKRISHNA Harave
Alderhey Children's Hospital, Liverpool, UNITED KINGDOM

Purpose:

To assess the imaging strategy employed in the assessment of children presenting with major trauma. Previously data from the Trauma & Research Network (2012), demonstrated that children imaged in a non-paediatric major trauma centre are more likely to undergo a whole body CT (9% vs 3%).

Regional practice is being compared to the UK national guidelines as recommended by the Royal Colleges of Radiologists (RCR) and Paediatric and Child Health and National Institute of Clinical Excellence. The key recommendation by these bodies is that a blanket whole body CT is inappropriate in children presenting after trauma, and a more targeted approach based on clinical examination and using the lowest possible exposure to ionising radiation be used. When CT of the abdomen is performed a dual phase protocol is recommended.

Methods:

We are performing a retrospective analysis of the imaging strategy employed in the assessment of paediatric trauma over a course of 5 years in a major paediatric trauma centre and 6 other hospitals in the Merseyside region of the UK.

Results:

Preliminary results show that the hospitals seem to be following paediatric imaging guidelines (RCR/RCPCH) to a large extent, but full analysis (including dose data) will be available in time for the conference.

Conclusions:

Trauma is a leading cause of mortality and morbidity in children and understandably causes anxiety in clinicians. Imaging plays a key role in the assessment of injuries. However, unlike in adults, in whom there is some evidence that prompt whole body CT is associated with more favourable outcomes, no such data exists for children and such blanket approach to imaging is inappropriate in children. This is because injury patterns in children are different than those in adults due to differences in size and physiological factors, for example, higher elasticity of tissues, narrow calibre of vessels and a higher vasoconstrictive response which can limit bleeding. Indeed in many trauma centres the decision to pursue surgical treatment is based on the patient's haemodynamic status over the severity of injury based on imaging. Importantly the developing tissues are more radiosensitive and the stochastic effects of exposure to extensive ionising radiation is an important consideration, as children have a longer potential lifespan to develop radiation induced neoplasms. Therefore an imaging strategy tailored to the individual case is essential in delivering a high standard of care.

Poster: SCI-198

THE EFFECT OF THE UK LOCKDOWN ON EMERGENCY RADIOLOGY PRACTICE IN A TERTIARY CHILDREN'S HOSPITAL

GARETH Davies, ANDREW Fitzsimons, ANNE Paterson
Royal Belfast Hospital for Sick Children, Belfast, UNITED KINGDOM

Aim: UK lockdown started on 23.03.2020, twelve days following the WHO's declaration of a global pandemic due to Covid-19. Schools and play parks closed, team sports ceased and social circles shrank. And the number of children presenting to the Emergency Department (ED) fell. Our aim was to assess the impact of reduced ED attendance on the Radiology Department (RD), paying particular attention to delayed presentation of injury.

M+M: Retrospective cohort study. All children referred from ED to RD between 24.03.20 – 23.04.20 were compared with the same period in 2019. Information pulled from PACS and ED database.

Referrals for trauma radiographs and CT were included. Demographic data, mechanism/time of injury, and results of imaging were recorded.

Results: In 2019, 596 children had trauma radiographs and 22 children CT exams. In 2020, this fell to 246 radiographs and 11 CT exams, 41.3% and 50% less respectively.

106-17.8% and 44-17.9% children presented >24 hours after injury in 2019 and 2020 respectively. All 2019 fractures were acute. In 2020, 3 children presented with healing fractures. There were no cases of suspected inflicted injury in either group.

There were 217/582-37.3% children in 2019 and 124/232-53.4% children in 2020 with fractures on their radiographs.

134/582-23% children in 2019 were injured in ways not accessible to children during lockdown: at schools or in play areas and during team sports. All children in the 2020 group had 'Covid compliant' injury mechanisms.

Conclusions: During the first month of UK lockdown, the number of children requiring imaging following trauma fell by over 40%, with a greater percentage of those imaged showing fractures on their radiographs; 3 children had a delayed presentation. Our study figures imply that children with more minor injuries were being cared for by their families rather than attending the ED, but also that attendance numbers fell due to the reduction in available play and sports activities.

Poster: SCI-199

MR IMAGING IN PEDIATRIC KNEE LYME ARTHRITIS

SURAJ Parikh¹, JOSHUA Powell¹, JEAN-KIMBERLY Rongo¹, AMISHA Shah²

¹ University of Pittsburgh Medical Center Department of Radiology, Pittsburgh, USA

² Children's Hospital of Pittsburgh Department of Radiology, Pittsburgh, USA

Introduction:

With a growing incidence, Lyme disease has reached endemic levels in Southwestern Pennsylvania. The early differentiation of Lyme arthritis from septic arthritis has profound implications on patient management. Lyme arthritis is treated with outpatient antibiotics, while septic arthritis requires emergent irrigation and drainage. A diagnostic dilemma exists in differentiating the two arthritides, and a reliable diagnostic test may prevent unnecessary surgery. MRI may assist in equivocal cases; however, definitive characterization of MRI imaging features in Lyme arthritis is limited at this time. Our objective of this study is to further elaborate on the MRI features of knee Lyme arthritis in serologically positive Lyme patients at our tertiary care Children's Hospital within a Lyme-endemic region of the USA.

Materials and Methods:

After IRB approval, we retrospectively reviewed all pediatric cases of serologically positive Lyme Arthritis from 2010 to 2020. Inclusion criteria included those aged less than or equal to 18, a positive serologic Lyme titer and Western blot, and the presence of knee magnetic resonance imaging. Exclusion criteria included patients older than 18. A

fellowship-trained pediatric radiologist retrospectively reviewed the imaging of all cases. Each case was analyzed for patient demographics, use of Gadolinium-based IV contrast, MRI features including joint effusions, synovitis, muscle and soft tissue edema, and lymphadenopathy. Non-parametric univariate analysis was completed on the aggregate with an alpha set at 0.05.

Results:

A total of 32 images were obtained with contrast used in 19 of the cases. Joint effusion and synovitis were seen in nearly all of the patients evaluated. Moderate to large effusions were seen in 65% of cases. Synovitis was not correlated with the size of the effusion. In those cases, the synovial lining was uneven in thickness and showed intense bilaminar enhancement. Other significant findings included myositis (65%) and popliteal lymphadenopathy (69%). Minimal subcutaneous edema (25%), bone marrow edema (6%), or bony erosion was seen (0).

Conclusion:

The most frequently seen MRI features of knee Lyme arthritis were joint effusion, synovitis, myositis, and lymphadenopathy, while less frequently seen features included subcutaneous edema and bone marrow abnormality. Our preliminary data suggests that MRI can be an important diagnostic tool in the diagnosis of pediatric knee Lyme arthritis.

Poster: SCI-200

MAGNETIC RESONANCE IMAGING SACROILIAC JOINT SCORING SYSTEM FOR JUVENILE IDIOPATHIC ARTHRITIS: ARE WEIGHTS FOR ITEMS NEEDED? MULTICENTRIC MULTIDISCIPLINARY OMERACT INITIATIVE

TARIMOBO Ootobo¹, MIRKAMAL Tolend¹, SAYALI Joshi¹, MICHAL Znajdek², JENNIFER Stimec¹, ARTHUR Meyers³, NELE Herregods⁴, JACOB Jaremko⁵, LENNART Jans⁴, SHIRLEY Tse⁶, MARION van Rossum⁷, APPENZELLER Simone⁸, PAMELA Weiss⁹, DAX Rumsey¹⁰, OLYMPIA Papakonstantinou¹¹, JOHN Carrino¹², EVA Kirkhus¹³, NIKOLAY Tzaribachev¹⁴, ALOYSIUS Ligha¹⁵, EMILIO Inarejos¹⁶, PHILIP Conaghan¹⁷, ROBERT Lambert⁵, WALTER Maksymowych¹⁰, MANUELA Perez¹⁸, RAHIM Moineddin¹⁹, NIGIL Haroon²⁰, IWONA Sudol-Szopinska², ANDREA Doria¹

¹ Hospital for SickKids, Diagnostic Radiology, Toronto, CANADA

² National Institute of Geriatrics Rheumatology and Rehabilitation, Radiology, Warsaw, POLAND

³ Cincinnati Children's Hospital Medical Center Department of Radiology and Medical Imaging, Cincinnati, USA

⁴ Universitair Ziekenhuis Gent, Radiology; Prinses Elisabeth Children's Hospital, Division of Pediatric Radiology, Ghent, BELGIUM

⁵ University of Alberta, Radiology, Edmonton, CANADA

⁶ Hospital for SickKids, Rheumatology, Toronto, CANADA

⁷ Reade and Emma Children's Hospital Amsterdam University Medical Center, Amsterdam Rheumatology and Immunology Center, Amsterdam, NETHERLANDS

⁸ Universidade Estadual de Campinas, Rheumatology, Campinas, BRAZIL

⁹ Children's Hospital of Philadelphia, Rheumatology; University of Pennsylvania Perelman School of Medicine, Pediatrics, Philadelphia, USA

¹⁰ University of Alberta, Rheumatology, Edmonton, CANADA

¹¹ Attikon General Hospital, National and Kapodistrian University of Athens, Radiology, Athens, GREECE

¹² Hospital for Special Surgery, Department of Radiology and Imaging, New York, USA

¹³ Oslo University Hospital, Radiology, Oslo, NORWAY

¹⁴ Medical Center Bad Bramstedt, Pediatric Rheumatology, Bramstedt, GERMANY

¹⁵ Niger Delta University, Anatomy, Amassoma, NIGERIA

¹⁶ Sant Joan de Deu, Radiology, Barcelona, SPAIN

¹⁷ University of Leeds, Rheumatology, Leeds, UNITED KINGDOM

¹⁸ University of Toronto, Radiology, Toronto, CANADA

¹⁹ University of Toronto, Family Medicine, Toronto, CANADA

²⁰ Toronto Western Hospital, Rheumatology, Toronto, CANADA

Background. The sacroiliac joint (SIJ) is difficult to be assessed clinically in children with juvenile idiopathic arthritis (JIA). Hence, MRI becomes an essential diagnostic tool for assessment of the joint status for guiding management. Without standardization of measurements of pathology in SIJs, it is not possible to compare results of clinical trials in SIJ MRI conducted in different centres and to properly follow SIJs of patients over time. This study focuses on the face validity of the recently developed JIA MRI scoring system for SIJs (JAMRIS-SIJ).

Objective. To determine the relative importance of weights for measurement items of the JAMRIS-SIJ.

Methods. An adaptive multi-criteria decision-making application was used to conduct two discrete choice experiment (DCE) surveys to determine the relative importance weights of the items in the JAMRIS-SIJ inflammation and damage domains. These DCE surveys were completed independently by members of the outcome measure in rheumatology (OMERACT) juvenile arthritis MRI (JAMRI) working group, which comprise of international experts in imaging, rheumatology, and outcome measure methodology. Each DCE survey question asked the expert to compare two hypothetical patient profiles which are otherwise similar but different at two items at a time and select which item shows a more severe stage of inflammation or osteochondral damage. Weights obtained from each of the expert participants were averaged across the expert group to serve as the template importance weights for the scoring system for future phases of its validation.

Results. Seventeen experts completed the DCE survey (8 radiologists and 9 rheumatologists). Concerning the inflammation domain, osteitis (24.7%) and bone marrow edema (24.3%) reported higher group-averaged percentage weights compared to inflammation in erosion cavity (16.9%), joint space enhancement (13.1%), joint space fluid (9.1%), capsulitis (7.3%) and enthesitis (4.6%). Similarly, concerning the damage domain, ankylosis (41.3%) and erosion (25.1%) showed higher group-averaged weights compared to backfill (13.9%), sclerosis (10.7%), and fat metaplasia lesion (9.1%).

Conclusions. The DCE method identified differences in relative weights between the JAMRIS-SIJ measurement items. Determination of the relative weights provided expert-opinion-driven score scaling and face validity for the JAMRIS-SIJ, enabling the subsequent evaluation of its longitudinal construct validity.

Poster: SCI-201

CORRELATING CLINICAL EXAM FINDINGS TO IMAGING FINDINGS FOR NEWBORNS WITH SUSPECTED HIP DYSPLASIA

DONALD Lee

Staten Island University Hospital, NYC, USA

Purpose

Developmental hip dysplasia in a healthy newborn involves abnormal development of the hip joint. This can be detected as hip instability on clinical exam, which in most newborns resolve within the first 2 months of age. However, untreated hip dislocation has serious functional consequences, with patients developing problems such as accelerated hip osteoarthritis, impaired gait, and lifelong back problems. Due to such serious consequences, several

screening strategies involving physical exam findings and diagnostic imaging have been proposed to diagnose hip dysplasia for subsequent treatment. Dynamic hip ultrasound is the standard imaging modality for diagnosing hip dysplasia due to its utility in functional assessment of hip movement. Given that physical examination is the primary assessment tool in the physician office, several studies have compared physical exam findings with ultrasound imaging to assess their diagnostic predictability. One study described that 17.8% of newborns with a hip click were found to have concurrent hip abnormalities on ultrasound. One recent article described 25/66 newborns with asymmetric skin folds were found to have dysplastic hips on ultrasound or radiographs. This single institutional study will attempt to correlate the predictability of various physical exam findings to radiologic imaging for newborns with suspected hip dysplasia.

Methods

Retrospective chart review of newborns with suspected hip dysplasia. Clinical information such as physical exam findings and ultrasound/radiograph/MR imaging reports will be obtained. Each physical exam finding will then be assessed for its diagnostic predictability based on how prevalent it is in newborns with radiologically defined developmental hip dysplasia.

Results

This study is in the process of data collection.

Conclusion/Significance

To determine the diagnostic value of various physical exam findings based on their prevalence in newborns with radiological evidence of developmental hip dysplasia.

Poster: SCI-202

3D SCOLIOSIS ANGLE PROVIDED BY RASTER-STEREOGRAPHY VERSUS 3D RECONSTRUCTION OF LOW DOSE RADIOGRAPHY (EOS) IN ADOLESCENT IDIOPATHIC SCOLIOSIS: A PRELIMINARY STUDY

MERYLE Laurent ¹, ANNE Tabard-Fougère ², CHARLOTTE de Bodman ³, SYLVIANE Hanquinet ¹, ALICE Bonnefoy-Mazure ², STÉPHANE Armand ², SEEMA Toso ¹, ROMAIN Dayer ²

¹ Geneva University Hospital - Children Hospital - Unit of Pediatric Radiology, Geneva, SWITZERLAND

² Geneva University Hospital - Children Hospital - Pediatric Orthopedics, Geneva, SWITZERLAND

³ Lausanne University Hospital - Children Hospital - Pediatric Orthopedics, Lausanne, SWITZERLAND

Purpose:

Gold standard practice of care for imaging scoliosis consists of low dose radiography (EOS) with anteroposterior and lateral views to analyze the Cobb angle for treatment planning. As scoliosis is a 3-dimensional (3D) deformity, a 3D imaging tool can improve evaluation of the true scoliosis angle. The 3D reconstruction of EOS images can be used to evaluate the 3D scoliosis angle. Another emerging technique is 3D modeling of the spine with raster-stereography (RASTER) that avoids radiation. It allows for the measurement of spinal deformity using the back's surface topography, the shape of the patient's back being recorded in a standing position by projecting parallel light raster lines onto the skin surface.

This study aimed to compare the value of 3D scoliosis angle (SA) as computed by RASTER with 3D-EOS in adolescent idiopathic scoliosis (AIS) patients.

Materials and Methods :

53 AIS children (female = 32) aged 13.5±1.9 years were recruited. The scoliosis angle of the major curve provided by the RASTER (SAR) and the 3D-EOS was extracted. Mean differences between measurements provided by each system were evaluated. Agreement and correlation were computed with intraclass correlation coefficient (ICC) and Pearson correlation coefficient (Cor), respectively.

Results :

Scoliosis angles with those 2 techniques were strongly correlated (Cor > 0.85) with high agreement (ICC > 0.85). But mean difference between SAR and 3D-EOS was 7.5+/-6.4° and 56 % patients had a difference superior to 5°, considered as clinically relevant.

Conclusion :

This preliminary study showed an excellent correlation in scoliosis angle measurements by RASTER compared to EOS. However, the mean difference value between these systems was clinically relevant with more than 50% patients with a difference > 5°. Further studies are needed to see if a conversion factor could be applied, so that RASTER could be used in clinical practice as a complementary or alternative radiation-free technique to monitor 3D scoliosis angle.

Poster: SCI-203

“STAY HOME, STAY SAFE” - HOW SAFE IS HOME?

HARSIMRAN Laidlow-Singh, JONATHAN Colledge, ANOUSHKA Ljutikov, CHARLOTTE A. Roberts
Department of Imaging, The Royal London Hospital, London, UNITED KINGDOM

Purpose: In March 2020, the British Prime Minister decreed that everybody should stay at home to stay safe, as the UK went into lockdown due to the novel Coronavirus pandemic. However, what did that mean for those most vulnerable in our society, where home is not a safe place? Our institution serves some of the most deprived families in the country. The objectives of this work are to retrospectively review the frequency of children under two years of age being investigated for non-accidental injury during that time period, and identify the effect of this time of extraordinary pressures when London's Metropolitan Police Service received an increased number of calls-for-service regarding domestic incidents.

Poster: SCI-204

A REVIEW OF THE EFFECT OF THE SARS-COV-2 PANDEMIC ON PAEDIATRIC TRAUMA IN A MAJOR TRAUMA CENTRE

HARSIMRAN Laidlow-Singh, ANOUSHKA Ljutikov, JONATHAN Colledge, SUSAN Cross, CHARLOTTE A. Roberts
Department of Imaging, The Royal London Hospital, London, UNITED KINGDOM

Purpose: This poster will look at the epidemiology of paediatric trauma patients imaged at one of Europe's busiest major trauma centres. The frequency of attendances, mechanism of injury, and injury severity score will be compared for 12 months from the start of the first UK lockdown and contrasted with the same period for the preceding year. As well as highlighting how enforced changes in behaviour affected the occurrence of trauma, we will review the trends throughout the 12 month periods, demonstrating how the incidence of paediatric trauma changed with the public's shifting tolerance for the restrictions.

Poster: SCI-205

REVIEW OF PEDIATRIC HIP ULTRASOUNDS: ARE WE PERFORMING TO NORTH AMERICAN STANDARDS?

TYSON Keddie, EILEEN Tu, TERESA Liang
University of Alberta, Edmonton, CANADA

Summary of presentation: Presenting results of a 1st stage clinical audit identifying areas not meeting North American recommendations for paediatric hip ultrasounds. 2nd stage re-audit currently being performed to assess compliance.

Educational objectives: Review and identify shortcomings of current departmental paediatric hip ultrasonography. Highlight the importance and current standards for developmental dysplasia of the hips screening.

Purpose: No absolute contraindications exist for assessing developmental hip dysplasia (DDH) ultrasounds, however; recommendations in North America suggest performing scans after 4 weeks to minimize physiological hip laxity findings, and before 6 months (femoral head ossification limits utility), with accepted indications/risk factors. Non-compliance can lead to unnecessary studies, increased follow-ups, and potentially erroneous interventions. The aim was to assess adherence to these recommendations.

Methods: 12 consecutive months of paediatric hip ultrasounds at the University of Alberta Hospital were reviewed, with 599 total scans for 474 patients. Trauma studies were excluded. Each study was assessed for age, indication/risk factor, documented descriptors, diagnosis.

Results: Our audit indicated that 53/474 patients ages were below 4 weeks and 4/474 patients were over 6 months. For less than 4 weeks old, 41/53 were identified as abnormal. For those identified abnormal under 4 weeks old, 9/41 normalized without treatment by 12 weeks of age. In total 22/41 identified abnormal under 4 weeks normalized without treatment. 91/474 patient scans did not include clinical reasoning/history. 163/599 scans did not annotate acetabular morphology. Of the 474 initial patient scans, 17/474 were identified as subluxated, while 14/474 were identified as dislocated. The targets for the appropriate age, necessary indication/risk factors, and inclusion of acetabular morphology were not achieved.

Conclusion: The target was not achieved. Results were discussed in a subgroup presentation. Departmental protocol was revised to perform DDH ultrasounds between 4 weeks and 6 months unless orthopedic referral. Indications/risk factors are now required for all referrals. A standardized template has been updated for DDH reporting.

Poster: SCI-206

IMPACT OF COVID-19 PANDEMIC ON MUSCULOSKELETAL EXAMINATIONS IN A PAEDIATRIC EMERGENCY RADIOLOGY DEPARTMENT

MARIANTONIETTA Francavilla¹, GIAMPIERO Bottari², BIAGIO Solarino², ALESSANDRO Dell'Erba², MAURIZIO Aricò³, GIANDOMENICO Stellacci¹

¹ U.O.S.D. Radiodiagnostica Ospedale Giovanni XXIII-A.O.U. Policlinico, Bari, Italy, Bari, ITALY

² Dipartimento Interdisciplinare di Medicina - Università degli Studi di Bari - U.O.S. Rischio Clinico, Bari, Italy, Bari, ITALY

³ U.O. Malattie Metaboliche e Genetiche Ospedale Giovanni XXIII - A.O.U. Policlinico, Bari, Italy, Bari, ITALY

SUMMARY

During the Covid-19 pandemic, the number of accesses to the paediatric Emergency Department (pED) in Italy sharply decreased to nearly 70% compared to the last years.

Purpose

To evaluate the difference in imaging examination in musculoskeletal (MSK) traumatic injury in the pED comparing the Covid era with the previous years, focusing on the possible impact that Covid-19 pandemic had on imaging in the field of trauma.

Materials and Methods

All MSK imaging studies performed in the pED of a tertiary children's Hospital during the first wave of the Covid-19 pandemic (between March and May 2020) were collected. Data were compared with those retrospectively collected from a control time interval (March to May 2019).

Results

In the pre-Covid control era, the execution of 669 imaging studies revealed the presence of bone fractures in 145/568 children (25,5%). In the study Covid-era, 79/177 (44,6%) paediatric patients showed bone fractures after the evaluation of 193 radiological surveys.

Comparative analysis shows a 71% decrease of imaging studies in paediatric patients for evaluation of alleged trauma at the pED. The proportion of imaging studies with no evidence of bone fractures dropped in 2020 by 19% compared to the 2019 control era.

Conclusions

During the first wave of the current Covid-19 pandemic children and adolescents underwent much fewer MSK imaging studies at the pED ($p < 0.00001$), this reflecting a strong decrease in physical activity. On the other hand, the sharp decrease of negative studies suggests a new approach to the pED by the general population. Nevertheless, the impact of a pandemic on emergency medicine may offer a unique opportunity to revisit diagnostic and therapeutic protocols also in paediatrics, including appropriateness of imaging prescription.

LIST OF EDUCATIONAL OBJECTIVES:

- To display how the first wave of COVID-19 pandemic affected musculoskeletal traumatic imaging in children in Italy;
- To demonstrate how the pandemic has affected patients' access to the paediatric emergency department;
- To examine and discuss the appropriateness of imaging prescription in traumatic injury of children.

Poster: SCI-207

OPTIMIZATION OF ULTRASOUND PLANES FOR ASSESSMENT OF JOINTS OF PATIENTS WITH BLOOD-INDUCED ARTHRITIS: A MULTICENTRIC STUDY

JYOTI Panwar¹, MIRKAMAL Tolend¹⁴, ELOY Fernandes², SONIA Mitraud², VICTOR Blanchette⁴, JORGE Carneiro⁵, PAULO Daruge⁶, ELBIO D'Amico⁵, SERGIO Dertkigil⁷, ARTUR Fernandes², AIHUA Huo⁸, JOSE Jarrin⁹, YING-JIA Li¹⁰, ARUN Mohanta⁹, JOSE Negrao², MARGARETH Ozelo¹¹, SANUJ Panwar¹², YUN Peng⁸, MARCELO Bordalo Rodrigues⁶, EMERSON Sakuma⁷, JIN Sung¹³, SANDRA Antunes³, PAULA Villaca⁵, RUNHUI Wu¹⁵, NINGNING Zhang⁸, ALEX Zhou⁹, FANG Zhou¹⁰, ANDREA Doria⁹

¹ Christian Medical college - Diagnostic Imaging, Vellore, INDIA

² Universidade Federal de Sao Paulo - Imaging Department, Sao Paulo, BRAZIL

³ Universidade Federal de Sao Paulo - Hematology and Blood Transfusion, Sao Paulo, BRAZIL

⁴ The Hospital for Sick Children - Department of Hematology and Oncology, Toronto, CANADA

⁵ Hospital das Clínicas da Universidade de São Paulo - Thrombosis and Hemostasis, Sao Paulo, BRAZIL

⁶ Hospital das Clínicas da Universidade de São Paulo -The Orthopedic Institute, Sao Paulo, BRAZIL

⁷ Universidade Estadual de Campinas - Radiology Department, Campinas, BRAZIL

⁸ Beijing Children's Hospital - Department of Radiology, Beijing, CHINA

⁹ The Hospital for Sick Children - Diagnostic Imaging, Toronto, CANADA

¹⁰ Nanfang Hospital - Department of Radiology, Guangzhou, CHINA

¹¹ Universidade Estadual de Campinas - Hematology Department, Campinas, BRAZIL

¹² Krishna Advanced M.R.I & C.T Research center, Tirupati, INDIA

¹³ Nanfang Hospital - Department of Hematology, Guangzhou, CHINA

¹⁴ The Hospital for Sick Children - Research Institute, Toronto, CANADA

¹⁵ Beijing Children's Hospital - Department of Hematology, Beijing, CHINA

Background: Optimization of ultrasound (US) scanning planes for evaluation of different joint components of subjects with blood-induced arthropathy can decrease scanning time without compromising diagnostic information.

Purpose: To identify the most diagnostically informative set of US planes for assessment of arthropathy in growing joints of persons with hemophilia based on frequency of findings.

Methods: Unilateral knees (n=32), ankles (n=47) and elbows (n=11) of boys with hemophilia A and B (median/range age,13/7-17 years) were evaluated by US in five treatment centers (Brazil, n=3; China, n=2). US scans were performed by two operators at each center. All examinations were blindly reviewed and final results agreed upon by consensus. Soft-tissue (effusion, synovial hypertrophy, synovial hyperemia, and hemosiderin) and osteochondral (erosions, subchondral cysts, and cartilage loss) joint components were analyzed using different US planes.

Results: Synovial hypertrophy was the most frequent finding in all index joints. For knees, L1-sagittal-posterior-central, L2-coronal-medial/lateral, L2-sagittal-anterior-lateral and L1-sagittal-anterior-central planes demonstrated highest frequencies of synovial hypertrophy, followed by hemosiderin-rich synovium and synovial hyperemia. Soft tissue findings were most frequently observed in L2-sagittal-anterior and posterior-central/medial planes in the ankles, and L1-sagittal-anterior-medial, L2-sagittal-anterior-lateral, L1-sagittal-posterior-central, and L2-sagittal-posterior-medial planes in the elbows. Osteochondral findings were most commonly noted in L1-sagittal-anterior-lateral, L2-sagittal-posterior-lateral and medial, and L1-sagittal-anterior-medial planes in all joints.

Conclusion: L1 and L2 sagittal US planes showed highest frequencies of abnormalities in all joints. Future research investigating different levels of severity is needed for developing practical protocols for US assessment of joints of subjects with blood-induced arthropathy receiving different treatment strategies.

Poster: SCI-208

RADIOLOGIC FEATURES OF SCURVY: A CASE REPORT

MARIA FERNANDA Dien Esquivel, CARMEN Rotaru
CHEO-University of Ottawa, Ottawa, CANADA

Introduction: Until recently scurvy has been viewed in developed countries as a disease of the past. Most recent cases reported in the literature are associated with underlying conditions such as iron overload, bone marrow transplant, and neurological disorders. Musculoskeletal symptoms are a common presenting feature in children with scurvy. However, they are often nonspecific and may mimic several other common conditions, therefore, most children undergo an extensive imaging workup. Our purpose is to summarize the imaging features of scurvy.

Methods and Materials: The patient's electronic medical record was reviewed, including clinical history, laboratory data, and treatment. Diagnostic imaging studies were reviewed, including plain-films, NM, and MRI.

Results: 4-year-old male, presented with a history of gradually worsening gait problems for 7 months and malnutrition, secondary to worsening food aversion since 1 year of age. An extensive workup was completed during his admission, including x-rays of the tibia-fibula, metabolic survey, MR of the head and spine, NM bone mineral density, MRI of the whole body, and NM bone scan. Radiographic findings included alternating dense and lucent bands in the metaphyses of the distal femurs and subtle lucency within the distal femoral epiphyses. MRI revealed symmetric bone marrow signal changes in the metaphyses of long bones, more prominent in the lower extremities. NM bone scan showed increased uptake in the metaphyses of the long bones, with similar distribution to that of the MRI. The differential diagnosis included scurvy, other metabolic disorders, leukemia, metastatic neuroblastoma, and CRMO. Vitamin C levels at < 5 umol/L confirmed the diagnosis. The

remainder of the laboratory results were reassuring. The patient's symptoms improved soon after Vitamin C supplementation.

Conclusion: Although scurvy is a rare entity, it is important to include it in the differential diagnosis in a child with musculoskeletal ailments and typical imaging features, in the context of underlying malnutrition and after exclusion of other ominous pathologies.

Poster: SCI-209

KAPOSIFORM HAEMANGIOENDOTHELIOMA OF THE SPINE WITH FIXED HYPERLORDOTIC DEFORMITY AND KASABACH MERRITT SYNDROME: A RARE ATYPICAL CASE REPORT AND REVIEW OF THE LITERATURE

LEANNE HAN QING Chin¹, KEVIN KIN FEN Fung², JOYCE PUI KWAN Chan², MING KEUNG Yuen², AMANDA Kan³, ELAINE YEE LING Kan²

¹ Department of Radiology, Queen Mary Hospital, Hong Kong, HONG KONG

² Department of Radiology, Hong Kong Children's Hospital, Hong Kong, HONG KONG

³ Department of Pathology, Hong Kong Children's Hospital, Hong Kong, HONG KONG

Kaposiform haemangioendothelioma (KHE) is a rare disease of childhood, classified as a locally aggressive vascular tumour by the International Society for the Study of Vascular Anomalies (ISSVA). It is known to affect any sites, with predilection for the extremities and trunk. Its classical presentation is of an enlarging cutaneous or soft tissue lesion, but less than 10% of cases may not have any skin involvement, with retroperitoneum being the most frequent extracutaneous site. To date, less than 20 cases of KHE with bony involvement have been reported in the literature, with only 5 of the cases specifically involving spine.

In this exhibit, we report an unique, rare and atypical case of KHE in a child presenting with progressive fixed hyperlordotic deformity associated with multiple non-specific bony lesions in the thoracolumbosacral spine and abnormal blood tests that posed as both a clinical and radiological diagnostic challenge. We also performed a comprehensive review of the literature to compare and contrast the different multimodality imaging appearances of KHE involving the spine.

Poster: SCI-210

FOCAL FIBROCARILAGINOUS DYSPLASIA AS A CAUSE OF PERIOSTEAL TETHERING: RADIOLOGICAL FEATURES

JUNG-EUN Cheon, YOUNG HUN Choi, YEON JIN Cho, SEUNGHYUN Lee, SEULBI Lee, WOO SUN Kim

Seoul National University Children's Hospital, Seoul, SOUTH KOREA

Purpose: Focal fibrocartilaginous dysplasia (FFCD) is a rare and benign condition associated with unilateral genu varum in early childhood. The aims of this study are to evaluate radiological features of FFCD including MRI and to describe long term follow-up results of FFCD.

Materials and Methods: Radiological features in 19 cases of FFCD which involved the tibia (n=13), femur (n=5) and ulna (n=1) (M:F=12:7, median age at diagnosis: 16 months) were retrospectively reviewed. Spontaneous resolution of the lesion was observed in 12 tibiae and 3 femurs. One ulnar, one tibial and two femoral, lesions with progressed angular deformities were managed with osteotomies. We evaluated the typical features and temporal changes of the FFCD on radiography and findings of periosteal tethering and adjacent growth plate configuration as well as perichondrial abnormalities on MR imaging.

Results

All patients showed typical radiographic pattern of focal fibrocartilaginous dysplasia: focal area of radiolucency and adjacent cortical thickening with

sclerosis and angular deformities of the involved long tubular bones. MR image demonstrated dense fibrous inclusion within the thick cortical bone which showed low signal intensity on all imaging sequences and adjacent periosteal thickening. We also found the thin linear cartilage invagination from the peripheral margin of the growth plate, at the level of perichondrium. Histological findings obtained in four cases comprised of dense fibrous tissue, of fibrocartilage and of sclerotic bone.

Conclusion

FFCD shows typical radiographic and MRI features. We postulated that FFCD might be a developmental abnormalities of the perichondrium which plays important role in the development of cartilage and osseous structures.

Poster: SCI-211

PAEDIATRIC HIP ULTRASOUND OF DDH DURING THE COVID-19 PANDEMIC

STACEY Castle, RICHARD Jenkins, AFSHIN Alavi, MAYAI Seah, SUFI Sadigh, DANIN Joanna

Imperial Healthcare NHS Trust. St Mary's Hospital. Department of Radiology., London, UNITED KINGDOM

Introduction

Developmental Hip Dysplasia (DDH) is currently screened for under the NHS New-born and Infant Physical Examination (NIPE) programme. Newborn babies who screen positive for dislocation should be referred for an ultrasound within 2 weeks of life. Infants that have a normal clinical examination but have positive risk factors for DDH require an ultrasound within 6 weeks of life. Undetected DDH or delayed treatment can result in complex surgery or long-term disability, pain as well as reduced quality of life.

During the first Covid-19 pandemic ultrasound appointment bookings were amended for several months and this study was designed to assess the effect this has had on management of these babies.

Aim

The primary aim of this audit was to identify whether newborns with potential hip dysplasia had a screening paediatric hip ultrasound in the recommended time frame as per NIPE guidance during COVID pandemic at an academic teaching hospital.

The secondary aim of the audit was to evaluate the rate of abnormal hip ultrasound findings during the COVID pandemic, and the time point at which this was identified.

Method

Data was collected retrospectively from the Radiology database of newborn and infants who had paediatric hip ultrasounds as part of the screening program for DDH at our centre between February 2020 and Dec 2020. Due to Covid-19 all outpatient routine work was put on hold with the exception of Urgent referrals between the months of March and August 2020.

Results

708 paediatric hip ultrasound examinations (for hip screening ie. first USS appointment) were undertaken during the Covid 19 pandemic between February and December 2020.

32 (4.4%) hips required follow up of these 3 (0.004%) were dislocated. 1 dislocation was noted at under 6 weeks, 1 at under 8 weeks and one over 12 weeks. 14 abnormal hips were noted at under 6 weeks whilst 18 abnormal hips were noted at over 6 weeks.

Discussion and Conclusion

In our series during COVID only 14.8 % of newborns and infants had screening ultrasound scans at under 6 weeks. The first COVID wave resulted in 47% having scans at greater than 12 weeks and contributing to the 56% of abnormal scans were noted at greater than 6 weeks.

Our results highlight the importance of performing time sensitive examinations during a global pandemic and we highly recommend that if any further pandemic is to occur paediatric hip ultrasounds should continue to

be screened in a timely fashion in keeping with NIPE for DDH.

Poster: SCI-212

HUGE FEMORAL ARTERY PSEUDOANEURYSM AS A SWELLING MASS: CASE REPORT

ZUHAL Bayramoglu, EZGI Kara, ESHGIN Sahibli, SEÇKIN Çobanoğlu
Istanbul University, Istanbul Medical Faculty, Radiology Department, Istanbul, TURKEY

Pseudoaneurysms common vascular abnormalities caused by a disruption in arterial wall continuity after trauma. Various causes such as inflammation, and iatrogenic injuries may cause pseudoaneurysms. They may be asymptomatic but rupture, thrombosis, and compression of adjacent structures are potential complications. We present a rare case of pseudoaneurysm resulted from autoinflammation with radiological imaging findings.

A 16-year-old male patient presented with left thigh swelling for two months without a history of trauma. On physical examination, there was a huge pulsatile mass at the medial aspect of the left mid-thigh. Also, he had a positive history of recurrent oral ulcers. Gray-scale ultrasonography (US) demonstrated a hypoechoic cystic structure adjacent to the left superficial femoral artery. Color Doppler US showed blood flow within a cystic structure is characterized by turbulent forward and backward flow called the “yin-yang sign”. CT angiography of the left thigh vessels revealed a 90x88x70 mm pseudoaneurysm in the inferior distal part of the left superficial femoral artery with partial mural thrombosis. F-18 FDG PET/CT was ordered to assess the prevalence of the inflammatory process. Intense F-18 FDG uptake was detected in the pseudoaneurysm wall supporting the vasculitis. It was thought that there was a pseudoaneurysm due to vasculitis in the foreground. Surgical treatment was performed due to the size of the arterial pseudoaneurysm.

The diagnosis of pseudoaneurysms has become more common and easier due to the presence of various imaging modalities. The rupture of an arterial pseudoaneurysm is the most serious cause of morbidity from pseudoaneurysms. All clinicians and radiologists should keep in mind the differential diagnosis of pseudoaneurysm to prevent serious complications.

Poster: SCI-213

PILOMATRIXOMA OF THE MOLAR REGION: A CASE REPORT

ZUHAL Bayramoglu, EZGI Kara, ARAZ Gafarli, SINAN Seyrek
Istanbul University, Istanbul Medical Faculty, Radiology Department, Istanbul, TURKEY

A pilomatricoma is an uncommon, benign neoplasm derived from hair cortex cells. This subepidermal tumor is usually found on the face, neck or upper extremities. We present a case of pilomatricoma of the left molar region on the face in a healthy 1-year-old boy.

Pilomatricoma is a benign neoplasm which is thought to be caused by skin extensions. Commonly seen in the head and neck region and less frequently localized in the torso and the lower extremities. Usually, it is solitary, asymptomatic, firm nodule and painless on palpation and most commonly seen in children and young adults.

A 1 year old healthy boy presented with a 3 month history of a firm to hard swelling which gradually increased in size of the left molar region on the face. It was learned that the swelling did not occur from birth and appeared later. On examination, a hard and mobile to palpation mass was found in the subcutaneous tissue of the left molar region and reddish discoloration of the skin as well as swelling. Gray-scale ultrasound image showed well-

circumscribed heterogeneous echogenicity mass measuring 14x10 mm in the superficial subcutaneous soft tissues of left molar region. It had a well-defined hypoechoic rim and multiple tiny hyperechoic foci, likely calcifications, were seen in it. Color Doppler ultrasound image showed vascularity in periphery and center of lesion.

Pilomatricoma, also known as pilomatricoma or calcifying epithelioma of Malherbe. Pilomatricoma is a rare, benign, skin neoplasm that is superficially located and most commonly occurs in the head and neck. They are usually diagnosed on the basis of clinical history and physical examination findings. Since it doesn't spontaneously regress, surgical excision is both curative and the treatment of choice. Recurrence is rare. Ultrasound is usually the initial and only imaging modality used in preoperative evaluation of these tumors.

Poster: SCI-214

A CASE REPORT ON ENDOCHONDRAL OSSIFIED THYROID CARTILAGE AS A SUSPICIOUS LESION

ZUHAL Bayramoglu, EZGI Kara, SINAN Seyrek, ARAZ Gafarli
Istanbul University, Istanbul Medical Faculty, Radiology Department, Istanbul, TURKEY

Endochondral ossification of the thyroid cartilage may mimic a neoplasia. Our case report is focused on this entity of the thyroid cartilage.

Ossification and calcification of laryngeal cartilages are an anatomical problem that has been going on for a very long time. Thyroid, cricoid, and larger parts of the arytenoid cartilages are made up of hyaline cartilage which undergoes calcification and ossification as part of the aging process. Generally, the endochondral ossification process of the thyroid cartilage begins in the first decade.

We present a case of rhabdomyosarcoma in the parapharyngeal space with newly developed thyroid cartilage lesions in the follow-up.

A 12-year-old female patient who was diagnosed with parapharyngeal rhabdomyosarcoma was referred for follow-up neck ultrasonography. She received treatment approximately two years ago. New lesions were revealed in the thyroid cartilage on the neck ultrasound. On ultrasound, we noted two expansile homogeneously hypoechoic well-defined avascular foci on each side of the thyroid cartilage. On MRI, small well-defined structures with intermediate T1-weighted signal and high signal on the fat-suppressed sequence were seen on each side of the thyroid cartilage. In absence of any other lymphadenopathy or a cervical mass, we evaluated these findings as to the normal endochondral ossification process of the thyroid cartilage.

Knowledge of the endochondral ossification process of the thyroid cartilage is important, especially while evaluating of the neck region. All radiologists should be aware of this entity that can be misdiagnosed as malignancy.

Poster: SCI-215

CHRONIC RECURRENT MULTIFOCAL OSTEOMYELITIS (CRMO): RADIOLOGICAL IMAGING FINDINGS OF AN EXTREMELY YOUNGER CHILD

ZUHAL Bayramoglu, RANA GUNOZ Comert
Istanbul University, Istanbul Medical Faculty, Radiology Department, Istanbul, TURKEY

Objective: Chronic recurrent multifocal osteomyelitis (CRMO) is an osseous inflammatory disease of autoinflammatory origin, affecting children and young adults, more common in females and progressing with relapses and remissions with no bacterial or other detectable infectious etiology.

Case: A 13-month-old baby girl was brought with the complaint of swelling in her left foot; She was examined for swelling on the right mandible 3

months ago. Leukocytosis (WBC: 15.2), increased sedimentation (ESR: 42), and acute phase reactants (CRP: 71) were detected at the time of admission. Blood culture was negative in terms of bacteremia. In the neck and abdomen ultrasound evaluation: bilateral parotid gland expansion, edema, and inflammation were found. On the foot radiograph (Figure 1) performed due to the complaint of swelling in the left foot; 5. metatarsal expansion and sclerosis; a continuous solid-type periosteal reaction is observed in the second metatarsal of the right foot. The subsequent whole-body MR examination showed asymmetric expansion and oedematous signal increase in the right parotid region (Figure 3.a, 3.b) and focal signal anterior part of the left 8th rib, focal signal increase in the left iliac wing (Figure 3.d) in the coronal short tau version recovery sequence (STIR). Besides, the left foot on the 2nd and 5th metatarsal bones (Figure 3.d, 3.e) the right foot on the 2nd metatarsal (Figure 3.e), and the bilateral calcaneus bone (Figure 3.f) marrow edema has been detected in STIR sequence. With these findings, CRMO was considered in the differential diagnosis. Biopsy performed to confirm the diagnosis from the area with swelling in the 5th metatarsal of the left foot revealed osteoblastic activity, new bone formation, inflammation, and osteoclast proliferation, and microbiological tissue culture was negative. Histopathologically, osteoclastic activity increase, bone resorption, multinuclear giant cells, and nonspecific granulocytic infiltration are detected in the early stage, while osteoblastic activity, lymphocytes, and granuloma formation are observed in the late recovery stage. Lytic bone lesions, bone marrow edema, surrounding soft tissue swelling, and increase contrast enhancement are observed in radiological imaging in the early phase while new bone formation, hyperostosis, sclerosis, and periosteal thickening are observed in the late healing period. A whole-body MRI could contribute to clearly demonstrate involved bones.

Poster: SCI-216

ENDOCHONDRAL OSSIFICATION OF THE THYROID CARTILAGE

ZUHAL Bayramoglu, EZGI Kara

Istanbul University, Istanbul Medical Faculty, Radiology Department, Istanbul, TURKEY

Abstract

Endochondral ossification of the thyroid cartilage may mimic neoplasia. Our case report is focused on this entity of the thyroid cartilage.

Introduction

Ossification and calcification of laryngeal cartilages are an anatomical problem that has been going on for a very long time. Thyroid, cricoid, and larger parts of the arytenoid cartilages are made up of hyaline cartilage which undergoes calcification and ossification as part of the aging process. Generally, the endochondral ossification process of the thyroid cartilage begins in the first decade. We present a case of rhabdomyosarcoma in the parapharyngeal space with newly developed thyroid cartilage lesions in the follow-up.

Case Report

A 12-year-old female patient who was diagnosed with parapharyngeal rhabdomyosarcoma was referred for follow-up neck ultrasonography. She received treatment approximately two years ago. New lesions were revealed in the thyroid cartilage on the neck ultrasound (Fig. 1). On ultrasound, we noted two expansile homogeneously hypoechoic well-defined avascular foci on each side of the thyroid cartilage. On MRI, small well-defined structures with intermediate T1-weighted signal and high signal on the fat-suppressed sequence were seen on each side of the thyroid cartilage (Fig. 2). In absence of any other lymphadenopathy or a cervical mass, we evaluated these findings as to the normal endochondral ossification process of the thyroid cartilage.

Discussion

Knowledge of the endochondral ossification process of the thyroid cartilage is important, especially while evaluating the neck region. All radiologists should

be aware of this entity that can be misdiagnosed as malignancy.

Poster: SCI-217

FIBROUS HAMARTOMA OF INFANCY: MRI FINDINGS IN FOUR CASES

AMADEO Arango-Diaz ¹, VIRGINIA Trujillo-Ariza ¹, MARIA MERCEDES Liñares-Paz ¹, SONSOLES Junquera-Olay ¹, ANA Ecenarro-Montiel ¹, PABLO Caro-Dominguez ²

¹ Complejo Hospitalario Universitario de Santiago de Compostela, Santiago de Compostela, SPAIN

² Hospital Universitario Virgen del Rocío, Sevilla, SPAIN

Purpose

The purpose of this poster is to report the MRI findings of four patients with histopathologically proven fibrous hamartoma of infancy.

Materials and methods

We retrospectively review the clinical, histopathological and imaging data of four children with fibrous hamartoma of infancy seen at our institution since 2010 focusing on the MRI characteristics.

Results

All four children had a histopathologically proven fibrous hamartoma of infancy arising from the subcutaneous fat of the left axilla (n=1), left arm (n=1), left groin (n=1) and lumbar region (n=1). All were boys ranging in age from 4 to 11 months (mean age, 7.75 months). The four patients underwent surgical resection of the lesion, either total (n=2) or partial (n=1). Tumor recurrence has not been reported in any of them. They were imaged with MRI (n=4), US (n=4), CT (n=1) and x-ray (n=3). The MRI showed in all cases a non-encapsulated mass with layers of fat interspersed with fibres of soft-tissue. This soft tissue demonstrated isointensity to muscle on T2 and T1-weighted images, enhancement after the administration of intravenous contrast material and areas markedly hyperintense on STIR images (n=2), T2-weighted fat-saturated images (n=1) and DP-weighted fat-saturated images (n=1). The mean tumoral size was 4.1 cm.

Conclusions

Our findings are consistent with previously reported cases of fibrous hamartoma of infancy, which is a rare soft-tissue tumor that generally occurs in the first year of life. This case series emphasizes the role of MRI, since it may help in the differential diagnosis with other lesions such as infantile hemangiomas or subcutaneous lipomas.

Poster: SCI-218

ASSESSING THE PREVALENCE OF SPINAL INVOLVEMENT IN OUR COHORT OF CHRONIC RECURRENT MULTIFOCAL OSTEOMYELITIS PATIENTS: ARE DEDICATED SPINAL IMAGING SEQUENCES REQUIRED?

TOBI Aderotimi, NIK Barnes, CAREN Lande

Alder Hey Children's Hospital, Liverpool, UNITED KINGDOM

Purpose:

Chronic Recurrent Multifocal Osteomyelitis (CRMO) is an auto-inflammatory condition affecting children and adolescents. Radiological imaging primarily utilises Whole-body MRI (WBMRI), which is normally performed as coronal short Tau inversion recovery (STIR).

A 2020 paper by Andronikou et al regarding WBMRI protocols in CRMO recommends including dedicated sagittal STIR of the spine, as spinal involvement is characteristic of CRMO with a reported prevalence of 8- 33% in the literature. Spinal involvement can lead to pathological vertebral fractures, therefore early detection is important.

Currently, sagittal STIR spinal imaging is not performed at our institution when imaging CRMO patients. Our study aims to assess the prevalence of spinal involvement in our cohort of CRMO patients compared to the literature, and assess whether the spinal involvement is identifiable on the current coronal WBMRIs we perform.

Methods:

Patients with a diagnosis of CRMO were identified using a paediatric rheumatology database, and by searching the RIS system at our institution. Only patients who had WBMRI as part of their investigation or follow up were included.

This identified 57 patients, (32 female, 25 male). The median age at diagnosis was 10 years old (range 3–17 years). In total 97 WBMRIs were performed in this cohort, with most of the patients having had multiple scans.

All WBMRIs will be independently reviewed by two consultant paediatric radiologists, specialising in musculoskeletal radiology, and a paediatric radiology fellow, who are all blinded to the original reports. Using body maps, sites of involvement will be drawn with particular focus on the spine. These will then be compared to the original reports to identify any ‘missed’ lesions.

Disagreements between the observers will be reviewed by the team and decided by consensus.

Additionally, review of separate spinal MRI imaging if performed, and clinical notes, will be performed to identify patients with spinal pathology not found on the WBMRIs.

Results/Conclusions:

Pending. Study on-going

Poster: SCI-219

HEAD INJURY IN CHILDREN DUE TO NEGLECT

KHAWAJA BILAL Waheed, MUHAMMAD ZIA Ul Hassan
King Fahad Military Medical Complex, Dhahran, SAUDI ARABIA

Background and Objective:

Child abuse comprises physical, sexual, and psychological abuse. Many children evaluated for child abuse have noninjured injuries due to supervisory neglect. The aim of this study is to evaluate the imaging findings in children with isolated head injuries due to neglect and to highlight the vulnerable age group.

Subjects and Method:

A retrospective study was performed in Radiology department at our Hospital in Dhahran, collecting imaging data of children (under 18 years) from January 2017 to 2020. Isolated head injury cases were selected that occurred due to negligence and were notified under Domestic Violence and Neglect Protection Prevention Program set by the Medical Services Department. Skull radiographs and computed tomography of the brains were evaluated, and findings were labeled as “E” (extracranial, subgaleal hematoma, and scalp injury), “C” (cranial; fracture, and its location), and “I” (intracranial, extradural and subdural hematoma, brain contusion, etc.). Imaging findings were documented in children aged under 5 years and between 5 and 18 years. Chi square test was used to determine association.

Results:

Among 85 children with isolated head injuries, abnormal imaging findings were seen in more than half of children (n = 47, 55.2%). Children under 5 years were mostly affected with fractures (C) seen as common findings (n = 34, 72.3%), whereas 19 (40.4%) had intracranial (I) abnormalities (P = 0.89).

Conclusion:

Head injuries resulting from negligence occur mostly in children under 5 years. Fractures account for more than two thirds of injuries.

Limitations

Single center, retrospective study.

Only isolated head injuries were only taken.

Indoor and outdoor cases of neglect were not separated.

Poster: SCI-220

NEUROIMAGING OF CNS MYELOID SARCOMA IN INFANTILE ERYTHROID LEUKEMIA

SANNA Toiviainen-Salo
Helsinki University Children's Hospital, Helsinki, FINLAND

Case report and pictorial assay of an infant with prenatally diagnosed brain malformations and neonatal acute erythroid leukemia with associated intra-axial myeloid sarcomas

Myeloid sarcoma (previously called Chloroma) is a leukemic mass in organs outside of bone marrow.

It is a rare presentation of acute myeloid leukemia (AML). Most commonly myeloid sarcomas appear in children and young adults.

CNS myeloid sarcoma may involve subperiosteum and leptomeninges but on rare occasions it may invade also brain parenchyma and appear as intra-axial masses. Prevalence of myeloid sarcoma in AMLs 9,7%, but in CNS it is very rare (prevalence of CNS MS 0,4%).

The imaging appearances of CNS myeloid sarcoma offers a large variety of differential diagnosis and, especially if presenting prior to the diagnosis of leukemia, risks of lacking timely correct diagnosis.

Acute erythroid leukemia (AER) is a rare form of acute myeloid leukemia accounting less than 5 % of acute myeloid leukemia. There are only few reports of infantile AER with paucity of reports of associated CNS myeloid sarcoma.

The report demonstrates sequential CNS imaging features (including brain ultrasound and MRI) and their evolution over time prior to and after diagnosis and post-therapy in an extremely rare case of an infant with prenatally detected brain malformations and infantile acute erythroid leukemia with associated myeloid sarcomas in the brain.

Poster: SCI-221

TWO DIFFERENT MRI PATTERNS IN PEDIATRIC PARECHOVIRUS ENCEPHALITIS – FROM THE NEWBORN TO THE ADOLESCENT

LUIS OCTAVIO Tierradentro-García, ALIREZA Zandifar, JORGE DU UB Kim, SAVVAS Andronikou
Division of Neuroradiology, Department of Radiology, Children's Hospital of Philadelphia, Philadelphia, USA

Summary of the presentation

Parechovirus encephalitis is an underrecognized condition that may lead to significant neurological impairment. A characteristic white matter (WM) pattern of injury has been described in previous case series, mostly focused on newborns/infants; however, there is paucity of literature on older children's neuroimaging findings

We will present two cases of parechovirus encephalitis, showing distinctive MRI brain patterns of injury in a newborn and an adolescent

Case 1. A 15-day-old male presented with poor feeding, fever and seizures. Parechovirus RNA PCR tested positive in plasma, CSF and urine. Brain MRI exhibited restriction of diffusion involving both cerebral hemispheres asymmetrically, involving the deep and periventricular WM (sparing the subcortical U-fibers) distributed in the frontal zones predominantly but also affecting the parietal and temporal lobes, and sparing the occipital lobes. There was also restricted diffusion involving the corpus callosum; the thalami were swollen/expanded and demonstrated an unequal degree of restricted diffusion bilaterally. The WM showed a typical radiating linear appearance (sunburst pattern), starting at the ventricular edge and following a perivasculor/radiogial distribution of the brain

Case 2. A 17-year-old female with history of lupus presented with left-side weakness, unsteady gait and headache. Parechovirus RNA PCR was positive in serum and CSF. Brain MRI showed bilateral symmetric WM high signal involving the deep and periventricular WM of the centrum semiovale and corona radiata, running in continuity through the posterior

limb of the internal capsule, along the corticospinal tracts of the brainstem and into the decussation in the pons; no corresponding regions of enhancement were visualized. There were also features of cerebellar and cerebral bilateral volume loss symmetrically

Educational objectives

- To demonstrate two different patterns of parechovirus encephalitis at two different pediatric age groups: newborn and adolescent
- To demonstrate a typical radiating sunburst pattern of restriction diffusion in association with corpus callosum signal abnormality and bilateral swollen thalami, in a newborn
- To demonstrate a different pattern of WM signal abnormality in the corona radiata in continuity with the corticospinal tracts, in an adolescent
- To consider parechovirus in the differential diagnosis of WM involvement with typical distribution in both neonates and adolescents

Poster: SCI-222

WHEN SKULL GROWTH GOES WILD: A CASE REPORT OF HYPEROSTOSIS CRANIALIS INTERNA

SUSAN Taylor¹, CHRISTABELL Ndibe¹, KARTIK Reddy^{1,2}, ADAM Goldman-Yassen^{1,2}, KRISTAN Alfonso^{1,2}

¹ Department of Radiology and Imaging Sciences, Emory University School of Medicine, Atlanta, USA

² Department of Radiology, Children's Healthcare of Atlanta, Atlanta, USA

We present a case of hyperostosis cranialis interna (HCI). A 16-year-old male was referred to our facility for right-sided monocular vision loss for 1 month. His physical exam was remarkable in his right eye for the perception of light only. Extra-ocular muscles were intact bilaterally, and the remainder of his cranial nerve examination was unremarkable. CT of the head demonstrated ground glass density and diffuse thickening of the diploe throughout the calvarium and skull base with narrowing of the bilateral orbital apices. Skeletal survey demonstrated no evidence of skeletal dysplasia.

HCI is a bone disorder that involves progressive osteosclerosis and hyperostosis. The exact etiology is unknown. While HCI often involves the calvarium and skull base, it can also involve the mandible. The calvarial endosteal hyperostosis preferentially involves the inner table. When HCI involves the skull base, it can cause cranial nerve deficits due to hyperostotic narrowing of the neuroforamina. Due to the progressive nature of HCI, patients become symptomatic as they become older. In younger patients, the paranasal sinuses and petrous bones tend to be pneumatized at an earlier age, although this is generally replaced by secondary sclerosis as the patient ages. Differential diagnoses for calvarial hyperostosis also include Paget disease, fibrous dysplasia, phenytoin use, or acromegaly. While there is no treatment for the underlying cause of HCI, symptomatic treatment such as surgical decompression for cranial nerve palsies can be pursued.

Our patient underwent right pterional craniotomy for optic nerve decompression; however, his vision did not significantly improve in his right eye. Approximately 6 months later, vision in the patient's left eye had worsened, and the patient underwent left pterional craniotomy and anterior clinoidectomy for optic nerve decompression. The ultimate outcome of the second optic nerve decompression is not yet known as he is 1 week out from the surgery at time of this abstract.

Poster: SCI-223

LARGE POSTERIOR DURAL VENOUS SINUS MALFORMATION: A CONCERNING RARE CONGENITAL INTRACRANIAL VASCULAR MALFORMATION

LETICIA Schaefer Abu Hana, CHRISTINE Saint-Martin, AWS Kamona

Montreal Children's Hospital - McGill - Department of Radiology, Montreal, CANADA

Purpose: Dural sinus malformations (DSMs) are rare pediatric vascular anomalies that have variable presentations and outcomes. It is typically associated with dural arteriovenous (AV) fistula. Common clinical manifestations include heart failure, macrocephaly and seizure. Prognosis is reserved for the cases involving the confluence of central dural sinus. We present a case of midline DSMs involving the torcula herofili and superior sagittal sinus (SSS), discuss the different types of dural AV shunts and review the literature.

Material and Methods: Retrospective review of the clinical presentation, imaging studies and treatment performed for our patient.

Results: We present a case of a 7-month-old patient who had history of increased head circumference. Head US was initially performed in an outside institution, showing a large cystic lesion in the posterior fossa/occipital region. A head MRI was subsequently performed, showing massive dilatation of the dural venous sinuses, centered at the torcula herofili, involving the posterior SSS and the medial transverse sinuses (left more than right, with significant mass effect, causing herniation of the cerebellar tonsils and massive hydrocephalus. AV fistula was demonstrated on vascular MRI sequences with feeders arising from branches of the bilateral external carotid arteries. Diagnosis of DSM was made. Further evaluation of the angioarchitecture was made by cerebral angiogram, confirming the MRI findings. The main AV feeding branches were partially embolized using coils and embolization glue in order to have decrease in size of the enlarged veins without complete occlusion. Follow-up MRI done 1 month after the procedure showed decreased size of the dural venous pouch and improved hydrocephalus with resolution of transependymal resorption signal changes.

Conclusion: Early diagnosis, understanding of this rare condition, appropriate imaging studies with visualization of the angioarchitecture, and the treatment (if necessary) of DSMs are important to prevent cardiac failure or parenchymal injury. Management should be individualized for each case.

Poster: SCI-224

PEDIATRIC HIGH-GRADE GLIOMAS - DIFFERENTIATING THE GENETIC SUBTYPES OF HISTONE H3G34 MUTANT, HISTONE H3K27 MUTANT, AND IDH-1 MUTANT TUMORS

GRACE Renshaw, AUDREY Fazel, RYAN Bruhns, BEN Renshaw, JEFFERY Bennett

Banner University Medical Center, Tucson, USA

Introduction:

- Pediatric high-grade gliomas have different genetic profiles from adult glioblastomas. Imaging of histone H3K27M mutant, histone H3G34 mutant, and IDH-1 mutant tumors are presented.
- The pathologic diagnosis involves evaluation of histology and immunohistochemistry (IHC), as well as genomic testing.

Discussion:

- Diffuse midline glioma most commonly occurs in the brainstem where it is referred to as DIPG (diffuse intrinsic pontine glioma). It may also occur in the thalami, or more rarely in the cerebellum or spinal cord. It is listed in the 2016 WHO brain tumor classification as diffuse midline glioma with histone H3K27M mutation. The prognosis is poor.
- Pediatric high-grade glioma or glioblastoma with histone H3G34 mutation likely has a different cell of origin than the H3K27M tumors. It occurs at different locations, specifically the cerebral hemispheres, most commonly the temporal and parietal lobes. There are two appearances of this tumor - either similar to an adult glioblastoma or similar to an undifferentiated embryonal tumor. This tumor is not yet part of the WHO classification of brain tumors, and it is less well understood.

- The common adult glioblastoma with IDH-1 mutant or IDH-1 wildtype is very rare in children. Adult IDH-1 mutant glioblastoma occurs at an earlier age than the IDH-1 wildtype, and when seen in older pediatric patients, it likely represents early presentation of the adult variety of glioblastoma.

- While cellular morphology alone may help differentiate and diagnose pediatric high-grade gliomas, IHC is generally required for diagnostic certainty. IHC may be performed as an alternate to or in conjunction with genomic testing via molecular studies, which are not always performed but likely to become more routine.

- Despite the heterogeneous morphology of some pediatric high-grade gliomas many exhibit typical IHC profiles. For example the IHC profile for H3G34 mutant gliomas includes the loss of nuclear ATRX, strong nuclear p53, a high Ki-67 index and the absence of cytoplasmic IDH-1 R132H.

References:

- Gianno F, Antonelli M, et al. Pediatric high-grade glioma: A heterogeneous group of neoplasms with different molecular drivers. *Glioma* 2018;1:117-24.

- Sturm D, Pfister S, et al. Pediatric gliomas: Current concepts on diagnosis, biology, and clinical management. *J Clin Oncol* 2017;38;21:2370-77.

- Barkovich AJ. Pediatric neuroimaging. Lippincott Williams & Wilkins. (2005)

Poster: SCI-225

CLINICAL AND RADIOLOGIC MANIFESTATIONS OF SMART SYNDROME: A CASE REPORT

ANTHONY Radosevich¹, ELIZABETH Ryals², CORY Pfeifer²

¹ Baylor University Medical Center/Children's Medical Center, Dallas, USA

² Children's Medical Center, Dallas, USA

Background:

Stroke-like Migraine Attacks After Radiation Therapy (SMART) syndrome is a delayed, often reversible, complication of cerebral radiation therapy related to microvascular effects of radiation. Patients present with seizure or transient focal neurologic deficit often associated with headache. Focal gyriform edema and enhancement with mild mass effect are observed with variable diffusion restriction on MRI. The differential diagnosis includes tumor recurrence, subacute infarct, and posterior reversible encephalopathy syndrome. Clinicians and neuroradiologists should be aware of the clinical and radiologic features of SMART syndrome to provide the best care for our patients with previously irradiated intracranial disease processes.

Case Presentation:

Starting approximately two years after finishing radiation therapy for medulloblastoma, a 12-year-old male experienced two episodes of altered mental status six months apart. MRI demonstrated diffuse left cerebral hemisphere expansile cortical FLAIR hyperintensity. During the patient's ensuing hospitalizations, clinical evaluations for recurrent tumor, stroke, or seizures as the cause of the altered mental status and imaging findings were nonrevealing. He fully recovered and was discharged. A follow-up MRI in three months demonstrated cortical laminar necrosis and chronic volume loss in the same distribution. He remained asymptomatic. Based on clinical and imaging characteristics, both episodes were attributed to "Stroke-like Migraine Attacks After Radiation Therapy" (SMART) Syndrome.

Discussion:

The clinical and radiological picture of this patient is compatible with SMART syndrome. The underlying pathophysiology of SMART syndrome is poorly understood, but thought to be related to microvascular effects of radiation. Its clinical presentation, course and imaging findings are important to recognize and distinguish from other disease processes as it is a potential cause of transient or non-progressive focal neurologic deficit in patients with prior history of radiation.

Poster: SCI-226

CONGENITAL FACIAL NERVE DISORDERS: A CASE SERIES

TREY Mitchell, BRIAN Pando, BRITTANY Matthews, DHARUV Patel
Memorial Health University Medical Center, Department of Radiology, Savannah, USA

BACKGROUND INFORMATION/PURPOSE:

Congenital facial nerve palsy is a rare condition most often caused by birth trauma, presenting as unilateral or bilateral weakness of the facial muscles. Developmental forms of facial nerve palsy are rarer and are often associated with syndromic conditions, with very few cases reported on isolated facial nerve disorders.

Our purpose is to present two rare cases of isolated congenital facial nerve aplasia and hypoplasia and, using these exemplary cases, review MRI assessment of the facial nerve.

EDUCATIONAL GOALS/TEACHING POINTS:

- Review anatomy of the facial nerve.
- Review MRI protocol and sequences to best assess the facial nerve.
- Review normal MRI appearance of the facial nerve.
- Review MRI appearance of congenital facial nerve palsy.

CASES:

A 5 month old infant was referred to a neurologist due to persistent left sided facial weakness since birth. The patient was born via cesarean section with no trauma noted. Physical exam revealed isolated left sided facial weakness with flattening of the left nasolabial fold with no dysmorphic features visualized. Chromosomal micro-array revealed no abnormalities. A MRI brain revealed left facial nerve aplasia with no other abnormality present.

A 4 year old patient was referred to a neurologist due to concerns about delayed motor milestones from poor coordination. Mild facial weakness was noted at 3 months of age. The patient was born at term via cesarean section due to non-reassuring heart tones, with no complications thereafter. Physical exam revealed an asymmetric smile, but no overt facial weakness. Mildly dysmorphic features were also noted with poor coordination in the upper extremities. Chromosomal micro-array as Fragile X testing revealed no abnormalities. MRI Brain revealed a hypoplastic left facial nerve with no other abnormal findings.

CONCLUSION:

Learners will become familiar with MRI appearance of congenital facial nerve palsy.

Poster: SCI-227

IMAGING OF MIDLINE CONGENITAL MALFORMATIONS OF BRAIN

RAHUL Nikam¹, ASHRITH Kandula¹, SNIGDHA Puram¹, BEN Paudyal¹, XUYI Yue¹, SACHIN Kumbhar²

¹ Nemours Alfred I. duPont Hospital for Children, Wilmington, USA

² Medical College of Wisconsin, Milwaukee, USA

Purpose:

The midline congenital malformations of brain are complex, and poses a significant difficulty and confusion to the radiologists and trainees alike. In this exhibit, we aim to describe the embryological basis, and imaging phenotypes of various midline congenital malformations of brain. Where relevant, we will describe the underlying genetic abnormalities.

Objectives/Materials and Methods:

In this educational exhibit, we will discuss the imaging phenotypes and embryology of following midline malformations.

1. Nasal Gliomas, nasal dermoids, and dermal sinus
2. Midline cephaloceles: anterior and posterior
3. Anomalies of the olfactory bulbs, and olfactory sulcus: Kallmann syndrome
4. Congenital midline cleavage anomalies: Holoprosencephaly spectrum (alobar, semilobar, lobar, syntelencephaly, septo-optic dysplasia)
5. Anomalies of corpus callosum
6. Intracranial lipomas
7. Hypothalamic-pituitary anomalies: Ectopic posterior pituitary, pituitary stalk interruption syndrome, Rathke's cleft cyst, hypothalamic hamartoma, inter-hypothalamic fusion
8. Posterior fossa malformations:
 - Cystic posterior fossa malformations (Dandy-Walker continuum, Blake pouch cyst, mega cisterna magna, arachnoid cyst)
 - Cerebellar hypoplasia
 - Pontocerebellar hypoplasia
 - Rhombencephalosynapsis
 - Molar tooth malformations
 - Arnold Chiari Malformations

Results/Conclusion:

After review of the exhibit, the reader will be well versed with the embryological basis and imaging phenotypes of various complex, midline congenital malformations of the brain.

Poster: SCI-228

VENTRICULAR MORPHOMETRY AND RESISTIVE INDEX IN PRE AND POST-TREATMENT EVALUATION OF HYDROCEPHALUS

DHANANJAYA KOTEB Narayana Vamyanmane, VINODH D, RAMESH R L, SHRAMANA Bagchi
Indira Gandhi Institute of Child Health, Bengaluru, INDIA

Objectives

- To accurately measure the size of lateral ventricles using ultrasound
- To assess the resistive index of anterior cerebral artery using doppler sonography

Background knowledge:

To measure the acute reversible cerebrovascular changes, and thus improve indication and timing of drainage procedure in non-invasive way, there is a need for examination technique, which could be used in daily clinical practice. This is the potential of transcranial Doppler sonography. It can analyze blood flow in the cerebral arteries and thus enables to perform noninvasive assessment of hemodynamic parameters of cerebral circulation.

Material and methods

Neonates who presented to the Department of Pediatric Radiology, Indira Gandhi Institute of Child Health, Bangalore, for ultrasonography with intracranial hemorrhage and hydrocephalus. Samsung Accuvix XG ultrasound machine with L 5-13 IS probe is used to perform Ultrasound and Doppler.

Inclusion criteria

Neonates presenting to the department of pediatric radiology for ultrasound with Intracranial hemorrhage and hydrocephalus

Exclusion criteria

Neonates with myelomeningocele.

Patients who are lost to follow up.

Conclusion:

Increased intracranial pressure in progressive neonatal hydrocephalus leads to the alteration of cerebral circulation (decreased cerebral blood

flow, hypoperfusion and ischemia). Transcranial color Doppler sonography provides a noninvasive method of monitoring of the blood flow velocities in cerebral vessels. In general, there is a good correlation between the increase of intracranial pressure and changes in Doppler curve parameters. Before the drainage procedure there was confirmed increased basal and compressive values of resistive index of cerebral arteries. After the successful drainage procedure, the significant decrease of basal and compressive values of resistive index was found.

Poster: SCI-229

Withdrawn

Poster: SCI-230

PERINATAL ARTERIAL ISCHEMIC STROKE IN FETAL VASCULAR MALPERFUSION: A CASE SERIES AND LITERATURE REVIEW

ANA Geraldo ¹, ALESSANDRO Parodi ², MARTA Bertamino ³, FRANCESCA Buffeli ⁴, SARA Uccella ⁵, DOMENICO Tortora ⁶, PAOLLO Moretti ³, LUCA Ramenghi ^{2,7}, ENZIO Fulcheri ^{4,8}, ANDREA Rossi ^{6,9}, MARIASAVINA Severino ⁶

¹ Diagnostic Neuroradiology Unit, CHVNG/E, Vila Nova de Gaia, PORTUGAL

² Neonatal Intensive Care Unit, IRCCS Istituto Giannina Gaslini, Genoa, ITALY

³ Physical Medicine and Rehabilitation Unit, IRCCS Istituto Giannina Gaslini, Genoa, ITALY

⁴ Gynaecologic and Fetal-Perinatal Pathology Unit, IRCCS Istituto Giannina Gaslini, Genoa, ITALY

⁵ Child Neuropsychiatry Unit, IRCCS Istituto Giannina Gaslini, Genoa, ITALY

⁶ Neuroradiology Unit, IRCCS Istituto Giannina Gaslini, Genoa, ITALY

⁷ Departments of Neurosciences, Rehabilitation, Ophthalmology, Genetics, Maternal and Child Health (DINO GMI), University, Genoa, ITALY

⁸ Surgical Sciences and Integrated Diagnostics, Pathology Division of Anatomic Pathology, University of Genoa, Genoa, ITALY

⁹ Health Sciences (DISSAL), University of Genoa, Genoa

Introduction: Fetal vascular malperfusion includes a continuum of placental histologic abnormalities increasingly associated with perinatal brain injury, namely arterial ischemic stroke. Here, we describe the clinical-neuroimaging features of 5 neonates with arterial ischemic stroke and histologically proved fetal vascular malperfusion.

Materials and methods: Five patients with PAIS and histologically proved fetal vascular malperfusion were identified from the institutional database of pediatric patients treated for stroke at the Gaslini Children's Hospital between 2012 and 2019.

Results: All infarcts involved the anterior territories and were multiple in 2 patients. In 2 neonates, there were additional signs of marked dural sinus congestion, thrombosis, or both. A mixed pattern of chronic hypoxic-ischemic encephalopathy and acute infarcts was noted in 1 patient at birth. Systemic cardiac or thrombotic complications were present in 2 patients.

Conclusion: These peculiar clinical-radiologic patterns may suggest fetal vascular malperfusion

and should raise the suspicion of this rare, underdiagnosed condition carrying important implications in patient management, medicolegal actions, and future pregnancy counseling.

Poster: SCI-231

DEEP CERVICAL LYMPH NODES ON PEDIATRIC HEAD AND NECK MRI SCANS – A PICTORAL REVIEW

RIDDHIKA Chakravarty, SARAH Watson
Royal Surrey Hospital NHS Foundation Trust, Guildford, UNITED KINGDOM

We present a pictorial review of deep cervical lymph nodes – incidental findings in a series of paediatric head and neck MRI scans. The clinical importance of these nodes was first highlighted in a radiology events and learning meeting where one of these nodes was mistaken for a dissection. We will also present the results of a matched case control study between paediatric and adult head and neck MRI scans which confirmed anecdotal evidence that these nodes are seen in the paediatric population and rarely in adults.

Poster: SCI-232

MR SIALOGRAPHY AT A DISTRICT GENERAL HOSPITAL: OUR JOURNEY

RIDDHIKA Chakravarty, SARAH Watson
Royal Surrey Hospital NHS Foundation Trust, Guildford, UNITED KINGDOM

Background: A recent review article (2018) suggested that MR Sialography could be the optimal imaging modality to assess for salivary calculi in children. It scores over conventional fluoroscopy given its lack of radiation, anatomical detail and availability of three dimensional imaging. However practical difficulties in offering this service at the district general hospital level include optimisation of available MR hardware and imaging protocols, in addition to the other challenges of paediatric MR imaging.

Educational exhibit: We discuss our journey in setting up a paediatric MR sialography service on our existing 1.5T scanner with representative images documenting the various steps to optimise the protocol. This involved the addition of FIESTA sequence to the protocol to best visualise the salivary glands and ducts. We also then acquired a new head coil which has considerably improved imaging quality. Motion artefacts continue to pose challenges in interpretation.

Poster: SCI-233

CONGENITAL INTRADURAL SPINAL LIPOMATOSIS WITH INTRACRANIAL EXTENSION

EMILY Evans¹, HUMA Haseeb¹, GUIRISH Solanki², MARK Bishay¹
¹ Birmingham Children's Hospital - Department of Radiology, Birmingham, UNITED KINGDOM
² Birmingham Children's Hospital - Department of Neurosurgery, Birmingham, UNITED KINGDOM

A ten month old girl was referred to a paediatrician with concerns of abnormal tone and severe developmental delay (there was some delay in accessing medical assessment due to the coronavirus pandemic). She was found to have gross motor and fine motor delay affecting the trunk and all limbs. She was not able to sit up or hold a rattle. She had no smile and difficulty swallowing. On examination, she had a disproportionately large head (91st centile for head circumference, 9th centile for weight), but was not dysmorphic. Upper and lower limbs were hypertonic and hyperreflexic. Fat folds were noted at the back of the neck and base of the spine. She was found to have respiratory insufficiency, and required supplemental oxygen. Sleep study demonstrated a number of hypopneas.

Subsequent MRI of the head and spine demonstrated extensive intradural spinal lipomatosis, extending into the posterior fossa and causing severe spinal cord compression, especially in the cervical region, as well as hydrocephalus. There was expansion of the spinal canal. Subcutaneous lipomatosis

was also noted overlying the cervical and lumbar spine. She underwent initial decompression with posterior fossa craniotomy and cervicothoracic laminoplasty, followed by later thoracolumbar laminoplasty and debulking of intradural lipoma. Histology demonstrated benign mature adipose tissue in keeping with lipomatosis. Postoperative imaging demonstrated spinal decompression and debulking with some improvement in ventricular dilatation.

Following surgery, she no longer required oxygen, and made encouraging neurodevelopmental progress, gained motor milestones and is beginning to sit with support using a brace.

Intradural spinal lipomatosis is a rare condition, accounting for less than 1% of spinal tumours. It is even more unusual in the paediatric population and should be considered as a rare but important cause of severe developmental delay with spastic quadriplegia.

The combination of intracranial and intradural lipomatosis with subcutaneous lipomatosis seen here is suggestive of the even more rare diagnosis of encephalocraniocutaneous lipomatosis (ECCL). ECCL is characterised by central nervous system, skin and ocular anomalies, particularly lipomatosis (including intracranial and intraspinal lipomatosis).

Poster: SCI-234

LYMPHANGIOMA OF THE PEDIATRIC TEMPORAL BONE

PASCALE Aouad, MAURA Ryan
Lurie Children's Hospital, Northwestern University, Department of Radiology, Chicago, USA

Summary of the presentation: Lymphangiomas are benign congenital tumors commonly encountered in the head and neck region. Osseous involvement is rare but can present clinical and diagnostic difficulties when occurring in the temporal bone. Lymphangiomas in the temporal bone present as destructive lesions that may be misinterpreted as more common lytic lesions in the pediatric population, such as otomastoiditis or Langerhans Cell Histiocytosis. Lymphangiomatous involvement of the temporal bone is associated with CSF leaks and can mimic more common clinical causes of ear drainage. Here, we present a case based pictorial review of temporal bone lymphangiomas presenting with CSF leak.

List of educational objectives:

- Recognize characteristic imaging features of lymphangioma that can help distinguish from more commonly encountered destructive processes of the temporal bone.
- Increase awareness of temporal bone lymphangioma to enable earlier diagnosis, guide appropriate management and help prevent potential complications of CSF leak and recurrent meningitis.

Purpose: To review the imaging and clinical findings of temporal bone lymphangioma with CSF leak.

Methods: We are presenting the imaging findings in children with lymphangioma involving the temporal bone with CT, MRI and cisternography. We will compare with imaging examples of coalescent otomastoiditis, Langerhans cell histiocytosis and cholesteatoma to highlight imaging differences that distinguish from more common pediatric temporal bone lesions.

Results: Lymphangiomas are uncommon benign congenital tumors that mainly involve the soft tissues of the head and neck region. Bone involvement is rare and usually results from extension of a primary soft tissue lesion (1). Histologically, these appear as lymph-filled multilocular cavities with endothelial lining (2). CT typically shows bone destruction without sclerotic margins (3). On MRI, they may be macrocystic or microcystic but typically show marked T2 hyperintensity and may demonstrate fluid-fluid levels (4). Involvement of the skull base may lead to CSF leak. The typical course of the disease is long standing with slow progression (2). Treatment depends on location and associated complications, but is primarily surgical.

Conclusion: Lymphatic malformations are a rare cause of lucent lesions in the temporal bone but have distinct imaging features. Awareness and

recognition of this entity can help prevent delayed diagnosis, guide appropriate management.

Poster: SCI-235

ANATOMICAL CORRELATION OF HUMAN VS. MOUSE MODEL ON MRI

CESAR Alves, MEAGAN Mcmanus, NINA Duncan, ABHAY Ramachandran, WALT McHugh, SERGEY Magnitsky, TODD Kilbaugh, SAVVAS Andronikou
Children's Hospital of Philadelphia, Philadelphia, USA

Purpose:

Leigh syndrome is the most commonly presenting primary mitochondrial disease and the brainstem is one of the main sites affected, along with basal ganglia lesions. The brainstem itself is not diffusely involved, and more often, specific gray matter nuclei are affected.

Significant advances in the metabolomics of mitochondrial disorders have triggered advanced analysis and management strategies for Leigh syndrome. Animal models are being created with the purpose of testing potential treatments. However, there is a deficiency in the literature for the translation of imaging findings observed in animal models as compared to humans. This study aims to correlate the distribution of brain MR imaging abnormalities in Leigh Syndrome animal models (mice) with imaging of humans with Leigh syndrome.

Methods

In this IRB approved imaging study, electronic medical records were reviewed to confirm the diagnosis of Leigh syndrome among all PMD individuals from 2000 to 2019. In parallel, the mice Leigh syndrome models (NDUFS4 KO, MT-ND6 KO) were imaged at 7.0 T MRI (2019-2020). The distribution of the lesions was correlated between humans and mice models.

Results

MRI scans of 57 patients with typical imaging features of Leigh syndrome and 20 MRI scans of Leigh syndrome mice models correlated well in the brainstem, demonstrating selective involvement of the vestibular nuclei (Figure 1). All lesions observed were hyperintense in T2 weighted imaging sequences in both humans and mice. Selected imaging correlations are presented in a pictorial anatomic format as a reference map for future studies.

Conclusions

MRI scans showing a distribution of lesions in the same gray matter nuclei in humans and Leigh syndrome mice models, support the use of MRI scans in Leigh syndrome mice models for future studies focusing on treatment response in this disease.

Poster: SCI-236

DOSE REDUCTION WITH SPECTRAL SHAPING FOR PEDIATRIC PARANASAL SINUS CT

WEI Zhou¹, ILANA Neuberger², JOHN Maloney², CHRISTINA White², DONGLAI Huo¹, JASON Weinman²

¹ University of Colorado, Anschutz Medical Campus, Aurora, USA

² Children's Hospital Colorado, Aurora, USA

Purpose: To investigate the effects of spectral shaping using tin filtration on radiation dose and image quality of pediatric paranasal sinus CT exams on a 2.5th generation dual-source CT (DSCT).

Methods: An anthropomorphic head phantom was scanned on a 128-slice commercial DSCT system (SOMATOM Drive, Siemens Healthcare) using a conventional pediatric protocol (120kV, 50 quality reference mAs). The same phantom was also scanned using 100 kV with additional 0.4 mm tin filter (Sn100kV) and 350 quality reference mAs. An ion chamber (10X6-0.6,

Radcal) was placed on the phantom surface of eye and parotid gland region at both sides to measure entrance skin doses (ESD). Identical image reconstruction parameters were utilized for both the Sn100kV and conventional 120kV protocols. Image noise was measured as the standard deviation of CT number from a uniform soft tissue. Regions of interest were placed with the same size and location for both protocols. Line profile of CT number across the nasal bone structure of phantom was measured. The average CT number of nasal bone structure was also calculated.

Results: The CTDIvol values from phantom acquisitions using Sn100kV and 120kV were 4.35 and 5.73 mGy, respectively. The ESDs from Sn100kV acquisitions (eye lens: 3.94 mGy; parotid gland: 4.03 mGy) were lower than those of 120kV acquisitions (eye lens: 5.00 mGy; parotid gland: 4.92 mGy). The phantom image noises of Sn100kV and 120kV protocols were 80.6 HU and 83.5 HU at the same head dedicated sharp kernel (Hr60). Radiation dose and noise comparison results indicated that Sn100kV can provide approximately 27% dose reduction for routine sinus CT exams, compared to conventional 120kV acquisitions. The line profile of CT number across nasal bone from Sn100kV was closely matched to that of 120kV. The average CT numbers of nasal bone mimicking materials were 1383.0 HU and 1378.6 HU, respectively. This implies that though low energy photons were removed by spectral shaping, using lower kV could preserve CT image contrast of bony structures.

Conclusion: Spectral shaping using lower kV and additional tin filtration, which is available in the newest CT scanner, can reduce radiation dose for pediatric non-contrast sinus CT exams without compromising image quality. Our results provide a new strategy to minimize CT radiation dose to pediatric sinus patients.

Poster: SCI-237

THE EVALUATION OF ANATOMIC STRUCTURES' VOLUME OF THE BRAIN IN PEDIATRIC PATIENTS WITH EPILEPSY – PRELIMINARY STUDY

MONIKA Zbroja¹, WERONIKA Cyranka¹, KATARZYNA Drelich¹, OLGA Pustelniak¹, MALGORZATA Matuszek¹, EWA Kopyto¹, ANDRZEJ Materniak², MAGDALENA Wozniak²

¹ Students Scientific Society at the Department of Pediatric Radiology, Medical University of Lublin, Lublin, POLAND

² Department of Pediatric Radiology, Medical University of Lublin, Lublin, POLAND

Purpose:

Epilepsy has recently been increasingly viewed as a generalized disorder of neuronal networks with progressive atrophy of brain structures with incompletely understood causes, patterns, and rate. Published articles have focused so far on evaluating changes in adult patients. The aim of the study was to evaluate anatomic structures' volume of the brain in pediatric patients with epilepsy.

Materials and Methods:

A group of 14 pediatric patients aged 8-17 years with clinical symptoms of epilepsy (study group) and 10 healthy patients (experimental group) were enrolled in the study. Brain MR imaging was performed in all children according to a dedicated protocol (epilepsy specific protocol). Individual anatomical structures of the central nervous system were analyzed on the basis of T1-weighted 3D isometric 1 mm sequence and volume changes of specific structures were compared between the epilepsy group and the control group.

Results:

In the study group, the ratio of brain tissue to CSF was 87.63% to 12.37%, while in the control group it was 90.08% to 9.92%. In the research group compared to the control group, the volumes of each brain structure were: cerebrum – 77,08%/78,88%, cerebellum – 9,18%/9,78%, brainstem – 1,37%/1,43%, lateral ventricle – 2,28%/0,57%, caudate – 0,53%/0,58%,

putamen – 0,63%/0,67%, thalamus – 0,75%/0,89%, globus pallidus – 0,17%/0,20%, hippocampus – 0,41%/0,49%, amygdala – 0,10%/0,10%, accumbens – 0,04%/0,05%.

Conclusion:

During the course of epilepsy in pediatric patients, there is a decrease in the volume of brain tissue, with particular emphasis on the cerebrum, cerebellum, brainstem, caudate, putamen, thalamus, globus pallidus, hippocampus and accumbens, moreover an increase in the volume of lateral ventricles. Preliminary findings indicate cortical and subcortical atrophy in pediatric patients with epilepsy. The data obtained have important clinical and prognostic significance, but need to be confirmed on a large study group with taking into account changes in the volume of anatomical structures of the brain in relation to age and disease duration.

Poster: SCI-238

CLINICAL UTILITY OF THE DIFFUSION WEIGHTED IMAGING (DWI) RATIO IN CHARACTERIZING PRIMARY BRAIN NEOPLASMS IN PEDIATRIC PATIENTS: A 5-YEAR RETROSPECTIVE STUDY IN A TERTIARY HOSPITAL IN THE PHILIPPINES

SHEEN Urquiza, RYAN JASON Urgel, ALVIN Camacho, ROSANNA Fragante
University of the Philippines - Philippine General Hospital, Manila, PHILIPPINES

Objective: The goal of this study was to determine the accuracy of DWI ratio in characterizing primary brain tumors among pediatric patients in the Philippine General Hospital from January 2013 to July 2018.

Methods: Magnetic resonance images of pediatric brain tumors were reviewed. A standardized ROI was placed on the solid portion of the tumor that presented the highest signals on DWI (DWI T), the normal appearing white matter of the contralateral frontal lobe (DWI WM), and the normal-appearing homologous area of the ROI of the tumor in the contralateral hemisphere or adjacent region (DWI N). The DWI ratios were determined and analyzed. Data gathered were then subjected to statistical analysis to determine the accuracy of the DWI ratios.

Results: Thirty cases of pediatric brain tumors were included in this study. Upon analysis, there was a significant difference in the median DWI(T/N) and DWI (T/WM) ratios between Grades II-IV neoplasms; with the Grade IV tumors exhibiting a higher median ratio compared to Grade II. There was significant difference in the median DWI (T/N) and DWI(T/WM) values between low- and high-grade neoplasms, with the median DWI (T/N) and DWI (T/WM) ratios significantly higher among those with high grade neoplasms.

Conclusion: The DWI ratios presented relatively high sensitivity, high specificity, and relatively high diagnostic accuracies in grading or classifying pediatric intracranial tumors. The method will be useful for clinical neuro-oncology imaging services, and is applicable to guiding diagnostic and therapeutic strategies, such as biopsies and surgeries.

Poster: SCI-239

MRI FINDINGS OF AICA LOOPS IN CHILDREN: INCIDENCE AND ASSOCIATION WITH AUDIOVESTIBULAR SYMPTOMS

BIRSEL Sen Akova¹, SUAT Fitoz¹, EMRE Ocak²

¹ Ankara University, Department of Pediatric Radiology, Ankara, TURKEY

² Ankara University, Department of Otolaryngology, Ankara, TURKEY

Purpose:

Vascular loops in internal auditory canal (IAC) has been widely studied in adults. In this study, we aimed to investigate the incidence of vascular

loops in different pediatric age groups and association of audio-vestibular and facial symptoms with the presence of vascular loops.

Materials and Methods:

This retrospective study included 400 ears of 200 pediatric patients. Exclusion criteria included the patients with congenital inner ear anomaly, tumors at cerebellopontine angle (CPA), history of surgery including CPA, temporal bone trauma and neuritis.

43 ears enrolled the study group and 357 ears formed the control group. The patients formed the study group had symptoms include sensory neural hearing loss (SNHL), peripheral facial paralysis or vertigo in one or both of the ears.

All MRI examinations included thin slice axial 3D balanced fast-field echo (bFFE) sequence through IAC which was used for the assessments. Vascular loops were graded according to Chavda classification based on anatomical location of loop and were also documented nerve contact and angulation of the VII. and VIII. nerves if present.

Frequency, percentage, mean and standard deviation were used in descriptive statistics.

Results:

In 251 (62.57%) of total 400 ears, no visible vascular loop at CPA or internal auditory meatus (IAM) was identified (grade 0). In 106 (26.5%) ears a vascular loop was detected at CPA or IAM (grade I). Grade II vascular loop as it runs less than 50% of IAC was detected in 40 ears (10%). Grade III vascular loop described as running more than 50% of IAC was identified in 3 ears (0.8%). In comparison of control and study groups; grade 0, I, and III were more common in study group and grade II was more common in control group (p<0.01).

In comparison of control and study groups; contact with VII. or VIII. nerves of vascular loop was more common in study group (44.2%, 26.6%, p<0.05).

The difference was insignificant for the right or left ears about vascular loop incidence or grade in both control and study groups.

The only patient in study group, who had a grade III vascular loop with a contact with nerves, complained of peripheral facial paralysis of ipsilateral face.

Conclusions:

In our study, we showed that vascular loops, especially with nerve contact was more common in patients with audiovestibular system complaints. However, this finding must be evaluated in larger study groups.

Poster: SCI-240

NEONATAL BRAIN EVALUATION WITH MRI AND NEUROSONOGRAM WITH HISTORY OF DYSTOCIA

RAMESH R L¹, DHANANJAYA KOTEB Narayana Vamyanmane¹, BALAKRISHNA Shetty²

¹ Indira Gandhi Institute Child Health, Bengaluru, INDIA

² Sri Siddhartha medical college, Tumakuru, INDIA

Purpose:

Usefulness of combined MRI and Neurosonogram evaluation in all the cases of Dystocia.

Effectiveness of combined MRI and Neurosonogram over individual studies.

Establishing advantages of MRI and Neurosonogram in different clinical settings.

Materials and Methods:

Prospective study of 71 neonates with history of dystocia.

All the cases with following history were included in our study:

- Delayed cry
- Birth Asphyxia
- Seizures
- Delayed activities.
- Slow motor activity and reduced power for age
- Mechanical injury.

Results:

- Total of 71 neonates were studied with inclusion criteria.
- 31 neonates were Female and 40 neonates were male.
- Youngest baby scanned was 3rd day and oldest baby was 90th day.
- Out of 70 babies positive findings were seen in 20 neonates on MRI and 16 neonates on Neurosonogram.
- Incidental findings were noted in 4 Neurosonogram study.
- Neonatal death was seen in 1 baby due to severe intraparenchymal hemorrhage.

Conclusion:

- MRI and Neurosonogram are both used as complimentary in evaluation of neonate with history of dystocia.
- Incidental findings are not well evaluated in MRI alone.
- Although MRI is best modality, Neurosonogram is adjunctive.
- Periventricular leukomalacia is better seen on MRI.
- MRI and Neurosonogram should be done between 24 hrs and 7 days to expected date of delivery.

Poster: SCI-241

EVALUATION OF MAJOR INTRACRANIAL ARTERY RESISTIVE INDEX IN MANAGEMENT OF NEONATAL HYDROCEPHALUS

DHANANJAYA KOTEB Narayana Vamyanmane, RAMESH R L, MANU S, VINODH D, SHRAMANA Bagchi
Indira Gandhi Institute Child Health, Bengaluru, INDIA

AIM OF THE STUDY:

- Comparing the Resistive Index (RI) of Anterior Cerebral Artery (ACA) and Middle cerebral artery (MCA) in hydrocephalic infants.
- Studying the changes in RI of ACA and MCA in hydrocephalic infants before and after drainage of cerebrospinal fluid (CSF).
- Establishing the standard value for considering surgical interventions in hydrocephalus.
- Application of Resistive Index as marker tool for non-surgical management.

Materials and Methods:

Prospective study of neonates with various degree of hydrocephalus.

Inclusion: All the cases with hydrocephalus included in our study.

Exclusion: Intracranial space occupying lesions, trauma and congenital anomalies of brain were excluded. Frontal ventricular/ intracranial diameter Ratio of less than 0.26.

Technique:

Duplex Doppler /Ultrasonography of cranium done. Resistive index (RI) from Anterior cerebral and Middle cerebral arteries were taken pre and post drainage of CSF. Both anterior fontanelle and temporal/mastoid window used for Doppler study of anterior and middle cerebral artery.

Drainage of CSF done with following methods: CSF Tapping done from EVD with reservoir, lumbar puncture and ventricular-peritoneal shunting

Results:

- Neonates with clinically suspected hydrocephalus with inclusion criteria were studied.
- Mild, moderate, severe and extreme hydrocephalus was classified according to V/H ratio.
- RI of 0.75 with clinical symptoms of increased intracranial pressure was considered as threshold for CSF drainage.
- RI of 0.85 without clinical symptoms of increased intracranial pressure was considered as threshold for CSF drainage.
- There is 10 to 15% reduction in RI after CSF drainage and improvement in clinical condition.

- Clinically significant positive correlation between degree of hydrocephalus and Resistive index (RI) in the MCA and/ or ACA.

Conclusion:

- Resistive index of ACA and / or MCA provides a reliable measure of cerebrovascular resistance in hydrocephalus.
- Ultrasonography and Duplex Doppler study is a useful noninvasive means of monitoring cerebrohaemodynamic change in infantile hydrocephalus.

Poster: SCI-242

BRAIN MRI FINDINGS IN PAEDIATRIC PATIENTS WITH DEVELOPMENTAL DELAY AT A TERTIARY HOSPITAL IN JOHANNESBURG, SOUTH AFRICA

FARZAANA Badat³, HALVANI Moodley^{1,3}, HEATHER CLARE Thomson^{1,3}, JACQUELINE KIM Bezuidenhout^{1,3}, SHEETAL Daya^{2,3}

¹ Charlotte Maxeke Johannesburg Academic Hospital, Johannesburg, SOUTH AFRICA

² Helen Joesph Hospital, Johannesburg, SOUTH AFRICA

³ University of the Witwatersrand, Johannesburg, SOUTH AFRICA

Purpose: Developmental delay (DD) in children should be diagnosed as early as possible for intervention, as it has a significant impact on communication, mobility, schooling and societal participation. The worldwide prevalence of developmental delay is 2 – 5%, however the prevalence in South Africa is unknown. Neuroimaging is an adjunct to the clinical, biochemical and genetic work up of children with DD. MRI of the brain is the modality of choice with a positive yield of 54 – 84 %. We assessed the findings and utility of MRI brain studies at first presentation of DD, in a resource limited environment by comparing this to the primary-, secondary complaints and clinical diagnosis.

Methods: A retrospective study was conducted for children under the age of 5 years presenting to the Charlotte Maxeke Johannesburg Academic Hospital to the neurodevelopmental clinic from January 2018 to December 2019. Ninety - five patients with complete clinical work up and MRI brains exams were enrolled consecutively.

Results: The median age was 34,07 months, with 57 (60%) children being male. DD (51, 53,68%) and speech delay/abnormality (18, 18,95%) were the most common primary presenting problems respectively. Cerebral palsy (CP) was the most common primary diagnosis (51, 53,68%), followed by autism spectrum disorder (14, 14,74%). Eighty - three children (83/95, 87,37%) had abnormal MRIs with abnormalities of the white matter (77, 81,05%), corpus callosum specifically (61, 64,21%) and ventricular abnormalities (54, 56,84%) being the most common. Abnormal MRIs were more likely with primary complaints of DD (48/51, 94,12%, p=0.027) and speech delay/abnormality (12/18, 66,67%, p=0.008). Children with a diagnosis of CP were more likely to have an abnormal MRI (49/51, 96,08% p=0.0059). Hypoxic ischaemic injury patterns on MRI were most common in CP (p=0.1351).

Conclusion: We are the first to document the spectrum of MRI brain findings at first assessment of DD in South Africa with a high diagnostic yield. In our resource - constrained environment, this is an effective use of MRI in the investigation of DD with guidance for clinicians on which presenting complaints and diagnoses could potentially benefit from MRI.

Poster: SCI-243

PROTOCOL-BASED IMAGING OF PAEDIATRIC BRAIN TUMOURS WITH MAGNETIC RESONANCE IMAGING (MRI) USING COMPRESSED SENSE: IMPACT ON IMAGE QUALITY AND EXAMINATION TIME

RIEKE LISA Meister¹, MICHAEL Groth¹, JULIAN Jürgens¹, SHUO Zhang², CHRISTOPH Katemann², THOMAS Amthor³, JAN HENDRIK Buhk⁴, JOCHEN Herrmann¹

¹ Department of Diagnostic and Interventional Radiology and Nuclear Medicine, Section of Paediatric Radiology, University, Hamburg, GERMANY

² Philips Healthcare, Hamburg, GERMANY

³ Philips Research, Hamburg, GERMANY

⁴ Department of Diagnostic and Interventional Neuroradiology, University Medical Center Hamburg-Eppendorf, Hamburg, GERMANY

Purpose

To compare a dedicated MRI brain tumour protocol for children with and without Compressed SENSE (C-SENSE) with regards to image quality, artefacts, examination time and specific energy dose (SED).

Material and Methods

Two consecutive MRI studies of 22 patients from 2.33 to 18.83 years with different brain tumour entities were assessed. The standardized MRI protocols included each a 3D T1-weighted turbo-field-echo pre- and post-contrast, a T2-weighted turbo-spin-echo (TSE), and a fluid attenuated inversion recovery (FLAIR) sequence. Main imaging parameters were kept comparable between both studies. C-SENSE FLAIR was adjusted additionally for best fluid suppression.

Exam duration and SED of all sequences were evaluated with a dedicated analysis tool based on scanner logfiles. Image quality and artefacts of the C-SENSE and standard/SENSE study were assessed for each patient in a consensus reading by two experienced paediatric radiologists with a dedicated scoring system for different anatomical regions.

Results

Total scan duration of the C-SENSE was significantly shorter than the standard protocol (20.94 ± 1.85 min vs. 16.52 ± 1.60 min, $p = 0.001$) with C-SENSE T2 benefiting the most. Total SED was reduced by 53.8 % (1703.6 ± 116.9 J/kg vs. 786.3 ± 150.3 J/kg, $p < 0.001$). Image quality and sharpness were improved in C-SENSE T1 pre- and post-contrast and FLAIR ($p = 0.001$), while deemed similar in C-SENSE T2. Different C-SENSE-related artefacts with no impairment of assessment were observed in C-SENSE T1. CSF artefacts were mitigated sufficiently in C-SENSE FLAIR with help of the additional parameter adjustments ($p = 0.001$).

Conclusion

The Compressed SENSE technique can significantly reduce the scan time required for a MRI protocol of paediatric brain tumours while maintaining or even improving the image quality. The benefits for daily clinical routine have been demonstrated with promise in shortened examination and sedation time, reduced energy deposit as well as improved compliance of paediatric patients.

Poster: SCI-244

POLYTRAUMA IN CHILDREN - COMPUTED TOMOGRAPHY ASSESSMENT OF CRANIOCEREBRAL PATHOLOGIES

MALGORZATA Matuszek ¹, EWA Kopyto ¹, MONIKA Zbroja ¹, MAGDALENA MARIA Wozniak ²

¹ Students' Scientific Association at The Department of Pediatric Radiology, Medical University of Lublin, Lublin, POLAND

² The Department of Pediatric Radiology, Medical University of Lublin, Lublin, POLAND

Purpose: Traumatic injuries are common in all age groups, especially in children and are the leading cause of death in children aged 10–19 years. The multi-organ damage is known as polytrauma. One of the most serious complications is traumatic brain injury that significantly deteriorates the patient's prognosis. The aim of this study was the retrospective assessment of head traumatic changes occurrence in the pediatric patients referred to computed tomography (CT) polytrauma examination.

Materials and methods: The study included 67 consecutive patients, aged 1 to 17 years, examined in the Department of Pediatric Radiology, Medical University of Lublin, who underwent CT examination in

polytrauma protocol during the period from January to November 2020. The examination was performed with Siemens Definition AS+ in spiral acquisition. Preliminary analysis identified 29 patients (53.3%) with post-traumatic craniocerebral changes, excluding 38 patients without head injury.

Results: Imaging findings were divided into 4 main groups: 1. cerebral oedema (n=16), 2. subgaleal hematoma (n=16), 3. intracranial hemorrhage (n=9), 4. skull fracture (n=12). Cerebral oedema most often accompanied a subgaleal haematoma (n=6) and bone fractures (n=6). The subgaleal hematoma was usually located in the parietal area (n=9). Intracranial hemorrhage occurred only in the form of intracerebral haemorrhages. Fractures affected neurocranium (n=8) and facial bones (n=4).

Conclusions: Head traumatic lesions often occur in the course of multi-organ trauma. Most post-traumatic deaths occur during the first hour after the injury, therefore quick and complex diagnosis and low CT invasiveness is crucial to reduce mortality.

Poster: SCI-245

MAGNETIC RESONANCE SPECTROSCOPY STUDY OF ACUTE MILD TRAUMATIC BRAIN INJURY

ANDREI Manzhurtsev ¹, MAXIM Ublinskiy ^{1,2}, PETR Bulanov ¹, OLGA Bozhko ¹, TOLIB Akhadov ¹, NATALIA Semenova ^{1,2}

¹ Clinical and Research Institute of Emergency Pediatric Surgery and Trauma, Moscow, RUSSIA

² Emanuel Institute of Biochemical Physics of the Russian Academy of Sciences, Moscow, RUSSIA

Introduction

To date, the mechanisms of post-traumatic disorders in mTBI are studied poorly and require additional research. Clinical and experimental data demonstrate that the row of molecular and cellular processes following mTBI. The balance between major neurotransmitters (excitatory – glutamate (Glu), and inhibitory – gamma-aminobutyric acid, GABA), is crucial for the normal functioning of CNS.

Materials & Methods:

Eighteen patients with acute mTBI (up to 72 hours since the injury, aged 16.2 ± 1.9 , 8f+10m) and fifteen healthy age-matched controls (9f+6m) participated in the study. MRI scanner Philips Achieva dStream 3.0T was used with receive SENSE head coil. Standard MRI protocol revealed no pathological lesions in brain tissue of any subject.

The MEGA-PRESS spectra of GABA and TE averaged PRESS spectra to study glutamate (Glu) were acquired. GABA spectra were processed in Gannet 3.1. A single lorentzian line was used to fit Glu resonance peaks in TEav PRESS spectra.

Results:

No statistically significant change in GABA was found from individual spectra processing. The fit error for averaged GABA signal was ~3 times lower than for a typical individual GABA spectrum (see fig.1). From the group-averaged MEGA-PRESS spectra, GABA was increased by $9 \pm 5\%$ in mTBI group. For Glu, the results are opposite: from the individually processed data Glu decreased by 3% ($p < 0.05$), while the averaged spectra demonstrated the lack of Glu change: 0.5% decrease with 0.9% error.

Conclusions:

The accuracy of the group-averaged spectral processing is significantly higher than of individual processing. The 9% change in GABA is rather low, keeping in mind the magnitude of the individual spectrum processing error (up to ~15%). In our study, the improved processing allowed to detect the effect of acute mTBI on the GABA levels in PCC. On the other hand, the $p < 0.05$ statistically significant Glu change seems to be false positive. The results of the study draw attention to the data quality and indicate that the statistical significance of the effect may be not enough for the confidence in results.

To sum up, the excitatory-inhibitory neurotransmitter balance is shifted towards excitation in the region of posterior cingulate cortex after acute mTBI. Long-term studies may be of interest in order to connect the mTBI outcome with the [GABA] and [Glu] dynamics.

Poster: SCI-246

LATE-ONSET SUBVENTRICULAR ECHOGENICITY ON CRANIAL SONOGRAPHY IN EXTREMELY LOW BIRTH WEIGHT INFANTS WITH INTESTINAL PERFORATION

SARA Janos¹, ADRIAN Epstein², ERIC Benner², CHARLES MICHAEL Cotten², LOGAN Bisset¹, JOSEPH Davis¹, CHARLES Maxfield¹

¹ Duke University Hospital - Department of Radiology, Durham, USA

² Duke University Hospital - Department of Pediatrics, Durham, USA

Purpose:

To report clinical associations and possible neurodevelopmental significance of a previously uncharacterized cranial ultrasound finding in premature infants.

Materials and Methods:

We performed a retrospective review of all extremely low birth weight infants (< 1000 grams) born at our institution between 1/1/2017 and 12/31/2019. Infants included in the study had a baseline cranial ultrasound at the end of the first week of life that was negative for germinal matrix hemorrhage and at least one additional follow-up cranial ultrasound (n=132). The ultrasounds were assessed by three pediatric radiologists for the presence of subventricular echogenicity after the first week of life, as defined by bilateral and symmetric, homogeneously increased echogenicity in the expected location of the germinal matrix: along the foramina of Monro, tracking variably up the lateral wall of the frontal horns. The positive cases were subsequently compared to an equal number of matched negative controls (n = 52) to assess for clinical associations and differences in neurodevelopmental outcomes, retrieved through medical record review.

Results:

26/132 (20%) patients were positive for late-onset subventricular echogenicity with an average gestational age of 25.2 weeks (range 23.4–28.4). There were no statistically significant differences in gestational age, birth weight, or gender between the case and control groups (p values range from 0.17–1.0). 13/26 (50%) of the positive cases had intestinal perforation prior to the appearance of subventricular echogenicity. 3/26 (12%) in the control group had intestinal perforation (p = 0.003). There were no statistically significant differences between the two groups in the number of patients with positive blood cultures, clinical sepsis requiring prolonged antibiotic therapy, adrenal insufficiency, bronchopulmonary dysplasia, or surgical PDA ligation. Insufficient clinical follow-up data precluded meaningful comparison of neurodevelopmental outcomes.

Conclusions:

Bilateral and symmetric subventricular echogenicity occurring after the first week in extremely low birth weight infants is associated with intestinal perforation and may reflect systemic inflammation affecting the germinal matrix.

Poster: SCI-247

THE IMPACT OF CEREBELLAR VOLUME ON BRAIN NETWORKS IN CHILDREN WITH EPILEPSY

KATJA GLUTIG Glutig¹, LUISA KAROLINE Lange¹, CHRISTIAN Gaser², HEIKE de Vries³, HANS-JOACHIM Mentzel¹

¹ Section of Pediatric Radiology, Institute of Diagnostic and Interventional Radiology, Jena University Hospital, Jena, GERMANY

² Department of Neurology Biomagnetic Center, Jena University Hospital, Jena, GERMANY

³ Department of Neuropediatrics, Jena University Hospital, Jena, GERMANY

PURPOSE:

The relationship between cerebellar volume and different neuronal networks in children with epilepsy should be clarified.

METHODS:

High resolution MRI including T1w 3D MPRAGE at 1.5 and 3T in a group of children with epilepsy of unknown etiology (N 16 f, 25 m; median 11 years (3.1 – 18.8)) and in a control group of children with headache but without pathology in cMRI (N 15 f, 11 m; median 12.1 years (5.3–17.1)) were analyzed retrospectively.

Patients were divided into subgroup A with one antiepileptic drug (N=31) and subgroup B with more than one antiepileptic drug (N=10).

Evaluation of the total cerebellar white and grey matter and 48 different cerebellar subregions was performed using region-based morphometry technique (Computational Anatomy Toolbox (CAT12)). Volume analysis was carried out using generalized linear models (GEE).

RESULTS:

Children with epilepsy showed significantly less volume in the whole cerebellar white matter

(p = 0.04).

Analysis of different cerebellar subregions revealed significant less volume in 5 different white matter areas: lobulus V (right p=0.03, left p=0.01), lobulus VIIIA (left p=0.01), lobulus VIIIB (right p=0.01, left p=0.02).

Analysis of subgroup A showed additionally significant volume loss in left Crus I (p=0.01).

Subgroup B had significant volume loss of white matter in the right Lobulus X (p=0.02).

CONCLUSION

A single consideration is not sufficient to understand disturbed network interactions in children with epilepsy. Lobulus V, VIII A and B in the anterior lobe of the cerebellum are interconnected with sensorimotor areas. Crus I as part of the posterior lobe is associated with higher cognitive functions. Lobulus X had vestibular afferences from the inner ear for controlling of head and ear movement.

Our study in children with epilepsy was able to demonstrate a reduced volume in areas connected to sensorimotor and higher cognitive function areas. The results indicate a contribution of epilepsy to the disruption of neuronal development in children.

Poster: SCI-248

THE ROLE OF ADVANCED EPILEPSY-SPECIFIC MRI PROTOCOL IN THE DIAGNOSIS OF PHARMACORESISTANT EPILEPSY IN CHILDREN

WERONIKA Cyranka¹, MONIKA Zbroja¹, KATARZYNA Drelich¹, MAGDALENA Wozniak²

¹ Students' Scientific Society at the Department of Pediatric Radiology, Medical University of Lublin, Lublin, POLAND

² Department of Pediatric Radiology, Medical University of Lublin, Lublin, POLAND

Purpose: Magnetic resonance imaging (MRI) has a well-established role in the diagnosis of epilepsy being crucial modality in identification of a wide spectrum of epileptogenic conditions, particularly in patients with pharmacoresistant disease. However, standard brain MRI is often not specific enough to reveal epileptogenic lesions, particularly small or subtle. The aim of the current preliminary study was the assessment of the usefulness in children of the epilepsy-specific MRI protocol called Essential Six, determined based on a large European presurgical epilepsy program.

Methods One hundred and eight children with pharmacoresistant epilepsy underwent MRI according to the epilepsy-specific MRI protocol including 3D T1-weighted images at 1 mm isotropic voxels size and 5 sequences of < 3 mm slice thickness, a hemosiderin/calcification-sensitive sequence in axial section and T2-weighted/STIR and FLAIR images in axial and coronal sections. All examinations were performed with Siemens Aera 48-channel 1.5T MRI scanner.

Results: 34 of 108 children (31, 4%) included into the study presented the spectrum of epileptogenic lesions. Heterotopy was diagnosed in 14 patients (41%), cortical dysplasia in 6 patients (18%), and polymicrogyria in 4 patients (12%). The presence of cysts near the hippocampus was found in 3 patients (9%). One child had hypoplasia of the cerebral hemispheres (3%). In 6 children (18%), MRI of the head showed coexisting abnormalities in the CNS.

Conclusions: The advanced epilepsy-specific MRI protocol can contribute to improved and earlier identification of epileptogenic lesions in children with pharmacoresistant epilepsy and seems to be more sensitive compared to standard brain MRI protocol.

Poster: SCI-249

COMPARING MEASUREMENTS ON STANDARD AND ULTRAFAST MRI SEQUENCES

CAI LING Yong, PHUA HWEE Tang
KK Women's and Children's Hospital, Singapore, SINGAPORE

Purpose

To compare the length of brain structures on ultrafast and standard brain sequences as slice thickness and imaging planes differ between the ultrafast and standard brain protocols.

Materials and Methods

MRI sequences of all patients scanned with ultrafast and standard MRI brain protocol at the same sitting on 3T MRI scanner were retrieved. Single operator performed measurements on both sets of MRI data using ITK-SNAP. There were 14 patients with normal brains and 35 patients had brain abnormalities.

Anteroposterior length of corpus callosum on sagittal T1 MRI sequences, distance between tips of the frontal horns on axial T2 weighted sequences, transverse dimension of cerebellum (on axial FLAIR ultrafast and coronal standard brain sequences) were obtained as these structures are clearly defined on MRI. T test was performed to check for statistical differences with $p < 0.05$ considered significant.

Results

Forty-nine participants took part in this Institute Review Board prospective and they consisted of 28 males, 21 females, with average age of 10.3 +/- 4.7 years (age range 1.0 to 18.0).

Corpus callosum measure 65.8 +/- 5.9mm (48.3 to 75.5mm) on 5mm thick sagittal T1 ultrafast compared to 65.8 +/- 5.9mm (48.2 to 76.1mm) on 1mm thick sagittal T1 standard sequence ($p=0.90$).

Transverse dimension of cerebellum measure 103.6 +/- 6.6mm (range 82.2 to 115.9mm) on axial FLAIR ultrafast compared to 103.8 +/- 6.6mm (82.2 to 116.2mm) on coronal FLAIR standard ($p=0.03$).

Distance between frontal horns measure 35.3 +/- 7.2mm (range 25.4 to 66.9mm) on axial T2 ultrafast compared to 35.1 +/- 7.2mm (25.2 to 66.6mm) on axial T2 standard sequence ($p < 0.01$).

Conclusion

Linear measurements performed on ultrafast and standard MRI brain sequences in our cohort are comparable despite differences in slice thickness and imaging planes.

Poster: SCI-250

LACRIMAL SACK PATHOLOGY: THE ROLE OF ULTRASOUND - A CASE PRESENTATION

ELENI Koutrouveli¹, RODANTHI Sfakiotaki¹, GEORGIOS Daniil², IRENE Vraka¹, ANNA Chountala¹, MARINA Vakaki¹, CHRYSOULA Koumanidou¹

¹ Children's Hospital of Athens P&A Kyriakou, Athens, GREECE

² General Hospital of Thessaloniki G. Gennimatas, Thessaloniki, GREECE

Purpose:

The role of ultrasound in lacrimal sack pathology in children. A bedside diagnostic approach and follow up. Case Presentation.

Materials:

A 10 year-old boy with no significant past medical history presented with left medial canthal and periorbital swelling, periorbital erythema, sticky eyes, epiphora and one-week onset of mild fever.

Methods:

Facial CT revealed left-sided homogenous periorbital and suborbital soft tissue edema. No bone erosion was noted.

Ultrasound showed diffuse periorbital edema and a well-circumscribed ovoid lesion at the tip of the nasolacrimal duct, filled with echogenic fluid and no internal vascularity on color Doppler. No calculi or soft tissue mass was depicted along the lacrimal duct course. History, Clinical and ultrasonographic findings supported the diagnosis of Dacryocystitis complicated by lacrimal abscess.

Results:

Patient was treated with intravenous antibiotics and anti-inflammatories which resulted in spontaneous drainage of the lacrimal abscess into the nasal cavity after three days. On follow up ultrasonography all signs of inflammation were absent and normal sonographic anatomy of the region was restored.

Conclusion:

Ultrasound is a radiation-free, readily available and inexpensive modality for a bedside diagnostic approach and follow up of everyday periorbital pathology, allowing differentiation of benign from malignant dacryocystitis, identification of lacrymal sack abscess and evaluation of the adjacent and periorbital soft tissues, offering a significant advantage in depicting soft tissue anatomical details of the lacrimal apparatus compared to CT. Awareness about potential thermal effects to the orbit and optimization of scanning settings is a prerequisite for patient safety.

Poster: SCI-251

RAPID MAGNETIC RESONANCE IMAGING OF THE BRAIN IN A PEDIATRIC EMERGENCY DEPARTMENT: AN ANALYSIS OF USAGE FOR HEADACHE

MARIA Velez-Florez, ARASTOO Vossough, SUMMER Kaplan
Children's Hospital of Philadelphia, Philadelphia, USA

Purpose: Headache is the third most common cause of visits to pediatric Emergency Departments (ED), and as many as 36% of patients get imaged. Neuroimaging should be reserved for children with headache and red flag findings such as vomiting, worsening with Valsalva, altered mental status, seizures, fever, awakening pain, change of the character of headache, increased head circumference, neurological deficits, and first or worst ever. Rapid magnetic resonance imaging of the brain (rMRI) is a popular pediatric technique because it avoids ionizing radiation and decreases time and sedation needs of MRI, but it may have limited diagnostic range. Most rMRI literature focuses on hydrocephalus and nonaccidental trauma. Although headache is the most common indication for pediatric ED MRI, there are no known studies comprehensively evaluating the use of rMRI for the study of headache in children. We assessed ED rMRI for headache for the first year it was widely offered at our

institution through a unique ordering code in the electronic health record in order to understand its clinical utility.

Methods: We retrospectively reviewed rMRI reports at our pediatric hospital between January–December 2019. We recorded demographics and coded radiology reports in terms of indication and diagnostic impression. We used descriptive statistics and studied categories association using Fisher exact test.

Results: rMRI was performed 524 times by the ED (78% of all cases). Median age was 11.6 years old (range 0–22 years), 51% were female. Headache was the most common indication (40%), and 49% were associated with red flag findings. Most of these were nausea and vomiting (16%), focal neurological deficits (11%), visual abnormalities (8%), and seizures or fever (4%). The most common radiology report impressions were normal (66%) and paranasal sinus disease (10%). There was a significant association of headache with the radiology impressions normal, paranasal sinus disease, cerebellar tonsillar ectopia, and no acute findings ($p < 0.005$).

Conclusion: Our results suggest ED rMRI brain is used commonly for patients with headache, only half of them with associated red flag findings, and mostly with inconsequential results. In normal neurological examination in pediatric headache, the yield of neuroimaging is low. It is imperative to standardize protocols and policies for this technique in order to harness its potential and reduce unnecessary imaging costs.

Poster: SCI-252

DYNAMICS OF MICROSTRUCTURAL AND METABOLIC PARAMETERS IN CHILDREN WITH SEVERE TBI AND HYPOXIC-ISCHEMIC BRAIN INJURY

MAXIM Ublinskiy¹, ANDREI Manzhurtsev^{1,2}, ILYA Melnikov¹, TOLIBDZHON Akhadov¹, NATALIA Semenova^{1,2}, ALEXEI Yakovlev^{1,2}

¹ Clinical and Research Institute of Emergency Pediatric Surgery and Trauma, Moscow, RUSSIAN FEDERATION

² Institute for Biochemical Physics (IBCP), Russian Academy of Sciences (RAS), Moscow, RUSSIAN FEDERATION

Purpose / Learning Objectives: Aim of this study was to explore the dynamics of microstructure and brain metabolism parameters in children with severe traumatic brain injury (sTBI) and hypoxic-ischemic brain injury (HIBI).

Methods and materials / Background: 8 patients (mean age = 12.5) with sTBI comprised group 1. 4 children (mean age = 13.6) with HIBI caused by drowning in fresh water. MR studies of patients from both groups were carried out twice: first - during the first seven days after injury (period 1); second - a month after injury (period 2). All studies were performed at Phillips Achieva 3.0T MRI scanner. DT MR images were acquired with diffusion gradients applied in 32 non-collinear directions. 1H-MRS voxel (TR/TE = 1500 ms/ 40 ms, NSA = 128) was localized in left and right thalamus (for groups 1 and 2) and in brain stem (for group 2).

Results: 1H MRS analysis in thalamus revealed significant decrease in dynamics of NAA/Cho value in group 1 (41% decrease) and absence in dynamics of this index in group 2. Significant increases in dynamics of ADC and FA values were found in corpus callosum in group 1. In group 2 we detected increase in dynamics of ADC value and NAA/Cho ratio in brain stem.

Conclusion: The significant decrease of NAA/Cho dynamics in thalamus in group 1 may indicate an active NAA intake in synthesis of oligodendrocytes to restore myelin sheath. Dynamics of spectroscopy and DTI parameters in brain stem correlates with the restoration of CNS functions in patients after drowning.

Poster: SCI-253

DYSFUNCTION OF FUNCTIONAL CONNECTIVITY BETWEEN DEFAULT MODE NETWORK AND CEREBELLAR STRUCTURES IN PATIENTS WITH MTBI IN ACUTE STAGE. RSFMRI AND DTI STUDY

MAXIM Ublinskiy¹, ANDREI Manzhurtsev^{1,2}, ILYA Melnikov¹, TOLIBDZHON Akhadov¹, NATALIA Semenova^{1,2}, ALEXEI Yakovlev^{1,2}

¹ Clinical and Research Institute of Emergency Pediatric Surgery and Trauma, Moscow, RUSSIA

² Institute for Biochemical Physics (IBCP), Russian Academy of Sciences (RAS), Moscow, RUSSIA

Introduction: Mild traumatic brain injury (mTBI) occupies one of the first places in children injuries. Among all brain networks at the resting state, the Default Mode Network (DMN) is the most widely studied network. The aim of this study is to examine functional connectivity in normal-appearing cortex in acute period of mTBI using rsfMRI.

Material & Methods: 34 MR negative participants were studied in age from 12 to 17 years (mean age – 14.5 years). Group of patients consisted of 17 children with mild traumatic brain injury in acute stage. 17 age-matched healthy volunteers comprised control group. All studies were performed at Phillips Achieva 3.0T MRI scanner using 32-channel head coil. fMRI data were processed using functional connectivity toolbox CONN. Seed-based analysis was performed in order to reveal disturbances in functional connectivity. Statistical processing was performed using Statistica 12.

Results: DTI analysis didn't show any changes in values of apparent diffusion coefficient (ADC) and fractional anisotropy (FA) between two groups. No statistically significant differences in correlation strength between DMN parts were observed in two groups. Intergroup seed-based analysis revealed statistically significant ($p < 0.05$) difference in neural correlations between DMN parts and vermis (cerebellum structural part): positive link in control group and negative link in group of patients.

Conclusions: One of the most common symptoms of mTBI is dizziness as a result of impaired movements coordination. Vermis as an essential cerebellum part plays an important role in the vestibulo-ocular system which is involved in the learning of basic motor skills in the brain. Vermis aids in the synchronization of eye and motor functions in order for the visual field and the motor skills to function together. Our results show that mTBI appears to be a possible reason of connectivity malfunction in normal-appearing vermis.

Poster: SCI-254

CEREBROSPINAL FLUID FLOW DETECTION IN POST-HEMORRHAGIC HYDROCEPHALUS WITH NOVEL MICROVASCULAR IMAGING MODALITY

LUIS OCTAVIO Tierradentro-García¹, BRANDI L. Kozak¹, KASSA Darge², MISUN Hwang²

¹ Department of Radiology, Children's Hospital of Philadelphia, Philadelphia, USA

² Department of Radiology, Children's Hospital of Philadelphia, Perelman School of Medicine, University of Pennsylvania, Philadelphia, USA

Purpose: Microvascular imaging is an innovative advancement of Doppler ultrasound (US) designed to detect slow blood flow in microvessels and reveal important insights into various pathologies affecting tissue perfusion. This technology uses a clutter suppression algorithm to better depict low-speed flow signals with color or monochrome maps while discarding motion-related artifacts. The potential utility of this technology in non-vascular pathologies is largely unknown. We will show for the first time that cerebrospinal fluid (CSF) flow may be depicted using brain US by implementing highly sensitive microvascular

imaging technology. This novel application could potentially expand the use of this technology beyond depiction of vascular flow pathologies in newborns.

Methods: We evaluated two patients wherein microvascular imaging technology detected turbulent CSF jetting from the cerebral aqueduct into the third ventricle. Brain US with B-flow (microvascular imaging technology from GE Healthcare), using L2-9 probe and Logiq E10 system, were performed in both patients.

Results: The first case (19-day-old term male) had hypoplastic left heart syndrome (status post stage I palliative surgery) and presented with post-operative seizures and ventriculomegaly. Prior brain US and MRI showed bilateral choroid plexus hemorrhage and acute ventriculomegaly. Brain US with microvascular imaging revealed a turbulent influx of CSF jet from the cerebral aqueduct into the third ventricle, retrograde than expected of normal CSF flow. The second case (16-day-old preterm female) had post-hemorrhagic hydrocephalus from bilateral grade 3 intraventricular hemorrhage. Coronal and sagittal brain US demonstrated marked ependymal echogenicity and thickening, as well as avid flow in the ventricular ependymal lining and turbulent flow jets across the cerebral aqueduct and third ventricle also in retrograde fashion.

Conclusion: Our findings suggest that microvascular imaging technology may be used beyond vascular imaging to assess the direction and turbulence of CSF flow in infants with post-hemorrhagic hydrocephalus. The potential clinical and prognostic significance of CSF flow detection with microvascular imaging technology warrants further investigation.

Poster: SCI-255

BENIGN DEVELOPMENTAL CHANGES OF THE THYROID CARTILAGE MIMICKING PATHOLOGICAL NODULES

TIMOTHY SHAO ERN Tan, SARAT KUMAR Sanamandra
Department of Diagnostic Radiology, Singapore General Hospital, Singapore, SINGAPORE

PURPOSE/BACKGROUND

A previously well 30-year-old man presenting with clinical and biochemical (Serum T4: 34.2pmol/L, Thyroid stimulating hormone: <0.010MU/L, TSH receptor antibodies: 14.50IU/L) features of hyperthyroidism was referred for sonographic evaluation of his thyroid gland. No palpable neck lump was felt on examination.

RESULTS:

Sonography revealed a normal appearing thyroid gland with no focal lesion or abnormal vascularity evident. Several small subcentimetre well-defined focal oval anechoic-hypoechoic dilatations were however noted in both laminae of thyroid cartilage. No associated abnormal vascularity or discrete calcification was seen within. No enlarged cervical lymph nodes were detected. Overall features were consistent with cystic change in the thyroid cartilage, a normal variant.

The thyroid cartilage is formed by two lateral hyaline laminae joining ventrally to form a V-shaped cartilaginous sling. From its embryological development, it undergoes multiple processes of mineralisation and ossification in the posteroinferior lamina, secondary to micro-traumatism by the extralaryngeal musculature, resulting in progressive calcification. In some cases, this process does not evolve completely, and the thyroid cartilage may show cyst-like cavities, especially in the anterior half. These are usually incidentally discovered on imaging studies and may be symmetrical, affecting both thyroid laminae, mainly described in adolescents.

The differential diagnosis of these cyst-like changes in the thyroid cartilage include degenerative thyroid cartilage cysts, post-traumatic or post-radiotherapy cysts, chondromas, chondrosarcomas or metastases. Where there is doubt, clinical correlation and further evaluation with dedicated MRI neck would be useful.

CONCLUSION:

Knowledge and recognition of this rare anatomical variant is essential to avoid misdiagnosis and further unnecessary examinations or intervention.

Poster: SCI-256

AFTER-HOURS MRI AT CHILDREN'S HOSPITALS: EMERGENT VP SHUNT EVALUATION AS A JUSTIFICATION FOR 24-HOUR STAFFING

LELIA Williams¹, ELIZABETH Ryals², ANTHONY Radosevich³, CORY Pfeifer²

¹ UT Southwestern, Dallas, USA

² Children's Medical Center, Dallas, USA

³ Baylor University Medical Center, Dallas, USA

Background:

As children's hospitals have grown in size, the demand for 24-hour MRI services has increased. In the USA, few children's hospitals staff MRI technologists at all times, but the use of MRI in pediatrics to evaluate frequent emergency department complaints such as ventriculoperitoneal shunt dysfunction can avoid ionizing radiation while providing diagnostic specificity.

Methods:

A retrospective review of all emergently performed MRI's after hours at a large children's hospital (490 beds) during a 365-day period in which the MRI department was not staffed (between 2300 and 0700) was performed. MRI may only be performed when considered emergent by the ordering provider and the covering radiologist. The rate of those with positive findings was computed. This was determined via review by an attending pediatric radiologist and pediatric neuroradiologist with a positive finding representing an acute abnormality or a change from a prior study. The total number of CT's performed to evaluate shunt function between 2300 and 0700 in a 365-day period were also assessed.

Results:

121 emergent MRI's were performed over 365 days (33% of all 8-hour call shifts). The positive rate was 52%, with a positive MRI occurring on 17% of all 8-hour shifts. The total number of CT examinations performed to evaluate shunt function was 140 for an average of 38%. On average, a head CT to evaluate shunt function or emergent MRI is ordered after hours on 72% of all 8-hour shifts in which there is no regularly-scheduled MRI technologist coverage.

Conclusions:

Encouraging the use of rapid MRI of the head rather than CT could increase the number of procedures and justification for 24-hour coverage. Considering emergent evaluation for appendicitis and scanning inpatients could add additional justification. With a positive rate of 52%, it is conceivable that there are additional acute abnormalities missed under the present system due to restriction of afterhours access to MRI.

Poster: SCI-257

'TWO-IN-ONE' – IN-BORE CHILD AND PARENT POSITIONING FOR NON-ANESTHESIA PEDIATRIC MRI

ROMAN Melamed¹, AVIAD Rabinowich^{1,3}, SHELLY I Shiran^{1,3}, JONATHAN Roth^{2,3}, SHLOMI Constantini^{2,3}, LIAT Ben-Sira^{1,3}

¹ Department of Radiology, Tel Aviv Medical Center, Tel Aviv, ISRAEL

² Departments of Neurosurgery and Pediatric Neurosurgery, Tel Aviv Medical Center, Tel Aviv, ISRAEL

³ Sackler Faculty of Medicine, Tel Aviv University, Tel Aviv, ISRAEL

Purpose

MRI is a robust and effective diagnostic tool in pediatric imaging due to high-quality image contrast and tissue characterization without ionizing radiation. However, images can be substantially corrupted due to patient movement and noncooperation. Thus, the common use of anesthesia in young children. However, anesthesia is associated with a higher

prevalence of adverse outcomes, longer access times, and safety concerns. We present a method to achieve quality studies, with parental and patient positioning inside the magnet bore for complex cases when cooperation was not achieved with other measures.

Materials and Methods

We reviewed data collected from nine patients undergoing no anesthesia MRI, with a parent joining the patient inside the magnet bore. Criteria for inclusion were a) outpatient MRI referral, b) ages of 1-6 years and c) patient cooperation not achieved using other methods. Image quality was evaluated by an experienced pediatric radiologist and was ranked on a three-point scale: 'not acceptable', 'acceptable', or 'excellent'. Scans were also classified as diagnostic or not diagnostic, based on whether they answered the clinical question. The patient's gender, age, scanning protocol, clinical indication, study time, and the use of contrast were recorded.

Results

We analyzed nine children using our protocol (median age – 4.2 years, range – 1-5.7 years). Seven children underwent brain imaging, one child underwent brain and neck imaging, and one child had a knee scan. Intravascular contrast was injected in 2 cases. The average scan time was 29.1±10.2 minutes. Diagnostic image quality was obtained in all cases, and no anesthesia appointment rescheduling was needed. The average image quality was ranked 2.56±0.68. Only one scan was ranked as not acceptable image quality, although the clinical question was answered. No safety issues were recorded.

Conclusions

In-bore parent and child positioning is an effective tool for achieving child cooperation and good image quality. Future large-scale studies and comparisons with other methods are needed to evaluate this method's potential efficiency in image quality, scan time, and safety issues.

Poster: SCI-258

DO CHILDREN WITH SUSPECTED SHUNT FAILURE ALSO REQUIRE A RADIOGRAPHIC SHUNT SERIES IF HEAD CT IS GOING TO BE, OR HAS BEEN, PERFORMED?

MICHAEL Paddock¹, GEORGE Beattie¹, SAURABH Sinha², SUZANNE Mason¹, DANIEL JA Connolly²

¹ Barnsley Hospital NHS Foundation Trust, Barnsley, UNITED KINGDOM

² Sheffield Children's NHS Foundation Trust, Sheffield, UNITED KINGDOM

PubMed and Medline databases on NHS Evidence were searched which returned 3 eligible studies.

VP shunts are prone to complications with reported failure rates up to 50% within 2 years of placement and up to 87.5% of shunts failing by 10 years. No single symptom is diagnostic of shunt failure which can be life threatening if untreated. Both radiographic shunt series (ShS) and head CT are often employed to assess shunt function

Poor ShS sensitivity is reported (estimated 19.4%, true sensitivity <31% (95% CI)), a prediction that 10.46% of future SS will be expected to demonstrate the cause of shunt failure and that the SS is even less likely to agree with the findings from CT, MRI and nuclear cisternography (Cohen's kappa =0.02) than by chance alone. ShS is not advocated as an acceptable modality in the investigation of suspected shunt failure.

Cumulative lifetime exposure to ionising radiation can be significant and should be reduced wherever possible. Infants and children are more vulnerable to the accumulative risks of ionising radiation than adults. Single-view site-specific radiographs can reduce the number of complete ShS without compromising clinical care when performed for: 1) localised swelling or pain along the path of the shunt tubing, 2) externalised shunt tubing from distal migration (rare) or 3) surgical planning.

Head CT examinations are approximately 4 times the dose of ShS. Children with VP shunts reportedly undergo a median of 8.5 head CT and 3 ShS and have a head CT in nearly 50% of emergency attendances.

It is necessary to reduce exposure to ionising radiation by adhering to ALARA. Fast-sequence MRI is more cost-effective and definitive in the diagnosis of acute shunt failure when compared with head CT: improved access to MRI is required.

In children with long-term indwelling VP shunts, the absence of change in intracranial appearances does not signify shunt dysfunction nor that there has been a significant alteration in intracranial pressure. If there is persistent clinical concern, a neurosurgical opinion is required.

From the available retrospective evidence, ShS should not be used as a first-line investigation for suspected shunt failure and not been performed when a head CT is going to be, or has been, performed failure. If there is clinical concern for mechanical shunt failure (tubing disconnection, kink or breakage), specific single-view radiographs may be performed following proven shunt failure on cross-sectional imaging.

Poster: SCI-259

AVOIDING SKULL RADIOGRAPHS IN INFANTS WITH SUSPECTED INFLICTED INJURY WHO ALSO UNDERGO HEAD CT: "A NO-BRAINER?"

MICHAEL Paddock¹, ANDREW Martin², CHRISTOPHER Johns², JESSICA Smith³, ASHOK Raghavan⁴, DANIEL JA Connolly², AMAKA C Offiah⁴

¹ Barnsley Hospital NHS Foundation Trust, Barnsley, UNITED KINGDOM

² Royal Hallamshire Hospital, Sheffield, UNITED KINGDOM

³ University of Sheffield Medical School, Sheffield, UNITED KINGDOM

⁴ Sheffield Children's NHS Foundation Trust, Sheffield, UNITED KINGDOM

OBJECTIVES:

To assess whether head CT with 3D reconstruction can replace skull radiographs (SXR) in the imaging investigation of suspected physical abuse (SPA)/abusive head trauma (AHT).

METHODS:

PACS was interrogated for antemortem skeletal surveys performed for SPA, patients younger than 2 years, SXR and CT performed within 4 days of each other. Paired SXR and CT were independently reviewed. One reviewer analysed CT without and (3 months later) with 3D reconstructions. SXR and CT expert consensus review formed the gold standard. Observer reliability was calculated.

RESULTS:

A total of 104 SXR/CT examination pairs were identified, mean age 6.75 months (range 4 days to 2 years); 21 (20%) had skull fractures; two fractures on CT were missed on SXR. There were no fractures on SXR that were not seen on CT. For SXR and CT, respectively: PPV reviewer 1, 95% confidence interval (CI) 48-82% and 85-100%; reviewer 2, 67-98% and 82-100%; and NPV reviewer 1, 95%, CI 88-98% and 96-100%; reviewer 2, 88-97% and 88-98%. Inter- and intra-observer reliability were respectively the following: SXR, excellent (kappa=0.831) and good (kappa=0.694); CT, excellent (kappa=0.831) and perfect (kappa=1). All results were statistically significant (p<0.001).

CONCLUSIONS:

CT has greater diagnostic accuracy than SXR in detecting skull fractures which is increased on concurrent review of 3D reconstructions and should be performed in every case of SPA/AHT. SXR does not add further diagnostic information and can be omitted from the skeletal survey when CT with 3D reconstruction is going to be, or has been, performed.

KEY POINTS:

Head CT with 3D reconstruction is more sensitive and specific for the diagnosis of skull fractures.

Skull radiographs can be safely omitted from the initial skeletal survey performed for suspected physical abuse when head CT with 3D

reconstruction is going to be, or has been, performed.

Poster: SCI-260

MENINGIOANGIOMATOSIS IN A 5 YEAR OLD: A CASE REPORT

CHRISTABELL Ndibe, SUSAN Taylor, ADAM Goldman-Yassen, KARTIK Reddy
Emory University School of Medicine, Atlanta, USA

EDUCATIONAL OBJECTIVES:

1. Review the clinical and imaging findings of meningoangiomas as described in the literature.
2. Present a successfully treated case of meningoangiomas.
3. Summarize differential diagnosis and potential mimics of meningoangiomas.

SUMMARY OF PRESENTATION:

Meningioangiomas (MA) is a rare non-neoplastic brain lesion of unknown etiology. Meningioangiomas can be sporadic or syndromic, with the syndromic form associated with neurofibromatosis type 2. Most symptomatic patients with meningoangiomas have the sporadic form and typically present with medically refractory seizure. The imaging findings of MA are variable, making it a diagnostic dilemma. An understanding of the various imaging features, as well as the clinical presentation of MA is pivotal in ensuring accurate diagnosis and timely management.

We present the case of a 5-year-old girl without significant past medical history who presented to the emergency room after increasing frequency of multiple episodes of dysarthria lasting approximately 10-15 seconds each. The episodes were followed by confusion. EEG was normal. There was no history of trauma. Physical examination was within normal limits, revealing no focal neurologic deficits.

Computed Tomography of the head without contrast showed a calcified mass in the left temporal lobe. Magnetic Resonance Imaging obtained the same day showed focal cortical T1 and T2 hypointense signal, susceptibility and small foci of enhancement involving the left middle and inferior temporal gyri. There was no associated restricted diffusion.

The patient was initially managed conservatively with antiepileptic medications and discharged home. A left craniotomy was performed 2 months post-discharge for resection of the left temporal lesion. Pathology was consistent with meningoangiomas. The patient has remained seizure free since her surgery and continues treatment with an antiepileptic drug.

Poster: SCI-261

SIMULATION OF REDUCED-DOSE IMAGES USING NOISE-INSERTION PROGRAM FOR PEDIATRIC BRAIN CT

HYUN GI Kim¹, SEONGYONG Pak², JISEON Lim³

¹ The Catholic University of Korea, Seoul, SOUTH KOREA

² Siemens Healthineers Ltd., Seoul, SOUTH KOREA

³ Hankuk University of Foreign Studies, Yongin, SOUTH KOREA

Purpose: The purpose of this study was to simulate reduced-dose images with different levels of iterative reconstruction using a noise-insertion reconstruction program for pediatric brain CT.

Methods: Brain CT of children (< 16 years of age) were taken using tube voltage of 80 and different tube currents (range, 322 mA - 720 mA) depending on the patient's weight. With raw brain CT data, reduced-dose images were generated using a noise-insertion reconstruction program. Tube current reduction rate of 0%, 5%, 10%, and 15% from the original tube current was applied. Iterative reconstruction was done from level 1 to 5 in each image. Contrast-to-noise ratios (CNRs) and signal-to-noise ratios (SNRs) were calculated.

Results: Two hundred and eighty sets of images from 14 children's (mean weight, 24.8 kg; range, 3.6 kg – 68.0 kg) brain CT were reconstructed. CNR of 0% and 5% reduced-dose images increased with higher iterative reconstruction levels (0%, 0.227 to 0.565; 5%, 0.138 to 0.386). CNR of 10% reduced-dose images decreased with iterative reconstruction level increment from 4 to 5 (level 4, 0.207; level 5, 0.119). SNR of 0%, 5%, and 10% reduced-dose images increased with higher iterative reconstruction levels (0%, 6.794 to 11.174; 5%, 5.332 to 9.660; 10%, 4.889 to 7.490). In 15% reduced-dose images, SNR decreased with iterative reconstruction level increment from 1 to 2 (level 1, 4.422; level 2, 4.223). CNR and SNR of 5% reduced-dose images with iterative reconstruction level 4 were higher than those of original images (CNR, 0.238 vs. 0.227; SNR, 6.993 vs. 6.794).

Conclusion: Using noise-insertion reconstruction program, simulation of reduced-dose images with different levels of iterative reconstruction was possible for pediatric brain CT. Higher iterative reconstruction levels resulted in the different trends of image quality change, depending on the dose reduction rate. Five percentage dose reduction was possible without degrading image quality.

Poster: SCI-262

NEONATAL NEUROSONOGRAM – SPECTRUM OF CASES IN A TERTIARY CARE CENTRE IN INDIA

PRASANNA KARPAGA Kumaravel, NITIN ASHok, abirami krithiga
Rainbow Childrens Hospital, Hyderabad, INDIA

Purpose

Neurosonography is a simple, non-invasive technique without any radiation exposure and the first line of investigation for the intracranial assessment of neonates. A bedside neurosonogram is a vital investigation in the case of a critically ill infant. This pictorial essay attempts to highlight the sonographic anatomy and the spectrum of pathological imaging appearances seen in neonates.

Materials and Methods;

A compilation of neurosonogram cases with findings over a period of 6 months. All preterms and neonates are scanned early to diagnose intracerebral hemorrhages, hypoxic-ischemic encephalopathy (HIE), infections, and congenital problems. Bedside and OPD basis neurosonogram was performed with a dedicated neurosonogram and linear probes through anterior fontanelle and additional view whenever required. Images were obtained in coronal, sagittal, and parasagittal views. In this presentation, we present you images for normal anatomy, variants, and intracranial pathologies - intracranial hemorrhages, periventricular leukomalacia, obstructive and non-obstructive hydrocephalus, corpus callosal agenesis, cerebritis, cerebral abscess, subdural empyema, conatal cyst, choroid plexus cysts, porencephalic cyst, lenticulostriate artery calcifications.

Conclusion

Many general radiologists are not quite familiar with the spectrum of imaging appearances of the neonatal intracranium due to inadequate exposure. Many specific clinical questions can be resolved by optimally utilizing this simple informative tool. Despite the advances in computed tomography and MRI, NSG is the most commonly used first baseline modality for examining the neonatal brain. Neonatal NSG still remains a mainstay of imaging in the neonatal brain.

Poster: SCI-263

VOLUMETRIC ANALYSIS OF CAUDATE, LENTIFORM NUCLEI, THALAMIC VOLUMES OF CHILDREN WHO UNDERWENT MRI FOR HEADACHE

ABIGAIL Ho, PHUA HWEE Tang

KK Women's and Children's Hospital, Singapore, SINGAPORE

Purpose:

Aim to quantify the caudate, lentiform and thalami volumes of children with headache who have undergone MRI with normal brains on T2 weighted sequences to determine if they can be used as controls as the volumes of such structures show high variability in the published literature.

Material and methods:

In this retrospective pilot MRI study, T2 weighted MRI of children with headache and structurally normal brains had volumes of thalami, caudate, lentiform nuclei, quantified using ITK-SNAP by single operator. Volumes of caudate, lentiform nuclei and thalami were plotted with respect to age and compared between the genders. T-test was performed to check for statistical significance.

Results:

There were 316 children (129 males, 187 females) with average age of 12 years (range 3 to 15 years).

Caudate, lentiform and thalami volumes show stability across the ages of 3 to 15 years.

Average volume of right thalamus is 6.23 ± 1.63 for males compared to 5.97 ± 1.50 for females ($p = 0.07$)

Average volume of left thalamus is 6.39 ± 1.68 for males compared to 6.09 ± 1.67 for females ($p = 0.05$)

Average volume of right caudate is 4.88 ± 0.82 for males compared to 4.47 ± 0.61 for females ($p < 0.05$)

Average volume of left caudate is 4.56 ± 0.76 for males compared to 4.25 ± 0.57 for females ($p < 0.05$)

Average volume of right lentiform is 7.96 ± 0.76 for males compared to 7.39 ± 0.69 for females ($p < 0.05$)

Average volume of left lentiform is 7.95 ± 0.69 for males compared to 7.45 ± 0.73 for females ($p < 0.05$)

Conclusion:

Volumes of caudate, lentiform nuclei and thalami of children with headache show no significant difference across ages 3 to 15 years. Volumes of caudate, lentiform nuclei and thalami are smaller in females compared to males, reaching statistical significance for the caudate and lentiform nuclei.

Poster: SCI-264

GANGLIONEUROMA WHICH IS RARELY LOCATED ON THE NECK: A CASE REPORT

ZUHAL Bayramoglu, EZGI Kara, ESHGIN Sahibli, ELIF HAZAL Karli
Istanbul University, Istanbul Medical Faculty, Radiology Department,
Istanbul, TURKEY

Neck masses are frequently encountered in the pediatric population in daily radiology practice. We report a case of neck mass in a 5-year-old female, who presented with painless, gradually progressive mass in the right anterolateral side of the neck.

Neck masses are common in the pediatric population. A careful evaluation of the clinical history and detailed physical examination have an important place in the diagnosis and management of neck masses in pediatric patients. These masses may occur as a result of many conditions of congenital, acquired inflammatory, neoplastic, or vascular origin.

A 5-year-old female patient was referred to our hospital for further evaluation of neck mass. She presented with a neck swelling that persisted for two years. On physical examination, a painless mass was found on the right side of her neck. There was no history of rash, hoarseness, or dysphagia. It was learned that the patient had previously undergone lymph node excision and pathological evaluation was compatible with Rosai-Dorfman disease. Doppler ultrasonography demonstrated a well-defined, encapsulated, highly vascularised solid hypoechoic mass located at the carotid bifurcation and contained microcalcification. Magnetic resonance imaging (MRI) evaluation revealed a well-defined mass, isointense on T1-weighted imaging, and hyperintense on T2-weighted imaging,

involving the right carotid space, and intense enhancement following gadolinium was seen. Also, that mass was completely encasing the internal carotid artery (ICA) and enveloped external carotid artery (ECA). Differential diagnoses included Rosai-Dorfman disease, ganglioneuroma and carotid body tumor. The patient underwent US guided tru-cut biopsy and histopathological examination confirmed diagnose as a ganglioneuroma.

Ganglioneuromas should be considered in differential diagnosis of pediatric soft tissue tumors of the neck which located in the immediate vicinity of main neurovascular structures such as carotid arteries, vagus and jugular vein. They are normally asymptomatic, slow-growing and well-differentiated tumors of the autonomic nervous system. Cervical region is a rare localization for ganglioneuromas. Ultrasound, Computed tomography (CT), and MRI are radiological tools that are useful in diagnosis. The preferred method of treatment is surgical excision.

Poster: SCI-265

CEREBRAL VASCULAR FINDINGS IN CHILDREN WITH NEUROFIBROMATOSIS TYPE 1 USING TIME-OF-FLIGHT MRA

LAURA Acosta-Izquierdo¹, BRUNO MARINO Monarim¹,
CHRISTIAN ALFRED OBrien², ERICK Sell³, NAGWA Wilson¹

¹ Medical Imaging Department, CHEO, University of Ottawa, Ottawa, CANADA

² Faculty of Medicine, University of Ottawa, Ottawa, CANADA

³ Department of Pediatrics, Division of Neurology, CHEO, University of Ottawa, Ottawa, CANADA

Background: Cerebral vasculopathy is associated with NF1, and is seen as aneurysms, stenoses, AVM and Moyamoya syndrome. Vasculopathy is rare in NF1, but has potential impact on clinical care, as there is a lack of guidelines about initial and follow-up evaluation for its detection.

Objective: The aim of this retrospective study in patients with NF1 is to describe a group of patients with NF1-related cerebral vasculopathy and assess its stability/progression over time, as well as to assess NF1 patients without cerebral vasculopathy and evaluate its course over time. Additionally, to characterize the arterial anatomical variants in the cerebral circulation of NF1 patients.

Materials and Methods: Retrospective analysis was conducted over 13 years, TOF-MRA of 68 patients with NF1 were evaluated for the presence of cerebral vasculopathy related to NF1. Imaging was reviewed for their presence and for follow-up and progression with time.

Results: On initial imaging, there were 4 cases (5.8%) of NF1-related cerebral vasculopathy. Throughout the study period, one had a silent infarct and a spontaneous intraparenchymal hemorrhage. Remainder of the 64 patients with NF1, none had cerebral vasculopathy in the initial study, 34 patients were followed-up without development of vasculopathy.

The NF1 group had a higher rate of arterial anatomical variants at 75%, compared to the 50% of the control group; the difference between the groups had 95% confidence interval [0.05,0.45], $p=0.01$.

Conclusion: TOF-MRI might be a good tool for initial evaluation and follow up of NF1 related vasculopathy as there is lack of guidelines about initial and follow-up evaluation for the detection but given the small number of vasculopathy patients in our cohort larger studies are needed to validate the necessity of a baseline TOF-MRA and follow-up in NF1-patients.

Figure. 12-year-old boy with NF 1 at the time of the initial study in our institution. A) 3D TOF-MRA showing absence of the right anterior and middle cerebral arteries, as well as hypoplastic left anterior cerebral artery (arrow). B) Axial source image displaying Moyamoya vessels extending into the anterior perforated substance from the left internal carotid termination and proximal middle cerebral artery.

Poster: SCI-266

BIOMETRY OF THE CEREBRAL VENTRICLES IN EXTREMELY LOW GESTATIONAL AGE NEONATESLAURA Acosta-Izquierdo¹, EMANUELA Ferretti², MARIA FERNANDA Dien Esquivel¹, ELKA Miller¹, NICK Barrowman^{3,4}, VID Bijelic^{3,4}, CLAUDIA Martinez-Rios¹¹ Medical Imaging Department, CHEO, University of Ottawa, Ottawa, CANADA² Division of Neonatology, CHEO, University of Ottawa, Ottawa, CANADA³ Department of Pediatrics, University of Ottawa, Ottawa, CANADA⁴ Clinical Research Unit, CHEO Research Institute, Ottawa, CANADA

Reference values of measurement of the cerebral ventricles in the premature newborn have been described. However, previous studies have focused on infants born after 24 weeks gestational age (GA), with limited data on the extremely low gestational age (ELGA) infants, born between 22 and 24 weeks' GA. The purpose of this study was to assess by cranial ultrasound (cUS) the ventricles' linear measurements at baseline and subsequent cUS in a cohort of ELGA neonates, and to evaluate associations between ventricular size and gender, delivery mode and complications.

Institutional Research Ethics Board-approved retrospective study of 28 ELGA neonates that underwent cUS, born in a tertiary care pediatric institution, during January 2000 to September 2020. 16 infants (7 girls, 9 boys) had cUS between 22 and 24 weeks corrected GA. The ventricular axis (VA), index (VI), anterior horn width (AHW), calculated frontal horn ratio (FHR), thalamo-occipital distance (TOD), atria, third (3V) and fourth (4V) ventricles measurements were acquired systematically. Descriptive analysis, growth curves and statistical comparison were obtained.

At baseline, median size (millimeters) were for VA, right (r) 6.7, left (l) 7.3; AHW, (r) 1.70, (l) 2.0; VI (r) 8.0, (l) 8.25; atrium (r), 5.5, (l) 6.0; TOD (r) 13.0, (l) 14.0; 3V, 1.0; and 4V, 3.3, and calculated FHR (r) 0.34, (l) 0.36. Delivery was vaginal in thirteen and cesarian-section in three infants. Complications for the whole cohort included germinal matrix-intraventricular hemorrhage Grades 1-3 (2, 11, and 2, respectively), one parenchymal hemorrhagic infarct, three cerebellar hemorrhages, and one post-hemorrhagic ventricular dilatation. Results can be used to inform larger confirmatory studies.

ELGA infants are commonly seen in intensive care units. Norms for ventricular size will allow for prompt identification of dramatic changes, should a complication occur, to guide further management. Data on associations of ventricular size with peri and postnatal factors in larger cohorts of ELGAs is still needed.

Poster: SCI-267

EXPECT THE UNEXPECTED: A PICTORIAL REVIEW OF UNEXPECTED PET/MR FINDINGS IN COMMON CHILDHOOD MALIGNANCIES AND THEIR CLINICAL SIGNIFICANCEJAYNE Seekins, HELEN Nadel, JESSE Sandberg
Lucile Packard Children's Hospital, Palo Alto, USA

PURPOSE: To present a pictorial review of unexpected findings and their clinical significance on PET/MR in common childhood malignancies.

MATERIAL AND METHODS: A retrospective review of unexpected findings on PET/MR studies in children with malignancies that were performed at a large tertiary children's hospital. The series of cases range in age from infancy to early adulthood.

RESULTS: Unexpected findings on PET/MRI can range from findings in the brain, heart, subcutaneous soft tissue and peritoneum. Knowing the normal appearance and common pitfalls can assist in knowing when a true unexpected finding is present. Cases will

include but are not limited to lymphoma, neuroblastoma and Langerhans Cell Histiocytosis.

CONCLUSIONS: Knowing the when to recognize unexpected findings on PET/MRI in commonly imaged childhood malignancies will strengthen the differential diagnosis, help effect changes in patient care and decrease the need for re-imaging.

Poster: SCI-268

MRI APPARENT DIFFUSION COEFFICIENT (ADC) AND 123-I-MIBG UPTAKE IN LOW-RISK NEUROBLASTOMA: CASE REPORTANNA LISA Martini¹, MICHELA Allocca¹, MARIA Dipaolantonio¹, ANNALISA Tondo², ANNA Perrone², CATIA Olianti¹¹ AUOC CAREGGI Nuclear Medicine Department, FLORENCE, ITALY² Azienda Ospedaliero Universitaria Meyer, FLORENCE, ITALY

Functional imaging with catecholamine analogue 123I-metaiodobenzylguanidine (123I-MIBG) has been widely used in evaluation of tumors of the sympathetic nervous system such as neuroblastoma (NB). The accuracy of 123I-MIBG scan was well proved for diagnosis, staging, assessment of chemotherapy (CHT) response and recurrence detection of NB. The evolution assessment of the primitive mass could be studied by the uptake ratio between tumor and liver. The apparent diffusion coefficient (ADC) on magnetic resonance imaging (MRI) can also be used, correlating directly to the differentiation of neoplastic cells. We report a case of localized, unresectable, not differentiated NB, 13-months child, with negative bone marrow, not amplified NMYC, no genomic alteration, normal VAM, but with hypertension controlled with ACE-inhibitors. Abdomen MRI showed heteroplastic lesion of 42*50*27 mm localized in the epigastric region, enclosing the celiac artery, with ADC of 0.5. The 123I-MIBG whole body scan confirmed the diagnosis of NB, showing an avid area in the epigastrium characterized by radiotracer uptake twice than the liver. After three months and four cycles of CHT (VP16 and CARBO), the 123I-MIBG scan showed a reduction of the uptake extent, but an increase of its intensity (mass/liver=2.46). MRI demonstrated a mild reduction of the mass size (42*44*27 mm) with a little increase of ADC values to 0.75. According to the european study protocol in low-risk NB, and because of the resolution of hypertension, a short-term reevaluation was decided. After two months, lesion dimensions and 123I-MIBG uptake were clearly reduced (mass/liver=1.07) at the scintigraphy. The MRI confirmed the reduction in mass size to 34*42*24 mm, and the ADC index increased to 1.6. The 123I-MIBG uptake increase in the early post-CHT scan may suggest a selection of cellular clone with greater differentiation just before the involution process, associated with only mild dimensional response at the first MRI, but subsequently confirmed by the increased ADC value. Many studies demonstrated a proportional increasing of ADC value with cellular differentiation, and its decreasing in case of anaplasia. Moreover, high123I-MIBG uptake seemed to be more associated to highly differentiated tumor with better prognosis. Monitoring both with 123I-MIBG uptake and ADC index could help predicting modifications of NB biological features, with possible interesting prognostic implications.

Poster: SCI-269

THYROID INVOLVEMENT OF LANGERHANS CELL HISTIOCYTOSIS: IMAGING FINDINGS OF RARE DISEASESÜKRIYE Yılmaz¹, BERRIN Demir¹, BIRSEL Sen Akova¹, KORAY Ceyhan², ISINSU Kuzu³, EMEL Unal⁴, ÖMER SUAT Fitoz¹

¹ Ankara University Faculty of Medicine, Department of Pediatric Radiology, Ankara, TURKEY

² Ankara University Faculty of Medicine, Department of Cytology, Ankara, TURKEY

³ Ankara University Faculty of Medicine, Department of Pathology, Ankara, TURKEY

⁴ Ankara University Faculty of Medicine, Department of Pediatric Oncology, Ankara, TURKEY

Langerhans cell histiocytosis (LCH) is a rare multisystem disease. Demonstration of involvement sites and accurate staging are crucial. Isolated thyroideal involvement is very rare and it is difficult to diagnose. In this report, radiological findings of involvement are presented and differential diagnoses were discussed.

Materials and Methods: A 14-year-old man who has maintained complete remission for over 4 years was admitted to radiology department for routine yearly follow-up chest CT imaging for stable lung cysts. Thorax CT also revealed an incidental hypodense lesions within the both lobes of thyroid gland. Retrospective evaluation of previous CT examination was normal and he did not have a history of thyroid disease. Sonography identified patchy hypoechoic areas with variable vascularity which was typical for thyroiditis. However, laboratory results for thyroid markers were completely negative for thyroiditis. The F-18 FDG PET / CT examination revealed non-homogeneous FDG uptake in the thyroid gland and thymus. Fine needle aspiration cytology and cell block material of thyroid lesion was diagnostic for Langerhans cell histiocytosis involvement. Immunohistochemically histiocytic cells were stained with S-100, CD1a and langerin antibodies, characteristic for LCH involvement. Residual thyrocytes in the background were also stained with TTF-1. In light of the new findings the patient was accepted as multisystem involvement of LCH and treatment was initiated.

Results: Review of the literature showed that LCH involvement of thyroid gland is usually involved in multisystem disease and misdiagnosis as benign goiter or hypothyroidism is very common. In our case the diagnosis was confirmed in the early phase of the disease and patient's thyroid gland size and hormone levels were within normal limits.

Conclusion: It is important to distinguish the extent of the disease because single organ involvement is associated with an excellent survival rate. The majority of thyroid involvement of LCH in pediatric patients is associated with multi-system disease. Although it is extremely rare, the thyroid gland involvement should be kept in mind in patients who have recently developed lesions and negative history for thyroid disease.

Poster: SCI-270

PAPILLARY CARCINOMA IN A CHILD, RARE BUT AGGRESSIVE

PRADEEP RAJ Regmi ¹, ISHA Amatya ¹

¹ Hospital for Advanced Medicine and Surgery (HAMS), Kathmandu, NEPAL

² Kathmandu Medical College (KMC), Kathmandu, NEPAL

INTRODUCTION

Thyroid nodules are uncommon in childhood than the adult population comprising only 1-1.5% of paediatric age groups. Thyroid malignancies are more common in the detected nodules comprising 22-26% in paediatric age groups in comparison to 5-15% of the adult population. In addition, thyroid malignancies are more aggressive in children than in adults with nodal and pulmonary metastasis. The differentiated thyroid carcinoma accounts for 0.5-3% of all the malignancies in the paediatric population. In addition, the child who received the radiotherapy is vulnerable to thyroid malignancies.

FINDINGS

Ultrasound of the neck showed diffuse hyper-echoic non-mass like lesions with scattered micro-calcifications involving the bilateral lobes. The right lobe appeared larger than the left. No evidence of increased vascularity in the hyper-echoic areas in the right lobe. Ultrasound with colour Doppler showed the enlarged node in the right level IV of the cervical region. The node appeared purely solid with no calcifications. The axial non-contrast CT showed diffusely scattered micro-calcifications within bilateral lobes of the thyroid. Axial contrast CT showed homogenous enhancement of both lobe of the thyroid without any mass like focal lesions within. HRCT images showed multiple randomly distributed nodules in the visible lung fields.

EDUCATIONAL OBJECTIVES

Papillary carcinoma in children is rare but aggressive in contrast to adults. Sclerosing variant of papillary carcinoma as in our case is also one of the common presentations of papillary carcinoma of the thyroid in children. Therefore, a case with diffuse micro-calcifications in bilateral lobes of thyroid in children warrants cytological analysis for the timely workup and management.

CONCLUSION

Papillary carcinoma in a child is rare but aggressive in presentation than in the adult population. Despite having a more recurrent rate than in adults, survival seems to be better. However, in some literature, a child less than 10 years are said to have the worst prognosis than the older and pre-pubertal age groups. Therefore, diagnosing a case with papillary carcinoma of the thyroid in children is very challenging and demanding expertise. For this, a pediatric radiologist could play a vital role in diagnosis which leads to proper management.

Keywords: Children, CT, Ultrasound, Papillary carcinoma

Poster: SCI-271

LANGERHANS CELL HISTIOCYTOSIS: A GREAT MIMICKER!

RAHUL Nikam ¹, ASHRITH Kandula ¹, SNIGDHA Puram ¹, XUYI Yue ¹, BEN Paudyal ¹, SACHIN Kumbhar ²

¹ Nemours Alfred I. duPont Hospital for Children, Wilmington, USA

² Medical College of Wisconsin, Milwaukee, USA

Purpose:

Langerhans cell Histiocytosis (LCH) represents a spectrum of diseases characterized by neoplastic clonal proliferations of dendritic cells, with an annual incidence of 2.6 – 5.4 cases per million children. The pattern of involvement of LCH can be single system (either unifocal or multifocal), or multisystem. The purpose of this education exhibit is to describe the pathophysiology, familiarize the audience with various radiologic features of osseous and extra-osseous LCH, and formulate appropriate differential diagnosis for various imaging morphologies. In addition, we will also describe the current role of whole body MRI, PET/CT, and PET/MRI for treatment monitoring and follow-up of LCH.

Materials and Methods:

In this educational exhibit, we will discuss the following.

1. General features including demographics, clinical presentation, historic classification, histology, and diagnostic immunohistochemistry.
2. Imaging findings of LCH: Craniofacial including orbital, salivary and temporal, skeletal, central nervous system, pulmonary, and hepatosplenic.
3. Role of multimodality imaging in diagnosis, management and follow-up of LCH.
4. Differential considerations for various imaging manifestations.

Conclusions:

After review of this exhibit, the audience will be well versed with clinical presentation, histopathology, and imaging findings of LCH, and will be able to formulate appropriate differential diagnosis.

Poster: SCI-272

WHEN LIQUID TUMORS TURN SOLID...

HOI MING Kwok¹, KAI YAT KENNETH Cheung², YEE LING ELAINE Kan³, CHUN KIT Shiu⁴, KEVIN KIN FEN Fung³, KWOK CHUN Wong³, PUI KWAN JOYCE Chan³, WING KEI CAROL Ng³

¹ Department of Diagnostic and Interventional Radiology, Princess Margaret Hospital, Hong Kong, HONG KONG

² University of British Columbia, Vancouver, CANADA

³ Department of Radiology, Hong Kong Children's Hospital, Hong Kong, HONG KONG

⁴ Medical Imaging Department, Union Hospital, Hong Kong, HONG KONG

Introduction

Leukemias are neoplasms that arise from the hematopoietic cells of bone marrow and usually spread first to the peripheral blood. These 'liquid' tumors occasionally involve extramedullary sites forming solid tumors. When they present as such, they are easily misdiagnosed. These rare clinical encounters pose diagnostic challenges to the radiologists.

Purpose

- To illustrate the presentation of acute leukemia as solid masses using various imaging modalities in 3 pathological-proven cases.
- To increase radiologists' awareness that acute leukemia is a possible differential for solid masses in children.

Methodology

Cases were retrospectively identified from Radiology Information System of a regional tertiary children's hospital over 1 year from March 2020 to March 2021. All cases are pathologically proven.

Results

1. A 5-year-old boy diagnosed with B-cell Acute Lymphoblastic Leukemia (B-ALL) was treated but presented as a knee mass in his first relapse and epidural mass in second relapse. Radiographs and ultrasound of both knees revealed aggressive soft tissue masses with bone destruction. MRI spine revealed enhancing epidural mass at mid thoracic level and left L5/S1 level causing spinal cord and nerve root compression. Together with bone marrow examination confirming bone marrow relapse with >50% blast, these are most likely leukemic infiltrates.

2. A 16-month-old girl had mediastinal, peritoneal and omental masses as initial presentation of Acute Megakaryoblastic Leukemia. FDG-PET showed a hypermetabolic anterior mediastinal mass, gross ascites with diffuse hypermetabolic peritoneal and omental masses, suggesting underlying malignancy. Bone marrow examination revealed 24% blasts. Core biopsy of the left upper quadrant peritoneal mass confirmed granulocytic sarcoma.

3. A 10-year-old girl was with relapsed B-ALL presented with an ovarian mass and bone marrow involvement. Pelvic ultrasound and MRI showed a large ovarian mass. Additionally, MRI showed focal areas abnormal bone marrow signal at lumbar spine, anterior left iliac bone and right proximal femur. No blasts were detected in the peripheral blood smear and bone marrow aspiration performed at posterior iliac spine. Left salpingo-oophorectomy confirmed the diagnosis.

Conclusion

Acute leukemia is a treatable and potentially curable condition. Recognition of solid mass presentation of leukemia in the appropriate clinical setting by radiologists is essential for early diagnosis and treatment.

Poster: SCI-273

DIFFERENTIAL DIAGNOSIS OF SKIN NODULES OR MASSES IN CHILDREN. ROLE OF ULTRASONOGRAPHY

CRISTIAN Garcia¹, FLORENCIA De Barbieri¹, DIEGO Bazaes², MARIA SOLEDAD Zegoi³, SERGIO Gonzalez⁴

¹ Pontificia Universidad Catolica, Department of Radiology, Santiago, CHILE

² Pontificia Universidad Catolica, School of Medicine, Santiago, CHILE

³ Pontificia Universidad Catolica, Department of Dermatology-Radiology, Santiago, CHILE

⁴ Dermatopatologia SG., Santiago, CHILE

Purpose. The purpose of this exhibit is to show the different skin nodules or masses that can be seen in children, emphasizing the sonographic appearance and clinical and pathological correlation.

Material and methods. We reviewed retrospectively our experience with Ultrasonography (US) in the study of superficial soft tissue nodules or masses in children for the last 17 years, including clinical and pathological findings. Vascular anomalies were not considered.

Results. All lesions were examined with high-resolution US and color Doppler study, which was the first imaging study in the great majority of patients. Selected examples of different lesions are shown, including epidermal cysts, dermoid cyst, epidermal inclusion cyst, trichilemmal cyst, fibroma, pilomatricoma, neurofibroma, papiloma, granuloma, Langerhans cell histiocytosis, pyogenic granuloma, keloid, xanthoma, congenital myofibromatosis, plantar wart, neurocystic hamartoma, spiradenoma, congenital blue nevus, septic emboli, post vaccination nodules, subcutaneous fat necrosis, metastatic neuroblastoma, granuloma annulare, pyogenic granuloma, congenital nodular melanocytic nevi, juvenile xanthogranuloma, erythema pernio, blue nevus, villous nevus, cutaneous mastocytosis. In most cases, no additional imaging studies were necessary.

Conclusions. High-resolution color-Doppler US is helpful in the characterization and the differential diagnosis of skin nodules or masses in children. Although findings might be nonspecific, they may suggest a diagnosis, especially when correlated with clinical findings and could avoid doing other more sophisticated studies, such as MRI.

Poster: SCI-274

WILMS TUMOR UPDATE

DARRAGH Brady, NARENDRA Shet¹, RAMON Sanchez-Jacob¹, JEFFREY Dome¹

Children National Hospital, Washington, D.C., USA

Wilms tumor, also known as nephroblastoma, is the commonest childhood renal tumor outside of infancy. Radiological evaluation is central to its diagnosis, staging, treatment decisions, and surveillance. In the last ten years there have been advances that have affected imaging recommendations.

We performed a systematic evaluation of the literature for papers relevant to the imaging of nephroblastoma during the years 2010–2020. This search identified 1636 articles. The abstracts of 1573 studies were screened after removal of duplicates. 1430 studies were deemed irrelevant. 143 full text studies were screened and 10 studies were excluded for various reasons. 133 studies were included.

We present up to date data on initial diagnosis, staging by modality, surveillance recommendations, cost effectiveness, and treatment complications.

Poster: SCI-275

EXTRARENAL WILMS TUMOUR WITH PULMONARY METASTASES: A RARE PRESENTATION OF A COMMON PAEDIATRIC TUMOUR

MARK Bishay, EMILY Evans, SHRUTI Moholkar, MOTI Chowdhury
Birmingham Children's Hospital - Department of Radiology,
Birmingham, UNITED KINGDOM

A 5 year old girl presented to the emergency department with abdominal distension. She was found to have a palpable abdominal mass. Ultrasound demonstrated a large abdominopelvic mass, displacing the aorta and inferior vena cava. The ovaries and kidneys were seen separate to the mass.

MRI confirmed a large highly cellular abdominopelvic lobulated mass. Some high signal within the mass on T1 weighted imaging was considered in keeping with haemorrhage. T2 weighted imaging demonstrated a low signal rim, which was breached anterolaterally on the right. There was no evidence of calcification. The lesion demonstrated heterogenous contrast enhancement. The origin of the mass remained unclear. CT of the thorax revealed five round nodules measuring up to 7 mm, in keeping with metastases. Ultrasound guided biopsy was performed and histology showed a small round blue cell tumour with features of triphasic Wilms tumour/nephroblastoma. Pre-operative chemotherapy was commenced. The child then became unwell with severe abdominal pain, and was found to have an increase in abdominal distension and a drop in haemoglobin, raising suspicion of haemorrhage within the tumour. Abdominal CT demonstrated an increase in size of the tumour, together with developing bowel and ureteric obstruction. Urgent surgery was scheduled and the tumour was resected in a long and difficult operation. The tumour was retroperitoneal and attached to the sacrum. Defunctioning colostomy was subsequently formed and bilateral ureteric stents inserted. Histology confirmed features again in keeping with nephroblastoma, presumably arising from extrarenal nephrogenic rests.

Following treatment with chemotherapy and radiotherapy, the patient remains well three years later without recurrence.

Extrarenal Wilms tumour is a rare entity which poses a significant diagnostic challenge. It is estimated to account for 0.5 – 1% of Wilms tumours. Reported sites include retroperitoneal, lumbosacral, inguinal, genital and even mediastinal and chest wall. Of reported cases, only 6% have presented with distant metastases.

Imaging features of extrarenal Wilms tumours are non-specific, and the diagnosis must be confirmed on histology. Nonetheless this rare presentation of a common paediatric tumour should be considered in the differential diagnosis of retroperitoneal tumours in children, particularly if pulmonary metastases are seen.

Poster: SCI-276

HEPATIC EPITHELIOID HAEMANGIOENDOTHELIOMA WITH PULMONARY INVOLVEMENT: A ONE IN A MILLION DIAGNOSIS

JOHN Adu¹, PAOLA Angelini², DANIEL Levine³, DAVID MacVicar⁴, ERIKA Pace⁴

¹ King's College Hospital, Department of Radiology, London, UNITED KINGDOM

² Royal Marsden Hospital, Department of Oncology, London, UNITED KINGDOM

³ Royal Marsden Hospital, Department of Nuclear Medicine, London, UNITED KINGDOM

⁴ Royal Marsden Hospital, Department of Radiology, London, UNITED KINGDOM

Purpose:

Epithelioid haemangioendothelioma (EHE) is an incredibly rare slow-growing, vascular malignant tumour of unknown aetiology, mostly affecting adults, and usually presenting with non-specific abdominal symptoms. It arises from the mesenchymal tissue of medium to large blood vessels and involves soft tissues, liver, lung, bone, head, and neck. We illustrate a case of paediatric EHE which presented with tumour-related thrombosis.

Educational Objective:

To alert the reader to this rare entity, which can mimic multi-systemic granulomatous disease or advanced neoplasms (angiosarcoma, multifocal hepatocellular carcinoma), and have an atypical presentation due to a complication.

Case Report:

A previously well 12-year-old girl presented with a 4-day history of left leg swelling. Colour-Doppler ultrasound examination identified occlusive thrombus in the left popliteal and femoral veins. An abdominopelvic ultrasound demonstrated multiple, well-defined hypoechoic bilobar peripheral liver lesions. Blood sampling revealed D-dimer: 510 ng/MI; Ca19-9: 54 kU/l; angiotensin converting enzyme: 60 IU/l; normal values of alpha-fetoprotein and beta-human chorionic gonadotropin. Chest radiography demonstrated bilateral subcentimetre scattered lung nodules confirmed on a subsequent CT examination alongside liver lesions, and prominent mesenteric lymph nodes. Echocardiography was normal.

A PET-CT performed at the regional paediatric oncology centre exhibited moderate FDG-avidity of the hepatic lesions (SUVmax 5.8) and pulmonary nodules (SUVmax 2.9). No metastatic marrow or bone involvement. Histopathology of an ultrasound-guided biopsied liver lesion was consistent with epithelioid haemangioendothelioma, nodular type.

Treatment strategy involved anticoagulation for the deep vein thrombosis and active observation in the first instance, with subsequent antiangiogenic agents upon completion of anticoagulation therapy. If the disease were confined to the liver, organ transplant would have been considered.

Conclusion:

Because of its rarity and varied presentation, EHE diagnosis might be difficult to promptly diagnose and treatment options are few. It should be considered in challenging cases with multi-system involvement. Tissue diagnosis and a paediatric oncology multidisciplinary team approach are vital in the management of this rare disease.

Poster: SCI-277

COMPARISON OF WHOLE BODY MRI AND PET-CT IN PEDIATRIC SOLID TUMORS

GOKALP Cikman, SUREYYA BURCU Gorkem
Erciyes University Department of Pediatric Radiology, Kayseri, TURKEY

Introduction-Goals

Whole-body MRI is an increasingly used imaging modality for screening metastasis and follow-up in pediatric oncology patients. It spares children from ionizing radiation transmitted by PET-CT. In this study, we aim to compare the diagnostic accuracy of Whole-Body MRI and PET-CT in children with solid tumors.

Keywords: whole-body MRI, pet-ct, solid tumors, children

Materials - Methods

We retrospectively enrolled 41 patients (18 girls, 23 boys, mean age 12 ±5.7 years) who were diagnosed with solid tumors. All patients underwent a whole-body MRI (coronal T2-W STIR (Short tau inversion

recovery)) and PET-CT (F-18 FDG and Ga68) at initial diagnosis (or follow-up which examination interval was not longer than 1 year. Patients who had chemotherapy/radiotherapy or operation history between whole-body MRI and PET-CT were excluded (n=5).

Results

With PET-CT as the reference standard, 29 of 41 (70%) patients had abnormal findings on PET-CT studies, including primary mass in 22 (53%) cases, 6 metastasis (14%) cases, 1 avascular necrosis (0.2 %), 12 postoperative negatives (29%). The overall diagnostic accuracy, sensitivity, and specificity of MRI for detecting metastasis were 97%, 92.3%, and 100%. One undiagnosed finding with MRI that was detected with PET-CT was bone metastasis.

Conclusion

Whole-body MRI is a radiation-free and comparable imaging method with PET-CT for evaluating pediatric oncology patients. Pediatric whole-body MRI protocol with shorter examination times and better image quality might be considered in lieu of PET-CT in screening metastasis of pediatric solid tumors.

References

- Greer MC. Whole-body magnetic resonance imaging: techniques and non-oncologic indications. *Pediatr Radiol.* 2018 Aug;48(9):1348-1363.
- Sandra Saade-Lemus, Andrew J. Degnan, Michael R. Acord, et al. Whole-body magnetic resonance imaging of pediatric cancer predisposition syndromes: special considerations, challenges, and perspective *Pediatric Radiology* volume 49, pages 1506–1515 (2019)

Poster: SCI-278

ULTRASOUND IN TONSILLAR LYMPHOMA: AN EMERGING FRONTLINE MODALITY - TWO CASE REPORTS.

ELENI Koutrouveli¹, IRENE Vraka¹, RODANTHI Sfakiotaki¹, MARINA Vakaki¹, GEORGIOS Daniil², ANNA Chountala¹, EKATERINI Haritou¹, KOUMANIDOU Chrysoula¹

¹ Children's Hospital of Athens P&A Kyriakou, Athens, GREECE

² General Hospital Of Thessaloniki G. Gennimatas, Thessaloniki, GREECE

PURPOSE:

We present two case studies of unilateral tonsillar lymphoma, in which transcutaneous ultrasound, as the initial imaging method, safely established the suspicion of tonsillar malignancy and contributed to post-operative follow-up.

MATERIALS AND METHODS:

Case 1: A 14-year old boy who complained of dysphagia. Physical examination revealed unilateral tonsillar enlargement and adjacent cervical lymphadenopathy.

Case 2: A 5-year old boy who reported recent weight loss accompanied by nocturnal snoring. Physical examination detected unilateral tonsillar enlargement. Laboratory tests were suspicious for tonsillar infection.

RESULTS:

Ultrasound performed revealed in both cases tonsillar asymmetry, with alteration of tonsillar appearance, echotexture and vascularity. The affected tonsil was enlarged (>2), medially displaced and rounded rather than ovoid. The tonsillar parenchyma had partially or completely lost its striated appearance, tonsillar capsule remained intact, peritonsillar tissues were normal. Internal vascularity was markedly increased. A regional enlarged lymph node was present in case 1 and enlarged mesenteric lymph nodes in case 2.

In both cases ultrasound findings established the suspicion of malignancy, further confirmed by CT scan. Tonsillectomy was performed and subsequent biopsy confirmed NH-Burkitt lymphoma.

Post-operative follow-up in case 1 showed no immediate complications and no signs of recurrence for the first two years and in case 2 fluid collection immediately after surgery, completely resolved two weeks later and no signs of recurrence after 6month follow-up.

CONCLUSION:

Transcutaneous ultrasound is a useful and efficacious imaging modality in the differential diagnosis of unilateral tonsillar enlargement and the crucial early diagnosis of tonsillar lymphoma.

Poster: SCI-279

IMAGING FINDINGS OF CONGENITAL-INFANTILE FIBROSARCOMA WITH A PICTORIAL REVIEW

NASIM Tahir

Leeds Children's Hospital, Leeds, UNITED KINGDOM

Background

Congenital-infantile fibrosarcoma (CIFS) is a rare soft tissue childhood tumour. Tumours usually involve the extremities and can be misdiagnosed as vascular anomalies. Unlike the adult counterpart, prognosis is usually excellent. Given their rarity, there is a lack of literature on imaging features.

Purpose

To review imaging features of biopsy proven CIFS at our institution and provide a pictorial review of findings.

Materials and methods

Patients with histologically proven CIFS were identified from our oncology database. Patient demographics and imaging findings were recorded.

Results

During January 2010 to October 2020 6 patients were identified. 3 were female and 3 were male. 2 patients had lesions apparent at birth. The average age of presentation for the other 4 was 4.5 weeks. In terms of location, the lesion was in the limbs in 4 patients, intra-abdominal in 1 patient and over the lumbosacral spine in the other patient. 4 patients had plain films on presentation: in 2 patients this showed a soft tissue opacity; in 1 patient there was soft tissue opacity with irregularity of the underlying bone; in 1 patient there was soft tissue opacity with areas of dystrophic calcification. All patients had ultrasound at presentation. 4 of these showed complex solid / cystic masses with increased vascularity; 1 showed a solid mass with increased vascularity and irregularity of the underlying bone; 1 showed a solid mass with internal vascularity and echogenic strands in the periphery. All patients also had MRI at presentation. This provided better anatomical detail of the lesion but appearances were otherwise similar to those seen on ultrasound. In 2 patients areas of haemorrhage were noted.

Conclusion

Our study has shown imaging findings of CIFS are non-specific but can show features similar to vascular anomalies. Biopsy should be considered in patients which do not show typical clinical and imaging features of vascular anomalies to exclude this diagnosis.

Poster: SCI-280

ADAPTATION OF TI-RADS TO A LARGE PEDIATRIC POPULATION

SUMMIT Shah, ADAM Bobbey, HIRA Ahmad, AMEER Al-Hadidi, JOSEPH Stanek, ANDREW Peachman, ROBERT Hoffman, KATHLEEN Nicol, JENNIFER Aldrick

Nationwide Children's Hospital, Columbus, USA

Background: Thyroid nodules are uncommon in pediatric patients. However, a thyroid nodule in a child poses a risk of malignancy up to 25-30%. A validated radiographic classification of thyroid nodules in adults, but not yet widely used in children, is Thyroid Imaging Reporting and Data System (TI-RADS). The purpose of this study was to determine the sensitivity, specificity and accuracy of TI-RADS in predicting thyroid malignancy for nodules with available cytopathology,

and to compare the diagnostic accuracy to the current American Thyroid Association (ATA) guidelines.

Methods: A single institution retrospective review was performed of patients younger than 21 years who underwent thyroid nodule FNAB, and who had ultrasound imaging available. Two radiologists were blinded to the pathology and independently classified all biopsied thyroid nodules based on TI-RADS. The reliability of radiologists' ratings was done using Spearman correlation. We then compared ATA guidelines to TI-RADS to determine the diagnostic sensitivity and specificity of both scoring systems in this cohort. All statistical analyses were conducted using SAS 9.4. **Results:** 115 patients (median age 15.5years, IQR (13-16.9), 90 females) with 138 nodules were retrospectively scored using TIRADS. There was moderate inter-rater agreement between radiologists (Kappa = 0.51; $p < .0001$). Using ATA guidelines, 82.6% of nodules were recommended for FNAB. Evaluating several potential TI-RADS criteria, 23.2%–68.1% of nodules were recommended for FNAB. Using TI-RADS ≥ 3 as an indication for FNA had 100% sensitivity with no missed suspicious or malignant nodules on cytology or pathology, respectively. Sensitivity, specificity, and accuracy for each system are displayed in Table 1.

Conclusions: Using TI-RADS for diagnostic management of pediatric thyroid nodules improves accuracy in predicting malignancy, thereby decreasing unnecessary biopsies. We recommend using TI-RADS ≥ 3 as an indication for FNA. Further efforts to validate TI-RADS for pediatric thyroid nodules are required.

Poster: SCI-281

BILOBED METANEPHRIC ADENOMA AND WILMS TUMOR: IDENTICAL EMBRYOLOGIC ORIGIN, DIVERGENT IMAGING APPEARANCE. FIRST REPORT WITH US, SPECTRAL CT, AND MRI

CHARLES Runyan, DIANNA M. E. Bardo
Phoenix Children's Hospital, Phoenix, Arizona, USA

CASE PRESENTATION:

We present a 2-year-old boy with abdominal pain in whom a complex, bilobed right upper pole renal mass was found on ultrasound exam. Subsequent spectral CT/W IV contrast revealed a two-part upper pole mass. Renal MRI WO/W IV gadolinium was performed to further distinguish tumor characteristics.

Imaging characteristics:

US - nearly anechoic superior and hyperechoic inferior components.

CT - hypoattenuating upper mass with enhancing septa, homogeneous inferior mass.

MRI - nearly identical T1 signal in both components, T2 hypointense signal, relatively more hypointense in the inferior component, and similar in enhancement pattern to CT. Only the upper component restricted diffusion.

Spectral analysis of the CT image data showed a qualitative and quantitative difference between the superior component, the inferior component, and the normal kidney.

Given mixed tumor components, the patient underwent US-guided percutaneous biopsy; histology revealed a diagnosis of metanephric adenoma. The patient returned 3 months later with hematuria, at which time the patient was reimaged. US and MRI then showed marked interval enlargement of the superior tumor component with more aggressive features including intense contrast enhancement on MRI.

Radical nephrectomy was performed. Histology showed Wilms tumor capsule rupture (Stage III) with adjacent metanephric adenoma.

DISCUSSION:

Wilms tumor is the most common primary renal malignancy in children, originating from nephrogenic rests which are characterized by persistent

embryonal cells. Metanephric adenoma is a rare, nearly always benign tumor typically found in middle-aged females, but is a rare occurrence in young males. Metanephric adenomas also originate from nephrogenic rests.

This is the first time that a composite metanephric adenoma and Wilms tumor has been reported as a bi-lobed renal mass in 2-year-old. It has never been reported with correlating imaging modalities, including US, Spectral CT, and MRI.

Poster: SCI-282

DO OTHERWISE WELL, HEALTHY CHILDREN WITH PALPABLE CERVICAL LYMPH NODES REQUIRE INVESTIGATION WITH NECK ULTRASOUND?

MICHAEL Paddock¹, AMY Ruffle², GEORGE Beattie¹, AMIT Prasai², ANNMARIE Jeanes²

¹ Barnsley Hospital NHS Foundation Trust, Barnsley, UNITED KINGDOM

² Leeds Teaching Hospitals NHS Trust, Leeds, UNITED KINGDOM

PubMed and Medline databases on NHS Evidence and Web of Science were searched which returned 8 eligible studies.

Palpable cervical lymph nodes (CLNs) are common in children with a reported prevalence of 45%–57% in otherwise healthy children. Lymphadenopathy is defined as abnormal lymph node(s) in terms of size, number and/or consistency. Cervical lymphadenopathy is reported to occur in up to 90% of children between the ages of 4 and 8 years and is a common reason for referral from primary care for 'suspected cancer' in children. A cancer diagnosis in children referred with isolated lymphadenopathy on a '2 week wait' pathway is rare. Mislabelling children as having 'lymphadenopathy' when they have normal palpable CLN may result in unnecessary parental anxiety, referral and investigations.

The evidence regarding which children require further investigation and/or biopsy is limited. The National Institute for Health and Care Excellence suspected cancer guidelines give no size or other criteria to differentiate between normal 'reactive' CLN and malignant lymphadenopathy. A Delphi process established that UK paediatric haematologists and oncologists would consider small (<10 mm) palpable cervical lymph nodes to be physiological, even if they are persistent for many months. The same process suggested that lymph nodes greater than 2 cm persisting for more than 6 weeks warrant referral from primary to secondary care.

The role of ultrasound is less clear. Nodal size is known to be an unreliable criterion for malignancy. No single sonographic criterion is able to determine the aetiology of an enlarged lymph node given that there are several overlapping sonographic characteristics among benign, malignant and infectious CLN. A combination of sonographic features may favour one diagnosis over another depending on the clinical context but it is also well recognised that ultrasound cannot reliably differentiate between reactive hyperplasia and lymph nodes involved by lymphoma. This further reinforces the limitations of ultrasound as a diagnostic tool in the assessment of palpable CLN and cervical lymphadenopathy.

Otherwise well, healthy children with palpable cervical lymph nodes do not require investigation with neck ultrasound. Ultrasound should not be used as a screening tool to 'exclude malignancy'. Children with palpable cervical lymph nodes greater than 2 cm persisting for more than 6 weeks, or supraclavicular nodes, warrant referral for specialist assessment.

Poster: SCI-283

NEUROBLASTOMA WITH KINSBOURNE SYNDROME: CASE SERIES OF SIXTEEN CASES AND REVIEW OF LITERATURE

PRASANNA Karpaga Kumaravel, ABIRAMI KRITHIGA Jayakumar
Rainbow Childrens Hospital, Hyderabad, INDIA

Purpose.

To identify Neuroblastoma in patients with Kinsbourne syndrome (Opsoclonus-myoclonus-ataxia syndrome - OMAS) or dancing eye syndrome.

Materials and Methods.

Retrospective study of neuroblastoma patients with Opsoclonus-myoclonus-ataxia syndrome in Rainbow Children's Hospital, Hyderabad, a tertiary care centre from October 2010 till October 2020. Patients with Opsoclonus-myoclonus-ataxia syndrome have undergone routine ultrasound and CT scans.

Results.

A total of 16 cases of Opsoclonus-myoclonus-ataxia syndrome had neuroblastoma with major number of cases (n=13) having intra abdominal neuroblastoma and remaining three cases presented with thoracic neuroblastoma. Onset of OMAS preceded the diagnosis of malignant tumour in all cases. The time interval between onset of OMAS and the diagnosis of neuroblastoma varied from 2 weeks to 14 months, median being around 4 months. All children except one, have normal development on follow up.

Conclusions

OMAS is a rare disorder, but it affects children more frequently than adults and exhibits an excellent rate of survival. Screening for an occult neuroblastoma is necessary in all children with Kinsbourne syndrome.

Poster: SCI-284

IMAGING PATTERNS OF GROWTH OF TUMORS IN LI-FRAUMENI SYNDROME: CASE SERIES

ROXANA Azma¹, THITIPORN Junhasavasdiku^{1,2}, NIPAPORN Tewattarat^{1,3}, ARMIN Nourmohammad¹, ARMIN Abadeh¹, SANUJ Panwar¹, ANITA Vilani¹, DAVID Malkin¹, ANDREA S. Doria^{1,4}

¹ Department of Medical Imaging, The Hospital for Sick Children, University of Toronto, Toronto, CANADA

² Department of Diagnostic and Therapeutic Radiology, Faculty of Medicine Ramathibodi Hospital, Mahidol University, Bangkok, THAILAND

³ Department of Radiology, Khon Kaen University, Mueang, Khon Kaen, THAILAND

⁴ Research Institute, Peter Gilgan Centre for Research and Learning, The Hospital for Sick Children, Toronto, CANADA

Purposes:

Background: Li-Fraumeni syndrome (LFS) is a rare but aggressive autosomal-dominant hereditary cancer predisposing syndrome, caused by germline mutations in the TP53 tumor suppressor gene. The affected individuals are highly prone to developing multiple cancers of both solid organs and hematological system, starting as early as childhood. Previous studies showed that most tumors of LFS have a pre-malignant or dormant phase which could be exploited by early detection techniques which include imaging modalities.

Purpose: To assess potential growth patterns of different tumors in Li-Fraumeni syndrome by imaging, which has been under-evaluated.

Methods & Materials: Between January 1999 and September 2017, the clinical features and imaging findings of 22 patients with LFS (carriers of a germline TP53 pathogenic variant), affected by 39 tumors and diagnosed in a single center, were retrospectively reviewed by independent radiologists. Temporal imaging characteristics of tumors in different imaging modalities including MRT, CT scan, sonography and X-rays were reviewed. Factors such as local invasion, time interval for developing primary cancer and/or recurrent disease and metastasis as well as factors that delayed the diagnosis of tumors were assessed.

Results: In patients with multiple tumors the median time interval for development of first, second and third primary cancers were 45.9, 79.8 and 28.1 months, respectively. The most frequently detected malignancies in our cohort were adrenocortical carcinoma (most common), followed by osteosarcoma and rhabdomyosarcoma. Five osteosarcomas detected in 4 patients were 3 high-grade conventional osteosarcomas with a telangiectatic variant, 1 intermediate- to high-grade surface growth pattern osteosarcoma and 1 low-grade osteosarcoma. The three rhabdomyosarcomas comprised of two anaplastic embryonal rhabdomyosarcomas and one anaplastic alveolar rhabdomyosarcoma. All of the observed adrenocortical carcinomas appeared as single well-defined lobulated and predominantly solid lesions with the larger tumor containing cystic parts. Superposition of anatomic structures on coronal views diffculted the visualization of very small tumors.

Conclusion: Although further studies with larger series should confirm this recommendation, the disease pattern of new cancer development observed in this study was variable both between and within histologic categories of tumors.

Poster: SCI-285

DIAGNOSTIC ACCURACY OF MRI FOR PEDIATRIC NEUROBLASTIC TUMOR DIFFERENTIATION: SYSTEMATIC REVIEW AND SUBGROUP META-ANALYSIS

DOMENICA Tambasco¹, MARIA Medeleanu², RAHIM Moineddin³, SHELLEY Harris⁴, DANIEL Morgenstern⁵, ANITA Villani⁵, DAVID Malkin⁵, ANDREA Doria⁶

¹ University of Toronto - Faculty of Medicine, Toronto, CANADA

² The Hospital for Sick Children - Research Institute, Toronto, CANADA

³ University of Toronto - Division of Family & Community Medicine, Toronto, CANADA

⁴ University of Toronto - Department of Epidemiology & Department of Occupational and Environmental Health, Toronto, CANADA

⁵ The Hospital for Sick Children -Department of Pediatric Oncology, Toronto, CANADA

⁶ The Hospital for Sick Children -Department of Diagnostic Imaging, Toronto, CANADA

Purpose: The purpose of our study is to review the evidence on MRI to diagnose pediatric neuroblastic tumors, in particular the discriminative ability of specific MRI features to distinguish malignant versus benign tumor types based on histopathologic diagnosis and characteristics.

Methods: Data extracted included: 1) Participant characteristics; 2) MRI parameters, techniques, or features used for detection, diagnosis, or differentiation of neuroblastic tumors; 3) Comparator (histology) diagnosis; 4) Outcomes (diagnostic accuracy calculations for ADC-MRI feature, descriptive summaries of other features). QUADAS-2 tool was used to assess risk of bias and STARD to assess reporting of diagnostic studies. GRADE was used to evaluate the evidence.

Results: 9 studies were included for final review with a total of 224 participants. Average age of participants was 3 years old. Female to male ratio was 0.75:1. A sub-group meta-analysis of 5 studies using similar population, intervention, methods, and outcomes showed that ADC was associated with tumor type based on level of cellular

differentiation. A low ADC was associated with more malignant (immature, poorly differentiated) histology type (Neuroblastoma +/- Ganglioneuroblastoma-nodular) while a higher ADC with more benign (mature, differentiated) histology type (Ganglioneuroma +/- Ganglioneuroblastoma-intermixed). The overall average ADC cut-off value was 1.04 (SD 0.19, 95% CI 0.65-1.22), with a mean ADC for Neuroblastoma of 0.78 (SD 0.14, 95% CI 0.53-0.92) and a mean ADC for Ganglioneuroma of 1.42 (SD 0.24, 95% CI 1.15-1.69). Overall accuracy of MRI to diagnose Neuroblastoma from suspected Neuroblastoma in solid extracranial tumors in children was 83% (95% CI 77-88%). Diagnostic accuracy of DWI-MRI using ADC to distinguish Neuroblastoma from Ganglioneuroma was 87% (95% CI 65-98%).

Conclusions : Diffusion-weighted MRI technique using ADC maps and analysis may aid in distinguishing more malignant neuroblastic tumor types from more benign by detecting level of cellularity and differentiation on histopathology. Overall quality of the evidence using GRADE approach was moderate, indicating that the true effect is likely to be close to the effect estimate, but further research with larger sample sizes is likely to have an important impact on our confidence and may change the effect estimates.

Poster: SCI-286

2D SHEAR WAVE ELASTOGRAPHY OF SUPERFICIAL LYMPH NODES IN CHILDREN WITH HODGKIN LYMPHOMA. ITS CONTRIBUTION IN EVALUATING RESPONSE TO CHEMOTHERAPY

ANNA Chountala¹, RODANTHI Sfakiotaki¹, EFI Alexopoulou³, MARINA Vakaki¹, NICKOS Spyridis², DIMITRIS Doganis⁴, CHRYSOULA Koumanidou¹, LYDIA Kossiva²

¹ Children's Hospital 'P&A Kyriakou' Radiology, Athens, GREECE

² Children's Hospital 'P&A Kyriakou', Medical School, National and Kapodistrian University of Athens, Athens, GREECE

³ General University Hospital Attikon, Medical School, National and Kapodistrian University of Athens, Athens, GREECE

⁴ Children's Hospital 'P&A Kyriakou' Oncology, Athens, GREECE

PURPOSE

The role of 2D shear wave elastography in evaluating superficial lymph nodes in children with Hodgkin Lymphoma, after chemotherapy.

MATERIAL AND METHODS

In our study, in a timespan of five (5) months, nine (9) children, aged 9-15years, with Hodgkin Lymphoma were examined with 2D shear elastography, after chemotherapy.

Ultrasonography was performed with a last generation GE system, designed for pediatric use (GE S8).

A high frequency (9MHz) linear transducer was used for 2D Shear wave elastography and stiffness was measured in kPa units.

RESULTS

In seven (7) subjects the lymph nodes were re-examined after the first chemotherapy.

2D shear wave elastography, at diagnosis, measured lymph node stiffness ranging between 102,24kPa -136,89kPa. After the first chemotherapy session, lymph node stiffness was ranging between 11,21kPa -31,31kPa. In two (2) subjects, 2D shear wave elastography interrogation of superficial lymph nodes was performed after the initial chemotherapy sessions with no prior 2D shear wave elastography control at the point of diagnosis. Lymph node stiffness was ranging between 10,76kPa-14,40kPa.

CONCLUSION

2D shear wave elastography is a modern and promising method.

However, it's important to underline that only a few studies on lymph node elastography exist and almost none of them addresses the specific problem in children, therefore more research on the topic is required.

In conclusion, taking into account our initial results, it seems that 2D shear wave elastography interrogation of superficial lymph nodes in children is a method with the known advantages of ultrasonography (readily available, noninvasive, no radiation, etc) that can significantly contribute in the evaluation of chemotherapy response.

Poster: SCI-287

CAN SUPERFICIAL LYMPH NODES' ELASTOGRAPHY CONTRIBUTE TO THE DIFFERENTIAL DIAGNOSIS OF THE TYPES OF PEDIATRIC MALIGNANCY?

ANNA CHOUNTALA¹, RODANTHI Sfakiotaki¹, EFI Alexopoulou³, MARINA Vakaki¹, ELENI Koutrouveli¹, IRENE Vraka¹, DIMITRIS Doganis⁴, CHRYSOULA Koumanidou¹, LYDIA Kossiva²

¹ Children's Hospital of Athens P&A Kyriakou, Radiology Department, Athens, GREECE

² Children's Hospital 'P&A Kyriakou', Medical School, National and Kapodistrian University of Athens, Athens, GREECE

³ General University Hospital Attikon, Medical School, National and Kapodistrian University of Athens, Athens, GREECE

⁴ Children's Hospital 'P&A Kyriakou', Oncology Department, Athens, GREECE

PURPOSE

To underline the role of 2D shear wave elastography in differentiating between different types of malignancies involving lymph nodes.

MATERIAL AND METHODS

In our study, in a time span of 6 months, 17 children, aged 6-15years, with enlarged and suspicious of malignant proliferation superficial lymph nodes, were evaluated with 2D shear wave elastography.

A modern GE ultrasonographic unit, designed for pediatric use (GE S8), was utilized.

A high frequency (9MHz) linear transducer was used for 2D Shear wave elastography and stiffness was measured in kPa units.

RESULTS

In 16 subjects enlarged lymph nodes were demonstrated.

2D shear wave elastography revealed:

- In seven (7) subjects with node stiffness 102,24kPa-136,89kPa, histology revealed Hodgkin Lymphoma.

- In one (1) subject with node stiffness 113kPa-148,57kPa, histology revealed Non-Hodgkin Lymphoma.

- In eight (8) subjects with node stiffness 4,25kPa-35,98kPa, bone marrow aspiration and immunophenotyping revealed acute lymphoblastic leukemia.

In one (1) subject two (2) inguinal ovoid, hypochoic lymph nodes of normal size and homogenous echotexture were depicted. Their stiffness values measured by 2D shear wave Elastography ranged between 100,70kPa-186,79kPa and histology revealed Langerhans Histiocytosis.

CONCLUSION

2D shear wave elastography is an innovative and promising technique.

Given the fact that only a few studies related to the subject have been published so far and almost none of them addresses the specific issue in children, more research on the topic is necessary.

Considering our initial findings, it seems that 2D shear wave elastography of superficial lymph nodes in children can contribute in the differential diagnosis of the types of malignancy, which has a direct correlation with the treatment plan and prognosis, as well.

A HARTUNG ERUM	S3.3.2	USA
A SURESH	Poster: SCI-152	INDIA
ABADEH ARMIN	Poster: SCI-284	CANADA
ABATE MASSIMO ERALDO	S5.3.3	ITALY
ABD AZIZ SURAYA	Poster: SCI-144	MALAYSIA
ABDELAZIZ OMAR	Poster: EDU-054	EGYPT
ABDUL GHANI NUR AZURAH	Poster: SCI-144	MALAYSIA
ABHAY SRINIVASAN	S7.1.4	USA
ABI ZEID FARAH	Poster: SCI-097	LEBANON
ABOUGHALIA HASSAN	Poster: SCI-099	USA
ABOUROKBAH NESREEN	Poster: SCI-114	SAUDI ARABIA
ABU ATA NADEEN	S6.2.1,S6.2.2	USA
ABU-EL-HAIJA MAISAM	Poster: SCI-098	USA
ABUSAMAAN SANDRA	Poster: EDU-005	QATAR
ACKER AMY	Poster: SCI-007	CANADA
ACORD MICHAEL	S8.2.4,S7.1.4,S7.1.2,Poster: SCI-149	USA
ACOSTA LAURA	Poster: EDU-003	CANADA
ACOSTA-IZQUIERDO LAURA	Poster: EDU-006, Poster: SCI-024, Poster: SCI-265, Poster: SCI-266	CANADA
ADALETI IBRAHIM	S2.1.4,S7.2.6	TURKEY
ADAMSBAUM CATHERINE	S4.2.5,S8.1.3	FRANCE
ADEROTIMI TOBI	Poster: SCI-218,Poster: EDU-029	UNITED KINGDOM
ADESALU OLUSEYI	Poster: SCI-133	UNITED KINGDOM
ADU JOHN	Poster: EDU-065,Poster: SCI-276	UNITED KINGDOM
ADZICK N. SCOTT	S8.4.4	USA
AERTS ISABELLE	S1.4.1,S5.3.1	FRANCE
AERTSEN M	S7.4.2	BELGIUM
AFACAN ONUR	Poster: SCI-073	USA
AGARWAL REEMA	Poster: EDU-020,Poster: EDU-072	USA
AGGARWAL RAJAN	Poster: SCI-152	INDIA
AGOSTINI HÉLÈNE	S4.2.5	FRANCE
AGUILAR HECTOR	Poster: SCI-042	USA
AHLIN JENNY	S4.2.3	SWEDEN
AHMAD HIRA	Poster: SCI-280	USA
AHYAD RAYAN	Poster: SCI-132	SAUDI ARABIA
AKHADOV TOLIB	S3.1.2,S3.1.4,Poster: SCI-245,	RUSSIAN FEDERATION
AKHADOV TOLIBDZHON	Poster: SCI-252,Poster: SCI-253	RUSSIA
AKINDOLIE OMOWUNMI	Poster: SCI-133	UNITED KINGDOM
AKPINAR YUNUS EMRE	S2.1.4	TURKEY
AKYOL SARI ZEYNEP NUR	S4.4.5,S7.2.6	TURKEY
AL FADHEL MAJID	Poster: EDU-107	SAUDI ARABIA
AL MEHDAR ABEER	Poster: EDU-107	SAUDI ARABIA
ALAMAR MARIANA	S3.1.6	SPAIN
ALAMO LEONOR	Poster: SCI-081	SWITZERLAND
ALAVI AFSHIN	Poster: SCI-089, Poster: SCI-175, Poster: SCI-211	UNITED KINGDOM
ALAZRAKI ADINA	S8.3.5, Poster: SCI-008, Poster: SCI-009	USA
ALBA-GARCIA EVA MARIA	Poster: SCI-070	MEXICO

(continued)

ALBOKHARI SHATHA	Poster: SCI-132	SAUDI ARABIA
AL-DAJANI MARIAM	Poster: SCI-020	CANADA
ALDRINK JENNIFER	Poster: SCI-280	USA
ALEID SHAIMA	Poster: SCI-167	SAUDI ARABIA
ALEO ELENA	Poster: SCI-055	ITALY
ALESSIO ADAM	Poster: SCI-016,Poster: SCI-019	USA
ALESSIO MARIA	S4.1.2	ITALY
ALEXANDER KAREN	Poster: SCI-020	USA
ALEXANDER TOWBIN	S8.3.5	USA
ALEXOPOULOU EFI	Poster: SCI-286,Poster: SCI-287	GREECE
ALEXOPOULOU EFTHYMIA	Poster: SCI-040	GREECE
ALFONSO KRISTAN	Poster: SCI-222	USA
AL-HADIDI AMEER	Poster: SCI-280	USA
ALHASHMI GHUFRAN	S6.2.3,Poster: SCI-132	SAUDI ARABIA
ALI HANEEN	S3.4.5	USA
ALI KAMRAN	Poster: SCI-082	USA
ALI SANA	Poster: EDU-001	UNITED KINGDOM
ALISON MARIANE	S4.1.6	FRANCE
ALIZAI NAVED	Poster: SCI-093	UNITED KINGDOM
ALJABR ALJOHARAH	Poster: SCI-091	CANADA
ALMEHDAR ABEER	Poster: SCI-114	SAUDI ARABIA
ALSAIKHAN NAIF	S7.1.2	USA
ALSHABANAT ABDULLAH	S6.2.3	SAUDI ARABIA
ALSRHANI HETAF	Poster: SCI-114	SAUDI ARABIA
ALVES CESAR	S4.1.5,S5.3.4,Poster: SCI-235,	USA
ALVES CESAR A P F	S8.4.6	USA
ALVES CESAR AUGUSTO	S4.1.1	USA
ALVES PEDRO	Poster: EDU-052,Poster: EDU-086	PORTUGAL
ALZAHER ASRAR	Poster: SCI-167	SAUDI ARABIA
ALZAHIRANI AMIN	Poster: SCI-139	SAUDI ARABIA
ALZAHIRANI NASSER	Poster: SCI-054	SAUDI ARABIA
AMAL MOHAMAD YANUAR	Poster: SCI-021	INDONESIA
AMARAL JOAO	Poster: EDU-074	CANADA
AMATYA ISHA	Poster: SCI-038,Poster: SCI-270	NEPAL
AMBS JAN-MALTE	S3.2.3	GERMANY
AMERICAN MAX	Poster: SCI-151	USA
AMIN RAOUF	Poster: SCI-043	USA
AMIRABADI AFSANEH	S6.2.3,Poster: SCI-003	CANADA
AMMENDOLA ROSA	S4.1.2	ITALY
AMTHOR THOMAS	Poster: SCI-243	GERMANY
ANAMIKA MEENA	Poster: EDU-113	INDIA
ANDERBERG PETER	S7.3.5,Poster: SCI-184	SWEDEN
ANDERS REBECCA	S3.2.6	GERMANY
ANDRADE DEFENDI LARISSA	Poster: EDU-019	BRAZIL
ANDRONIKOU SAVVAS	S1.1.5,S1.2.1,S4.1.5,S5.3.4	USA
	Poster: SCI-110,	
	Poster: SCI-186,	
	Poster: SCI-221,	
	Poster: SCI-235	
ANFIGENO LORENZO	S3.3.3,S3.3.5,	ITALY
	Poster: SCI-055,	
ANGELINI PAOLA	Poster: SCI-276	UNITED KINGDOM
ANGENETE OSKAR W.	Poster: SCI-191,	NORWAY
	Poster: SCI-192	
ANN ATWEH LAMYA	Poster: SCI-097	LEBANON
ANNAPRAGADA ANANTH	S6.2.4,S6.4.1	USA
ANNE-LAURE HERMANN	S1.4.1	FRANCE
ANTON CHRISTOPHER	S3.3.7,S3.4.3,	USA
	Poster: SCI-109,	
ANTUNES SANDRA	Poster: SCI-207	BRAZIL
ANUPINDI SUDHA	S8.2.4,	
	Poster: SCI-094,	
	Poster: SCI-095,	USA
AOKI TAKATOSHI	Poster: SCI-077	JAPAN

(continued)

AOUAD PASCALE	Poster: SCI-234	USA
APARICIO JAVIER	S3.1.6	SPAIN
AQUINO MICHAEL	S4.2.2	USA
ARANGO-DIAZ AMADEO	Poster: SCI-217	SPAIN
ARIA DAVID	Poster: SCI-164	USA MINOR OUTLYING ISLANDS
ARICÒ MAURIZIO	Poster: SCI-206	ITALY
ARKADER ALEXANDRE	S7.3.1	USA
ARKHANGELSKAYA ELENA	Poster: SCI-055	ITALY
ARMAND STÉPHANE	Poster: SCI-202	SWITZERLAND
ARMSTRONG AIMEE	Poster: SCI-166	USA
ARNON SHMUEL	Poster: SCI-117	ISRAEL
ARORA MUDIT	Poster: EDU-089	USA
ARTHURS OWEN	S5.4.3,S6.4.6, Poster: EDU-087, Poster: SCI-182	UNITED KINGDOM
ARTHURS OWEN JOHN	Poster: SCI-063	UNITED KINGDOM
ARYA SRIVIDYA	Poster: EDU-064	UNITED KINGDOM
ASHOK NITIN	Poster: SCI-262	INDIA
AUGDAL THOMAS	S6.2.6, Poster: SCI-191, Poster: SCI-192, Poster: SCI-055	NORWAY
AVANZINI STEFANO	Poster: SCI-194	ITALY
AVAR PINAR OZGE	S5.3.2,Poster: EDU-103	TURKEY
AVERILL LAUREN	Poster: EDU-035,	USA
AVNI FRED	Poster: EDU-071	BELGIUM
AW EDNA	S3.4.2	SINGAPORE
AWAN ATIF	Poster: EDU-067	IRELAND
AYERS LAUREN	Poster: SCI-068	USA
AYYALA RAMA	S8.2.4	USA
AYYILDIZ HAKAN	S1.3.8, Poster: SCI-113	TURKEY
AZIZ DAYANG ANITA	Poster: SCI-144	MALAYSIA
AZMA ROXANA	Poster: SCI-284	CANADA
BABAR JUDITH	Poster: SCI-025	UNITED KINGDOM
BACK SUSAN J	S8.2.6, Poster: SCI-106	USA
BADACHHAPE ANDREW	S6.4.1	USA
BADALLO RIVAS GIL	Poster: SCI-150	MEXICO
BADAT FARZAANA	Poster: SCI-242	SOUTH AFRICA
BAGCHI SHRAMANA	Poster: SCI-053,Poster: SCI-138, Poster: SCI-228, Poster: SCI-241	INDIA
BAILEY SMITA	Poster: SCI-128	USA
BAJNO LYDIA	Poster: SCI-145	CANADA
BALLANCO GERARD	Poster: SCI-060	USA
BALMER DORENE	S7.1.6	USA
BANDEIRA EDUARDO	Poster: EDU-063	PORTUGAL
BANKER HIRAL	Poster: EDU-018, Poster: EDU-062, Poster: EDU-112, Poster: EDU-050	USA
BAO SHANSHAN	S1.4.2,S4.4.3	USA
BARATTO LUCIA	Poster: EDU-003,	SPAIN
BARBER IGNACI	Poster: EDU-084	
BARDO DIANNA	S7.4.5	USA
BARDO DIANNA M. E.	S8.4.3, Poster: EDU-034, Poster: SCI-281,	USA
BARENO SANDRA	Poster: EDU-060, Poster: EDU-061	CHILE
BARLETTA ANTONINO	S8.1.5	ITALY
BARNES NIK	Poster: SCI-218	UNITED KINGDOM

(continued)

BARRERA CHRISTIAN	S6.3.5	USA
BARRERA CHRISTIAN A	S3.2.4	USA
BARROWMAN NICK	S6.4.5, Poster: SCI-266	CANADA
BARTH RICHARD	S2.1.2,S2.2.1,S8.4.5,	USA
BASSERI SANA	Poster: SCI-137	CANADA
BASSO LUCA	S3.3.3,S3.3.5, Poster: SCI-055,	ITALY
BAYRAMOGLU ZUHAL	S1.3.8,S2.1.4,S4.4.5,S7.2.6 S8.3.1, Poster: SCI-029, Poster: SCI-047, Poster: SCI-048, Poster: SCI-049, Poster: SCI-050, Poster: SCI-051, Poster: SCI-113, Poster: SCI-131, Poster: SCI-148, Poster: SCI-212, Poster: SCI-052, Poster: SCI-213, Poster: SCI-214, Poster: SCI-215, Poster: SCI-216, Poster: SCI-264	TURKEY
BAZAES DIEGO	Poster: SCI-273	CHILE
BEATTIE GEORGE	Poster: SCI-122, Poster: SCI-258, Poster: SCI-282,	UNITED KINGDOM
BECERRA CERVANTES ANGIE	Poster: SCI-090	MEXICO
BECERRA MARIA VICTORIA	S3.1.6	SPAIN
BECKER CAROL	Poster: SCI-060	USA
BECKER ROBERT	Poster: EDU-041	USA
BEDIR REEM	Poster: SCI-025	UNITED KINGDOM
BEDOYA MARIA ALEJANDRA	S7.3.6	USA
BEISHUIZEN AUKE	S1.4.4,S4.4.6	THE NETHERLANDS
BELLAH RICHARD	S1.3.2,S7.1.2, Poster: EDU-088,	USA
BENKERT THOMAS	S3.2.6	GERMANY
BENNER ERIC	Poster: SCI-246	USA
BENNETT BRITTANY	Poster: EDU-023	USA
BENNETT COLLEEN E	Poster: SCI-187	USA
BENNETT JEFFERY	Poster: SCI-224	USA
BENOIT STEFANIE	S3.3.6	USA
BEN-SIRA LIAT	Poster: SCI-257	ISRAEL
BERGER-KULEMANN VANESSA	S8.4.2	AUSTRIA
BERKOVICH RACHEL	Poster: EDU-020,Poster: EDU-072	USA
BERLANGA PABLO	S1.4.1	FRANCE
BERTAMINO MARTA	Poster: SCI-230	ITALY
BESLOW LAUREN A.	S3.1.7	USA
BEVAN JONATHAN	Poster: SCI-033	UNITED KINGDOM
BEZUIDENHOUT JACQUELINE KIM	Poster: SCI-242	SOUTH AFRICA
BHANDARI PRAJWAL	S6.4.1	USA
BHAT HIMANSHU	Poster: SCI-166	GERMANY
BHAT PAREEKSHITH	Poster: SCI-059	INDIA
BHATTI TRICIA	S3.3.2	USA
BHIMANIYA SUDHIR	S8.3.4	USA
BIASSONI LORENZO	Poster: EDU-114, Poster: EDU-115	UNITED KINGDOM
BIDDLE GARRICK	Poster: SCI-075	USA
BIJELIC VID	Poster: SCI-266	CANADA
BIKO DAVID M	S1.2.7,S2.1.1,S3.2.2,S3.2.4 S4.3.2,S7.3.1	USA
BILANIUK LARISSA T	S8.4.6	USA
BINKOVITZ LARRY	Poster: SCI-105	USA

(continued)

BIRDIR CHAHIT	Poster: SCI-072	GERMANY
BISHAY MARK	S1.2.2, Poster: EDU-001, Poster: SCI-233, Poster: SCI-275	UNITED KINGDOM
BISSET LOGAN	Poster: SCI-246	USA
BISWAS ROHAN	Poster: EDU-070	USA
BIXBY SARAH	S8.2.1, Poster: SCI-064	USA
BLANC RAPHAËL	S5.3.1	FRANCE
BLANCHETTE VICTOR	S7.3.2, Poster: SCI-207	CANADA
BLANCO CYNTHIA	Poster: SCI-037	USA
BLINMAN THANE A.	Poster: SCI-094,Poster: SCI-095	USA
BLOCK TOBIAS	S3.3.4	USA
BOBBEY ADAM	Poster: SCI-280	USA
BODO NICOLE	S7.1.6, Poster: SCI-061	USA
BODRIA MONICA	S3.3.3,S3.3.5	ITALY
BOLDRINI LUCA	S3.4.1	ITALY
BONAFFINI PIETRO ANDREA	S7.1.3,S8.1.5, Poster: SCI-134, Poster: SCI-202	ITALY
BONNEFOY-MAZURE ALICE	Poster: SCI-193	SWITZERLAND
BOORA NAVEENJYOTE	Poster: SCI-207	CANADA
BORDALO RODRIGUES MARCELO	S1.2.9	BRAZIL
BORDONARO VERONICA	S6.3.4,Poster: SCI-190	ITALY
BORN MARK	Poster: EDU-010, Poster: EDU-076	GERMANY
BORST ALEXANDRA	S4.2.3	USA
BOSTRÖM HÅKAN	Poster: SCI-206	SWEDEN
BOTTARI GIAMPIERO	Poster: EDU-056, Poster: EDU-057, Poster: EDU-058, S7.3.2	ITALY
BOUSKILL VANESSA	S7.4.3	USA
BOWMAN ROBIN	Poster: SCI-028	CANADA
BOYLE LUCY	S3.1.2, Poster: SCI-245	USA
BOZHKO OLGA	Poster: EDU-015,Poster: SCI-274	UNITED KINGDOM
BRADY DARRAGH	S3.3.7,S3.4.3,S7.1.5, Poster: SCI-006	RUSSIA
BRADY SAMUEL	Poster: EDU-047, Poster: EDU-055	USA
BRAITHWAITE KIERY	Poster: SCI-021	USA
BRAMANTYA IDO NARPATI	Poster: EDU-045, Poster: SCI-084, Poster: SCI-086, Poster: SCI-145	INDONESIA
BRAY HEATHER	S1.4.5	CANADA
BRECHT INES	Poster: SCI-166	GERMANY
BREUER CHRISTOPHER	S4.2.2	USA
BRIAN JAMES	Poster: SCI-039	USA
BRIASSOULIS GEORGE	Poster: SCI-015	GREECE
BRIGGS DANIEL	S4.2.3	USA
BRINK MELA	S1.4.1	SWEDEN
BRISSE HERVÉ	S5.3.1	FRANCE
BRISSE HERVÉ J.	Poster: SCI-092, Poster: SCI-154	FRANCE
BRODZISZ AGNIESZKA	Poster: SCI-028	POLAND
BROLUND-NAPIER CARINA	S6.4.3	UNITED KINGDOM
BROWN BRANDON	Poster: SCI-224	USA
BRUHNS RYAN	S1.4.4	USA
BRUIN MARRIE C.A.	S3.3.8	THE NETHERLANDS
BRUNO COSTANZA		ITALY

(continued)

BRUZONI MATIAS	S2.1.2	USA
BUFFELI FRANCESCA	Poster: SCI-230	ITALY
BUHK JAN HENDRIK	Poster: SCI-243	GERMANY
BULANOV PETR	S3.1.4,S8.3.3, Poster: SCI-245,	RUSSIAN FEDERATION
BULAS DOROTHY	S1.2.6	USA
BUNT CHRISTOPHER W.	Poster: SCI-006	USA
BURKHARDT BARBARA	S8.4.1	SWITZERLAND
BURKOW JONATHAN	Poster: SCI-016, Poster: SCI-019	USA
BUTTERWORTH ERIN	Poster: SCI-175	UNITED KINGDOM
BUTTERWORTH SONIA	Poster: SCI-086	CANADA
BYRNE ANGELA	S6.3.2	IRELAND
BYRNE ANGELA T.	Poster: EDU-068, Poster: SCI-123	IRELAND
C OFFIAH AMAKA	S7.4.6	UNITED KINGDOM
CABRAL ALÉXIA A.	Poster: SCI-177	BRAZIL
CADOGAN LAURA	S8.2.1	USA
CAFFARENA JOSE MARIA	Poster: EDU-003	SPAIN
CAHILL ANNE MARIE	S7.1.2,S7.1.4, Poster: SCI-149,	USA
CAJIGAS-LOYOLA STEPHANIE	S1.3.2	USA
CALDER ALISTAIR	S1.1.9	UNITED KINGDOM
CALLAGHAN FRASER	S8.4.1	SWITZERLAND
CALLAHAN MICHAEL	S6.2.5,S8.2.1, Poster: EDU-022, Poster: EDU-088, Poster: SCI-110	USA
CALLE TORO JUAN S.	Poster: SCI-238	PHILIPPINES
CAMACHO ALVIN	S3.3.8	ITALY
CAMOGGIO FRANCESCO	Poster: SCI-176	USA
CAMPION ANDREW	S3.3.3	ITALY
CAMPO IRENE	S3.1.6	SPAIN
CANDELA SANTIAGO	Poster: SCI-130	USA
CAO JOSEPH	S4.1.2	ITALY
CAORSI ROBERTA	S8.1.2	CANADA
CAOUILLE-LABERGE LOUISE	Poster: EDU-111	ITALY
CARAI ANDREA	ITALY	
CARBONE FRANCESCO SAVERI S7.1.3	S3.1.8,Poster: EDU-099, Poster: EDU-111,	ITALY
CARBONI ALESSIA	S5.3.1	FRANCE
CARDOEN LIESBETH	Poster: SCI-055	ITALY
CARLUCCI MARCELLO	S5.3.3	ITALY
CARMELA RUSSO	Poster: SCI-207	BRAZIL
CARNEIRO JORGE	Poster: EDU-019	BRAZIL
CARNEIRO MARQUES RODRIGO	Poster: EDU-063	PORTUGAL
CARNEIRO RITA	Poster: SCI-217	SPAIN
CARO-DOMINGUEZ PABLO	S5.1.5	USA
CAROTENUTO GIUSEPPE	Poster: SCI-020	CANADA
CARPIO OLGA	Poster: EDU-003	SPAIN
CARRETERO JUAN MANUEL	S3.1.6	SPAIN
CARRILLO ALBA	Poster: SCI-200	USA
CARRINO JOHN	Poster: EDU-059	UNITED KINGDOM
CARROLL ANNE	S3.3.2	USA
CARSON ROBERT	S1.4.1	FRANCE
CARTON MATTHIEU	Poster: EDU-104	USA
CARUSO PAUL	S8.1.1	USA
CASAR BERAZALUCE ALEJANDRA	S6.4.4	USA
CASHEN TY A.	Poster: EDU-071	USA
CASSART MARIE	S5.3.1	BELGIUM
CASSOUX NATHALIE	S3.4.1	FRANCE
CASTELLANO AURORA	Poster: SCI-057,Poster: SCI-089, Poster: SCI-169, Poster: SCI-175	ITALY
CASTLE STACEY		

(continued)

CASTRO DENISE	Poster: SCI-211	UNITED KINGDOM
CASTRO DENISE A	S6.2.3 S1.3.1,Poster: SCI-007, Poster: SCI-137,Poster: SCI-177	CANADA
CASTRO ROJAS CYD	S4.2.6	CANADA
CASTRO-ARAGON ILSE	Poster: SCI-116,Poster: SCI-141	USA
CAULO MASSIMO	Poster: EDU-099	USA
CECCHERINI ISABELLA	S4.1.2	ITALY
CEYHAN KORAY	Poster: SCI-269	ITALY
CHAIKA MARYANNA	S1.4.3	TURKEY
CHAIYACHATI BARBARA H.	Poster: SCI-187	GERMANY
CHAKRABORTY SANTANU	Poster: EDU-109	USA
CHAKRAVARTTY RIDDHKA	Poster: SCI-231,Poster: SCI-232	CANADA
CHAN JOYCE PUI KWAN	Poster: SCI-209	UNITED KINGDOM
CHAN PUI KWAN JOYCE	Poster: SCI-272	HONG KONG
CHAN SHERWIN	S1.1.8,S4.2.1,Poster: SCI-020,	HONG KONG
CHANG ALEX	Poster: SCI-018	USA
CHANG JENNIFER	Poster: SCI-075	CANADA
CHANG KENNETH	S3.4.2	USA
CHANG SAMUEL	S8.3.5	SINGAPORE
CHARALAMBOUS STAVROS	Poster: SCI-120	USA
CHATZI LEDA	Poster: SCI-120	GREECE
CHAUHAN ANKITA	Poster: EDU-056,Poster: EDU-057, Poster: EDU-058, Poster: SCI-171	USA
CHAUVIN NANCY	Poster: EDU-074	USA
CHAVAN GOVIND	S4.2.1,S4.2.2,S8.3.2,Poster: SCI-020	CANADA
CHAVHAN GOVIND	Poster: SCI-026	CANADA
CHAWLA SIDDHI	Poster: SCI-025	INDIA
CHEE YING HUI	Poster: SCI-134	UNITED KINGDOM
CHELI MAURIZIO	S1.3.5	ITALY
CHEN AARON	S8.2.6,Poster: SCI-106	USA
CHEN AARON E	Poster: SCI-102	USA
CHEN HAIYING	S4.1.4,S5.1.2,S5.4.2,Poster: SCI-004	CANADA
CHEON JUNG-EUN	Poster: SCI-005,Poster: SCI-163, Poster: SCI-210, Poster: SCI-272	SOUTH KOREA
CHEUNG KAI YAT KENNETH	Poster: EDU-007,Poster: EDU-008	CANADA
CHEUNG KENNETH	Poster: EDU-008	CANADA
CHIA NAM-HUNG	Poster: SCI-144	HONG KONG
CHIAM WOOI KEE	Poster: SCI-209	MALAYSIA
CHIN LEANNE HAN QING	S2.2.3	HONG KONG
CHIOTOS KATHLEEN	Poster: EDU-037, Poster: EDU-092	USA
CHITNAVIS MADHURA	Poster: SCI-010	USA
CHMIL MARGARITA	S4.1.4,S5.1.2,S5.4.2,Poster: SCI-004	SOUTH KOREA
CHO YEON JIN	Poster: SCI-005, Poster: SCI-163, Poster: SCI-210, S3.4.7	SOUTH KOREA
CHO YOUNG AH	S5.1.2,Poster: SCI-004	SOUTH KOREA
CHOI JAE WON	Poster: EDU-028	SOUTH KOREA
CHOI JOHN	S5.1.2,S5.4.2, Poster: SCI-004, Poster: SCI-104	USA
CHOI YOUNG HUN	Poster: SCI-163, Poster: SCI-210	SOUTH KOREA
CHOI YOUNGHUN	S4.1.4,Poster: SCI-005	SOUTH KOREA
CHOU JANET	S4.3.6	USA
CHOUDHARY ARABINDA	S1.3.3,S5.3.2,Poster: EDU-103, S1.1.9	USA
CHOUDHARY ARABINDA K	Poster: EDU-024, Poster: EDU-066, Poster: SCI-035,	USA
CHOUNTALA ANNA		GREECE

(continued)

	Poster: SCI-115	
	Poster: SCI-118,	
	Poster: SCI-119,	
	Poster: SCI-140,	
	Poster: SCI-250	
	Poster: SCI-278,	
	Poster: SCI-286,	
	Poster: SCI-287,	
CHOW JEANNE	S3.3.4	USA
CHOWDHURY MOTI	Poster: SCI-275	UNITED KINGDOM
CHRYSOULA KOUMANIDOU	Poster: SCI-278	GREECE
CHUANG JANET	S4.4.4	USA
CHUNG ELLEN	Poster: SCI-010	USA
CHUNG TAYLOR	S4.2.2	USA
CHUNG TIFFANY	Poster: EDU-008	HONG KONG
CIESLAK JOHN	Poster: SCI-160	USA
CIKMAN GOKALP	Poster: SCI-277	TURKEY
CINELLI CHRISTINA	Poster: SCI-058	USA
CLEMENT ANNICK	S1.2.8	FRANCE
CLIFFE HELEN	S6.3.1	UNITED KINGDOM
CLIFFORD SIMON	Poster: EDU-114,Poster: EDU-115	UNITED KINGDOM
ÇOBANOĞLU SEÇKİN	Poster: SCI-029,Poster: SCI-212	TURKEY
COCA DAVID	Poster: EDU-080	SPAIN
COHEN HARRIS L.	Poster: EDU-056,Poster: EDU-057,	
	Poster: EDU-058,	USA
COKER MICHAEL	Poster: SCI-136	USA
COLAFATI G. STEFANIA	S3.1.8,Poster: EDU-099,	
	Poster: EDU-111,	ITALY
COLE DENZEL	Poster: EDU-034	USA
COLEMAN BEVERLY	S8.4.4	USA
COLEY BRIAN	S3.3.7,Poster: SCI-109	USA
COLLEDGE JONATHAN	Poster: SCI-088,Poster: SCI-204,	
	Poster: SCI-203,	UNITED KINGDOM
COLLERAN GABRIELLE	S5.1.1,Poster: EDU-002,	
	Poster: EDU-030,Poster: SCI-123	IRELAND
COLLINGWOOD ELLEN	Poster: EDU-073,Poster: EDU-075,	
	Poster: SCI-161,	UNITED KINGDOM
COLLINS MARGARET	S6.2.1	USA
COMERT RANA GUNOZ	Poster: SCI-050,Poster: SCI-052,	
	Poster: SCI-148,Poster: SCI-215	TURKEY
CONAGHAN PHILIP	Poster: SCI-200	UNITED KINGDOM
CONNOLLY DANIEL JA	S6.3.1,Poster: EDU-100,	
	Poster: SCI-258,Poster: SCI-259	UNITED KINGDOM
CONSTANTINI SHLOMI	Poster: SCI-257	ISRAEL
CONTI GIOVANNI	S4.1.2	ITALY
CORDEIRO DE MACEDO PONTES IRLINE	Poster: EDU-019	BRAZIL
CORDER WILLIAM	S7.1.6	USA
CORDOEN LIESBETH	S1.4.1	FRANCE
CORNEJO PATRICIA	S7.4.5	USA
COSTIGAN CAOIMHE	Poster: EDU-067	IRELAND
COTTEN CHARLES MICHAEL	Poster: SCI-246	USA
COULOMB L HERMINÉ AURORE S1.2.8	FRANCE	
COURTIER JESSE	Poster: SCI-151	USA
CRIVELLI LAURENCE	Poster: SCI-081	SWITZERLAND
CRONENBER ROLAND	S8.4.2	AUSTRIA
CROOK TRAVIS	Poster: SCI-062	USA
CROSS SUSAN	Poster: SCI-204	UNITED KINGDOM
CROTHERS ABIGAIL	S4.4.4	USA
CROTTY ERIC	S3.4.3,Poster: SCI-065	USA
CRYAN JANE	Poster: EDU-108	IRELAND
CULHAM GORDON	Poster: EDU-007,Poster: SCI-031	CANADA
CURIONE DAVIDE	S1.2.9,S3.4.1	ITALY
CURRY JOE	Poster: EDU-059	UNITED KINGDOM
CYRANKA WERONIKA	Poster: SCI-092,Poster: SCI-154,	

(continued)

D VINODH	Poster: SCI-237,Poster: SCI-248 Poster: SCI-138,Poster: SCI-228, Poster: SCI-241,	POLAND
D'AMICO ALESSANDRA	S1.1.2	INDIA
DAHAB KATHERINE	S7.3.3	ITALY
DALDRUP-LINK HEIKE	S1.4.2	USA
DALE BRIAN	S4.2.1	USA
DALLA ROSA DAVIDE	Poster: SCI-134	ITALY
DALLORA ANA LUIZA	S7.3.5,Poster: SCI-184	SWEDEN
DAMASIO MARIA BEATRICE	S3.3.3,S3.3.5,Poster: SCI-055,	ITALY
D'AMICO ELBIO	Poster: SCI-207	BRAZIL
DAMPHOUSSE AMÉLIE	Poster: SCI-111	CANADA
D'ANDREA MARIA LUISA	Poster: EDU-111	ITALY
DANDRUPL HIEKE	S4.4.3	USA
DANEMAN ALAN	Poster: SCI-087,Poster: SCI-102	CANADA
DANIEL GEORGE	Poster: EDU-024	GREECE
DANIIL GEORGIOS	Poster: EDU-066,Poster: SCI-035, Poster: SCI-115,Poster: SCI-118 Poster: SCI-119,Poster: SCI-250, Poster: SCI-278, Poster: SCI-169	GREECE
DANIN JOANNA	S5.3.3	UNITED KINGDOM
D'ARCO FELICE	S8.2.6,Poster: SCI-094, Poster: SCI-095,Poster: SCI-106 Poster: SCI-254	UNITED KINGDOM
DARGE KASSA	Poster: SCI-207	USA
DARUGE PAULO	Poster: EDU-083	BRAZIL
DAS SREENA	S3.2.1	UNITED KINGDOM
DASI LAKSHMI PRASAD	Poster: SCI-146	USA
DAUGHERTY REZA	S3.1.1	USA
DAVATZIKOS CHRISTOS	S4.3.4	USA
DAVE HITENDU	S5.1.4	SWITZERLAND
DAVIDSON RICHARD	Poster: SCI-198	USA
DAVIES GARETH	Poster: EDU-115	UNITED KINGDOM
DAVIES THOMAS	Poster: EDU-117	UNITED KINGDOM
DAVIES TOM	Poster: EDU-006	UNITED KINGDOM
DAVILA JORGE	S4.4.2	CANADA
DAVIS J. CHRISTOPHER	Poster: SCI-246	USA
DAVIS JOSEPH	Poster: SCI-093	USA
DAWRANT MICHAEL	Poster: SCI-242	UNITED KINGDOM
DAYA SHEETAL	Poster: SCI-202	SOUTH AFRICA
DAYER ROMAIN	Poster: SCI-273	SWITZERLAND
DE BARBIERI FLORENCIA	Poster: SCI-202	CHILE
DE BODMAN CHARLOTTE	S7.4.2	SWITZERLAND
DE CATTE L	S4.2.4,S7.2.1	BELGIUM
DE HAAS ROBBERT	Poster: SCI-001	THE NETHERLANDS
DE JONG PIM A.	S1.4.4	THE NETHERLANDS
DE KEIZER BART	S4.2.4,S7.2.1	THE NETHERLANDS
DE KLEINE RUBEN	S3.3.1,S34:8	THE NETHERLANDS
DE KRIJGER RONALD R.	Poster: EDU-079	THE NETHERLANDS
DE LA HOZ POLO MARCELA	S1.4.4,S4.2.3	UNITED KINGDOM
DE LANGE CHARLOTTE	Poster: SCI-067	NORWAY
DE LISI GIOVANNI	Poster: SCI-105	ITALY
DE ST JEOR JEFFREY	Poster: SCI-001	USA
DE VOS BOB D.	Poster: SCI-247	THE NETHERLANDS
DE VRIES HEIKE	S8.4.4	GERMANY
DEBARI SUZANNE	Poster: SCI-055	USA
DEGL'INNOCENTI MARIALUDOVICA	S4.3.5	ITALY
DEGUZMAN MARIETTA	S1.4.1	USA
DELATTRE OLIVIER	Poster: SCI-069	FRANCE
DELLA GROTTA LYNN	Poster: SCI-206	USA
DELL'ERBA ALESSANDRO	S7.4.2	ITALY
DEMAEREL P	Poster: SCI-129,Poster: SCI-194, Poster: SCI-269,	BELGIUM
DEMIR BERRIN		TURKEY

(continued)

DENNIS REBECCA	Poster: SCI-094,Poster: SCI-095, Poster: SCI-110, S1.2.7	USA USA
DENNIS REBECCA A	S6.2.1,S6.2.2	USA
DENSON LEE A.	S7.4.2	UNITED KINGDOM
DEPREST J	Poster: SCI-207	BRAZIL
DERTKIGIL SERGIO	S5.4.1,Poster: SCI-022	USA
DESAI NILESH	S4.2.1	USA
DESHPANDE VIBHAS	Poster: SCI-082	USA
DESILET-DOBBS DEBBIE	S3.3.6	USA
DEVARAJAN PRASAD	S6.4.1	USA
DEVKOTA LAXMAN	S8.4.5	USA
D'HONDT AURÉLIE	Poster: SCI-183	USA
DHOUB AMIRA	S3.4.1	SWITZERLAND
DI GIANNATALE ANGELA	S3.4.1	ITALY
DI PAOLO PIER LUIGI	Poster: EDU-016	ITALY
DIAS JOÃO	Poster: SCI-023,Poster: SCI-027	PORTUGAL
DIAZ ERIC	Poster: SCI-074	USA
DIAZ JOANA	Poster: SCI-150	USA
DÍAZ MONTOYA MARCO ANTONIO	Poster: EDU-012	MEXICO
DIAZ RUIZ SANDRA	S1.1.6,S7.3.5,Poster: SCI-184,	SWEDEN
DIAZ SANDRA	Poster: EDU-055	SWEDEN
DICKSON PAULA	Poster: SCI-060	USA
DICKSON WILLIAM NOLAN DI	S8.4.4	USA
DIDIER RYNE	Poster: SCI-112,Poster: SCI-208, Poster: SCI-266,	USA
DIEN ESQUIVEL MARIA FERNANDA	S7.2.1	CANADA
DIKKERS RIKSTA	Poster: SCI-059	THE NETHERLANDS
DIKSHA DIKSHA	S3.3.6,S3.3.7,S3.4.3,S4.2.6	INDIA
DILLMAN JONATHAN	Poster: SCI-109	USA
DILLMAN JONATHAN R.	S6.2.1,S6.2.2	USA
DIMITRI PAUL	Poster: SCI-170	UNITED KINGDOM
DINA MATTHEW	Poster: SCI-045	USA
DINEEN ROBERT	S6.3.1	UNITED KINGDOM
DING AIPING	Poster: SCI-017	USA
DIPAOLANTONIO MARIA	Poster: SCI-268	ITALY
DITTMANN HELMUT	S4.4.1	GERMANY
DIXON RACHEL	S6.3.1	UNITED KINGDOM
DIYAOLU MODUPEOLA	S2.1.2	USA
DO BAO	Poster: SCI-176	USA
DOGANIS DIMITRIS	Poster: SCI-286,Poster: SCI-287	GREECE
DOME JEFFREY	Poster: SCI-274	USA
DONG PHUONG	S6.3.5	USA
DONNELLY AUSTIN	Poster: SCI-046	UNITED KINGDOM
DORI YOAV	S4.3.2	USA
DORI YOAV	S8.1.6	USA
DORIA ANDREA	S7.3.2,Poster: SCI-003, Poster: SCI-018,Poster: SCI-200 Poster: SCI-207,Poster: SCI-285	CANADA
DORIA ANDREA S.	Poster: SCI-284	CANADA
DOSHI JIMIT	S3.1.1	USA
DOTTA FRANCESCO	S3.1.8	ITALY
DOUGHERTY SHAUNA	Poster: SCI-061	USA
DOUROS KONSTANTINOS	Poster: SCI-040	GREECE
DOZ FRANÇOIS	S1.4.1,S5.3.1	FRANCE
DRAAISMA JOS MT	S4.3.1	THE NETHERLANDS
DRELICH KATARZYNA	Poster: SCI-237,Poster: SCI-248	POLAND
DRIVER CAMILLE	S6.4.2	USA
DUBOIS JOSÉE	S8.1.2,Poster: SCI-111, Poster: SCI-157,	CANADA
DUCOU LE POINTE HUBERT	S1.2.8	FRANCE
DUFFY PATRICK	S6.3.6	USA
DULCETTA LUDOVICO	S7.1.3	ITALY
DUNCAN NINA	Poster: SCI-235	USA

(continued)

DURAND RACHELLE	Poster: SCI-151	USA
DURVE DIPALEE	S1.2.4	UNITED KINGDOM
DUTT MOHINI	S3.3.2,Poster: SCI-014	USA
DYMARKOWSKI S	S7.4.2	BELGIUM
DZIEHCINSKA-POLETEK DARIA	Poster: SCI-079,Poster: SCI-080	POLAND
EASTY MARINA	Poster: EDU-114,Poster: EDU-115	UNITED KINGDOM
EBNER M	S7.4.2	UNITED KINGDOM
ECENARRO-MONTIEL ANA	Poster: SCI-217	SPAIN
ECKLUND KIRSTEN	S6.3.6	USA
EDWARDS HARRIET	S6.3.1	UNITED KINGDOM
EFTEKHARI ARASH	Poster: SCI-086	CANADA
EGBE TENIOLA	Poster: SCI-106	USA
EGBE TENIOLA I	S8.2.6,Poster: SCI-186,Poster: SCI-187,	USA
EING JULEE	Poster: SCI-002	USA
EKER OMEROGU RUKIYE	S7.2.6	TURKEY
EKVALL NILS	S4.2.3	SWEDEN
EL DEMELLAWY DINA	S6.4.5	CANADA
EL JALBOUT RAMY	Poster: SCI-111	CANADA
EL-ALI ALEXANDER	Poster: SCI-065	USA
ELBAALY HEBA	S7.2.3	UNITED KINGDOM
ELBAALY HEBA ELBAALY	S8.1.2,Poster: SCI-111,Poster: SCI-157,	CANADA
ELEGITI SAI	Poster: EDU-114	UNITED KINGDOM
ELETI SAIGEET	S7.2.2,Poster: EDU-115	UNITED KINGDOM
ELSINGERGY MOHAMED	S1.3.4,Poster: EDU-088, Poster: SCI-106,Poster: SCI-110 Poster: SCI-149	USA
EMAD-ELDIN SALLY	Poster: EDU-054	EGYPT
ENGLUND ERIN	S6.4.2	USA
ENRIQUEZ GOYA	S1.4.4	SPAIN
EPELMAN MONICA	S5.4.4	USA
EPSTEIN ADRIAN	Poster: SCI-246	USA
ERSOY BERKE	S1.3.8,Poster: SCI-113	TURKEY
ERUS GURAY	S3.1.1	USA
ESCALLARD CLÉMENT	S4.2.5	FRANCE
ESCOBAR FERNANDO	S7.1.2,S7.1.4,S7.1.6,S8.1.6 Poster: SCI-156	USA
ESCOBAR FERNANDO A	S4.3.2	USA
ESCOBAR-DIAZ MARIA CLARA	Poster: EDU-003,Poster: SCI-024	SPAIN
ESSER MICHAEL	S1.4.3,S1.4.5,S3.2.5,S4.4.1	GERMANY
ESTROFF JUDY	Poster: EDU-031	USA
EVANS EMILY	S6.3.1,Poster: EDU-001, Poster: SCI-233,Poster: SCI-275	UNITED KINGDOM
FADELL MICHAEL	S7.3.3,Poster: SCI-176	USA
FAGAN AISLING	Poster: EDU-087,Poster: EDU-114, Poster: EDU-115,Poster: EDU-117	UNITED KINGDOM
FAGAN NATHAN	Poster: SCI-159,Poster: SCI-165	USA
FAINGOLD RICARDO	Poster: SCI-087	CANADA
FANG CHARLES	Poster: SCI-176	USA
FARKAS AMY	S1.3.2,S5.1.4	USA
FARRAS LARA	S4.2.2	CANADA
FARSIANI YASAMAN	S3.2.1	USA
FAZEL AUDREY	Poster: SCI-224	USA
FEARON CONOR	Poster: EDU-108	IRELAND
FERGUSON POLLY	Poster: EDU-077,Poster: SCI-195	USA
FERNANDES ARTUR	Poster: SCI-207	BRAZIL
FERNANDES ELOY	Poster: SCI-207	BRAZIL
FERNANDES LÚCIA	Poster: EDU-016,Poster: EDU-086	PORTUGAL
FERRETTI ALESSANDRO	S3.1.8	ITALY
FERRETTI EMANUELA	Poster: SCI-266	CANADA
FEYGIN TAMARA	S3.1.5,S8.4.6	USA
FIANNACCA MARTINA	Poster: SCI-055	ITALY
FIDON L	S7.4.2	UNITED KINGDOM
FISCHER MADELEINE	S3.2.3	GERMANY
FITE JOHNSTON	S1.1.8	USA

(continued)

FITTOZ ÖMER SUAT	Poster: SCI-269	TURKEY
FITTOZ SUAT	Poster: SCI-129,Poster: SCI-194, Poster: SCI-239, S34:8	TURKEY THE NETHERLANDS
FITSKI MATTHIJS	Poster: SCI-198	UNITED KINGDOM
FITZSIMONS ANDREW	Poster: SCI-043	USA
FLECK ROBERT	S1.1.5	USA
FLEURY ANILAWAN S	S7.3.5,Poster: SCI-184	SWEDEN
FLODMARK CARL-JOHAN	S3.3.5	ITALY
FONTANA ANDREA	Poster: EDU-016,Poster: EDU-044, Poster: EDU-052,Poster: EDU-053 Poster: EDU-086	PORTUGAL
FORJACO ANA	S6.2.5	USA
FOUST ALEXANDRA	S6.4.1	USA
FOX KARIN	Poster: SCI-238	PHILIPPINES
FRAGANTE ROSANNA	S1.1.7	GERMANY
FRAHM JENS	Poster: SCI-206	ITALY
FRANCAVILLA MARIANTONIETTA	S5.1.4, Poster: EDU-026	USA
FRANCAVILLA MICHAEL	S4.2.5,S7.2.4,S8.1.3, Poster: SCI-109	FRANCE USA
FRANCHI ABELLA STÉPHANIE	Poster: SCI-058	USA
FRANKLAND MICHAEL	S8.3.5	USA
FRAZIER MICHAEL	S1.4.1,S5.3.1	FRANCE
FREEMAN ALVIN	S1.3.5	USA
FRENEAUX PAUL	Poster: SCI-019	USA
FRIEDLAENDER ERON	Poster: SCI-122	UNITED KINGDOM
FROST JAMIE	Poster: SCI-006,Poster: SCI-017	USA
FROSTE DANIEL	S1.4.6,S1.4.7	GERMANY
FRUSH DONALD	Poster: EDU-060,Poster: EDU-061	CHILE
FUCHS JOERG	Poster: SCI-121	USA
FUENTEALBA ISABEL	Poster: SCI-230	ITALY
FUJIMOTO JENA	Poster: SCI-209,Poster: SCI-272	HONG KONG
FULCHERI ENZIO	Poster: EDU-037,Poster: EDU-092	USA
FUNG KEVIN KIN FEN	Poster: SCI-037	GERMANY
FUNICIELLO LANDON	S1.3.4	USA
FÜRBÖTER-BEHNERT ISABEL	S7.1.2,Poster: SCI-156	USA
FURTH SUSAN	Poster: EDU-054	EGYPT
GABALLAH MARIAN	Poster: SCI-016	USA
GAD MUSTAFA	Poster: SCI-048,Poster: SCI-049, Poster: SCI-213,Poster: SCI-214	TURKEY
GADGEEL GAURAV	S4.3.6	USA
GAFARLI ARAZ	S1.2.2	UNITED KINGDOM
GAFFIN JONATHAN	S5.3.5	ITALY
GAGEN RICHARD	Poster: SCI-040	GREECE
GAGLIANO DOMENICO	Poster: SCI-015	USA
GALANI ANGELIKI	S3.3.6	USA
GALLO-BERNAL SEBASTIAN	S1.1.2,S3.1.8,S4.1.2,Poster: EDU-099 Poster: EDU-111	ITALY
GANDHI DEEP	Poster: EDU-111	ITALY
GANDOLFO CARLO	Poster: EDU-114,Poster: EDU-115, Poster: EDU-117, Poster: SCI-273	UNITED KINGDOM
GANGEMI EMMA	S22:4	CHILE
GARBERA DAVID	S8.1.3,Poster: EDU-035 Poster: EDU-110	USA FRANCE
GARCIA CRISTIAN	Poster: SCI-247	IRELAND
GARCIA TOMKINS KANDICE	S1.4.3,S1.4.6,S1.4.7, S1.4.3,S4.4.1,S1.4.7, S4.1.2	GERMANY GERMANY GERMANY
GAREL CATHERINE	Poster: EDU-036	ITALY
GARGAN MARY LOUISE	S1.4.1,S5.3.1	USA
GASER CHRISTIAN	S4.2.1,Poster: SCI-020, Poster: SCI-107,	FRANCE
GASSENMAIER SEBASTIAN		USA
GATIDIS SERGIOS		
GATTORNO MARCO		
GAUGUET JEAN-MARC		
GAUTHIER ARNAUD		
GEE MICHAEL		

(continued)

GEE MICHAEL S.	Poster: SCI-015	USA
GEIGER JULIA	S8.4.1,Poster: SCI-034	SWITZERLAND
GEOERGER BIRGIT	S1.4.1	FRANCE
GEORGE VERGHESE	S6.4.1	USA
GERALDO ANA	S1.1.2,S4.1.2,Poster: SCI-230,	PORTUGAL
GHAGHADA KETAN	S6.4.1	USA
GHANDI DEEP B.	S6.2.2	USA
GHIGGERI GIAN MARCO	S3.3.5,Poster: SCI-055	ITALY
GHOLIPOUR ALI	Poster: SCI-073	USA
GHOSH ADARSH	S3.3.2,S5.1.4,S5.3.4,Poster: SCI-014	USA
GIESEKE JÜRGEN	Poster: SCI-190	GERMANY
GIESTA ISABELA R. P.	Poster: SCI-177	BRAZIL
GILL ANNE	S1.3.9,S8.1.4,Poster: SCI-153, Poster: SCI-155	USA
GILL IRWIN	S4.1.3	IRELAND
GILL KANWAR	Poster: EDU-100	UNITED KINGDOM
GILL KARA	S6.4.4	USA
GILLIGAN LEAH	S3.4.3	USA
GILLMAN JENNIFER	S4.4.2	USA
GINADER ABIGAIL	S7.1.6,Poster: SCI-061	USA
GLUSIC MOJCA	S8.2.5	SLOVENIA
GLUTIG KATJA	S2.2.2	GERMANY
GLUTIG KATJA GLUTIG	Poster: SCI-147,Poster: SCI-247	GERMANY
GNANNT RALPH	S4.3.4	SWITZERLAND
GOKLI AMI	S3.4.5, Poster: EDU-070, Poster: EDU-082,Poster: SCI-006 Poster: SCI-061, Poster: SCI-065	USA
GOLDENBERG ANNA	Poster: SCI-018	CANADA
GOLDMAN-YASSEN ADAM	S3.1.5,Poster: SCI-222,Poster: SCI-260,	USA
GOLDSTEIN AMY	S4.1.1	USA
GÓMEZ GALLARDO GEORGINA	Poster: SCI-150	MEXICO
GOMEZ IRENE	Poster: EDU-003	SPAIN
GOMEZ-CHIARI MARTA	S3.1.6	SPAIN
GOMEZ-SAHAGUN MONICA HASSEL	Poster: SCI-070	MEXICO
GONCALVES FABRICIO	S4.1.1,S5.3.4	USA
GONCALVES LUIS	S7.4.5	USA
GONCALVES LUIS F.	S8.4.3,Poster: EDU-034	USA
GONZÁLEZ RODRÍGUEZ ANDREA PAOLA	Poster: SCI-150	MEXICO
GONZÁLEZ RODRÍGUEZ CARLOS HUMBERTO	Poster: SCI-150	MEXICO
GONZALEZ SERGIO	Poster: SCI-273	CHILE
GORKEM SUREYYA BURCU	S3.2.7,Poster: SCI-277	TURKEY
GOULD MARY	S1.3.3	USA
GOULD SHARON	S1.3.3,Poster: SCI-045,Poster: SCI-068,	USA
GOVAERT PAUL	S1.1.2	THE NETHERLANDS
GOVENDER THESHNI	Poster: SCI-085	SOUTH AFRICA
GRAEPLER MAINKA UTE	S3.2.5,S4.4.1	GERMANY
GRAF NORBERT	S3.3.1	GERMANY
GRÁFE DANIEL	S1.1.7,S3.2.6	GERMANY
GRAHAM ERIC	Poster: SCI-128	USA
GRANADOS MACÍAS MADELINNE	Poster: SCI-090	MEXICO
GRANATA CLAUDIO	S1.4.4,S5.3.5	ITALY
GRASSER MICHAEL GEORG	Poster: SCI-013	AUSTRIA
GRASSI DAPHINE	Poster: SCI-110	USA
GREEN NICOLE	S8.3.5	USA
GREENE ELTON	S1.4.2	USA
GREER MARY -LOUISE	S6.2.3, Poster: EDU-074, Poster: EDU-080,Poster: SCI-020	CANADA
GRÉVENT DAVID	Poster: SCI-081	FRANCE
GRIFFIN LINDSAY	S4.2.1	USA
GRIMM ROBERT	S1.4.7	GERMANY

(continued)

GRIPP EMILY	Poster: SCI-045	USA
GROTH MICHAEL	Poster: SCI-243	GERMANY
GRZEGORCZYK MAGDALENA	Poster: SCI-092,Poster: SCI-154	POLAND
GUARIENTO ALVES ANDRESSA	S7.3.1	USA
GUESSOUM MYRIAM	S7.2.2	UNITED KINGDOM
GUFFENS FREDERIC	S7.4.2	BELGIUM
GUILLEMOT DELPHINE	S1.4.1	FRANCE
GUILLERMAN PAUL	S2.1.3,S6.2.4	USA
GUILLERMAN R. PAUL	S3.2.8,S4.3.5	USA
GUIMARAES FABRICIO G	S8.4.6	USA
GUPTA NEETIKA	S6.4.5, Poster: EDU-006, Poster: EDU-109,	CANADA
GUR RAQUEL	S3.1.1	USA
GUR RUBEN	S3.1.1	USA
GURLEYEN HAZAL BERCEM	S3.2.7	TURKEY
GWAL KRITI	Poster: SCI-075,Poster: SCI-108	USA
HA AUDREY	Poster: SCI-176	USA
HA JI YOUNG	Poster: SCI-142	SOUTH KOREA
HAAS DAVID	S6.4.3	USA
HAAS EMILY	Poster: EDU-010	USA
HADIAN FATEMEH	Poster: EDU-001	UNITED KINGDOM
HAHN GABRIELE	Poster: SCI-037,Poster: SCI-071,Poster: SCI-072,	GERMANY
HAILU TIGIST	S7.1.6	USA
HALABI SAFWAN	S8.4.5	USA
HALEVY DAN	S8.3.2	CANADA
HALLIDAY KATH	S6.3.1	UNITED KINGDOM
HAMEED SHEMA	S1.2.4,S7.2.3,Poster: SCI-180,	UNITED KINGDOM
HAMILTON MARK	Poster: SCI-028	UNITED KINGDOM
HAMILTON THOMAS	S6.2.5	USA
HAMMAN SUSAN	Poster: SCI-011	USA
HAMMILL ADRIENNE	Poster: SCI-165	USA
HANAGANDI PRASAD	Poster: EDU-107	SAUDI ARABIA
HANEMANN CYNTHIA	Poster: SCI-060	USA
HANQUINET SYLVIANE	Poster: SCI-081,Poster: SCI-202	SWITZERLAND
HANSEN CARLY	S2.1.3	USA
HAQUE SAIRA	Poster: EDU-064,Poster: EDU-065,Poster: EDU-069,Poster: EDU-079 Poster: EDU-083,Poster: SCI-133	UNITED KINGDOM
HARA HIROKO	Poster: EDU-106	JAPAN
HARAVE SRIKRISHNA	S1.4.8,Poster: SCI-197	UNITED KINGDOM
HARCCKE H THEODORE	Poster: SCI-045,Poster: SCI-068	USA
HARITOU EKATERINI	Poster: EDU-024,Poster: EDU-066,Poster: SCI-035,Poster: SCI-140 Poster: SCI-278	GREECE
HAROON NIGIL	Poster: SCI-200	CANADA
HAROYAN HARUTYUN	Poster: EDU-015	USA
HARPER HOLLY	Poster: EDU-085	USA
HARRINGTON SAMANTHA	Poster: SCI-064,Poster: SCI-107	USA
HARRIS MATTHEW A	S3.2.2	USA
HARRIS SARAH	S7.3.4	USA
HARRIS SHELLEY	Poster: SCI-285	CANADA
HARTUNG ERUM	Poster: SCI-014	USA
HARTY MARY	Poster: SCI-068	USA
HARTY PATRICIA	Poster: SCI-045	USA
HASEEB HUMA	Poster: SCI-233	UNITED KINGDOM
HASHMI SAHAR	Poster: SCI-003	USA
HASKIYA HASAN	Poster: SCI-117	ISRAEL
HASSAN MAHMOUD MOHAMED	S7.4.6	EGYPT
HATTINGH LOUISE	Poster: EDU-105	UNITED KINGDOM
HAWKINS C. MATT	S8.1.4	USA
HAWKINS C. MATTHEW	Poster: SCI-155	USA
HAWKINS CLIFFORD MATTHEW	Poster: SCI-153	USA
HAWKINS MATT	S1.3.9	USA

(continued)

HAYASHIDA YOSHIKO	Poster: SCI-077	JAPAN
HAYES KARI	S7.3.3	USA
HEALY FIONA	S4.1.3	IRELAND
HEBELKA HANNA	S4.2.3	SWEDEN
HEDGES WILLIAM	Poster: EDU-001	UNITED KINGDOM
HEMMELMAYR ARIANE	Poster: SCI-013	AUSTRIA
HENNEBRY JENNIFER	Poster: EDU-108	IRELAND
HENRY M KATHERINE	S8.2.6,Poster: SCI-106,Poster: SCI-186,Poster: SCI-187	USA
HERKERT ELLEN	S1.1.2	THE NETHERLANDS
HERNÁNDEZ CRISTINA	Poster: EDU-084	SPAIN
HERNANZ-SCHULMAN MARTA	S1.1.4,Poster: SCI-096	USA
HERREGODS NELE	Poster: SCI-200	BELGIUM
HERRMANN JOCHEN	Poster: SCI-185,Poster: SCI-243	GERMANY
HERRMANN JUDITH	S1.4.5	GERMANY
HEWITT RICHARD	S5.3.3	UNITED KINGDOM
HIGGINS PETER D.	S6.2.1	USA
HILLIARD PAMELA	S7.3.2	CANADA
HILMES MELISSA	S5.4.5,Poster: EDU-027,Poster: EDU-085,Poster: SCI-062	USA
HILVERT NICOLE	S7.1.5,S8.1.1	USA
HINOJOSA JOSE	S3.1.6	SPAIN
HIREMATH SHIVAPRAKASH	Poster: EDU-109	CANADA
HIRSCH FRANZ WOLFGANG	S1.1.7,S3.2.6	GERMANY
HO ABIGAIL	Poster: SCI-263	SINGAPORE
HOARE SIBOHAN	Poster: EDU-002	IRELAND
HOBBINS JOHN	S6.4.2	USA
HOFFMAN CHRISTOPER	S1.3.5	USA
HOFFMAN ROBERT	Poster: SCI-280	USA
HOFFMANN RALF-THORSTEN	Poster: SCI-071,Poster: SCI-072	GERMANY
HO-FUNG VICTOR	Poster: SCI-106,Poster: SCI-171	USA
HOLSTE GREGORY	Poster: SCI-019	USA
HONG SHIJIE	S6.3.5	USA
HONG YOUNGTAEK	S5.4.2	SOUTH KOREA
HOOD-WATSON KRISTEN	Poster: SCI-006	USA
HOPMAN WILMA M.	S1.3.1	CANADA
HOPPE BERND	Poster: SCI-190	GERMANY
HOR KAN	Poster: SCI-166	USA
HORN PAUL	S7.4.4	USA
HOSKING MARTIN	Poster: EDU-007	CANADA
HOWELL DAVID	S7.3.3	USA
HU HARRY	S1.1.8	USA
HUANG DEAN	Poster: EDU-069	UNITED KINGDOM
HUANG HAO	S5.1.4	USA
HUANG SUIYUAN	S8.3.5	USA
HUISMAN THIERRY	S5.4.1,Poster: SCI-022	USA
HULL NATHAN	Poster: SCI-105	USA
HULSHOFF JAN BINNE	S4.2.4	THE NETHERLANDS
HUMPHREY TERRY	S8.2.2,Poster: SCI-093	UNITED KINGDOM
HUO AIHUA	S7.3.2,Poster: SCI-207	CHINA
HUO DONGLAI	Poster: SCI-236	USA
HUSSAIN ADAM	Poster: EDU-097	AUSTRALIA
HUSSAINI SYED	Poster: SCI-012	USA
HWANG JAE-YEON	S4.1.4,Poster: SCI-104	SOUTH KOREA
HWANG MISUN	S1.1.1,S2.2.3,S3.1.3,Poster: SCI-094	USA
	Poster: SCI-095,Poster: SCI-254	
HWANG ROSA	S1.3.5	USA
IBIS AYSE	S8.3.1	TURKEY
IHEZAGIRE IGOR	S2.1.4	TURKEY
ILIA STAVROULA	Poster: SCI-039	GREECE
INAREJOS EMILIO	Poster: SCI-200	SPAIN
INAREJOS EMILIO J	Poster: EDU-080	SPAIN
INSALACO ANTONELLA	S4.1.2	ITALY
IRAHARA SAHO	Poster: SCI-077	JAPAN
ITHIER GHISLAINE	S4.1.6	FRANCE
ITO YUSHI	Poster: SCI-077	JAPAN

(continued)

ITRAGO LEON PEDRO	S4.2.1	USA
IV MICHAEL	S4.4.3	USA
J. OTERO HANSEL	S3.3.2	USA
JACKSON KANDISE	S6.3.1	UNITED KINGDOM
JACOB JOHN	Poster: EDU-007	CANADA
JADHAV SID	Poster: SCI-008,Poster: SCI-009	USA
JADHAV SIDDHARTH	S5.4.1	USA
JAIMES CAMILO	S7.4.1,Poster: EDU-028, Poster: SCI-064, Poster: SCI-073	USA
JAIN AMIT	S1.1.8	USA
JAKAB ANDRAS	S8.4.1	SWITZERLAND
JANOS SARA	Poster: SCI-246	USA
JANS LENNART	Poster: SCI-200	BELGIUM
JANSSEN JAN JAAP	S4.3.3	THE NETHERLANDS
JARA HERNAN	Poster: SCI-116	USA
JARAMILLO DIEGO	S5.1.5,S6.3.5,S7.3.6,	USA
JAREMKO JACOB	Poster: SCI-193, Poster: SCI-200	CANADA
JARRIN JOSE	S7.3.2,Poster: SCI-207	CANADA
JAYAKUMAR ABIRAMI KRITHIGA	S1.3.6,Poster: SCI-283	INDIA
JEANES ANNMARIE	Poster: SCI-054,Poster: SCI-282	UNITED KINGDOM
JEFFERY TIMOTHY JAMES	Poster: SCI-127	AUSTRALIA
JENKINS RICHARD	Poster: SCI-057,Poster: SCI-089, Poster: SCI-169,Poster: SCI-175 Poster: SCI-211	UNITED KINGDOM
JENNIFER KUCERA	Poster: SCI-074	USA
JENNINGS RUSSELL	S6.2.5	USA
JENNISKENS SJOERD	S4.3.3	THE NETHERLANDS
JENSEN ERIK A	S3.2.4	USA
JEONG DAWUN	S5.4.2	SOUTH KOREA
JO JONATHAN	Poster: SCI-151	USA
JOANNA DANIN	Poster: SCI-211	UNITED KINGDOM
JOGEESVARAN HARAN	S7.2.3	UNITED KINGDOM
JOHNS CHRISTOPHER	Poster: SCI-259	UNITED KINGDOM
JOHNSON CURTIS	S5.3.2,Poster: EDU-103	USA
JOHNSON LAURA A.	S6.2.1	USA
JOHNSON OLIVER	Poster: EDU-073	UNITED KINGDOM
JOHNSTON PATRICK R	Poster: SCI-036	USA
JONES KATHRYN	Poster: EDU-037,Poster: EDU-092	USA
JOSEPHS SHELLIE	Poster: SCI-160	USA
JOSHI SAYALI	Poster: SCI-018,Poster: SCI-200	CANADA
JULIA SAIDMAN	Poster: EDU-051	ARGENTINA
JULIA UDAQUIOLA	Poster: EDU-051	ARGENTINA
JUNEWICK JOSEPH	Poster: SCI-016,Poster: SCI-019	USA
JUNG AH YOUNG	S3.4.7	SOUTH KOREA
JUNGE CARL-MARTIN	S3.2.3	GERMANY
JUNHASAVASDIKU THITIPORN	Poster: SCI-284	CANADA
JUNQUERA-OLAY SONSOLES	Poster: SCI-217	SPAIN
JÜRGENS JULIAN	Poster: SCI-185,Poster: SCI-243	GERMANY
JYOTHISH DEEPTHI	S1.2.2	UNITED KINGDOM
KAHANOWITCH RYAN	Poster: SCI-042	USA
KALAITZAKIS GEORGIOS	Poster: SCI-120	GREECE
KAMEL IHAB	S8.3.5	USA
KAMIYAMA NAOHISA	Poster: SCI-103	JAPAN
KAMONA AWS	Poster: SCI-223	CANADA
KAN AMANDA	Poster: SCI-209	HONG KONG
KAN ELAINE	Poster: EDU-008	HONG KONG
KAN ELAINE YEE LING	Poster: SCI-209	HONG KONG
KAN HERMAN	S2.1.3	USA
KAN YEE LING ELAINE	Poster: SCI-143,Poster: SCI-272	HONG KONG
KANAMORI YUTAKA	Poster: SCI-077	JAPAN
KANDEMIRLI SEDAT	Poster: EDU-077,Poster: SCI-195	USA
KANDULA ASHRITH	Poster: EDU-102,Poster: SCI-227,	

(continued)

KANDULA VINAY	Poster: SCI-271,	USA
KANE TIMOTHY	S5.3.2,Poster: EDU-103	USA
KANG JIHYUN	S1.2.6	USA
KAPLAN SUMMER	S3.4.5	USA
	S1.3.5,S4.2.2,Poster: SCI-106,	
	Poster: SCI-251	USA
KAPRAL NICOLE	Poster: SCI-146	USA
KAR ERICA	Poster: SCI-066	USA
KARA EZGI	Poster: SCI-029,	TURKEY
	Poster: SCI-047,	
	Poster: SCI-048,	
	Poster: SCI-049	
	Poster: SCI-212,	
	Poster: SCI-213,	
	Poster: SCI-214,	
	Poster: SCI-216	
	Poster: SCI-148,	
	Poster: SCI-264	
KARAKAS ROTHEY PINAR	S4.2.2	USA
KARIA SUMIT	Poster: SCI-025	UNITED KINGDOM
KARLI ELIF HAZAL	S8.3.1,	TURKEY
	Poster: SCI-047,	
	Poster: SCI-048,	
	Poster: SCI-051	
	Poster: SCI-131,	
	Poster: SCI-148,	
	Poster: SCI-264,	
	S8.3.5	USA
KARMAZYN BOAZ	S8.3.5	USA
KARNSAKUL WIKROM	S1.3.6,Poster: SCI-262,	
KARPAGA KUMARAVEL PRASANNA	Poster: SCI-283,	INDIA
	Poster: SCI-139,	SAUDI ARABIA
KASHGARI AMNA	Poster: EDU-107	
	Poster: SCI-243	GERMANY
KATEMANN CHRISTOPH	S5.3.2,	USA
KAUR GURCHARANJEET	Poster: EDU-103	
	S1.3.3	USA
KECSKEMETHY HEIDI	Poster: SCI-205	CANADA
KEDDIE TYSON	S1.2.5,S4.3.4,S8.4.1,Poster: SCI-034	SWITZERLAND
KELLENBERGER CHRISTIAN	S5.1.1,Poster: EDU-002	IRELAND
KELLY BRENDAN	Poster: SCI-166	USA
KELLY JOHN	Poster: SCI-126	UNITED KINGDOM
KHAIR ALMUZAMEL	S8.3.4	USA
KHANNA GEETIKA	Poster: EDU-065,Poster: SCI-133	UNITED KINGDOM
KHARA SAYANI	Poster: SCI-097	USA
KHASAWNEH HALA	S3.1.3	USA
KHAW KRISTINA	Poster: SCI-026	INDIA
KHERA PUSHPINDER	Poster: SCI-126	UNITED KINGDOM
KHOIJALI AHMED	S3.3.2,S3.3.4,S5.3.4,	USA
KHRICHENKO DMITRY	Poster: SCI-031	CANADA
KHUMALO ZONAH	Poster: SCI-094,Poster: SCI-095	USA
KHWAJA ASEF	S4.1.1	SOUTH AFRICA
KIDD MARTIN	S3.2.5	GERMANY
KIEFER LENA	S3.1.3,S2.2.3,Poster: SCI-235,	USA
KILBAUGH TODD	S5.1.1,Poster: EDU-002	IRELAND
KILLEEN RONAN	Poster: SCI-005	SOUTH KOREA
KIM DAE HEE	Poster: SCI-104,Poster: SCI-261	SOUTH KOREA
KIM HYUN GI	Poster: EDU-015	USA
KIM JANE	Poster: SCI-196	SOUTH KOREA
KIM JI YOUNG	S7.2.5,	
KIM JISOO	Poster: SCI-103,	
	Poster: SCI-178,	SOUTH KOREA
KIM JONG-HYO	Poster: SCI-005	SOUTH KOREA
KIM JORGE	S4.1.5,S5.3.4	USA

(continued)

KIM JORGE DU UB	S3.1.7, Poster: SCI-221	USA
KIM PYEONG HWA	S3.4.7	SOUTH KOREA
KIM WENDY G.	S8.2.3	USA
KIM WOO SUN	S4.1.4,S5.4.2,S5.1.2,Poster: SCI-004 Poster: SCI-005, Poster: SCI-163, Poster: SCI-210,	SOUTH KOREA
KINO AYA	S2.2.1	USA
KIRJAVAINEN TURKKA	Poster: EDU-013,Poster: SCI-032	FINLAND
KIRKHUS EVA	Poster: SCI-200	NORWAY
KIRSACLIOGLU CEYDA TUNA	Poster: SCI-129	TURKEY
KISHORE DIVYA	Poster: EDU-014	USA
KLEIBER NIINA	S8.1.2,Poster: SCI-157	CANADA
KLEIMEIER LOTTE ELISABETH	S4.3.1	THE NETHERLANDS
KLEIN WILLEMIJN	S4.3.3	THE NETHERLANDS
KLEIN WILLEMIJN M	S4.3.1	THE NETHERLANDS
KLINE-FATH BETH	S7.4.4	USA
KLJUCEVSEK DAMJANA	S8.2.5	SLOVENIA
KLOSS JENNY Y	Poster: SCI-106	USA
KNAPP JANINE	Poster: EDU-033	GERMANY
KNERR INA	Poster: EDU-110	IRELAND
KOBERLEIN GEORGE	Poster: SCI-069	USA
KOENIGSBERG ROBERT	Poster: EDU-096	USA
KOH HONG	Poster: SCI-103	SOUTH KOREA
KÖHLER THORSTEN	S6.2.6	NORWAY
KOKER OYA	S7.2.6	TURKEY
KOLBE AMY	Poster: SCI-105	USA
KOLLI K. PALLAV	Poster: SCI-151	USA
KOMÁR MATEJ	Poster: SCI-071	GERMANY
KOOIJMAN-KURFUERST HENDRIK	S8.4.2	GERMANY
KOPYTO EWA	Poster: SCI-237,Poster: SCI-244	POLAND
KORDING FABIAN	S8.4.2,Poster: EDU-033	GERMANY
KOSSIVA LYDIA	Poster: SCI-286, Poster: SCI-287	GREECE
KOUMANIDOU CHRISOULA	Poster: EDU-024, Poster: EDU-066, Poster: SCI-035, Poster: SCI-115 Poster: SCI-118, Poster: SCI-119, Poster: SCI-140, Poster: SCI-250 Poster: SCI-286, Poster: SCI-287	GREECE
KOUSHESH POURIA	Poster: SCI-130	USA
KOUTROUVELI ELENI	Poster: EDU-024, Poster: EDU-066, Poster: SCI-035, Poster: SCI-115 Poster: SCI-118, Poster: SCI-119, Poster: SCI-140, Poster: SCI-250 Poster: SCI-278, Poster: SCI-287	GREECE
KOYAMA TAKASHI	Poster: EDU-106	JAPAN
KOZAK BRANDI L.	Poster: SCI-254	USA
KOZLOVA POLINA	Poster: EDU-032,Poster: SCI-078	RUSSIAN FEDERATION
KRAUS MAREEN	S3.2.5,S4.4.1	GERMANY
KRAUSE MATTHIAS	S1.1.7	GERMANY
KRISHNAMURTHY GANESH	S4.3.2,S7.1.2,S7.1.4,S8.1.6 Poster: SCI-156	USA
KRISHNAMURTHY RAJESH	S3.2.1,S3.3.4,Poster: SCI-002,	USA

(continued)

	Poster: SCI-010	
	Poster: SCI-023,Poster: SCI-027,	
	Poster: SCI-166,	
KRISHNAMURTHY RAMKUMAR	S3.3.4,	
	Poster: SCI-023,	
	Poster: SCI-027,	USA
	Poster: SCI-166	
KRISHNASARMA REKHA	Poster: EDU-010	USA
KRITHIGA ABIRAMI	Poster: SCI-262	INDIA
KRÜGER PAUL -C	S2.2.2	GERMANY
KRÜGER PAUL CHRISTIAN	Poster: SCI-147	GERMANY
KUCERA JENNIFER	Poster: SCI-076	USA
KUCZYNSKA MARYLA	Poster: SCI-092,	POLAND
	Poster: SCI-154	
KUKUK GUIDO	Poster: SCI-190	GERMANY
KULOGLU ZARIFE	Poster: SCI-129	TURKEY
KUMAZAWA TAKAO	Poster: EDU-106	JAPAN
KUMBHAR SACHIN	Poster: EDU-102,	
	Poster: SCI-227,	
	Poster: SCI-271,	USA
KUPRIYANOV DMITRY	S8.3.3	RUSSIAN FEDERATION
KURUGOL SILA	S3.3.4	USA
KURZWEIL DINA	Poster: SCI-006	USA
KUZU ISINSU	Poster: SCI-269	TURKEY
KVIST OLA	S7.3.5,Poster: SCI-184	SWEDEN
KWEE THOMAS	S7.2.1	THE NETHERLANDS
KWEE THOMAS C.	S1.4.4	THE NETHERLANDS
KWOK HOI MING	Poster: SCI-272	HONG KONG
KWOK WAI-SIU	Poster: EDU-008	HONG KONG
LABORIE LENE BJERKE	Poster: SCI-183	NORWAY
LACANNA FRANCESCO	Poster: SCI-134	ITALY
LACEKOVA JANA	Poster: SCI-013	AUSTRIA
LADARRE DELPHINE	S7.2.4	FRANCE
LADERA ENRIQUE	Poster: EDU-003	SPAIN
LAFFAN EOGHAN E.	Poster: EDU-068	IRELAND
LAGERSTRAND KERSTIN	S4.2.3	SWEDEN
LAI LILLIAN	Poster: EDU-116	USA
LAILOW-SINGH HARSIMRAN	Poster: SCI-063,	
	Poster: SCI-088,	
	Poster: SCI-203,	UNITED KINGDOM
	Poster: SCI-204	
LALA SHAILEE	S5.4.4	USA
LAM CHRISTOPHER	Poster: EDU-074	CANADA
LAM MADELEINE	Poster: EDU-008	HONG KONG
LAM MARNIX G.E.H.	S4.4.6	THE NETHERLANDS
LAM YU HIN	Poster: SCI-143	HONG KONG
LAMBERT ROBERT	Poster: SCI-200	CANADA
LANDE CAREN	S6.3.1,	
	Poster: SCI-126,	
	Poster: SCI-218,	UNITED KINGDOM
LANGAN DEAN	S6.4.6	UNITED KINGDOM
LANGE LUISA KAROLINE	Poster: SCI-247	GERMANY
LANHAM SARAH	Poster: EDU-100	UNITED KINGDOM
LANKESTER EVELYN	Poster: SCI-145	CANADA
LAOR TAL	S7.3.6	USA
LAPIERRE CHANTALE	Poster: SCI-111,	CANADA
	Poster: SCI-157	
LARRY MATSUMOTO	Poster: SCI-074	USA
LARSEN ETHAN	S22.4,	
	Poster: EDU-023,	
	Poster: EDU-026,	USA
LARSON DAVID	S22.4	USA
LAU CHUI-KIN	Poster: EDU-008	HONG KONG
LAURENT MERYLE	Poster: SCI-202	SWITZERLAND

(continued)

LAWLOR AONGHUS	S5.1.1, Poster: EDU-002	IRELAND
LAWRENCE J. TODD	Poster: SCI-171	USA
LE CACHEUX CATALINA	Poster: SCI-087,Poster: SCI-102	CANADA
LE CAM SOLÈNE	S8.1.3	FRANCE
LE VIET	Poster: SCI-165	USA
LEBEL R. MARC	S6.4.4	CANADA
LEE ANNA	Poster: EDU-049	CANADA
LEE DONALD	Poster: SCI-201, Poster: SCI-125, Poster: SCI-174, S4.3.6	USA USA
LEE EDWARD	S8.2.3,Poster: SCI-030, Poster: SCI-036,	USA
LEE EDWARD Y.	Poster: EDU-008	HONG KONG
LEE FRANCIS	S3.4.7	SOUTH KOREA
LEE JIN SEONG	S7.2.5,Poster: SCI-101, Poster: SCI-103,Poster: SCI-178	SOUTH KOREA SOUTH KOREA
LEE MI-JUNG	S5.1.2,S5.4.2,Poster: SCI-004, Poster: SCI-005 Poster: SCI-163	SOUTH KOREA SOUTH KOREA
LEE SEUL BI	S4.1.4,Poster: SCI-210	SOUTH KOREA
LEE SEULBI	S4.1.4,S5.1.2,S5.4.2, Poster: SCI-004 Poster: SCI-005,Poster: SCI-210	SOUTH KOREA SOUTH KOREA
LEE SEUNGHYUN	Poster: SCI-104	SOUTH KOREA
LEE SO MI	S3.4.5	USA
LEI BRANDON	S1.4.1	FRANCE
LEMELLE LAURIANE	Poster: EDU-077,Poster: SCI-195	USA
LENERT ALEKSANDER	S3.4.1	ITALY
LENKOWICZ JACOPO	S4.1.3	IRELAND
LEONARD JANE	Poster: EDU-050	USA
LEONHARDT LEAH	S8.3.5	USA
LEUNG DANIEL	Poster: EDU-008	HONG KONG
LEUNG KA-HO	Poster: SCI-276	UNITED KINGDOM
LEVINE DANIEL	S4.2.4	THE NETHERLANDS
LEVOLGER STEF	S1.1.6	SWEDEN
LEWIS GABRIELLA	Poster: SCI-044	USA
LEWIS MICHAEL CHIGOZIR	Poster: EDU-032	RUSSIAN FEDERATION
LI OLGA	Poster: SCI-007	CANADA
LI TIN	S1.3.1	CANADA
LI TIN YAU	Poster: SCI-109	USA
LI YINAN	S7.3.2,Poster: SCI-207	CHINA
LI YING-JIA	Poster: SCI-205	CANADA
LIANG TERESA	Poster: SCI-200	NIGERIA
LIGHA ALOYSIUS	S1.1.6	SWEDEN
LILJEROTH MARIA	S7.2.5,Poster: SCI-101,Poster: SCI-178, Poster: SCI-261	SOUTH KOREA SOUTH KOREA
LIM HYUN JI	S1.2.2	UNITED KINGDOM
LIM JISEON	Poster: EDU-049,Poster: SCI-086	CANADA
LIM ZHIA	Poster: SCI-098	USA
LIMANTORO IONE	Poster: EDU-047,Poster: EDU-048	USA
LIN TOM	Poster: SCI-217	SPAIN
LINAM LEANN	S8.4.3	USA
LIÑARES-PAZ MARIA MERCEDES	S8.3.2	CANADA
LINDBLADE CHRISTOPHER L.	Poster: SCI-042	USA
LING SIMON	S1.4.2	USA
LINGURARU MARIUS GEORGE	Poster: SCI-168	CANADA
LINK MICHAEL	S1.4.4,S3.3.1,S34:8,S4.4.6 Poster: SCI-001	THE NETHERLANDS
LISTON MARIA	Poster: SCI-043	USA
LITTOOIJ ANNEMIEKE S.	S5.3.3	UNITED KINGDOM
LIU ISABELLA	Poster: SCI-088, Poster: SCI-203,	
LIVJA MERTIRI		
LJUTIKOV ANOUSHKA		

(continued)

LLOYD CLAIRE	Poster: SCI-204,	UNITED KINGDOM
LO RE GIUSEPPE	Poster: SCI-180	UNITED KINGDOM
LOCATELLI FRANCO	Poster: SCI-067	ITALY
LOEWEN JONATHAN	S3.4.1	ITALY
	S5.4.4,	
	Poster: EDU-048,	
LOHI JOUKO	Poster: SCI-179,	USA
LONG SARAH	Poster: EDU-013,Poster: SCI-032	FINLAND
LOPER PETER	Poster: SCI-060	USA
LOPEZ DIANA	Poster: SCI-011	USA
LOPEZ-GARCIA DIANA	S4.4.3	USA
LOW SAMANTHA	Poster: EDU-040	USA
LOYA MOHAMMED	Poster: EDU-001,Poster: EDU-025	UNITED KINGDOM
LU RONG	Poster: SCI-158	USA
LUKE BRIAN	S1.4.2	USA
LUKISH JEFFREY	S7.3.2	CANADA
LUMBROSO-LE ROUIC LIVIA	S1.2.6	USA
LUNGREN MATTHEW	S5.3.1	FRANCE
LUO YU	Poster: SCI-160	USA
LUTTERS GERD	Poster: EDU-085	USA
LYO SHAWN	S1.2.5	SWITZERLAND
LYON JANE	S1.1.1	USA
MA GRACE	S6.4.4	USA
MACCALLUM GAIL	S1.2.6	USA
	S8.2.3,	USA
	Poster: SCI-036	
MACHADO RIVAS FEDEL	S7.4.1,	
	Poster: EDU-028,	
	Poster: SCI-015,	USA
	Poster: SCI-064	
	Poster: SCI-073	
MACK LAUREN	Poster: SCI-002	USA
MACK TAKMAN	Poster: EDU-116	USA
MACKINNON GRANT	Poster: EDU-085,Poster: SCI-062	USA
MACVICAR DAVID	Poster: SCI-276	UNITED KINGDOM
MAENNLIN SIMON	S1.4.7	GERMANY
MAGEE JOHN	S8.3.5	USA
MAGHRABIA FADI	S1.3.7,Poster: EDU-105	UNITED KINGDOM
MAGISTRELLI ANDREA	S5.3.5	ITALY
MAGNAGUAGNO FRANCESCA	Poster: SCI-055	ITALY
MAGNITSKY SERGEY	Poster: SCI-235	USA
MAHALINGAM NEERAJA	S4.2.6	USA
MAHAN KELLYN	S8.2.1	USA
MAKIN ERICA	Poster: EDU-069,Poster: SCI-133	UNITED KINGDOM
MAKSYMOWYCH WALTER	Poster: SCI-200	CANADA
MALDONADO RAYAS JESUS	Poster: SCI-090	MEXICO
MALIK ARCHANA	Poster: EDU-096	USA
MALIK ULYA	Poster: EDU-001	UNITED KINGDOM
MALKIN DAVID	Poster: SCI-284,Poster: SCI-285	CANADA
MALONEY JOHN	Poster: SCI-236	USA
MALOVA MARIYA	S1.1.2	ITALY
MAMOUN SAEED	Poster: EDU-108	IRELAND
MAN CARINA	S7.3.2	CANADA
MANASHE SARAH	Poster: SCI-019	USA
MANGANAS GEORGIOS	Poster: EDU-093,	
	Poster: SCI-135,	
	Poster: SCI-172,	GREECE
MANKAD KSHITIJ	S1.1.9,S5.3.3	UNITED KINGDOM
MANN GURDEEP	Poster: EDU-005	QATAR
MANNES INÈS	S4.2.5	FRANCE
MÄNNLIN SIMON	S1.4.3	GERMANY
MANOPOULOU EVAGGELIA	Poster: EDU-093,	
	Poster: SCI-135,	
	Poster: SCI-172,	GREECE

(continued)

MANSOOR NINA	Poster: EDU-069	UNITED KINGDOM
MANZHURTS ANDREI	S3.1.4	RUSSIAN FEDERATION
MANZHURTSEV ANDREI	S3.1.2, Poster: SCI-245, Poster: SCI-252, Poster: SCI-253	RUSSIA
MAPUNDA ELLEN MARY	Poster: SCI-085	SOUTH AFRICA
MARESI EMILIANO	Poster: SCI-067	ITALY
MARGETAKI KATERINA	Poster: SCI-120	GREECE
MARIANA MEYERS	S6.4.2	USA
MARIS THOMAS G	Poster: SCI-120	GREECE
MARKHAM CHRISTINE	Poster: EDU-043	USA
MARRA PAOLO	S8.1.5	ITALY
MARRA PAOLO	S7.1.3	ITALY
MARRAZZO ANTONIO	S3.1.8, Poster: EDU-099, Poster: EDU-111, Poster: EDU-003	ITALY SPAIN
MARSICO SALVATORE	Poster: EDU-013, Poster: EDU-083, Poster: SCI-032,	UNITED KINGDOM
MARSLAND LAURA	Poster: SCI-259	UNITED KINGDOM
MARTIN ANDREW	S6.4.5, Poster: EDU-109, Poster: SCI-102, Poster: SCI-266	CANADA
MARTINEZ RIOS CLAUDIA	Poster: SCI-268	ITALY
MARTINI ANNA LISA	S4.1.2	ITALY
MARTINO SILVANA	bS4.1.1,S8.4.6	USA
MARTIN-SAAVEDRA JUAN SEBASTIAN	Poster: SCI-055	ITALY
MARZOLI ANNA	S8.3.5	USA
MASAND PRAKASH	Poster: EDU-032,Poster: SCI-078	RUSSIAN FEDERATION
MASHCHENKO IRINA	Poster: SCI-258	UNITED KINGDOM
MASON SUZANNE	Poster: EDU-111	ITALY
MASTRONUZZI ANGELA	Poster: SCI-237	POLAND
MATERNIAK ANDRZEJ	S5.3.1	FRANCE
MATET ALEXANDRE	Poster: EDU-098	USA
MATHEUS MARIA GISELE	Poster: SCI-226	USA
MATTHEWS BRITTANY	S3.3.3,Poster: SCI-055	ITALY
MATTIOLI GIROLAMO	Poster: SCI-237,Poster: SCI-244	POLAND
MATUSZEK MALGORZATA	Poster: EDU-007	CANADA
MAWSON JOHN	Poster: SCI-246	USA
MAXFIELD CHARLES	Poster: EDU-003	SPAIN
MAYOL JAVIER	Poster: SCI-136	USA
MCBEE MORGAN	Poster: EDU-031	USA
MCCLURE MEGHAN	S4.2.6	USA
MCCRARY JOSEPH	Poster: SCI-037	USA
MCCURNIN DONALD	Poster: EDU-067, Poster: EDU-068, Poster: SCI-123,	IRELAND
MCDONNELL CAOIMHE	S6.3.2	IRELAND
MCDONNELL CIARA	S7.4.6	IRELAND
MCGOVERN EIMEAR	Poster: EDU-007	CANADA
MCGRAW MARTY	Poster: EDU-081	USA
MCGUIRE CHARLES	Poster: SCI-082	USA
MCGUIRK SIMON	S1.2.2	UNITED KINGDOM
MCHUGH KIERAN	Poster: EDU-059,Poster: EDU-117	UNITED KINGDOM
MCHUGH WALT	Poster: SCI-235	USA
MCILVAIN GRACE	S5.3.2,Poster: EDU-103	USA
MCMANUS MEAGAN	Poster: SCI-235	USA
MCNAUGHTON RYAN	Poster: SCI-116	USA
MEDELEANU MARIA	Poster: SCI-285	CANADA
MEHOLLIN-RAY AMY	Poster: SCI-065	USA
MEISNER JAY	S6.2.5	USA

(continued)

MEISSNER CHRISTOPH	Poster: SCI-071,Poster: SCI-072	GERMANY
MEISTER RIEKE	Poster: SCI-185	GERMANY
MEISTER RIEKE LISA	Poster: SCI-243	GERMANY
MELAMED ROMAN	Poster: SCI-257	ISRAEL
MELLENDEZ SARAH	Poster: SCI-193	CANADA
MELETI CHRISTINA	Poster: EDU-093, Poster: SCI-135, Poster: SCI-172, Poster: SCI-252, Poster: SCI-253	GREECE RUSSIA
MELNIKOV ILYA	Poster: EDU-009	USA
MENASHE SARAH	Poster: EDU-078	CANADA
MENDES DA COSTA THOMAS	Poster: SCI-070	MEXICO
MENDOZA-CERPA CLAUDIA	S1.2.9	ITALY
MENNINI MARIA LUISA	Poster: SCI-037	GERMANY
MENSCHNER LEONHARD	S3.1.4,S8.3.3	RUSSIAN FEDERATION
MENSHCHIKOV PETR	S2.2.2,Poster: SCI-147, Poster: SCI-247, Poster: SCI-060	GERMANY USA
MENTZEL HANS -JOACHIM	S8.1.5 S3.4.2	ITALY
MERCADO-DEANE MARIA-GISELA	Poster: SCI-065	SINGAPORE
MERCANZIN ELISA	S3.2.1	USA
MERCHANT KHURSHID	S7.2.2, Poster: SCI-063, Poster: SCI-182, S1.1.2	USA
MERROW ARNOLD CARLSON	Poster: SCI-085	UNITED KINGDOM
MERY CARLOS	Poster: SCI-171	ITALY
MESHAKA RIWA	Poster: SCI-200	SOUTH AFRICA
MESSINA SIMONA	Poster: EDU-030	USA
METELO-LIQUITO LUKE DANIEL	S8.1.3	USA
METHRATTA SOSAMMA	Poster: SCI-268	FRANCE
METHRATTA SOSAMMA	S4.2.6	ITALY
MEYERS ARTHUR	S5.4.4	USA
MEYERS MARIANA	S5.4.4	USA
MEYRIGNAC OLIVIER	S1.4.4,S6.4.5, Poster: EDU-109, Poster: SCI-112	USA
MICHELA ALLOCCA	Poster: SCI-266	CANADA
MIETHKE ALEXANDER	Poster: EDU-116	USA
MILLA SARAH	Poster: SCI-081	FRANCE
MILLER ANGIE	Poster: SCI-117	ISRAEL
MILLER ELKA	Poster: EDU-013,Poster: SCI-032	FINLAND
MILLER JOSEPH	S1.2.1,S22:4,S4.1.5, Poster: SCI-111	USA
MILLISCHER ANNE-ELODIE	S4.2.5,S6.4.2	CANADA
MILNER ROTEM	Poster: SCI-006	USA
MIRAFTABI PÁRIA	Poster: SCI-226	USA
MIRANDA SCHAEUBINGER MONICA	Poster: SCI-207	BRAZIL
MIRON MARIE-CLAUDE	Poster: SCI-112	CANADA
MIRSKY DAVID	Poster: SCI-077	JAPAN
MITCHELL GRACE	Poster: SCI-077	JAPAN
MITCHELL TREY	S1.4.1	FRANCE
MITRAUD SONIA	Poster: SCI-037	GERMANY
MITSAKAKIS NICHOLAS	S1.3.3	USA
MIYASAKA MIKIKO	Poster: SCI-001	THE NETHERLANDS
MIYAZAKI OSAMU	S6.2.5	USA
MOALLA SALMA	S7.3.2,Poster: SCI-207	CANADA
MÖBIUS MARIUS	Poster: SCI-144	MALAYSIA
MODY TEJAL	Poster: SCI-275	UNITED KINGDOM
MOESKOPS PIM	S7.3.2, Poster: SCI-200, Poster: SCI-285,	CANADA
MOHAMMED SOMALA		
MOHANTA ARUN		
MOHD ZAKI FAIZAH MOHD ZAKI		
MOHOLKAR SHRUTI		
MOINEDDIN RAHIM		

(continued)

MOLLESTON JEAN	S8.3.5	USA
MOLOSSI SILVANA	S3.2.1	USA
MOLTER MOELLE	Poster: SCI-006	USA
MOLTO GARCIA JOSE FRANCISCO	Poster: SCI-042	USA
MOLTO JOSE	Poster: EDU-090	USA
MONARIM BRUNO MARINO	Poster: SCI-265	CANADA
MONSALVE JOHANNA	Poster: SCI-056	USA
MONSON MATTHEW	S7.3.3	USA
MONTEMEZZI STEFANIA	S3.3.8	ITALY
MOODLEY HALVANI	S6.3.3, Poster: SCI-085, Poster: SCI-181, Poster: SCI-242	SOUTH AFRICA
MOORE MICHAEL	S4.2.1	USA
MOORE TYLER	S3.1.1	USA
MOOTE DOUGLAS	S5.4.4, Poster: EDU-050	USA
MORANA GIOVANNI	S1.1.2	ITALY
MOREAU ANDREW	S6.3.5	USA
MORENO-MCNEILL DAVID	S3.2.8	USA
MORETTI PAOLLO	Poster: SCI-230	ITALY
MORGAN ERIC	Poster: SCI-023, Poster: SCI-027	USA
MORGENSTERN DANIEL	Poster: SCI-285	CANADA
MORIKI DAFNI	Poster: SCI-040	GREECE
MORIN CARA	S4.2.1,S4.2.2	USA
MOSCATELLI ANDREA	Poster: SCI-055	ITALY
MOSCHOVAKI ZEIGER ORNELLA	Poster: SCI-040	GREECE
MOSCOSO BOSCO ALEJANDRO	Poster: EDU-003	SPAIN
MOSTOUFI-MOAB SOGOL	S6.3.5	USA
MOTURU ABHISHEK	Poster: SCI-018	CANADA
MOUM SARAH	Poster: EDU-104	USA
MOURTOS EVANGELOS	Poster: EDU-012	SWEDEN
MPATZIOU IOANNA	Poster: SCI-039	GREECE
MUCHART JORDI	S3.1.6	SPAIN
MUELLER CLAUDIA	S2.1.2	USA
MUNAWAR SALEHA	Poster: SCI-007	CANADA
MUNUERA JOSEP	S3.1.6,Poster: EDU-003	SPAIN
MURARESKU COLLEEN	S4.1.1	USA
MURPHY ROBYN	Poster: EDU-095	USA
MUSCHOL NICOLE	Poster: SCI-185	GERMANY
MUSTAFA SHAMIMUNISA	Poster: SCI-037	USA
MYERS HANNAH	Poster: EDU-082	USA
MYLAVARAPU GOUTHAM	Poster: SCI-043	USA
NACE GARY	S1.3.5	USA
NADEL HELEN	Poster: EDU-040,Poster: SCI-267	USA
NAFFAA LENA	Poster: EDU-081	USA
NAGARAJ USHA	S7.4.4	USA
NANCE MICHAEL L	Poster: SCI-106	USA
NAOHISA KAMIYAMA	Poster: SCI-101	JAPAN
NAPOLITANO ANTONIO	S3.4.1	ITALY
NARAYANA VAMYANMANE DHANANJAYA KOTEB	Poster: SCI-228, Poster: SCI-240, Poster: SCI-241, Poster: SCI-055	INDIA
NARDI FRANCESCA	S8.3.5	ITALY
NARKEWICZ MICHAEL	S8.3.5	USA
NASHER OMAR	Poster: SCI-093	UNITED KINGDOM
NASR ALEXANDER	Poster: SCI-098	USA
NASSAR LARA	Poster: SCI-097	LEBANON
NASSER MICHAEL	S3.4.3,Poster: SCI-109	USA
NATHAN JAIMIE	Poster: SCI-098	USA
NATHAN NADIA	S1.2.8	FRANCE
NAVALLAS MARIA	Poster: EDU-003,Poster: EDU-080	SPAIN

(continued)

NAVARRO OSCAR	S6.2.3	CANADA
NAVARRO OSCAR M	Poster: EDU-080	CANADA
NAZAROVA EVELINA	S8.3.3	RUSSIAN FEDERATION
NDIBE CHRISTABELL	Poster: SCI-222,Poster: SCI-260	USA
NEGRAO JOSE	Poster: SCI-207	BRAZIL
NEUBERGER ILANA	Poster: SCI-236	USA
NEWMAN BEVERLEY	S2.1.2,Poster: EDU-004, Poster: EDU-011, Poster: SCI-143	USA HONG KONG
NG CAROL	Poster: EDU-008	HONG KONG
NG CAROL WING-KI	S1.3.4	USA
NG DEREK	Poster: EDU-008	HONG KONG
NG GEORGE	Poster: SCI-272	HONG KONG
NG WING KEI CAROL	Poster: SCI-006	USA
NGUYEN DANA R.	S1.2.3,S3.2.8,S4.3.5,	USA
NGUYEN HAITHUY	S5.1.4	USA
NGUYEN JIE	S7.3.1	USA
NGUYEN JIE C	S6.3.5	USA
NGUYEN JIE CHEN	Poster: SCI-100	AUSTRALIA
NGUYEN LAN	S6.3.5	USA
NGUYEN MICHAEL	S7.3.1	USA
NGUYEN MICHAEL K	Poster: EDU-030, Poster: EDU-067, Poster: SCI-123, Poster: SCI-122	IRELAND UNITED KINGDOM
NICHOLL RICHARD	S1.4.5	GERMANY
NICKEL MARCEL DOMINIK	Poster: SCI-280	USA
NICOL KATHLEEN	S1.4.1,S5.3.1	FRANCE
NICOLAS NAYLA	S1.4.4,S3.3.1,S4.4.6,Poster: SCI-001	THE NETHERLANDS
NIEVELSTEIN RUTGER A. J.	S5.3.2,Poster: EDU-102, Poster: EDU-103,Poster: SCI-227	USA
NIKAM RAHUL	Poster: SCI-271 S7.3.5,Poster: SCI-184	SWEDEN
NILSSON OLA	Poster: SCI-107	USA
NIMKIN KATHERINE	Poster: SCI-042	USA
NINO GUSTAVO	Poster: SCI-102	CANADA
NIRULLA GINA	Poster: SCI-164	USA MINOR OUTLYING ISLANDS
NISSIM LAVI	Poster: SCI-099	USA
NODA SAKURA	Poster: SCI-077	JAPAN
NOSAKA SHUNSUKE	Poster: SCI-284	CANADA
NOURMOHAMMAD ARMIN	S8.3.3	RUSSIAN FEDERATION
NOVICHKOVA GALINA	Poster: SCI-092, Poster: SCI-154	POLAND
NOWAKOWSKA MALGORZATA	S4.1.6	FRANCE
NTORKOU ALEXANDRA	Poster: EDU-044	PORTUGAL
NUNES ANA	Poster: SCI-056	USA
NURUZZAMAN FARZANA	S6.2.6	NORWAY
NYMO TRULSEN LENE	S6.3.1, Poster: EDU-001, Poster: EDU-025, S1.1.9	UNITED KINGDOM UNITED KINGDOM UNITED KINGDOM
OATES ADAM	Poster: SCI-173	CANADA
OATES ADAM J	Poster: SCI-265	AUSTRALIA
O'BOYLE ELAINE	Poster: SCI-100	TURKEY
OBRIEN CHRISTIAN ALFRED	Poster: SCI-239	UNITED KINGDOM
O'BRIEN KATHLEEN	Poster: SCI-170	
OCAK EMRE	S1.1.9,S6.3.1, Poster: SCI-054, Poster: SCI-122	UNITED KINGDOM
OFFIAH AMAKA	Poster: SCI-183, Poster: SCI-259	
OFFIAH AMAKA C	Poster: SCI-101, Poster: SCI-103	JAPAN

(continued)

OH SAELIN	Poster: SCI-041, Poster: SCI-142	SOUTH KOREA
O'HARA SARA	Poster: SCI-109	USA
OKAMOTO REIKO	Poster: SCI-077	JAPAN
OLGA SLATER	S5.3.3	UNITED KINGDOM
OLIANI CATIA	Poster: SCI-268	ITALY
OLIVER EDWARD	S8.4.4,S8.4.6	USA
OLOUKOI CAMELIA	S4.1.6	FRANCE
OLSEN ØSTEIN E.	S3.3.1	UNITED KINGDOM
O'NEIL ROSS	Poster: SCI-100	AUSTRALIA
ONO TAKAFUMI	Poster: EDU-106	JAPAN
ORBACH DANIEL	S1.4.1	FRANCE
OSMAN MARJMIN	Poster: SCI-144	MALAYSIA
O'SULLIVAN SIOBHAN	Poster: EDU-110	UNITED KINGDOM
OTERO HANSEL	S1.3.2, Poster: SCI-110, Poster: SCI-187,	USA USA
OTERO HANSEL J	S1.2.7,S2.1.1,S3.2.4,S4.3.2	
OTJEN JEFFREY	Poster: EDU-009, Poster: SCI-016, Poster: SCI-019, Poster: SCI-099	USA
OTOBO TARIMOBO	Poster: SCI-200	CANADA
OTTAVIANELLI ALESSANDRA	S1.2.9	ITALY
OTTO RANDOLPH	S8.3.5	USA
OUYANG MINUHI	S5.1.4	USA
OWOYELE ADEYINKA	Poster: EDU-101	USA
OZCAKAR BIRSIN	Poster: SCI-194	TURKEY
ÖZDEN ISMAIL	S1.2.5	SWITZERLAND
OZELO MARGARETH	Poster: SCI-207	BRAZIL
OZTEK MURAT ALP	Poster: SCI-099	USA
OZTURK ARZU	Poster: SCI-075	USA
PACE ERIKA	Poster: SCI-276	UNITED KINGDOM
PACE MARIO	S5.3.5	ITALY
PADDOCK MICHAEL	S6.3.1, Poster: EDU-100, Poster: SCI-054, Poster: SCI-122, Poster: SCI-258, Poster: SCI-259, Poster: SCI-282,	UNITED KINGDOM
PAHLKA RAYMOND	S2.1.3	USA
PAK SEONGYONG	Poster: SCI-261	SOUTH KOREA
PALERMO JOSEPH	S8.3.5	USA
PALMER EMILEE	Poster: SCI-006	USA
PALTIEL HARRIET J.	S8.2.3	USA
PAMPARINO SILVIA	Poster: SCI-055	ITALY
PANAYIOTOU ANDREAS	Poster: EDU-079, Poster: SCI-133	UNITED KINGDOM
PANDEY SALIL	Poster: SCI-152	INDIA
PANDO BRIAN	Poster: SCI-226	USA
PANWAR JYOTI	Poster: SCI-207	INDIA
PANWAR SANUJ	Poster: SCI-207, Poster: SCI-284	INDIA
PAPAIOANNOU GEORGIA	Poster: EDU-093, Poster: SCI-135, Poster: SCI-172,	
PAPAKONSTANTINO OLYMPIA	Poster: SCI-200	GREECE
PARIENTE DANIELE	S4.2.5	GREECE
PARIKH ASHISHKUMAR	Poster: EDU-014	FRANCE
PARIKH SURAJ	Poster: SCI-199	USA
PARK HALLEY	S8.2.3	USA
PARK JI EUN	Poster: SCI-104	USA
PARODI ALESSANDRO	S1.1.2,Poster: SCI-230	SOUTH KOREA ITALY

(continued)

PARTHASARATHY JAYANTHI	S3.2.1,S34:4	USA
PARTINGTON SARA L	S3.2.2	USA
PASETTI FRANCESCO	Poster: SCI-055	ITALY
PASTORE SERENA	S4.1.2	ITALY
PATANÈ SIMONE	S3.3.8	ITALY
PATEL DHRUV	Poster: SCI-226	USA
PATEL HITEN	Poster: EDU-001	UNITED KINGDOM
PATEL JAI	Poster: SCI-161	UNITED KINGDOM
PATEL MANISH	Poster: SCI-159,Poster: SCI-165	USA
PATEL PREET	Poster: SCI-017	USA
PATEL RUPESH	Poster: SCI-098	USA
PATERSON ANNE	Poster: SCI-046, Poster: SCI-173, Poster: SCI-198,	UNITED KINGDOM
PATINO MANUEL	Poster: EDU-028	USA
PATTON DANIELLA	S5.1.4	USA
PAUDYAL BEN	Poster: EDU-102, Poster: SCI-227, Poster: SCI-271,	USA
PAYETTE KELLY	S8.4.1	SWITZERLAND
PEACHMAN ANDREW	Poster: SCI-280	USA
PENG YUN	S7.3.2, Poster: SCI-207	CHINA
PENNO EVA	Poster: EDU-012	SWEDEN
PEREZ ALEX	Poster: EDU-003	SPAIN
PEREZ FRANCISCO	Poster: EDU-009, Poster: SCI-016, Poster: SCI-019,	USA
PEREZ LIZBET	Poster: EDU-060, Poster: EDU-061	CHILE
PEREZ MANUELA	Poster: SCI-200	CANADA
PERISSI SARA	Poster: SCI-055	ITALY
PERITO EMILY	S8.3.6	USA
PERRONE ANNA	Poster: SCI-268	ITALY
PETROSYAN MIKAEL	S1.2.6	USA
PFEIFER CORY	Poster: SCI-130, Poster: SCI-225, Poster: SCI-256,	USA
PHUONG JONATHAN	Poster: SCI-121	USA
PIAGGIO GIORGIO	S3.3.3, Poster: SCI-055	ITALY
PIANYKH OLEG	Poster: SCI-015	USA
PICARIELLO STEFANIA	S5.3.3	ITALY
PICCIRILLI ELEONORA	Poster: EDU-099	ITALY
PICCOTTI EMANUELA	Poster: SCI-055	ITALY
PICHÉ NELSON	Poster: SCI-157	CANADA
PIEKARSKA MONIKA	Poster: SCI-092, Poster: SCI-154	POLAND
PIERRO AGOSTINO	Poster: SCI-087	CANADA
PIERRON GAËLLE	S1.4.1	FRANCE
PIFARRE FERRAN	S3.1.6, Poster: EDU-003	SPAIN
PIMS TS WORKING GROUP EVELINA	S1.2.4	UNITED KINGDOM
PINA PRATA RITA	Poster: EDU-044	PORTUGAL
PINTO ERIN	S4.3.2	USA
PINTO OLGA	Poster: SCI-003	CANADA
PIO LUCA	Poster: SCI-055	ITALY
PISTORIO ANGELA	S3.3.3,S3.3.5	ITALY
PITSOULAKI DESPINA	Poster: EDU-024, Poster: SCI-140	GREECE
PITTS JOHN	S1.1.8	USA
PLASENCIA JONATHAN D.	S8.4.3	USA
PLUT DOMEN	S8.2.3,Poster: SCI-030, Poster: SCI-162,	SLOVENIA

(continued)

PLYUKHIN ALEXEY	S7.1.1	RUSSIAN FEDERATION
POHL ERIN	Poster: EDU-023	USA
POLETTI ERICA	Poster: EDU-092, Poster: EDU-096	USA
POLLOCK AVRUM	S3.1.5,S8.4.6	USA
POMMIER ROMAIN	S8.1.3	FRANCE
PONGIGLIONE MARTA	Poster: SCI-055	ITALY
POON MEI YU	Poster: EDU-008, Poster: SCI-143	HONG KONG
PORTO LUCIANA	S3.4.6	GERMANY
POSSELT ANDREW	S8.3.6	USA
POWELL JOSHUA	Poster: SCI-199	USA
POWELL JULIE	S8.1.2	CANADA
POZNICK LAURA	S2.2.3,S8.2.6	USA
PRABHU SANJAY	S1.1.3	USA
PRADA FREDY	Poster: EDU-003	SPAIN
PRASAI AMIT	Poster: SCI-282	UNITED KINGDOM
PRASHER SPARSH	S1.4.8, Poster: SCI-197	UNITED KINGDOM
PRATA RITA	Poster: EDU-016, Poster: EDU-063	PORTUGAL
PRAYER DANIELA	S8.4.2	AUSTRIA
PRINCE DANIEL NICHOLAS	Poster: SCI-181	SOUTH AFRICA
PRONO VALENTINA	Poster: SCI-055	ITALY
PROUNTZOS SPYRIDON	Poster: SCI-040	GREECE
PRÜFER FRIEDERIKE	Poster: EDU-094	SWITZERLAND
PRUTHI SUMIT	S1.1.4, Poster: SCI-096	USA
PRYOR WILLIAM WATKINS	Poster: SCI-171	USA
PSYCHOGIOS MARIOS-NIKOS	Poster: EDU-094	SWITZERLAND
PURAM SNIGDHA	Poster: EDU-102, Poster: SCI-227, Poster: SCI-271, Poster: SCI-237	USA
PUSTELNIAK OLGA	S6.2.3	POLAND
PUTRA JUAN	Poster: SCI-076	CANADA
QUINTANA JAVIER	Poster: SCI-228, Poster: SCI-240, Poster: SCI-241, Poster: SCI-257	USA
R L RAMESH	S7.1.5,S8.1.1	INDIA
RABINOWICH AVIAD	S8.1.2	ISRAEL
RACADIO JOHN	S6.4.3	USA
RACICOT JEAN -NICOLAS	Poster: SCI-225, Poster: SCI-256	CANADA
RADHAKRISHNAN RUPA	Poster: SCI-259	USA
RADOSEVICH ANTHONY	Poster: SCI-039, Poster: SCI-120	USA
RAGHAVAN ASHOK	Poster: SCI-026	UNITED KINGDOM
RAISSAKI MARIA	Poster: SCI-152	GREECE
RAJAGOPAL RENGARAJAN	Poster: EDU-056, Poster: EDU-057, Poster: EDU-058, Poster: SCI-193	INDIA
RAJASEKARAN MUTHUSUBRAMANIAN		INDIA
RAJU ANAND		
RAKKUNEDETH HAREENDRANATH		USA
ABHILASH		CANADA
RAMACHANDRAN ABHAY	Poster: SCI-235	USA
RAMEH VANESSA	Poster: SCI-097	LEBANON
RAMENGGHI LUCA	S1.1.2,Poster: SCI-230	ITALY
RAMIREZ ALIA	S3.1.6	SPAIN
RAMIREZ KAREN I.	S2.1.1	USA
RAMIREZ SUAREZ KAREN	S1.2.1	USA
RAMIREZ-SUAREZ KAREN I	S1.2.7,S3.2.2,S3.2.4, Poster: SCI-070	USA
RAMOS-RUBIO GONZALO		MEXICO
RAMSEY JACOB	S5.4.5	USA

(continued)

RAMZAN ZAHRA	Poster: EDU-073	UNITED KINGDOM
RAND ELIZABETH	S7.1.2	USA
RANGINWALA SAAD	S7.4.3	USA
RAO PADMA	Poster: EDU-097	AUSTRALIA
RAPP JORDAN	S1.2.1	USA
RAPP JORDAN B	S1.2.7,S2.1.1,S3.2.2,S3.2.4 S4.3.2	USA
RASHIDI ALI	S1.4.2,S4.4.3	USA
RASLAN OSAMA	Poster: SCI-075	USA
RAUCCI UMBERTO	S3.1.8	ITALY
RAYA JOSE	S6.3.5	USA
RAZAVI ATEFE	S3.2.1	USA
REBOLLO MONICA	S3.1.6	SPAIN
REBSAMEN SUSAN	S6.4.4	USA
REDDY KARTIK	Poster: SCI-222,Poster: SCI-260	USA
REES MITCHELL	S34:4	USA
REGA ANA	Poster: EDU-052	PORTUGAL
REGMI PRADEEP RAJ	Poster: SCI-038, Poster: SCI-270	NEPAL
REID ALISTAIR	Poster: SCI-046	UNITED KINGDOM
REID CATRIONA	S7.2.3, Poster: SCI-180	UNITED KINGDOM
REID JANET	S8.2.4, Poster: SCI-012, Poster: SCI-061, Poster: SCI-065	USA
REID JANET R.	Poster: SCI-011	USA
RENSHAW BEN	Poster: SCI-224	USA
RENSHAW GRACE	Poster: SCI-224	USA
RENZ DIANE M.	S2.2.2	GERMANY
RETROUVEY MICHELLE	Poster: SCI-061	USA
REYNOSO-TOPETE ABRAHAM	Poster: SCI-070	MEXICO
RIAZ FARHANA R.	Poster: EDU-036	USA
RICHER EDWARD	Poster: EDU-014, Poster: EDU-055, Poster: SCI-179,	USA
RIEDEL ERICA	Poster: EDU-014, Poster: SCI-179	USA
RIEMANN MONIQUE	Poster: EDU-043, Poster: SCI-128	USA
RIGBY VALERIE	S22:4	USA
RISPOLI JOANNE	S1.1.3	USA
RISSMILLER JULIA	Poster: EDU-036	USA
RISTAGNO ROSS	Poster: SCI-165	USA
RIZZO FRANCESCA	Poster: SCI-055	ITALY
ROBERTS CHARLOTTE A.	Poster: SCI-088, Poster: SCI-203, Poster: SCI-204,	UNITED KINGDOM
ROBERTSON RICHARD	Poster: SCI-064	USA
ROBINSON AMIE	S1.1.8, Poster: SCI-020	USA
ROBINSON IAN	Poster: EDU-030	IRELAND
ROBSON CAROLINE	S5.3.3, Poster: EDU-028, Poster: SCI-064,	USA
ROEM JENNIFER	S1.3.4	USA
ROHDE JULIA	S7.4.1	USA
ROLLINS CAITLIN K	S7.4.1	USA
ROMBERG ERIN	Poster: EDU-009, Poster: SCI-019	USA
RONGO JEAN-KIMBERLY	Poster: SCI-199	USA
ROSENBAUM DANIEL	Poster: EDU-049, Poster: EDU-078, Poster: SCI-086,	CANADA

(continued)

ROSENBERG JARRETT	S8.4.5	USA
ROSENDAHL KAREN	S6.2.6, Poster: SCI-183, Poster: SCI-191, Poster: SCI-192	NORWAY
ROSSI ANDREA	S1.1.2,S4.1.2, Poster: SCI-230,	PORTUGAL
ROTARU CARMEN	Poster: SCI-208	CANADA
ROTH CHRISTIAN	S1.1.7	GERMANY
ROTH JONATHAN	Poster: SCI-257	ISRAEL
ROUECHE ALICE	S1.2.4	UNITED KINGDOM
ROUMELIOTAKI THEANO	Poster: SCI-120	GREECE
ROYALL IVEY	S1.2.3	USA
ROYERO ARIAS MONICA	Poster: EDU-042	COLOMBIA
ROYLE LEANNE	Poster: EDU-078, Poster: SCI-031	CANADA
RUBERT NICHOLAS	S8.4.3,S7.4.5, Poster: EDU-034,	USA
RUBESOVA ERIKA	S7.3.4,S8.4.5	USA
RUBIN JONATHAN M.	S6.2.1	USA
RÜDIGER MARIO	Poster: SCI-037	GERMANY
RUSS LYNN	Poster: SCI-002, Poster: SCI-010	USA
RUFFLE AMY	Poster: SCI-282	UNITED KINGDOM
RUMSEY DAX	Poster: SCI-200	CANADA
RUNYAN CHARLES	Poster: SCI-281	USA
RUTTEN CAROLINE	S7.2.4	FRANCE
RYALS ELIZABETH	Poster: SCI-225, Poster: SCI-256	USA
RYAN MAURA	Poster: EDU-104, Poster: SCI-234	USA
RYAN STEPHANIE	S4.1.3, Poster: EDU-067, Poster: EDU-110, Poster: SCI-123	IRELAND
RYCHIK JACK	S3.2.2	USA
RYPENS FRANÇOISE	S8.1.2, Poster: SCI-157	CANADA
RYU YOUNG JIN	Poster: SCI-104, Poster: SCI-196	SOUTH KOREA
S MANU	Poster: SCI-241	INDIA
SA MARIO	S1.2.4	UNITED KINGDOM
SAADAI PAYAM	Poster: SCI-108	USA
SA'ADEDIN FIRAS	Poster: SCI-133	UNITED KINGDOM
SABADO CONSTANTINO	S1.4.4	SPAIN
SADHASIVAM SENTHILKUMAR	S6.4.3	USA
SADHWANI ANJALI	S7.4.1	USA
SADIGH SUFI	Poster: SCI-057, Poster: SCI-211	UNITED KINGDOM
SAEBEOM HUR	Poster: SCI-163	SOUTH KOREA
SAEED SAAD	Poster: EDU-005	QATAR
SAFFARI SEYED EHSAN	S3.4.2	SINGAPORE
SAGO HARUHIKO	Poster: SCI-077	JAPAN
SAHIBLI ESHGIN	Poster: SCI-029, Poster: SCI-212, Poster: SCI-264,	
SAIGEET ELETI	S1.4.9	TURKEY
SAINT-MARTIN CHRISTINE	Poster: SCI-223	UNITED KINGDOM
SAIT SAIF	Poster: EDU-065	CANADA
SAITO YUKI	Poster: SCI-077	UNITED KINGDOM
SAKUMA EMERSON	Poster: SCI-207	JAPAN
SALEEM SHEENA	Poster: SCI-044	BRAZIL
SALERNO SERGIO	S5.3.5,Poster: SCI-067	USA
SÄLL MATS	Poster: SCI-191,	ITALY
		NORWAY

(continued)

SALLEMI CLAUDIO	Poster: SCI-192 S7.1.3	ITALY
SALMAN RIDA	Poster: EDU-081	USA
SAMEI EHSAN	Poster: SCI-017	USA
SAMIM ATIA	Poster: SCI-001	THE NETHERLANDS
SAMMER MARLA	S1.2.3,S2.1.3,S5.4.1,S6.2.4 Poster: SCI-008, Poster: SCI-009, Poster: SCI-022, Poster: SCI-255	USA
SANAMANDRA SARAT KUMAR	Poster: SCI-255	SINGAPORE
SANCHEZ DE TOLEDO JOAN	Poster: EDU-003	SPAIN
SANCHEZ RAMON	Poster: EDU-089, Poster: SCI-042 Poster: SCI-274	USA
SANCHEZ-JACOB RAMON	S7.3.4, Poster: EDU-040, Poster: SCI-267,	USA
SANDBERG JESSE	Poster: EDU-018, Poster: EDU-056, Poster: EDU-057, Poster: EDU-058 Poster: EDU-062, Poster: EDU-112	USA
SANDHU PREET	Poster: SCI-158	USA
SANKHLA TINA	S7.3.5, Poster: SCI-184	SWEDEN
SANMARTIN BERGLUND JOHAN	S1.2.9	ITALY
SANTANGELO TERESA PIA	Poster: SCI-067	ITALY
SANTORO MICHELE	S7.2.3	UNITED KINGDOM
SANTOS RUI	Poster: SCI-017	USA
SAPP ARMISTEAD	Poster: SCI-040	GREECE
SARDELI OLYMPIA	S6.4.1	USA
SARKAR POONAM	Poster: EDU-010, Poster: EDU-076	USA
SARMA ASHA	Poster: EDU-077, Poster: SCI-195	USA
SATO SHAWN	Poster: EDU-106	JAPAN
SATO SHINICHI	Poster: EDU-041	USA
SATO TAKASHI SHAWN	S3.1.1	USA
SATTERTHWAITE THEODORE	S1.2.1	USA
SAUL DAVID	S8.3.2	CANADA
SAYED BLAYNE	Poster: EDU-098	USA
SCAGGIANTE JACOPO	Poster: SCI-223	CANADA
SCHAEFER ABU HANA LETICIA	S1.4.7	GERMANY
SCHAEFER JUERGEN FRANK	S1.4.3,S1.4.5,S1.4.6,S4.4.1	GERMANY
SCHÄFER JÜRGEN	S3.2.5	GERMANY
SCHÄFER JÜRGEN F	S34:4	USA
SCHARSCHMIDT THOMAS	S1.4.7	GERMANY
SCHERER MONIKA	S1.2.5	SWITZERLAND
SCHERER STEPHAN	S3.3.1	GERMANY
SCHENK JENS-PETER	S5.4.4	USA
SCHENKER KATHLEEN	Poster: SCI-064	USA
SCHERRER BENOIT	S4.3.4	SWITZERLAND
SCHLAPBACH LUREGN	S1.4.1	FRANCE
SCHLEIERMACHER GUDRUN	Poster: EDU-027	USA
SCHLOTMAN ALYSSA	S1.4.7	GERMANY
SCHMIDT ANDREAS	Poster: SCI-037	GERMANY
SCHÖNFELD JULIA	Poster: EDU-033	GERMANY
SCHÖNNAGEL BJÖRN	S4.3.3	THE NETHERLANDS
SCHULTZE KOOL LEO	S3.2.5,S4.4.1	GERMANY
SCHWARZ RICARDA	S7.4.3	USA
SCORLETTI FEDERICO	S8.2.6, Poster: SCI-106, Poster: SCI-186,	USA
SCRIBANO PHILIP V		

(continued)

SEAH MAYAI	Poster: SCI-211	UNITED KINGDOM
SEAH MAY-AI	Poster: SCI-169	UNITED KINGDOM
SEBAALY MIKHAEL	Poster: EDU-041, Poster: EDU-077, Poster: SCI-195, S6.4.6, Poster: EDU-087	USA UNITED KINGDOM
SEBIRE NEIL	S1.2.9,S3.4.1 Poster: EDU-040, Poster: SCI-017, Poster: SCI-267, S2.2.2	ITALY
SECINARO AURELIO	Poster: SCI-008,Poster: SCI-009	USA GERMANY
SEEKINS JAYNE	S2.1.3,S5.4.1,S6.2.4, Poster: SCI-008 Poster: SCI-009, Poster: SCI-022 Poster: SCI-037	USA CANADA
SEIDNER STEVEN	Poster: SCI-265	USA
SELL ERICK	S34.4 Poster: EDU-032, Poster: SCI-078	RUSSIAN FEDERATION
SELVARAJ BHAVANI	S3.1.2,S3.1.4, Poster: SCI-245, Poster: SCI-252 Poster: SCI-253	RUSSIA
SEMEANOVA ELENA	Poster: SCI-129, Poster: SCI-194, Poster: SCI-239, Poster: SCI-269	TURKEY
SEMEANOVA NATALIA	S3.3.2,S4.2.1, Poster: SCI-014, Poster: SCI-018	USA
SERAI SURAJ	S3.2.2	USA
SERAI SURAJ D	S3.1.6	SPAIN
SERRANO SILVIA	S3.3.3,S3.3.5, Poster: SCI-055, S8.2.6, Poster: SCI-186	ITALY
SERTORIO FIAMMETTA	Poster: SCI-166	USA
SERVAES SABAH	Poster: SCI-141 Poster: SCI-163	GERMANY USA
SETSER RANDOLPH	S1.1.2,S4.1.2, Poster: SCI-230, Poster: SCI-049, Poster: SCI-213, Poster: SCI-214, Poster: EDU-024, Poster: EDU-066, Poster: SCI-035, Poster: SCI-115, Poster: SCI-118, Poster: SCI-119, Poster: SCI-140, Poster: SCI-250 Poster: SCI-278, Poster: SCI-286, Poster: SCI-287, S7.4.3	SOUTH KOREA PORTUGAL
SETTY BINDU N.	Poster: SCI-214, Poster: EDU-024, Poster: EDU-066, Poster: SCI-035, Poster: SCI-115, Poster: SCI-118, Poster: SCI-119, Poster: SCI-140, Poster: SCI-250 Poster: SCI-278, Poster: SCI-286, Poster: SCI-287, S7.4.3	TURKEY GREECE
SEUNGHYUN LEE	Poster: SCI-115, Poster: SCI-118, Poster: SCI-119, Poster: SCI-140, Poster: SCI-250 Poster: SCI-278, Poster: SCI-286, Poster: SCI-287, S7.4.3	USA
SEVERINO MARIASAVINA	Poster: SCI-002	USA
SEYREK SINAN	Poster: SCI-066, Poster: SCI-199	USA
SFAKIOTAKI RODANTHI	S1.3.9, Poster: SCI-158	USA
SHAABAN AIMEN		
SHAFFER REBECCA		
SHAH AMISHA		
SHAH JAY		

(continued)

SHAH SUMMIT	Poster: SCI-280	USA
SHAIKH FURQAN	S8.3.2	CANADA
SHALOF HEBA SALEH SHALO	Poster: SCI-170	UNITED KINGDOM
SHAPIRA GALI	Poster: SCI-091	CANADA
SHAPIRA-ZALSTBERG GALI	Poster: EDU-074, Poster: SCI-112	CANADA
SHARMA KARUN	Poster: SCI-042	USA
SHARP SUSAN	S4.4.4	USA
SHASHI KUMAR	S8.2.1,S8.2.3, Poster: EDU-021, Poster: EDU-022	USA
SHEA KEVIN	Poster: SCI-176	USA
SHEEHAN MATYLDA	S4.1.3	IRELAND
SHEEKA ALEX	Poster: SCI-089	UNITED KINGDOM
SHEEKA ALEXANDER	Poster: SCI-057, Poster: SCI-169	UNITED KINGDOM
SHEIKH ZISHAN	Poster: EDU-097	UNITED KINGDOM
SHELEPOVA EKATERINA	Poster: EDU-032	RUSSIAN FEDERATION
SHELMERDINE SUSAN	S5.4.3,S6.4.6, Poster: EDU-087, Poster: SCI-182	UNITED KINGDOM
SHELMERDINE SUSAN CHENG	Poster: SCI-063	UNITED KINGDOM
SHER ANDREW	S5.4.1,S6.2.4, Poster: SCI-008, Poster: SCI-009 Poster: SCI-022	USA
SHER ANDY	S2.1.3	USA
SHER NARENDRA	Poster: EDU-015, Poster: EDU-089, Poster: SCI-274, Poster: SCI-240	USA
SHETTY BALAKRISHNA	Poster: SCI-191,Poster: SCI-192	INDIA
SHI XIEQI	S3.1.5	NORWAY
SHIFRIN ANNA	S5.4.2	USA
SHIM HACKJOON	S3.4.7,	SOUTH KOREA
SHIN HYUN JOO	Poster: SCI-104	SOUTH KOREA
SHIRAN SHELLY I	Poster: SCI-257	ISRAEL
SHIU CHUN KIT	Poster: SCI-272	HONG KONG
SHIVAMURTHY VINAY	S7.2.3	UNITED KINGDOM
SHUAIB TAGHREED	Poster: SCI-132	SAUDI ARABIA
SHUWEIHDI FARAG	Poster: SCI-054, Poster: SCI-170	UNITED KINGDOM
SICO RITA	Poster: SCI-066	USA
SIDDIQUI IRAM	S8.3.2	CANADA
SIDPRA JAI	S1.1.9	UNITED KINGDOM
SIEDEK FLORIAN	S4.4.3	USA
SIEJKA KAROLINA	Poster: SCI-092, Poster: SCI-154	POLAND
SIEN MAURA	S1.1.8	USA
SIGNA SARA	S4.1.2	ITALY
SILEO CHIARA	S1.2.8	FRANCE
SILVA CECÍLIA P.	Poster: SCI-177	BRAZIL
SILVA CICERO	S5.4.4	USA
SILVA-CARMONA MANUEL	S3.2.8,S4.3.5	USA
SILVERIO PERROTTA	S5.3.3	ITALY
SILVESTRO ELIZABETH	Poster: EDU-023, Poster: EDU-026	USA
SIMCOCK IAN	S6.4.6	UNITED KINGDOM
SIMONE APPENZELLER	Poster: SCI-200	BRAZIL
SIMONI PAOLO	Poster: SCI-183	BELGIUM
SINGH RUCHI	S4.2.6	USA
SINGH SUDHA	S5.4.5, Poster: EDU-027, Poster: EDU-085,	USA

(continued)

SINGH SUSAN	Poster: EDU-108	IRELAND
SINHA SAURABH	Poster: EDU-100, Poster: SCI-258	UNITED KINGDOM
SIQQIQUI IRAM	S6.2.3	CANADA
SIRONI SANDRO	S7.1.3,S8.1.5, Poster: SCI-134,	ITALY
SIU NAVARRO YOUCK JEN	Poster: EDU-096	USA
SLAK PETER	Poster: SCI-162	SLOVENIA
SMITH CHRISTOPHER	S8.1.6	USA
SMITH CHRISTOPHER L	S4.3.2	USA
SMITH JESSICA	Poster: SCI-259	UNITED KINGDOM
SMITH KATHERINE	Poster: SCI-036	USA
SMITTHIMEDHIN ANILAWAN	S8.2.4	USA
SNYDER ELIZABETH	S1.1.4, Poster: EDU-010, Poster: EDU-076, Poster: SCI-096	USA
SO ERIC	Poster: EDU-008	HONG KONG
SOARES EUGÉNIA	Poster: EDU-044, Poster: EDU-063	PORTUGAL
SOBEIH AHMED M.	Poster: EDU-036	USA
SOBOLESKI DON	Poster: SCI-007, Poster: SCI-137	CANADA
SOBOLESKI DONALD A.	S1.3.1	CANADA
SOBOTA AMY	Poster: SCI-141	USA
SODHI KUSHALJIT	S1.2.1	INDIA
SOLANKI GUIRISH	Poster: SCI-233	UNITED KINGDOM
SOLARINO BIAGIO	Poster: SCI-206	ITALY
SOMASUNDARAM ELANCHEZHIAN	S3.3.7	USA
SOMCIO RAY	S2.1.3	USA
SOMMER MISCHA	S3.2.3	GERMANY
SONI SHELLY	S8.4.4	USA
SONIGO PASCALE	Poster: SCI-081	FRANCE
SORANTIN ERICH	Poster: SCI-013	AUSTRIA
SORGE INA	S1.1.7	GERMANY
SOTARDI SUSAN	S3.1.1,S4.2.1,S5.1.4, S5.3.3	USA
SOTIRIOS BISDAS		UNITED KINGDOM
SOUZA MICHELINE A. R.	Poster: SCI-177	BRAZIL
SPAMPINATO MARIA VITTORIA	Poster: EDU-098	USA
SPARKS CHRISTINA	S6.4.3	USA
SPIETH STEPHANIE	Poster: SCI-071, Poster: SCI-072	GERMANY
SPIJKERS SUZANNE	S1.4.4,S4.4.6, Poster: SCI-001,	THE NETHERLANDS
SPRINKART ALOIS	Poster: SCI-190	GERMANY
SPRUCE REBECCA	S1.2.4	UNITED KINGDOM
SPUNT SHERI	S1.4.2	USA
SPYRIDIS NICKOS	Poster: SCI-286	GREECE
SQUIRE SANDRA	S7.3.2	CANADA
SRIDHARAN ANUSH	S3.1.3	USA
SRINIVASAN ABHAY	S7.1.2,S8.1.6,Poster: SCI-156,	USA
SRIVASTAVA MAYANK	S6.4.1	USA
STABELL NIKLAS	S6.2.6	NORWAY
STACKIEVICZ RODICA	Poster: SCI-117	ISRAEL
STAFFA STEVEN	S6.2.5	USA
STAGNARO NICOLA	Poster: SCI-055	ITALY
STANCO FRANCESCO	S8.1.5	ITALY
STANEK JOSEPH	Poster: SCI-280	USA
STATES LISA	Poster: SCI-008, Poster: SCI-009, Poster: SCI-018,	USA
STATES LISA J.	S4.4.2	USA
STEFANO CONGIU	Poster: EDU-003	SPAIN
STEIN JILL	S7.3.3	USA

(continued)

STEINER ZVI	Poster: SCI-117	ISRAEL
STEIN-WEXLER REBECCA	Poster: SCI-108, Poster: SCI-121	USA
STELLACCI GIANDOMENICO	Poster: SCI-206	ITALY
STEPHENS LINDA	Poster: SCI-033	UNITED KINGDOM
STEVENS KENDALL	Poster: EDU-095	USA
STIMEC JENNIFER	Poster: SCI-200	CANADA
STIVAROS STAVROS	S6.3.1	UNITED KINGDOM
STOODLEY NEIL	S6.3.1	UNITED KINGDOM
STORER SILVIA	S3.3.8	ITALY
STRATAKIS NIKOS	Poster: SCI-120	USA
STRECKER RALPH	S1.4.5	GERMANY
SUBRAMANIAN SUBRAMANIAN	S4.2.2	USA
SUDOL-SZOPINSKA IWONA	Poster: SCI-200	POLAND
SULEMAN NAGEENA	Poster: EDU-001, Poster: EDU-025	UNITED KINGDOM
SULKOWSKI JASON	Poster: EDU-037	USA
SUN JING	S7.3.2	CHINA
SUNDER B VENKATAKRISHNA, SHYAM	Poster: SCI-014	USA
SUNG JIN	Poster: SCI-207	CHINA
SUPAKUL NUCHARIN	Poster: EDU-091	USA
SURIYAKUMAR VINITH	Poster: SCI-018	CANADA
SWEENEY KIERON	S4.1.3	IRELAND
SWERDLIN RACHEL	S8.1.4	USA
SZABO SARAH	S4.4.4	USA
SZE ALYSSA	S7.1.6,S7.3.1	USA
SZE RAYMOND	S22.4,S5.1.4,S7.1.6, Poster: EDU-023 Poster: EDU-026 Poster: EDU-108	USA
T. BYRNE ANGELA	Poster: EDU-108	IRELAND
TABARD-FOUGÈRE ANNE	Poster: SCI-202	SWITZERLAND
TAGALAKIS PANAGIOTIS	Poster: EDU-093, Poster: SCI-135, Poster: SCI-172, S1.4.9, Poster: EDU-073, Poster: EDU-075, Poster: SCI-161 Poster: SCI-279	GREECE UNITED KINGDOM
TAHIR NASIM	S5.3.3	ITALY
TALENTI GIACOMO	Poster: SCI-058	USA
TALMADGE JENNIFER	Poster: EDU-019	BRAZIL
TAMAKI SAMESHIMA YOSHINO	Poster: EDU-051	ARGENTINA
TAMARA KREINDEL	Poster: SCI-285	CANADA
TAMBASCO DOMENICA	Poster: SCI-097	USA
TAMER CHRISTEL	S3.4.2	SINGAPORE
TAN EELIN	Poster: SCI-083,Poster: SCI-255	SINGAPORE
TAN TIMOTHY SHAO ERN	Poster: EDU-009	USA
TANG ELIZABETH	S3.4.2, Poster: SCI-249, Poster: SCI-263, S6.4.1	SINGAPORE USA
TANG PHUA HWEE	Poster: SCI-123	IRELAND
TANIFUM ERIC	S1.3.4	USA
TARRANT AILBHE	Poster: EDU-033	GERMANY
TASIAN GREGORY	Poster: SCI-179, Poster: SCI-222, Poster: SCI-260, Poster: EDU-029	USA UNITED KINGDOM
TAVARES DE SOUSA MANUELA	S5.3.4	USA
TAYLOR SUSAN	S4.1.1,S8.4.6	USA
TAYLOR-ROBSINSON KATE	Poster: EDU-074	CANADA
TEIXEIRA SARA	Poster: EDU-038, Poster: EDU-039	SINGAPORE
TEIXEIRA SARA REIS		
TEMPLE MICHAEL		
TEO HARVEY		

(continued)

TEO HARVEY EU LEONG	Poster: SCI-083	SINGAPORE
TERESHCHENKO GALINA	S8.3.3	RUSSIAN FEDERATION
TEWATTANARAT NIPAPORN	Poster: SCI-018,Poster: SCI-284	CANADA
THACKER PAUL	Poster: SCI-105	USA
THAKOR AVNESH	Poster: SCI-160	USA
THALER MARTIN	S8.2.5	SLOVENIA
THAPALIYA SAMJHANA	S3.3.7,S3.4.3	USA
THEBAULD BERNARD	Poster: SCI-037	CANADA
THERUVATH ASHOK	S1.4.2	USA
THOMAS KRISTEN	Poster: SCI-105	USA
THOMPSON LYNN	S7.1.6	USA
THOMSON HEATHER CLARE	Poster: SCI-242	SOUTH AFRICA
THORPE MATTHEW	Poster: SCI-105	USA
THYAGARAJAN MANIGANDAN	Poster: EDU-001	UNITED KINGDOM
TIERRADENTRO GARCIA LUIS	S4.1.5,S5.3.4	USA
TIERRADENTRO-GARCÍA LUIS O.	S3.1.7	USA
TIERRADENTRO-GARCIA LUIS OCTAVIO	S1.1.1,S2.2.3,S4.1.1, Poster: SCI-094 Poster: SCI-095, Poster: SCI-221, Poster: SCI-254, Poster: SCI-061	USA
TIGIST HAILU	Poster: SCI-030,Poster: SCI-036,	USA
TIVNAN PATRICK	Poster: SCI-116, Poster: SCI-141	USA
TKACH JEAN	S3.3.6	USA
TKACH JEAN A.	S6.2.2	USA
TODEA RAMONA-ALEXANDRA	Poster: EDU-094	SWITZERLAND
TOIVIAINEN-SALO SANNA	Poster: SCI-220	FINLAND
TOLBOOM NELLEKE	S1.4.4	THE NETHERLANDS
TOLEND MIRKAMAL	Poster: SCI-200, Poster: SCI-207	CANADA
TOMA' PAOLO	S1.2.9,S3.1.8,S3.4.1,S5.3.5 Poster: EDU-111, Poster: EDU-099, Poster: SCI-183, S8.1.6	ITALY
TOMASULO CATHERINE	S8.1.6	USA
TOMLINSON CHRISTOPHER	Poster: SCI-087	CANADA
TONDO ANNALISA	Poster: SCI-268	ITALY
TOR DIEZ CARLOS	Poster: SCI-042	USA
TORTORA DOMENICO	S1.1.2,S4.1.2, Poster: SCI-230, Poster: SCI-202	ITALY
TOSO SEEMA	Poster: SCI-202	SWITZERLAND
TOWBIN ALEX J.	Poster: SCI-006	USA
TOWBIN ALEXANDER	S3.3.7	USA
TOWBIN RICHARD	Poster: SCI-164	USA MINOR OUTLYING ISLANDS
TRAN QUYNH	Poster: EDU-117	UNITED KINGDOM
TREAT JAMES	Poster: EDU-088	USA
TROUT ANDREW	S3.3.6,S3.3.7,S3.4.3,S4.2.6 S4.4.4, Poster: SCI-008, Poster: SCI-009, Poster: SCI-098 Poster: SCI-109	USA
TRUELOVE-HILL MONICA	S3.1.1	USA
TRUFANOV GENNADIY	Poster: EDU-032, Poster: SCI-078	RUSSIAN FEDERATION
TRUJILLO-ARIZA VIRGINIA	Poster: SCI-217	SPAIN
TSAI ANDY	S5.1.3, Poster: EDU-022, Poster: SCI-168, S1.2.5	USA
TSCHAUNER SEBASTIAN	S1.2.5	AUSTRIA
TSE SHIRLEY	Poster: SCI-200	CANADA

(continued)

TSEMBERIS ELENA	S1.3.5	USA
TSIFLIKAS ILIAS	S4.4.1,S1.4.3,S1.4.5,S1.4.6 S3.2.5	GERMANY
TSUKAMOTO JUN	Poster: SCI-077	JAPAN
TSUTSUMI YOSHIYUKI	Poster: SCI-077	JAPAN
TU EILEEN	Poster: SCI-205	CANADA
TUNACAO JESSA M.	Poster: SCI-056	USA
TUURA RUTH	S8.4.1	SWITZERLAND
TWOMEY EILIS	Poster: EDU-067	IRELAND
TZARIBACHEV NIKOLAY	Poster: SCI-200	GERMANY
TZAROUCHI LOUKIA	Poster: EDU-093, Poster: SCI-135, Poster: SCI-172, S3.1.2,S3.1.4, Poster: SCI-245, Poster: SCI-252	GREECE
UBLINSKIY MAXIM	Poster: SCI-253	RUSSIA
UCCELLA SARA	Poster: SCI-230	ITALY
UL HASSAN MUHAMMAD ZIA	Poster: SCI-219	SAUDI ARABIA
ULLOA-GONZALEZ JOSE MARIA	Poster: SCI-070	MEXICO
ULM BARBARA	S8.4.2	AUSTRALIA
UNAL EMEL	Poster: SCI-269	TURKEY
UNNIKRISHNAN SUNIL	S3.1.3	USA
URBINE JACQUELINE	Poster: EDU-037, Poster: EDU-092	USA
URGEL RYAN JASON	Poster: SCI-238	PHILIPPINES
URLA CHRISTIAN	S1.4.3,S1.4.6	GERMANY
URQUIZA SHEEN	Poster: SCI-238	PHILIPPINES
UTZ PHILIPP	S3.2.5,S4.4.1	GERMANY
VAFEIADI MARINA	Poster: SCI-120	GREECE
VAID DIVYA	Poster: SCI-025	UNITED KINGDOM
VAKAKI MARINA	Poster: EDU-024, Poster: EDU-066, Poster: SCI-035, Poster: SCI-115 Poster: SCI-118, Poster: SCI-119, Poster: SCI-140, Poster: SCI-250 Poster: SCI-278, Poster: SCI-286, Poster: SCI-287, S1.2.6	GREECE
VALAPARLA SUNIL	S1.2.6	USA
VALLE CLARISSA	Poster: SCI-134	ITALY
VALLE MAURA	Poster: SCI-055	ITALY
VALLS ARNAU	Poster: EDU-003	SPAIN
VALSANGIACOMO EMANUELA	S8.4.1	SWITZERLAND
VAN DEN HEUVEL-EIBRINK MARRY M.	S3.3.1,S34:8	THE NETHERLANDS
VAN DER BEEK JUSTINE N.	S3.3.1,S34:8	THE NETHERLANDS
VAN DER DOEF HUBERT	S4.2.4,S7.2.1	THE NETHERLANDS
VAN DER STEEG ALIDA F.W.	S34:8	THE NETHERLANDS
VAN GEYZEL LISA	S1.2.2	UNITED KINGDOM
VAN ROSSUM MARION	Poster: SCI-200	NETHERLANDS
VAN SANTEN HANNEKE M.	Poster: SCI-001	THE NETHERLANDS
VAN SCHAİK CAROLINE	S4.3.3	THE NETHERLANDS
VAN SCHAİK KATHERINE	Poster: SCI-168	USA
VARGAS SARA	S4.3.6	USA
VARIYAM DARSHAN	S1.3.9	USA
VASANAWALA SHREYAS	S2.2.1	USA
VASSALOU EVANGELIA	Poster: SCI-039	GREECE
VATSKY SETH	S7.1.2,S7.1.4, Poster: SCI-156,	USA
VATSKY SETH E.	S2.1.1	USA
VAUGHN JENNIFER	S7.4.5	USA

(continued)

VEALE SIMONE	S1.3.3	USA
VELASCO-ANNIS CLEMENTE	Poster: SCI-073	USA
VELDHUIS WOUTER B.	Poster: SCI-001	THE NETHERLANDS
VELEZ-FLOREZ MARIA	S1.3.5, Poster: EDU-023, Poster: EDU-026, Poster: SCI-012 Poster: SCI-061, Poster: SCI-251	USA
VELLEMA JEANINE	Poster: SCI-181	SOUTH AFRICA
VENKATAKRISHNA SHYAM	S5.1.4	USA
VENKATESAN CHARU	S7.4.4	USA
VERCAUTEREN T	S7.4.2	UNITED KINGDOM
VERHAGE THOMAS RICHARD	Poster: SCI-076	USA
VERHAGEN MARTIJN	S4.2.4,S7.2.1	THE NETHERLANDS
VERLHAC SUZANNE	S4.1.6	FRANCE
VERZEGNASSI FEDERICO	S1.4.4	ITALY
VIAENE ANGELA	S1.1.1,S5.3.4	USA
VIAL YVAN	Poster: SCI-081	SWITZERLAND
VICTORIA TERESA	S4.2.1,S8.4.4,S8.4.6,	USA
VIDDELEER ALAIN	S4.2.4	THE NETHERLANDS
VIGGIANO TAMARA	Poster: SCI-002, Poster: SCI-010	USA
VIGNALE ELISABETTA	Poster: SCI-055	ITALY
VILANI ANITA	Poster: SCI-284	CANADA
VILLACA PAULA	Poster: SCI-207	BRAZIL
VILLANI ANITA	Poster: SCI-285	CANADA
VIOLA ILARIA	Poster: SCI-067	ITALY
VIOLARI ELENA	Poster: SCI-160	USA
VIRANI KARIM VIRANI	Poster: SCI-153	USA
VITALE DAVID	Poster: SCI-098	USA
VITERI BERNARDA	S1.3.4,S3.3.2	USA
VOGEL TIPHANIE	S3.2.8,S4.3.5	USA
VOICU IOAN PAUL	Poster: EDU-111	ITALY
VOIT DIRK	S1.1.7	GERMANY
VON ALLMEN DANIEL	S8.1.1	USA
VON COSSEL KATHARINA	Poster: SCI-185	GERMANY
VON ROHDEN LUDWIG	Poster: SCI-185	GERMANY
VORONA GREGORY	Poster: EDU-037, Poster: EDU-092	USA
VOSS STEPHAN	Poster: EDU-021	USA
VOSSOUGH ARASTOO	S3.1.7,S4.1.1,S5.3.4, Poster: SCI-251	USA
VRAKA IRENE	Poster: EDU-024, Poster: EDU-066, Poster: SCI-035, Poster: SCI-115 Poster: SCI-118, Poster: SCI-119, Poster: SCI-140, Poster: SCI-250 Poster: SCI-278, Poster: SCI-287	GREECE
VUMA MAKHETHE	Poster: SCI-094, Poster: SCI-095	USA
VYSHEDKEVICH ELENA	Poster: SCI-078	RUSSIAN FEDERATION
WAGINGER MATTHIAS	S2.2.2,Poster: SCI-147	GERMANY
WAHEED KHAWAJA BILAL	Poster: SCI-219	SAUDI ARABIA
WALLACE ELLEN CHRISTINE	Poster: EDU-036	USA
WALLACE JACOB	Poster: SCI-082	USA
WALSH AOIBHINN	S4.1.3	IRELAND
WALSH CATHARINE	S6.2.3	CANADA
WALTER ANDREW	S5.3.2	USA
WANG GARY	Poster: SCI-107	USA

(continued)

WANG JOYE	Poster: SCI-056	USA
WARADY BRADLEY	S1.3.4	USA
WARFIELD SIMON	Poster: SCI-064	USA
WARFIELD SIMON K.	Poster: SCI-073	USA
WARMANN STEVEN	S1.4.3,S1.4.6	GERMANY
WARNE RICHARD	Poster: SCI-127	AUSTRALIA
WATSON SARAH	S1.4.1, Poster: SCI-231, Poster: SCI-232, Poster: SCI-028	FRANCE
WATSON SOPHIE	S7.2.2,Poster: EDU-117	UNITED KINGDOM
WATSON TOM	S3.3.1	UNITED KINGDOM
WATSON TOM A.	Poster: EDU-092	USA
WAY EWA	S3.4.5	USA
WEBB RYAN	Poster: SCI-159	USA
WEBER JONATHON	Poster: SCI-236	USA
WEINMAN JASON	Poster: SCI-042	USA
WEINSTOCK JERED	Poster: SCI-200	USA
WEISS PAMELA	Poster: EDU-020,	USA
WERMERS JOSHUA	Poster: EDU-072	
WERNER MAUREEN	S4.2.4	THE NETHERLANDS
WERNER MYRIAM	Poster: SCI-117	ISRAEL
WESSELS ROBYN MERYL	S6.3.3	SOUTH AFRICA
WETSCHEREK MARIA TA	Poster: SCI-025	UNITED KINGDOM
WEUM SVEN	S6.2.6	NORWAY
WEYLAND MATHIAS S.	S1.2.5	SWITZERLAND
WHITE AMMIE	S22:4, Poster: SCI-186	USA
WHITE AMMIE M	S1.2.7,S3.2.4,S4.3.2,	USA
WHITE AMMIE M.	S2.1.1	USA
WHITE CHRISTINA	Poster: SCI-236	USA
WHITEHEAD KEVIN K	S3.2.2	USA
WHITEHEAD MATHEW	Poster: EDU-090	USA
WHITMORE MORGAN	Poster: SCI-158	USA
WHITTAM FERN	S7.2.2,Poster: EDU-114, Poster: EDU-115, Poster: EDU-117	UNITED KINGDOM
WICAKSONO KRISHNA PANDU	Poster: SCI-021	JAPAN
WIJNEN MARC H.W.A.	S34:8	THE NETHERLANDS
WILDES DERMOT	Poster: EDU-067	IRELAND
WILKE UNDINE	S3.2.3	GERMANY
WILKINSON NICK	Poster: SCI-180	UNITED KINGDOM
WILLARD SCOTT	Poster: SCI-164	USA MINOR OUTLYING ISLANDS
WILLEMS RAFAEL	S3.4.6	GERMANY
WILLIAMS ALEXANDRA	Poster: EDU-029	UNITED KINGDOM
WILLIAMS FARIBA	Poster: EDU-117	UNITED KINGDOM
WILLIAMS LELIA	Poster: SCI-256	USA
WILSON NAGWA	Poster: SCI-091, Poster: SCI-265	CANADA
WINANT ABBEY	S4.3.6	USA
WINANT ABBEY J	S8.2.3, Poster: SCI-030, Poster: SCI-036,	USA
WISE RACHEL	S6.4.3	USA
WOLF DANIEL	S3.1.1	USA
WOLF LILY	Poster: EDU-091	USA
WONG CHRIS KWOK CHUN	Poster: SCI-143	HONG KONG
WONG DEREK	Poster: EDU-006	CANADA
WONG JAMES	S1.2.4,S7.2.3	UNITED KINGDOM
WONG KWOK CHUN	Poster: SCI-272	HONG KONG
WONG MICHELA	Poster: SCI-055	ITALY
WONG MICHELA CING YU	S3.3.3	ITALY
WONG YEE HING ERICA	Poster: SCI-144	MALAYSIA

(continued)

WOOD JOANNE N	S8.2.6, Poster: SCI-106, Poster: SCI-186, Poster: SCI-187	USA
WOODLEY HELEN	S8.2.2,Poster: SCI-093	UNITED KINGDOM
WOREDE FIKADU	S7.1.2	USA
WOREDE FIKADU WOREDE	S7.1.4, Poster: SCI-149	USA
WOZNIAK MAGDALENA	Poster: SCI-092, Poster: SCI-237, Poster: SCI-248,	POLAND
WOZNIAK MAGDALENA MARIA	Poster: SCI-154, Poster: SCI-244	POLAND
WU BOSCO	Poster: SCI-100	AUSTRALIA
WU RUNHUI	S7.3.2, Poster: SCI-207	CHINA
WUSIK KATIE	Poster: SCI-165	USA
XU CHEN XILEI	Poster: SCI-042	USA
YADAV TARUNA	Poster: SCI-026	INDIA
YAKOVLEV ALEXEI	Poster: SCI-252, Poster: SCI-253	RUSSIA
YAKOVLEV ALEXEY	S3.1.2,S3.1.4	RUSSIAN FEDERATION
YALLAMPALLI CHANDRASEKHAR	S6.4.1	USA
YAMAMURA JIN	Poster: EDU-033	GERMANY
YANG EDWARD	Poster: EDU-031	USA
YANG JOSEPH	S6.2.3, Poster: SCI-007	CANADA
YANG SHENG	S7.3.2	CHINA
YAP SAMUEL	Poster: SCI-121	USA
YARMENITIS SPYROS	Poster: EDU-093	GREECE
YARMENITIS SPYROS	Poster: SCI-135, Poster: SCI-172	GREECE
YAZDANI MILAD	Poster: EDU-098	USA
YE WEN	S8.3.5	USA
YEKELER ENSAR	S3.2.2,S4.3.2	USA
YEN ADAM	S8.3.6	USA
YEPURI APARNA DEVI	Poster: EDU-090	USA
YILMAZ SUKRIYE	Poster: SCI-129	TURKEY
YILMAZ SÜKRIYE	Poster: SCI-194, Poster: SCI-269	TURKEY
YONEYAMA MASAMI	S3.2.3	JAPAN
YONG CAI LING	Poster: SCI-249	SINGAPORE
YOON HAESUNG	S7.2.5, Poster: SCI-101, Poster: SCI-103, Poster: SCI-178	SOUTH KOREA
YOON HEE MANG	S3.4.7, Poster: SCI-104	SOUTH KOREA
YOSUPH AZZA	Poster: SCI-139	SAUDI ARABIA
YOU SUN KYUNG	Poster: SCI-104	SOUTH KOREA
YOUNG VICTORIA	Poster: SCI-160	USA
YUE XUYI	Poster: EDU-102, Poster: EDU-103, Poster: SCI-227, Poster: SCI-271	USA
YUEN MING KEUNG	Poster: SCI-209	HONG KONG
YUSUFOV AKIF	S7.1.1	RUSSIAN FEDERATION
ZAKANI SIMA	Poster: EDU-007	CANADA
ZALCMAN MAX	S7.3.4,S8.4.5	USA
ZAMPIERI NICOLA	S3.3.8	ITALY
ZANDIFAR ALIREZA	S3.1.7,S5.3.4,S7.1.4,Poster: SCI-094 Poster: SCI-095, Poster: SCI-221	USA
ZAPALA MATTHEW	S8.3.6,	USA

(continued)

ZARANKO ELVIRA	Poster: SCI-151	
ZARCHAN ADAM	Poster: SCI-134	ITALY
ZAVALETTA VAZ	Poster: SCI-082	USA
ZBOJNIEWICZ ANDREW	S8.1.4	USA
ZBOJNIEWICZ ANDY	Poster: SCI-016	USA
ZBROJA MONIKA	Poster: SCI-019	USA
	Poster: SCI-092,	
	Poster: SCI-154,	
	Poster: SCI-237,	POLAND
	Poster: SCI-244	
	Poster: SCI-248	
ZECH JOHN	S5.1.5	USA
ZEGOI MARIA SOLEDAD	Poster: SCI-273	CHILE
ZEIMPEKIS KONSTANTINOS	Poster: SCI-034	SWITZERLAND
ZELLNER MICHAEL	S1.2.5	SWITZERLAND
ZEMBER JONATHAN	Poster: SCI-042	USA
ZENDEJAS-MUMMERT BENJAMIN	S6.2.5	USA
ZHANG BIN	S4.4.4	USA
ZHANG JACK	Poster: SCI-193	CANADA
ZHANG NINGNING	S7.3.2,	CHINA
	Poster: SCI-207	
ZHANG SHUO	S3.2.3,S8.4.2,	
	Poster: EDU-033,	
	Poster: SCI-243	GERMANY
ZHANG ZHONGWEI	S8.3.4	USA
ZHAO JOSEPH	S3.4.2	SINGAPORE
ZHOU ALEX	S7.3.2,	CANADA
	Poster: SCI-207	
ZHOU FANG	S7.3.2,	CHINA
	Poster: SCI-207	
ZHOU WEI	Poster: SCI-236	USA
ZIMMERMANN PETER	S1.1.7	GERMANY
ZINGULA SHANNON	Poster: SCI-105	USA
ZNAJDEK MICHAL	Poster: SCI-200	POLAND
ZOURIDAKI CHRISTINA	Poster: SCI-035,	
	Poster: SCI-119,	
	Poster: SCI-140,	GREECE
ZUCCARINO FLAVIO	Poster: EDU-003,Poster: SCI-024	SPAIN
ZUCKER EVAN	S2.2.1	USA
ZURAKOWSKI DAVID	S6.2.5	USA
ZWAGEMAKER ANNE-FLEUR	S7.3.2	NETHERLANDS

Publisher's note Springer Nature remains neutral with regard to jurisdictional claims in published maps and institutional affiliations.